Facultad de Ciencias
Sede Bogotá

UNIVERSIDAD
NACIONAL
DE COLOMBIA

REVISTA COLOMBIANA DE CIENCIAS QUÍMICO-FARMACÉUTICAS

Universidad Nacional de Colombia
Facultad de Ciencias
Departamento de Farmacia

REVISTA COLOMBIANA DE CIENCIAS QUÍMICO-FARMACÉUTICAS
Universidad Nacional de Colombia, Facultad de Ciencias, Departamento de Farmacia.
ISSN 0034-7418, Fax: 3165060, Cra. 30 No. 45-03, Bogotá, D. C., Colombia.
Correo electrónico: *rcciquifa_fchog@unal.edu.co*
http://www.revistas.unal.edu.co/index.php/rccquifa
http://www.scielo.org.co/scielo.php?script=sci_serial&pid=0034-7418&rep=
https://scholar.google.com/citations?user=TvBT68sAAAAJ&hl=es

Edición, armada electrónica e impresión: Proceditor Ltda., Bogotá.
Teléfono: 757 9200. Fax: ext. 102.
Correo electrónico: *proceditor@yahoo.es*

MISIÓN

La *Revista Colombiana de Ciencias Químico-Farmacéuticas* es un órgano de difusión en el cual se publican investigaciones científicas, comunicaciones técnicas y revisiones temáticas originales en las áreas de las ciencias farmacéuticas (véanse Normas para publicación). La revista está destinada principalmente a químicos farmacéuticos, químicos, ingenieros químicos, médicos cirujanos, médicos veterinarios, y a otros profesionales de las ciencias físicas y naturales, de la ingeniería y de las profesiones sanitarias relacionadas con el uso de medicamentos.

VISIÓN

En pro de la difusión de las investigaciones, los contenidos de la *Revista Colombiana de Ciencias Químico-Farmacéuticas* son de acceso libre, con ello se espera llegar a un número mayor de lectores, propiciando la consolidación de comunidades académicas. Además, se proyecta que los contenidos publicados contribuyan al desarrollo e innovación de las ciencias farmacéuticas.

ÉTICA

La responsabilidad de lo expresado en cada artículo es exclusiva de los autores y no representa ni compromete posiciones de la revista ni del cuerpo editorial. Los contenidos publicados pueden reproducirse siempre que se cite la fuente respectiva. Esta revista sigue los lineamientos del COPE (Committee on Publication Ethics), que pueden ser consultados en *http://publicationethics.org/*

LICENCIA CREATIVE COMMONS

Contenido

Clinical research article / https://doi.org/10.15446/rcciquifa.v53n2.114422

Epidemiological profile of infections caused by *Helicobacter pylori* diagnosed through histopathological examinations conducted at a reference University Hospital

Davi Azevedo Ferreira [1a*], Carlos Márcio Moura Ponce de Leon [2b], Egberto Santos Carmo [2c]

[1]Postgraduate Program in Bioactive Natural and Synthetic Products, Department of Pharmaceutical Sciences, Federal University of Paraíba, 58050-585, João Pessoa, Paraíba, Brazil.

[2]Center for Education and Health of the Federal University of Campina Grande, 58175-000, Cuité, Paraíba, Brazil.

E-mail addresses: [a]daviazevedoferreira@ltf.ufpb.br, [b]carlos.marcio@professor.ufcg.edu.br, [c]egberto.santos@professor.ufcg.edu.br

*Correspondent author.

Received: October 23, 2023
Corrected: February 9, 2024
Accepted: February 15, 2024

Summary

Introduction: This study analyzed cases of *Helicobacter pylori* infection diagnosed through histopathological examinations. **Aim:** to analyze the results of anatomopathological examinations of gastric mucosa performed in the Pathology Department. **Methods:** It was an epidemiological, retrospective, descriptive and analytical study with a quantitative approach. The sample consisted of all the histopathological examinations of gastric mucosa obtained by upper digestive endoscopy (UDE) carried out at the Alcides Carneiro University Hospital between 01/01/2017 and 31/12/2019, for which there was a suspicion of *H. pylori* infection. **Results:** A total of 2028 reports and their respective requests were analyzed. The year with the highest prevalence of reports was 2018, with 798 (39.3%) tests carried out. The female sex prevailed with 1313 (64.7%) analyzes. The highest concentration of individuals was between 40 and 59 years of age, with 784 (38.7%). The main endoscopic finding presented by the doctor was gastritis, with 801 cases (39.5%). However, positive results proving clinical suspicion of *H. pylori* represented a smaller proportion of the findings, with 686 (33.7%). In addition, positive cases for *H. pylori* were more associated with the 20-59 age group (n=471; 23.2%) and it was found that patients with an endoscopic diagnosis of ulcers were more associated with positive results proving clinical suspicion for *H. pylori* on pathology examination

(n=106; 5.2%). **Conclusion:** We conclude that one third of the population seen at the hospital for EDA with biopsy and who had clinical suspicion of *H. pylori* infection were positive for the bacterium in the anatomopathological study subsequently carried out at the hospital during the period studied, corroborating the bacterial association with inflammatory processes of the gastric mucosa already described in previous studies.

Keywords: Gastric mucosa, Gastritis, Inflammation, *Helicobacter pylori*, Biopsy.

Resumo

Perfil epidemiológico das infecções causadas pelo *Helicobacter pylori* diagnosticadas através de exames histopatológicos realizados em um Hospital Universitário de referência

Introdução: O presente estudo analisou os casos de infecção causada por *Helicobacter pylori* diagnosticados através de exames histopatológicos. **Objetivo:** analisar os resultados dos exames anatomopatológicos da mucosa gástrica realizados no Serviço de Patologia. **Métodos:** Tratou-se de estudo epidemiológico, retrospectivo, descritivo e analítico, com abordagem quantitativa. A amostra foi composta por todos os exames anatomopatológicos de mucosa gástrica obtida por endoscopia digestiva alta (EDA) realizados no Hospital Universitário Alcides Carneiro entre 01/01/2017 e 31/12/2019, cuja solicitação foi apresentada suspeita de infecção por *H. pylori*. **Resultados:** Foram analisados 2028 laudos, com suas respectivas requisições. O ano com maior prevalência de laudos foi 2018, com 798 (39,3%) exames realizados. O sexo feminino prevaleceu com 1313 (64,7%) análises. A maior concentração dos indivíduos foi entre 40 a 59 anos de idade, com 784 (38,7%). O principal achado endoscópico apresentada(o) pelo médico foi gastrite, com 801 casos (39,5%). Contudo, os resultados positivos que comprovam a suspeita clínica para *H. pylori* representaram menor parcela dos achados, com 686 (33,7%). Além disso, os casos positivos para *H. pylori* associam-se mais com a faixa etária de 20 a 59 anos (n=471; 23,2%) e constatou-se que os pacientes com diagnóstico endoscópico de úlcera apresentaram maior associação com resultados positivos que comprovam a suspeita clínica para *H. pylori* ao exame anatomopatológico (n=106; 5,2%). **Conclusão:** Conclui-se que um terço da população atendida no Hospital para realização de EDA com biópsia e que apresentavam suspeita clínica de infecção por *H. pylori* apresentou positividade para a bactéria ao estudo anatomopatológico

subsequentemente realizado no hospital no período estudado, corroborando a associação bacteriana com processos inflamatórios de mucosa gástrica já descrita em estudos anteriores.

Palavras-chave: Mucosa gástrica, Gastrite, Inflamação, *Helicobacter pylori*, Biópsia.

Resumen

Perfil epidemiológico de las infecciones por *Helicobacter pylori* diagnosticadas mediante exámenes histopatológicos realizados en un Hospital Universitario de referencia

Introducción: El presente estudio analizó casos de infección por *Helicobacter pylori* diagnosticados mediante exámenes histopatológicos. **Objetivo:** analizar los resultados de los exámenes anatomopatológicos de la mucosa gástrica realizados en el Servicio de Patología. **Métodos:** Se trató de un estudio epidemiológico, retrospectivo, descriptivo y analítico, con enfoque cuantitativo. La muestra estuvo compuesta por todos los exámenes anatomopatológicos de la mucosa gástrica obtenidos por endoscopia digestiva alta (EDA) realizados en el Hospital Universitário Alcides Carneiro entre el 01/01/2017 y el 31/12/2019, cuya solicitud fue sospechosa de infección por *H. pylori*. **Resultados:** Se analizaron 2028 informes, con sus respectivas solicitudes. El año con mayor prevalencia de reportes fue 2018, con 798 (39,3%) exámenes realizados. Predominaron las mujeres con 1.313 (64,7%) análisis. La mayor concentración de individuos se registró entre 40 y 59 años, con 784 (38,7%). El principal hallazgo endoscópico presentado por el médico fue la gastritis, con 801 casos (39,5%). Sin embargo, los resultados positivos que confirman la sospecha clínica de *H. pylori* representaron una porción menor de los hallazgos, con 686 (33,7%). Además, los casos positivos para *H. pylori* se asocian más con el grupo etario de 20 a 59 años (n=471; 23,2%) y se encontró que los pacientes con diagnóstico endoscópico de úlceras tuvieron una mayor asociación con resultados positivos que confirman sospecha clínica de *H. pylori* en el examen patológico (n=106; 5,2%). **Conclusión:** Se concluye que un tercio de la población atendida en el Hospital por EDA con biopsia y que tuvo sospecha clínica de infección por *H. pylori* resultó positiva a la bacteria en el estudio anatomopatológico realizado posteriormente en el hospital durante el período estudiado, corroborando la asociación bacteriana con procesos inflamatorios de la mucosa gástrica ya descritos en estudios previos.

Palabras clave: Mucosa gastrica, Gastritis, Inflamación, *Helicobacter pylori*, Biopsia.

Introduction

In the world, there are thousands of microorganism species, including fungi, bacteria, and protozoa, but only a small fraction of these species have the potential to be pathogenic to humans [1].

One common bacterial infection worldwide is caused by *Helicobacter pylori*, a Gram-negative bacillus that infects the human stomach and can lead to gastritis, ulcers, and even more serious conditions such as cancer. It is estimated that a portion of the world's population may have this microorganism infecting their gastric mucosa, with the prevalence varying by region, affecting 46.3% of men, with a prevalence of 48.6% in adults compared to children [2].

Histopathological examinations are used in the diagnosis of various infections, including those caused by Helicobacter pylori, enabling the prescription of specific treatment [3].

The present study aimed to analyze the results of anatomopathological examinations of gastric mucosa performed in the Pathology Department of Alcides Carneiro University Hospital (ACUH), using tissue samples obtained via endoscopy, where the request indicated suspicion of *H. pylori* infection. The study is retrospective and includes examinations conducted from 01/01/17 to 31/12/2019, aiming to determine the profile of patients concerning age, gender, clinical hypotheses, endoscopic findings, and biopsy topography.

Materials and methods

The research consisted of an epidemiological, retrospective, descriptive, and analytical study with a quantitative approach [4]. Data collection was carried out in the physical archive of requests and reports from the Pathology Department of HUAC.

To constitute the sample, all anatomopathological examinations of gastric mucosa with tissue samples obtained through endoscopy were included, where there was a suspicion of *H. pylori* infection, while documents with incomplete information or outside the predefined time frame were excluded.

The data selected for analysis included the year of the examination, patient's gender, patient's age, diagnostic hypothesis (+/- endoscopic findings), biopsy topography, and the result of the *H. pylori* investigation.

The collected data were organized into a Microsoft Office Excel 2013 spreadsheet and later processed in the Statistical Package for Social Sciences (SPSS) software version

20.0, obtaining their absolute and relative frequencies and calculating adjusted residuals, considering ≥ 1.96.

Adjusted residuals can be used as a tool for interpreting data displayed in contingency tables. With this statistical tool, it is possible to analyze how the possible values in the tables contribute to the Chi-square value and, consequently, to the associations between the variables analyzed. For a 95% significance level, the adjusted residual with statistical significance is one greater than 1.96 times the standard deviation. When significant residual values are positive, it indicates a tendency of more observed cases than expected in the statistics, while significant residuals [5].

The adjusted residual (R) has a normal distribution with a mean of zero and a standard deviation of 1. Thus, if the adjusted residual is greater than 1.96 in absolute value, it can be said that there is evidence of a significant association between the two categories. The higher the adjusted residual, the stronger the association between the categories, with a 95% confidence interval and a p-value ≤ 0.05, using the Pearson Chi-Square Test. Additionally, the Graphpad Prism program was used to create graphs of the variables under study.

Information such as year, month, gender, age group, type of biopsy (incision, excision, absent when the patient's record did not specify the biopsy type, and others when the patient's record marked "other" as the biopsy type), clinical hypothesis (the diagnostic hypothesis raised by the doctor), positive or negative microorganism, and removal location were collected.

In accordance with Resolution N°. 466 of December 12, 2012, and Resolution N°. 510 of April 7, 2016, this research complied with the guidelines and norms for research involving human subjects. The project was approved by the ethics committee on February 8, 2022, under opinion number 5.231.298, and data collection began shortly thereafter, with due respect to the confidentiality of sensitive patient data and the caution not to harm the Pathology service, the patients it serves, and the research results. Furthermore, the project received approval from the Education and Research Management (ERM) of ACUH under Process N°. 23769.010333/2021-01 SEI N°. 18173742.

Results

Within the analyzed time frame, the Pathology department of HUAC had 10600 anatomopathological reports in its archives, and those that met the objectives of this study were selected, totaling 2028 records (19%).

The year 2018 had the highest number of examinations, with 798 (39.3%). Concerning the months, there were more examinations in the months of August, with 100 (5%), November with 114 (6%), and December with 106 (5%), as shown in Figure 1. Regarding gender, there was a higher number of anatomopathological examinations of gastric mucosa for females, with 1313 (64.7%) exams (Figure 1B). As for age groups, the highest concentration was among individuals aged 40 to 59 years, with 784 (7%), followed by those aged 20 to 39 years, with 495 (24.4%) in anatomopathological examinations of gastric mucosa (Figure 1C).

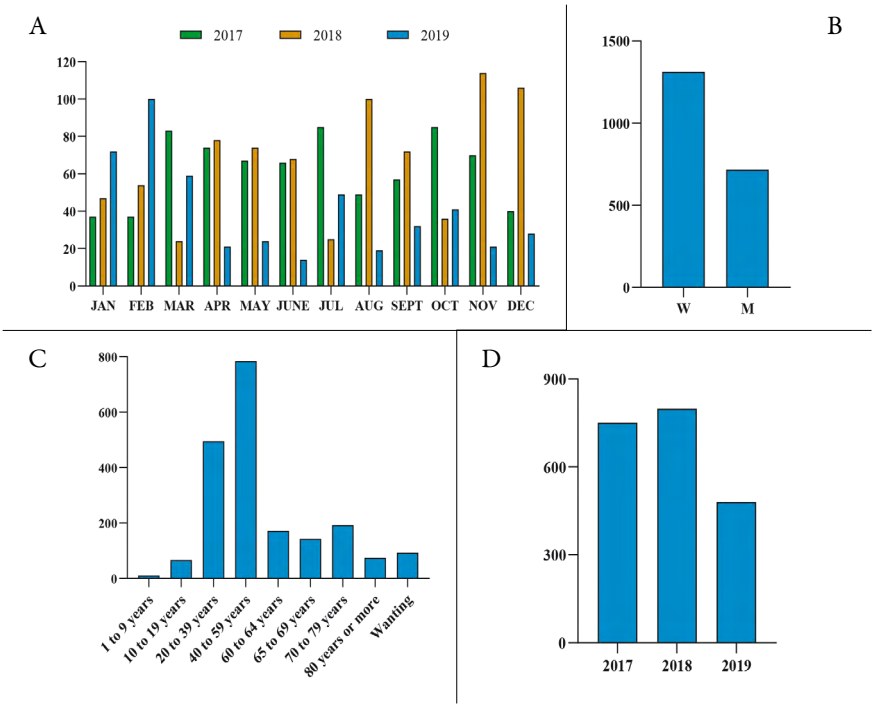

Figure 1. Frequencies of years, months, gender, and age groups of histopathological results for bacteria and fungi performed at ACUH from 2017 to 2019. Fig. 1A - Distribution of histopathological examinations by months and years. Fig. 1B - Frequency by gender. Fig. 1C - Frequency of the study's age groups. Fig. 1D - Analyzed time period. M - Male; W - Women. JAN - January. FEB - February. MAR - March. APR - April. MAY - May. JUNE - June. JUL - July. AUG - August. SEPT - September. OCT - October. NOV - November. DEC - December.

In this study, a greater number of biopsies were performed by incision (n=1,217; 60%), followed by biopsies by excision (n=458; 22.6%) (Figure 2A). Among the examined cases, 686 (33.7%) tested positive for *H. pylori* (Figure 2B). Regarding the diagnostic

hypotheses presented by the requesting physician, pangastritis prevailed (n=801; 39.5%), followed by gastritis (n=510; 25.1%) (Figure 2C). As for the biopsy topography, the body and antrum of the stomach were the most frequent sites (n=1,097; 54.1%), followed by biopsies from the antrum alone (n=610; 30.1%) (Figure 2D).

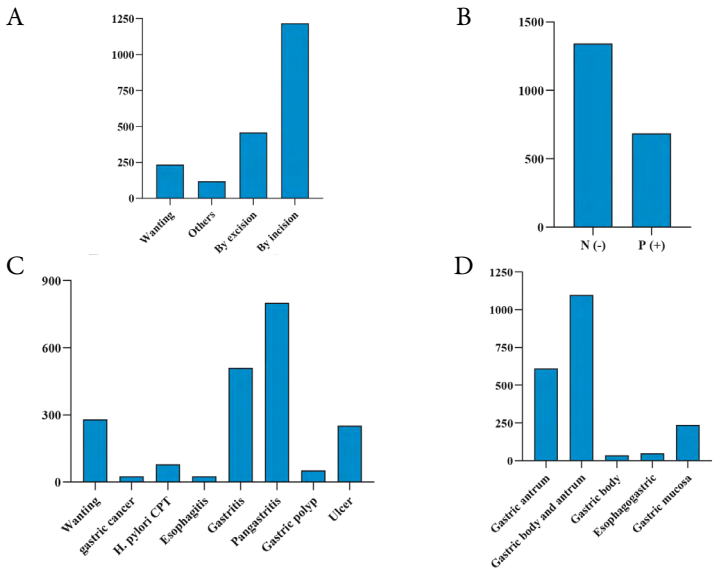

Figure 2. Laboratory Aspects. Fig. 2A - Type of lesion removal for subsequent biopsy. Fig. 2B - Distribution of positive or negative results for *H. pylori*. Fig. 2C - Clinical hypothesis raised by the physician. Fig. 2D - Anatomical locations removed for histopathological examination. N - Negative. P - Positive.

In Table 1, it was observed that the male gender is positively associated with biopsies for *H. pylori* in the esophagogastric region (n=29; 1.4%). Furthermore, it can be noted that patients with endoscopic findings of gastric ulcers had a stronger association with histopathological positivity for *H. pylori* (n=106; 5.2%).

It was found that the age group of 60 years or older is positively associated with excision biopsies (n=145; 7.1%), and the age group of 20 to 59 years is associated with incision biopsies (n=778; 38.4%). Regarding the removal location, the age group of 20 to 59 years was positively associated with removals in the gastric antrum (n=410; 20.2%). Additionally, cases positive for *H. pylori* were more associated with the age group of 20 to 59 years (n=471; 23.2%) (Table 2)

Table 1. Association between the removal site and the patients' sex, as well as between the microorganism and clinical hypothesis.

Removal location	**Sex**						
	Women		**Male**		**TOTAL**		**p**
	N	**%**	**N**	**%**	**N**	**%**	
Gastric antrum	399	19.7	211	10.4	610	30.1	0.008
Gastric body and antrum	716	35.3	381	18.8	1097	54.1	
Gastric body	25	1.2	11	0.5	36	1.8	
Esophagogastric	19	0.9	29+	1.4	48	2.4	
Gastric mucosa	154	7.6	83	4.1	237	11.7	
TOTAL	1313	64.7	715	35.3	2028	100	
Clinical hypothesis	**Positive or negative microorganism**						
	Negative		**Positive**		**TOTAL**		**p**
	N	%	N	%	N	%	
Wanting	211	10.4	69	3.4	280	13.8	0.006
Gastric cancer	19	0.9	7	0.3	26	1.3	
Control after *H. pylori* treatment	49	2.4	31	1.5	80	3.9	
Esophagitis	19	0.8	7	0.3	26	0.8	
Gastritis	344	17	166	8.2	510	25.1	
Pangastritis	518	25.5	283	14	801	39.5	
Gastric polyp	38	1.9	15	0.7	53	2.6	
Ulcer	146	7.2	106+	5.2	252	12.4	
TOTAL	1344	66.3	684	33.7	2028	100	

+ – Adjusted residual; *p* – Pearson's Chi-square test.

Table 2. Association of removal type, removal site, and microorganism (positive or negative) with age group.

Type of Biopsy	**Age range**										
	1-19 years		**20-59 years**		**60 years or more**		**Wanting**		**TOTAL**		**p**
	N	%	N	%	N	%	N	%	N	%	
By excision	16	0.8	293	14.4	146+	7.1	5	0.2	460	22.7	<0.001
By incision	48	2.4	778+	38.4	332	16.4	59	2.9	1217	60	
Wanting	11	0.5	160	7.9	68	3.4	0	0	235	11.9	
Others	1	0	48	2.4	34	1.7	29	1.4	110	5.5	
TOTAL	76	3.7	1279	63.1	580	28.6	93	4.6	2028	100	

(*Continued*)

Type of Biopsy	**Age range**										
	1-19 years		**20-59 years**		**60 years or more**		**Wanting**		**TOTAL**		**p**
	N	%	N	%	N	%	N	%	N	%	
Removal location	Age range										
	1-19 years		20-59 years		60 years or more		Wanting		TOTAL		p
	N	%	N	%	N	%	N	%	N	%	
Gastric antrum	21	1	410+	20.2	175	8.6	4	0.2	610	30.1	<0.001
Gastric body and antrum	44	2.2	675	33.3	307	15.1	71	3.5	1097	54.1	
Gastric body	2	0.1	21	1	13	0.6	0	0	36	1.8	
Esophagogastric	3	0.1	34	1.7	11	0.5	0	0	48	2.4	
Gastric mucosa	6	0.3	139	6.9	74	3.6	18	0.9	237	11.7	
TOTAL	76	3.7	1279	63.1	580	28.6	93	4.6	2028	100	
Positive/ negative microorganism	Age range										
	1-19 years		20-59 years		60 years or more		Wanting		TOTAL		p
	N	%	N	%	N	%	N	%	N	%	
Negative	59+	2.9	808	39.8	419+	20.7	58	2.9	1344	66.3	<0.001
Positive	17	0.8	471+	23.2	161	7.9	35	1.7	684	33.7	
TOTAL	76	3.7	1279	63.1	580	28.6	93	4.6	2028	100	

+ – Adjusted residual; *p* – Pearson's Chi-square test.

Discussion

In the present study, a higher number of anatomopathological examinations of gastric mucosa were observed for females. The lower number of male patients can be justified by social and cultural factors contributing to a reduced utilization of healthcare services by men, potentially leading to delays in diagnosing and treating diseases [6, 7].

Regarding age groups, the predominant group was individuals aged 40 to 59 years, consistent with another study conducted in two reference services in the southern region of Santa Catarina, which showed that individuals undergoing histopathological examinations of stomach tissue had an average age between 40 and 60 years [8].

In the current study, there was a higher number of incision biopsies, followed by excision biopsies. Histopathological biopsies can be classified based on the type of lesion removal, with the most common methods being incision (removing only a part of the lesion), excision (removing the entire lesion, including adjacent cells), puncture (removing part of the material using needles, including Fine Needle Aspiration Biopsy - FNA), scraping (ideal for evaluating small local infections like fungal infections and dermatitis), and surgical specimen (removing organs or parts of them) [9].

The choice of the lesion removal site for biopsy should be based on the region with the highest number of possible alterations detectable in the tissue, while avoiding necrotic tissues. In the incision biopsy format, the removal should be elliptical, in a "V" shape. Excision biopsies are typically performed on theoretically small-sized materials, which are often benign [10].

Histopathological testing for *H. pylori* was positive in 33.7% of suspected cases of infection by the bacterium. Histopathological examinations can assist in diagnosing various infections, including *H. pylori* infections in regions such as the stomach, esophagus, gastroduodenal regions, and esophagogastric regions [3].

Regarding the clinical hypothesis raised by the physician, pangastritis prevailed, followed by gastritis. As for the removal location for *H. pylori* biopsy, the removal of both the body and antrum of the stomach was more frequent, followed by the removal of just the gastric antrum. Gastritis, pangastritis, and ulcers are more common than other clinical hypotheses because a larger number of examinations were conducted to investigate *H. pylori*, a pathogen that can cause the aforementioned diseases. Most removals occurred in the stomach, in the body and antrum region, due to material collection for *H. pylori* research. Typically, two samples are collected from different locations in each region of the body and gastric antrum, depending on the level of inflammation observed in the endoscopy [11]. The treatment of ulcers and diseases acid-peptics, associated the proton pump inhibitors (PPIs) which have fully replaced antacids, parasympatholytics and histamine H2 receptor antagonists. The most effective approach is to administer PPIs in the morning on an empty stomach, in a single daily dose. This therapy is generally considered very safe. However, potential adverse effects of long-term PPI treatment on the efficacy of other medications (such as clopidogrel), bone metabolism, and the development of respiratory infections have been discussed recently. PPIs also play an essential role in the eradication treatment of *H. pylori* infection, as well as in the prevention and treatment of gastropathy induced by nonsteroidal anti-inflammatory drugs. Additionally, they are utilized in relation to some rare hypersecretory conditions [12].

Table 1 showed that the male gender was positively associated with biopsies for *H. pylori* in the esophagogastric region. One of the main characteristics developed when *H. pylori* is present in gastrointestinal regions is gastric atrophy [13]. A study by Chiang *et al.* (2021) [14] that demonstrated the association between *H. pylori* and gastric junction atrophy observed that this atrophy is more strongly associated with the male gender.

In Table 2, it was found that the age group of 60 years or older is positively associated with excision biopsies, and the age group of 20 to 59 years is associated with incision biopsies. In excision, it is important to consider the removal direction in line with local tension to reduce the need for skin grafts and reconstructive skin procedures. Large lesions undergoing excision should be carefully considered, as this procedure can interfere with lymphatic mapping, affecting lymphoscintigraphy accuracy. To mitigate this issue with excision, other techniques such as incision are used; however, incision has some disadvantages, like the potential loss of malignant material in the analyzed lesions [15].

As seen in Table 2, histopathological examinations that were positive for *H. pylori* were associated with the age group of 20 to 59 years, while negative results for *H. pylori* were associated with the age group of 60 years or older. This bacterium has several mechanisms that enhance its mobility, adhesion, and manipulation of the gastric microenvironment, including a variety of virulence factors that increase its pathogenicity, such as the antigen A associated with cytotoxin, vacuolating cytotoxin, A-promoter duodenal ulcer gene protein, and urease, which enables the bacterium to survive in an acidic environment. The host's immune system may react with a polarized Th1-type immune response. Therefore, it is essential to use diagnostic methods for this infection to prevent future health problems [16].

Patients with the presence of *H. pylori*, leading to chronic gastritis, have various factors contributing to this health issue. Foods can affect gastric motility, for example, hot foods can cause gastric mucosa congestion, leading to increased acid secretion. In addition, the consumption of alcoholic beverages also increases gastric acid secretion [17].

Conclusion

With the present study, it was possible to observe that, within the analyzed time frame, the year 2018 had the highest number of histopathological examinations for the diagnosis of *H. pylori* infections, with a predominance of females in the age group of 40 to 59 years. Positive results for the bacterium occurred in a lower proportion, accounting for 33.7% of suspected cases, especially in those with a clinical hypothesis of gastritis and biopsies of the body and antrum of the stomach. Furthermore, in esophagogastric

region removals for investigative *H. pylori* biopsies, males are more likely to undergo these procedures. The age group of 60 years or older is more prone to excision biopsies, while the age group of 20 to 59 years is more associated with incision biopsies and removals in the gastric antrum. Additionally, the age group of 20 to 59 years is more associated with positive results for *H. pylori*, while the age group of 60 years or older is more associated with negative results.

The present study allowed for an epidemiological assessment of histopathological diagnoses of *H. pylori* infections. There is a lack of epidemiological studies related to histopathological diagnosis of *H. pylori* infection. In the current study, there was a higher proportion of males and adults, especially in the age group of 40 to 59 years, with positive results for *H. pylori*, which aligns with studies described in the literature. However, more studies of this nature are still necessary, or the observation that there is a need for better completion of requests for anatomopathological examinations.

Conflict of interest

No potential conflicts of interest were reported by the authors.

Ethics approval

This research was approved by the Research Ethics Committee of the Center for Education and Health at the Federal University of Campina Grande - CES/UFCG, under opinion number 5.231.298.

References

1. G. Atiwesh, C.C. Parrish, J. Banoub, T.-A.T. Le, Lignin degradation by microorganisms: A review. *Biotechnology Progress*, **38**(2), e3226 (2022). Doi: https://doi.org/10.1002/btpr.3226

2. M. Zamani, F. Ebrahimtabar, V. Zamani, W.H. Miller, R. Alizadeh-Navaei, J. Shokri-Shirvani, M.H. Derakhshan, Systematic review with meta-analysis: the world wide prevalence of *Helicobacter pylori* infection, *Alimentary Pharmacology & Therapeutics*, **47**(7), 868-876 (2018). Doi: https://doi.org/10.1111/apt.14561

3. G.B. Vasconcelos de Souza, E. Rezende-Moura, Y.T. Delmondes-Trindade, D.J.d. Santana-Neto, L. Gonçalves-Moreira, G.P. Santos de Carvalho, Í.D.d. Carvalho-Barreto, D. Fragata da Silva, L. Meurer, L.M.D. Freitas-Trindade, Prevalência de

achados histopatológicos de mucosa esofágica e sua correlação com *Helicobacter pylori*, *Research, Society and Development*, **11**(2), e33811225769 (2022). Doi: https://doi.org/10.33448/rsd-v11i2.25769

4. J. Trevisan-Martins, R. Perfeito-Ribeiro, M.C. Cescatto-Bobroff, M.H. Palucci-Marziale, M.L.d.C. da Cruz-Robazzi, Pesquisa epidemiológica da saúde do trabalhador: uma reflexão teórica, *Semina: Ciências Biológicas e da Saúde*, **35**(1), 163-174 (2014). Doi: https://doi.org/10.5433/1679-0367.2014v35n1p163

5. G. Carreiro-Pinasco, A. Brunelli-Sales, C.V. Aguilar-Santos, E. Cola, F.N. Barcellos Filho, J.B. Francalino da Rocha, E.M.J. de Mattos-Farina, W. França-Fiorotti, L.C. de Abreu, Maternal perception of the child's nutritional status from the perspective of adjusted residual analysis, *Journal of Human Growth and Development*, **30**(3), 389-397 (2020). Doi: https://doi.org/10.7322/jhgd.v30.11102

6. A. Costa-Souza, F. Rodrigues-Custódio, O. Ferreira-Melo, Cenário epidemiológico da tuberculose no município de Sobral (CE) entre os anos de 2013 e 2017, *Revista Eletrônica Acervo Saúde*, **23**, e445 (2019). Doi: https://doi.org/10.25248/reas.e445.2019

7. L. Rodrigues-Bosqui, S. Santos-Silva, R. Arruda-Sanfelice, M.M. Miranda-Sapla, D. Sapede-Alvarenga, B.B. Lucas, L.F. Machado, F. Nesello-Melanda, L.A. Custodio, W.R. Pavanelli, I. Conchon-Costa, I.N. Costa, Perfil clínico de pacientes com diagnóstico de tuberculose atendidos no Hospital universitário de Londrina, Paraná, *Semina: Ciências Biológicas e da Saúde*, **38**(1), 89-98 (2017). Doi: https://doi.org/10.5433/1679-0367.2017v38n1p89

8. S.d.R. Sousa, G.d.O. Bernardo, A.J. Faraco, C.d.O. Bernardo, Perfil epidemiológico dos pacientes diagnosticados com úlcera gástrica e/ou duodenal em dois serviços de referência do extremo sul catarinense no período de um ano, *Arquivos Catarinenses de Medicina*, **46**(3), 59-69 (2017). URL: https://revista.acm.org.br/index.php/arquivos/article/view/127

9. A. Figueiredo-Caubi, R.L.d. Freitas-Xavier, M.A.d. Lima Filho, J. Ferreira-Chalegre, Biópsia, *Revista de Cirurgia e Traumatologia Buco-Maxilo-Facial*, **4**(1), 39-46 (2004). URL: https://www.revistacirurgiabmf.com/2004/v4n1/pdf/v4n1.5.pdf

10. M.M.M.G. Romero-Antelo, *Biópsias: diferentes abordagens cirúrgicas*, Artigo de Revisão Bibliográfica, Mestrado Integrado de Medicina Dentária, Universidade do Porto, Porto, 2020, 36 p. URL: https://repositorio-aberto.up.pt/bitstream/10216/130072/2/428822.pdf

11. M.C. Freitas-Coelho, H. Gomes-Ribeiro, C.G. de Oliveira-Gomes, F. Passos-Marinho, A.J.A. Barbosa, L.G. Vaz-Coelho, *Helicobacter pylori* chronic gastritis on patients with premalignant conditions: OLGA and OLGIM evaluation and serum biomarkers performance, *Arquivos de Gastroenterologia*, **58**(1), 39-47 (2021). Doi: https://doi.org/10.1590/S0004-2803.202100000-08

12. M. Lukáš, Therapy for peptic ulcer disease [Terapie peptického vředu], *Vnitřní lékařství*, **64**(6), 595-599 (2018). URL: https://casopisvnitrnilekarstvi.cz/pdfs/vnl/2018/06/03.pdf

13. E. Lahner, M. Carabotti, B. Annibale, Treatment of *Helicobacter pylori* infection in atrophic gastritis, *World Journal of Gastroenterology*, **24**(22), 2373-2380 (2018). Doi: https://doi.org/10.3748/wjg.v24.i22.2373

14. T.-H. Chiang, W.-J. Chang, S.L.-S. Chen, A.M.-F. Yen, J.C.-Y. Fann, S.Y.-H. Chiu, Y.-R. Chen, S.-L. Chuang, C.-F. Shieh, C.-Y. Liu, H.-M. Chiu, H. Chiang, C.-T. Shun, M.-W. Lin, M.-S. Wu, J.-T. Lin, C.-C. Chan, D.Y. Graham, H.-H. Chen, Y.-C. Lee, Mass eradication of *Helicobacter pylori* to reduce gastric cancer incidence and mortality: A long-term cohort study on Matsu Islands, *Gut*, **70**(2), 243-250 (2021). Doi: https://doi.org/10.1136/gutjnl-2020-322200

15. J.K.Y. Hooi, W.Y. Lai, W.K. Ng, M.M.Y. Suen, F.E. Underwood, D. Tanyingoh, P. Malfertheiner, D.Y. Graham, V.W.S. Wong, J.C.Y. Wu, F.K.L. Chan, J.J.Y. Sung, G.G. Kaplan, S.C. Ng, Global prevalence of Helicobacter pylori infection: Systematic review and meta-analysis, *Gastroenterology*, **153**(2), 420-429 (2017). Doi: https://doi.org/10.1053/j.gastro.2017.04.022

16. B. Bittencourt de Brito, F.A. França da Silva, A. Silva-Soares, V.A. Pereira, M.L. Cordeiro-Santos, M. Miranda-Sampaio, P.H. Moreira-Neves, F. Freire de Melo, Pathogenesis and clinical management of *Helicobacter pylori* gastric infection, *Word Journal of Gastroenterology*, **25**(37), 5578-5589 (2019). Doi: https://doi.org/10.3748/wjg.v25.i37.5578

17. L. Chamse-Ddine, C. Chamse-Ddine, C.C.R. Rodrigues, V. Ramos-Kirsten, E. Colpo, Factors associated with chronic gastritis in patients with presence and absence of *Helicobacter pylori*, *ABCD Arquivos Brasileiros de Cirurgia Digestiva* (São Paulo), **25**(2), 96-100 (2012). Doi: https://doi.org/10.1590/S0102-67202012000200007

How to cite this article

D. Azevedo-Ferreira, C.M. Moura-Ponce de Leon, E. Santos-Carmo, Epidemiological profile of infections caused by *Helicobacter pylori* diagnosed through histopathological examinations conducted at a reference University Hospital, *Rev. Colomb. Cienc. Quim. Farm.*, **53**(2), 291-305 (2024). https://doi.org/10.15446/rcciquifa.v53n2.114422

Artículo de revisión / https://doi.org/10.15446/rcciquifa.v53n2.114423

Plantas medicinales de la familia Verbenaceae activas frente a hongos levaduriformes: Revisión sistemática y perspectivas 2015-2022

Linda Roxana Jaimes Duarte[1], Sara Emilia Giraldo Quintero[1], Jesús Fredy Hoyos Argote[1], María Consuelo Bernal Lizarazú[2*]

[1]Escuela de Ciencias Básicas y Aplicadas. Universidad de La Salle. Carrera 2 No. 10-70. Bogotá D.C., Colombia. Código postal 111711. PBX (601) 353 53 60.

[2]Universidad Nacional Abierta y a Distancia. Transversal 31 No. 12-38 Sur. Bogotá D.C., Colombia. Código Postal 111511. PBX (601) 203 83 38.

*Autor de correspondencia: maria.bernal@unad.edu.co

Recibido: 27 de junio de 2023
Revisado: 12 de febrero de 2024
Aceptado: 19 de febrero de 2024

Resumen

Introducción: Las infecciones fúngicas oportunistas han aumentado en las últimas décadas requiriéndose la búsqueda de alternativas terapéuticas, considerando además la aparición de nuevas especies y el aumento de la resistencia a los antifúngicos. **Objetivo:** Este estudio describe plantas de la familia Verbenaceae con potencial terapéutico frente a hongos levaduriformes. **Metodología:** Se realizó una revisión sistemática de 2015 a 2020 empleando bases de datos, aplicando criterios de inclusión y exclusión, explorando además perspectivas recientes a 2022. **Resultados y discusión:** Se encontraron 5 géneros y 14 especies con potencial actividad antifúngica, resaltándose el género *Lippia* el cual demostró mayor actividad. El aceite esencial de hojas fue el producto natural más estudiado, principalmente activo frente a *Candida albicans* y *Cryptococcus neoformans;* los análisis fitoquímicos reportan en su mayoría metabolitos tipo terpeno como carvacrol, timol, linanol y geraniol. Para la determinación de CIM, la técnica *in vitro* de microdilución en caldo fue la más reportada. Estudios recientes respaldan la importancia de especies, entre ellas *Lantana montevidensis* (Spreng.) Briq., por su actividad moduladora de fármacos antifúngicos. **Conclusión:** Se encontraron cinco géneros con potencial actividad: *Aloysia*, *Lantana, Lippia*, *Stachytarpheta* y *Verbena*; siendo de interés las especies *Lippia berlandieri* Schauer y *Lippia graveolens* Kunth por su alta actividad frente

a *C. albicans* y *C. neoformans.* Se reconoce la importancia de especies de la familia Verbenaceae para futuras investigaciones, que permitan desarrollar alternativas terapéuticas naturales contra infecciones causadas por hongos levaduriformes.

Palabras clave: Infecciones micóticas, plantas medicinales, agentes antifúngicos, extractos vegetales, aceites esenciales, Verbenaceae.

Summary

Medicinal plants of the Verbenaceae family active against yeast fungi: Systematic review and perspectives 2015-2022

Introduction: Opportunistic fungal infections have increased in recent decades, requiring the search for therapeutic alternatives, also considering the appearance of new species and the increase in resistance to antifungals. **Objective**: This study describes plants of the Verbenaceae family with therapeutic potential against yeast fungi. **Methodology**: A systematic review was carried from 2015 to 2020, using different databases, applying inclusion and exclusion criteria, also exploring recent perspectives to 2022. **Results and discussion**: 5 genera and 14 species with potential antifungal activity were found, highlighting the genus *Lippia* which showed greater activity. The essential oil of the leaves was the most studied natural product, mainly active against *Candida albicans* and *Cryptococcus neoformans*. Phytochemical analysis report mostly terpene-type metabolites such as carvacrol, thymol, linanol, and geraniol. For the determination of MIC, the *in vitro* technique of microdilution in broth was the most reported. Recent studies support the importance of species, including *Lantana montevidensis* (Spreng.) Briq., for their modulating activity of antifungal drugs. **Conclusions**: Five genera with potential activity were found: *Aloysia*, *Lantana*, *Lippia*, *Stachytarpheta* and *Verbena*; being of interest the species *Lippia berlandieri* Schauer and *Lippia graveolens* Kunth for its high activity against *C. albicans* and *Cryptococcus neoformans*. The importance of species of the Verbenaceae family for future research is recognized, which will allow the development of natural therapeutic alternatives against infections caused by yeast-like fungi.

Keywords: Mycosis, medicinal plants, antifungal agents, plant extracts, essential oils, Verbenaceae.

Resumo

Plantas medicinais da família Verbenaceae ativadas frente a hongos levaduriformes: Revisão sistemática e perspectivas 2015-2022

Introdução: As infecções fúngicas oportunistas aumentaram nas últimas décadas, exigindo a busca de alternativas terapêuticas, considerando também o aparecimento de novas espécies e o aumento da resistência aos antifúngicos. **Objetivo:** Este estudo descreve plantas da família Verbenaceae com potencial terapêutico frente a grandes levaduriformes. **Metodologia:** Foi realizada uma revisão sistemática de 2015 a 2020, empregando bases de dados, aplicando critérios de inclusão e exclusão, explorando outras perspectivas recentes para 2022. **Resultados e discussão**: Encontrar 5 gêneros e 14 espécies com potencial atividade antifúngica, resaltando o gênero *Lippia* el cual demostró mayor actividad. O óleo essencial de folhas de chá foi o produto natural mais estudado, principalmente ativo contra *Candida albicans* e *Cryptococcus neoformans*; a análise fitoquímica relatada em seus principais metabólitos, como terpeno, como carvacrol, timol, linanol e geraniol. Para a determinação do CIM, a técnica de microdiluição in vitro em caldo foi mais relatada. Estudos recentes respaldaram a importância das espécies, entre elas *Lantana montevidensis* (Spreng.) Briq., por sua atividade moduladora de medicamentos antifúngicos. **Conclusão:** Foram encontrados cinco gêneros com atividade potencial: *Aloysia*, *Lantana*, *Lippia*, *Stachytarpheta* e *Verbena*; sendo de interesse as espécies *Lippia berlandieri* Schauer e *Lippia graveolens* Kunth por sua alta atividade frente a *C. albicans* e *C. neoformans*. Se você reconhecer a importância das espécies da família Verbenaceae para futuras investigações, permitirá desenvolver alternativas terapêuticas naturais contra infecções causadas por fungos levaduriformes.

Palavras-chave: Infecções micóticas, plantas medicinais, agentes antifúngicos, extratos vegetais, óleos essenciais, Verbenaceae.

Introducción

Las infecciones fúngicas oportunistas han ido en incremento en las últimas décadas; dentro de los principales géneros se destacan *Candida* spp.*, Cryptococcus* spp.*, Aspergillus* spp. y *Pneumocystis* spp., para los cuales Schmiede *et al.* reportan un estimado de dos millones de personas infectadas por año a nivel mundial [1]. Estas cifras se ven favorecidas por el aumento de pacientes inmunocomprometidos, entre ellos pacientes receptores de trasplantes, así como aquellos que reciben inmunomoduladores o quie-

nes tienen diagnóstico de VIH o cáncer [2]. Más recientemente con el advenimiento del SARS-CoV-2 datos publicados reportan la tendencia emergente de infección fúngica en pacientes con COVID-19, principalmente cuadros de aspergillosis pulmonar, candidiasis sistémica y mucormicosis, que adicionalmente pueden aumentar la gravedad de la infección viral y la mortalidad [3, 4].

La aparición de resistencia a los antifúngicos cobra mayor importancia con el tiempo por el aumento en la prevalencia de cepas resistentes, su impacto en los costos de tratamiento y muy alta mortalidad. Datos reportados por Zurita *et al.* en 2018, muestran a nivel global una resistencia del 1,4 %, 16,7 % y 4,0 % para *Candida albicans, Candida glabrata y Candida tropicalis* respectivamente. Específicamente para América Latina, se reportó una resistencia al fluconazol del 0,7 % para *C. albicans* y del 2,9 % para *Candida parapsilosis* [5]. En Colombia, varían los datos de resistencia reportados; para el caso de Bogotá se ha encontrado un 30 % de resistencia al fluconazol, en los aislamientos clínicos de *Candida* spp. [6]. De otro lado a nivel mundial aislamientos de *Cryptococcus* sp. han reportado resistencia hasta del 50 % frente al tratamiento con antifúngicos de uso clínico, las más altas en Sur Africa, Taiwan y España [7]. Adicionalmente el metaanálisis realizado por Bongomin *et al.* en 2018, reporta una resistencia *in vitro* promedio al fluconazol para aislamientos clínicos de *Cryptococcus neoformans* del 18,7 % [8].

La aparición de especies patógenas emergentes resistentes a los antifúngicos ha tomado relevancia en los últimos años; tal es el caso de *Candida auris*, que para el 2018 reportó una mortalidad del 60 % con un incremento del 318 % en la incidencia, informándose además una alta tasa de resistencia a todos los antifúngicos convencionales [9].

Durante la pandemia, los hongos también cobraron importancia clínica. Estudios informaron infección por *C. albicans* entre otras especies de *Candida*, en pacientes hospitalizados con COVID-19 [10]; también se resaltó la presencia de cepas multifármaco-resistentes de *C. auris* en India generando una tasa de letalidad del 60 % de la infección [11] así como el reporte de *C. glabrata* resistente a equinocandinas [12].

En general el arsenal terapéutico disponible para el tratamiento de las micosis es limitado y más aún el de las micosis oportunistas. El reducido número de grupos farmacoterapéuticos, su toxicidad, su espectro de actividad y la aparición de cepas multifármaco-resistentes, ha promovido la investigación para el desarrollo de otras alternativas, como la combinación de fármacos [13]. Si bien el uso de la terapia combinada puede ser eficaz, podría traducirse en un mayor reporte de efectos adversos y altos costos de tratamiento, por lo que la búsqueda de alternativas más seguras y asequibles es necesaria, especialmente para países en vía de desarrollo donde las comunidades aún acuden a la medicina tradicional a base de plantas [14].

Un estudio reciente orientado hacia la revisión sistemática de la información científica sobre plantas medicinales con actividad *in vitro*, eficaces frente a microorganismos resistentes a antimicrobianos en África, entre 1980 a 2019, reportó un total de 138 especies pertenecientes a 50 familias siendo las principales Asteraceae, Fabaceae Lamiaceae, Moraceae y Myrtaceae. Dentro de los microorganismos se reportaron 52 especies de bacterias y 27 especies de hongos, siendo *C. albicas* el hongo filamentoso más estudiado [15]. Dentro de este estudio, para la familia Verbenaceae se reportó la evaluación antimicrobiana del aceite esencial de las hojas de diferentes quimiotipos de *Lippia javanica*, demostrando una alta actividad frente a microorganismos patógenos implicados en infecciones respiratorias, *Klebsiella pneumoniae*, *Bacillus cereus* y *C. neoformans,* dando así soporte a su uso tradicional [16]. Por otro lado, en un estudio de revisión reciente sobre la investigación de agentes antimicrobianos prometedores obtenidos de plantas medicinales en Latinoamérica entre el 2000 al 2020, se encontró que *Staphylococcus aureus* y *Candida* spp. fueron los microorganismos con mayor número de reportes, mientras que entre las especies se destacaron *Bidens pilosa* (Asteraceae), *Lippia origanoides* (Verbenacea), *Piper regnellii* (Piperaceae), *Ziziphus joazeiro* (Rhamnaceae), *Amphipterygium adstringens* y *Schinus terebinthifol*, estas dos últimas de la familia Anacardiaceae. Entre otras especies, *L. origanoides*, se destacó dentro de los estudios reportados en Colombia por su actividad antimicrobiana frente a bacterias y hongos. Dentro de sus usos tradicionales medicinales se emplea para el tratamiento de resfriados, asma, tos, infecciones pulmonares y diarrea, también como expectorante y antiséptico oral. El aceite esencial de esta especie nativa de Centroamérica (México y Guatemala) y Suramérica (especialmente región amazónica de Guayana, Venezuela, Brasil y Colombia), comúnmente conocida como "oregano" presenta metabolitos secundarios distribuidos en al menos tres quimiotipos, carvacrol (37–52%), timol (30–87%) y (E)-cariofileno (9–16%)/p-cimeno (11–20%), responsables de su actividad tanto antibacteriana como antifúngica [17]. Estudios demostraron que el aceite esencial del quimiotipo timol presentó una alta actividad frente a *C. parapsilosis*, *Candida krusei*, *Aspergillus flavus* y *Aspergillus fumigatus* en ensayos de actividad antifúngica como valores de Concentración Inhibitoria Mínima (CIM) de 157,5, 198,4, 125,0 y 31,0 μg/mL respectivamente [18]. En otros estudios extractos medianamente polares (en hexano y diclorometano) de *L. origanoides* demostraron potencial actividad antifúngica frente a *C. albicans* en técnicas de difusión en disco, atribuida a la presencia de metabolitos tipo esteroides, glicósidos cardiotónicos y carotenoides en estos extractos [19].

Estudios etnobotánicos han permitido conocer el potencial terapéutico de recursos vegetales, identificando diferentes especies pertenecientes a la familia Verbenaceae, citadas por su uso tradicional atribuido especialmente a sus aceites esenciales [20]. Esta familia encierra alrededor de 100 géneros y 2600 especies con una distribución pan-

tropical (África, Asia y América), muchas nativas de Suramérica, con una variedad de biocompuestos que le brindan amplio uso en la farmacopea vegetal como antimicrobianos, [20, 21]. Diferentes publicaciones han reportado su potencial en estudios *in vitro* orientados ya sea hacia su actividad antibacteriana, [22-24], pero también antifúngica, siendo de interés *Aloysia gratissima* (Gillies & Hook.) Tronc. [25], *Lippia alba* (Mill.) N.E.Br. ex Britton & P. Wilson [26], *Lippia origanoides* Kunth [27] y *Lantana camara* L. [28], contemplando además para estas dos últimas especies la evaluación de extractos.

A partir del estudio etnobotánico realizado por Giraldo *et al.* (2015) en mercados populares de Bogotá (Colombia) [29], surge el interés en la búsqueda y evaluación de plantas medicinales con potencial antimicrobiano resaltándose los extractos etanólicos de *L. camara* L. y *Lippia dulcis* T., ambas pertenecientes a la familia Verbenaceae, por su actividad *in vitro* frente a las bacterias patógenas *S. aureus* y *Proteus vulgaris* [30].

Considerando los antecedentes previamente descritos y los resultados e intereses del grupo de investigación, se propone hacer un estudio de revisión enfocado en la búsqueda sistemática, recopilación y descripción de estudios orientados a la evaluación de la actividad antifúngica de especies de la familia Verbenaceae frente a hongos levaduriformes entre 2015 a 2020, el cual permitirá seleccionar las plantas de la familia Verbenaceae con potencial antifúngico describiéndolas desde la composición de sus metabolitos, la naturaleza de sus extractos o aceites y su bioactividad, resaltando además la importancia de la familia Verbenaceae en Suramérica. El estudio busca también dar un acercamiento a las perspectivas de investigación actuales sobre plantas de la familia Verbenaceae, como precursores de productos naturales para el desarrollo de alternativas terapéuticas con actividad antifúngica a 2022.

Metodología

Según el estudio reportado por Jaimes y Hoyos [31], se realizó una revisión sistemática estableciendo los siguientes criterios de búsqueda: Intervalo de búsqueda entre los años 2015 a 2020; bases de datos: Pubmed, ScienceDirect, Web of Science, Biblioteca Virtual en Salud (BVS), Red de Revistas Científicas de América Latina y el Caribe, España y Portugal (Redalyc) y el motor de búsqueda Google Académico; palabras clave: "actividad antifúngica", "plantas medicinales", "hongos levaduriformes", "extractos vegetales o extractos de plantas" y "Verbenaceae". La búsqueda se hizo en idioma inglés mediante ecuaciones de búsqueda por tema de la siguiente manera ("Antifungal activity" AND "Verbenaceae" AND "plant extract" OR "medicinal plants" AND "yeast") o (Antifungal activity, Verbenaceae, yeast, plant extract, medicinal plants). Se tuvieron en cuenta tanto artículos de investigación como artículos de revisión.

Como criterios de inclusión y exclusión, se tomó en consideración que en el título o resumen de cada artículo se mencionara algún tipo de hongo levaduriforme patógeno para humanos; que los géneros o especies de plantas medicinales mencionadas pertenecieran a la familia Verbenaceae; que el estudio estuviera enfocado en la evaluación antifúngica de las plantas a nivel *in vitro* y por último que los artículos se encontraran entre los más citados (para Web of Science, BVS y Redalyc) o entre los más relevantes dentro de la búsqueda (para ScienceDirect, Pubmed y Google Académico). Se excluyeron los documentos pertenecientes a trabajos de grado o tesis y estudios anteriores a 2015.

Los artículos seleccionados se clasificaron en una matriz (Microsoft Excel, versión 15-2013), asignando una hoja independiente a cada género de interés de la familia Verbenaceae. La información se organizó según: Título del artículo, planta medicinal (especie), año de publicación, revista, naturaleza de cada extracto o aceite evaluado, composición de sus metabolitos o compuestos fitoquímicos, el(los) microorganismo(s) estudiado(s), bioactividad frente a las especies de levaduras evaluadas, resumen, base de datos, número de citaciones y el link o DOI.

Las perspectivas actuales en investigación se orientaron a partir de la búsqueda y selección de estudios relacionados con los 5 artículos más citados en la presente revisión sistemática, publicados entre 2021 a 2022 en las mismas bases de datos y que en su título o resumen se mencionara al menos una especie de la familia Verbenaceae en relación con actividad antimicrobiana frente a hongos levaduriformes de interés en salud humana.

Resultados y discusión

la ecuación de búsqueda "Antifungal activity" AND "Verbenaceae" AND "plant extract" OR "medicinal plants" AND "yeast" arrojó en Web of Science 134 resultados, en BVS 3 resultados, en Redalyc 2 resultados y en Google Académico 322 resultados. La ecuación de búsqueda "Antifungal activity", "Verbenaceae", "yeast", "plant extract", "medicinal plants" mostró en Science Direct 35 resultados y en Pubmed 76 resultados. A partir de los resultados anteriores y después de aplicar los criterios de inclusión y exclusión finalmente se obtuvo por cada base de datos: Science Direct 3, Pubmed 6, Web of Science 2, BVS 2, Redalyc 2 y Google Académico 22, siendo en total 37 artículos, los cuales fueron tomados en cuenta para la revisión.

Del total de estudios se encontraron 31 artículos de investigación y 6 artículos de revisión, para los siguientes años, 2015: 7, 2016: 11, 2017: 4, 2018: 6, 2019: 8 y 2020:1, siendo el 2016 el año con más estudios realizados; teniendo en cuenta las filiaciones institucionales de los autores los artículos fueron publicados en los siguientes países: Brasil: 14, México: 5, Argentina: 2, Ecuador: 1, Colombia: 1, Guyana Francesa: 2,

India: 1, Indonesia: 1, Malasia: 1, Pakistán: 1, Irak: 1, Irán: 2, Etiopia: 1, Nigeria: 2, Tanzania: 1, Túnez: 1. 25 estudios se publicaron en Suramérica y 12 estudios en países extranjeros (África y Asia).

Cuatro artículos se publicaron en el *Journal of Essential Oil Research* y 3 en *Molecules*, los demás artículos se distribuyeron en 30 revistas diferentes. En la tabla 1 se muestran los cinco artículos más citados a partir de la revisión.

Tabla 1. Artículos más citados sobre plantas de la familia Verbenacea con potencial actividad antifúngica entre 2015 a 2020.

Título	Doi	Referencia	Revista	Base de datos	# citas
Antimicrobial properties of plant essential oils against human pathogens and their mode of action: An updated review	https://doi.org/10.1155/2016/3012462	[32]	Evidence-Based Complementary and Alternative Medicine	Google Académico	300
Phytosynthesis of silver nanoparticles using aqueous leaf extracts of *Lippia citriodora*: Antimicrobial, larvicidal and photocatalytic evaluations	https://doi.org/10.1016/j.msec.2017.02.161	[33]	Materials Science and Engineering	ScienceDirect	52
The antibacterial and antifungal activity of essential oils extracted from Guatemalan medicinal plants	https://doi.org/10.3109/13880209.2014.932391	[34]	Pharmaceutical biology	Biblioteca Virtual en Salud	38
Stachytarpheta jamaicensis (L.) Vahl: From traditional usage to pharmacological evidence	https://doi.org/10.1155/2016/7842340	[35]	Hindawi Publishing Corporation	Google Académico	18

(*Continúa*)

Título	Doi	Referencia	Revista	Base de datos	# citas
Antimicrobial activity of Mexican oregano (*Lippia berlandieri*), thyme (*Thymus vulgaris*), and mustard (*Brassica nigra*) essential oils in gaseous phase	https://doi.org/10.1016/j.indcrop.2019.01.036	[36]	Industrial Crops and Products	ScienceDirect	16

Realizada la búsqueda, recopilación, organización y revisión de la información, se encontraron cinco géneros (*Aloysia*, *Lantana*, *Lippia*, *Stachytarpheta* y *Verbena*) pertenecientes a la familia Verbenaceae, resaltándose 14 especies que demostraron potencial actividad antifúngica con valores de CIM menores o iguales a 1000 μg/mL. Para seleccionar estas especies se tuvieron en cuenta los estudios de Sartoratto *et al.* quienes refieren actividades "fuertes" (0,05–0,5 mg/mL) y "moderadas" (0,6–1,50 mg/mL) [37] y de Almeida *et al.* [38] quienes establecen actividades "buenas" (<100 μg/mL) y "moderadas" (100-500 μg/mL) para productos naturales con actividad antifúngica obtenidos a partir de plantas medicinales. En la tabla 2 se resume la información para estas 14 especies, se muestra la especie y parte(s) de la planta estudiada, microorganismo(s), aceite y/o extracto(s) evaluado(s), metabolitos mayoritarios detectados, método de evaluación antifúngica *in vitro*/bioactividad (CIM) y referencia.

Dentro de los géneros de la familia Verbenaceae con potencial antifúngico se destacó el género *Lippia* resaltándose el aceite esencial comercial de *L. berlandieri* que demostró mediante el método de difusión en fase de vapor un valor de CIM de 0,25 μg/mL de aire frente a *C. albicans* y *C. neoformans* siendo la más alta actividad inhibitoria reportada. Según los autores bajo este método se aprovecha la volatilidad de los aceites por lo que en fase de vapor se obtienen mayores efectos antifúngicos a menores dosis que los obtenidos cuando los aceites se prueban en contacto directo con los hongos ya sea en soluciones acuosas o en agares sólidos. Por lo general es un método que se emplea cuando el interés es evaluar la actividad antifúngica frente a mohos, sin embargo, en este estudio se evaluó la actividad antibacteriana y antifúngica (mohos y levaduras) de aceites esenciales comerciales. En el aceite esencial de *L. berlandieri* se detectaron de forma mayoritaria p-cimeno (35,54 %) y carvacrol (26,86%) [36]. También se destacó el aceite esencial de hojas de *L. graveolens*, cuyo análisis fitoquímico mediante cromatografía de gases acoplada a espectrometría de masas (CG-EM) detectó la presencia de

timol (31,7%), cimeno (18,7%) y carvacrol (16,4%) [50]. El aceite esencial se evaluó frente a *C. albicans* mediante el método de dilución en tubo obteniendo una CIM de 0,31 µL/mL [34]. Otras plantas de importancia pertenecientes al género *Lippia* con valores de actividad inhibitoria menores a 100 µg/mL, evaluadas mediante el método de microdilución en caldo fueron: *L. junelliana* cuyo aceite esencial de partes aéreas (hojas, flores ó tallos) demostró ser activo frente *C. krusei* y *C. parapsilosis* (CIM 3,12 mg/L) [40], *L. origanoides* (aceite esencial de partes aéreas) activa frente a *C. neoformans* con CIM 78 µg/mL [42] y el aceite esencial de hojas de *L. sidoides* activo contra *C. krusei* (CIM 64 µg/mL) [43]; en otro estudio sobre esta última especie, se destacó la evaluación mediante microdilución de su fracción hexánica de hojas, demostrando actividad antifúngica frente a *Cryptococcus* sp. (CIM 31,25 µg/mL) y *Cryptococcus gattii* (CIM 62,5 µg/mL) [45].

Con respecto a extractos vegetales, se resalta el extracto acuoso en nanopartículas de plata de *L. citriodora* el cual alcanzó un valor de CIM de 100 µg/mL frente a *C. albicans* mediante difusión en disco [33]. Con actividades moderadas entre 0,6 a 1,50 mg/mL, se resaltaron los extractos etanólico y en diclorometano de los tallos de *L. vibrinoides* con CIM de 0,625 mg/mL y 0,313 mg/mL respectivamente frente a *C. neoformans* [46]; los extractos etanólicos de hojas de *L. adoensis* var. *adoensis* y *L. citriodora* con CIM de 512 µg/mL y 625 µg/mL respectivamente frente a *C. albicans* evaluados por microdilución [47, 48] y el extracto metanólico de las partes aéreas de *Verbena carolina* que demostró actividad frente a *C. albican*s con MIC de 0,7 mg/mL mediante dilución en agar. Técnicas de fraccionamiento por cromatografía en columna permitieron aislar diferentes compuestos de interés a partir de este extracto resaltándose compuestos de tipo terpenoide y fenólicos, entre ellos verbenalina, hastatosido, verbascosido, hispidulina-7-O-β-D-glucuronopiranosido y pectinolaringenina-7-O-α-D-glucuronopiranosido [49].

Dentro de los métodos de microdilución se destacó también el estudio de dos Santos *et al.* (2015), donde el aceite esencial de flores de *L. camara* mostró un % de inhibición del 95 % a una concentración de 15,6 µg/mL, mientras que los controles positivos (miconazol y nistatina) fueron menos activos a la misma concentración alcanzando un 92 % y 91 % de inhibición respectivamente. En el aceite fueron mayoritarios germacreno B, germacreno D, β-cariofileno y longicicleno [51].

Tabla 2. Especies de la familia Verbenaceae con potencial antifúngico frente a hongos levaduriformes.

Especie y parte de la planta estudiada	Microrganismo(s)	Aceite y/o extracto evaluado	Metabolitos mayoritarios detectados	Método(s)/ Bioactividad (CIM)[a]	Referencia
Aloysia gratissima (Gillies & Hook.) Tronc. hojas	*C. albicans ATCC 10231* *C. neoformans ATCC 32264*	Aceite esencial	1,8-cineol, germacreno-D, β-cariofileno, β-pineno	Microdilución en caldo CIM 1000 µg/mL	[25]
Lippia alba (Mill.) N.E.Br. ex Britton & P.Wilson Hojas	*C. dubliniensis ATCC 7978*	Aceite esencial	Nerol, geraniol, citral (neral/ geranial), 6-metil-5-hepten-2-ona, E-cariofileno	Difusión en disco y microdilución en caldo CIM 0,5 mg/mL	[39]
Lippia berlandieri Schauer	*C. albicans ATCC 900,028* *C. neoformans* var. *grubii* (Provided by Dr. Karen Bartlett, UBC)	Aceite esencial (muestra comercial)	p-cimeno, carvacrol	Difusión en fase de vapor CIM 0,25 µg/mL de aire	[36]
Lippia graveolens Kunth hojas	*C. albicans ATCC 90028*	Aceite esencial	ND	Dilución en tubo CIM 0,31 µL/mL	[34]
Lippia junelliana (Moldenke) Tronc. hojas, flores ó tallos	*C. krusei,* *C. albicans,* *C. glabrata,* *C. parapsilosis* (aislados clínicos)	Aceite esencial	Cis-davanona, mircenona, mirceno, Z-ocimenona E-ocimenona	Microdilución en caldo - *C. krusei* CIM_{90} 3,12 mg/L - *C. albicans* CIM_{90} 400 mg/L - *C. glabrata* CIM_{90} 800 mg/L) - *C. parapsilosis* CIM_{90} 3,12 mg/L	[40]

(*Continúa*)

Especie y parte de la planta estudiada	Microrganismo(s)	Aceite y/o extracto evaluado	Metabolitos mayoritarios detectados	Método(s)/ Bioactividad (CIM)[a]	Referencia
Lippia lasiocalycina Cham. hojas	*C. albicans ATCC 10231*	Aceite esencial	Óxido de piperitenona, limoneno	Microdilución en caldo CIM 512 µg/mL	[38]
Lippia micromera Schauer ramas florales	*C. albicans ATCC 24433* *C. parapsilosis ATCC 22019* *C. tropicalis ATCC 200956*	Aceite esencial	Carvacrol, p-cimeno, γ-terpineno, timol metil eter, timol, trans-β-cariofileno	Microdilución en caldo - *C. albicans* CIM 500 µg/mL - *C. parapsilosis* CIM 125 µg/mL - *C. tropicalis* CIM 125 µg/mL	[41]
Lippia origanoides Kunth partes aéreas	*C. albicans ATCC 10231* *C. neoformans* (aislado clínico)	Aceite esencial	(E)-Cinamato de metilo, hedicariol, α-eudesmol, β-eudesmol	Microdilución en caldo *C. neoformans* (CIM 78 µg/mL)	[42]
Lippia sidoides Cham. hojas	*C. albicans,* *C. tropicalis* *C. krusei* (muestras biológicas codificadas)	Aceite esencial	Timol (muestra adquirida comercial)	Microdilución en caldo - *C. krusei* CIM 64 µg/mL CFM[b] 128 µg/mL - *C. tropicalis* CIM 128 µg/mL - *C. albicans* CIM 256 µg/mL	[43]
Stachytarpheta indica (Linn.) Vahl partes aéreas	*C. albicans ATCC 10231*	Aceite esencial	β - cariofileno, 1-8 cineol, limoneno, β – turmerona	Microdilución en caldo *C. albicans* CIM 625 µg/mL	[44]

(*Continúa*)

Especie y parte de la planta estudiada	Microrganismo(s)	Aceite y/o extracto evaluado	Metabolitos mayoritarios detectados	Método(s)/ Bioactividad (CIM)[a]	Referencia
Lippia sidoides Cham. hojas	*C. albicans* *63U* *C. parapsilosis* *ATCC* *22019, 86U* *Cryptococcus sp. ATCC* *D* *C. gattii* *L48* *C. neoformans* *L3*	Aceite esencial, extracto etanólico y fracciones (hexánica, de diclorometano, de acetato de etilo y acuosa)	En aceite esencial: isoborneol, acetato de bornilo, *α*-humuleno, *α*-fencheno, 1.8-cineol	Microdilución en caldo - Aceite esencial: *C. parapsilosis* *Cryptococcus* sp. y *C. gattii* CIM 500 µg/mL - Extracto etanólico: *Cryptococcus* sp., *C. gattii, C. neoformans y C. parapsilosis* CIM 125–250 µg/mL - Fracción hexánica: *Cryptococcus* sp. CIM 31,25 µg/mL *C. gattii* CIM 62,5 µg/mL *C. neoformans* y *C. parapsilosis* CIM 250 µg/mL - Fracción de diclorometano: *Cryptococcus* sp. CIM 125–250 µg/mL, *C. albicans* CIM 500 µg/mL	[45]

(*Continúa*)

Especie y parte de la planta estudiada	Microrganismo(s)	Aceite y/o extracto evaluado	Metabolitos mayoritarios detectados	Método(s)/ Bioactividad (CIM)[a]	Referencia
Lantana vibrinoides tallos	*C. neoformans ATCC 90112*	Extracto etanólico, extracto de diclorometano, extracto en éter de petróleo	ND	Microdilución en caldo - Extracto etanólico: CIM 0,625 mg/mL - Extracto de diclorometano: CIM 0,313 mg/mL	[46]
Lippia adoensis var. *adoensis* Hojas	*C. albicans ATCC 10231*	Extracto etanólico	ND	Microdilución en caldo CIM 512 µg/mL	[47]
Lippia citriodora (Lam.) Kunth hojas	*C. albicans PTCC 5027*	Extracto etanólico	ND	Difusión en disco, difusión en pozo, microdilución en caldo CIM 625 µg/mL	[48]
	C. albicans (aislados clínicos, University College Hospital, Ibadan, Nigeria)	Extracto acuoso en nanopartículas de plata	ND	Microdilución en caldo CIM 100 µg/mL	[33]
Verbena carolina L. partes aéreas	*C. albicans ATCC 10231*	Extracto metanólico	Verbenalina, hastatosido, verbascosido, hispidulina-7-O -β- D-glucuronopiranosido, pectinolaringenina-7-O-α-D-glucuronopiranosido	Dilución en agar CIM 0,7 mg/mL	[49]

[a] CIM: Concentración Inhibitoria Mínima; [b]CFM: Concentración Fungicida Mínima; ND: no determinado

También se encontraron estudios orientados a la determinación de zonas de inhibición mediante difusión en disco, resaltándose el aceite esencial de las partes aéreas de *Aloysia triphylla* obtenido de diferentes regiones geográficas de Túnez. Los aceites de la región geográfica de Kairouan reportaron diámetros de inhibición frente a *C. albicans* (85±8,3 mm), *C. parapsilosis* (85±6,6 mm), *C. glabrata* (85±8,6 mm). Y los aceites de la región geográfica Siliana, reportaron diámetros de inhibición frente a *C. albicans* (85±8,0 mm), *C. parapsilosis* (85±8,5 mm) y *C. glabrata* (85±8,8 mm). Estas zonas de inhibición fueron más altas que las reportadas para el control de nistatina (25±2,68 mm). Los autores atribuyeron a la presencia de citral (geranial), la alta actividad demostrada por el aceite [52].

La búsqueda arrojó un total de 5 géneros de la familia Verbenaceae con potencial actividad antifúngica: *Aloysia*, *Lantana, Lippia*, *Stachytarpheta* y *Verbena*; este resultado es acorde con otros estudios de revisión sobre plantas con actividad antimicrobiana donde especies de los géneros *Aloysia, Lantana, Lippia* y *Stachytarpheta* se resaltaron por su actividad frente a hongos levaduriformes [24, 53].

A partir de la revisión se obtuvo una mayor cantidad de artículos publicados en Suramérica, lo cual puede tener relación con la distribución geográfica de esta familia que presenta un mayor número de especies en esta región gracias a la diversidad de ecosistemas, favoreciendo amplios rangos de distribución en la zona neotropical [20]. Especialmente para Colombia, se reportó la evaluación *in vitro* de aceites esenciales e hidrosoles de *L. alba*, *Rosmarinus officinalis* y *Thymus vulgaris* frente a bacterias y hongos por su potencial actividad preservante. Para cada planta se evaluaron los aceites e hidrosoles de forma individual y en combinación, evaluando además la combinación de aceites de diferentes plantas. Dentro de los resultados se destacó la mezcla de aceites esenciales de *L. alba* y *T. vulgaris* frente a *C. albicans y A. niger,* calculando un valor de Concentración Microbicida Fraccional (CMF) de 1 y una interacción de tipo Adición (0,5 < CMF ≤ 1,0), siendo una alternativa para ser utilizados de forma combinada como preservantes en productos terminados de la industria cosmética o fitoterapéutica incluso con sus respectivas indicaciones terapéuticas [54]. Recientemente, Pájaro-González *et al.* (2022) publicaron un estudio de revision sobre plantas medicinales de uso tradicional como antimicrobianos en Colombia, endémicas o no para el tratamiento de enfermedades infecciosas. En el rango de búsqueda establecido (1990 a 2020) las plantas con mayor uso tradicional fueron *Austroeupatorium inulifolium* Kunth. y *Xanthium strumarium* L. (Asteraceae), *Jacaranda caucana* Pittier (Bignoniaceae), *Hymenaea courbaril* L. (Leguminosae), *Guazuma ulmifolia* Lam. (Malvaceae), *Cymbopogon citratus* (DC.) Stapf (Poaceae) y *Solanum nudum* Hassl (Solanaceae). Cabe mencionar que en ese estudio se encontraron plantas promisorias por reportar actividad antibacteriana (CIM ≤5 μg/mL), antiviral (CIM ≤5.5 μg/mL) o antiparasitaria (DE_{50} ≤5 μg/mL),

mas no actividad antifúngica [55]. Aunque la familia Verbenacea no es de las mas abundantes en Colombia, Stashenko y Martínez (2019) resaltaron esta familia junto con la familia Labiatae por reunir especies útiles en la medicina tradicional como antibacterianos, antifúngicos, antivirales e insecticidas [56]. Dentro de la familia Verbenacea son de interés en Colombia los estudios adelantados con el aceite esencial de tallos y hojas de *L. origanoides* activo frente a *C. albicans* (CIM: 157,5 µg/mL) [27] y con el aceite esencial de los tallos, hojas, flores y raíces de *L. citriodora* activo contra *C. krusei y A. fumigates* (CIM: 99,21 µg/mL y 62,5 µg/mL respectivamente) [57]. Estos estudios no se encontraban dentro del rango de búsqueda propuesto para la presente revisión sistemática.

Los resultados reportados en la tabla 2, evidencian una mayor cantidad de estudios con aceites esenciales que con extractos y/o fracciones vegetales. Solo en uno se evalúa el aceite esencial pero también el extracto etanólico y las fracciones de las hojas de *L. sidoides* frente a diferentes microorganismos [45]. Una razón de ello puede atribuirse a los procedimientos de extracción de aceites volátiles (hidrodestilación o fluido supercrítico) los cuales son más sencillos, rápidos y seguros implicando menos costos económicos y técnicos en su investigación y desarrollo, más aún si se contempla su incorporación en un producto terminado. Aunque es fundamental determinar la composición y proporción de sus metabolitos, los aceites esenciales son muchas veces considerados de por sí un producto final con valor comercial que no requiere de procesos de purificación posteriores [58], mientras que la obtención de extractos vegetales o fracciones enriquecidas, puede requerir el empleo de diferentes solventes de extracción, (algunos de ellos tóxicos) y mayores procesos de purificación y análisis. Aun así, los resultados promisorios obtenidos en esta revisión sugieren adelantar estudios sobre el análisis y evaluación de extractos de especies de la familia Verbenaceae, orientados ya sea hacia su estandarización o al aislamiento de biocompuestos con actividad antifúngica.

Tanto los aceites esenciales como los extractos fueron obtenidos de diferentes partes de las plantas, para esta revisión se reportó una mayor cantidad de estudios donde empleaban las hojas, seguido de las partes aéreas, flores y tallos. La parte de la planta o droga vegetal puede influir en los diferentes resultados en cuanto a bioactividad y metabolitos secundarios, dependiendo también del método de extracción, el lugar de recolección, el suelo y factores climáticos, entre otros [59]. Para las especies de la familia Verbenaceae, la parte de la planta más usada en la medicina tradicional son las hojas, empleándose principalmente para tratar diferentes afecciones como bronquitis, trastornos digestivos y nerviosos ó como antipirético, antihipertensivo, analgésico, sedante, para la dermatitis, la malaria, las úlceras, como antiséptico para heridas, para tratar la diarrea, para el asma y como antimicrobiano, entre muchos otros usos [20].

Se observó como factor común la evaluación de actividad antifúngica sobre especies del género *Candida*, especialmente *C. albicans* que fue incluida en la mayoría de los estudios, demostrando que sigue siendo una especie de importancia clínica y el agente etiológico principal de las infecciones y enfermedades producidas por especies de *Candida* [60]. En el estudio publicado por Chin *et al.* (2016), se reporta que en los hospitales de Estados Unidos *C. albicans* es la especie más común en infecciones del torrente sanguíneo representando una tasa de mortalidad hasta del 55 % [61]. Otra especie de interés fue *C. neoformans*, también de importancia clínica por su mortalidad y difícil manejo especialmente en pacientes inmunocomprometidos, como lo reporta Bongomin *et al.* (2018) quien mediante un estudio de revisión tipo meta-análisis que incluyó estudios desde 1988 a 2017, documentó la prevalencia de resistencia *in vitro* al fluconazol de aislados clínicos de especies de *Cryptococcus* obtenidos de pacientes infectados con VIH, reportando un 18,7 % para aislados de *C. neoformans*. En su estudio también destaca que las más altas tasas de resistencia se presentaron en Sudáfrica (50 %), España (46,6 %) y Taiwán (33,7 %) [8]. *Saccharomyces cerevisiae* fue poco evaluado en los estudios; aunque sigue siendo una especie de mayor interés en la industria alimentaria, se está reportando también como patógeno emergente [62].

El método que más se resaltó para la evaluación de la actividad antifúngica fue microdilución en caldo seguido del método de difusión (en disco y en pozo de agar). En 17 de los 31 estudios de investigación revisados se contempló el método de microdilución para la evaluación tanto de extractos como de aceites. Este método es uno de los más usados gracias a que su reproducibilidad requiere menos reactivos y espacio, por lo que resulta bastante económico; arroja además resultados cuantitativos respecto a los valores de CIM, según lectura visual en el ensayo estandarizado por el Instituto de Estándares Clínicos y de Laboratorio (CLSI) y cuantificación espectrofotométrica de acuerdo a las directrices del Comité Europeo de Pruebas de Susceptibilidad a los Antimicrobianos (EUCAST). Por otro lado, los métodos de difusión en disco y en pozo son bien conocidos y también bastante usados en los laboratorios; se usan debido a su bajo costo, simplicidad y facilidad para leer e interpretar los resultados, sin embargo, no ofrecen un valor de CIM específico debido a la dificultad de cuantificar la cantidad de agente difundido en el agar [63, 64].

Perspectivas actuales en investigación

En estudios recientes se reconoce el creciente aumento de la resistencia de los microorganismos a los medicamentos actuales, siendo necesaria la búsqueda y desarrollo de nuevos agentes antimicrobianos entre ellos los antifúngicos. Según Vaou *et al.*, aunque se hace complejo determinar la interacción entre los diversos compuestos que se encuentran en una planta hay que tener en cuenta que cerca del 74 % de los compuestos

bioactivos son derivados de éstas; es pertinente realizar investigaciones orientadas a la obtención de los compuestos químicos con mayor bioactividad y así lograr comprender los mecanismos de acción implicados, ya que muchos de estos compuestos son inexplorados y pueden contribuir a hallazgos interesantes en medicina [65].

En este sentido, dentro de las especies de la familia Verbenacea, el orégano mexicano (*L. graveolens*), sigue teniendo reconocimiento como una fuente de compuestos bioactivos con potencial aplicación en la industria farmacéutica, cosmética, de alimentos funcionales y de nutracéuticos, siendo su aceite esencial el más estudiado a partir del cual se han aislado metabolitos, especialmente monoterpenos responsables de su sabor y aroma, pero también de su actividad antifúngica, entre ellos timol y carvacrol, como se ha reportado [50]. Otros compuestos de interés detectados en *L. graveolens* son los compuestos fenólicos, especialmente flavonoides y ácidos fenólicos, presentes en extractos hidroalcohólicos los cuales han demostrado actividad antioxidante, antiinflamatoria y citotóxica [66]. Estos compuestos podrían ser promisorios para su estudio como agentes antifúngicos, siendo una actividad poco explorada.

Estudios recientes se han orientado a la evaluación de aceites esenciales, demostrando ser más activos que los fármacos control o modulando su actividad mediante mecanismos sinérgicos; tal es el caso del estudio de Jaradat *et al.* (2021) quienes evaluaron la actividad antimicrobiana de los aceites esenciales de hojas de *Aloysia citriodora* Palau recolectadas en las regiones de Palestina: Umm al-Fahm y Baqa al-Gharbiyye. Su actividad antifúngica se evaluó frente al crecimiento de *C. albicans* (ATCC 90028) mediante el método de microdilución en RPMI e incubación de 18 a 24 horas, empleando fluconazol como control. Los resultados mostraron una CIM (µg/mL) para el aceite esencial de Baqa al-Gharbiyye de 0,625 y de 0,312 para el aceite esencial de Umm al-Fahm; mientras que para el fluconazol se estableció en 1,56 µg/ml. Esto evidencia la capacidad de los aceites esenciales de *A. citriodora* de inhibir el crecimiento de *C. albicans* con mayor actividad que el fluconazol, existiendo diferencias en relación con los lugares de recolección de las muestras estudiadas [67]. Por otro lado, de Lima *et al*., reporta la capacidad del aceite esencial de *Lantana montevidensis* para modular la actividad antifúngica del fluconazol. En este trabajo se evalúo el aceite esencial de las hojas de *L. montevidensis* obtenido por hidrodestilación frente a cepas estándar y aislamientos clínicos de *C. albicans* y *C. tropicalis* por medio de microdilución, evaluando la actividad antifúngica pero también moduladora en combinación con fluconazol. Si bien el aceite esencial no evidenció actividad antifúngica de forma independiente superior al fluconazol frente a las cepas evaluadas, si se observó capacidad para modular la actividad del fluconazol frente a *C. tropicalis* con un efecto sinérgico, siendo el mejor valor de reducción del crecimiento del 48% (±0.1913), a una concentración de 128 µg/mL [68]. Estos reportes sugieren que la administración de fármacos en combinación con

aceites esenciales brinda nuevas opciones para mejorar ya sea la eficacia o potencia de los antifúngicos.

Bajo este panorama, dentro de las especies de plantas medicinales de la familia Verbenacea descritas en este estudio, con registros en Colombia según el Sistema Global de Información sobre Biodiversidad (GBIF), se encuentran especialmente dentro del género *Lippia*, *L. alba*, *L. citriodora*, *L. graveolens*, *L. micromera*, *L. origanoides*; además de las especies *A. citriodora*, *L. montevidensis* y *Stachytarpheta indica*, las cuales son promisorias por su actividad antifúngica *in vitro,* siendo una fuente de metabolitos para el estudio y evaluación de productos naturales y el desarrollo de bioproductos. Cabe resaltar, además, según los estudios de Bernal *et al*. (2011), la familia Verbenacea se encuentra dentro de las principales familias botánicas de las especies medicinales de uso en Colombia. En su trabajo reporta a *Verbena valerianoides* Kunth como una especie medicinal exclusiva de Colombia y a *Lantana cuyanbensis* (*Lantana cujabensis* Schauer) como una especie nativa del neotrópico presente en Colombia [69], lo que sugiere adelantar estudios etnobotánicos de estas plantas explorando usos medicinales antimicrobianos.

Por último, es importante resaltar estudios orientados a la evaluación de extractos vegetales, obtenidos de familias diferentes a Verbenaceae. En un estudio realizado con plantas medicinales de Republica Dominicana, se evaluaron extractos etanólicos crudos de 48 especies pertenecientes a 32 familias diferentes, hallando una actividad antifúngica importante para 3 especies de plantas *Eleutherine bulbosa* (Mill.) Urb., *Xanthium strumarium* L. y *Zingiber cassumunar* Roxb., de las familias Iridaceae, Asteraceae y Zingiberaceae respectivamente. Los extractos fueron activos frente a *C. albicans* con halos de inhibición de 16-20 mm de diámetro, reconociendo la amplia diversidad de plantas medicinales que pueden tener un potencial en cuanto a metabolitos precursores de compuestos bioactivos para desarrollar nuevos productos terapéuticos, a partir de familias diferentes a Verbenaceae [70].

Conclusión

Se encontraron cinco géneros de la familia Verbenaceae con potencial actividad antifúngica, *Aloysia*, *Lantana, Lippia*, *Stachytarpheta* y *Verbena*, resaltándose el género *Lippia* con un número mayor de especies evaluadas. Dentro de este género fueron de interés el aceite esencial de *L. berlandieri* activo (CIM de 0,25 µg/mL) frente a *C. albicans* y *C. neoformans,* y el aceite esencial de *L. graveolens* activo (CIM de 0,31 µL/mL) frente a *C. albicans*. Los metabolitos mayoritarios a los cuales podría atribuirse la acti-

vidad antifúngica de estas dos especies son p-cimeno (35,54 %) y carvacrol (26,86 %) y timol (31,7 %), cimeno (18,7 %) y carvacrol (16,4 %) respectivamente.

Se evidenció que hay una diversidad de especies de la familia Verbenaceae con potencial antifúngico, resaltando de tal manera la importancia de esta familia en especial para Suramérica teniendo en cuenta que dentro de las especies encontradas la mayoría se distribuyen en zonas neotropicales. Los aceites esenciales jugaron un papel de gran importancia en las valoraciones de bioactividad, que por lo general se realizó mediante el método de microdilución en caldo, sin embargo, es pertinente adelantar estudios orientados a la evaluación de extractos como una fuente también importante de metabolitos con actividad antifúngica, siendo de interés los compuestos fenólicos.

El estudio de revisión permitió un acercamiento al reconocimiento de biocompuestos prometedores para el desarrollo de nuevos fármacos o productos naturales derivados, que ayuden en el control y tratamiento de las infecciones fúngicas, dentro de la problemática del aumento de incidencias de dichas infecciones y la resistencia que están generando especies patógenas de hongos levaduriformes a los fármacos convencionales, especialmente en pacientes inmunocomprometidos.

Agradecimientos

Los autores agradecen al programa de Biología de la Escuela de Ciencias Básicas y Aplicadas de la Universidad de La Salle y a la Escuela de Ciencias de la Salud de la Universidad Nacional Abierta y a Distancia – UNAD.

Conflicto de intereses

Los autores del estudio manifestamos no presentar ningún conflicto de interés.

Referencias

1. Y. Schmiedel, S. Zimmerli, Common invasive fungal diseases: an overview of invasive candidiasis, aspergillosis, cryptococcosis, and *Pneumocystis pneumonia*, *Swiss Medical Weekly*, **146**, w14281 (2016). Doi: https://doi.org/10.4414/smw.2016.14281

2. S. Vallabhaneni, R.K. Mody, T. Walker, T. Chiller, The global burden of fungal diseases, *Infectious Disease Clinics of North America*, **30**(1), 1-11 (2016). Doi: https://doi.org/10.1016/j.idc.2015.10.004

3. O.T. Ezeokoli, O. Gcilitshana, C.H. Pohl, Risk factors for fungal co-infections in critically ill COVID-19 patients, with a focus on immunosuppressants, *Journal of Fungi*, **7**(7), 545 (2021). Doi: https://doi.org/10.3390/jof7070545

4. G. Segrelles-Calvo, G.R. de Araújo, S. Frases, Systemic mycoses: a potential alert for complications in COVID-19 patients, *Future Microbiology*, **15**(14), 1405-1413 (2020). Doi: https://doi.org/10.2217/fmb-2020-0156

5. S. Zurita, Situation of anti-fungal resistance of species of the genus *Candida* in Peru, *Revista Peruana de Medicina Experimenal y Salud Pública*, **35**(1), 126-131 (2018). Doi: https://doi.org/10.17843/rpmesp.2018.351.3563

6. J.A. Cortés, P. Reyes, C.H. Gómez, S.I. Cuervo, P. Rivas, C.A. Casas, *et al*., Clinical and epidemiological characteristics and risk factors for mortality in patients with candidemia in hospitals from Bogotá, Colombia, *The Brazilian Journal of Infectious Diseases*, **18**(6), 631-637 (2014). Doi: https://doi.org/10.1016/j.bjid.2014.06.009

7. R. Selb, V. Fuchs, B. Graf, A. Hamprecht, M. Hogardt, L. Sedlacek, R. Sánchez, Molecular typing and *in vitro* resistance of *Cryptococcus neoformans* clinical isolates obtained in Germany between 2011 and 2017, *Int. J. Med. Microbiol*., **309**(6), 1-8 (2019). Doi: https://doi.org/10.1016/j.ijmm.2019.151336

8. F. Bongomin, R.O. Oladele, S. Gago, C.B. Moore, M.D. Richardson, A systematic review of fluconazole resistance in clinical isolates of *Cryptococcus* species, *Mycoses*, **61**(5), 290-297 (2018). Doi: https://doi.org/10.1111/myc.12747

9. S.R. Lockhart, J. Guarner, Emerging and reemerging fungal infections, *Seminars in Diagnostic Pathology*, **36**(3), 177-181 (2019). Doi: https://doi.org/10.1053/j.semdp.2019.04.010

10. M. Nucci, G. Barreiros, L.F. Guimarães, V.A.S. Deriquehem, A.C. Castiñeiras, S.A. Nouér, Increased incidence of candidemia in a tertiary care hospital with the COVID-19 pandemic, *Mycoses*, **64**(2), 152-156 (2021). Doi: https://doi.org/10.1111/myc.13225

11. A. Chowdhary, B. Tarai, A. Singh, A. Sharma, Multidrug-resistant *Candida auris* infections in critically ill coronavirus disease patients, India, April–July 2020, *Emerging Infectious Diseases*, **26**(11), 2694-2696 (2020). Doi: https://doi.org/10.3201/eid2611.203504

12. B. Posteraro, R. Torelli, A. Vella, P.M. Leone, G. De Angelis, E. De Carolis, G. Ventura, M. Sanguinetti, M. Fantoni, Pan-echinocandin-resistant *Candida glabrata* bloodstream infection complicating COVID-19: A fatal case report, *Journal of Fungi*, **6**(3), 163-174 (2020). Doi: https://doi.org/10.3390/jof6030163

13. I. Quiles, J. García, Antifúngicos de uso sistémico, *Revista Iberoamericana de Micología*, **38**(2), 42-46 (2021). Doi: https://doi.org/10.1016/j.riam.2021.04.004

14. A. Rasool, K.M. Bhat, A.A. Sheikh, A. Jan, S. Hassan, Medicinal plants: Role, distribution and future, *Journal of Pharmacognosy and Phytochemistry*, **9**(2), 2111-2114 (2020). URL: https://www.phytojournal.com/archives/2020.v9.i2.11165/medicinal-plants-role-distribution-and-future

15. C.C. Achilonu, O.U. Udensi, Systematic review of antimicrobial activities of medicinal plants against bacterial and fungal microbes: a research trend in Africa from 1980 to 2019, *Research Square*, 1-22 (2022). Doi: https://doi.org/10.21203/rs.3.rs-1529001/v1

16. A.M. Viljoen, S. Subramoney, S.F. van Vuuren, K.H.C Başer, B. Demirci, The composition, geographical variation and antimicrobial activity of *Lippia javanica* (Verbenaceae) leaf essential oils, *Journal of Ethnopharmacology*, **96**(1-2), 271-277 (2005). Doi: https://doi.org/10.1016/j.jep.2004.09.017

17. A. Muñoz-Acevedo, M.C. González, O.J. Castillo, C.P, Guzmán, S. Rodríguez-Acosta, M. Cervantes-Díaz, *et al.*, Promising antimicrobial agents from some Latin American medicinal plants against disease-causing pathogens in humans and animals, en: M. Rai, I. Kosalec (editores), *Promising Antimicrobials from Natural Products*, Springer, Cham, Switzerland, 2022, pp. 241-279. URL: https://link.springer.com/chapter/10.1007/978-3-030-83504-0_11

18. L. Betancur-Galvis, B. Zapata, A. Baena, J. Bueno, C.A. Ruíz-Nova, E. Stashenko, A.C. Mesa-Arango, Antifungal, cytotoxic and chemical analyses of essential oils of *Lippia origanoides* HBK grown in Colombia, *Revista Salud UIS*, **43**(2), 141-148 (2011). URL: https://revistas.uis.edu.co/index.php/revistasaluduis/article/view/2397

19. J. Henao, L.J. Muñoz, E. Ríos, L. Padilla, G.A. Giraldo, Evaluación de la actividad antimicrobiana de los extractos de la planta *Lippia origanoides* H.B.K. cultivada en el Departamento del Quindío, *Revista de Investigaciones Universidad del Quindío*, **19**(1), 159-164 (2009). Doi: https://doi.org/10.33975/riuq.vol19n1.784

20. C.M. Pérez-Zamora, C.A. Torres, M.B. Nuñez, Antimicrobial activity and chemical composition of essential oils from Verbenaceae species growing in South America, *Molecules*, **23**(3), 544 (2018). Doi: https://doi.org/10.3390/molecules23030544

21. Z. Xu, L. Chang, Verbenaceae, en: *Identification and Control of Common Weeds*, Vol. 3, Springer Netherlands, Dordrecht, 2017, p. 163. Doi: https://doi.org/10.1007/978-981-10-5403-7_7

22. E.O. Sousa, F.S.S. Barreto, F.F.G. Rodrigues, A.R. Campos, J.G.M. Costa, Chemical composition of the essential oils of *Lantana camara* L. and *Lantana montevidensis* Briq. and their synergistic antibiotic effects on aminoglycosides, *Journal of Essential Oil Research*, **24**(5), 447-452 (2012). Doi: https://doi.org/10.1080/10412905.2012.703494

23. U. Nogueira de Aguiar, S.G. de Lima, M.d.S. Rocha, A.M.d.G. Lopes-Citó, A.J. Pereira-Sousa, R. Morais-Silva, I.S. Alcantara-Silva, J.G. Martins da Costa, Chemical composition and modulation of antibiotic activity of essential oil of *Lantana caatingensis* M. (Verbenaceae), *Industrial Crops and Products*, **74**, 165-170 (2015). Doi: https://doi.org/10.1016/j.indcrop.2015.04.011

24. C.M. Pérez-Zamora, C.A. Torres, M.I. Aguado, A.J. Bela, M.B. Nuñez, C. Bregni, Actividad antibacteriana de los aceites esenciales de *Aloysia polystachya* y *Lippia turbinata* (Verbenaceae), *Boletín Latinoamericano y del Caribe de Plantas Medicinales y Aromáticas*, **15**(4), 199-205 (2016). URL: https://www.blacpma.ms-editions.cl/index.php/blacpma/article/view/274

25. T.G. Santos, J. Laemmle, R.A. Rebelo, E.M. Dalmarco, B. Cruz, A.P. Schmit, A.L.B. Zeni, Chemical composition and antimicrobial activity of *Aloysia gratissima* (Verbenaceae) leaf essential oil, *Journal of Essential Oil Research*, **27**(2), 125-130 (2015). Doi: https://doi.org/10.1080/10412905.2015.1006737

26. J. Acero-Godoy, T. Guzmán-Hernández, C. Muñoz-Ruiz, Revisión documental de uso de los aceites esenciales obtenidos de *Lippia alba* (Verbenaceae), como alternativa antibacteriana y antifúngica, *Revista Tecnología en Marcha*, **32**(1), 3-11 (2019). URL: https://www.scielo.sa.cr/pdf/tem/v32n1/0379-3982-tem-32-01-3.pdf

27. V. Tangarife-Castaño, J. Correa-Royero, B. Zapata-Londoño, C. Durán, E. Stashenko, A.C. Mesa-Arango, Anti-*Candida albicans* activity, cytotoxicity and interaction with antifungal drugs of essential oils and extracts from aromatic and medicinal plants, *Infectio*, **15**(3), 160-167 (2011). Doi: https://doi.org/10.1016/S0123-9392(11)70080-7

28. A.K. Pardo, J.J. Arenas, M. Gómez, F.M. Lora, J.E. Gómez, Determinación de la actividad antifúngica de extractos de *Lantana camara* frente a *Candida* spp., *Infectio*, **15**(4), 235-242 (2011). Doi: https://doi.org/10.1016/S0123-9392(11)70737-8

29. S.E. Giraldo-Quintero, M.C. Bernal-Lizarazú, A. Morales-Robayo, A.Z. Pardo-Lobo, L. Gamba-Molano, Descripción del uso tradicional de plantas medicinales en mercados populares de Bogotá, D.C., *Nova*, **13**(23), 73-80 (2015). Doi: https://doi.org/10.22490/24629448.1707

30. N.A. Navarrete-Barragán, E.F. Pita-Ospina, R.M. Sánchez-Mora, S.E. Giraldo-Quintero, M.C. Bernal-Lizarazú, Actividad *in vitro* de los extractos etanólicos de *Lantana camara* L., *Petiveria alliacea* L. y *Lippia dulcis* T. frente a bacterias patógenas, *Nova*, **18**(33), 53-71 (2020). Doi: https://doi.org/10.22490/24629448.3700

31. L.R. Jaimes-Duarte, J.F. Hoyos-Argote, *Plantas medicinales de la familia Verbenaceae con potencial antifúngico contra hongos levaduriformes*, Trabajo de grado, Universidad de la Salle, Bogotá D.C., 2020. 54 p. URL: https://ciencia.lasalle.edu.co/biologia/91

32. M.K. Swamy, M.S. Akhtar, U.R. Sinniah, Antimicrobial properties of plant essential oils against human pathogens and their mode of action: An updated review, *Evidence-Based Complementary and Alternative Medicine*, **2016**, 3012462 (2016). Doi: https://doi.org/10.1155/2016/3012462

33. E.E. Elemike, D.C. Onwudiwe, A.C. Ekennia, R.C. Ehiri, N.J. Nnaji, Phytosynthesis of silver nanoparticles using aqueous leaf extracts of *Lippia citriodora*: Antimicrobial, larvicidal and photocatalytic evaluations, *Materials Science and Engineering: C*, **75**, 980-989 (2017). Doi: https://doi.org/10.1016/j.msec.2017.02.161

34. A.B. Miller, R.G. Cates, M. Lawrence, J.A.F. Soria, L.V. Espinoza, J.V. Martinez, D.A. Arbizú, The antibacterial and antifungal activity of essential oils extracted from Guatemalan medicinal plants, *Pharmaceutical Biology*, **53**(4), 548-554 (2015). Doi: https://doi.org/10.3109/13880209.2014.932391

35. P.M. Liew, Y.K. Yong, *Stachytarpheta jamaicensis* (L.) Vahl: from traditional usage to pharmacological evidence, *Evidence-Based Complementary and Alternative Medicine*, **2016**, 7842340 (2016). Doi: https://doi.org/10.1155/2016/7842340

36. F. Reyes-Jurado, T. Cervantes-Rincón, H. Bach, A. López-Malo, E. Palou, Antimicrobial activity of Mexican oregano (*Lippia berlandieri*), thyme (*Thymus vulgaris*), and mustard (*Brassica nigra*) essential oils in gaseous phase, *Industrial Crops and Products*, **13**, 90-95 (2019). Doi: https://doi.org/10.1016/j.indcrop.2019.01.036

37. A. Sartoratto, A.L.M. Machado, C. Delarmelina, G.M. Figueira, M.C.T. Duarte, V.L.G. Rehder, Composition and antimicrobial activity of essential oils from aromatic plants used in Brazil, *Brazilian Journal of Microbiology*, **35**(4), 275-280 (2004). Doi: https://doi.org/10.1590/S1517-83822004000300001

38. W. Sales de Almeida, S.G. de Lima, H. Medeiros-Barreto, L.M. de Sousa-Andrade, L. Fonseca, C. Athayde-Sobrinho, A.R. Beserra-Santos, M.C. Sanches-Muratori, Chemical composition and antimicrobial activity of the essential oil of *Lippia lasiocalycina* Cham. (Verbenaceae), *Industrial Crops and Products*, **125**, 236-240 (2018). Doi: https://doi.org/10.1016/j.indcrop.2018.09.007

39. N. Santos, R.C. Pascon, M.A. Vallim, C.R. Figueiredo, M.G. Soares, J.H.G. Lago, P. Sartorelli, Cytotoxic and antimicrobial constituents from the essential oil of *Lippia alba* (Verbenaceae), *Medicines*, **3**(3), 22 (2016). Doi: https://doi.org/10.3390/medicines3030022

40. S. Córdoba, W. Vivot, W. Szusz, G. Albo, Antifungal activity of essential oils against *Candida* species isolated from clinical samples, *Mycopathologia*, **184**(5), 615-623 (2019). Doi: https://doi.org/10.1007/s11046-019-00364-5

41. C. Scotto, P. Burger, M. Khodjet, M. Ginouves, G. Prevot, D. Blanchet, P.G. Delprete, X. Fernandez, Corrigendum of the article: Composition and antifungal activity of the essential oil of *Nashia inaguensis* Millsp. (Verbenaceae) cultivated in French Guiana, *Journal of Essential Oil Research*, **29**(6), 507-509 (2017). Doi: https://doi.org/10.1080/10412905.2017.1369466

42. W.H. Perera, H.R. Bizzo, P.E. Gama, C.S. Alviano, F.R.G. Salimena, D.S. Alviano, S.G. Leitão, Essential oil constituents from high altitude Brazilian species with antimicrobial activity: *Baccharis parvidentata* Malag., *Hyptis monticola* Mart. ex Benth. and *Lippia origanoides* Kunth, *Journal of Essential Oil Research*, **29**(2), 109-116 (2016). Doi: https://doi.org/10.1080/10412905.2016.1210039

43. D.I.V. Brito, M.F. Morais-Braga, F.A.B. Cunha, R.S. Albuquerque, J.N.P Carneiro, M.S. Lima, N.F. Leite, C.E.S. Souza, J.C. Andrade, L.B.B. Alencar, A.K.L.S. Lavor, F.G. Figueredo, L.F. Lima, H.D.M. Coutinho, Análise fitoquímica e atividade antifúngica do óleo essencial de folhas de *Lippia sidoides* Cham. e do Timol contra cepas de *Candida* spp., *Revista Brasileira de Plantas Medicinais* (Campinas), **17**(4), 836-844 (2015). Doi: https://doi.org/10.1590/1983-084X/14_060

44. E.E. Essien, T.M. Walker, J.S. Newby, W.N. Setzer, O. Ekundayo, Characterization and antimicrobial activity of essential oils of *Stachytarpheta indica* (Linn.) Vahl and *Mariscus alternifolius* Vahl, *Journal of Medicinally Active Plants*, **5**(2), 47-52 (2017). Doi: https://doi.org/10.7275/R5DR2SNN

45. S.R. De Morais, T.L.S. Oliveira, L.P. De Oliveira, L.M. Faustino, E. Cardoso, M.H. Rezende, T.d.S. Fiuza, E.A. Costa, P.H. Ferri, J.R. de Paula, Essential oil composition, antimicrobial and pharmacological activities of *Lippia sidoides* Cham. (Verbenaceae) from São Gonçalo do Abaeté, Minas Gerais, Brazil, *Pharmacognosy Magazine*, **12**(48), 262-270 (2016). URL: https://www.ncbi.nlm.nih.gov/pmc/articles/PMC5096271/pdf/PM-12-262.pdf

46. M.V.N. Mbunde, F. Mabiki, E. Innocent, P.G. Andersson, Antifungal activity of single and combined extracts of medicinal plants from Southern Highlands of Tanzania, *Journal of Pharmacognosy and Phytochemistry*, **8**(1), 181-187 (2019). URL: https://www.phytojournal.com/archives?year=2019&vol=8&issue=1&ArticleId=6722

47. A. Teka, J. Rondevaldova, Z. Asfaw, S. Demissew, P. Van Damme, L. Kokoska, W. Vanhove, *In vitro* antimicrobial activity of plants used in traditional medicine in Gurage and Silti Zones, south central Ethiopia, *BMC Complementary Medicine and Therapies*, **15**, 286 (2017). Doi: https://doi.org/10.1186/s12906-015-0822-1

48. M. Ghasempour, S.M. Omran, A.A. Moghadamnia, F. Shafiee, Effect of aqueous and ethanolic extracts of *Lippia citriodora* on *Candida albicans*, *Electronic Physician*, **8**(8) 2752-2758 (2016). Doi: https://doi.org/10.19082/2752

49. G. Lara-Issasi, C. Salgado, J. Pedraza-Chaverri, O.N. Medina-Campos, A. Morales, M.A. Águila, M. Avilés, B.E. Rivero-Cruz, V. Navarro, R. Ríos-Gómez, M.I. Aguilar, Antimicrobial, antioxidant activities, and HPLC determination of the major components of *Verbena carolina* (Verbenaceae), *Molecules*, **24**(10), 1970 (2019). Doi: https://doi.org/10.3390/molecules24101970

50. S. Herrera, R. López, E. García, M. Estarrón, Mexican oregano (*Lippia graveolens*) essential oil-in-water emulsions: impact of emulsifier type on the antifungal activity of *Candida albicans*, *Food Science and Biotechnology*, **28**, 441-448 (2019). Doi: https://doi.org/10.1007/s10068-018-0499-6

51. R.C. dos Santos, A.A. de Melo Filho, E.A. Chagas, J.A. Takahashi, V.P Ferraz, I.M. Fernandez, P.R.E. Ribeiro, A.C.G. Reis de Melo, L.C. Holanda, Chemical composition, antimicrobial and anti-acetylcholinesterase activities of essential oil from *Lantana camara* (Verbenaceae) flowers, *Journal of Medicinal Plants Research*, **9**(35), 922-928 (2015). Doi: https://doi.org/10.5897/JMPR2015.5919

52. L. Rezig, M. Saada, N. Trabelsi, S. Tammar, H. Limam, I. Bettaieb-Rebey, A. Smaoui, G. Sghaier, G. Del Re, R. Ksouri, K. Msaada, Chemical composition, antioxidant and antimicrobial activities of *Aloysia triphylla* L. Essential oils and methanolic extract, *Italian Journal of Food Science*, **31**(3), 556-572 (2019). Doi: https://doi.org/10.14674/IJFS-1373

53. C. Giordani, R. Santin, M.B. Cleff, Levantamento de extratos vegetais com ação anti-*Candida* no período de 2005-2013, *Revista Brasileira de Plantas Medicinais*, (Campinas), **17**(1), 175-185 (2015). Doi: https://doi.org/10.1590/1983-084X/12_072

54. Y.O. Hay, M.A. Abril-Sierra, L.G. Sequeda-Castañeda, C. Bonnafous, C. Raynaud, Evaluation of combinations of essential oils and essential oils with hydrosols on antimicrobial and antioxidant activities, *Journal of Pharmacy & Pharmacognosy Research*, **6**(3), 216-230 (2018). Doi: https://doi.org/10.56499/jppres17.310_6.3.216

55. Y. Pájaro-González, A.F. Oliveros-Díaz, J. Cabrera-Barraza, J. Cerra-Dominguez, F. Díaz-Castillo, F, Chapter 1 - A review of medicinal plants used as antimicrobials in Colombia, en: F. Chassagne (editor), *Medicinal Plants as Anti-Infectives*, Academic Press, Toulouse, 2022, p. 3-57. Doi: https://doi.org/10.1016/B978-0-323-90999-0.00005-7

56. E. Stashenko, J.R Martínez, Chapter 8. Study of essential oils obtained from tropical plants grown in Colombia, en: H. El-Shemy (editor), Essential oils: oils of nature, IntechOpen Limited, London, 2019, p. 1-28. Doi: https://doi.org/10.5772/intechopen.87199

57. J. Correa-Royero, V. Tangarife, C. Durán, E. Stashenko, A. Mesa-Arango, *In vitro* antifungal activity and cytotoxic effect of essential oils and extracts of medicinal and aromatic plants against *Candida krusei* and *Aspergillus fumigatus*, *Revista Brasileira de Farmacognosia*, **20**(5), 734-741 (2010). Doi: https://doi.org/10.1590/S0102-695X2010005000021

58. A.L. Bandoni, D. Retta, P.M.D.L. Lira, C.M. van Baren, ¿Son realmente útiles los aceites esenciales?, *Boletin Latinoamericano y del Caribe de Plantas Medicinales y Aromáticas*, **8**(5), 317-322 (2009). URL: https://www.redalyc.org/pdf/856/85611977001.pdf

59. P.S. Costa, E.B. de Souza, E.H. Salles, R.O. dos Santos, Atividade antimicrobiana e potencial terapêutico do gênero *Lippia sensu lato* (Verbenaceae), *Hoehnea*, **44**(2), 158-171 (2017). Doi: https://doi.org/10.1590/2236-8906-68/2016

60. T. Vila, J.A. Romo, C.G. Pierce, S.F. McHardy, S.P. Saville, J.L. Lopez-Ribot, Targeting *Candida albicans* filamentation for antifungal drug development, *Virulence*, **8**(2), 150-158 (2017). Doi: https://doi.org/10.1080/21505594.2016.1197444

61. V.K. Chin, T.Y. Lee, B. Rusliza, P.P. Chong, Dissecting *Candida albicans* infection from the perspective of *C. albicans* virulence and omics approaches on host–pathogen interaction: A review, *Internationl Journal of Molecular Sciences*, **17**(10), 1643 (2016). Doi: https://doi.org/10.3390/ijms17101643

62. R. Pérez-Torrado, A. Querol, Opportunistic strains of *Saccharomyces cerevisiae*: A potential risk sold in food products, *Frontiers in Microbiology*, **6**, 1522 (2016). Doi: https://doi.org/10.3389/fmicb.2015.01522

63. M. Balouiri, M. Sadiki, S.K. Ibnsouda, Methods for *in vitro* evaluating antimicrobial activity: A review, *Journal of Pharmaceutical Analysis*, **6**(2), 71-79 (2016). Doi: https://doi.org/10.1016/j.jpha.2015.11.005

64. L. Scorzoni, F. Sangalli-Leite, J.de Lacorte-Singulani, A.C.A. de Paula e Silva, C.B. Costa-Orlandi, A.M. Fusco-Almeida, M.J.S. Mendes-Giannini, Searching new antifungals: The use of in *vitro* and *in vivo* methods for evaluation of natural compounds, *Journal of Microbiological Methods*, **123**, 68-78 (2016). Doi: https://doi.org/10.1016/j.mimet.2016.02.005

65. N. Vaou, E. Stavropoulou, C. Voidarou, C. Tsigalou, E. Bezirtzoglou, Towards advances in medicinal plant antimicrobial activity: A review study on challenges and future perspectives, *Microorganisms*, **9**(10), 2041 (2021). Doi: https://doi.org/10.3390/microorganisms9102041

66. I. Bautista-Hernández, C.N. Aguilar, G.C.G. Martínez-Ávila, C. Torres-León, A. Ilina, A. C. Flores-Gallegos, D.K. Verma, M.L. Chávez-González, Mexican oregano (*Lippia graveolens* Kunth) as source of bioactive compounds: A review, *Molecules*, **26**(17), 5156 (2021). Doi: https://doi.org/10.3390/molecules26175156

67. N. Jaradat, M. Hawash, M.N. Abualhasan, M. Qadi, M. Ghanim, E. Massarwy, S.A. Ammar, N. Zmero, M. Arar, F. Hussein, L. Issa, A. Mousa, A. Zarour, Spectral characterization, antioxidant, antimicrobial, cytotoxic, and cyclooxygenase inhibitory activities of *Aloysia citriodora* essential oils collected from two Palestinian regions, *BMC Complementary Medicine and Therapies*, **21**, 143 (2021). Doi: https://doi.org/10.1186/s12906-021-03314-1

68. J.d.L. Silva, P.S. Pereira, C.V. Barros-Oliveira, M.A. de Freitas, J.R. de Lima-Silva, A. Rodrigues-Costa, C.D.d.M. Oliveira-Tintino, M.F.B. Morais-Braga, A.E. Duarte, H.D. Melo-Coutinho, L.M. Barros, Study of the capacity of the essential oil of *Lantana montevidensis* to modulate the action of fluconazole on *Candida albicans* and *Candida tropicalis* strains, *Journal of Medical Mycology*, **31**(3), 101171 (2021). Doi: https://doi.org/10.1016/j.mycmed.2021.101171

69. H.Y. Bernal, H. García-Martínez, G.F. Quevedo-Sánchez, *Pautas para el conocimiento, conservación y uso sostenible de las plantas medicinales nativas en Colombia. Estrategia Nacional para la Conservación de Plantas*, Instituto de Investigación de Recursos Biológicos Alexander von Humboldt, Bogotá, 2011, 236 p. URL: http://repository.humboldt.org.co/handle/20.500.11761/31427

70. C.M. Lozano, M.A. Vasquez-Tineo, M. Ramírez, M.I. Infante, *In vitro* antimicrobial activity of tropical medicinal plants used in Santo Domingo, Dominican Republic: Part 2, *Pharmacognosy Communications*, **11**(1), 52-60 (2021). Doi: https://doi.org/10.5530/pc.2021.1.11

Como citar este artículo

L.R. Jaimes-Duarte, S.E. Giraldo-Quintero, J.F. Hoyos-Argote, M.C. Bernal-Lizarazú, Plantas medicinales de la familia Verbenaceae activas frente a hongos levaduriformes: Revisión sistemática y perspectivas 2015-2022, *Rev. Colomb. Cienc. Quim. Farm.*, **53**(2), 306-335 (2024). https://doi.org/10.15446/rcciquifa.v53n2.114423

Artigo de pesquisa cientifica / https://doi.org/10.15446/rcciquifa.v53n2.114424

A descrição teórica da detecção eletroanalítica de resveratrol em vinhos e sucos, assistida pelo oxihidróxido de cobalto

Volodymyr V. Tkach[1,2*], Marta V. Kushnir[1], Nataliia M. Storoshchuk[1], Olga V. Luganska[3], Vira V. Kopiika[3], Nataliia V. Novosad[3], Svitlana M. Lukanova[1], Yana G. Ivanushko[4], Valentyna G. Ostapchuk[4], Svitlana P. Melnychuk[4], Petro I. Yagodynets'[1], Sílvio C. de Oliveira[5], José I. Ferrão de Paiva Martins[2], Isabel O´Neill de Mascarenhas Gaivão[6], Maria João Monteiro[6], Zholt O. Kormosh[7], Jarem R. Garcia[8], Eloi A. da Silva Filho[9], Oksana P. Vitriak[10]

[1]Universidade Nacional de Chernivtsi, 58012,Rua de Kotsyubyns'ky., 2, Chernivtsi, Ucrânia

[2]Faculdade de Engenharia da Universidade do Porto, 4200-465, Rua Dr. Roberto Frias, s/n, Porto, Portugal

[3]Universidade Nacional de Zaporizhzhia, 69600, Rua de Zhukovsky, 66, Zaporizhzhya, Ucrânia

[4]Universidade Estatal de Medicina de Bucovina, 58001, Praça Teatral, 9, Chernivtsi, Ucrânia

[5]Universidade Federal de Mato Grosso do Sul, Av. Sen. Felinto. Müller, 1555, C/P. 549, 79074-460, Campo Grande, MS, Brasil

[6]Universidade de Trás-os-Montes e Alto Douro, Quinta de Prados, 5001-801, Folhadela, Vila Real, Portugal

[7]Universidade Nacional Leste-Europeia, 43000, Av. da Liberdade, 13, Luts'k, Ucrânia

[8]Universidade Estadual de Ponta Grossa, Campus de Uvaranas, Av. Gal. Carlos Cavalcanti, 4748, 84030-900, Ponta Grossa, PR, Brasil

[9]Universidade Federal de Espírito Santo, Av. Fernando Ferrari, 514, 29075-910, Vitória, ES, Brasil

[10]Universidade Nacional de Comércio e Economia de Kiev, 02156, Rua de Quioto, 19, Kiev, Ucrânia

*Correio eletrônico: nightwatcher2401@gmail.com

Recebido: 3 de julho de 2022
Revisado: 20 de fevereiro de 2024
Aceto: 26 de fevereiro de 2024

Resumo

Introdução: A possibilidade da detecção eletroanalítica de resveratrol, assistida pelo oxihidróxido de cobalto e seus compósitos com polímeros condutores tem

sido avaliada do ponto de vista teórico. **Metodologia:** O modelo matemático correspondente tem sido desenvolvido e analisado mediante a teoria de estabilidade linear e análise de bifurcações. **Resultados:** A análise do modelo confirma que o oxihidróxido de cobalto pode servir de uma substância ativa eficaz na detecção eletroanalítica de resveratrol. **Conclusão:** A depender das condições da análise, o processo eletroanalítico pode ser controlado tanto pela difusão como pela cinética do processo. Por outro lado, o comportamento oscilatório também é possível, sendo, ademais, mais provável que nos casos mais simples, haja vista o impacto das etapas químicas e eletroquímica na dupla camada eléctrica.

Palavras-chave: resveratrol, sensor eletroquímico, oxihidróxido de cobalto, polímeros condutores, estado estacionário estável.

Summary

The theoretical description for cobalt oxyhydroxide-assisted resveratrol electrochemical determination in vines and juices

Introduction: The possibility of resveratrol electrochemical determination, assisted by cobalt (III) oxyhydroxide and its composites with conducting polymers has been evaluated from the theoretical point of view. **Methodology:** The correspondent mathematical model has been developed and analyzed by means of the linear stability theory and bifurcation analysis. **Results:** The analysis of the model confirms that the cobalto oxyhydroxide may serve as an efficient electrode modifier for resveratrol electroanalytical determination. **Conclusion:** Depending on the analysis conditions, the electroanalytical process may be either diffusion- or kinetically controlled. On the other hand, the oscillatory behavior is also possible being even more probable than in the simplest cases, due to the impact of the chemical and electrochemical stages on DEL.

Keywords: resveratrol, electrochemical sensor, cobalt oxyhydroxide, conducting polymer, stable steady-state.

Resumen

La descripción teórica de la detección electroanalítica de resveratrol en vinos y jugos, asistida por el oxihidróxido de cobalto

Introducción: La posibilidad de la detección electroanalítica de resveratrol, asistida por el oxihidróxido de cobalto y sus compuestos con polímeros conductores ha sido teóricamente evaluada. **Metodología:** El modelo matemático correspondiente ha sido desarrollado y analizado mediante la teoría de estabilidad lineal y análisis de bifurcaciones. **Resultados:** El análisis del modelo confirma que el oxihidróxido de cobalto puede ser eficaz en la detección electroanalítica de resveratrol. **Conclusión:** Dependiendo de las condiciones de análisis, el proceso electroanalítico puede ser controlado tanto por la difusión como por la cinética del proceso. Por otro lado, el comportamiento oscilatorio también es posible, siendo, además, más probable que en los casos más simples, visto el impacto de las etapas químicas y la electroquímica en la doble capa eléctrica.

Palabras-clave: resveratrol, sensor electroquímico, oxihidróxido de cobalto, polímeros conductores, estado estacionario estable.

Introdução

O resveratrol, ou seja (E)-5-(4-hidroxiestiril) benzen-1,3-diol ou 3,4,5-trihidroxiestilbeno (M = 228,23 g·mol^{-1}, CAS RN: 501-306-0, Fig. 1) é o principal composto polifenólico do vinho tinto e do suco e uva *(Vitis vinífera)* e o seu antioxidante mais importante [1-4]. Outra fonte ainda maior de resveratrol é uma hortaliça chamada azeda. Quanto mais intensa é a cor do vinho ou suco, tanto mais resveratrol ele possui.

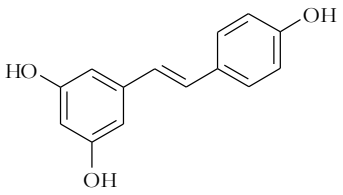

Figura 1. Resveratrol

A biossíntese de resveratrol dá-se a partir do aminoácido essencial fenilalanina, codificando-se pelos genes *TAL, C4H* e *STS*. Na primeira etapa, a fenilalanina fica

desaminada pela ensima fenilalaninamonioliase (PAL), transformando-se no ácido *trans*-cinâmico. Este, posteriormente, serve de substrato para as enzimas cinamato--4-hidroxilase (C4H) e é convertido no ácido *p*-cumárico, que é convertido pelo 4CL em *p*-cumaroil-CoA, que é condensado com três unidades de malonil-CoA (uma interação sequencial, assistida pela enzima STS, codificada pelo gene *STS),* o que produz resveratrol.

O resveratrol desempenha papel de antioxidante, favorece a formação, no fígado, de HDL e a redução de LDL, desentope, destarte, os vasos sanguíneos e contribui na prevenção de doenças cardiovasculares. Na própria produção de vinhos e cervejas [5, 6] o resveratrol também é importante, pois prolonga a vida das leveduras, cujo metabolismo transforma a glicose em álcool etílico, conforme a reação famosa (1):

$$C_6H_{12}O_6 \rightarrow 2C_2H_5OH + 2CO_2 \qquad (1),$$

aumentando o teor alcoólico em vinhos. Assim, a concentração do etanol em vinhos depende da sua idade e o resveratrol, prorrogando a longevidade das leveduras, promove o aumento do teor alcoólico no vinho "maduro".

Por outro lado, o estudo dos efeitos das concentrações excessivas de resveratrol ainda não tem sido concluído, o que pode servir de advertência [7, 8] sobre o risco das concentrações altas de resveratrol para consumo humano. Assim, o desenvolvimento de um método de quantificação eficaz de resveratrol é realmente atual [9-12], e os métodos eletroquímicos podem servir de ótima resposta a este desafio [13-15], por serem rápidos, baratos e precisos.

Possuindo grupos hidroxila fenólicos, além dos fragmentos aromáticos e ligação dupla, o resveratrol pode ser facilmente oxidado. Outrossim, visto que a eletropolimerização de vários compostos polifenólicos, incluindo catecol, resorcinol, ácido gálico e floroglucinol já tem sido feita nos cinco últimos anos [16-20], o resveratrol também poderia ser eletropolimerizado, com vistas à formação de um material sensível a analitos, que se oxidam mediante a transferência de prótons e com propriedades eletrocatalíticas e eletroanalíticas.

Um dos problemas da maioria dos processos eletroanalíticos, que é a sobretensão, pode ser resolvido pelo uso dos elétrodos quimicamente modificados (EQM), cujo modificador, além de reduzir a sobretensão, aumenta a afinidade entre o eléctrodo e o analito, o que providencia a maior seletividade da detecção. Dentre os modificadores de elétrodos para compostos (poli)fenólicos destacam-se os polímeros condutores [21-24],

materiais de carbono [25-28], óxidos de metais e derivados [29-32]. Existe também um processo eletroanalítico, baseado na incorporação de um fragmento da casca de banana [33, 34], que, contendo enzimas específicas, oxida hidroquinonas em quinonas.

Neste caso, um dos modificadores de eléctrodo plausíveis para a detecção eletroanalítica do resveratrol pode ser o oxihidróxido de cobalto [35, 36], material semicondutor, frequentemente usado nos aparelhos semicondutores como substituição para o dióxido de titânio, porém, ao contrário deste, é eletroquimicamente ativo. Ele, sozinho ou em compósito com polímeros condutores [37-40], podia ter um desempenho eficiente como modificador de elétrodo para a detecção da nereistoxina.

No entretanto, o seu uso poderia acarretar uma influência comportamental, nociva à estabilidade do sistema e à sua eficiência eletroanalítica [41-44]. Destarte, o uso prático deste sistema eletroanalítico não pode ser realizado sem uma descrição teórica prévia do comportamento do sistema, o que se faz neste trabalho.

Assim, neste trabalho, pela primeira vez, faz-se uma análise comportamental do sistema eletroanalítico da detecção eletroquímica do resveratrol sobre o oxihidróxido de cobalto, estabilizado pelo polímero condutor. A análise comportamental do sistema eletroanalítico faz-se mediante o desenvolvimento e a análise do modelo correspondente. Com isto também se faz a comparação do comportamento do sistema eletroanalítico com o dos semelhantes [45-48].

O sistema e o seu modelo

Para o resveratrol, a depender do potencial aplicado, são possíveis três possibilidade de eletrooxidação:

- Reação de Wagner, rendendo um derivado substituído de etilenglicol, que, posteriormente se oxida;
- Incorporação de uma hidroxila no sítio mais eletrofílico na unidade aromática do resorcinol com a formação de um derivado do ácido gálico e a oxidação ulterior para a quinona correspondente ou um composto semelhante;
- Eletropolimerização, rendendo um composto macromolecular.

Esquematicamente, o processo eletroanalítico poder-se-á expor conforme na Fig. 2:

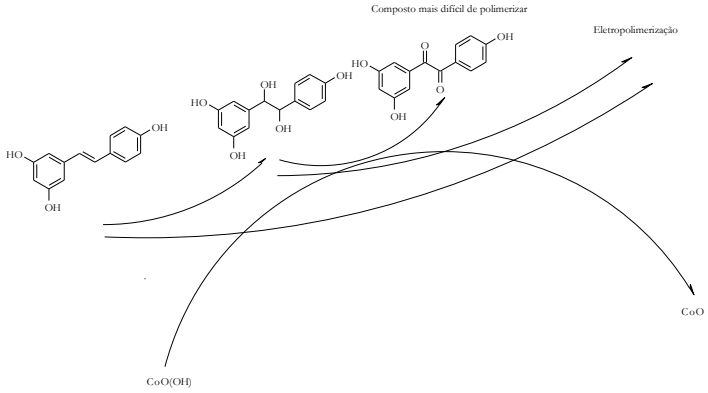

Figura 2. Oxidação gradual de resveratrol pela reação de Wagner

ou Fig. 3:

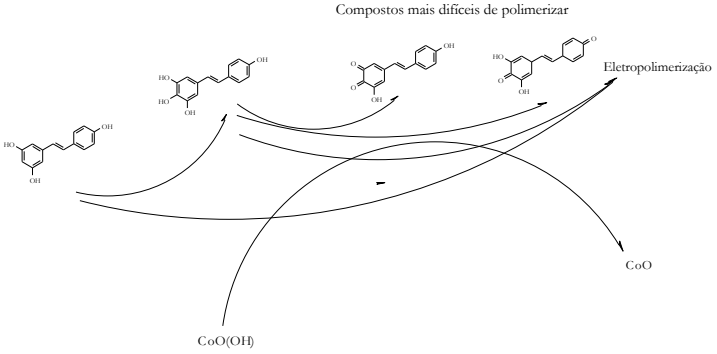

Figura 3. Oxidação gradual de resveratrol pelo derivado do ácido gálico

Como a reação de Wagner requer condições específicas para a realização, os processos, descritos na Fig. 2 e 3 se realizam em condições diferentes, e isto se reflete não só na cinética do processo eletroanalítico, mas também na condição diferencial e, por conseguinte, nas propriedades do polímero (aliás, do copolímero do resveratrol com um dos seus produtos de oxidação) resultantes. O modelo, correspondente à cinética da reação de Wagner será descrito e analisado num dos nossos próximos trabalhos. Neste trabalho descrever-se-á a eletrooxidação pelo derivado do ácido gálico. De qualquer modo, o comportamento em ambos os casos será semelhante.

Considerando os processos, descritos na Fig. 3, para descrever o compostamento do sistema eletroanalítico introduzimos três variáveis:

ρ – a concentração do resveratrol na camada pré-superficial;

ρ^* - a concentração do produto de oxidação micromolecular na camada pré-superficial;

c – o grau de recobrimento da matriz polimérica pelo óxido de cobalto.

Considerando as suposições, aceitas em [46 – 48], descrevemos o comportamento do sistema eletroanalítico pelo conjunto de três equações de balanço (2):

$$\begin{cases} \frac{d\rho}{dt} = \frac{2}{\delta}\left(\frac{\Delta}{\delta}(\rho_0 - \rho) - r_{31} - r_p\right) \\ \frac{d\rho*}{dt} = \frac{2}{\delta}\left(r_{31} - r_{32} - r_{33} - r_{34} - r_p\right) \\ \frac{dc}{dt} = \frac{1}{C}(r_{31} + r_{32} + r_{33} + r_{34} + r_p - r_o) \end{cases} \quad (2)$$

Sendo Δ o coeficiente de difusão, p_0 a concentração do resveratrol no interior da solução, C a concentração superficial máxima do óxido de cobalto na matriz polimérica e os parâmetros r são velocidades de reações correspondentes, que se podem calcular como:

$$r_{31} = k_{31}\rho(1 - c)^2 \exp(-\alpha\rho) \quad (3)$$

$$r_{32} = k_{32}\rho*(1 - c)^2 \exp(-\beta\rho*) \quad (4)$$

$$r_{33} = k_{33}\rho*(1 - c)^2 \exp(-\beta\rho*) \quad (5)$$

$$r_{34} = k_{34}\rho*(1 - c)^2 \exp(-\beta\rho*) \quad (6)$$

$$r_p = k_p\rho^x\rho*^y (1 - c)^w \exp(-\alpha\rho) \exp(-\beta\rho*) \quad (7)$$

$$r_o = k_o c \exp\left(\frac{F\varphi_0}{RT}\right) \quad (8)$$

Em que os parâmetros k são constantes de velocidades das respectivas reações, α e β são parâmetros, que relacionam a cinética das etapas químicas com as propriedades eletrofísicas da DCE, x, y e w são ordens de cada um dos componentes da reação da eletropolimerização, F é o número de Faraday, φ é o salto do potencial, relativo ao potencial da carga zero, R é a constante universal de gases e T é temperatura absoluta do vaso.

O comportamento do sistema com a detecção eletroanalítica de resveratrol sobre o ânodo, modificado pelo oxihidróxido de cobalto é mais complexo que em sistemas semelhantes. O comportamento oscilatório é muito mais provável. Entretanto, o processo eletroanalítico da detecção de resveratrol pode ser feito eficazmente sobre o oxihidróxido de cobalto, conforme descrito abaixo.

Resultados e discussão

Para investigar o comportamento do sistema com a detecção eletroanalítica do resveratrol, analisamos o conjunto de equações diferenciais de balanço (2) mediante a teoria de estabilidade linear. Os elementos estacionários da matriz Jacobiana podem ser expostos como (9):

$$\begin{pmatrix} a_{11} & a_{12} & a_{13} \\ a_{21} & a_{22} & a_{23} \\ a_{31} & a_{32} & a_{33} \end{pmatrix} \tag{9}$$

Sendo:

$$a_{11} = \frac{2}{\delta}\Big(-\frac{A}{\delta} - k_{31}(1-c)^2\exp(-\alpha\rho) + \alpha k_{31}\rho(1-c)^2\exp(-\alpha\rho) - xk_p\rho^{x-1}\rho_*^{\,y}(1-c)^w\exp(-\alpha\rho)\exp(-\beta\rho_*) + \alpha k_p\rho^x\rho_*^{\,y}(1-c)^w\exp(-\alpha\rho)\exp(-\beta\rho_*)\Big) \tag{10}$$

$$a_{12} = \frac{2}{\delta}\Big(-yk_p\rho^x\rho_*^{\,y-1}(1-c)^w\exp(-\alpha\rho)\exp(-\beta\rho_*) + \beta k_p\rho^x\rho_*^{\,y}(1-c)^w\exp(-\alpha\rho)\exp(-\beta\rho_*)\Big) \tag{11}$$

$$a_{13} = \frac{2}{\delta}\big(2k_{31}\rho(1-c)\exp(-\alpha\rho) + wk_p\rho^x\rho_*^{\,y}(1-c)^{w-1}\exp(-\alpha\rho)\exp(-\beta\rho_*)\big) \tag{12}$$

$$a_{21} = \frac{2}{\delta}\big(k_{31}(1-c)^2\exp(-\alpha\rho) - \alpha k_{31}\rho(1-c)^2\exp(-\alpha\rho) - xk_p\rho^{x-1}\rho_*^{\,y}(1-c)^w\exp(-\alpha\rho)\exp(-\beta\rho_*) + \alpha k_p\rho^x\rho_*^{\,y}(1-c)^w\exp(-\alpha\rho)\exp(-\beta\rho_*)\big) \tag{13}$$

$$a_{22} = \frac{2}{\delta}\big(-k_{32}(1-c)^2\exp(-\beta\rho_*) + \beta k_{32}\rho_*(1-c)^2\exp(-\beta\rho_*) - k_{33}(1-c)^2\exp(-\beta\rho_*) + \beta k_{33}\rho_*(1-c)^2\exp(-\beta\rho_*) - k_{34}(1-c)^2\exp(-\beta\rho_*) + \beta k_{34}\rho_*(1-c)^2\exp(-\beta\rho_*) - yk_p\rho^x\rho_*^{\,y-1}(1-c)^w\exp(-\alpha\rho)\exp(-\beta\rho_*) + \beta k_p\rho^x\rho_*^{\,y}(1-c)^w\exp(-\alpha\rho)\exp(-\beta\rho_*)\big) \tag{14}$$

$$a_{23} = \frac{2}{\delta}\big(-2k_{31}\rho(1-c)\exp(-\alpha\rho) + 2k_{32}\rho_*(1-c)\exp(-\beta\rho_*) + 2k_{33}\rho_*(1-c)\exp(-\beta\rho_*) + 2k_{34}\rho_*(1-c)\exp(-\beta\rho_*) + wk_p\rho^x\rho_*^{\,y}(1-c)^{w-1}\exp(-\alpha\rho)\exp(-\beta\rho_*)\big) \tag{15}$$

$$a_{31} = \frac{1}{C}\big(k_{31}(1-c)^2\exp(-\alpha\rho) - \alpha k_{31}\rho(1-c)^2\exp(-\alpha\rho) + xk_p\rho^{x-1}\rho *^{y} (1-c)^{w}\exp(-\alpha\rho)\exp(-\beta\rho *) - \alpha k_p\rho^{x}\rho *^{y}(1-c)^{w}\exp(-\alpha\rho)\exp(-\beta\rho *)\big) \quad (16)$$

$$a_{32} = \frac{1}{C}\big(k_{32}(1-c)^2\exp(-\beta\rho *) - \beta k_{32}\rho *(1-c)^2\exp(-\beta\rho *) + k_{33}(1-c)^2\exp(-\beta\rho *) - \beta k_{33}\rho *(1-c)^2\exp(-\beta\rho *) + k_{34}(1-c)^2\exp(-\beta\rho *) - \beta k_{34}\rho *(1-c)^2\exp(-\beta\rho *) + yk_p\rho^{x}\rho *^{y-1}(1-c)^{w}\exp(-\alpha\rho)\exp(-\beta\rho *) - \beta k_p\rho^{x}\rho *^{y}(1-c)^{w}\exp(-\alpha\rho)\exp(-\beta\rho *)\big) \quad (17)$$

$$a_{33} = \frac{1}{C}\Big(-2k_{31}\rho(1-c)\exp(-\alpha\rho) - 2k_{32}\rho *(1-c)\exp(-\beta\rho *) - 2k_{33}\rho *(1-c)\exp(-\beta\rho *) - 2k_{34}\rho *(1-c)\exp(-\beta\rho *) - wk_p\rho^{x}\rho *^{y}(1-c)^{w-1}\exp(-\alpha\rho)\exp(-\beta\rho *) - k_o\exp\left(\frac{F\varphi_0}{RT}\right) + jk_oc\exp\left(\frac{F\varphi_0}{RT}\right)\Big) \quad (18)$$

O comportamento oscilatório é passível de realizar, desde que sejam satisfeitas as condições da bifurcação de Hopf. A sua condição necessária é a presença dos elementos positivos na diagonal principal da matriz Jacobiana (a formada pelos elementos (10), (14) e (18)). Como se vê, o comportamento oscilatório é ainda mais provável neste sistema que nos semelhantes [45-48], por haver mais de um elemento, que pode ter valores positivos.

Como foi mencionado na seção anterior, a estrutura da DCE está alterada não só durante a etapa eletroquímica, mas também aquando das etapas químicas, que causam alterações estruturais na composição química da DCE. Essas inbfluências, por conseguinte, se refletem nas propriedades eletrofísicas e eletroquímicas da camada. Isto se manifesta sob a forma do comportamento oscilatório. Estes elementos positivos são:

$jk_oc\exp\left(\frac{F\varphi_0}{RT}\right) > 0$, se j>0, que descreve as influências cíclicas da etapa eletroquímica, ou seja, da oxidação do óxido de cobalto, que regenera o oxihidróxido de cobalto, na DCE e: $\alpha k_{31}\rho(1-c)^2\exp(-\alpha\rho) > 0$, $\alpha k_p\rho^{x}\rho *^{y}(1-c)^{w}$, $\beta(k_{32}+k_{33}+k_{34})(1-c)^2 *\exp(-\beta\rho *) > 0$, $\beta k_p\rho^{x}\rho *^{y}(1-c)^{w} * \exp(-\alpha\rho)\exp(-\beta\rho *) > 0$, se α,β>0, que descrevem as influências das etapas químicas nas capacitâncias da DCE, que também podem ser responsáveis pelo comportamento oscilatório. No entretanto, a realização de todas essas influências desestabilizadoras na dupla camada dar-se-á nos valores paramétricos, afastados do limite de detecção, o que se mostrará abaixo.

Para investigar a estabilidade do estado estacionário, aplicamos ao conjunto de equações diferenciais (1 – 4) o critério Routh-Hurwitz. Evitando as expressões grandes, introduzimos as novas variáveis, reescrevendo o determinante conforme (19):

$$\frac{4}{\delta^2 C}\begin{vmatrix} -\kappa - \Xi - \Lambda & -P & \Phi \\ \Xi - \Lambda & P - \Sigma & -\Phi + A \\ \Xi + \Lambda & P + \Sigma & -\Phi - A - \Omega \end{vmatrix} \quad (19)$$

Segundo as propiedades do determinante, a expressão (19) pode ser rearranjada conforme (20):

$$\frac{4}{\delta^2 C}\begin{vmatrix} -\kappa-\Xi-\Lambda & -P & \Phi \\ \Xi-\Lambda & P-\Sigma & -\Phi+A \\ \Xi+\Lambda & P+\Sigma & -\Phi-A-\Omega \end{vmatrix} \sim \frac{4}{\delta^2 C}\begin{vmatrix} -\kappa-\Xi-\Lambda & -P & \Phi \\ 2\Xi & 2P & -2\Phi-\Omega \\ \Xi+\Lambda & P+\Sigma & -\Phi-A-\Omega \end{vmatrix} \sim \frac{4}{\delta^2 C}\begin{vmatrix} -\kappa-\Lambda & 0 & -\frac{\Omega}{2} \\ 2\Xi & 2P & -2\Phi-\Omega \\ \Xi+\Lambda & P+\Sigma & -\Phi-A-\Omega \end{vmatrix} \tag{20}$$

Abrindo os parênteses retos e aplicando o critério Det J<0, saliente do critério, e trocando os signos pelos opostos, obtemos o requisito de estabilidade do estado estacionário, escrito conforme (21):

$$\Xi(\Omega P+\Omega\Sigma)-2P(\kappa\Phi+\kappa A+\kappa\Omega+\Xi A+K\Omega+\Lambda A+\Lambda\Omega)+(2\Phi-\Omega)(\kappa P+\Lambda P+\kappa\Sigma+\Lambda\Sigma)>0 \tag{21}$$

Ou então (22):

$$\Xi(\Omega P+\Omega\Sigma)+(2\Phi+\Omega)(\kappa P+\Lambda P+\kappa\Sigma+\Lambda\Sigma)>2P(\kappa\Phi+\kappa A+\kappa\Omega+\Xi A+K\Omega+\Lambda A+\Lambda\Omega) \tag{22}$$

E representará um processo eletroanaliticamente eficiente, controlado tanto pela difusão do analito, como pela cinética do processo, com a prevalência do segundo fator. Isto se realiza, mantendo-se positivos os valores dos parâmetros das etapas químicas e eletroquímica Ξ, Σ, Λ, Ω e P. Deveras, se se supuser que todos os mencionados parâmetros têm valores positivos, ver-se-á que o lado esquerdo da inequação (22) terá valores mais positivos e maiores que a do lado direito. Havendo vista que os estados estacionários instáveis se consideram deviações dos estáveis, assim como a representação exponencial dessas deviações, que, nas inequações (21 – 22) se descrevem pelos signos opostos, o estado estacionário é considerado estabilizado.

Haja vista o serem usadas as condições de pH, correspondentes ao meio neutro ou levemente básico, a estabilidade do analito, das suas formas ionizadas e do oxihidróxido de cobalto não é comprometida em reações laterais. Assim, o estado estacionário estável é eletroanaliticamente eficiente, o que corresponde à linearidade da dependência entre a concentração do analito e o parâmetro eletroquímico (neste caso, corrente).

A condição da instabilidade monotônica, relativa ao limite de detecção, para este sistema descreve-se conforme:

$$\Xi(\Omega P+\Omega\Sigma)+(2\Phi+\Omega)(\kappa P+\Lambda P+\kappa\Sigma+\Lambda\Sigma)=2P(\kappa\Phi+\kappa A+\kappa\Omega+\Xi A+K\Omega+\Lambda A+\Lambda\Omega) \tag{23}$$

realizando-se, neste ponto, a igualdade das influências estabilizadoras a desestabilizadoras.

O corante esquaraínico pode ser usado na fase orgânica do material compósito como oligômero com propriedades (semi)condutoras [49]. Ele pode ser tanto sozinho como monômero ou dopante do polímero condutor. A sua função não se limita à mediação de transferência de elétrons, mas também à estabilização do oxihidróxido de cobalto, mediante a formação das ligações de coordenação (Fig. 4):

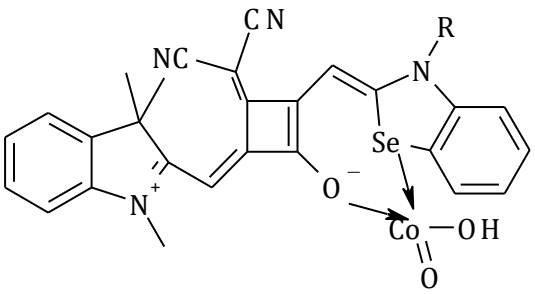

Figura 4. Coordenação do corante com o oxihidróxido de cobalto

A presença de outros substituintes, assim como do nitrogênio piridínico, aumentará a possibilidade da formação de compostos de coordenação de outra configuração. Isto também contribuirá para o desempenho eletroanalítico do sensor.

Conclusões

Da análise do comportamento do sistema eletroanalítico, baseado em oxihidróxido de cobalto na detecção eletroquímica do resveratrol nas condições da oxidação "hidroquinônica", pode-se concluir que:

- o oxihidróxido de cobalto pode ser um modificador eficiente na determinação do resveratrol no ânodo. Realiza-se a formação de um derivado do ácido gálico, que, posteriormente, se oxida. O cenário da eletropolimerização assistida também não é descartável. A reversibilidade de CoO(OH) obtém-se na etapa eletroquímica;
- o processo eletroanalítico é eficiente e controlado maioritariamente pela cinética do processo, minoritariamente pela difusão do analito;
- o comportamento oscilatório neste sistema é mais provável que nos semelhantes, haja vista o existirem mais processos a influenciarem a dupla camada elétrica e as suas capacitâncias. A realização deste tipo de comportamento obtém-se quando os valores dos parâmetros estão além do limite de detecção.

Nota de agradecimento

Volodymyr V. Tkach agradece à Faculdade de Engenharia da Universidade do Porto e à Universidade de Trás-os-Montes e Alto Douro o seu apoio nos tempos difíceis para a Ucrânia e a sua ciência.

Conflitos de interesse

Os autores não têm conflitos de interesse a declarar.

Referências

1. G.d.N. Barbosa de Souza, J.C.d. Sales-Ferreira, Efeitos do resveratrol nas células cancerígenas, *Research, Society and Development*, **11**(6), e3711628841 (2022). Doi: https://doi.org/10.33448/rsd-v11i6.28841

2. Y. Bian, X. Wang, Z. Zheng, G. Ren, H. Zhu, M. Qiao, G. Li, Resveratrol drives cancer cell senescence via enhancing p38MAPK and DLC1 expressions, *Food & Function*, **13**(6), 3283-3293 (2022). Doi: https://doi.org/10.1039/d1fo02365a

3. R. Haunschild, W. Marx, On health effects of resveratrol in wine, *International Journal of Environmental Research and Public Health*, **19**(5), 3110 (2022). Doi: https://doi.org/10.3390/ijerph19053110

4. M. Mikolajkova, N. Ladicka, M. Janusova, K. Ondrova, H.K. Mikulaskova, D. Dordevic, Resveratrol content in wine – resveratrol biochemical properties, *MASO International – Journal of Food Science and Technology*, **11**, 31-38 (2021). Doi: https://doi.org/10.2478/mjfst-2022-0005

5. R. Vejarano, M. Luján-Corro, Red wine and health: Approaches to improve the phenolic content during winemaking, *Frontiers in Nutrition*, **9**, e809066 (2022). Doi: https://doi.org/10.3389/fnut.2022.890066

6. M. Naiker, S. Anderson, J.B. Johnson, J.S. Mani, L. Wakeling, V. Bowry, Loss of *trans*-resveratrol during storage and ageing of red wines, *Australian Journal of Grape and Wine Research*, **26**(4), 385-387 (2020). Doi: https://doi.org/10.1111/ajgw.12449

7. F. Hajizadeh-Sharafabad, A. Sahebkar, F. Zabetiah-Targhi, V. Maleki, The impact of resveratrol on toxicity and related complications of advanced glycation end products: A systematic review, *BioFactors*, **45**(5), 651-665 (2019). Doi: https://doi.org/10.1002/biof.1531

8. A. Shaito, A.M. Posadino, N. Younes, H. Hasan, S. Halabi, D. Alhababi, A. Al-Mohannadi, W.M. Abdel-Rahman, A.H. Eid, G.K. Nasrallah, G. Pintus, Potential adverse effects of resveratrol: A literature review, *International Journal of Molecular Sciences*, **21**(6), 2084 (2020). Doi: https://doi.org/10.3390%2Fijms21062084

9. Z.S. Erdemir Tıraş, H.H. Okur, Z. Günay, H.K. Yıldırım, Different approaches to enhance resveratrol content in wine, *Ciência e Técnica Vitivinícola*, **37**(1), 13-28 (2022). Doi: https://doi.org/10.1051/ctv/ctv20223701013

10. A.L. Crăciun, G. Gutt, Study on kinetics of trans-resveratrol, total phenolic content, and antioxidant activity increase in vine waste during post-pruning storage, *Applied Sciences*, **12**(3), 1450 (2022). Doi: https://doi.org/10.3390/app12031450

11. I. Bononi, P. Tedeschi, V. Mantovani, A. Maietti, E. Mazzoni, C. Pancaldi, V. Brandolini, M. Tognon, Antioxidant activity of resveratrol diastereomeric forms assayed in fluorescent-engineered human keratinocytes, *Antioxidants*, **11**(2), 196 (2022). Doi: https://doi.org/10.3390/antiox11020196

12. W. Wu, K. Li, C. Zhao, X. Ran, Y. Zhang, T. Zhang, Rapid HPLC-MS/MS method for the simultaneous determination of luteolin, resveratrol and their metabolites in rat plasma and its application to pharmacokinetic interaction studies, *Journal of Chromatography B*, **1191**, 123118 (2022). Doi: https://doi.org/10.1016/j.jchromb.2022.123118

13. R.S. Klein, M.M. Taniguchi, P.D. Dos Santos, E.G. Bonafe, A.F. Martins, J.P. Monteiro, Trans-resveratrol electrochemical detection using portable device based on unmodified screen-printed electrode, *Journal of Pharmaceutical and Biomedical Analysis*, **207**, 114399 (2022). Doi: https://doi.org/10.1016/j.jpba.2021.114399

14. I.G. Munteanu, C. Apetrei, A review on electrochemical sensors and biosensors used in assessing antioxidant activity, *Antioxidants*, **11**(3), 584 (2022). Doi: https://doi.org/10.3390/antiox11030584

15. Ö. Güngör, C.B.A. Hassine, M. Burç, S.T. Duran, Voltammetric determination of resveratrol using poly(l-phenylalanine)-modified gold electrode, *Macedonian Journal of Chemistry and Chemical Engineering*, **39**(2), 177 (2020). Doi: https://doi.org/10.20450/mjcce.2020.2073

16. R. Pourghobadi, D. Nematollahi, M.R. Baezzat, S. Alizadeh, H. Goljani, Electropolymerization of catechol on wireless graphite electrode. Unusual cathodic polycatechol formation, *Journal of Electroanalytical Chemistry*, **866**, 114180 (2020). Doi: https://doi.org/10.1016/j.jelechem.2020.114180

17. A.M. Gavrila, E.B. Stoica, T.V. Iordache, A. Sarbu, Modern and dedicated methods for producing molecularly imprinted polymer layers in sensing applications, *Applied Sciences*, **12**(6), 3080 (2022). Doi: https://doi.org/10.3390/app12063080

18. G. Ziyatdinova, E. Guss, E. Yakupova, Electrochemical sensors based on the electropolymerized natural phenolic antioxidants and their analytical application, *Sensors*, **21**(24), 8385 (2021). Doi: https://doi.org/10.3390/s21248385

19. C. White, *Electropolymerization and Characterization of Thin Film Dielectrics*, M. Sc. Thesis, University of Nebraska, Lincoln, Nebraska, 2019. URL: https://digitalcommons.unl.edu/cgi/viewcontent.cgi?article=1102&context=chemistrydiss

20. M. Bonechi, M. Innocenti, D. Vanossi, C. Fontanesi, The fundamental and underrated role of the base electrolyte in the polymerization mechanism. The resorcinol case study, *Journal of Physical Chemistry A*, **125**(1), 34-42 (2021). Doi: https://doi.org/10.1021/acs.jpca.0c07702

21. K.-l. Song, R. Li, K. Li, H. Yu, Simultaneous determination of dihydroxybenzene isomers using a three-dimensional over-oxidized polypyrrole–reduced graphene oxide composite film electrode prepared by an electrochemical method, *New Journal of Chemistry*, **44**, 20294-20302 (2020). Doi: https://doi.org/10.1039/d0nj01613f

22. L. Ji, Q. Wang, L. Peng, X. Li, X. Zhu, P. Hu, Cu-TCPP nanosheets-sensitized electrode for simultaneous determination of hydroquinone and catechol, *Materials*, **15**(13), 4625 (2022). Doi: https://doi.org/10.3390/ma15134625

23. Z. Khalifa, K. Hassan, M.F.A. Oura, A. Hathoot, M.A. Azzem, Individual and simultaneous voltammetric determination of ultratrace environmental contaminant dihydroxybenzene isomers based on a composite electrode sandwich-like structure, *ACS Omega*, **5**(30), 18950-18957 (2020). Doi: https://doi.org/10.1021/acsomega.0c02228

24. J. Zuo, Y. Shen, J. Gao, H. Song, Z. Ye, Y. Liang, S. Zhang, Highly sensitive determination of paracetamol, uric acid, dopamine, and catechol based on flexible plastic electrochemical sensors, *Analytical and Bioanalytical Chemistry*, **414**, 5917-5928 (2022). Doi: https://doi.org/10.1007/s00216-022-04157-6

25. S. Xue, K. Wang, Y. Cheng, B. Tu, Y. Xia, S. Yuan, H. Tao, Simultaneous determination of catechol and hydroquinone with L-cysteine and nickel cobaltite Co-functionalised graphene oxide modified glassy carbon electrode, *International Journal of Environmental Analytical Chemistry*, **103**(4), 899-914 (2023). Doi: https://doi.org/10.1080/03067319.2020.1865330

26. M. Yang, H. Guo, L. Sun, N. Wu, M. Wang, F. Yang, T. Zhang, J. Zhang, Z. Pan, W. Yang, Simultaneous electrochemical detection of hydroquinone and catechol using MWCNT-COOH/CTF-1 composite modified electrode, *Colloids and Surfaces A: Physicochemical and Engineering Aspects*, **625**, 126917 (2021). Doi: https://doi.org/10.1016/j.colsurfa.2021.126917

27. M.M. Rao, R. Settu, Sh.-M. Chen, P. Alagarsamy, T.-W. Chen, I.-S. Hong, Electrochemical determination of catechol using functionalized multiwalled carbon nanotubes modified screen printed carbon electrode, *International Journal of Electrochemical Science*, **13**(6), 6126-6134 (2018). https://doi.org/10.20964/2018.06.121

28. S. Piña, Ch. Candia-Onofray, N. Hassan, P. Jara-Ulloa, D. Contreras, R. Salazar, Glassy carbon electrode modified with C/Au nanostructured materials for simultaneous determination of hydroquinone and catechol in water matrices, *Chemosensors*, **9**(5), 88 (2021). Doi: https://doi.org/10.3390/chemosensors9050088

29. B. Dalkiran, C. Brett, Poly(safranine T)-deep eutectic solvent/copper oxide nanoparticle-carbon nanotube nanocomposite modified electrode and its application to the simultaneous determination of hydroquinone and catechol, *Microchemical Journal*, **179**, 107531 (2022). Doi: https://doi.org/10.1016/j.microc.2022.107531

30. I. Maor, S. Asadi, S. Korganbayev, D. Dahis, Y. Shamay, E. Schena, H. Azhari, P. Saccomandi, I.S. Weitz, Laser-induced thermal response and controlled release of copper oxide nanoparticles from multifunctional polymeric nanocarriers, *Science and Technology of Advanced Materials*, **22**(1), 218-233 (2021). Doi: https://doi.org/10.1080/14686996.2021.1883406

31. M.A. Sheikh-Mohseny, S. Pirsa, Simultaneous determination of dopamine and acetaminophen by a carbon paste electrode doubly modified with poly (pyrrole) and CuO nanoparticles, *Analytical & Bioanalytical Electrochemistry*, **8**(6), 777-789 (2016). URL: http://abechem.ir/No.%206-2016/2016,%208(6),%20777-789.pdf

32. E. Fazio, S. Spadaro, C. Corsaro, G. Neri, S.G. Leonardi, F. Neri, N. Lavanya, C. Sekar, N. Donato, G. Neri, Metal-oxide based nanomaterials: Synthesis, characterization and their applications in electrical and electrochemical sensors, *Sensors*, **21**(7), 2494 (2021). Doi: https://doi.org/10.3390/s21072494

33. Zs. Őri, A. Kiss, A.A. Ciucu, C. Mihailciuc, C.D. Stefanescu, L. Nagy, G. Nagy, Sensitivity enhancement of a "bananatrode" biosensor for dopamine based on SECM studies inside its reaction layer, *Sensors and Actuators B: Chemical*, **190**, 149-156 (2014). Doi: https://doi.org/10.1016/j.snb.2013.08.063

34. G. Selvollini, C. Lazzarini G. Marazza, Electrochemical composite single use sensor for dopamine detection, *Sensors*, **19**(14), 3097 (2019). Doi: https://doi.org/10.3390/s19143097

35. N. Stasiuk, O. Smutok, O. Demkiv, T. Prokopiv, G. Gayda, M. Nisnevitch, M. Gonchar, Synthesis, catalytic properties and application in biosensorics of nanozymes and electronanocatalysts: A review, *Sensors*, **20**(16), 4509 (2020). Doi: https://doi.org/10.3390/s20164509

36. Y. Zou, J. Chen, Q. Chai, T. Zhu, S. Zeng, Y. Liu, Stimuli-responsive colorimetric sensor based on bifunctional pyrophosphate-triggered controlled release and enhancing activity of CoOOH nanozyme, *Sensors and Actuators B: Chemical*, **369**, 132215 (2022). Doi: https://doi.org/10.1016/j.snb.2022.132215

37. Garima, G.A. Sachdev, I. Matai, An electrochemical sensor based on cobalt oxyhydroxide nanoflakes/reduced graphene oxide nanocomposite for detection of illicit drug clonazepam, *Journal of Electroanalytical Chemistry*, **919**, 116537 (2022). Doi: https://doi.org/10.1016/j.jelechem.2022.116537

38. K. Tyszczuk-Rotko, J. Kozak, B. Czech, Screen-printed voltammetric sensors—Tools for environmental water monitoring of painkillers, *Sensors*, **22**(7), 2437 (2022). Doi: https://doi.org/10.3390/s22072437

39. G. Balkourani, Th. Damartzis, A. Brouzgou, P. Tsiakaras, Cost effective synthesis of graphene nanomaterials for non-enzymatic electrochemical sensors for glucose: A comprehensive review, *Sensors*, **22**(1), 355 (2022). Doi: https://doi.org/10.3390/s22010355

40. J. Li, Z-P. Li, Y-F. Bai, S.-X. Luo, Y. Guo, Y.-Y. Bao, R. Li, H.-Y. Liu, F. Feng, A flexible enzymeless glucose sensor via electrodepositing 3D flower-like CoS onto self-supporting graphene tape electrode, *Journal of Electrochemistry*, **28**(1), 2104211 (2022). URL: https://jelectrochem.xmu.edu.cn/cgi/viewcontent.cgi?article=1169&context=journal

41. I. Das, N.R. Agrawal, S.A. Ansari, S.K. Gupta, Pattern formation and oscillatory electropolymerization of thiophene, *Indian Journal of Chemistry*, **47**A, 1798-1803 (2008). URL: https://nopr.niscpr.res.in/bitstream/123456789/2565/1/IJCA%2047A(12)%201798-1803.pdf

42. K. Aoki, I. Mukoyama, J. Chen., Competition between polymerization and dissolution of poly(3-methylthiophene) films, *Russian Journal of Electrochemistry*, **40**, 280-285 (2004). Doi: https://doi.org/10.1023/b:ruel.0000019665.59805.4c

43. I. Das, N. Goel, N.R. Agrawal, S.K. Gupta, Growth patterns of dendrimers and electric potential oscillations during electropolymerization of pyrrole using mono and mixed surfactants, *Journal of Physical Chemistry B*, **114**(40), 12888-12896 (2020). Doi: https://doi.org/10.1021/jp105183q

44. M. Bazzaoui, E.A. Bazzaoui, L. Martins, J.I. Martins, Electropolymerization of pyrrole on zinc-lead-silver alloys' electrodes in neutral and acid organic media, *Synthetic Metals*, **130**(1), 73-83 (2002). Doi: https://doi.org/10.1016/S0379-6779(02)00101-7

45. V.V. Tkach, M.V. Kushnir, I.M. Shevchuk, S.d. Oliveira, V.V. Lystvan, A.O.V. Luganska, P.I. Yagodynets, Z.O. Kormosh, Y.G. Ivanushko, The theoretical description for ecopipam electrochemical determination on a Cobalt (III) oxyhydroxide based material, *Applied Journal of Environmental Engineering Science*, **8**(2), 123-129 (2022). Doi: https://doi.org/10.48422/imist.prsm/ajees-v8i2.27095

46. V.V. Tkach, M.V. Kushnir, S.C. de Oliveira, I.M. Shevchenko, V.M. Odyntsova, V.M. Omelyanchik, *et al.*, Theoretical description for anti-COVID-19 drug molnupiravir electrochemical determination over the poly(1,2,4-triazole)-co-squaraine dye composite with Cobalt (III) oxyhydroxide, *Biointerface Research in Applied Chemistry*, **13**(1), 74 (2023). Doi: https://doi.org/10.33263/briac131.074

47. V.V. Tkach, M.M. Kucher, N. Slyvka *et al.,* The modeling for anti-Covid-19 drug molnupiravir electrochemical sensing on C_3N_4, *Biointerface Research in Applied Chemistry*, **13**(5), 446 (2023). Doi: https://doi.org/10.33263/briac135.446

48. D. Lynch, Pyrrolyl squaraines–Fifty golden years, *Metals*, **5**(3), 1349 (2015). Doi: https://doi.org/10.3390/met5031349

49. E. Lima, R.E. Boto, D. Ferreira, J.R. Fernandes, P. Almeida, L.F.V. Ferreira, E.B. Souto, A.M. Silva, L.V. Reis, Quinoline- and benzoselenazole-derived unsymmetrical squaraine cyanine dyes: Design, synthesis, photophysicochemical features and light-triggerable antiproliferative effects against breast cancer cell lines, *Materials*, **13**(11), 2646 (2020). Doi: https://doi.org/10.3390/ma13112646

Como citar este artigo

V.V. Tkach, M.V. Kushnir, N.M. Storoshchuk, O.V. Luganska, V.V. Kopiika, N.V. Novosad, S.M. Lukanova, Y.G. Ivanushko, V.G. Ostapchuk, S.P. Melnychuk, P.I. Yagodynets', S.C. de Oliveira, J.I.F. de Paiva Martins, I.O'N.d.M. Gaivão, M.J. Monteiro, Z.O. Kormosh, J.R. Garcia, E.A. da Silva Filho, Oksana P. Vitriak, A descrição teórica da detecção eletroanalítica de resveratrol em vinhos e sucos, assistida pelo oxihidróxido de cobalto, *Rev. Colomb. Cienc. Quim. Farm.*, **53**(2), 336-353 (2024). https://doi.org/10.15446/rcciquifa.v53n2.114424

Review article / https://doi.org/10.15446/rcciquifa.v53n2.114447

The random forest machine learning model performs better in predicting drug repositioning using networks: Systematic review and meta-analysis

Darlyn Juranny García Marín[a], Jerson Alexander García Zea[b]

Universidad EAFIT, Carrera 49, N° 7 Sur -50, Medellín, Antioquia, Colombia

E-mail adresses: [a]djgarciam@eafit.edu.co, [b]jagarciaz2@eafit.edu.co

Received: February 5, 2024
Corrected: March 10, 2024
Accepted: March 12, 2024

Summary

Introduction: The lengthy and costly process of drug development can be expedited through drug repositioning (DR), a strategy that identifies new therapeutic targets using existing products. Supervised machine learning (SML) models, incorporating interaction networks, offer a promising approach for DR. This study aims to systematically review and meta-analyze SML models predicting DR, identifying key characteristics influencing their performance. **Methodology:** A systematic review was conducted to identify SML models that used networks to predict DR, which were evaluated by comparing their performance through a random-effects meta-analysis. **Results:** 19 studies were included in the qualitative synthesis and 17 in the quantitative evaluation, The Random Forest (RF) model emerged as the predominant classifier (63%), yielding the highest performance in AUC ROC comparisons (overall value: 0.91, 95% CI: 0.86 – 0.96). Validation efforts in 18 studies confirmed the predictions of the SML models, affirming the proposed drugs. The incorporation of chemical structure in model training was found to enhance performance by aiding in prediction discrimination. **Conclusion:** SML models can predict DR, the RF model was the most widely used SML model with the best performance results, which underscores the potential use of FR models for predicting DR using network form biomedical information.

Keywords: Drug Repositioning, Drug development, Biological Networks, Machine Learning, Random Forest.

Resumen

El modelo de aprendizaje automático bosque aleatorio presenta un mejor desempeño para predecir el reposicionamiento de medicamentos usando redes: Revisión sistemática y Meta-análisis

Introducción: El proceso de investigación y desarrollo de fármacos se puede acelerar mediante el reposicionamiento de medicamentos (DR), una estrategia que identifica nuevos objetivos terapéuticos utilizando productos existentes. Los modelos de aprendizaje automático supervisado (SML), que incorporan redes de interacción, ofrecen un enfoque prometedor para DR. Este estudio tiene como objetivo revisar y meta-analizar sistemáticamente los modelos SML que predicen DR, identificando características clave que influyen en su desempeño. **Metodología:** Se realizó una revisión sistemática para identificar modelos SML que utilizaran redes para predecir DR, los cuales se evaluaron comparando su desempeño mediante un meta-análisis de efectos aleatorios. **Resultados:** Se incluyeron 19 estudios en la síntesis cualitativa y 17 en la evaluación cuantitativa. El modelo Bosque aleatorio surgió como el clasificador predominante (63%), obteniendo el mayor rendimiento en las comparaciones AUC ROC (valor general: 0,91, 95% IC: 0,86 – 0,96). Los esfuerzos de validación en 18 estudios confirmaron las predicciones de los modelos SML, afirmando los medicamentos propuestos. Se descubrió que la incorporación de estructura química en el entrenamiento de modelos mejora el rendimiento al ayudar en la discriminación de predicciones. **Conclusión:** Los modelos SML pueden predecir la DR, el modelo RF fue el modelo SML más utilizado con los mejores resultados de rendimiento, lo que resalta el uso potencial de modelos FR para predecir el DR utilizando redes de información biomédica.

Palabras clave: Reposicionamiento de medicamentos, Desarrollo de medicamentos, Redes biológicas, Aprendizaje automático, Bosque aleatorio.

Resumo

O modelo de aprendizado de máquina Floresta Aleatória apresenta melhor desempenho para prever o reposicionamento de medicamentos utilizando redes: Revisão Sistemática e Meta-análise

Introdução: O processo longo e custoso de desenvolvimento de medicamentos pode ser acelerado por meio do reposicionamento de medicamentos (DR), uma estratégia

que identifica novos alvos terapêuticos usando produtos existentes. Modelos de aprendizado de máquina supervisionado (SML), incorporando redes de interação, oferecem uma abordagem promissora para o DR. Este estudo tem como objetivo revisar sistematicamente e realizar meta-análises de modelos SML que preveem DR, identificando características-chave que influenciam seu desempenho. **Metodologia:** Foi realizada uma revisão sistemática para identificar modelos SML que usaram redes para prever DR, os quais foram avaliados comparando seu desempenho por meio de uma meta-análise de efeitos aleatórios. **Resultados:** 19 estudos foram incluídos na síntese qualitativa e 17 na avaliação quantitativa, o modelo Floresta Aleatória (RF) emergiu como o classificador predominante (63%), apresentando o melhor desempenho em comparações de AUC ROC (valor geral: 0,91, IC 95%: 0,86 - 0,96). Os esforços de validação em 18 estudos confirmaram as previsões dos modelos SML, afirmando os medicamentos propostos. A incorporação da estrutura química no treinamento do modelo mostrou-se capaz de melhorar o desempenho ao auxiliar na discriminação das previsões. **Conclusão:** Os modelos SML podem prever DR, o modelo RF foi o modelo SML mais amplamente utilizado com os melhores resultados de desempenho, o que destaca o potencial uso dos modelos FR para prever DR usando informações biomédicas de rede.

Palavras-chave: Reposicionamento de medicamentos, Desenvolvimento de medicamentos, Redes biológicas, Aprendizado de máquina, Floresta Aleatória.

Introduction

The research and development of new drugs constitute a lengthy and costly process. Given the varying complexities of therapeutic fields, it proves challenging to universally quantify the approximate cost in terms of both time and money for all drugs. Nevertheless, available data indicates that the investment required to bring a drug to market ranges from $161 million to $4.5 billion dollars [1] and can take 10 to 15 years [2]. Despite the substantial efforts invested in this process, approximately 90% of drugs experience failure during their clinical phase. This outcome leads to prolonged waiting periods for many patients, anticipating a successful approval process for a treatment molecule [3]. Given the extended timeline and a relatively low success rate, it becomes crucial to adopt strategies aimed at enhancing the efficiency and success of the drug development and approval process.

Drug repositioning (DR) is an approach that enables the identification of new therapeutic targets from products that are already known or currently in the market. This

approach facilitates an expedited drug approval process [4]. This characteristic makes DR an advantageous strategy compared to the traditional pharmaceutical product development process. Typically, for a repositioned drug, a significant portion of non-clinical research has already been explored. This includes aspects such as chemical analysis, manufacturing and control, animal toxicology, and clinical pharmacology. Consequently, it can progress more directly to the clinical phase, where there is already existing basic clinical information that could prove beneficial for the new treatment. This streamlined process has the potential to significantly reduce the overall development costs by 50 – 60%. Moreover, given that this medicine already possesses a known safety profile, the risk of failure in later stages of the process is significantly reduced [5].

DR can be conducted through experimental work where the drug is evaluated in the laboratory. However, it may not be the most optimal path to take initially in the research for drug repositioning. This is because it demands time, facilities, equipment, and personnel dedicated to experimentation, along with the physical product, to conduct the necessary assessments for each specific analysis [6]. This, added to the high number of molecules available on the market, makes it strategically better to have computational tools that initiate the DR process. In this regard, high-performance computing and artificial intelligence can help accelerate the identification of potential active substances for repositioning and reduce high failure rates [7].

Thanks to the different open data initiatives, the extensive pharmaceutical knowledge in the literature, large databases of diseases, drugs and adverse effects, it has been possible to develop computational tools for the repositioning of drugs [7]. Computational prediction between drugs and diseases has emerged as a crucial process in drug repositioning research. Advances in systems biology and interaction networks have facilitated the evolution of network pharmacology, transforming the paradigm of drug interaction. Initially perceived as a linear path "one drug – one therapeutic target – one disease", it has evolved into a network model: "Multiple Drug" network, involving multiple therapeutic targets and multiple diseases. This shift represents a fundamental change in our understanding of drug interactions [8].

In general, in the study of drug repositioning, it is assumed that chemical structures, target proteins, and even adverse effects enrich the information to establish new indications [9]. The chemical structure of a drug provides information based on its structural function, target proteins provide information on the direct effect of the drug at the molecular level, and adverse effects establish key points in relation to the undesired effect at the level of the drug phenotype [10]. Understanding the rules, patterns, and similarities within existing data facilitates comprehending the interaction between a drug and its efficacy in treating a disease. In the same vein, exploring these data sets

can lead to the discovery of new relationships. Studies have demonstrated that drugs sharing similar chemical structures, target proteins, or exhibiting comparable adverse effects have an increased probability of effectively treating the same disease [10, 11]. In this sense, the use of biological networks provides the opportunity to know those topological characteristics between nodes and edges that predict unknown associations between drugs and diseases [9].

For making predictions, Supervised Machine Learning (SML) models have been implemented. These models are trained using the characteristics of the network extracted from biomedical databases to measure similarities in conjunction with known drug-disease interactions. Through this approach, the model becomes capable of generating new potential candidate drugs for repositioning [12]. On the other hand, the use of SML is an efficient strategy that provides predictions on a larger scale, which broadens the scope of repositioning evaluation, allowing screening to be made to a greater number of drugs [13]. In addition, Machine Learning models are not limited to the total knowledge of the three-dimensional structure of chemical ligands and protein targets, which is the main disadvantage of the well-known molecular docking modeling [14].

The utilization of SML for suggesting drug candidates for repositioning based on network information has seen substantial growth. This presents an opportune scenario to synthesize information, discern strategic data pertaining to the models and algorithms employed, the origin of the data utilized, and identify potential performance moderators influencing the prediction of new therapeutic targets. In addition, to be able to establish the reliability of the different models based on their validation strategies in the candidate drugs for repositioning.

Thus, in this work, a systematic review and meta-analysis [15] was developed in order to synthesize the available information on the use of SML in proposing candidate drugs for repositioning, using network information and provide a tool for academia or industry with key synthesized information for the development of computational models for DR.

Methodology

The systematic review was conducted following the guidelines in the Preferred Reporting Items for Systematic Reviews and Meta-Analyses (PRISMA) statement 2020 [16].

Literature search strategy

A literature search was executed in English in the Scopus and PubMed databases, where studies up to April 2023 were included. The search syntax related the terms net-

works (Network*) and drug repurpose* joined with the AND operator, and the Boolean operator OR was used to include the synonyms. The complete search strategy for both databases can be reviewed in Supplementary Table 1. Employing search engine filters, articles in languages other than English, conference abstracts, and reviews were excluded.

Study selection and eligibility criteria

The initial screening of studies was conducted using the Rayyan platform [17]. Leveraging the tools provided by Rayyan, duplicates between the two databases were identified and removed. Two review authors independently conducted the title and abstract screening. To be included, a study had to explicitly indicate the use of at least one network model to predict drug repositioning (or any of its synonyms). Any discrepancies in this initial review were resolved through discussions among the review authors.

In a subsequent step, one of the authors categorized the studies that emerged from the initial screening based on the identified computational strategy, a classification that was verified by the second reviewer. The primary focus of interest was on SML models, encompassing any technique within this category employed for predicting drug repositioning through interaction networks. For encoding SML, the Python programming language's SciKit Learn library was utilized [18]. The models incorporated into this package served as a reference for classifying the studies.

The full-text review and data collection process was carried out in all studies using at least one MLS model. One author conducted this review, and the findings were corroborated by the second author to address any discrepancies. Data extraction involved populating a matrix in Microsoft Excel 2010, including author data, country, year of publication, objectives, model type, data source for model development, network type, performance metrics, details on whether the model was compared against other prediction models, and information on validation. At this stage, the reasons for exclusion were documented in each case.

The studies that were eligible in the qualitative analysis met the following criteria:

- The primary objective was to use networks to predict drug repositioning, employing at least one SML strategy.
- The study specified the name of the algorithm utilized.
- The developed model targeted more than one therapeutic specialty (screening) for medication repositioning.
- The developed model focuses on more than one drug.

- The data used for training the model was not veterinary.
- The study did not center on herbal medicines.
- The study did not center on traditional Chinese medicine.

The full article was accessible.

Studies were eligible in the quantitative analysis if they met the following criteria:

- Fulfill all the criteria mentioned above.
- Evaluate the performance of the model with available results.

Studies were excluded if they met the following criteria:

- The article did not meet the inclusion criteria.
- The article was in a language other than English.
- The article was a review.
- The article was a conference summary.
- The article was a book chapter.

Quality assessment of study

The quality of the publications was measured after the final selection process. The following list of questions was used to assess the credibility of the selected publications.

Question 1: Specify type of model, model-building procedures, and method for internal validation.

Question 2: Specify measures used to assess model performance and, to compare multiple models.

Question 3: Discuss the results with reference to performance and any other validation data.

Question 4: Give an overall interpretation of the results, considering objectives, limitations, results from similar studies, and other relevant evidence.

Each of the above questions was assessed with responses categorized as "Yes," "Partially," or "No." These responses were assigned numerical values: "Yes"=1, "Partially"=0.5 and "No"=0. For each selected study, its quality score was determined by summing the

scores of the responses to the four questions. This evaluation process was conducted by one of the authors of this article. The quality levels were classified as High (score = 4), Medium (2 ≤ score <4) and Low (score <2). Studies with scores greater than or equal to 3 were included in the final selection [19]. In cases where studies assessed performance using only one parameter, question two was marked "partially".

Performance measurement and meta-Analysis

The AUC-ROC (Area Under the Curve - Receiver Operator Characteristics) was chosen as the primary metric to assess the models' performance in the quantitative analysis, given its prevalent inclusion in nearly all articles (19 out of 17). While additional metrics were gathered, they were not incorporated into the quantitative analysis. In cases where a study reported results from multiple predictive models, performance parameters were collected exclusively for the model with the most favorable outcome.

The random effects meta-analysis model employing the DerSimonian-Laird model [20] was selected for the corresponding statistical analyses. This approach involved estimating the variability between studies (τ^2) and applying Cochrane's Q and I^2 tests to assess heterogeneity across studies. In the calculations, "n" was defined as the number of interactions during network construction. Statistical analysis was conducted in R Studio version 4.2.3 [21] using the metafor package.

Results

Article Selection for Synthesis

Following the application of search terms in the databases and the use of filter tools, reviews, conference papers, and articles not in English were excluded. The initial total of articles was 941 (PubMed) and 861 (Scopus). After removing duplicates across both databases, a total of 1057 articles were obtained and included in the initial screening process. Within this set, articles utilized at least one network model for predicting DR. These articles were categorized according to the computational strategy identified (see Table 1). Among these publications, we identified 44 articles that used SML models for the prediction of DR and were included in the full article review process. A comprehensive review of the 44 publications disclosed that 19 fulfilled all the inclusion criteria for synthesis. All 19 studies were incorporated in the qualitative synthesis and only 17 were included in the meta-analysis, with 2 studies [22, 23] being excluded. At this point, the reasons for exclusion were recorded and can be reviewed in Figure 1.

Table 1 Classification of articles by computational strategy.

Model Classification	Number of articles
Deep Learning (DL)	67
Supervised Machine Learning	44
Graph theory	21
Network based	20
Semi supervised machine learning	7
Undetermined	37

Model Categorization

The 196 studies were categorized into the six groups outlined in Table 1 and the frequency of model publication per year was determined (Figure 2). The initial publication appeared in 2009 with the most recent in 2023. DL emerged as the predominant modeling strategy, representing 34% of the total publications, and the 84% of its articles were published between 2020 and 2023, with the peak occurring in 2022, marking it as the year with the highest number of publications. This trend positions DL as the strategy that has experienced the most significant increase in the last three years. In contrast, SML constituting 22% of the articles, had publications spanning from 2013 to 2022, with representation in all years except 2015. Similarly, Network Based and Graph Theory models made their appearances in 2012 and 2013, respectively. While Figure 2 visually illustrates the distribution of studies up to 2023, it's crucial to note that the data for this year only includes articles published up to April.

Articles included in the synthesis/Study characteristics

Table 2 outlines the characteristics of the 19 studies. These were published between 2013 and 2022, 11 were conducted in China and the remainder in Thailand, Iran, Korea, the United Kingdom, Canada, and the United States.

To delineate the relationship between drugs and therapeutic targets, the 19 studies incorporated drug-target interaction databases. The most frequently utilized database was DrugBank (14 out of 19 articles), followed by the Kyoto Encyclopedia of Genes and Genomes (KEGG). In studies aimed at establishing the known relationship between drugs and diseases (drug-disease), the Comparative Toxicogenomics Database (CTD) was commonly employed. To determine the protein-disease relationship (Protein-disease), DisGeNET was implemented. When microRNAs and long noncoding RNAs were included, data from LncRNA2Target, LncRNADisease, lncRNASNP2, miRTarBase, and lncRNASNP2 were utilized. The protein-protein relationship was defined using the Search Tool for the Retrieval of Interacting Genes/Proteins (STRING). In studies that incorporated adverse effects to establish relation-

ships, SIDER (Side effect Resource) was employed, enabling the tracing of adverse effects associated with medications.

To characterize and establish similarities between chemical structures, molecule/drug repositories such as FDA-approved drugs, DrugBank or PubChem were implemented. The similarity of the chemical structure of the drugs was made based on the chemical language SMIleS or in other cases the molecular descriptor MACCS (Molecular ACCess System).

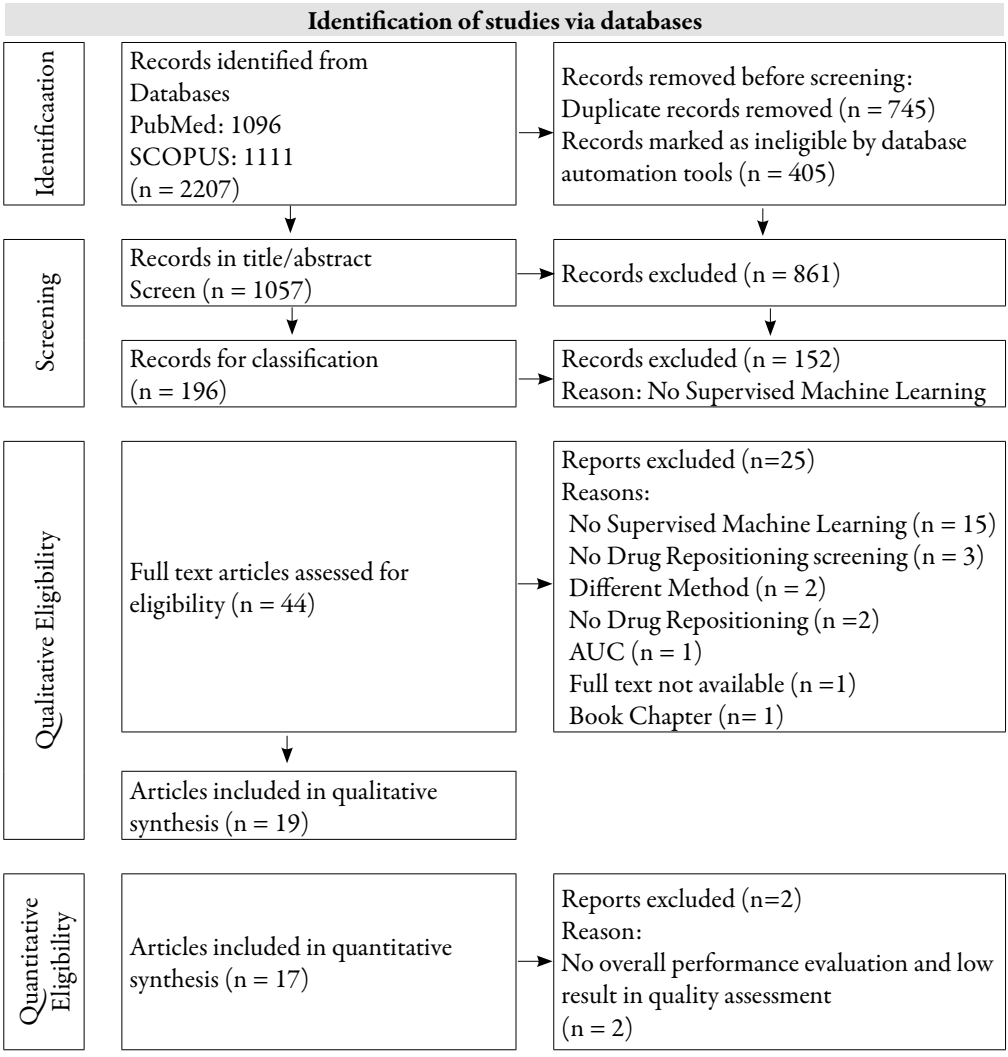

Figure 1. PRISMA Flow diagram. Papers identified in databases, title/abstract screened, read full text, and included in the synthesis. Reasons for exclusion are listed.

To establish relationships between genes and diseases, the studies utilized information available in Online Mendelian Inheritance in Man (OMIM) in some cases or DisGeNET (a database of gene-disease associations) in others, using them as compendiums of human genes and genetic disorders. For detailed information on the articles and their databases/libraries, see supplementary table 2.

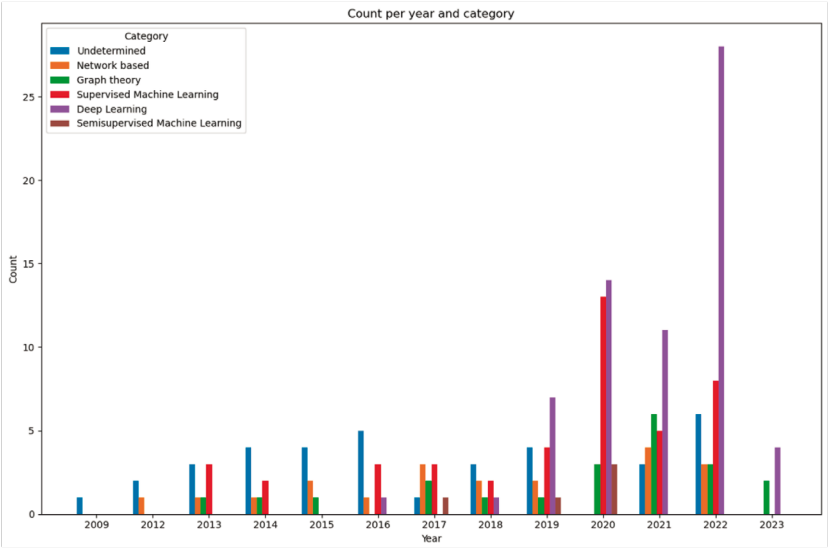

Figure 2. Categorization of studies resulting from screening that used at least one network model to predict drug repositioning.

In each study, considering the database utilized, various types of networks were constructed. The studies generated networks between drugs and targets with up to 9,400,000 interactions, 11 defined the interaction between drug and disease, 3 focused on the relationship between diseases and proteins. Additionally, 12 studies incorporated chemical structure in the development of the model. Moreover, in other instances, networks of interaction between genes and diseases or genes and drugs, as well as networks between adverse effects and drugs, were constructed. The strategy employed varied across studies; a single network was created to train the models, while in others, different networks were developed within the same study for training the model and establishing new indications for drugs (refer to Table 2 for more details).

Concerning the SML models, the most frequently employed classifier was Random Forest (RF) (63%), implemented in 12 studies. Other models included Support Vector Machine (SVM) (16%), logistic regression (11%), Gradient Boosting (5%) and XGBoost (5%). Each of the studies had a unique networking process to train the models and predict new therapeutic targets in medicines.

Table 2. Characteristics of the included studies

ID	Reference	Study Location	Year	Algorithm	Network	Models for Comparison (Name if available)	Model validation
2	Wang *et al.* (2013) [10]	China	2013	SVM	1,933 Interactions among 593 drugs and 313 diseases	PREDICT	ClinicalTrials.gov
4	Cao *et al.* (2014) [24]	China	2014	RF	5127 Drug target interactions	BGL, BLM, NetLapRLS, RLS	Literature searching
5	Qabaja *et al.* (2014) [22]	Canada	2014	LR	2343 genes and 22 diseases Network, 2343 genes and 406 drugs Network	-	Literature searching
8	Moghadam *et al.* (2016) [25]	iran	2016	SVM	1933 Drugs diseases interactions	PReDICT, a- PreDR	ClinicalTrials.gov
12	Lee and Yoon (2018) [23]	Korea	2018	RF	4248 Drugs and targets interactions, 7083 drugs and diseases interactions	PREDICT, PreDR	ClinicalTrials.gov and PubMed
16	Wei *et al.* (2019) [9]	China	2019	SVM	5868 Side effect for 1430 drugs, 19.906 drug target interactions	-	ClinicalTrials.gov and PubMed
18	Chen *et al.* (2020) [26]	China	2020	RF	105546 Drug target interactions	PREDICT, TL-HGBI, MBiRW, LRSSL, SCMFDD, a- EMP-SVD	-
20	Liu *et al.* (2020) [12]	China	2020	RF	4642 Drug protein interactions, 1365 disease protein interactions, 1827 drug disease interactions	HGBI, LDB, TL-HGB, a- Drug Net	Literature searching

(Continued)

ID	Reference	Study Location	Year	Algorithm	Network	Models for Comparison (Name if available)	Model validation
21	Fahimian *et al.* (2020) [27]	Iran	2020	RF	9400000 Drug disease interactions	MBiRW, DTINet, HGBI, NBI, a- JUST	A Cell toxicity assay to assess the effectiveness of the repurposed drug on breast cancer stage II (HER2 cell line)
23	Zhou *et al.* (2020) [28]	China	2020	RF	1933 Drug disease interactions	PREDICT	Literature searching
25	Gilvary *et al.* (2020) [29]	United States	2020	Gradient Boosting	22,399 Protein coding genes, 6,679 drugs	DDR, NEDD, NRLMF, DTINet, CMF, BLM-NII, a-NetLapRLS	Literature searching
28	Yue and Because (2021) [30]	China	2021	RF	90 Nuclear receptors, 1476 Ion channels, 635 GPCR, 2926 Enzymes, 9881 drugs	Pathima Nusrath Hameed *et al.*, Lei Chen *et al.*, methods, SPACE	Literature searching
29	Yang *et al.* (2021) [31]	China	2021	LR	8969 Substructure drug target domain interactions, 8053 indication drug target domain interactions	Lee and Yoon, Wu *et al.* methods	Literature searching
31	Kitsiranuwat *et al.* (2021) [32]	Thailand	2021	RF	14264 Drug disease interactions	DNILMF, DT-Hybrid, DDR	ClinicalTrials.gov, PubMed and AACT data base
32	Amiri-Souri *et al.* (2022) [33]	United kingdom	2022	XGBoost	2057 Real negative drug target interactions, 1721 Positive interaction	LAGCN, DTINet, a-deepDR	Drug-protein docking simulation and literature searching

(Continued)

ID	Reference	Study Location	Year	Algorithm	Network	Models for Comparison (Name if available)	Model validation
33	Zhao *et al.* (2022) [34]	China	2022	RF	18416 Drug disease interactions, 11107 drug protein interactions, 25.087 protein disease interactions	DeepDR, DTINet, GIPAE, a- HINGRL	Literature searching
34	Zhang *et al.* (2022) [35]	China	2022	RF	18416 Drug disease interactions, 5898 Disease protein interactions, 3110 Drug protein interactions	-	Literature searching
35	Kitsiranuwat *et al.* (2022) [36]	Thailand	2022	RF	27,683 Drug protein interactions	SCMFDD, LNS	Literature searching
36	Jiang and Huang (2022) [37]	China	2022	RF	6528 Drug target interactions	PREDICT, TL-HGBI, MBiRW, LRSSL, SCMFDD, a- EMP-SVD	Literature searching

RF– Random Forest / SVM – Support Vector Machine / LR – Logistic Regression

For the prediction of new drug targets, accuracy was assessed using AUC ROC ranging between 0.83 and 0.99 for the RF model and 0.88 to 0.90 for the SVM model.

Of the 19 articles selected after the full review of the study, 17 met all the final requirements to be included in the quantitative evaluation, while articles [22] and [23] were excluded. Despite the fact that all 17 articles presented model performance measures, there was no homogeneity in the performance parameters evaluated. The only common parameter in all 17 articles was the AUC ROC; Accuracy, F Measure, Sensitivity, and Precision were reported in 10 articles, Matthews' correlation coefficient was reported in 5, and specificity and AUPR were reported in 3 (see Table 3). Additionally, out of the 17 articles, all performed cross-validation, and 15 of 17 studies compared their prediction models with other models reported in the literature. Among these, 13 made the comparison by calculating the AUC ROC.

Table 3. Model Performance Overview

ID	AUC ROC	Acc	F measure	MCC	Its	Spe	For	AUPR	Cross validation / folds
2	0.902	0.823	0.822	-	0.847	-	0.808	-	Yes/10
4	0.986	0.948	-	-	0.965	0.930	-	-	Yes/5
8	0.88	0.83	0.82	0.66	-	-	-	-	Yes/10
16	0.903	0.853	0.779	-	-	-	0.778	-	Yes/10
18	0.920	0.854	-	0.713	0.796	0.912	0.900	-	Yes/5
20	0.966	0.919	0.918	0.840	0.939	-	0.899	-	Yes/5
21	0.83	-	0.72	-	0.79	-	0.66	-	Yes/10
23	0.923	-	-	-	-	-	-	-	Yes/10
25	0.841	-	-	-	-	-	-	-	Yes/5
28	0.998	-	-	-	-	-	-	-	Yes/10
29	0.876	-	-	-	-	-	-	-	Yes/-
31	0.879	0.967	1.00	-	-	-	-	-	Yes/5
32	0.940	-	0.928	-	0.928	-	0.927	0.894	Yes/10
33	0.876	-	0.794	0.589	0.796	-	0.793	0.866	Yes/10
34	0.963	0.900	0.900	-	0.897	-	0.903	-	Yes/10
35	0.938	0.857	0.866	-	0.928	-	0.812	0.932	Yes/5
36	0.879	0.798	-	0.596	0.800	0.796	0.797	-	Yes/5

AUC ROC: Area Under the Curve - Receiver Operator Characteristics / Acc: Accuracy / MCC: Matthews Correlation Coefficient / Sen: Sensitivity / Spe: Specificity / Pre: Precision/ AUPR: Area Under Precision-Recall Curve.

After evaluating the performance of the developed models, tests were conducted to validate the veracity of the predictions, and since the models aimed to predict new indications for the drugs, confirming the effectiveness of the newly established relationships became crucial. Out of the 19 studies, 18 presented validation results for their models. The most commonly employed strategy was consulting the literature to identify whether the new indication for the drug(s) had been reported at any time. In this exercise, the most cited sources of information were ClinicalTrials.gov and PubMed, in other cases the source consulted was not specified. In all the studies that used this way of validating the candidate drugs for repositioning, they presented citations of clinical studies or other references where this new indication for repositioned drugs had already been mentioned in the scientific literature. Finally, 2 studies presented different strategies to literature searching [27, 33], in the case of Amiri-Souri *et al.* (2022) [33], an *in vitro* study was done and in the Fahimian *et al.* (2020) [27] work, a simulation with molecular docking was performed (reference to Table 2 for more details).

Assessing the quality of the evidence

10 studies were rated as high quality, 8 as medium quality and 1 as low quality. For those studies that only assessed performance focused on a single metric, they were assigned "Partially" in question 2. In cases where there were no validation results, "Partially" was assigned in question 4. Since studies with a score equal to or greater than 3 were included in the quantitative assessment, 2 studies were excluded at this point in the process. The full result of the quality assessment of the studies can be found in Supplementary Table 3.

Meta-analysis

A total of 17 studies were included in the quantitative assessment after removing two studies due to quality assessment outcome and lack of overall model performance. The studies were evaluated using a random-effects model and compared based on their AUC ROC (95% CI), the summary of the results can be seen in Figure 3. We assessed inter-study variability τ^2 = 0.0103 (SE 0.0104) and Cochrane's Q=223772.7841, p-val <.0001, I^2 = 99.99% for heterogeneity.

The AUC ROC is measured on the scale 0 – 1, the closer to 1, the better the classifier [38]. The overall analysis of the results obtained from the meta-analysis showed that the mean AUC ROC for the included studies was 0.91 (95% CI 0.86 – 0.96). The highest AUC ROC result was obtained by Yue and He (2021) [30] with a value of 1.00 who implemented an RF model. The model with the lowest accuracy was Fahimian *et al.* (2020) [27] with 0.83 AUC ROC, which also used RF for prediction. Regard-

ing the studies that used SVM, the highest accuracy value was obtained by Wang *et al*. (2013) [10] and Wei *et al.* (2019) [9] with 0.90 and the lowest for Moghadam *et al.* (2016) [25] with a result of 0.88 in the meta-analysis. The model that implemented the highest number of interactions to build the network was Fahimian *et al.* (2020) [27], which obtained a result of 0.83. In contrast, the models implemented by Moghadam *et al*. (2016) [25], Wang *et al*. (2013) [10] and Zhou *et al*. (2020) [28] generated the lowest number of network drug-target interactions (1933) and showed a value for AUC ROC of 0.88, 0.90 and 0.92 respectively.

The study developed by Yue and He (2021) [30] obtained the highest result (1.00 AUC ROC) among the models that included databases that established a relationship between Drug–Target and Drug–Disease. Among the studies that used the Protein-Disease relationship in the construction of interactions, the highest result was AUC ROC of 0.96 [35]. As for those that included the Protein-Protein ratio, Kitsiranuwat *et al.* (2022) [36] obtained 0.94 as the highest value. The chemical structure of the drugs was integrated into the development of 12 models. Among these, Cao *et al.* (2014) [24], achieved the highest accuracy (0.99). Additionally, the association between genes and diseases was used in 10 articles, Liu *et al.* (2020) [12] obtained 0.97 in this category. Wang *et al*. (2013) [10] and Wei *et al*. (2019) [9] with 0.90, integrated adverse effects in drugs into the development of the model. Furthermore, both Jiang and Huang (2022) [37] and Chen *et al.* (2020) [26] were the only studies that included RNA and obtained values of 0.88 and 0.92 for AUC ROC, respectively.

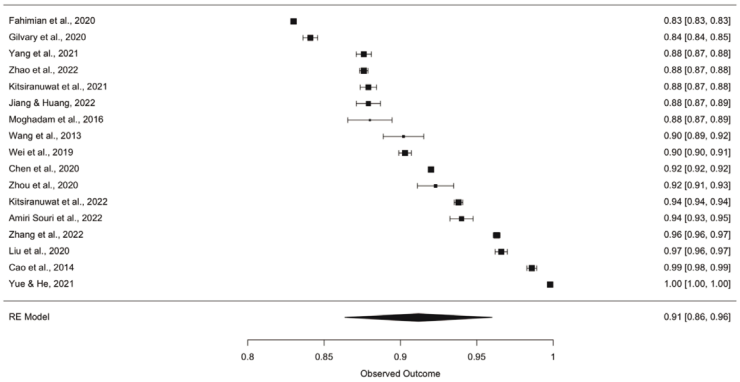

Figure 3. Forest plot comparing the papers by AUC ROC, in a random effects model. Overview of meta-analysis under a random effects model, comparing the AUC ROC of SML studies for drug repositioning. The data is organized in ascending order.

Discussion

Generally, in drug repositioning studies, it is assumed that chemical structures, target proteins, and even adverse effects enrich and provide valuable information for the identification of new indications [9]. Drugs with similar structures have been shown to have a high probability of treating the same disease [11] and in conjunction with the integration of biological networks offers the opportunity to understand the topological characteristics between nodes and edges, predicting previously unknown associations between drugs and diseases [9].

In this context, studies aimed at predicting drug repositioning use biomedical databases that relate information from the target to the drug. These databases are combined with various sources of information to build the network, measure similarities, and obtain the characteristics needed to train the prediction model. These predictions are based on the idea that drugs or diseases with similar topological network properties may be functionally related. Figure 2 illustrates the increase in studies predicting drug repositioning using interaction networks from 2009 to 2022. It highlights the increase in studies implementing SML from 2013 to 2020, with continuity in publications during 2021 and 2022. At this point, it is opportune to conduct a systematic review of the available information on these prediction models that implement SML methods. These models are designed to identify new candidate indications for drug repositioning, taking into account the various types of relationships between biomolecules and known drug-disease interactions. In addition, a quantitative evaluation of these models through a meta-analysis was proposed.

Considerable efforts have been devoted to demonstrating that drugs with similar chemical structure, similar adverse effects, and drugs that target the same target protein can treat the same specific disease. In a previous study, Wang *et al*. (2013) [10], showed that adopting this perspective favors the process of drug repositioning. It highlights that an SML model designed for repositioning can be trained using information from databases, such as chemical structures, target proteins, or adverse effects. In addition, various data, such as genes, expression profiles [22], microRNAs and long noncoding RNAs [26, 37], have proven to be valuable in the construction of these models. However, when evaluating performance, it has been observed that merging all these resources during the training process significantly improves the model compared to the individual use of information [10, 25]. Therefore, it can be considered that making a comprehensive characterization of drugs at multiple levels (chemical structure, target protein/gene or adverse effects) can substantially expand and improve the quality of predictions in drug repositioning.

Regarding the development of the models, the predominant approach in the reviewed studies consisted of the creation of interaction networks, the identification of their characteristics and the incorporation of this information into SML models, addressing the problem as a classification task. In this way, it can be determined whether a drug might be linked to a new disease, based on available training information. In several models developed, it has been shown that including the networks significantly improves the overall performance of the model. In these cases, network profiles provide valuable additional information compared to databases that do not incorporate interaction profiles [11, 24, 26]. This finding suggests that the consideration of network characteristics enriches the predictive capacity of the models, offering a more complete perspective in the identification between drugs and diseases.

In this study, papers were considered in the quantitative assessment if they reported at least AUC ROC. Some studies used a variety of performance measures (see Table 3), while others limited to report only the AUC ROC. The quantitative analysis was conducted using a meta-analysis, using a random-effects model that considers the variability both intra-study and between-studies. For this purpose, the measure τ^2 was calculated, which provides an estimate of the variance in effects between studies, while I^2 describes the percentage of variability attributable to heterogeneity, assessing the extent to which the studies agree with each other [39]. In our case, a high value for heterogeneity was obtained, which can be manifested through statistical uncertainty or random variability, which could be derived from methodological diversity due to different strategies in the construction of the network, variations in training data, differences in data sources, the definition of similarities in interactions and the use of different SML models.

In the resulting quantitative analysis, it was observed that the most frequently used classifier was RF, being not only the most common alternative, but also the model with the highest accuracy measured by the AUC ROC in the general summary of the meta-analysis (see Figure 3). In fact, the four highest values of this performance measure, ranging from 0.96 to 1.00, corresponded to models developed with RF. Additionally, studies comparing RF performance with other supervised learning models found that this strategy was shown to have more consistent performance and prediction [26, 37]. This finding becomes relevant when making large-scale predictions about the association between drugs and diseases. It is plausible that the preference for RF implementation in various studies is due to its suitability for larger datasets, as this method excels in the detection of Out-Of-Bag errors, the proximity between features, and the handling of unbalanced datasets [40].

In this sense, the model with the highest AUC ROC was the one developed by Yue and He (2021) [30], however, this study only reported the AUC ROC as a performance measure, other parameters such as sensitivity or specificity were not provided, and had a quality assessment classified as medium. In addition, other databases such as genes, adverse effects or chemical structures were not explored to create the network or establish similarities, which could have enriched the model. This fact was demonstrated by Cao *et al*. (2014) [24], where in their study, the drug-target relationship can be influenced by characteristics of the chemical structure in relation to the structural and physicochemical properties of the targets, greatly helping the discrimination of predictions. Similarly, studies that included adverse effects as part of the data to build the network, generated better predictive results in relation to the other data sources commonly used as a drug-target [10, 25].

Regarding the databases used in the development of the prediction models for DR, all studies incorporated databases that linked drugs to their targets. In addition, some authors explored the inclusion of information to understand the topology and similarities of their network. For example, Cao *et al*. (2014) [24], developed the model with the highest AUC ROC (0.99) among those who evaluated the chemical structures of drugs. This performance measure outperforms other studies that included additional information, such as genes and diseases, like Liu *et al.* (2020) [12] with AUC ROC of 0.97 or the protein-disease interaction [35] with an AUC ROC of 0.96; protein-protein [36] with an AUC ROC of 0.94; the inclusion of RNA [26] with an AUC ROC of 0.92, or the integration of adverse drug effects by Wang *et al.* (2013) [10] and Wei *et al.* (2019) [9], both with AUC ROC of 0.90. The observation that the inclusion of chemical structures obtained a higher AUC ROC value may be linked to what Cao *et al.* (2014) [24] defined. In this study, they suggest that the drug-target relationship may be influenced by characteristics of the chemical structure and its relationship with the properties of the targets, which helps in the discrimination of predictions.

A limitation of models that used supervised learning to make predictions is their need for both positive and negative training data. However, most data sources allow positive therapeutic relationships between drugs and diseases to be established but lack the ability to determine negative relationships between them. Therefore, one of the main challenges when defining a drug repositioning model lies in obtaining reliable negative data for training. To address this issue, many models chose to take unlabeled data or unrelated pairs (drug-targets) as negative examples. However, this strategy may introduce some possible positive drug-disease pairs into negative samples, generating noisy training data and decreasing the reliability of predictions. In contrast, studies such as that by Amiri-Souri *et al.* (2022) [33] and Liu *et al*. (2020) [12] adopted a more careful and realistic strategy when selecting negative training data, which contributed

to improved model performance compared to strategies that took unlabeled data randomly. Despite these advances, the study by Liu *et al.* (2020) [12] emphasizes the need to consider even more reliable strategies when employing supervised learning models in drug repositioning.

Regarding the validation of the results of the models, the most common strategy was the confirmation of predictions in scientific databases, where the main purpose was to identify references where the relationship between the repositioned drug and its new disease had previously been established. In some cases, the literature validation took a more focused approach to the study of the repositioned drug. This included the exploration of genes related to the disease, and the review of information related to the metabolic pathways in which the drug might be involved. This approach made it possible to determine whether the repositioned drug could be associated with the same pathways that lead to the treatment of the disease [10]. In addition, another strategy was to compare the new drug with those currently used to treat the disease, looking for similarities at the molecular or metabolic level to evaluate its potential effectiveness in treatment [10].

In some cases, the validations went beyond the literature review. An example is the study by Fahimian *et al*. (2020) [27], which carried out a structural comparative analysis between new molecules repositioned to treat breast cancer and those already approved for this indication. In addition, they conducted an *in vitro* study to demonstrate the efficacy of the newly repositioned drug in the treatment of this pathology [27]. Another highlight is the study by Amiri-Souri *et al*. (2022) [33], which performed a simulation with molecular docking and an exhaustive literature review to validate the new interactions between target proteins and drugs predicted by the SML model for cancer treatment.

In short, the application of an integrative approach, including multiple sources of biomolecules and validation of results using various methodologies, not only proposes promising candidates to treat various diseases, but also plays an important role in the understanding of effective therapies that influence multifactorial diseases. These models, apart from predicting new indications, can contribute significantly to clinical pharmacogenomics research, defining relationships between drugs–gene and disease–gene [22, 26]. Likewise, the repositioning of drugs can be very useful for the development of knowledge regarding adverse effects since, by discovering possible new indications for medicines, it is easier to conduct studies more focused on the mechanisms of action of drugs, reducing the gap between medical indications and the understanding of the effects of drugs [10].

Conclusions

This systematic review and meta-analysis of the published literature to predict drug repositioning by using SML models presents relevant aspects that may be useful for future studies in this field. This review suggests that SML models can predict the repositioning of drugs with high performance values, which underscores the potential use of RF in DR. It was identified that the inclusion of chemical structures in the development of the model can improve performance, which allows us to suggest the evaluation of this parameter in future studies. It is suggested to explore how the drug repositioning prediction could contribute to better understand multifactorial diseases and adverse drug effects in future studies. It should be noted that the RF model was the most widely used SML model to predict drug repositioning and with the best performance results compared to AUC ROC. It recognizes that it is important to define strategies to define negative samples when training SML models so as not to incur the increased risk of false negatives. Finally, it could be interesting to study the DL models developed to predict new indications for medications, given that its publications have considerably increased since 2019.

Acknowledgments

We would like to thank EAFIT University and the Master's Degree in Biosciences program. We would like to thank Professor Nicolas Pinel for his guidance on this work.

Conflict of interest

The authors report that they have no conflict of interest.

References

1. M. Schlander, K. Hernandez-Villafuerte, C.Y. Cheng, J. Mestre-Ferrandiz, M. Baumann, How much does it cost to research and develop a new drug? A systematic review and assessment, *Pharmacoeconomics*, **39**, 1243-1269 (2021). Doi: https://doi.org/10.1007/s40273-021-01065-y

2. PhRMA, *Research and Development Policy Framework*. URL: https://phrma.org/policy-issues/Research-and-Development-Policy-Framework, accessed May 2023.

3. D. Sun, W. Gao, H. Hu, S. Zhou, Why 90% of clinical drug development fails and how to improve it? *Acta Pharmaceutica Sinica B*, **12**(7), 3049-3062 (2022). Doi: https://doi.org/10.1016/j.apsb.2022.02.002

4. H. Luo, M. Li, M. Yang, F.X. Wu, Y. Li, J. Wang, Biomedical data and computational models for drug repositioning: A comprehensive review, *Briefings in Bioinformatics*, **22**(2), 1604-1619 (2021). Doi: https://doi.org/10.1093/bib/bbz176

5. M. Rudrapal, S.J. Khairnar, A.G. Jadhav, Drug repurposing (DR): An emerging approach in drug discovery, in: Badria, F.A., *Drug Repurposing - Hypothesis, Molecular Aspects and Therapeutic Applications*, IntechOpen Limited, London, 2020. Doi: https://doi.org/10.5772/intechopen.93193

6. B. Turanli, M. Grøtli, J. Boren, J. Nielsen, M. Uhlen, K.Y. Arga, A. Mardinoglu, Drug repositioning for effective prostate cancer treatment, *Frontiers in Physiology*, **9**, 500 (2018). Doi: https://doi.org/10.3389/fphys.2018.00500

7. J. Li, S. Zheng, B. Chen, A.J. Butte, S.J. Swamidass, Z. Lu, A survey of current trends in computational drug repositioning, *Briefings in Bioinformatics*, **17**(1), 2-12 (2016). Doi: https://doi.org/10.1093/bib/bbv020

8. J.L. Medina-Franco, M.A. Giulianotti, G.S. Welmaker, R.A. Houghten, Shifting from the single- to the multitarget paradigm in drug discovery, *Drug Discovery Today*, **18**(9-10), 495-501 (2013). Doi: https://doi.org/10.1016/j.drudis.2013.01.008

9. X. Wei, Y. Zhang, Y. Huang, Y. Fang, Predicting drug–disease associations by network embedding and biomedical data integration, *Data Technologies and Applications*, **53**(2), 217-229 (2019). Doi: https://doi.org/10.1108/dta-01-2019-0004

10. Y. Wang, S. Chen, N. Deng, Y. Wang, Drug repositioning by kernel-based integration of molecular structure, molecular activity, and phenotype data, *PLoS One*, **8**(12), e78518 (2013). Doi: https://doi.org/10.1371/journal.pone.0078518

11. C. Gilvary, J. Elkhader, N. Madhukar, C. Henchcliffe, M.D. Goncalves, O. Elemento, A machine learning and network framework to discover new indications for small molecules, *PLoS Computational Biology*, **16**(8), e1008098 (2020). Doi: https://doi.org/10.1371/journal.pcbi.1008098

12. J. Liu, Z. Zuo, G. Wu, Link prediction only with interaction data and its application on drug repositioning, *IEEE Transactions in NanoBioscience*, **19**(3), 547-555 (2020). Doi: https://doi.org/10.1109/TNB.2020.2990291

13. H. Ding, I. Takigawa, H. Mamitsuka, S. Zhu, Similarity-based machine learning methods for predicting drug–target interactions: A brief review, *Briefings in Bioinformatics*, **15**(5), 734-747 (2014). Doi: https://doi.org/10.1093/bib/bbt056

14. M.L. Shahreza, N. Ghadiri, S.R. Mousavi, J. Varshosaz, J.R. Green, A review of network-based approaches to drug repositioning, *Briefings in Bioinformatics*, **19**(5), 878-892 (2018). Doi: https://doi.org/10.1093/bib/bbx017

15. A.B. Haidich, Meta-analysis in medical research, *Hippokratia*, **14**(Suppl. 1), 29-37 (2010). URL: https://www.ncbi.nlm.nih.gov/pmc/articles/PMC3049418/, accessed May 2023.

16. M.J. Page, J.E. McKenzie, P.M. Bossuyt, I. Boutron, T.C. Hoffmann, C.D. Mulrow, L. Shamseer, J.M. Tetzlaff, E.A. Akl, S.E. Brennan, R. Chou, J. Glanville, J.M. Grimshaw, A. Hróbjartsson, *et al.*, PRISMA 2020 statement: an updated guideline for reporting systematic reviews, *BMJ*, **372**, 71 (2021). Doi: https://doi.org/10.1136/bmj.n71

17. M. Ouzzani, H. Hammady, Z. Fedorowicz, A. Elmagarmid, Rayyan -A web and mobile app for systematic reviews, *Systematic Reviews*, **5**, 210 (2016). Doi: https://doi.org/10.1186/S13643-016-0384-4

18. Supervised learning — SciKit-Learn 1.4.0 documentation. URL: https://scikit-learn.org/stable/supervised_learning.html, accessed January, 2024.

19. M.I. Azeem, F. Palomba, L. Shi, Q. Wang, Machine learning techniques for code smell detection: A systematic literature review and meta-analysis, *Information and Software Technology*, **108**, 115-138 (2019). Doi: https://doi.org/10.1016/j.infsof.2018.12.009

20. R. DerSimonian, N. Laird, Meta-analysis in clinical trials, *Controlled Clinical Trials*, **7**(3), 177-188 (1986). Doi: https://doi.org/10.1016/0197-2456(86)90046-2

21. R Core Team, *R: A Language and Environment for Statistical Computing*, R Foundation for Statistical Computing, Vienna, Austria, 2023. URL: https://lib.stat.cmu.edu/R/CRAN/doc/manuals/r-devel/fullrefman.pdf, accessed January, 2024.

22. A. Qabaja, M. Alshalalfa, E. Alanazi, R. Alhajj, Prediction of novel drug indications using network driven biological data prioritization and integration, *Journal of Cheminformatics*, **6**, 1 (2014). Doi: https://doi.org/10.1186/1758-2946-6-1

23. T. Lee, Y. Yoon, Drug repositioning using drug-disease vectors based on an integrated network, *BMC Bioinformatics*, **19**, 446 (2018). Doi: https://doi.org/10.1186/S12859-018-2490-X

24. D.-S. Cao, L.-X. Zhang, G.-S. Tan, Z. Xiang, W.-B. Zeng, Q.-S. Xu, A.F. Chen, Computational prediction of drug target interactions using chemical, biological, and network features, *Molecular Informatics*, **33**(10), 669-681 (2014). Doi: https://doi.org/10.1002/minf.201400009

25. H. Moghadam, M. Rahgozar, S. Gharaghani, Scoring multiple features to predict drug disease associations using information fusion and aggregation, *SAR and QSAR in Environment Research*, **27**(8), 609-628 (2016). Doi: https://doi.org/10.1080/1062936X.2016.1209241

26. Z.-H. Chen, Z.-H. You, Z.-H. Guo, H.-C. Yi, G.-X. Luo, Y.-B. Wang, Prediction of drug–target interactions from multi-molecular network based on deep walk embedding model, *Frontiers in Bioengineering and Biotechnology*, **8**, 338 (2020). Doi: https://doi.org/10.3389/fbioe.2020.00338

27. G. Fahimian, J. Zahiri, S.S. Arab, R.H. Sajedi, RepCOOL: Computational drug repositioning via integrating heterogeneous biological networks, *Journal of Translational Medicine*, **18**, 375 (2020). Doi: https://doi.org/10.1186/S12967-020-02541-3

28. R. Zhou, Z. Lu, H. Luo, J. Xiang, M. Zeng, M. Li, NEDD: A network embedding based method for predicting drug-disease associations, *BMC Bioinformatics*, **21**, 387 (2020). Doi: https://doi.org/10.1186/S12859-020-03682-4

29. C. Gilvary, J. Elkhader, N. Madhukar, C. Henchcliffe, M.D. Goncalves, O. Elemento, A machine learning and network framework to discover new indications for small molecules, *PLoS Computational Biology*, **16**(8), e1008098 (2020). Doi: https://doi.org/10.1371/journal.pcbi.1008098

30. Y. Yue, S. He, DTI-HeNE: A novel method for drug-target interaction prediction based on heterogeneous network embedding, *BMC Bioinformatics*, **22**, 418 (2021). Doi: https://doi.org/10.1186/S12859-021-04327-W

31. J. Yang, D. Zhang, L. Liu, G. Li, Y. Cai, Y. Zhang, H. Jin, X. Chen, Computational drug repositioning based on the relationships between substructure–indication, *Briefings in Bioinformatics*, **22**(4), bbaa348 (2021). Doi: https://doi.org/10.1093/bib/bbaa348

32. S. Kitsiranuwat, A. Suratanee, K. Plaimas, Multi-data aspects of protein similarity with a learning technique to identify drug-disease associations, *Applied Sciences* (Basel), **11**(7), 2914 (2021). Doi: https://doi.org/10.3390/app11072914

33. E. Amiri-Souri, R. Laddach, S.N. Karagiannis, L.G. Papageorgiou, S. Tsoka, Novel drug-target interactions via link prediction and network embedding, *BMC Bioinformatics*, **23**, 121 (2022). Doi: https://doi.org/10.1186/S12859-022-04650-W

34. B.-W. Zhao, L. Hu, Z.-H. You, L. Wang, X.-R. Su, HINGRL: predicting drug–disease associations with graph representation learning on heterogeneous information networks, *Briefings in Bioinformatics*, **23**(1), bbab515 (2022). Doi: https://doi.org/10.1093/bib/bbab515

35. M.-L. Zhang, B.-W. Zhao, X.-R. Su, Y.-Z. He, Y. Yang, L. Hu, RLFDDA: a meta-path based graph representation learning model for drug–disease association prediction, *BMC Bioinformatics*, **23**, 516 (2022). Doi: https://doi.org/10.1186/S12859-022-05069-Z

36. S. Kitsiranuwat, A. Suratanee, K. Plaimas, Integration of various protein similarities using random forest technique to infer augmented drug-protein matrix for enhancing drug-disease association prediction, *Science Progress*, **105**(3), 1-30 (2022). Doi: https://doi.org/10.1177/00368504221109215

37. H. Jiang, Y. Huang, An effective drug-disease associations prediction model based on graphic representation learning over multi-biomolecular network, *BMC Bioinformatics*, **23**, 9 (2022). Doi: https://doi.org/10.1186/S12859-021-04553-2

38. A.P. Bradley, The use of the area under the ROC curve in the evaluation of machine learning algorithms, *Pattern Recognition*, **30**(7), 1145-1159 (1997). Doi: https://doi.org/10.1016/S0031-3203(96)00142-2

39. J.J. Deeks, J.P.T. Higgins, D.G. Altman, Chapter 10: Analysing data and undertaking meta-analyses, Cochrane Training: Online Learning. URL: https://training.cochrane.org/handbook/current/chapter-10#section-10-10, accessed: January 2024.

40. M. Zakariah, Classification of large datasets using Random Forest Algorithm in various applications: Survey, *International Journal of Engineering and Innovative Technology (IJEIT)*, **4**(3), 2277-3754 (2008). URL: https://faculty.ksu.edu.sa/sites/default/files/classification_of_large_datasets_using_random.pdf

Supplementary Archive

Supplementary Table 1. Full search syntax for each database

PubMed	
Search	Syntax
#1	("Network*"[Title/Abstract])
#2	(("drug repurpos*"[Title/Abstract]) OR ("drug redirecting"[Title/Abstract]) OR ("drug reposition*"[Title/Abstract]) OR ("drug retasking"[Title/Abstract]) OR ("drug reprofiling"[Title/Abstract]) OR ("drug retargeting"[Title/Abstract]) OR ("drug relocation"[Title/Abstract]) OR ("Drug re-profiling"[Title/Abstract]) OR ("drug re-tasking"[Title/Abstract]) OR ("drug rescue"[Title/Abstract]) OR ("indication expansion"[Title/Abstract]) OR ("indication switching"[Title/Abstract]) OR ("drug rescuing"[Title/Abstract]) OR ("drug recycling"[Title/Abstract]) OR (drug redirection[Title/Abstract]) OR ("therapeutic switching"[Title/Abstract]) OR ("Novel drug us*"[Title/Abstract]) OR ("novel drug rediscovery"[Title/Abstract]) OR ("Novo drug us*"[Title/Abstract]) OR ("novo drug rediscovery"[Title/Abstract]))
#3	#1 and #2
SCOPUS	
Search	Syntax
#1	TITLE-ABS ("Network*")
#2	TITLE-ABS (("drug reposition*") OR ("drug repurpos*") OR ("drug redirecting") OR ("drug reposition*") OR ("drug retasking") OR ("drug reprofiling") OR ("drug retargeting") OR ("drug relocation") OR ("Drug re-profiling") OR ("drug re-tasking") OR ("drug rescue") OR ("indication expansion") OR ("indication switching") OR ("drug rescuing") OR ("drug recycling") OR (drug redirection) OR ("therapeutic switching") OR ("Novel drug us*") OR ("novel drug rediscovery") OR ("Novo drug us*") OR ("novo drug rediscovery"))
#3	#1 and #2

Supplementary Table 2. Databases and libraries used in the articles.

ID	Drug–Target	Drug–Disease	Protein–Disease	Protein–Protein	Side effects	Chemical structure	Gen - Disease	RNA
2	KEGG BRITE/ Brenda Supertarget/ DrugBank	-	-	-	CIDER	PubChem	OMIM	-
4	The Meaning of Meaning / Meaning	-	-	-	-	MACCS	-	-
5	DrugBank	-	-	-	-	-	OMIM, Reactome database STRING	-
8	-	ClinicalTrials.gov / DrugBank/ OMIM	-	-	CIDER	SMILES	-	-
12	DrugBank	CTD	-	-	-	-	DisGeNet BioCarta/ Reactome/ PID/ KEGG	-
16	DrugBank	mimMiner/ FDA approved drugs	-	-	CIDER	SMILES	OMIM, mimMiner	-
18	DrugBank	CTD	DisGeNET	STRING	-	-	-	LncRNA2Target/ LncRNADisease / lncRNASNP2/ miRTarBase/ HMDD / lncRNASNP2
20	DrugBank	PREDICT	-	-	-	-	OMIM	-
21	DrugBank	-	-	IntAct	-	-	OMIM/CTD/ DisGeNET/ COXPRESdb	-
23	-	PREDICT/ MeSH	-	-	-	SMILES	-	-

(*Continued*)

ID	Drug–Target	Drug–Disease	Protein–Disease	Protein–Protein	Side effects	Chemical structure	Gen - Disease	RNA
25	DrugBank	FDA approved drugs/ DrugBank/ PubChem	-	-	-	SMILES	MSigDB	-
28	Yamanishi	Olayan	-	-	-	-	-	-
29	DrugBank/ Uniprot	-	-	-	-	PubChem	-	-
31	DrugBank	CTD	-	STRING	-	-	DisGeNET	-
32	The Meaning / ChEMBL	-	-	-	-	MACCS	-	-
33	DrugBank	CTD	DisGeNET	-	-	SMILES	-	-
34	DrugBank	CTD/ MeSH	DisGeNET	-	-	SMILES	-	-
35	DrugBank/ KEGG	CTD	-	STRING	-	DD.chem.data	DisGeNET	-
36	DrugBank	SCMFDD-S/ MeSH	-	STRING	-	SMILES	DisGeNET	LncRNA2Target/ LncRNADisease/ lncRNASNP2/ miRTarBase/ HMDD/ lncRNASNP2

KEGG: Kyoto Encyclopedia of Genes and Genomes / Brenda: the enzyme database / Yamanishi: enzymes, ion channels, G-protein-coupled receptors and, nuclear receptors [Y. Yamanishi, M. Araki, A. Gutteridge, W. Honda, M. Kanehisa, Prediction of drug–target interaction networks from the integration of chemical and genomic spaces, *Bioinformatics*, 24(13), i232–i240 (2008). Doi: https://doi.org/10.1093/bioinformatics/btn162] / Uniprot: Universal Protein Resource / CTD: Comparative Toxicogenomics Database / Olayan: FDA-approved drugs and human target proteins [R.S. Olayan, H. Ashoor, V.B. Bajic, DDR: Efficient computational method to predict drug-target interactions using graph mining and machine learning approaches, *Bioinformatics*, 34(7), 1164–1173 (2018). Doi: https://doi.org/10.1093/bioinformatics/btx731] / PREDICT [A. Gottlieb, G.Y. Stein, E. Ruppin, R. Sharan, PREDICT: A method for inferring novel drug indications with application to personalized medicine, *Molecular Systems Biology*, 7, 496 (2011). Doi: https://doi.org/10.1038/msb.2011.26] / SCMFDD-S: similarity constrained matrix factorization method for the drug-disease association prediction data set collected by Zhang *et al.* [W. Zhang, X. Yue, W. Lin, W. Wu, R. Liu, F. Huang, F. Liu, Predicting drug-disease associations by using similarity constrained matrix factorization, *BMC Bioinformatics*, 19, 233 (2018). Doi: https://doi.org/10.1186/S12859-018-2220-4] / IntAct: Molecular Interaction Database / SIDER: Side Effect Resource / PID: the Pathway Interaction Database / MACCS: Molecular ACCess System / SMILES: Simplified Molecular Input Line Entry System / OMIM: Online Mendelian Inheritance in Man / STRING: Search Tool for the Retrieval of Interacting Genes-Proteins / MeSH: Medical Subject Headings / HMDD: the Human microRNA Disease Database.

Supplementary Table 3. Quality of evidence assessment

ID	1. Specify type of model, model-building procedures, and method for internal validation.		2. Specify measures used to assess model performance and, to compare multiple models.		3. Discuss the results with reference to performance and any other validation data.		4. Give an overall interpretation of the results, considering objectives, limitations, results from similar studies, and other relevant evidence.		Total
	Concept	Score	Concept	Score	Concept	Score	Concept	Score	
2	Yes	1	Yes	1	Yes	1	Yes	1	4
4	Yes	1	Yes	1	Yes	1	Yes	1	4
5	Partially	0,5	No	0	No	0	Partially	0,5	1
8	Yes	1	Yes	1	Yes	1	Yes	1	4
12	Yes	1	Partially	0,5	Partially	0,5	Partially	0,5	2,5
16	Yes	1	Yes	1	Yes	1	Yes	1	4
18	Yes	1	Yes	1	Yes	1	No	0	3
20	Yes	1	Yes	1	Yes	1	Yes	1	4
21	Yes	1	Yes	1	Partially	0,5	Partially	0,5	3
23	Yes	1	Partially	0,5	Yes	1	Yes	1	3,5
25	Yes	1	Partially	0,5	Yes	1	Yes	1	3,5
28	Yes	1	Partially	0,5	Yes	1	Yes	1	3,5
29	Partially	0,5	Partially	0,5	Yes	1	Yes	1	3
31	Yes	1	Yes	1	Yes	1	Yes	1	4
32	Yes	1	Yes	1	Yes	1	Yes	1	4
33	Yes	1	Yes	1	Yes	1	Yes	1	4
34	Yes	1	Yes	1	Yes	1	Yes	1	4
35	Yes	1	Yes	1	Yes	1	Partially	0,5	3,5
36	Yes	1	Yes	1	Yes	1	Yes	1	4

How to cite this article

D.J. García-Marín, J.A. García-Zea, The random forest machine learning model performs better in predicting drug repositioning using networks: Systematic review and meta-analysis, *Rev. Colomb. Cienc. Quim. Farm.*, 53(2), 354-384 (2024). https://doi.org/10.15446/rcciquifa.v53n2.114447

Scientific research article / https://doi.org/10.15446/rcciquifa.v53n2.114448

A repositioning approach: nitazoxanide inhibits inflammation and nociceptive response in mice models via a reduction of paw oedema, cellular migration and early TNF-α production

Livian Rabelo Lopes[1], Fellipe Alexandre Alves Moraes[1], João Paulo Costa Rodrigues[1], Flávio Martins de Oliveira[2], Débora de Oliveira Lopes[2], Flávia Carmo Horta Pinto[3], Aline Aparecida Saldanha[1], Adriana Cristina Soares[1]*

[1]Pharmacology of Pain and Inflammation Laboratory, Federal University of São João del-Rei, Divinópolis, Brazil

[2] Molecular Biology Laboratory, Federal University of São João del-Rei, Divinópolis, Brazil

[3]Experimental Pathology Laboratory, Federal University of São João del-Rei, São João del-Rei, Brazil

*Corresponding author E-mail: adrianasouza@ufsj.edu.br,
*ORCID: https://orcid.org/0000-0002-7953-8692

Received: February 20, 2024
Corrected: March 12, 2024
Accepted: March 12, 2024

SUMMARY

Introduction: Various studies have evaluated the *in vitro* anti-inflammatory effect of nitazoxanide (NTZ), suggesting new therapeutic functions for this drug. **Aims:** To evaluate the *in vivo* anti-inflammatory and antinociceptive activities of NTZ in acute mice models. **Methods:** Mice models of paw oedema, abdominal writhing, formalin and the rota-rod test were used. **Results:** Oral treatment with NTZ induced inhibition of paw oedema (60.00% and 66.67% at doses of 10 and 30 mg/kg, respectively) in the first hour after inflammatory stimulus, carrageenan (Cg). There was also a significant inhibition of 60.71% and 40.00% at the 30 mg/kg dose after 4h and 6 h, respectively after inflammation. Four hours after inflammation, the histological analysis of the footpad of animals treated with 30 mg/kg of NTZ showed a reduction in the migration of inflammatory cells by 65.77%. It is also important to highlight that there was a significant reduction of tumor necrose factor-alfa (TNF-α) in the initial phase of inflammation, 2 h after administration of the Cg. There was an inhibition in abdominal contortions by 54.14% and 56.21% at 30 and 90 mg/kg doses,

respectively. In the formalin test only the dose of 90 mg/kg showed antinociceptive action (54.85%; first phase and 45.67%; second phase). The results from rota-rod test showed that motor coordination was not affected with NTZ. **Conclusions:** This anti-inflammatory activity of NTZ appears to be a consequence of its ability to reduce the levels of an important mediator of the inflammatory response and pain the TNF-α.

Keywords: Nitazoxanide, repositioning, anti-inflammatory, antinociceptive, paw oedema, tumour necrosis factor-alpha.

RESUMEN

Un enfoque de reposicionamiento: la nitazoxanida inhibe la inflamación y la respuesta nociceptiva en modelos de ratones mediante una reducción del edema de la pata, la migración celular y la producción temprana de TNF-α

Introducción: Diversos estudios han evaluado el efecto antiinflamatorio *in vitro* de la nitazoxanida (NTZ), sugiriendo nuevas funciones terapéuticas para este fármaco. **Objetivos:** Evaluar las actividades antiinflamatorias y antinociceptivas *in vivo* de NTZ en modelos de ratones agudos. **Métodos:** Se utilizaron modelos en ratones de edema de pata, contorsiones abdominales, de formalina y prueba de rota-rod. **Resultados:** El tratamiento oral con NTZ indujo la inhibición del edema de la pata (60,00% y 66,67% a dosis de 10 y 30 mg/kg, respectivamente) en la primera hora después del estímulo inflamatorio con carragenano (Cg). También hubo una inhibición significativa del 60,71% y 40,00% con la dosis de 30 mg/kg después de 4 h y 6 h, respectivamente, después de la inflamación. Cuatro horas después de la inflamación, el análisis histológico de la almohadilla plantar de los animales tratados con 30 mg/kg de NTZ mostró una reducción de la migración de células inflamatorias del 65,77%. También es importante resaltar que hubo una reducción significativa del factor de necrosis tumoral alfa (TNF-α) en la fase inicial de la inflamación, 2 h después de la administración del Cg. Hubo una inhibición en las contorsiones abdominales de 54,14% y 56,21% con dosis de 30 y 90 mg/kg, respectivamente. En la prueba de formalina sólo la dosis de 90 mg/kg mostró acción antinociceptiva (54,85%; primera fase y 45,67%; segunda fase). Los resultados de la prueba rota-rod

mostraron que la coordinación motora no se vio afectada con NTZ. **Conclusiones:** Esta actividad antiinflamatoria de NTZ parece estar relacionada con su capacidad para reducir los niveles de un importante mediador de la respuesta inflamatoria y del dolor el TNF-α.

Palabras clave: Nitazoxanida, reposicionamiento, antiinflamatorio, antinociceptivo, edema de pata, factor de necrosis tumoral alfa.

Resumo

Uma abordagem de reposicionamento: a nitazoxanida inibe a inflamação e a resposta nociceptiva, em modelos com camundongos através da redução do edema da pata, da migração celular e da produção precoce de TNF-α

Introdução: Diversos estudos avaliaram o efeito antiinflamatório *in vitro* da nitazoxanida (NTZ), sugerindo novas funções terapêuticas para esta droga. **Objetivos:** Avaliar as atividades anti-inflamatória e antinociceptiva *in vivo* da NTZ em modelos agudos com camundongos. **Métodos:** Foram utilizados modelos de camundongos com edema de pata, contorções abdominais, teste de formalina e teste rota-rod. **Resultados:** O tratamento oral com NTZ induziu inibição do edema de pata (60,00% e 66,67% nas doses de 10 e 30 mg/kg, respectivamente) na primeira hora após o estímulo inflamatório, carragenina (Cg). Houve também uma inibição significativa de 60,71% e 40,00% na dose de 30 mg/kg após 4h e 6h, respectivamente, após a inflamação. Quatro horas após a inflamação, a análise histológica da pata dos animais tratados com 30 mg/kg de NTZ mostrou redução na migração de células inflamatórias em 65,77%. É importante destacar também que houve redução significativa do fator de necrose tumoral alfa (TNF-α) na fase inicial da inflamação, 2 horas após a administração do Cg. Houve inibição nas contorções abdominais em 54,14% e 56,21% nas doses de 30 e 90 mg/kg, respectivamente. No teste da formalina apenas a dose de 90 mg/kg apresentou ação antinociceptiva (54,85%; primeira fase e 45,67%; segunda fase). Os resultados do teste rota-rod mostraram que a coordenação motora não foi afetada com NTZ. **Conclusões:** Esta atividade anti-inflamatória da NTZ parece ser consequência da sua capacidade de reduzir os níveis de um importante mediador da resposta inflamatória e da dor o TNF-α.

Palavras-chave: Nitazoxanida, reposicionamento, antiinflamatório, antinociceptivo, edema de pata, fator de necrose tumoral alfa.

Introduction

Drug repositioning refers to the identification of new therapeutic indications for drugs already used in clinical practice and their application in the treatment of diseases that were not initially indicated. The advantages of this practice are evident: the drug has already been tested in all preclinical and clinical phases of drug development, has been used by humans and has well-established toxicology, pharmacology and safety data. The targeting of approved drugs is believed to be one of the most efficient and economical strategies for new drug development [1-3].

Nitazoxanide (NTZ) and tizoxanide (TIZ) are synthetic thiazolide derivatives discovered by Jean Francois Rossingnol [4]. NTZ is an anti-protozoal medicine clinically approved in the USA since 2002 and in Brazil since 2004 for treating various parasitic diseases in adults and children [5-10], being well tolerated, even at high doses [11, 12], with mild adverse reactions [5, 12, 13].

In addition to having a broad antiparasitic activity, NTZ and its circulating active metabolite, TIZ, have also been shown to have antimicrobial activity against various viruses [7-9, 14-20] and various aerobic and anaerobic bacteria [16, 21, 22].

Due to the broad spectrum of pathogens targeted by NTZ and TIZ, thiazolides might possess other pharmacological properties in addition to antimicrobial activity [23-26]. Although several *in vitro* studies have already demonstrated the anti-inflammatory effect of NTZ and its main active metabolite TIZ, the potential effect of these compounds on inflammation response, mainly *in vivo* inflammatory mouse models, has not been widely investigated [23-26]. There is only one *in vivo* study evaluating specifically the anti-inflammatory effect of NTZ in mice models of inflammation. In this study the NTZ reduced the plasma interleukin (IL)-6 levels in a mice model of thioglycollate-induced inflammation, but other inflammatory parameters were not evaluated [26].

The inflammatory response is a fundamental biological process that not only protects the host against infections by pathogens, but also promotes repair and healing after an injury [27, 28]. Failing to properly regulate inflammation results in a multitude of complications that are extremely harmful to the pulmonary, cerebrovascular and cardiovascular systems [27, 29-31]. The inflammatory process is part of the pathophysiology of several clinically important chronic diseases, such as asthma, obesity, cancer, cardiovascular diseases and diabetes [27, 29, 30, 32].

Non-steroidal anti-inflammatory drugs (NSAIDs) and glucocorticoids are the most commonly used drugs for the treatment of various types of inflammation and pain.

However, the chronic use of NSAIDs and glucocorticoids commonly induces gastrointestinal, cardiovascular, renal, hepatic, cerebral and pulmonary problems [33, 34]. In turn, analgesic opioids can cause constipation, nausea, vomiting, sedation, respiratory depression and dependence [35].

It is necessary to search for safer alternative therapies, since the inflammatory process is part of the pathophysiology of several important diseases [29, 30, 36]. Thus, the present study aimed to investigate the potential anti-inflammatory and antinociceptive activities of NTZ using *in vivo* mice models.

Materials and methods

Animals

Experiments were conducted using adult male Swiss (28–30 g) mice. Animals were housed in temperature-controlled rooms (22–25 °C), under a 12:12 h light-dark cycle, with free access to food and water, maintained for at least 7 days for acclimatization before the experiments. The feed was suspended 2 h before each experiment, leaving free access to water. The animals were randomly allocated to groups of six and seven animals each, for anti-inflammatory and antinociceptive tests, respectively. Each mouse was used only once during the study. All experimental protocols were by the guidelines adopted by the International Association for the Study of Pain and the Brazilian National Council for the Control of Animal Experimentation. The experiments were approved by the Ethics Committee in Animal Experimentation of the Federal University of São João del-Rei, Brazil (CEUA/UFSJ, protocol 016/2020 on 10/07/2020 and protocol 1699010321, on 04/01/2021). All efforts were made to minimize the number of animals and their suffering.

Anti-inflammatory activity

Carrageenan-induced mouse paw oedema

The antioedematogenic effect of NTZ was evaluated using Carrageenan (Cg)-induced mouse paw oedema. The Swiss mice were pre-treated orally with the vehicle (10 mL/kg, control group), NTZ (3, 10 and 30 mg/kg) or indomethacin (Ind; 10 mg/kg), 1 h before the intraplantar injection of Cg (400 μg/paw, 30 μL) into the left hind paw. The paw volume was measured by a blind evaluator using a plethysmometer (Insight®, Brazil) before treatment (basal) and 1, 2, 3, 4 and 6 h after injection of the Cg. The difference between paw volume before and after inflammatory stimulus injection was taken as the volume of oedema (μL). The percentage of oedema inhibition in treated mice was calculated in comparison with the respective the control group [37]. Carrageenan

λ type IV (22049) and indomethacin (I7378) were purchased from Sigma-Aldrich, Inc. (MO, USA) and NTZ (DCB 06413) was supplied by Eurofarma (SP, Brazil). Ind and Cg was dissolved in phosphate buffer saline (PBS) and Tween 20 solution and NTZ was diluted in PBS. The naive and control groups were treated with PBS.

Histopathological analysis

The animals were treated orally as follows: naive (PBS), control (PBS), NTZ (30 mg/kg) or Ind (10 mg/kg). One hour after oral treatment, Cg (400 μg/paw, 30 μL) was administered to the left hind paw of the animals, except for the naive group, which received an intraplantar injection of PBS. Samples of the footpad tissue were collected 4 h after the inflammatory stimulus and fixed in 4% Paraformaldehyde solution for 24 h. Paraffin blocks were then prepared, cut into 4 μm thick tissue sections and subsequently stained with hematoxylin-eosin (H&E) [38]. Images of the infiltration of inflammatory cells were obtained using a conventional optical microscope (Motic®) coupled to a capture system (Moticam 3000®), amplified 40x and 400x, and evaluated by two investigators using ImageJ® software, version 1.44 (Research Services Branch, U.S. National Institute of Health, Bethesda, MD, USA). The photomicrographs were used for the quantitative analysis of cell infiltration. The inflammatory cells were identified based on their characteristic morphology, in six different regions randomly selected for each animal, at 400x magnification. Subsequently, the total number of leukocytes was expressed as the number of cells/area analysed in μm^2.

Tumour necrosis factor alpha (TNF-α) levels in the tissue

The animals were treated orally as follows: naive (PBS), control (PBS), NTZ (30 mg/kg), Ind (10 mg/kg) or Dexamethasone (Dex; 1.5 mg/kg). One hour after treatment, Cg (400 μg/paw, 30 μL) was administered to the left hind paw of the animals, except for the naive group, which received an intraplantar injection of PBS. Samples of the plantar pads were collected 2 h after the inflammatory stimulus. The tissues from the pads were homogenised in 1 mL of cytokine extraction solution containing protease inhibitors (1 mL of solution for 50 mg of tissue) and 0.05% Tween 20. The samples were immediately ground and centrifuged at 3000 rpm for 8 minutes. The supernatant was then collected and stored in a -80 °C freezer until required. The TNF-α levels were determined using an enzyme-linked immunosorbent assay (ELISA), according to the kit manufacturer's instructions (eBioscience - 88-7324-88, San Diego, CA, USA) [39]. Dexamethasone (DCB02817) was purchased from Aché (SP, Brazil) and used as a commercial suspension.

Antinociceptive activity

Acetic acid-induced abdominal writhing test

The animals were treated orally as follows: control (PBS), NTZ (10, 30 and 90 mg/kg) or Ind (10 mg/kg). One hour after treatment, 1% acetic acid (10 mL/kg) was administered intraperitoneally (*ip*). The amount of abdominal writhing (abdominal contraction and/or simultaneous contraction of the abdomen with stretching of the hind limbs) was recorded 10 minutes after administration of the nociceptive stimulus, over 20 minutes, by a blind evaluator [40]. Acetic acid 96% (695092) was supplied by Merck KGaA (Darmstadt, Germany) and was diluted in PBS.

Formalin-induced nociception test

The animals were treated orally as follows: control (PBS), NTZ (10, 30 and 90 mg/kg) or Ind (10 mg/kg). Morphine (Mor; 7.5 mg/kg) was administered via *ip* injection. One hour after the oral treatments and 30 minutes after the *ip* treatment, 20 µL of 2.50% formaldehyde (formalin) was injected into the subplantar region of the left hind paw. The animals were then placed individually in an acrylic box and observed by a blind evaluator in two stages: 0-5 minutes (the first, neurogenic phase) and 15-30 minutes (the second, inflammatory phase). The time that the animal spent licking, biting or shaking their paw was timed and considered to be indicative of nociception [41]. Morphine (DCB 06090) sulphate was obtained from Cristália (SP, Brazil) and was used as a commercial injectable solution. Formaldehyde 37% (252549) were supplied by Merck KGaA (Darmstadt, Germany) and was diluted in PBS.

Rota-rod test

The day before the experiment, each animal was placed on a rotating bar at a speed of 24 rpm/min, using a cut-off time of 120 seconds (s). The time that each animal remained on the bar was recorded (the basal time). The following day, the animals were treated orally as follows: control group (PBS), NTZ (10, 30 and 90 mg/kg) or alprazolam (2 mg/kg). One hour after oral administration, the animals were placed on the rotating bar at the same speed, and the time the animals remained on the device was recorded at 30, 60, 120 and 150 minutes after treatments. Time until the first fall was recorded in seconds with a cut-off time of 120 s [42]. Alprazolam (DCB 00597) was supplied by Eurofarma (SP, Brazil) and was diluted in PBS.

Statistical analysis

The results are expressed as mean ± standard error of the mean (SEM). Statistical significance between groups was determined by one-way analysis of variance (ANOVA)

followed by Bonferroni's test. The level of significance ($p<0.05$, 0.01 or 0.001) was employed for each experimental model. The analyses were carried out using GraphPad Prism™ software, version 5.01 (GraphPad® Software Inc., San Diego, CA).

Results

Anti-inflammatory activity

Antioedematogenic effect of NTZ

The NTZ showed antioedematogenic activity at a dose of 10 mg/kg from the first hour (60.00%, $p<0.001$) to the fourth hour (21.43%, $p<0.05$) compared to the control group. At the 30 mg/kg dose, the inhibition of oedema occurred from the first hour (66.67%, $p<0.001$) and remained until the sixth hour (40.00%, $p<0.001$). Ind (10 mg/kg) inhibited oedema by 66.67% in the first hour ($p<0.001$), which was similar to the effect produced by NTZ at a dose of 10 mg/kg (Fig. 1a). In Fig.1b it is possible to confirm the antioedematogenic effect of NTZ compared to the control group. A greater thickening of the dermis and epidermis is evident in the control group in relation to the NTZ, Ind and naive groups. It is important to highlight that the antioedematogenic effect of NTZ was more noticeable compared to Ind.

Effect of NTZ on inflammatory infiltrate

In Fig. 2a, only discrete leukocytes are present in the naive group, probably indicating defence cells residing in the plantar tissue. On the other hand, the footpads of the control group show a significant infiltration of polymorphonuclear leukocytes, probably neutrophils, as they are the first cells to migrate in acute inflammatory processes. NTZ (30 mg/kg) and Ind (10 mg/kg) reduced the accumulation of leukocytes in the footpad. In Fig. 2b, it is important to note that, in comparison to the control group, NTZ reduced leukocyte migration (65.77%, $p<0.001$) in a similar manner to Ind (64.44%, $p<0.001$).

Effect of NTZ on TNF-α levels in the tissue

The level of TNF-α significantly increased in the footpads of the control group animals following Cg-induced inflammation. Treatment with NTZ (30 mg/kg) promoted a local decrease of TNF-α in the initial phase of the inflammatory response, 2 h after Cg, reducing the TNF-α level by 63.96% ($p<0.001$) (Fig. 3).

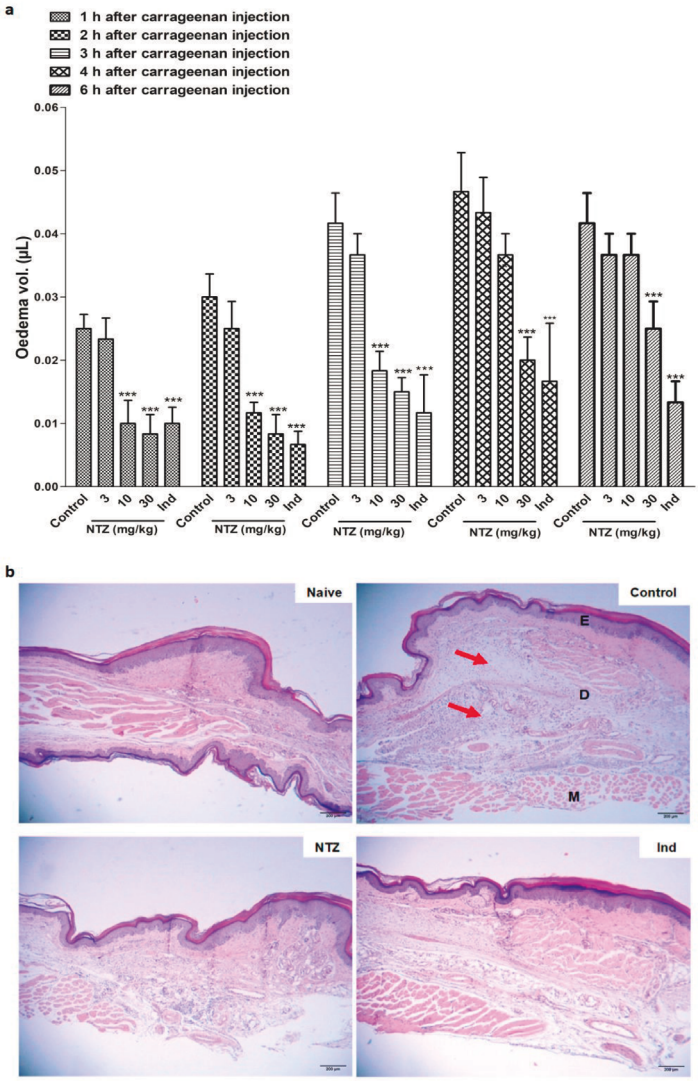

Fig. 1. a) Effect of NTZ (3, 10 and 30 mg/kg) and Ind (10 mg/kg) on Cg-induced paw oedema. NTZ and Ind were administered orally and Cg was administered via intraplantar. Each value represented as mean ± SEM (n = 6 per group). *p<0.05, and ***p<0.001 versus the respective control group (one-way ANOVA followed by Bonferoni's test). b) Effect of oral treatment with NTZ and Ind on paw oedema and leukocyte migration 4 hours after Cg stimulus. Representative histologic images from different experimental groups: Naive; Control; NTZ (30 mg/kg) and Ind (10 mg/kg). The arrows indicate the areas of oedema in the dermis and epidermis leading to increased thickness of the footpad. E: epidermis, D: dermis, M: muscle. Staining: haematoxylin-eosin (H&E). Magnification: 40x. Bar: 200 µm.

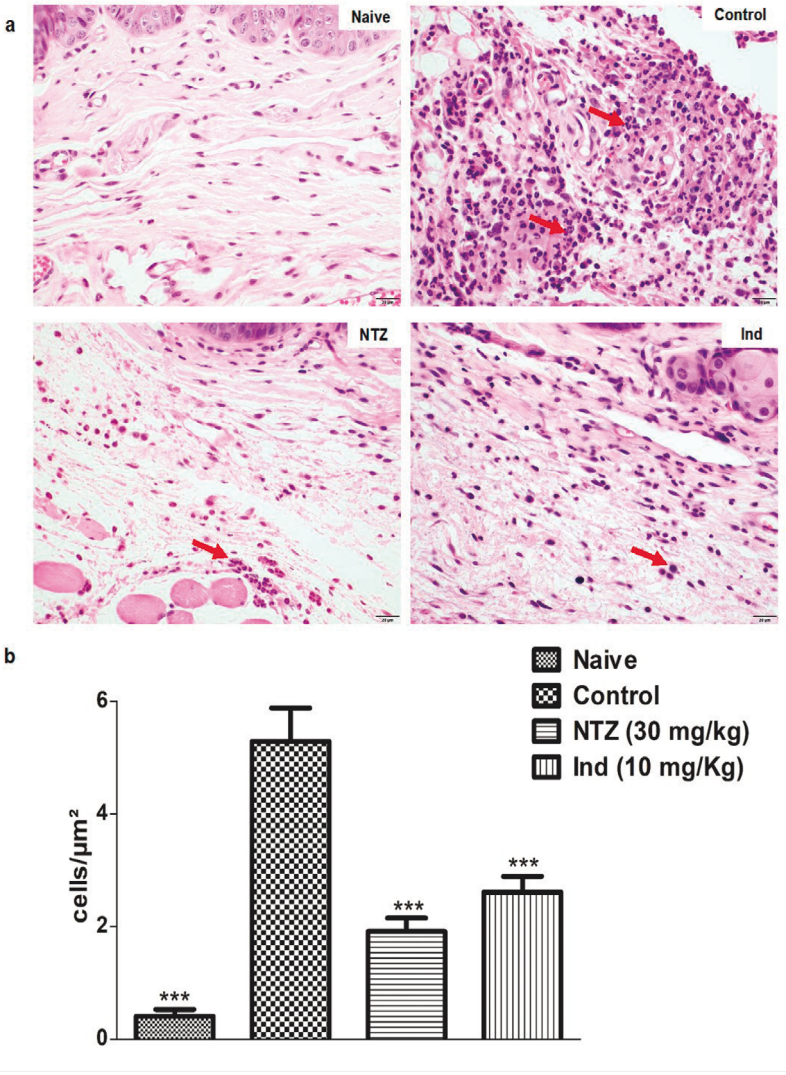

Fig. 2. a) Histopathological evaluation of mouse footpad tissue sections 4 h after the Cg intraplantar injection, demonstrating the effect of NTZ (30 mg/kg) and Ind (10 mg/kg), administered orally, on cellular migration. The arrows indicate leukocytes. Colour: haematoxylin-eosin (H&E). Magnification: 400x. Bar: 20 µm. b) Quantitative analysis of footpad sections collected 4 h post Cg injection, demonstrating the effect of NTZ (30 mg/kg) and Ind (10 mg/kg) on cellular migration. Each value represented as mean ± SEM (n = 6 per group). ***p<0.001 versus the control group (one-way ANOVA followed by Bonferroni's test).

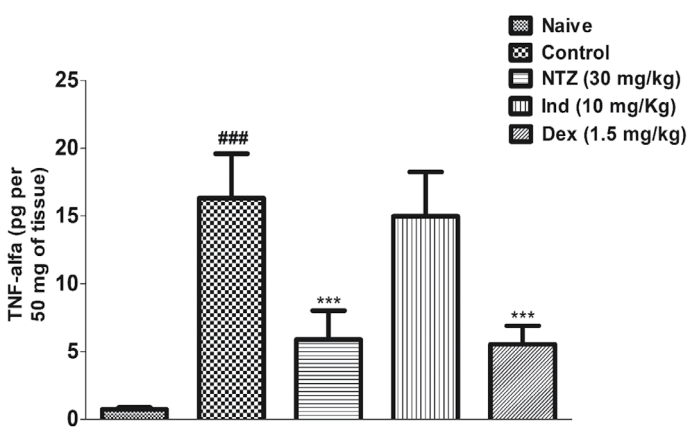

Fig. 3. Effect of NTZ (30 mg/kg), Ind (10 mg/kg) and Dex (1.5 mg/kg), administered orally, on TNF-α levels in footpads, 2 h following Cg-induced inflammation. Each value represented as mean ± SEM (n = 6 per group) ###p<0.001 control versus naive group; ***p<0.001 NTZ versus the control group (one-way ANOVA followed by Bonferroni's test).

Antinociceptive activity

Effect of NTZ on abdominal contortions

As the lowest dose of NTZ (3 mg/Kg) showed no activity on Cg-induced paw edema, doses of 10, 30 and 90 mg/Kg were used to assess antinociceptive activity. The administration of NTZ at doses of 30 and 90 mg/kg induced a statistically significant reduction in the number of abdominal contortions induced by acetic acid, with reductions of 54.14% (p<0.001), and 56.21% (p<0.001), respectively, compared to the control group. Meanwhile, Ind (10 mg/kg) caused a decrease of 73.20% (p<0.001) compared to the control group (Fig. 4).

Effect of NTZ on formalin-induced nociception

The Fig. 5 shows that only the group treated with the highest dose of NTZ (90 mg/kg) was able to significantly reduce the reaction time of the animals, by 54.85% (p<0.01) and 45.67% (p<0.05) in the first and second phases of the test, respectively, compared to the control group. As expected, Ind (10 mg/kg), being a NSAID, showed a reduction in reaction time only in the inflammatory phase, by 59.48% (p<0.05), while Mor (7.5 mg/Kg), being an opioid, was able to act in the first and second phases of the formalin test (p<0.001).

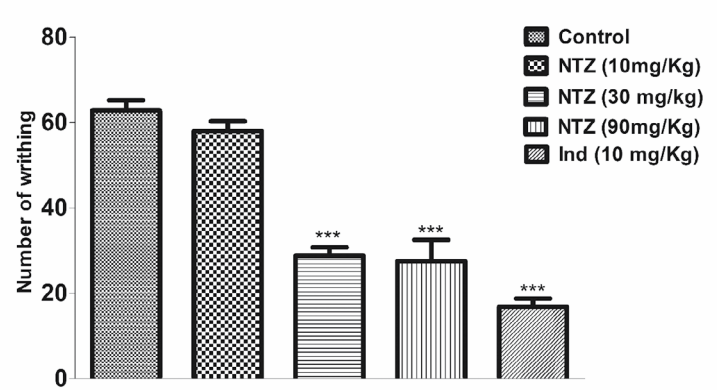

Fig. 4. Effect of NTZ (10, 30 and 90 mg/kg) and Ind (10 mg/kg), administered orally, on acetic acid-induced abdominal writhing. Each value represented as mean ± SEM (n = 7 per group). ***p<0.001 versus the control group (one-way ANOVA followed by Bonferroni's test).

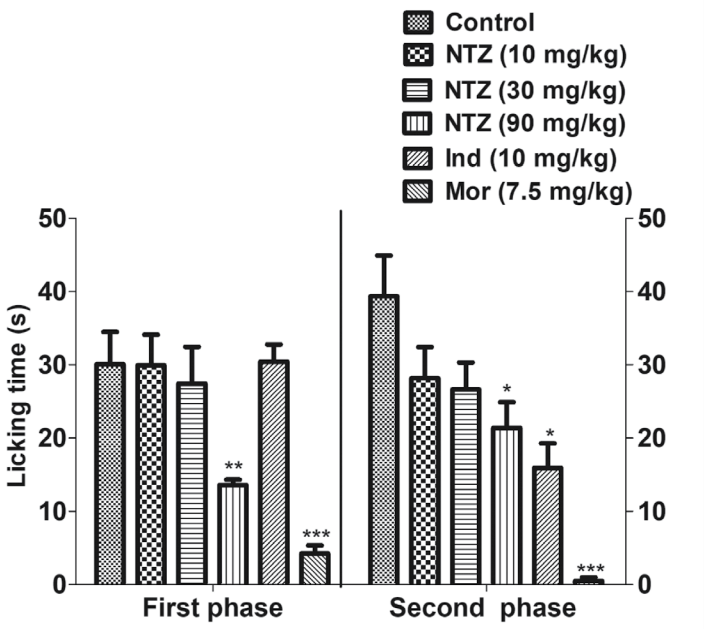

Fig. 5. Effect of NTZ (10, 30 and 90 mg/kg), Ind (10 mg/kg), administered orally, and Mor (7.5 mg/kg), via intraperitoneal, on the animals' reaction time in the formalin test. Each value represented as mean ± SEM (n = 7 per group). *p<0.05, **p<0.01 and ***p<0.001 versus the respective control group (one-way ANOVA followed by Bonferroni's test).

Effect of NTZ on motor coordination and balance

The results showed no statistical difference between the control groups and all tested doses of NTZ (10, 30 and 90 mg/kg) at any of the analysed times, after oral treatments (30, 60, 120 and 150 minutes). In contrast, animals treated with alprazolam remained on the bar for a significantly shorter period in seconds (s) ($p<0.001$) compared to the control group, as shown in Table 1.

Table 1. Effect of NTZ on motor coordination

Treatment	Time after treatment (min)			
	30	60	120	150
	Time on rod (s)	Time on rod (s)	Time on rod (s)	Time on rod (s)
Control	120±0.00	120±0.00	120±0.00	120±0.00
NTZ (10 mg/kg)	120±0.00	120±0.00	120±0.00	120±0.00
NTZ (30 mg/kg)	120±0.00	120±0.00	120±0.00	120±0.00
NTZ (90 mg/kg)	120±0.00	120±0.00	120±0.00	113.714±6.286
Alprazolam (2 mg/kg)	3.000±0.707*	14.250±3.425*	26.000±10.384*	28.250±16.332*

Each value represented as mean ± SEM (n = 7 per group). *$p<0.001$ versus the control group (one-way ANOVA followed by Bonferroni's test).

Discussion

The present study demonstrates that NTZ has an anti-inflammatory and antinociceptive activity in these *in vivo* models of inflammation and pain. NTZ was able to inhibit oedema and reduce leukocyte migration and TNF-α levels in tissue inflamed with Cg. NTZ also reduced the number of abdominal contortions induced by acetic acid and reduced the reaction time in the formalin-injected paw model, without altering motor function or balance.

Several previous works have demonstrated the ability of NTZ and TIZ to modulate the inflammatory response due to their anti-inflammatory activity. However, most of these studies evaluated the anti-inflammatory or modulatory effect of NTZ or TIZ in cell cultures [5, 14, 23-26, 43, 44], contributing to the decision to evaluate the possible anti-inflammatory and antinociceptive effect of NTZ using *in vivo* mice models.

To evaluate the anti-inflammatory activity, the Cg-induced paw oedema model was initially used, which is a classic, simple and effective experimental model to study inflammation and inflammatory pain. This model consists of two phases and is associated with the release of several inflammatory mediators. The first, (or initial) phase

mainly involves the release of serotonin, histamine, bradykinin and cyclooxygenase (COX) products. The second (or late) phase is related to leukocyte infiltration, further prostaglandin release, and the production of oxygen-derived free radicals, nitric oxide (NO) and cytokines [38, 45, 46]. Our results showed that NTZ significantly inhibited the formation of paw oedema, indicating that this compound has a potential anti-inflammatory effect since oedema is one of the main signs of inflammation.

To confirm the anti-inflammatory effect of NTZ, cell migration was also evaluated to verify whether the antioedematogenic activity is also associated with a decrease in leukocyte migration. The histological results indicated that Cg-induced inflammation is associated with intense oedema and migration of the infiltrate of inflammatory polymorphonuclear cells, probably neutrophils. This is in line with our previous studies, which also demonstrated an increase in cell migration to the Cg-inflamed site [47, 48]. The NTZ treatment significantly diminished oedema and the cell tissue migration, which is another important parameter of inflammation.

During the acute inflammatory response, leukocytes are important for tissue repair and are an essential part of the immune response. However, during diapedesis, these cells can attack the vessel wall and cause the extravasation of interstitial fluid, inducing the formation of oedema, and their support favours the permanence of cytokines at the site. Therefore, large amounts of leukocytes can have deleterious effects on tissue. Thus, drugs that decrease the passage of blood cells to extravascular tissue may be useful in therapy [28, 49]. Neutrophil migration is considered to be one of the central reactions of inflammation because they are innate effector cells and can respond quickly to danger signals. Neutrophils stimulate the release of several inflammatory mediators, such as NO, attracting more leukocytes to the site of injury, and initiating and maintaining the inflammatory process, thus being an important component of the immune response. Neutrophils can also release TNF-α and other cytokines that can also, indirectly, stimulate the arrival of more neutrophils [50]. The effect of NTZ suggests an association between the reduction of oedema and consequently in tissue cell migration, with a modulation in the production of cytokines.

One *in vivo* study evaluated the potential anti-inflammatory effect of NTZ in a mice model of thioglycollate-induced inflammation; the only anti-inflammatory parameter evaluated was the production of IL-6, which was also shown to be reduced [26].

Cytokines play an important role in the inflammatory response and some, such as TNF-α, deserve to be highlighted. TNF-α creates positive feedback to increase the production of NO, which acts as a vasodilator and induces the activation of adhesion molecules, favouring the continuation and amplification of oedema, cell tissue migra-

tion and inflammation. TNF-α also exerts several other biological effects that influence the development and maintenance of chronic inflammatory conditions, such as activating an important cell signalling pathway, the nuclear factor-kappa B (NF-κB) pathway [51-56]. Previous studies conducted by our group have already demonstrated the important participation of TNF-α in the inflammatory responses induced in this *in vivo* model [47, 48, 57, 58].

The NTZ was also able to reduce tissue TNF-α levels in the early stage of the inflammatory response. This decrease in TNF-α, 2 hours after the Cg inflammatory stimulus, seems to be important for the reduction in inflammatory cell migration observed later, 4 hours after the inflammatory stimulus.

This result is in agreement with several other studies that have also demonstrated the ability of NTZ and/or its active metabolite TIZ to inhibit TNF-α levels and other important inflammatory mediators. One of these studies showed that NTZ inhibited the production of pro-inflammatory cytokines such as TNF-α, IL-5, IL-6 and IL-8 in peripheral blood mononuclear cells [14]. Blum *et al*. also demonstrated a reduction of inflammatory markers such as TNF-α, IL-6 and IL-8 in a small pilot trial in patients with moderate COVID-19 treated with NTZ [20]. In another study on the LPS-induced inflammatory response in cells of microglia, TIZ treatment also decreased the release of pro-inflammatory cytokines, including TNF-α, IL-1β and IL-6, and chemokines, such as CCL-2 and CCL-3, as well as the extrinsic expression of inducible nitric oxide synthase (iNOS) and COX-2 expression [59, 60]. Fan *et al*. also demonstrated that NTZ reduced the levels of TNF-α, IL-1β and iNOS in the LPS-induced inflammatory response in cells of microglia [61]. Meanwhile, Hong *et al*. demonstrated that NTZ decreased IL-6 production in LPS-stimulated RAW 264.7 cells and peritoneal macrophages, and also showed that NTZ was able to suppress LPS-induced IL-6 messenger ribonucleic acid (mRNA) expression [26]. Salazar *et al.* found that NTZ was able to reduce the concentration of pro-inflammatory cytokines such as IL-2, IL-6 and IL-1β in cultures of human peripheral blood mononuclear cells and decrease the monocyte/macrophage M1/M2 ratio [62]. In addition, Tantawy *et al*. demonstrated that NTZ induces a decrease of IL-6 via the inhibition of JAK 2/STAT3, an important signal transduction pathway in the inflammatory response [63]. Thus, these studies suggest that NTZ has potential immunomodulatory and anti-inflammatory effects by inhibiting cell proliferation and reducing the levels of pro-inflammatory cytokines.

The inhibition of cytokines and their signalling pathways may indicate an effective therapy against inflammatory diseases [64, 65]. Shou *et al*. demonstrated that treatment with TIZ, the active metabolite of NTZ, reduced the inflammatory response in macrophage cell lines by suppressing the NF-κB, mitogen-activated protein kinase

(MAPK) [25] and PI3K/Akt/mTOR [23] signalling pathways. Fan *et al*. also demonstrated that NTZ inhibits NF-κB and PI3K/Akt/mTOR pathway signalling *in vitro* [61]. These signalling pathways are of particular importance in immune and inflammatory responses. Numerous stimuli are responsible for activating these pathways, such as protein kinase C, viruses, oxidants and pro-inflammatory cytokines, such as TNF-α, IL-1 and IL-6. Among the genes regulated by these signalling pathways are those involved in the production of pro-inflammatory cytokines, such as TNF-α, chemokines and adhesion molecules. Activation of these pathways therefore leads to a coordinated increase in the expression of numerous genes, whose products are related to the modulation of inflammatory and immune responses [66-70].

In this sense, through modulation of the signal transduction pathways of the inflammatory response, NTZ can reduce the tissue production of numerous inflammatory mediators, such as TNF-α.

The inhibition of inflammatory cytokines by signalling pathway suppression has been identified as a key step in the treatment of inflammation and therefore serves as an important target for drug development [23, 25, 67]. Thus, a good strategy in fighting inflammation is to search for new drugs with a multifactorial mode of anti-inflammatory action [23, 25, 71], and NTZ exhibits polypharmacological actions [11, 16, 72].

As NTZ has been shown to have an anti-inflammatory effect, and pain is a cardinal sign of inflammation, there is also a need to investigate the antinociceptive activity of NTZ, since these properties are shared by several NSAIDs. In our study, the investigation of antinociceptive activity started with a test of the abdominal writhing induced by acetic acid. This is a nonspecific test, in which even weak analgesics can present antinociceptive effects. In addition, with this test, it is not possible to determine the specific pharmacological pathways involved in the effect [73, 74]. The acid induces an increase in the release of inflammatory mediators, such as TNF-α and prostaglandins, which sensitise nociceptive fibers and lead to nociception [51, 73, 75, 76].

Our results demonstrated that NTZ showed significant antinociceptive activity in this model at doses of 30 and 90 mg/kg. This effect may be related to the inhibition of the inflammatory mediators. Thus, at least in part, the antinociceptive effect of NTZ may be a consequence of the suppression of TNF-α. Blum *et al*. evaluated the safety and efficacy of NTZ in patients with moderate COVID-19 and observed that NTZ statistically reduced the levels of TNF-α and IL-8 [20], which cytokines are known to be important for nociception. TNF-α promotes nociception in mice by two independent correlated pathways: (1) stimulation of interleukin (IL-1) release that leads to prostanoid production; and (2) keratinocyte-derived chemokines (KC/CXCL1/IL-8) that induce

both prostanoids and sympathetic amine release [77]. TNF-α can also induce nociception through direct action on the nociceptors, via tumour necrosis factor receptor 1 (TNFR1) activation [78].

The next step was to perform the formalin test, which is a more refined test capable of evaluating the central and peripheral activities of NTZ and confirming whether the antinociception was related to an anti-inflammatory effect. The formalin test is divided into two phases of nociceptive stimulation, the first being neurogenic (central) and the second being the inflammatory (peripheral) phase. The primary or neurogenic phase reflects centrally mediated pain with the release of substance P, being related to the direct stimulation of primary sensory neurons. The secondary or inflammatory phase is associated with peripheral sensitization, when pro-inflammatory cytokines are released, including TNF-α, histamine, serotonin and prostaglandins [79, 80]. Only at the highest dose (90 mg/kg) did NTZ significantly suppress the response in the neurogenic and inflammatory phases, leading to the hypothesis that NTZ has weak central and peripheral antinociceptive activity. Ai *et al*. demonstrated that the intraperitoneal administration of NTZ significantly reversed mechanical hyperalgesia in a model of neuropathic pain in rats [81]. The anti-inflammatory effect of NTZ, previously observed in the present study, corroborates the inhibitory effect of NTZ on the second phase of formalin-induced nociception.

Once the effect of NTZ had been shown in both phases of the formalin test, it was interesting to assess whether this inhibition in response could be due to the muscle relaxant action of NTZ, via its action on the central nervous system. The rota-rod test is widely used to assess central nervous system depression, possible muscle relaxation, and loss of balance [82]. The results of the rota-rod test suggest that NTZ was not able to change the motor capacity or balance of the animals, indicating that the minor antinociceptive effect presented by NTZ in the first phase of formalin test does not interfere with these characteristics.

Conclusion

The present study demonstrated that NTZ exhibits a significant anti-inflammatory activity in *in vivo* acute models of inflammation and pain. This effect appears to be a consequence of its ability to reduce the levels of an important polymorphonuclear leucocyte-derived inflammatory and pain mediator, TNF-α, reducing the oedema and leucocyte migration.

Acknowledgments

livian Rabelo Lopes acknowledges the Higher Education Personnel Improvement Coordination (CAPES) for the postgraduate fellowship.

Compliance with ethical standards

Ethical approval: The experiments were approved by the ehics committee in animal experimentation of the Federal University of São João del-Rei, Brazil (CEUA/UFSJ, protocol 016/2020 on 10/07/2020 and protocol 1699010321, on 04/01/2021).

Funding: This research receive funding from Federal University of São João del-Rei.

Author contributions: All authors contributed to the development, analysis, writing and review of this article.

Conflict of interest

The authors declare that they have no conflict of interest.

References

1. Y. Hua, X. Dai, Y. Xu, G. Xing, H. Liu, T. Lu, Y. Chen, Y. Zhang, Drug repositioning: Progress and challenges in drug discovery for various diseases, *European Journal of Medicinal Chemistry*, **234**, 114239 (2022). Doi: https://doi.org/10.1016/j.ejmech.2022.114239

2. J.-P. Jourdan, R. Bureau, C. Rochais, P. Dallemagne, Drug repositioning: A brief overview, *Journal of Pharmacy and Pharmacology*, **72**(9), 1145-1151 (2020). Doi: https://doi.org/10.1111/jphp.13273

3. X. Hanqing, L. Jie, X. Haozhe, Y. Wang. Review of drug repositioning approaches and resources, *International Journal of Biological Sciences*, **14**(10), 1232-1244 (2018). Doi: https://doi.org/10.7150/ijbs.24612

4. V.S. Somvanshi, B.L. Ellis, Y. Hu, R.V. Aroian, Nitazoxanide: Nematicidal mode of action and drug combination studies, *Molecular and Biochemical Parasitology*, **193**(1), 1-8 (2014). Doi: https://doi.org/10.1016/j.molbiopara.2013.12.002

5. L.D. Jasenosky, C. Cadena, C.E. Mire, V. Borisevich, V. Haridas, S. Ranjbar, A. Nambu, S. Bavari, V. Soloveva, S. Sadukhan, G.H. Cassell, T.W. Geisbert, S. Hur, A.E. Goldfeld, The FDA-approved oral drug nitazoxanide amplifies host antiviral responses and inhibits Ebola virus, *iScience*, **19**, 1279-1290 (2019). Doi: https://doi.org/10.1016/j.isci.2019.07.003

6. G.A.R. Soriano, J. Blac, Nitazoxanide use as part of an empiric multidrug regimen in treating children with suspected *Helicobacter pylori* infection, *Case Reports in Gastroenterology*, **9**(1), 36-42 (2015). Doi: https://doi.org/10.1159/000375116

7. A.V. Stachulski, C. Pidathala, E.A. Row, R. Sharma, N.G. Berry, M. Iqbal, J. Bentley, S.A. Allman, G. Edwards, A. Helm, J. Hellier, B.E. Korba, J.E. Semple, J.-F. Rossignol, Thiazolides as novel antiviral agents: 1. Inhibition of hepatitis B virus replication, *Journal of Medicinal Chemistry*, **54**(12), 4119-4132 (2011). Doi: https://doi.org/10.1021/jm200153p

8. J.F. Rossignol, Thiazolides: A new class of antiviral drugs, *Expert Opinion on Drug Metabolism & Toxicology*, **5**(6), 667-674 (2009). Doi: https://doi.org/10.1517/17425250902988487

9. J.F. Rossignol, S.L. Frazia, L. Chiappa, A. Ciucci, M.G. Santoro, Thiazolides, a new class of anti-influenza molecules targeting viral hemagglutinin at the posttranslational level, *Journal of Biological Chemistry*, **284**(43), 29798-29808 (2009). Doi: https://doi.org/10.1074/jbc.M109.029470

10. L.M. Fox, L.D. Saravolatz, Nitazoxanide: A new thiazolide antiparasitic agent, *Clinical Infectious Diseases*, **40**(8), 1173-1180 (2005). Doi: https://doi.org/10.1086/428839

11. A.S. Lokhande, P.V. Devarajan, A review on possible mechanistic insights of nitazoxanide for repurposing in COVID-19, *European Journal of Pharmacology*, **891**, 173748 (2021). Doi: https://doi.org/10.1016/j.ejphar.2020.173748

12. L.E. Walker, R. FitzGerald, G. Saunders, R. Lyon, M. Fisher, K. Martin, I. Eberhart, C. Woods, S. Ewings, C. Hale, *et al.*, An open-label, adaptive, phase 1 trial of high-dose oral nitazoxanide in healthy volunteers: An antiviral candidate for SARS-CoV-2, *Clinical Pharmacology & Therapeutics*, **111**(3), 585-594 (2022). Doi: https://doi.org/10.1002/cpt.2463

13. S. Abd-Elsalam, Sherief, F. El-Kalla, N. Elwan, R. Badawi, N. Hawash, S. Soliman, S. Soliman, W. Elkhalawany, M.-A. ElSawaf, A. Elfert, A randomized controlled trial comparing nitazoxanide plus lactulose with lactulose alone in the treatment of overt hepatic encephalopathy, *Journal of Clinical Gastroenterology*, **53**(3), 226-230 (2019). Doi: https://doi.org/10.1097/MCG.0000000000001040

14. J.-F. Rossignol, Nitazoxanide, a new drug candidate for the treatment of Middle East respiratory syndrome coronavirus, *Journal of Infection and Public Health*, **9**(3), 227-230 (2016). Doi: https://doi.org/10.1016/j.jiph.2016.04.001

15. G. Belardo, O. Cenciarelli, S. La Frazia, J.-F. Rossignol, M.G. Santoro, Synergistic effect of nitazoxanide with neuraminidase inhibitors against influenza A viruses *in vitro*, *Antimicrobial Agents and Chemotherapy*, **59**(2), 1061-1069 (2015). Doi: https://doi.org/10.1128/AAC.03947-14

16. J.-F. Rossignol, Nitazoxanide: A first-in-class broad-spectrum antiviral agent, *Antiviral Research*, **110**, 94-103 (2014). Doi: https://doi.org/10.1016/j.antiviral.2014.07.014

17. J.-F. Rossignol, E.B. Keeffe, Thiazolides: A new class of drugs for the treatment of chronic hepatitis B and C, *Future Microbiology*, **3**(5), 539-545 (2008). Doi: https://doi.org/10.2217/17460913.3.5.539

18. J. Haffizulla, A. Hartman, M. Hoppers, H. Resnick, S. Samudrala, C. Ginocchio, M. Bardin, J.-F. Rossignol, Effect of nitazoxanide in adults and adolescents with acute uncomplicated influenza: A double-blind, randomized, placebo-controlled, phase 2b/3 trial, *The Lancet: Infectious Diseases*, **14**(7), 609-618 (2014). Doi: https://doi.org/10.1016/S1473-3099(14)70717-0

19. P.R.M. Rocco, P.L. Silva, F.F. Cruz, M.A.C. Melo-Junior, P.F.G.M.M. Tierno, M.A. Moura, L.F.G. De Oliveira, C.C. Lima, E.A. Dos Santos, W.F. Junior, A.P.S.M. Fernandes, K.G. Franchini, E. Magri, N.F. de Moraes, J.M.J. Gonçalves, M.N. Carbonieri, I.S. Dos Santos, N.F. Paes, P.V.M. Maciel, R.P. Rocha, A.F. de Carvalho, P.A. Alves, J.L. Proença-Módena, A.T. Cordeiro, D.B.B. Trivella, R.E. Marques, R.R. Luiz, P.Pelosi, J.R. Lapa e Silva, Early use of nitazoxanide in mild COVID-19 disease: A randomized, placebo-controlled trial, *European Respiratory Journal*, **58**(1), 2003725 (2021). Doi: https://doi.org/10.1183/13993003.03725-2020

20. V.F. Blum, S. Cimerman, J.R. Hunter, P. Tierno, A. Lacerda, A. Soeiro, F. Cardoso, N.C. Bellei, J. Maricato, N. Mantovani, M. Vassao, D. Dias, J. Galinskas, L.M. Ramos-Janini, J.R. Santos-Oliveira, A.M. Da-Cruz, R.S. Diaz, Show less Nitazoxanide superiority to placebo to treat moderate COVID-19 - A pilot prove of concept randomized double-blind clinical trial, *eClinicalMedicine*, **37**, 100981 (2021). Doi: https://doi.org/10.1016/j.eclinm.2021.100981

21. Y. Guttner, H.M. Windsor, C.H. Viiala, L. Dusci, B.J. Marshall, Nitazoxanide in treatment of *Helicobacter pylori*: A clinical and *in vitro* study, *Antimicrobial Agents and Chemotherapy*, **47**(12), 3780-3783 (2003). Doi: https://doi.org/10.1128/AAC.47.12.3780-3783.2003

22. L. Dubreuil, I. Houcke, Y. Mouton, J.-F. Rossignol, *In vitro* evaluation of activities of nitazoxanide and tizoxanide against anaerobes and aerobic organisms, *Antimicrobial Agents and Chemotherapy*, **40**(10), 2266-2270 (1996). Doi: https://doi.org/10.1128/AAC.40.10.2266

23. J. Shou, M. Wang, X. Cheng, X. Wang, L. Zhang, Y. Liu, C. Fei, C. Wang, F. Gu, F. Xue, J. Li, K. Zhang, Tizoxanide induces autophagy by inhibiting PI3K/Akt/mTOR pathway in RAW264.7 macrophage cells, *Archives of Pharmacal Research*, **43**(2), 257-270 (2020). Doi: https://doi.org/10.1007/s12272-019-01202-4

24. J. Shou, X. Cheng, X. Wang, F. Xue, M. Wang, Y. Liu, *et al.*, Effects of tizoxanide on oxidative stress and inflammatory cytokine on lipopolysaccharide induced in raw264.7 cells, *Chinese Journal of Animal Infectious Diseases*, **27**(2), 71-77 (2019).

25. J. Shou, X. Kong, X. Wang, Y. Tang, C. Wang, M. Wang, L. Zhang, Y. Liu, C. Fei, F. Xue, J. Li, K. Zhang, Tizoxanide inhibits inflammation in LPS-activated RAW264.7 macrophages via the suppression of NF-κB and MAPKs activation, *Inflammation*, **42**(4), 1336-1349 (2019). Doi: https://doi.org/10.1007/s10753-019-00994-3

26. S.K. Hong, H.J. Kim, C.S. Song, I.S. Choi, J.B. Lee, S.Y. Park, Nitazoxanide suppresses IL-6 production in LPS-stimulated mouse macrophages and TG-injected mice, *International Immunopharmacology*, **13**(1), 23-27 (2012). Doi: https://doi.org/10.1016/j.intimp.2012.03.002

27. C.J. Hall, S.M. Wicker, A.T. Chien, A. Tromp, L.M. Lawrence, X. Sun, G.W. Krissansen, K.E. Crosier, P.S. Crosier, Repositioning drugs for inflammatory disease – Fishing for new anti-inflammatory agents, *Disease Models & Mechanisms*, **7**(9), 1069-1081 (2014). Doi: https://doi.org/10.1242/dmm.016873

28. R. Medzhitov, C. Janeway, Jr., Innate immunity, *The New England Journal of Medicine*, **343**(5), 338-344 (2008). Doi: https://doi.org/10.1056/NEJM200008033430506

29. A. Roy, M. Srivastava, U. Saqib, D. Liu, S. M. Faisal, S. Sugathan, S. Bishnoi, M.S. Baig, Potential therapeutic targets for inflammation in toll-like receptor 4 (TLR4)-mediated signaling pathways, *International Immunopharmacology*, **40**, 79-89 (2016). Doi: https://doi.org/10.1016/j.intimp.2016.08.026

30. M.D. Howard, E.D. Hood, B. Zern, V.V. Shuvaev, T. Grosser, V.R. Muzykantov, Nanocarriers for vascular delivery of anti-inflammatory agents, *Annual Review of Pharmacology and Toxicology*, **54**, 205-226 (2014). Doi: https://doi.org/10.1146/annurev-pharmtox-011613-140002

31. D. Mathis, S.E. Shoelson, Immunometabolism: An emerging frontier, *Nature Reviews Immunology*, **11**, 81-83 (2011). Doi: https://doi.org/10.1038/nri2922

32. S. Alrdahe, A.H. Sadoun, T. Torbica, A.E. Mckenzie, F.L. Boliche, A.J.M. Boulton, K.A. Mace, Dysregulation of macrophage development and phenotype in diabetic human macrophages can be rescued by Hoxa3 protein transduction, *PLoS One*, **14**(10), e0223980 (2019). Doi: https://doi.org/10.1371/journal.pone.0223980

33. S. Bindu, S. Mazumder, U. Bandyopadhyay, Non-steroidal anti-inflammatory drugs (NSAIDs) and organ damage: A current perspective, *Biochemical Pharmacology*, **180**, 114147 (2020). Doi: https://doi.org/10.1016/j.bcp.2020.114147

34. C. Strehl, L. Ehlers, T. Gaber, F. Buttgereit, Glucocorticoids-all-rounders tackling the versatile players of the immune system, *Frontiers in Immunology*, **10**, 1744 (2019). Doi: https://doi.org/10.3389/fimmu.2019.01744

35. J. Zhao, S. Cai, L. Zhang, Y. Rao, X. Kang, Z. Feng, Progress, challenges, and prospects of research on the effect of gene polymorphisms on adverse reactions to opioids, *Pain and Therapy*, **11**(2), 395-409 (2022). Doi: https://doi.org/10.1007/s40122-022-00374-0

36. X.-M. Peng, G.V.L. Damu, C.-H. Zhou, Current developments of coumarin compounds in medicinal chemistry, *Current Pharmaceutical Design*, **19**(21), 3884-3930 (2013). Doi: https://doi.org/10.2174/1381612811319210013

37. L. Levy, Carrageenan paw edema in the mouse, *Life Sciences*, **8**(11, Part 1), 601-606 (1969). Doi: https://doi.org/10.1016/0024-3205(69)90021-6

38. H. Sadeghi, V. Hajhashemi, M. Minaiyan, A. Movahedian, A. Talebi, A. Ardeshir, A study on the mechanisms involving the anti-inflammatory effect of amitriptyline in carrageenan-induced paw edema in rats, *European Journal of Pharmacology*, **667**(1-3), 396-401 (2011). Doi: https://doi.org/10.1016/j.ejphar.2011.05.053

39. H.C. Santiago, M.F.B. Pires, D.G. Souza, E. Roffê, D.F. Côrtes, W.L. Tafuri, M.M. Teixeira, LQ. Vieira, Platelet activating factor receptor-deficient mice present delayed interferon-γ upregulation and high susceptibility to *Leishmania amazonensis* infection, *Microbes and Infection*, **8**(11), 2569-2577 (2006). Doi: https://doi.org/10.1016/j.micinf.2006.06.011

40. R. Koster, M. Anderson, E.J. De Beer, Acetic acid for analgesic screening, *Federation Procedures*, **18**, 412-417 (1959).

41. S. Hunskaar, K. Hole, The formalin test in mice: Dissociation between inflammatory and non-inflammatory pain, *Pain*, **30**(1), 103-114 (1987). Doi: https://doi.org/10.1016/0304-3959(87)90088-1

42. Z.R. Vaz, V.C. Filho, R.A. Yunes, J.B. Calixto, Antinociceptive action of 2-(4-bromobenzoyl)-3-methyl-4,6-dimethoxy benzofuran, a novel xanthoxyline derivative on chemical and thermal models of nociception in mice, *Journal of Pharmacology and Experimental Therapeutics*, **278**(1), 304-312 (1996). URL: https://jpet.aspetjournals.org/content/278/1/304

43. P.R. Martins-Filho, J.A. Barreto-Alves, R. Fakhouri, Potential role for nitazoxanide in treating SARS-CoV-2 infection, *American Journal of Physiology: Lung Cellular and Molecular Physiology*, **319**(1), L35-L36 (2020). Doi: https://doi.org/10.1152/ajplung.00170.2020

44. A. Shakya, H.R. Bhat, S.K. Ghosh, Update on nitazoxanide: A multifunctional chemotherapeutic agent, *Current Drug Discovery Technologies*, **15**(3), 201-213 (2018). Doi: https://doi.org/10.2174/1570163814666170727130003

45. K.R. Patil, B.M. Mahajan, S.B. Unger, N.S. Goyal, S. Belemkar, S.J. Surana, S. Ojha, C.R. Patil, Animal models of inflammation for screening of anti-inflammatory drugs: Implications for the discovery and development of phytopharmaceuticals, *International Journal of Molecular Sciences*, **20**(18), 4367 (2019). Doi: https://doi.org/10.3390/ijms20184367

46. I.G. Otterness, P.F. Moore, Carragenan foot edema test, *Methods in Enzymology*, **62**, 320-327 (1988). Doi: https://doi.org/10.1016/0076-6879(88)62086-6

47. A.A. Saldanha, L. Fernandes do Carmo, S. Batista do Nascimento, N. Alves de Matos, C. de Carvalho-Veloso, A.H. Fonsêca-Castro, R.C.H. De Vos, A. Klein, J.M. de Siqueira, C.A. Carollo, T. Vieira do Nascimento, M.C. Toffoli-Kadri, A.C. Soares, Chemical composition and anti-inflammatory activity of the leaves of *Byrsonima verbascifolia*, *Journal of Natural Medicines*, **70**(4), 760-768 (2016). Doi: https://doi.org/10.1007/s11418-016-1011-3

48. A.A. Saldanha, J.M. de Siqueira, A.H. Fonsêca-Castro, R.I.M. de Azambuja-Ribeiro, F. Martins de Oliveira, D. de Oliveira-Lopes, F.C.H. Pinto, D. Brentan-Silva, A.C. Soares, Anti-inflammatory effects of the butanolic fraction of *Byrsonima verbascifolia* leaves: Mechanisms involving inhibition of tumor necrosis factor alpha, prostaglandin E2 production, and migration of polymorphonuclear leucocyte *in vivo* experimentation, *International Immunopharmacology*, **31**, 123-131 (2016). Doi: https://doi.org/10.1016/j.intimp.2015.12.031

49. M.A. Sugimoto, L.P. Sousa, V. Pinho, M. Perretti, M.M. Teixeira, Resolution of inflammation: What controls its onset? *Frontiers in Immunology*, **7**, 160 (2016). Doi: https://doi.org/10.3389/fimmu.2016.00160

50. R.F. Kraus, M.A. Gruber, Neutrophils from bone marrow to first-line defense of the innate immune system, *Frontiers in Immunology*, **12**, 767175 (2021). Doi: https://doi.org/10.3389/fimmu.2021.767175

51. A.G.M. Pacheco, E.J. Pacheco, L.A.R.O. Macedo, J.C. Silva, S.R.G. Lima-Saraiva, V.P. Barros, A. Brancoa, J.S.S. Quintansd, L.J. Quintans-Junior, H.D.M. Coutinhoe, I.R.A. Menezese, J.R.G.S. Almeida, Antinociceptive and anti-inflammatory activities of *Hymenaea martiana* Hayne (Fabaceae) in mice, *Brazilian Journal of Biology*, **82**, e240359 (2022). Doi: https://doi.org/10.1590/1519-6984.240359

52. M.A.M. Bezerra-Medeiros, M. Gama e Silva, J. de Menezes Barbosa, É. Martins de Lavor, T. Feitosa-Ribeiro, C.A. Ferreira-Macedo, L.A.M. de Souza Duarte-Filho, T. Alves-Feitosa, J.d.J. Silva, H.H. Fokoue, C.R. Melo-Araújo, A.d.A. Gonsalves, L.A. de Araújo-Ribeiro, J.R.G. da Silva-Almeida, Antinociceptive and anti-inflammatory effects of hydrazone derivatives and their possible mechanism of action in mice, *PLoS One*, **16**(11), e0258094 (2021). Doi: https://doi.org/10.1371/journal.pone.0258094

53. B.M. de Campos-Facchin, J.S. da Rosa, A.B.G. Luz, Y.J.K. Moon, T.C. de Lima, R. Casoti, M. Weber-Biavatti, E. Monguilhott-Dalmarco, T.S. Fröde, Systemic administration of *Calea pinnatifida* inhibits inflammation induced by carrageenan in a murine model of pulmonary neutrophilia, *Mediators of Inflammation*, **2020**, 4620251 (2020). Doi: https://doi.org/10.1155/2020/4620251

54. X. Dai, M. Ding, W. Zhang, Z. Xuan, J. Liang, D. Yang, Q. Zhang, B. Su, H. Zhu, X. Jia, Anti-inflammatory effects of different elution fractions of Er-Miao-San on acute inflammation induced by carrageenan in rat paw tissue, *Medical Science Monitor*, **25**, 7958-7965 (2019). Doi: https://doi.org/10.12659/MSM.916977

55. M. Sobeh, S. Rezq, O.M. Sabry, M.A.O. Abdelfattah, M.A.E. Raey, W.A.E. Kashak, A.M. El-Shazly, M.F. Mahmoud, M. Wink, *Albizia anthelmintica:* HPLC-MS/MS profiling and *in vivo* anti-inflammatory, pain killing and antipyretic activities of its leaf extract, *Biomedicine & Pharmacotherapy*, **115**, 108882 (2019). Doi: https://doi.org/10.1016/j.biopha.2019.108882

56. C. Velázquez-González, R. Cariño-Cortés, J.A. Gayosso de Lucio, M.I. Ortiz, M.d.l.O. Arciniega, D.A. Altamirano-Báez, L. Jiménez-Ángeles, M. Bautista-Ávila, Antinociceptive and anti-inflammatory activities of *Geranium bellum* and its isolated compounds, *BMC Complementary and Alternative Medicine*, **14**, 506 (2014). Doi: https://doi.org/10.1186/1472-6882-14-506

57. A.A. Saldanha, L. Vieira, D.S. da Silva-Maia, F. Martins de Oliveira, R.I.M. de Azambuja-Ribeiro, R.G. Thomé, H. Batista dos Santos, D. de Oliveira Lopes, C.A. Carollo, D. Brentan-Silva, A.C. Soares, J.M. de Siqueira, Anti-inflammatory and antinociceptive activities of a phenylpropanoid-enriched fraction of *Duguetia furfuracea*, *Inflammopharmacology*, **29**(2), 409-422 (2021). Doi: https://doi.org/10.1007/s10787-020-00775-7

58. L. Vieira, A.A. Saldanha, A. Marinho-Moraes, F. Martins de Oliveira, D. Oliveira-Lopes, L.A. de Oliveira-Barbosa, R.I.M. de Azambuja-Ribeiro, R.G. Thomé, H. Batista dos Santos, J.A.F. Perez-Villar, A.C. Soares, 21-Benzylidene digoxin, a novel digoxin hemi-synthetic derivative, presents an anti-inflammatory activity through inhibition of edema, tumor necrosis factor alpha production, inducible nitric oxide synthase expression, and leukocyte migration, *International Immunopharmacology*, **65**, 174-181 (2018). Doi: https://doi.org/10.1016/j.intimp.2018.10.010

59. X.-M. Li, R.-Z. He, Y. Li, Z.-F. Ruan, Tizoxanide mitigates inflammatory response in LPS-induced neuroinflammation in microglia via restraining p38/MAPK pathway, *European Review for Medical and Pharmacological Sciences*, **24**(13), 6446-6454 (2020). Doi: https://doi.org/10.26355/eurrev_202006_21543

60. D. Trabattoni, F. Gnudi, S. V. Ibba, I. Saulle, S. Agostini, M. Masetti, M. Biasin, J.-F. Rossignol, M. Clerici, Thiazolides elicit anti-viral innate immunity and reduce HIV replication, *Scientific Reports*, **6**, 27148 (2016). Doi: https://doi.org/10.1038/srep27148

61. L. Fan, X.X. Qiu, Z.Y. Zhu, J.-L. Lv, J. Lu, F. Mao, J. Zhu, J.-Y. Wang, X.-W. Guan, J. Chen, J. Ren, J.-M. Ye, Y.-H. Zhao, J. Li, X. Shen, Nitazoxanide, an anti-parasitic drug, efficiently ameliorates learning and memory impairments in AD model mice, *Acta Pharmacologica Sinica*, **40**(10), 1279-1291 (2019). Doi: https://doi.org/10.1038/s41401-019-0220-1

62. M. Castillo-Salazar, F. Sánchez-Muñoz, R. Springall del Villar, G. Navarrete-Vázquez, A. Hernández-DiazCouder, C. Mojica-Cardoso, S. García-Jiménez, C. Toledano-Jaimes, G. Bernal-Fernández, Nitazoxanide exerts immunomodulatory effects on peripheral blood mononuclear cells from type 2 diabetes patients, *Biomolecules*, **11**(12), 1817 (2021). Doi: https://doi.org/10.3390/biom11121817

63. M.A. Tantawy, N.A. El-Sherbeeny, N. Helmi, R. Alazragi, N. Salem, S.M. Elaidy, Synthetic antiprotozoal thiazolide drug induced apoptosis in colorectal cancer cells: Implications of IL-6/JAK2/STAT3 and p53/caspases-dependent signaling pathways based on molecular docking and *in vitro* study, *Molecular and Cellular Biochemistry*, **469**(1-2), 143-157 (2020). Doi: https://doi.org/10.1007/s11010-020-03736-4

64. D.-i. Jang, A.-H. Lee, H.-Y. Shin, H.-R. Song, J.-H. Park, T.-B. Kang, S.-R. Lee, S.-H. Yang, The role of tumor necrosis factor alpha (TNF-α) in autoimmune disease and current TNF-α inhibitors in therapeutics, *International Journal of Molecular Sciences*, **22**(5), 2719 (2021). Doi: https://doi.org/10.3390/ijms22052719

65. Y. Wang, M. Guo, Y. Ren, L. Jia, G. Yu, Drug repositioning based on individual bi-random walks on a heterogeneous network, *BMC Bioinformatics*, **20**(Suppl 15), 547 (2019). Doi: https://doi.org/10.1186/s12859-019-3117-6

66. Y.T. Yeung, A. Faisal, A. Guerrero-Castilla, S. Arguelles, Signaling pathways in inflammation and anti-inflammatory therapies, *Current Pharmaceutical Design*, **24**(14), 1449-1484 (2018). Doi: https://doi.org/10.2174/1381612824666180327165604

67. J.P. Mitchell, R.J. Carmody, NF-κB and the transcriptional control of inflammation, *Internation Review of Cell and Molecular Biology*, **335**, 41-84 (2018). Doi: https://doi.org/10.1016/bs.ircmb.2017.07.007

68. Q. Zhang, M.J. Lenardo, D. Baltimore, 30 Years of NF-κB: A blossoming of relevance to human pathobiology, *Cell*, **168**(1-2), 37-57 (2017). Doi: https://doi.org/10.1016/j.cell.2016.12.012

69. P.J. Barnes, M. Karin, Nuclear factor-kappaB: A pivotal transcription factor in chronic inflammatory diseases, *The New England Journal of Medicine*, **336**(15), 1066-1071 (1997). Doi: https://doi.org/10.1056/NEJM199704103361506

70. B. Kaminska, MAPK signalling pathways as molecular targets for anti-inflammatory therapy – from molecular mechanisms to therapeutic benefits, *Biochimica et Biophysica Acta (BBA) - Proteins and Proteomics*, **1754**(1-2), 253-262 (2005). Doi: https://doi.org/10.1016/j.bbapap.2005.08.017

71. T.B. Tumer, F.C. Onder, H. Ipek, T. Gungor, S. Savranoglu, T.T. Tok, A. Celik, M. Ay, Biological evaluation and molecular docking studies of nitro benzamide derivatives with respect to *in vitro* anti-inflammatory activity, *International Immunopharmacology*, **43**, 129-139 (2017). Doi: https://doi.org/10.1016/j.intimp.2016.12.009

72. N. De Santo, J. Ehrisman, Research perspective: Potential role of nitazoxanide in ovarian cancer treatment. Old drug, new purpose? *Cancers*, **5**(3), 1163-1176 (2013). Doi: https://doi.org/10.3390/cancers5031163

73. V.M. Couto, F.C. Vilela, D.F. Dias, M.H. Santos, R. Soncini, C.G. Nascimento, A. Giusti-Paiva, Antinociceptive effect of extract of *Emilia sonchifolia* in mice, *Journal of Ethnopharmacology*, **134**(2), 348-53 (2011). Doi: https://doi.org/10.1016/j.jep.2010.12.028

74. D. Le Bars, M. Gozariu, S.W. Cadden, Animal models of nociception, *Pharmacological Reviews*, **53**(4), 597-652 (2001). URL: https://www.researchgate.net/publication/11621016_Animal_Models_of_Nociception

75. B.G. Pinheiro, A.S. Silva, G.E. Souza, J.G. Figueiredo, F.Q. Cunha, S. Lahlou, J.K.R. da Silva, J.G.S. Maia, P.J.C. Sousa, Chemical composition, antinociceptive and anti-inflammatory effects in rodents of the essential oil of *Peperomia serpens* (Sw.) Loud, *Journal of Ethnopharmacology*, **138**(2), 479-486 (2011). Doi: https://doi.org/10.1016/j.jep.2011.09.037

76. P.R. Verma, A.A. Joharapurkar, V.A. Chatpalliwar, A.J. Asnani, Antinociceptive activity of alcoholic extract of *Hemidesmus indicus* R.Br. in mice, *Journal of Ethnopharmacology*, **102**(2), 298-301 (2005). Doi: https://doi.org/10.1016/j.jep.2005.05.039

77. T.M. Cunha, W.A. Verri, D.A. Valerio, A.T. Guerrero, L.G. Nogueira, S.M. Vieira, D.G. Souza, M.M. Teixeira, S. Poole, S.H. Ferreira, F.Q. Cunha, Role of cytokines in mediating mechanical hypernociception in a model of delayed-type hypersensitivity in mice, *European Journal of Pain*, **12**(8), 1059-1068 (2008). Doi: https://doi.org/10.1016/j.ejpain.2008.02.003

78. F.A. Pinho-Ribeiro, W.A. Verri, Jr., I.M. Chiu, Nociceptor sensory neuron-immune interactions in pain and inflammation, *Trends in Immunology*, **38**(1), 5-19 (2017). Doi: https://doi.org/10.1016/j.it.2016.10.001

79. R. Afridi, A.U. Khan, S. Khalid, B. Shal, H. Rasheed, M.Z. Ullah, O. Shehzad, Y.S. Kim, S. Khan, Anti-hyperalgesic properties of a flavanone derivative poncirin in acute and chronic inflammatory pain models in mice (Retracted Article), *BMC Pharmacology and Toxicology*, **20**(1), 57 (2019). Doi: https://doi.org/10.1186/s40360-019-0335-5

80. K. Lopes, J. Oliveira, F.J.C. Sousa-Junior, T.d.F. Santos, D. Andrade, S.L. Andrade, W.L. Pereira, P.W.P. Gomes, M.C. Monteiro, C.Y. Yoshioka e Silva, M.N. da Silva, C.F. Maia, E.A. Fontes-Júnior, Chemical composition, toxicity, antinociceptive, and anti-inflammatory activity of dry aqueous extract of *Varronia Multispicata* (Cham.) Borhidi (Cordiaceae) leaves, *Frontiers in Pharmacology*, **10**, 1376 (2019). Doi: https://doi.org/10.3389/fphar.2019.01376

81. N. Ai, R.D. Wood, W.J. Welsh, Identification of nitazoxanide as a group I metabotropic glutamate receptor negative modulator for the treatment of neuropathic pain: An *in silico* drug repositioning study, *Pharmaceutical Research*, **32**(8), 2798-2807 (2015). Doi: https://doi.org/10.1007/s11095-015-1665-7

82. G.M. Abu-Taweel, A.-M. Mohsen-G., P. Antonisamy, S. Arokiyaraj, H.-J. Kim, S.-J. Kim, K.H. Park, Y.O. Kim, *Spirulina* consumption effectively reduces anti-inflammatory and pain-related infectious diseases, *Journal of Infection and Public Health*, **12**(6), 777-782 (2019). Doi: https://doi.org/10.1016/j.jiph.2019.04.014

How to cite this article

L. Rabelo-Lopes, F.A. Alves-Moraes, J.P. Costa-Rodrigues, F. Martins de Oliveira, D. de Oliveira-Lopes, F.C. Horta-Pinto, A.A. Saldanha, A.C. Soares, A repositioning approach: nitazoxanide inhibits inflammation and nociceptive response in mice models via a reduction of paw oedema, cellular migration and early TNF-α production, *Rev. Colomb. Cienc. Quim. Farm.*, **53**(2), 385-413 (2024). https://doi.org/10.15446/rcciquifa.v53n2.114448

Scientific research article / https://doi.org/10.15446/rcciquifa.v53n2.114449

Inhibitory effect of the essential oil of *Schinus molle* L. against pathogens causing periodontal disease

Carlos Cadena-Viteri[1], Miriam Lima-Illescas[1,2,3], Edisson-Mauricio Pacheco-Quito[1,2,3], Mariela Cumandá Balseca-Ibarra[4], Fernanda Sacoto-Figueroa[2], Katherine Cuenca-León [1,2,3,5*]

[1]Specialty in Orthodontics, Catholic University of Cuenca, Azogues 030102, Ecuador; carlos.cadena.47@est.ucacue.edu.ec (C.C.-V)

[2]Academic Unit of Health and Wellness, Faculty of Dentistry, Catholic University of Cuenca, Cuenca 010105, Ecuador; mlimai@ucacue.edu.ec (M.-V.L); epachecoq@ucacue.edu.ec (E..P.-Q.); kacuen-ca22@gmail.com (M.B.-I.); fsacotof@ucacue.edu.ec (F.S.-F.); kcuencal@ucacue.edu.ec (K.C.-L.)

[3]Research Group: Innovation and Pharmaceutical Development in Dentistry Research Group, Faculty of Dentistry, Head of Research and Innovation, Catholic University of Cuenca, Cuenca 010105, Ecuador

[4]Central University of Ecuador. Quito 170521, Ecuador.

[5]Pharmaceutical Sciences Department, University of Salamanca, 37007 Salamanca, Spain

*Correspondence: kcuencal@ucacue.edu.ec

Received: November 30, 2023
Corrected: March 10, 2024
Accepted: March 13, 2024

Summary

Introduction: There are several oral diseases caused by various microorganisms. In this work, we discuss periodontal pathogens, which cause chronic degenerative damage in the supporting tissues of teeth. This is why several treatments have been developed for their eradication, including phytocomponents and essential oils as an option in antimicrobial therapy. **Objective:** The aim of this study was to determine the inhibitory effect of the essential oil of the plant species *Schinus molle* L. native to Ecuador on strain of *Porphyromonas gingivalis* at different concentrations. **Methodology:** This was a laboratory and longitudinal study in which the *Porphyromonas gingivalis* ATCC 33277 strain was cultured in 20 Petri dishes, working with several exposure subgroups, including Group 1 - 50% essential oil of *Schinus molle* leaves; Group 2 - 100% essential oil of *Schinus molle* L.; Group 3 - 0.12% chlorhexidine (positive control); Group 4 - saline solution (negative control)

with different incubation periods of 24 and 72 hours. **Results:** The *Porphyromonas gingivalis* ATCC 33277 sample exposed to 100% plant species *Schinus molle* L. for 24 hours had an inhibition zone of 15 mm, demonstrating high sensitivity, and exposure for 72 hours produced a zone of 14 mm, also suggesting sensitivity. Exposure to *S. molle* L. at 50% for 24 hours produced a zone of inhibition of 9.65 mm, showing sensitivity; however, it is worthwhile to continue developing and evaluating this area of study. **Conclusions:** This study demonstrates that phytotherapy using the essential oil of the plant species *Schinus molle* L. represents a therapeutic option in cases of infections caused by *Porphyromonas gingivalis*.

Keywords: Oils, periodontal diseases, anti-bacterial agents

Resumen

Efecto inhibitorio del aceite esencial de *Schinus molle* L. contra patógenos causantes de la enfermedad periodontal

Introducción: Existen varias enfermedades orales causadas por diversos microorganismos. En este trabajo, discutimos los patógenos periodontales, que causan daños crónicos degenerativos en los tejidos de soporte de los dientes. Por ello, se han desarrollado diversos tratamientos para su erradicación, entre los que destacan los fitocomponentes y aceites esenciales como opción en la terapia antimicrobiana. **Objetivo:** El objetivo de este estudio fue determinar el efecto inhibitorio del aceite esencial de la especie vegetal *Schinus molle* L. nativa del Ecuador sobre una cepa de *Porphyromonas gingivalis* a diferentes concentraciones. **Metodología:** Se trató de un estudio de laboratorio y longitudinal en el que se cultivó la cepa *Porphyromonas gingivalis* ATCC 33277 en 20 placas Petri, se trabajó con varios subgrupos de exposición, tales como: Grupo 1 - 50% aceite esencial de hojas de *Schinus molle*; Grupo 2 - 100% aceite esencial de *Schinus molle* L.; Grupo 3 - clorhexidina al 0,12% (control positivo); Grupo 4 - solución salina (control negativo) a diferentes periodos de incubación de 24 a 72 horas. **Resultados:** La muestra de *Porphyromonas gingivalis* ATCC 33277 expuesta al 100% de la especie vegetal *Schinus molle* L. durante 24 horas presentó un halo de inhibición de 15 mm, lo que demuestra una alta sensibilidad, y la exposición durante 72 horas produjo un halo de 14 mm, lo que también sugiere sensibilidad. La exposición a *S. molle* L. al 50% durante 24 horas produjo un halo de inhibición de 9,65 mm, demostrando sensibilidad; sin embargo, vale la

pena continuar desarrollando y evaluando esta área de estudio. **Conclusiones:** Este estudio demuestra que la fitoterapia utilizando el aceite esencial de la especie vegetal *Schinus molle* L. representa una opción terapéutica, en casos de infecciones ocasionadas por *Porphyromonas gingivalis.*

Palabras clave: Aceites, enfermedades periodontales, agentes antibacterianos.

Resumo

Efeito inibitório do óleo essencial de *Schinus molle* L. contra patógenos causadores de doença periodontal

Introdução: Existem diversas doenças bucais causadas por diversos microrganismos. Neste trabalho, discutimos os patógenos periodontais, que causam danos degenerativos crônicos aos tecidos de suporte dos dentes. Por este motivo, vários tratamentos têm sido desenvolvidos para a sua erradicação, entre os quais se destacam os fitocomponentes e os óleos essenciais como opção na terapia antimicrobiana. **Objetivo:** O objetivo deste estudo foi determinar o efeito inibitório do óleo essencial da espécie vegetal *Schinus molle* L. nativa do Equador sobre uma cepa de Porphyromonas gingivalis em diferentes concentrações. M**etodologia:** Trata-se de um estudo laboratorial e longitudinal em que a cepa *Porphyromonas gingivalis* ATCC 33277 foi cultivada em 20 placas de Petri, trabalhando com diversos subgrupos de exposição, tais como: Grupo 1 - 50% de óleo essencial de folhas de *Schinus molle* L.; Grupo 2 - óleo essencial 100% de Schinus molle L.; Grupo 3 - clorexidina 0,12% (controle positivo); Grupo 4 - solução salina (controle negativo) em diferentes períodos de incubação de 24 a 72 horas. **Resultados:** A amostra de *Porphyromonas gingivalis* ATCC 33277 exposta a 100% da espécie vegetal *Schinus molle* L. por 24 horas apresentou zona de inibição de 15 mm, o que demonstra alta sensibilidade, e a exposição por 72 horas produziu zona de inibição de 14 mm, o que também sugere sensibilidade. A exposição a *S. molle* L. a 50% durante 24 horas produziu uma zona de inibição de 9,65 mm, demonstrando sensibilidade; no entanto, vale a pena continuar a desenvolver e avaliar esta área de estudo. **Conclusões:** Este estudo demonstra que a fitoterapia utilizando o óleo essencial da espécie vegetal *Schinus molle* L. representa uma opção terapêutica em casos de infecções causadas por *Porphyromonas gingivalis.*

Palavras-chave: Óleos, doenças periodontais, agentes antibacterianos.

Introduction

The mouth constitutes a reservoir for many microorganisms, including bacteria. These bacteria, along with mucus and other components, constantly form a sticky, color-less "plaque" that adheres to the teeth [1, 2]. Brushing and flossing help to remove this plaque, but in situations wherein plaque is not removed, it hardens and forms deposits called "calculus" or "tartar", which brushing alone cannot remove; only professional cleaning by a dentist or dental hygienist can re-move it [3-6].

Periodontitis is a chronic inflammatory condition in which the progressive destruction of the tissues that support the teeth prevails; the etiological factor of this is the bacterial interaction of cell groups and the susceptibility of individuals to suffer it [7, 8]. Among the bacteria that generate this disease, the most predominant is *Porphyromonas gingivalis*, which has been found in patients with compromised periodontium, and curiously also in healthy patients. This microorganism can evade the host's immune system because it features a conglomerate of virulence factors, which allow it to become an aggressive pathobiont [9, 10].

Global records indicate that the incidence rate of periodontal disease in the adult population is approximately 1% in all ethnic groups, while its prevalence in the female sex is two to three times that in the male sex [4, 11-13]. The numbers are increasing, and preventive measures are sometimes not enough to reduce these numbers. For this reason, other alternatives are sought to help reduce the percentage of these oral diseases [14]. In recent years, phytotherapy has become a possible solution to this complex of microbial resistance, and it has begun to feature more prominently among new therapeutic options, raising hope with respect to combating bacterial resistance and the secondary effects that arise in most cases [15-19].

Essential oils have demonstrated their antioxidant capacity to act in metabolic response to endogenous production of free radicals and other oxidative species [20], showing *in vitro* studies, antimicrobial properties against various pathogens. *Schinus molle* L., commonly known as pink pepper or American pepper, is a tree of the Anacardiaceae family native to the subtropical regions of South America. It was introduced and naturalized in southern Europe, including Portugal, as an ornamental plant. In the health field, *Schinus molle* has been used for its antibacterial, antiviral, topical antiseptic, antifungal, antioxidant, anti-inflammatory, antitumor, antispasmodic, analgesic, stimulant and antidepressant properties, so its activity on bacteria such as *Porphyromonas gingivalis* is the focus of this study [21, 22].

Thus, the use of adjuvants with natural components in the treatment of periodontal disease suggests advantages such as a decrease in side effects; as it is a different treatment, resistance to usual treatments would be eliminated, and in terms of costs it would be very beneficial [20]. Now, the formulation of pharmaceutical substances based on plant species should take a more central role and should move beyond the level of theory. For this reason, we suggest that these types of study be developed, since there is a very broad range of plant species whose applications are not yet known, and it is necessary to develop this field so as to extend our knowledge [21-24].

In this context, chlorhexidine gluconate at a concentration of 0.12% is currently still used to combat diseases such as periodontitis. This antiseptic has been traditionally used since the 1970s in periodontal odontology. It continues to be the mouthwash of first choice for cases of periodontal diseases [25]. Consequently, and due to the need to explore new forms of treatment that are less invasive and have low toxicity, this research has been proposed to evaluate the inhibitory effects of one of our country's own plants, with anti-septic antecedents, on the microorganism that predominantly generates periodontitis [15].

Methodology

This was a longitudinal laboratory study that tested the inhibitory efficacy of *Schinus molle* oil at different concentrations and times on *Porphyromonas gingivalis* strain [26]. The inhibition halos produced by *Schinus molle* oil at 50% and 100% at 24 and 72 hours were compared with those of the control (chlorhexidine 0.12%) and blank (physio-logical serum 0.9%) when applied on strain of *Porphyromonas gingivalis* (ATCC 33277).

Obtaining the essential oil

After the selection of the sample, 1.5 kg of fresh plant was subjected to dehydration to a final weight of 140 g, which was crushed. This was then subjected to hydrodistillation with the reflux of condensation vapors using a Dean Stark grid for greater efficiency in the collection of the oil. It was expected that from 140 g of *Schinus molle*, between 4 and 5 mL of oil could be obtained. This was stored and refrigerated in amber containers to avoid de-composition by exposure to atmosphere. A concentration of 100% was obtained by separating residual water via distillation. To obtain a concentration of 50%, dilution with dis-tilled water was performed. To obtain a 50% concentration, dilution was carried out with distilled water; vortex was used to homogenize the dilution. The discs were soaked with 25 mL of this compound. Thus, the discs that represented 100% concentration were soaked with undiluted essential oil, and those that represented 50% concentration were soaked with oil diluted in a 1:1 ratio (oil-distilled water) [27, 28] (Figure 1. A).

Strain activation

To develop the microbiological part, a periodontal pathogenic bacterium, *Porphyromonas gingivalis* (strain ATCC 33277), was acquired and activated in a class 2 laminar flow chamber type BII. The turbidity of the bacterial inoculum was standardized until a dilution of 1.5×10^8 CFU/mL was obtained, equivalent to 0.5 on the McFarland scale. The bacteria were seeded on Agar blood culture medium and incubated in an anaerobic jar for 48 hours at 37 °C.

Inoculation of *Porphyromonas gingivalis* strain ATCC® 3327 TM

Using a sterile loop or swab, a small sample of the previously reactivated *Porphyromonas gingivalis* strain was extracted and immersed in a test tube with saline solution. The test tube was shaken until a turbidity of 1×10^8 CFU/m was reached, equivalent to 0.5 on the McFarland scale. This process was carried out visually [28] (Figure 1.B).

Placement of white disks soaked in the extracts of the plant species under study.

We inoculated culture media in Mueller Hinton agar with two drops of blood and with the *Porphyromonas gingivalis* ATCC® 33277TM strain. In total, 20 white disks for each sub-stance studied were placed in labeled Petri dishes; into these disks we embedded *Schinus molle* L. extract in concentrations of 50% and 100%, using a micropipette (Figure 1.C).

Placement of the culture media with the embedded discs in a Gaspak jar

Four antibiogram disks were placed in each Petri dish and soaked in 100% essential oil of *Schinus molle,* as well as 50% and 0.9% saline solutions acting as the negative control, and 0.12% chlorhexidine as the positive control. Each disk had a minimum separation of 15 mm. After the inoculation of the disks, the 20 Petri dishes were incubated at 37 °C for 24 and 72 hours (Figure 1.D).

Measurement of inhibition halos

With the help of a millimeter measuring device, data on the inhibition zones generated by the essential oil of *Schinus molle* at different concentrations were obtained (Figure 1.E).

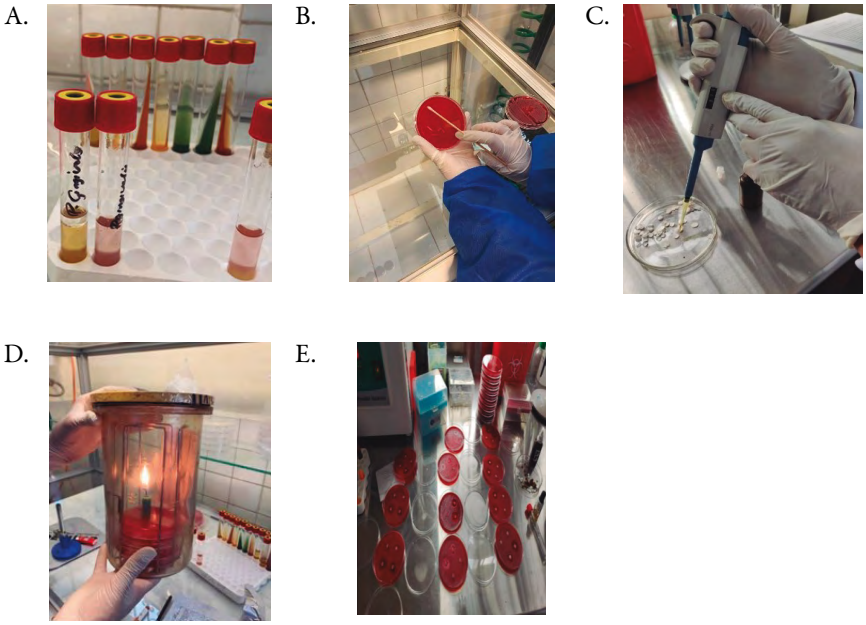

Figure 1. *In-vitro* study process of *Schinus molle* essential oil. A: Extraction of the essential oil. B: Inoculation of the *Porphyromonas gingivalis* ATCC® 3327 TM strain. C: White discs soaked in the study extracts. D: Placement of culture media with the discs soaked in the study substances in a Gaspak jar. E: Measurement of inhibition halos.

Results

The results of this research are based on the selection, preparation and extraction of essential oils from the plant species *A. Schinus molle*, evaluated on ATCC33277 strain of *Porphyromonas gingivalis*. Physiological serum and chlorhexidine were used as the controls. The following results were obtained according to the diameter of the inhibition halo, taking into account the exposure time (Table 1).

Descriptive statistical data for the inhibitory halo (mm) at 24 hours can be observed for the different substances evaluated, such as the essential oils of *Schinus molle* at 50% and 100%, and the physiological serum and chlorhexidine as negative and positive control groups, respectively. The average value of the inhibitory halo of chlorhexidine was the highest (20.80±1.64), and the lowest value was yielded by the control group (6.00±0.00).

Table 1. Concentration of the essential oil and exposure time on *Porphyromonas Gingivalis* strain

Time of exposure	Action composite	N	Mean mm	Standard deviation	Mediana	Minimum	Maximum	*p* value
24 hours	*E. Schinus* 50%	20	9.65	0.74	8	8	11	0.00
	E. Schinus 100%	20	15	0.85	14	13	17	
	Physiological saline solution (Negative Control)	20	6	0	6	6	6	
	Chlorhexidine (Positive Control)	20	20.8	1.64	18	19	25	
	Total	80	12.86	5.7	12	6	25	
72 hours	*E. Schinus* 50%	20	7.75	0.55	8	7	9	0.00
	E. Schinus 100%	20	14	0.64	14	13	15	
	Physiological saline solution (Negative Control)	20	6	0	6	6	6	
	Chlorhexidine (Positive Control)	20	17.5	0.82	18	16	19	
	Total	80	11.31	4.71	12	6	19	

The average inhibition halos of the different substances at 72 hours were the greatest for chlorhexidine (x=17.50±0.82), followed by the essential oil of *Schinus molle* at 100% (x=14.00±0.64) (Table 1). It was observed at 24 hours that the essential oil of the plant species at a concentration of 50% presented a halo of 9.65 mm; at a concentration of 100%, it showed an inhibitory halo of 15 mm, and with chlorhexidine, a halo of 20.80 mm was seen, surpassing all the previous ones. The Shapiro Wilk test determined a value of $p<0.05$; therefore, the non-parametric Kruskall Wallis test was used (Table 1). Significant differences were observed in all groups ($p=0.00$), thus the Dunn test was utilized to establish pairwise comparisons.

The average inhibition halos at 24 hours after subjecting the different substances to the PG strains were analyzed. For the negative control group, it was 6.00 mm, followed by 7.75 mm for *E. Schinus* 50%, 14.00 mm for *E. Schinus* 100%, and 17.50 mm for the

positive control group. Significant differences were found, prompting a further analysis using the Dunn test (Table 2).

It is important to point out that, according to the results presented, there were significant differences, and the effectiveness of *E. Schinus molle* was thus demonstrated. However, it is necessary to point out that according to the inhibition diameters, *E. Schinus* at 100% showed a greater inhibition diameter compared to *Schinus* at 50%.

On the other hand, chlorhexidine was more effective than the plant species *E. Schinus*, presenting a greater inhibitory diameter (Table 3).

Table 2. Dunn's test in the pairwise comparison of the inhibitory effects of essential oilsof *Schinus molle* L. at 50% and 100%, as well as physiological saline and chlorhexidine,at 72 hours on strain of *Porphyromonas gingivalis*.

		Contrast statistic	**Standard error**	**Deviation in contrast statistic**	**p**	**Adjusted p**
E. Schinus 50%	*E. Schinus* 100%	-20.00	7.25	-2.75	0.00	0.03
Control (-)	*E. Schinus* 50%	20.00	7.25	2.75	0.00	0.03
Control (-)	*E. Schinus* 100%	-40.00	7.25	5.51	0.00	0.00
E. Schinus 50%	Control (+)	-40.00	7.25	-5.51	0.00	0.00
E. Schinus 100%	Control (+)	-20.00	7.25	-2.75	0.00	0.03
E. Schinus 100%	Control (+)	-60.00	7.25	-8.27	0.00	0.00

Table 3. Comparison of the inhibitory effects of the essential oils of *Schinus molle* L. at 50% and 100%, as well as physiological saline and chlorhexidine, at 72 hours on strain of *Porphyromonas gingivalis*.

		Contrast statistic	Standard error	Deviation in contrast statistic	p	Adjusted p
Control (-)	*E. Schinus* 50%	20.00	7.25	2.75	0.00	0.03
Control (-)	*E. Schinus* 100%	40.00	7.25	5.51	0.00	0.00
Control (-)	Control (+)	-60.00	7.25	-8.27	0.00	0.00
E. Schinus 50%	*E. Schinus* 100%	-20.00	7.25	-2.75	0.00	0.03
E. Schinus 50%	Control (+)	-40.00	7.25	-5.51	0.00	0.0
E. Schinus 100%	Control (+)	-20.00	7.25	-2.75	0.00	0.03

Discussion

Phytotherapy has shown advancements in the field of health by taking advantage of the effects of active components on pathogenic bacteria. There is a diverse arsenal of essential oils obtained from plant species that have been used as adjuvants in oral problems and/or afflictions, with the bacteria that cause periodontal disease being of interest in this work. In this context, the essential oil of *Schinus molle* has been studied and applied due to its diverse properties, such as antibacterial, analgesic, diuretic, healing, and anti-inflammatory effects [29].

Several studies have evaluated the effectiveness of *Schinus molle* as an antibacterial agent in dentistry. An *in vitro* study conducted by Da Silva *et al.* in 2016, found that *Schinus molle* extracts significantly inhibited the growth of Streptococcus mutans, a bacteria commonly associated with dental caries. Furthermore, research by Turchetti *et al.* (2020) suggest that the active compounds of *Schinus molle* may interfere *in vitro* with the formation of bacterial biofilms, which could be relevant for the control of dental plaque and the prevention of periodontal diseases [30, 31].

Tahtamouni in 2018 [29] showed the antibacterial activity of the ethanolic, methanolic and essential oil extracts of *Schinus molle* leaves, compared to a positive control, which in their case was tetracycline. The ethanolic extract had a strong antibacterial effect against *Bacillus subtilis* and *Micrococcus luteus*, as did the positive control, but no significant differences were noted. On the contrary, in the present investigation, significant differences were found between the inhibitory effects of *Schinus molle* essential oil and 0.12% chlorhexidine as a positive control against *Porphyromonas gingivalis*, wherein the highest inhibitory effect was presented at the highest concentration of the oil (100%) in the first 24 hours.

Alfaro showed that the essential oil of *Schinus molle* at 60% presented a bactericidal effect due to its bioactive contents that are capable of inhibiting the bacterial development of *Staphylococcus aureus*; however, the use of penicillin as a positive control acted as a potent antibacterial agent. The data reported by Alfaro are similar to those obtained in this research, since applying the essential oil of *Schinus molle* at 50% and 100% had an inhibitory effect against *Porphyromonas gingivalis*, but there was no significant effect when com-pared with chlorhexidine 0.12% (positive control) [32].

On the other hand, Loyola and collaborators showed that extracts of *Schinus molle* at concentrations of 50% and 75%, applied for 24 h and 48 h, had inhibitory effects on *Streptococcus mutans*, due to the antibacterial and antifungal properties. This was also evidenced here, as the positive control manifested a halo with a diameter surpassing

that of the vegetable component. In this research, the *Schinus molle* essential oil applied at a concentration of 50% for 24 hours showed an increased inhibition halo according to the Duraffourd scale, and at 72 hours, its effect shifted from low to null, proving once again that applying 0.12% chlorhexidine leads to better bacterial inhibition [33].

Turchetti and Garzoli presented the results of an *in vitro* study carried out with extracts of *Schinus molle* leaves at various concentrations, classified into male and female leaves. They derived better inhibitory results with the extracts obtained from the female leaves against *Staphylococcus aureus*, *Enterococcus faecalis*, *Candida albicans* and *Bacillus subtilis*. In the present work, as mentioned, we used two concentrations (50-100%) and obtained an inhibitory effect equal to that obtained by Turchetti; however, it is necessary to emphasize that a comparison was made with chlorhexidine 0.12% as a positive control, with the latter showing a better inhibitory effect [31].

Despite the encouraging evidence, it is important to recognize the limitations of existing studies, which include the lack of standardization in extraction and evaluation methods, as well as the need for controlled clinical trials to validate their efficacy and safety in dental patients. In addition, a greater understanding of the mechanisms of action and possible interactions with other dental treatments is required.

In conclusion, *Schinus molle* emerges as a promising candidate for the development of antibacterial therapies in dentistry. However, more research is needed to establish its clinical efficacy and determine its exact role in the dental therapeutic armamentarium [15].

Conclusions

The use of the essential oil of *Schinus molle* against *Porphyromonas gingivalis* at a concentration of 50% for 24 hours and 72 hours showed sensitive and null inhibitory effects, respectively. The application of the essential oil at 100% for 24 hours showed high sensitivity, and it was sensitive for 72 hours. However, the chlorhexidine always showed greater sensitivity against the exposed bacteria according to the size of the inhibition halo. It is necessary to continue these studies, since this is a very wide field and can thus con-tribute new therapeutic options that will reduce the adverse effects associated with conventional pharmacological therapy.

In our country (Ecuador), there are innumerable plant species with curative properties that have not yet been studied. This research work represents a clear proposal to continue working in this area, carrying out more research on phytotherapy in relation to pathologies for which traditional treatment is no longer an option.

In the dental field the efficacy of chlorhexidine is clear, but there may also be other disinfection options, as proposed in this research, speaking specifically of the bacterium *Porphyromonas gingivalis*, but it is necessary to continue studying the phytotherapeutic area and in this way obtain new information, new alternatives.

Conflicts of interest

Authors declare that they have no conflicts of interest

References

1. S. Sharma, J. Mohler, S.D. Mahajan, S.A. Schwartz, L. Bruggemann, R. Aalinkeel, Microbial biofilm: A review on formation, infection, antibiotic resistance, control measures, and innovative treatment, *Microorganisms*, **11**(6), 1614 (2023). Doi: https://doi.org/10.3390/microorganisms11061614

2. W.H. Bowen, R.A. Burne, H. Wu, H. Koo, Oral biofilms: Pathogens, matrix, and polymicrobial interactions in microenvironments, *Trends in Microbiology*, **26**(3), 229-242 (2018). Doi: https://doi.org/10.1016/j.tim.2017.09.008

3. A. Pejcic, M. Kostic, I. Marko, R. Obradovic, I. Minic, M. Bradic-Vasic, N. Gligorijevic, D. Kurtagic, Tooth loss and periodontal status in patients with cardiovascular disease in the Serbian population: A randomized prospective study, *International Journal of Dental Hygiene*, **21**(2), 317-327 (2023). Doi: https://doi.org/10.1111/idh.12663

4. G. Schmalz, A.E. Hübscher, H. Angermann, J. Schmidt, J. Schmickler, T.J. Legler, D. Ziebolz, High prevalence of periodontitis in blood donors and the possibility of questionnaire-based screening – Results of a cross-sectional study, *Transfusion Medicine*, **29**(6), 394-400 (2019). Doi: https://doi.org/10.1111/tme.12633

5. D.T. Graves, J.D. Corrêa, T.A. Silva, The oral microbiota is modified by systemic diseases, *Journal of Dental Research*, **98**(2), 148-156 (2019). Doi: https://doi.org/10.1177/0022034518805

6. A. Akcalı, N.P. Lang, Dental calculus: The calcified biofilm and its role in disease development, *Periodontology 2000*, **76**(1), 109-115 (2018). Doi: https://doi.org/10.1111/prd.12151

7. L.M. Sedghi, M. Bacino, Y.L. Kapila, Periodontal disease: The good, the bad, and the unknown, *Frontiers in Cellular and Infection Microbiology*, **11**, 766944 (2021). Doi: https://doi.org/10.3389/fcimb.2021.766944

8. B. Dannewitz, B. Holtfreter, P. Eickholz, Periodontitis—therapy of a widespread disease [Parodontitis - Therapie einer Volkskrankheit], *Bundesgesundheitsblatt - Gesundheitsforschung – Gesundheitsschutz*, **64**(8), 931-940 (2021). Doi: https://doi.org/10.1007/s00103-021-03373-2

9. C.-M. Radu, C.C. Radu, S.-A. Bochiș, E.M. Arbănași, A.I. Lucan, V.R. Murvai, D.C. Zaha, Revisiting the therapeutic effects of essential oils on the oral microbiome, *Pharmacy* (Basel), **11**(1), 33 (2023). Doi: https://doi.org/10.3390/pharmacy11010033

10. L. Gao, T. Xu, G. Huang, S. Jiang, Y. Gu, F. Chen, Oral microbiomes: more and more importance in oral cavity and whole body, *Protein & Cell*, **9**(5), 488-500 (2018). Doi: https://doi.org/10.1007/s13238-018-0548-1

11. B.L. Mealey, Influence of periodontal infections on systemic health, *Periodontology 2000*, **21**(1), 197-209 (1999). Doi: https://doi.org/10.1111/j.1600-0757.1999.tb00176.x

12. L. Jamieson, M. Skilton, L. Maple-Brown, K. Kapellas, L. Askie, J. Hughes, P. Arrow, S. Cherian, D. Fernandes, B. Pawar, A. Brown, J. Boffa, W. Hoy, D. Harris, N. Mueller, A. Cass, Periodontal disease and chronic kidney disease among Aboriginal adults; an RCT, *BMC Nephrology*, **16**, 181 (2015). Doi: https://doi.org/10.1186/s12882-015-0169-3

13. R.G. Fischer, R. Lira-Junior, B. Retamal-Valdes, L.C. De Figueiredo, Z. Malheiros, B. Stewart, M. Feres, Periodontal disease and its impact on general health in Latin America. Section V: Treatment of periodontitis, *Brazilian Oral Research*, **34**(Suppl 11), e026 (2020). Doi: https://doi.org/10.1590/1807-3107bor-2020.vol34.0026

14. B. Mangal, A. Sugandhi, K.I. Kumathalli, R. Sridhar, Alternative medicine in periodontal therapy--A review, *Journal of Acupuncture and Meridian Studies*, **5**(2), 51-56 (2012). Doi: https://doi.org/10.1016/j.jams.2012.01.001

15. K. Cuenca-León, E.-M. Pacheco-Quito, Y. Granda-Granda, E. Vélez-León, A. Zarzuelo-Castañeda, Phytotherapy: A solution to decrease antifungal resistance in the dental field, *Biomolecules*, **12**(6), 789 (2022). Doi: https://doi.org/10.3390/biom12060789

16. M.A. Pfaller, Antifungal drug resistance: Mechanisms, epidemiology, and consequences for treatment, *The American Journal of Medicine*, **125**(Suppl 1), S3-S13 (2012). Doi: https://doi.org/10.1016/j.amjmed.2011.11.001

17. F. Bakkali, S. Averbeck, D. Averbeck, M. Idaomar, Biological effects of essential oils - A review, *Food and Chemical Toxicology*, **46**(2), 446-475 (2008). Doi: https://doi.org/10.1016/j.fct.2007.09.106

18. D.G.J. Larsson, C.F. Flach, Antibiotic resistance in the environment, *Nature Reviews Microbiology*, **20**(5), 257-269 (2022). Doi: https://doi.org/10.1038/s41579-021-00649-x

19. G.D. Antonio, C.D. Tesser, R.O. Moretti-Pires, Phytotherapy in primary health care, *Revista de Saúde Pública*, **48**(3), 541-553 (2014). Doi: https://doi.org/10.1590/S0034-8910.2014048004985

20. P. Kumar, S.H. Ansari, J. Ali, Herbal remedies for the treatment of periodontal disease--A patent review, *Recent Patents on Drug Delivery & Formulation*, **3**(3), 221-228 (2009). Doi: https://doi.org/10.2174/187221109789105603

21. K. Wińska, W. Mączka, J. Łyczko, M. Grabarczyk, A. Czubaszek, A. Szumny, Essential oils as antimicrobial agents—myth or real alternative? *Molecules*, **24**(11), 2130 (2019). Doi: https://doi.org/10.3390/molecules24112130

22. M. Abers, S. Schroeder, L. Goelz, A. Sulser, T. St. Rose, K. Puchalski, J. Langland, Antimicrobial activity of the volatile substances from essential oils, *BMC Complementary Medicine and Therapies*, **21**, 124 (2021). Doi: https://doi.org/10.1186/s12906-021-03285-3

23. G.S. Chatzopoulos, P. Karakostas, S. Kavakloglou, A. Assimopoulou, P. Barmpalexis, L. Tsalikis, Clinical effectiveness of herbal oral care products in periodontitis patients: A systematic review, *International Journal of Environmental Research and Public Health*, **19**(16), 10061 (2022). Doi: https://doi.org/10.3390/ijerph191610061

24. A. Bascones, S. Morante, Antisépticos orales. Revisión de la literatura y perspectiva actual, *Avances en Periodoncia e Implantología Oral*, **18**(1), 31-59 (2006). URL: https://scielo.isciii.es/pdf/peri/v18n1/original3.pdf

25. J. Soares de Oliveira, M.e.S. Conceição-Pinto, L.d.A. de Bastos-Santana, A.S. Bezerra-Pinto, D. di Lenardo, D.F. Pereira-Vasconcelos, Biological effects of medicinal plants on induced periodontitis: A systematic review, *International Journal of Dentistry*, **2016**, ID 3719879 (2016). Doi: https://doi.org/10.1155/2016/3719879

26. A. Geraci, V. Di Stefano, E. Di Martino, D. Schillaci, R. Schicchi, Essential oil components of orange peels and antimicrobial activity, *Natural Products Research*, **31**(6), 653-659 (2017). Doi: https://doi.org/10.1080/14786419.2016.1219860

27. U. Hazarika, B. Gosztola, Lyophilization and its effects on the essential oil content and composition of herbs and spices - A review, *Acta Scientiarum Polonorum Technologia Alimentaria*, **19**(4), 467-473 (2020). Doi: https://doi.org/10.17306/J.AFS.2020.0853

28. S. Bregaint, E. Boyer, S.B. Fong, V. Meuric, M. Bonnaure-Mallet, A. Jolivet-Gougeon, *Porphyromonas gingivalis* outside the oral cavity, *Odontology*, **110**(1), 1-19 (2022). Doi: https://doi.org/10.1007/s10266-021-00647-8

29. R.W. Tahtamouni, Investigating the antibacterial potential of ethanolic and methanolic extracts of the *Schinus molle* L tree, *Jordan Journal of Biological Sciences*, **11**(5), 527-531 (2018). URL: https://jjbs.hu.edu.jo/files/vol11n5/Paper%20Number%208.pdf

30. A.P. Sant'Anna da Silva, L.C. Nascimento da Silva, C.S. Martins da Fonseca, J.M. de Araújo, M.T. Dos Santos-Correia, M. da Silva-Cavalcanti, V.L. de Menezes-Lima, Antimicrobial activity and phytochemical analysis of organic extracts from *Cleome spinosa* Jaqc., *Frontiers in Microbiology*, **7**, 963 (2016). Doi: https://doi.org/10.3389/fmicb.2016.00963

31. G. Turchetti, S. Garzoli, V.L. Masci, C. Sabia, R. Iseppi, P. Giacomello, A. Tiezzi, E. Ovidi, Antimicrobial testing of *Schinus molle* (L.) leaf extracts and fractions followed by GC-MS investigation of biological active fractions, *Molecules*, **25**(8), 1977 (2020). Doi: https://doi.org/10.3390/molecules25081977

32. M.Y. Alfaro-Pérez, M.A. Ruiz-Barrueto, Efecto antibacteriano *in vitro* del extracto acuoso de *Schinus molle* (molle) sobre *Staphylococcus aureus* ATCC 25923, *Revista Científica de la Facultad de Ciencias Biológicas*, **38**(1), 4-16 (2018). URL: https://revistas.unitru.edu.pe/index.php/facccbiol/article/view/2145

33. D. Loyola, R. Mendoza, L. Chiong, M. Rueda, D. Alvítez-Temoche, W. Gallo, F. Mayta-Tovalino, Ethanol extract of *Schinus molle* L. (molle) and *Erythroxylum coca* Lam (coca): Antibacterial properties at different concentrations against *Streptococcus mutans*: An *in vitro* study, *Journal of International Society of Preventive & Community Dentistry*, **10**(5), 579-584 (2020). Doi: https://doi.org/10.4103/jispcd.jispcd_237_20

How to cite this article

C. Cadena-Viteri, M. Lima-Illescas, E.-M. Pacheco-Quito, M.C. Balseca-Ibarra, F. Sacoto-Figueroa, K. Cuenca-León, Inhibitory effect of the essential oil of *Schinus molle* L. against pathogens causing periodontal disease, *Rev. Colomb. Cienc. Quim. Farm.*, **53**(2), 414-429 (2024). https://doi.org/10.15446/rcciquifa.v53n2.114449

Scientific research article / https://doi.org/10.15446/rcciquifa.v53n2.114450

Drug delivery using doping of boron nitride nanosensor towards releasing chloroquine drug in the cells: A promising method for overcoming viral disease

Fatemeh Mollaamin[1],*, Majid Monajjemi[2]

[1]Department of Biomedical Engineering, Faculty of Engineering and Architecture, Kastamonu University, Kastamonu, Turkey

[2]Department of Chemical Engineering, Central Tehran Branch, Islamic Azad University, Tehran, Iran.

*Corresponding author E-mail: fmollaamin@kastamou.edu.tr, smollaamin@gmail.com

Received: December 19, 2023
Corrected: March 13, 2024
Accepted: March 16, 2024

Summary

Introduction: Chloroquine drug as the SARS-CoV-2's primary protease which can prevent *in vitro* viral duplication of all diverse experiments to now. Chloroquine drug is an anti-viral drug enlarged by Pfizer which can operate as an orally effective 3C-like protease inhibitor. **Materials and Methods:** In this work, chloroquine drug has been evaluated in forbiddance of coronavirus across trapping on the boron nitride nanocage (B_4N_{10}_NC) functionalized with some atoms as the drug delivery procedure owing to the direct electron transfer principle which can be illustrated by quantum mechanics method of density functional theory (DFT). **Results and Discussion:** As a matter of fact, it was performed the theoretical method of the B3LYP/6-311+G (d,p) to account the aptitude of B_4N_{10}_NC for grabbing Chloroquine drug via density of electronic states, nuclear quadrupole resonance, nuclear magnetic resonance, and thermodynamic specifications. Finally, the resulted amounts illustrated that using B_4N_{10}_NC functionalized with aluminum (Al), carbon (C), silicon (Si) for adsorbing Chloroquine drug towards formation of Chloroquine @Al–B_4N_{10}_NC, Chloroquine @C–B_4N_{10}_NC, Chloroquine @Si–B_4N_{10}_NC might provide the reasonable formula in drug delivery technique which is able to be fulfilled by quantum mechanics computations due to physicochemical properties of PDOS, NMR, NQR, and IR spectrum. **Conclusions:** Here, we used network pharmacology, metabolite analysis, and molecular simulation to figure out the biochemical basis of the health-raising influence of Chloroquine drug through

drug delivery with B_4N_{10}_NC. This research article peruses the drug ability, metabolites, and potential interaction of Chloroquine drug with Coronavirus-induced pathogenesis.

Keywords: Chloroquine, Drug delivery, COVID–19, X–B_4N_{10} (X=Al/C/Si)

Resumen

Administración de fármacos mediante dopaje de nanosensor de nitruro de boro para liberar el fármaco cloroquina en las células: un método prometedor para superar la enfermedad viral

Introducción: El fármaco cloroquina es la proteasa primaria del SARS-CoV-2 que puede prevenir la duplicación viral *in vitro* de todos los experimentos diversos hasta ahora. El fármaco cloroquina es un fármaco antiviral ampliado por Pfizer que puede funcionar como un inhibidor de la proteasa similar al 3C eficaz por vía oral. **Materiales y métodos:** en este trabajo, el fármaco cloroquina se ha evaluado para prevenir el coronavirus mediante la captura en la nanojaula de nitruro de boro (B_4N_{10}_NC) funcionalizada con algunos átomos como procedimiento de administración del fármaco debido al principio de transferencia directa de electrones que puede ilustrarse mediante la mecánica cuántica. Método de teoría funcional de la densidad (DFT). **Resultados y Discusión:** De hecho, se realizó el método teórico del B3LYP/6-311+G (d,p) para dar cuenta de la aptitud de B_4N_{10}_NC para capturar la droga cloroquina a través de la densidad de estados electrónicos, resonancia cuadrupolo nuclear, resonancia magnética nuclear y especificaciones termodinámicas. Finalmente, las cantidades resultantes ilustraron que el uso de B_4N_{10}_NC funcionalizado con aluminio (Al), carbono (C), silicio (Si) para adsorber el fármaco cloroquina hacia la formación de cloroquina @Al–B_4N_{10}_NC, cloroquina @C–B_4N_{10}_NC, cloroquina @Si–B_4N_{10}_NC podría proporcionar la fórmula razonable en la técnica de administración de fármacos que puede cumplirse mediante cálculos de mecánica cuántica debido a las propiedades fisicoquímicas de PDOS, NMR, NQR y espectro IR. **Conclusiones:** Aquí utilizamos farmacología de red, análisis de metabolitos y simulación molecular para descubrir la base bioquímica del efecto saludable del medicamento cloroquina a través de la administración de fármacos con B_4N_{10}_NC. Este artículo de investigación examina detenidamente la capacidad del fármaco, los metabolitos y la posible interacción del fármaco cloroquina con la patogénesis inducida por el coronavirus.

Palabras clave: cloroquina, administración de fármacos, COVID–19, X–B_4N_{10} (X=Al/C/Si)

Resumo

entrega de medicamentos usando dopagem de nanosensor de nitruro de boro para liberação de cloroquina nas células: um método promissor para superar doenças virais

Introdução: A droga cloroquina como a protease primária do SARS-CoV-2 que pode prevenir a duplicação viral *in vitro* de todos os diversos experimentos até agora. O medicamento cloroquina é um medicamento antiviral ampliado pela Pfizer que pode operar como um inibidor de protease semelhante ao 3C por via oral. **Materiais e Métodos:** Neste trabalho, a droga cloroquina foi avaliada na proibição do coronavírus através do aprisionamento na nanogaiola de nitruro de boro (B_4N_{10}_NC) funcionalizada com alguns átomos como procedimento de entrega da droga devido ao princípio de transferência direta de elétrons que pode ser ilustrado pela mecânica quântica, método da teoria do funcional da densidade (DFT). Resultados e **Discussão:** Na verdade, foi realizado o método teórico do B3LYP/6-311+G (d,p) para contabilizar a aptidão do B_4N_{10}_NC para capturar a droga Cloroquina via densidade de estados eletrônicos, ressonância quadrupolo nuclear, ressonância magnética nuclear e especificações termodinâmicas. Finalmente, os valores resultantes ilustraram que o uso de B_4N_{10}_NC funcionalizado com alumínio (Al), carbono (C), silício (Si) para adsorver o medicamento Cloroquina para a formação de Cloroquina @Al – B_4N_{10}_NC, Cloroquina @ C – B_4N_{10}_NC, Cloroquina @ Si – B_4N_{10}_NC pode fornecer a fórmula razoável na técnica de entrega de medicamentos que pode ser realizada por cálculos de mecânica quântica devido às propriedades físico-químicas do espectro PDOS, RMN, NQR e IR. **Conclusões:** Aqui, usamos farmacologia de rede, análise de metabólitos e simulação molecular para descobrir a base bioquímica da influência do medicamento Cloroquina na melhoria da saúde por meio da entrega de medicamentos com B4N10_NC. Este artigo de pesquisa examina a capacidade do medicamento, os metabólitos e a interação potencial do medicamento Cloroquina com a patogênese induzida pelo Coronavírus.

Palavras-chave: Cloroquina, Drug delivery, COVID–19, X–B_4N_{10} (X=Al/C/Si)

Introduction

The arrival of a recent coronavirus, known as the severe acute respiratory syndrome coronavirus 2 (SARS–CoV–2) has involved a pandemic of Coronavirus Disease of 2019 (COVID–19) [1-9]. After its precedent reported sample in Wuhan, China in

December 2019, recent explored proof by both medical doctors and scientists have supported some ideas on the malady pathogenesis and the nature of the virus itself [10]. The intensity of the COVID-19 pandemic has waned since the beginning of 2022, in parallel with a significantly reduced risk for disease progression and death due to widespread vaccination, hybrid immunity, and the intrinsic low virulence of the Omicron subvariants [11]. The use of early therapies (antiviral monoclonal antibodies and small molecules) has been approved for the prevention of disease progression and hospitalizations among high-risk outpatients with comorbidities [12]. Gottlieb *et al.* have investigated on early treatment of COVID-19 outpatients with oral antivirals or with short daily infusions is considered a treatment strategy that assisted in turning the tides of the pandemic by reducing hospital admissions and mortality [13]. Furthermore, Kim *et al.* have indicated that, while treatment options for patients with severe disease requiring hospitalization are now available, with corticosteroids emerging as the treatment of choice for critically ill patients, interventions that can be administered early during infection to prevent disease progression and longer-term complications are urgently needed [14]. There is not a certain therapy or vaccine receivable to battle versus SARS-CoV-2 [15]. Lately, antibodies have been almost all created in human cells and metamorphosed animal cells which are programs with many tools that are very difficult to run [16, 17]. In addition, SARS-CoV-2 is a current major challenge for researchers, and they are still working on the development of antiviral drugs against SARS-CoV-2 [18-20]. Currently, researchers and scientists are working on the development of a drug against COVID-19 in the following ways such as the prevention of self-assembly (structural proteins), viral replications (Nsps), viral entry, and the blocking of the signaling pathways required for viral infection [21-23].

Chloroquine with formula $C_{18}H_{26}ClN_3$ has antiviral and anti-inflammatory specifications which has been used in MERS-CoV, Zika virus, enterovirus EV–A71, OC43, influenza A H5N1, SARS-CoV, and SARS-CoV-2 infection treatment [24, 25].

Recently, some studies have done to investigate the possibility advantages of chloroquine or the derivative hydroxychloroquine, an economical anti-malaria medication that has been applied for years for COVID-19 therapy [26, 27].

Daolin *et al.* have exhibited that chloroquine with a dual function in antiviral immunity can be critical to remark for introducing the COVID-19 cure [28].

There is a regard to augmenting the bioavailability and interval of operation for a medication to correct remedial outcomes. Drug delivery approach can alter a medication's pharmacokinetics and quality by providing it with diverse components, medication transfers, and medical tools [29-38].

Amongst nanoparticles, boron nitride (BN) nanomaterials have shown excellent physical and chemical properties [39] and a wide usage perspective in drug delivery system [40]. In this work, it was concentrated on Chloroquine drug attached to functionalized B_4N_{10}_NC with Al, C, and Si atoms towards formation of Chloroquine @Al–B_4N_{10}_NC, Chloroquine @C–B_4N_{10}_NC, Chloroquine @Si–B_4N_{10}_NC complexes for decreasing the function of COVID–19 (Figure 1).

Figure 1. Adsorption of Chloroquine by functionalized B_4N_{10}_NC with Al, C, and Si atoms towards formation of Chloroquine @Al–B_4N_{10}_NC, Chloroquine @C–B_4N_{10}_NC, Chloroquine @Si–B_4N_{10}_NC complexes.

Theory, materials and approaches

The theoretical method of density functional theory (DFT) is one of the most utilized approximations of Hohenberg, Kohn and Sham which permits the theoretical investigation of material specifications [41]. DFT approach titrates a beneficial level for estimating the chemical systems [42-48].

In this work, the structures of Chloroquine drug adsorbed on the X–B_4N_{10} (X=Al/C/Si) were minimized at the skeleton of DFT approach accompanying the three-parameter Becke's exchange [49] and Lee–Yang–Parr's correlation non-local functional [50], introduced as B3LYP level of theory and basis set of 6–311+G(d,p). In fact, molecular modeling techniques are used to describe the process of interaction between Chloroquine drug and X–B_4N_{10} (X=Al/C/Si) towards formation of Chloroquine @Al–B_4N_{10}_NC, Chloroquine @C–B_4N_{10}_NC, Chloroquine @Si–B_4N_{10}_NC complexes as the drug delivery system for treatment of Covid-19 disease (Figure 1).

In this research, the Onsager pattern was carried out which was extended by Frisch, Wong and Wiberg by applying spherical cavities [51]. This model conveys a less accurate explanation of the solute/solvent interface, but it can lighten the assessment of energy derivatives in optimizing of geometries and analyzing the frequencies. Furthermore, Cramer and Truhlar developed this pattern at the dipole level [52]. As a matter

of fact, a cavity should have a physical impression like Onsager design, and has a mathematical susceptibility as frequently occurred in other definitions of solvent influences [53-58]. So, the cavity must maintain the solvent and its neighbors as the greatest possibility section of the solute charge diffusion [59, 60].

The compound of CNT is discoursing drug delivery programs that might be enforced with a variety of biomaterials containing DNA, proteins, and antibodies. This gives clearance the own aim for assignment the special cells, tissues, and organs. These substances might lightly interpenetrate cells, releasing medications straightly to the nucleus or cytoplasm. Drug releasing platforms ameliorate the pharmacological and therapeutic profile and influence of the medication and pull down the occurrence of off-targets [61-67].

In fact, a mass of quantum mechanical technics can accomplish discovering certain properties aspect of physicochemical specifications extracted from minimized frame of Chloroquine drug attached to X–B_4N_{10} (X=Al/C/Si) consisting of density of electrical states, electric potential, Bader charge distribution, vibrational computations and nuclear magnetic resonance analysis owing to running a drug delivery model using Gaussian 16 revision C.01 program [68]. In addition, the level of gauge including atomic orbitals (GIAO) has been dedicated to work out the gauge difficulty in the measurement of nuclear magnetic shielding for [Chloroquine @ X–B_4N_{10} (X=Al/C/Si)] complexes using DFT approach.

Results

PDOS study

The electronic structures of Chloroquine drug attached to the X–B_4N_{10} (X=Al/C/Si) nanocage were evaluated to explain the interfacial electronic parameters using quantum methods.

Figure 2a-d introduces the projected density of state (PDOS) of Chloroquine drug, Al–B_4N_{10}, C–B_4N_{10}, Si–B_4N_{10}, respectively. It is obvious from the figure that after adsorption of Chloroquine drug on the X–B_4N_{10} (X=Al/C/Si), there is a significant contribution of *p*-orbitals of Al, C, Si, N and Cl atoms in the unoccupied stage. Population analysis and PDOS indicate that C, N and Cl atoms of Chloroquine remain in the linkage with X–B_4N_{10} (X=Al/C/Si) and it can grab more electrons from other elements. So, the graph of PDOS has discovered that the *p* states of the adsorption of C, N and Cl atoms on the X–B_4N_{10} (X=Al/C/Si) are significant through the conduction band (Figure 2a-d). Furthermore, the existence of covalent features for [Chloroquine

@ X–B_4N_{10} (X=Al/C/Si)] complex has shown the equal energy content and configuration of the PDOS for the *p* orbitals of Al, C, Si, N and Cl atoms (Figure 2a-b).

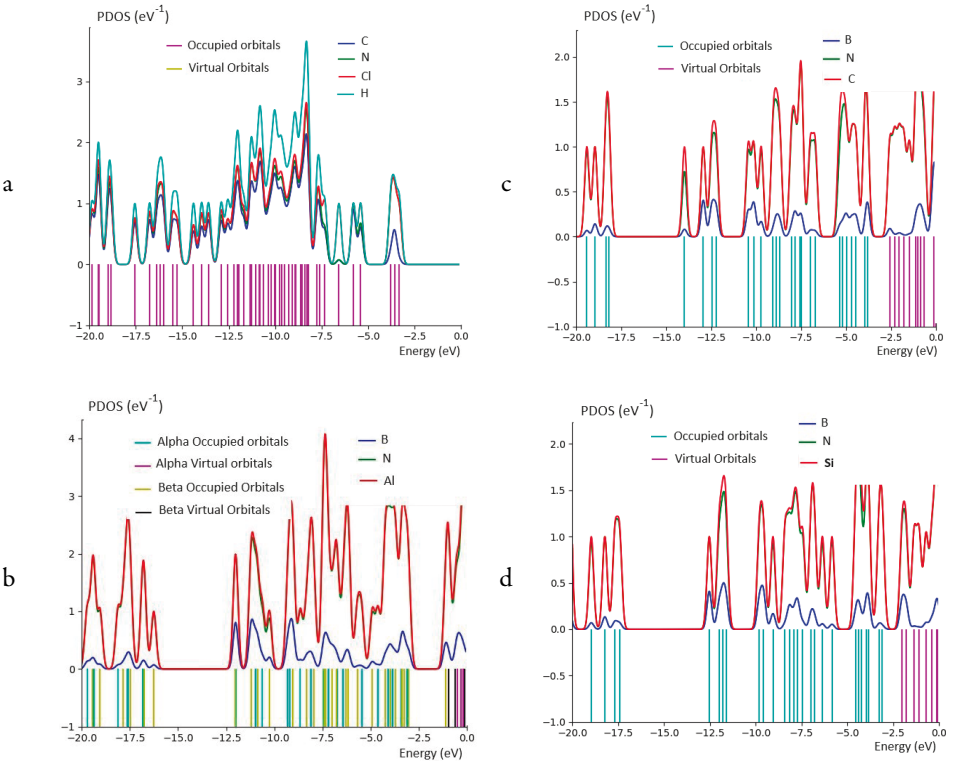

Figure 2. Electronic properties of Partial Density of States (PDOS) for **a)** Chloroquine drug adsorbed on **b)** Al–B_4N_{10} **c)** C–B_4N_{10} and **d)** Si–B_4N_{10}.

Figure 2a-d shows that the Chloroquine drug states adsorbed onto X–B_4N_{10} (X=Al/C/Si) complexes have more contribution at the middle of the conduction band between −5eV to −15eV, while contribution of C, N, Cl states in Chloroquine drug are expanded and close together (Figure 2a), and Al states in Al–B_4N_{10}_NC (Figure 2b), C in C–B_4N_{10}_NC (Figure 2c) and Si in Si–B_4N_{10}_NC (Figure 2d) approximately have the most contributions.

As a matter of fact, the mentioned consequences display that the principal complex and a certain degree of covalent traits can describe ameliorating of the straight conducting band gap of Chloroquine drug absorbing on the X–B_4N_{10} (X=Al/C/Si) complexes.

Spectroscopy of NMR

The nuclear magnetic resonance (NMR) information of shielding tensors (ppm) containing isotropic (σ_{iso}) and anisotropic (σ_{aniso}) for Chloroquine drug linked to X–B_4N_{10} (X=Al/C/Si) complexes were computed (Table 1). The accomplished consequences have demonstrated the "SCF/GIAO" magnetic shielding tensor for Al, C, Si, N and Cl atoms discovering the active zone of Chloroquine material as the medication for viral disease therapy. The measurements were run on "B3LYP/6–311+G (d, p)" level of theory using Gaussian 16 revision C.01 program [68] and were announced in Table 1.

The [Chloroquine @ X–B_4N_{10} (X=Al/C/Si)] complexes have reflected the significance of chemical shielding consisting of σ_{iso} and σ_{aniso} (ppm) for diverse elements of B, Al, C, Si, N and Cl atoms in the active zones of the system owing to the NMR curve (Table 1).

Furthermore, the ^{13}C–NMR considerations on Chloroquine drug have approved the active zones of this compound owing to unraveling the most electron donor elements during Chloroquine drug adsorption onto X–B_4N_{10} (X=Al/C/Si) complexes which expose the major shift in tetramethylsilane (TMS) using quantum methods (Figure 3a-d).

The most alterations were declared for atoms of N11 in Chloroquine drug (Figure 3a), N11, Al13 in Chloroquine @Al–B_4N_{10} (Figure 3b), N11, C13 in Chloroquine @C–B_4N_{10} (Figure 3c), N11, Si13 in Chloroquine @Si–B_4N_{10} (Figure 3d).

The progress of impressive DFT methods including electronic correlation effects has illustrated to be a significant key in the field of shielding computations. By DFT theory, which measures N^2 (N=number of electrons), it is feasible to compute shielding in molecular systems of practical interest consisting of electronic correlation impacts. Furthermore, new DFT approaches with linear scaling are accessible and these will supply further developments in the implementation of these technics to compute magnetic shielding in the large the large groups [69].

This skeleton based on the theory analyses the solvent effects on magnetic shielding. The real computation of these impacts is quite puzzling because any model that seeks to indicate these interactions must estimate both the electromagnetic iterations produced by the solvent molecules as well as their dynamic parameters.

Table 1. Data of nuclear magnetic resonance (NMR) tensors (ppm) for Chloroquine drug attached to Al–B_4N_{10}_NC, C–B_4N_{10}_NC, and Si–B_4N_{10}_NC by quantum methods. SCF GIAO Magnetic shielding tensors (ppm) consisting of isotropic shielding tensor (σ_{iso}) and anisotropic shielding tensor (σ_{aniso}).

Chloroquine			Al–B_4N_{10}			C–B_4N_{10}			Si–B_4N_{10}		
Atom	σ_{iso}	σ_{aniso}	Atom	σ_{iso}	σ_{aniso}	Atom	σ_{iso}	σ_{aniso}	Atom	σ_{iso}	σ_{aniso}
C (1)	132.52	130.65	B1	96.71	82.91	B1	103.95	91.64	B1	69.65	66.87
C (2)	134.71	115.73	N2	259.30	626.11	N2	111.66	621.75	N2	211.97	928.02
C (3)	154.14	132.97	N3	58.49	79.64	N3	1655.31	2921.16	N3	890.97	2652.00
C (4)	133.90	120.89	B4	105.97	72.42	B4	99.38	130.29	B4	93.00	40.07
C (5)	129.01	112.43	B5	94.94	58.17	B5	111.94	44.71	B5	56.79	52.74
C (6)	121.43	90.28	B6	78.48	78.26	B6	111.96	63.24	B6	55.44	76.88
C (7)	135.35	119.43	N7	180.32	573.04	N7	268.02	362.56	N7	147.71	1114.40
C (8)	145.64	85.83	N8	79.95	253.36	N8	557.61	1335.78	N8	1417.29	2153.41
C (9)	124.85	112.78	N9	460.09	832.80	N9	601.87	1305.01	N9	588.36	4046.60
N (10)	76.90	440.22	N10	558.79	717.03	N10	877.08	1752.31	N10	575.52	2937.29
N (11)	236.30	37.80	N11	512.23	941.85	N11	1094.84	1854.46	N11	88.60	3677.85
C (12)	179.56	34.90	N12	283.32	712.10	N12	637.42	1166.30	N12	300.50	2936.03
C (13)	204.91	29.29	Al13	488.58	206.97	C13	99.65	87.81	Si13	670.58	157.49
C (14)	198.50	27.14	N14	28.48	599.67	N14	35.63	1510.04	N14	123.22	1007.9
C (15)	200.92	22.42	N15	21.33	591.87	N15	262.85	1199.51	N15	40.17	1170.06
C (16)	179.88	55.74									
N (17)	274.67	37.68									
C (18)	184.27	51.36									
C (19)	208.57	23.61									
C (20)	186.65	40.51									
C (21)	208.71	17.64									
Cl (22)	920.80	169.33									

Note: Isotropic chemical-shielding (σ_{iso}/ppm) & anisotropic chemical-shielding (σ_{aniso}/ppm) [70]:

$$\sigma_{iso} = (\sigma_{33} + \sigma_{22} + \sigma_{11})/3$$

$$\sigma_{aniso} = \sigma_{33} - (\sigma_{22} + \sigma_{11})/2.$$

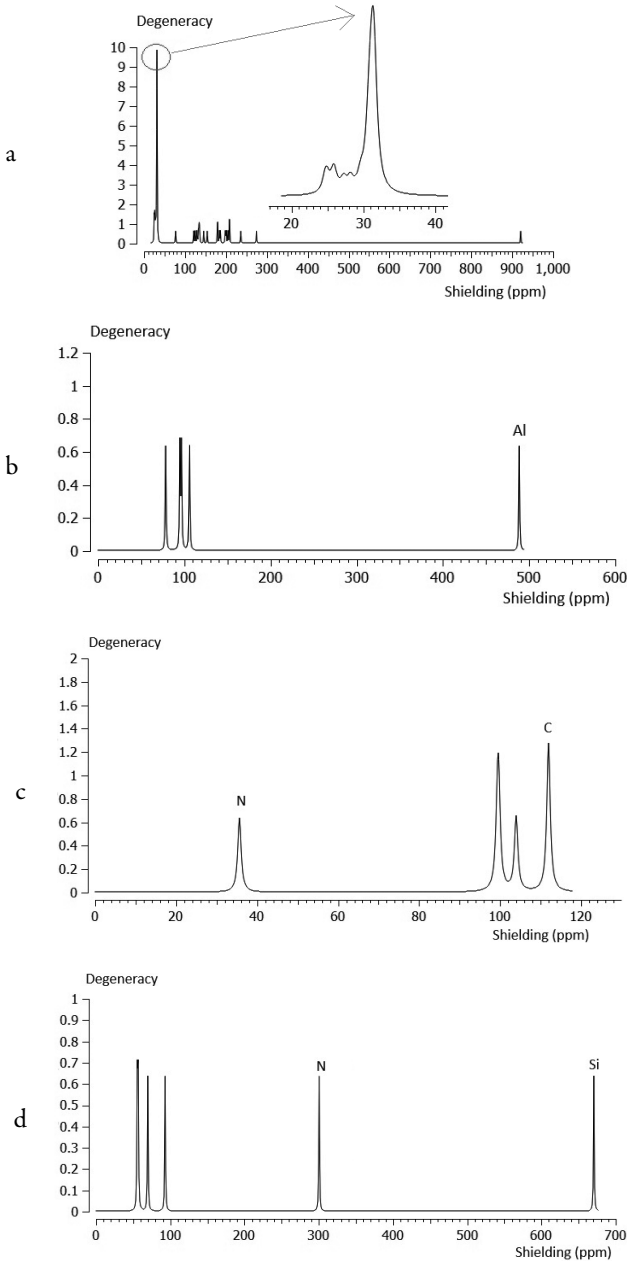

Figure 3. The NMR spectrums for **a)** Chloroquine drug, **b)** Chloroquine @Al–B_4N_{10}_NC, **c)** Chloroquine @C–B_4N_{10}_NC, **d)** Chloroquine @Si–B_4N_{10}_NC.

NQR analysis

The Nuclear Quadrupole Resonance (NQR) spectrums can prepare exact data on the structural and composition properties of active groups in biological reactions. It presents a special probability of identifying the quadrupole coupling constants and impressive charges which lets us knowledge of the electronic structure of the system. In fact, NQR spectrums become visible to propose an intense approach for the inquiry of diverse chemical influences in the solid phase of many nitrogen possessing substances. Analyzing the quadrupole coupling constants of nitrogen atoms permits an assessment of the electron density distribution on the nitrogen nuclei and authorizes the analysis of charge distribution in chemical bonding dealing with nitrogen atom.

So, "nuclear quadrupole resonance" or "NQR" was evaluated for Chloroquine drug trapped by the surface of X–B_4N_{10} (X=Al/C/Si) nanocages towards formation of [Chloroquine @X–B_4N_{10} (X=Al/C/Si)] complexes based on the "nuclear quadrupole moment", and the "electric field gradient" or "EFG" [70].

As the "EFG" at the citation of the nucleus in Chloroquine drug is allocated by the valence electrons twisted in the particular attachment with close nuclei of X–B_4N_{10} (X=Al/C/Si) nanocages, the "NQR" frequency at which transitions occur is particular for of [Chloroquine @(5,5) B_4N_{10} (X=Al/C/Si)] complexes (Table 2).

Furthermore, in Figure 4a-d, it was drawn the electric potential versus Bader charge of nuclear quadrupole resonance for some atoms in the attachment of Chloroquine drug onto X–B_4N_{10} (X=Al/C/Si) nanocages which was measured by theoretical method. In Figure 4a, it was exhibited the fluctuation of the charge distribution for all atoms in the Chloroquine drug towards understanding which atoms have more electron donating tendency in the attachment to the X–B_4N_{10} (X=Al/C/Si) complexes.

On the other hand, the element of N in Chloroquine drug acts like an electron donor which has a high energy orbital with one or more electrons. So, in X–B_4N_{10} (X=Al/C/Si) complexes, the elements of Al, C and Si can be considered as the electron acceptors which have a low energy orbital with one or more vacancies (Figure 4b,c,d).

In fact, it was presented the influence of the linkage between N11 in Chloroquine drug (Figure 4a) and Al13, C13 and Si13 in Al–B_4N_{10}_NC (Figure 4b), C–B_4N_{10}_NC (Figure 4c) and Si–B_4N_{10}_NC (Figure 4d) complexes, respectively during adsorbing Chloroquine owing to achieved data of E_p from NQR spectroscopy. The competence of X–B_4N_{10} (X=Al/C/Si) complexes for sensing of Chloroquine is oscillated by their selectivity and sensitivity which can indicate the yield of these materials as the engaged detectors.

Table 2. The electric potential (E_p/a.u.) and Bader charge (Q/coulomb) through NQR calculation for functionalized elements of Chloroquine drug attached to Al–B_4N_{10}, C–B_4N_{10}, and Si–B_4N_{10} nanocages using CAM-B3LYP/EPR-III,6-311+G(d,p) calculation.

Chloroquine			Al-B_4N_{10}			C-B_4N_{10}			Si-B_4N_{10}		
Atom	Q	E_p	Atom	Q	E_p	Atom	Q	E_p	Atom	Q	E_p
C (1)	0.01	−14.54	B1	−0.42	−11.30	B1	0.29	−11.27	B1	0.33	−11.26
C (2)	0.00	−14.54	N2	0.32	−18.14	N2	−0.15	−18.09	N2	−0.16	−18.11
C (3)	−0.04	−14.53	N3	−1.49	−18.12	N3	−0.13	−18.07	N3	−0.16	−18.10
C (4)	0.09	−14.51	B4	−0.37	−11.30	B4	0.29	−11.26	B4	0.33	−11.27
C (5)	0.04	−14.55	B5	−0.54	−11.30	B5	0.30	−11.28	B5	0.33	−11.26
C (6)	0.00	−14.50	B6	−0.26	−11.28	B6	0.29	−11.27	B6	0.33	−11.26
C (7)	0.10	−14.47	N7	0.58	−18.14	N7	−0.15	−18.09	N7	−0.16	−18.12
C (8)	0.04	−14.57	N8	1.57	−18.13	N8	−0.13	−18.08	N8	−0.15	−18.09
C (9)	0.10	−14.53	N9	0.47	−18.20	N9	−0.10	−18.08	N9	−0.33	−18.18
N (10)	−0.28	−18.14	N10	−0.24	−18.20	N10	−0.10	−18.09	N10	−0.33	−18.17
N (11)	−0.07	−18.01	N11	−0.02	−18.18	N11	−0.09	−18.08	N11	−0.31	−18.16
C (12)	0.12	−14.46	N12	0.20	−18.18	N12	−0.10	−18.07	N12	−0.32	−18.15
C (13)	0.02	−14.52	Al13	−0.00	−43.70	C13	0.11	−14.53	Si13	0.96	−48.39
C (14)	0.02	−14.52	N14	0.73	−18.12	N14	−0.14	−18.08	N14	−0.18	−18.12
C (15)	0.01	−14.52	N15	0.46	−18.13	N15	−0.14	−18.08	N15	−0.18	−18.12
C (16)	0.08	−14.51	Note:								
N (17)	−0.25	−18.10									
C (18)	0.08	−14.51									
C (19)	0.00	−14.55									
C (20)	0.08	−14.51									
C (21)	0.01	−14.54									
Cl (22)	−0.10	−63.31									

Electric potential: E_p/a.u.
Bader charge: Q/coulomb

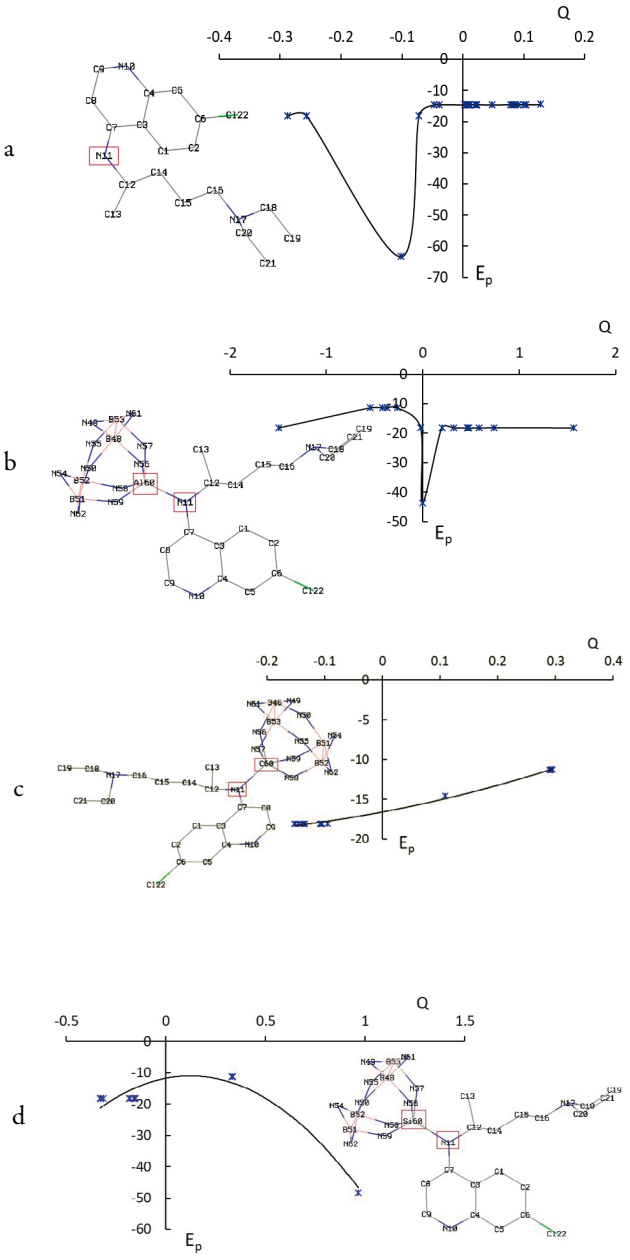

Figure 4. The amounts of electric potential (E_p/a.u.) versus Bader charge (Q/coulomb) through NQR calculation for **a)** Chloroquine drug, **b)** Chloroquine @Al–B_4N_{10}_NC, c) Chloroquine @C–B_4N_{10}_NC, **d)** Chloroquine @Si–B_4N_{10}_NC.

Spectroscopy of IR

The spectroscopy of infrared (IR) through some computations were completed for Chloroquine drug (Figure 5a) attached to X–B_4N_{10} (X=Al/C/Si) complexes by DFT approach to catch a more stable system accompanying thermodynamic attributes. Therefore, it has been simulated the several complexes containing Chloroquine @Al–B_4N_{10}_NC (Figure 5b), Chloroquine @C–B_4N_{10}_NC (Figure 5c), Chloroquine @ Si–B_4N_{10}_NC (Figure5d), respectively.

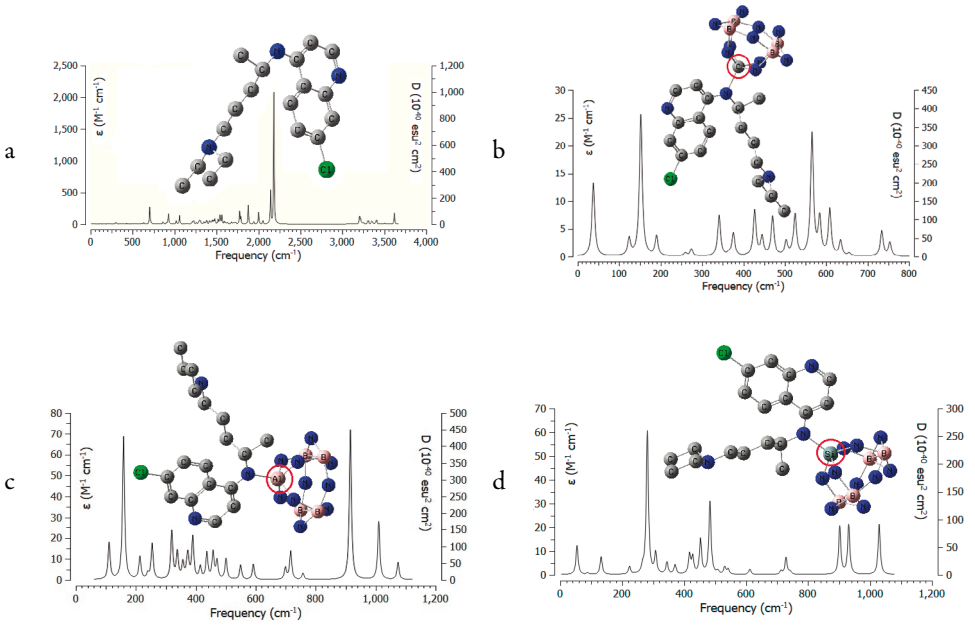

Figure 5. The Frequency (cm^{-1}) amounts of IR spectrums for a) v drug, b) Chloroquine @Al–B_4N_{10}_NC, c) Chloroquine @C–B_4N_{10}_NC, d) Chloroquine @Si–B_4N_{10}_NC.

The curve of Figure 5a was shown in the frequency limitation across 500–3500 cm^{-1} for v drug with a sharp peak around 2183.43 cm^{-1}. Figure 5b has shown the frequency range between 100–1500 cm^{-1} for Chloroquine @Al–B_4N_{10}_NC with two sharp peaks around 158.81 and 915.64 cm^{-1}. Figure 5c has indicated the fluctuation of frequency between 50–750 cm^{-1} for Chloroquine @C–B_4N_{10}_NC with the sharp peaks around 37.34, 152.01 and 565.57 cm^{-1}. Figure 5d has showed the fluctuation of frequency between 100–1100 cm^{-1} for Chloroquine @Si–B_4N_{10}_NC with sharp peaks around 281.19, 483.33, 902.26, 931.18 and 1029.57 cm^{-1}.

The outlook of Figure 5a-d introduces the proof for different frequencies of [Chloroquine @ X–B_4N_{10} (X=Al/C/Si)] complexes which indicate the active sites in the Chloroquine drug and functionalized atoms in X–B_4N_{10} (X=Al/C/Si) that can transfer the charge of electrons in polar Chloroquine into the X–B_4N_{10} (X=Al/C/Si) complexes.

Furthermore, Table 3 through the thermodynamic specifications concluded that X–B_4N_{10} (X=Al/C/Si) due to adsorption of Chloroquine drug might be more efficient sensor for a drug delivery system.

Table 3. The thermodynamic characters thermal energy ($\Delta E°$), thermal enthalpy ($\Delta H°$), Gibbs free energy ($\Delta G°$), entropy ($S°$) and dipole moment of Chloroquine drug, Chloroquine @Al–B_4N_{10}_NC, c) Chloroquine @C–B_4N_{10}_NC, Chloroquine @Si–B_4N_{10}_NC using CAM-B3LYP/6-311+G (d, p), LANL2DZ calculation.

Compound	Dipole moment (Debye)	$\Delta E°\times10^{-4}$ (kcal/mol)	$\Delta H°\times10^{-4}$ (kcal/mol)	$\Delta G°\times10^{-4}$ (kcal/mol)	$S°$ (cal/K.mol)
Chloroquine drug	5.83	–821.87	–821.87	–821.91	129.09
Chloroquin @Al–B_4N_{10}	3.42	–55.03	–55.03	–55.04	98.17
Chloroquine @C–B_4N_{10}	1.41	–42.35	–42.35	–42.35	99.09
Chloroquine @Si–B_4N_{10}	1.29	–57.95	–57.95	–57.95	99.25

It is remarkable that polarization functions into the practical basis set in the enumerations indicate a notable prosperity on the quantum theoretical technics. The outcomes of the mentioned perceptions intensely offer that Chloroquine attached to X–B_4N_{10} (X=Al/C/Si) complex which are persuades by a mutation in the polarization of the ambiance. It can be found that a growth in the dielectric constant augments the endurance and turnover of this medication for curing COVID-19 viral malady.

The adsorption process of Chloroquine drug on the surface of functionalized B_4N_{10}_NC by Al, C, and Si elements is affirmed by $\Delta G°_R$ the quantity:

$$\Delta G°_R = \Delta G°_{\text{Chloroquine@ X–B4N10\_\_NC}} - (\Delta G°_{\text{Chloroquine-adsorbed}} + \Delta G°_{\text{X–B4N10\_\_NC}}); \text{X= Al, C, Si}$$

As seen in Table 3, all accounted amounts of Al–B_4N_{10}_NC, C–B_4N_{10}_NC and Si–B_4N_{10}_NC are close which can demonstrate an appropriate potential of these functionalized nanocages for Chloroquine drug adsorption as a drug delivery technique (Figure 6).

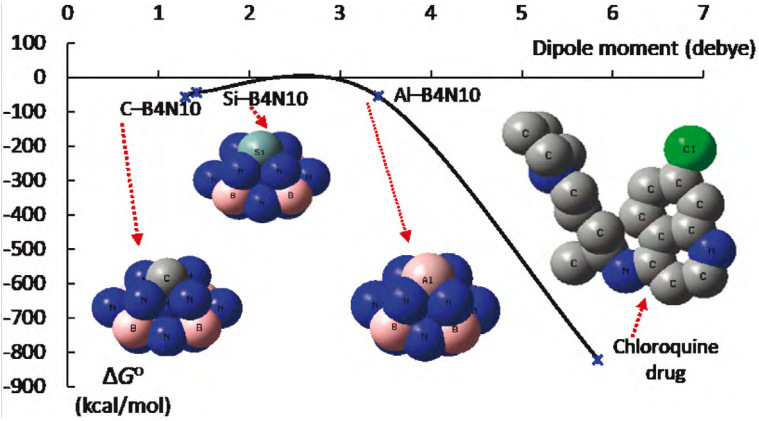

Figure 6. Gibbs free energy (ΔG°_{R}) versus dipole moment (Debye) for Chloroquine drug, Al–B_4N_{10}_NC, C–B_4N_{10}_NC, Si–B_4N_{10}_NC complexes using CAM-B3LYP/6-311+G (d,p), LANL2DZ.

Figure 6 has shown the fluctuation of ΔG° versus dipole moment for different functionalized nanocages of Al–B_4N_{10}_NC, C–B_4N_{10}_NC and Si–B_4N_{10}_NC as electron acceptors (adsorbents) for trapping Chloroquine drug as an electron donor (adsorbate) during interaction process as a promising drug delivery system.

Conclusions

In this work, the effect of Chloroquine drug on the COVID-19 treating has been studied owing to attaching to the X–B_4N_{10} (X=Al/C/Si) complex surrounds by periodic box of H_2O as the drug delivery technics. Chloroquine drug has motivated the scientists for investigation on the clinical therapy of viral coronavirus malady (COVID-19) using linkage to the B_4N_{10}_NC which can engage an impressive drug delivery approach due to computational analysis on the optimized structure extracted from DFT measurements. The progress of impressive DFT methods including electronic correlation effects has illustrated to be a significant key in the field of shielding computations. On the other hand, the element of N in Chloroquine drug acts like an electron donor which has a high energy orbital with one or more electrons. So, in X–B_4N_{10} (X=Al/C/Si) complexes, the elements of Al, C and Si can be considered as the electron acceptors which have a low energy orbital with one or more vacancies. In addition, thermodynamic properties have exhibited that functionalized nanocages of Al–B_4N_{10}_NC, C–B_4N_{10}_NC and Si–B_4N_{10}_NC as electron acceptors (adsorbents) for trapping Chloroquine drug as an electron donor (adsorbate) during interaction process can b promising drug delivery system. Concerning boron-based drug delivery

systems applied as a specific drug transport, as well as other essential drug delivery system design necessities, the authors have purposed to give readers a detailed conception of these systems.

Acknowledgment

In successfully completing this paper and its research, the authors are grateful to Kastamonu University.

Conflicts of interest

Authors declare that they have no conflicts of interest

References

1. A. Sharma, S. Tiwari, M.K. Deb, J.L. Marty, Severe acute respiratory syndrome coronavirus-2 (SARS-CoV-2): a global pandemic and treatment strategies, *International Journal of Antimicrobial Agents*, **56**(2), 106054 (2020). Doi: https://doi.org/10.1016/j.ijantimicag.2020.106054

2. F. Mollaamin, M. Monajjemi, Thermodynamic research on the inhibitors of coronavirus through drug delivery method, *Journal of the Chilean Chemical Society*, **66**(2), 5195-5205 (2021). Doi: https://doi.org/10.4067/S0717-97072021000205195

3. B. Hu, H. Guo, P. Zhou, Z.-L. Shi, Characteristics of SARS-CoV-2 and COVID-19, *Nature Reviews Microbiology,* **19**(3), 141-154 (2021). Doi: https://doi.org/10.1038/s41579-020-00459-7

4. S. Shahriari, M. Monajjemi, F. Mollaamin, Determination of proteins specification with SARS- COVID-19 based ligand designing, *Journal of the Chilean Chemical Society*, **67**(2), 5468-5476 (2022). Doi: https://doi.org/10.4067/S0717-97072022000205468

5. F. Mollaamin, Physicochemical investigation of anti-COVID19 drugs using several medicinal plants, *Journal of the Chilean Chemical Society*, **67**(2), 5537-5546 (2022). Doi: https://doi.org/10.4067/S0717-97072022000205537

6. F. Mollaamin, S. Shahriari, M. Monajjemi, Treating omicron BA.4 & BA.5 via herbal antioxidant asafoetida: A DFT study of carbon nanocarrier in drug delivery, *Journal of the Chilean Chemical Society*, **68**(1), 5781-5786 (2023). Doi: https://doi.org/10.4067/S0717-97072023000105781

7. F. Mollaamin, S. Shahriari, M. Monajjemi, Monkeypox disease treatment by tecovirimat adsorbed onto single-walled carbon nanotube through drug delivery method, *Journal of the Chilean Chemical Society,* **68**(1), 5796-5801 (2023). Doi: https://doi.org/10.4067/S0717-97072023000105796

8. M. Monajjemi, F. Mollaamin, S. Shojaei, An overview on coronaviruses family from past to COVID-19: Introduce some inhibitors as antiviruses from Gillan's plants, *Biointerface Research in Applied Chemistry*, **10**(3), 5575-5585 (2020). Doi: https://doi.org/10.33263/BRIAC103.575585

9. F. Mollaamin, M. Monajjemi, Molecular drug discovery of potential inhibitor of Covid–19 using several medicinal plant ingredients: A promising therapy for viral disease, *Revista de la Facultad de Ciencias*, **13**(1), 141-158 (2024). Doi: https://doi.org/10.15446/rev.fac.cienc.v13n1.111288

10. U. Anand, C. Cabreros, J. Mal, F. Ballesteros, Jr., M. Sillanpää, V. Tripathi, E. Bontempi, Novel coronavirus disease 2019 (COVID-19) pandemic: From transmission to control with an interdisciplinary vision, *Environmental Research*, **197**, 111126 (2021). Doi: https://doi.org/10.1016/j.envres.2021.111126

11. R. Rana, R. Kant, R.S. Huirem, D. Bohra, N.K. Ganguly, Omicron variant: Current insights and future directions, *Microbiological Research*, **265**, 127204 (2022). Doi: https://doi.org/10.1016/j.micres.2022.127204

12. P.C. Taylor, A.C. Adams, M.M. Hufford, I. de la Torre, K. Winthrop, R.L. Gottlieb, Neutralizing monoclonal antibodies for treatment of COVID-19, *Nature Reviews Immunology,* **21**(6), 382-393 (2021). Doi: https://doi.org/10.1038/s41577-021-00542-x

13. R.L. Gottlieb, C.E. Vaca, R. Paredes, J. Mera, B.J. Webb, G. Perez, G. Oguchi, P. Ryan, B.U. Nielsen, M. Brown, A. Hidalgo, Y. Sachdeva, et al., Early remdesivir to prevent progression to severe Covid-19 in outpatients, *The New England Journal of Medicine*, **386**(4), 305-315 (2022). Doi: https://doi.org/10.1056/NEJMoa2116846

14. P.S. Kim, S.W. Read, A.S. Fauci, Therapy for early COVID-19: A critical need, *JAMA,* **324**(21), 2149-2150 (2020). Doi: https://doi.org/10.1001/jama.2020.22813

15. Z. Plavec, A. Domanska, X. Liu, P. Laine, L. Paulin, M. Varjosalo, P. Auvinen, S.G. Wolf, M. Anastasina, S.J. Butcher, SARS-CoV-2 Production, purification methods and UV inactivation for proteomics and structural studies, *Viruses*, **14**(9), 1989 (2022). Doi: https://doi.org/10.3390/v14091989

16. N.Z. Zabidi, H.L. Liew, I.A. Farouk, A. Puniyamurti, A.J.W. Yip, V.N. Wijesinghe, Z.Y. Low, J.W. Tang, V.T.K. Chow, S.K. Lal, Evolution of SARS-CoV-2 variants: Implications on immune escape, vaccination, therapeutic and diagnostic strategies, *Viruses*, **15**(4), 944 (2023). Doi: https://doi.org/10.3390/v15040944

17. O.I. Yarovaya, D.N. Shcherbakov, S.S. Borisevich, A.S. Sokolova, M.A. Gureev, E.M. Khamitov, N.B. Rudometova, A.V. Zybkina, E.D. Mordvinova, A.V. Zaykovskaya, A.D. Rogachev, O.V. Pyankov, R.A. Maksyutov, N.F. Salakhutdinov, Borneol ester derivatives as entry inhibitors of a wide spectrum of SARS-CoV-2 viruses, *Viruses*, **14**(6), 1295 (2022). Doi: https://doi.org/10.3390/v14061295

18. A. Majeed, X. Zhang, On the adoption of modern technologies to fight the COVID-19 pandemic: A technical synthesis of latest developments, *COVID*, **3**(1), 90-123 (2023). Doi: https://doi.org/10.3390/covid3010006

19. G. Bonaccorsi, F. Pierri, M. Cinelli, A. Flori, A. Galeazzi, F. Porcelli, A.L. Schmidt, C.M. Valensise, A. Scala, W. Quattrociocchi, F. Pammolli, Economic and social consequences of human mobility restrictions under COVID-19, *Proceedings of the National Academy of Sciences of the United States of America*, **117**(27), 15530-15535 (2020). Doi: https://doi.org/10.1073/pnas.2007658117

20. A. Barakat, A. Mostafa, M. Ali, A.M. Al-Majid, L.R. Domingo, O. Kutkat, Y. Moatasim, K. Zia, Z. Ul-Haq, Y.A.M.M. Elshaier, Design, synthesis and *in vitro* evaluation of spirooxindole-based phenylsulfonyl moiety as a candidate anti-SAR-CoV-2 and MERS-CoV-2 with the implementation of combination studies, *International Journal of Molecular Sciences*, **23**(19), 11861 (2022). Doi: https://doi.org/10.3390/ijms231911861

21. F. Zeng, Y. Huang, Y. Guo, M. Yin, X. Chen, L. Xiao, G. Deng, Association of inflammatory markers with the severity of COVID-19: a meta-analysis, *International Journal of Infectious Diseases*, **96**, 467-474 (2020). Doi: https://doi.org/10.1016/j.ijid.2020.05.055

22. Q.M.S. Jamal, Antiviral potential of plants against COVID-19 during outbreaks—An update, *International Journal of Molecular Sciences*, **23**(21), 13564 (2022). Doi: https://doi.org/10.3390/ijms232113564

23. S. Bibi, M.S. Khan, S.A. El-Kafrawy, T.A. Alandijany, M.M. El-Daly, Q. Yousafi, D. Fatima, A.A. Faizo, L.H. Bajrai, E.I. Azhar, Virtual screening and molecular dynamics simulation analysis of Forsythoside A as a plant-derived inhibitor of SARS-CoV-2 3CLpro, *Saudi Pharmaceutical Journal*, **30**(7), 979-1002 (2022). Doi: https://doi.org/10.1016/j.jsps.2022.05.003

24. M. Wang, R. Cao, L. Zhang, X. Yang, J. Liu, M. Xu, Z. Shi, Z. Hu, W. Zhong, G. Xiao, Remdesivir and chloroquine effectively inhibit the recently emerged novel coronavirus (2019-nCoV) *in vitro*, *Cell Research*, **30**(3), 269-271 (2020). Doi: https://doi.org/10.1038/s41422-020-0282-0

25. F. Touret, X. de Lamballerie, Of chloroquine and COVID-19, *Antiviral Research*, **177**, 104762 (2020). Doi: https://doi.org/10.1016/j.antiviral.2020.104762

26. P. Colson, J.M. Rolain, J.C. Lagier, P. Brouqui, D. Raoult, Chloroquine and hydroxychloroquine as available weapons to fight COVID-19, *International Journal of Antimicrobial Agents*, **55**(4), 105932 (2020). Doi: https://doi.org/10.1016/j.ijantimicag.2020.105932

27. A. Cortegiani, G. Ingoglia, M. Ippolito, A. Giarratano, S. Einav, A systematic review on the efficacy and safety of chloroquine for the treatment of COVID-19, *Journal of Critical Care*, **57**, 279-283 (2020). Doi: https://doi.org/10.1016/j.jcrc.2020.03.005

28. D. Tang, J. Li, R. Zhang, R. Kang, D.J. Klionsky, Chloroquine in fighting COVID-19: good, bad, or both? *Autophagy*, **16**(12), 2273-2275 (2020). Doi: https://doi.org/10.1080/15548627.2020.1796014

29. *J. Li, M. Zeng, H. Shan, C. Tong,* Microneedle patches as drug and vaccine delivery platform*, Current Medicinal Chemistry,* **24**(22), 2413-2422 (2017). Doi: https://doi.org/10.2174/0929867324666170526124053

30. *A.P. Singh, A. Biswas, A. Shukla, P. Maiti,* Targeted therapy in chronic diseases using nanomaterial-based drug delivery vehicles, *Signal Transduction and Targeted Therapy*, **4**, 33 (2019). Doi: https://doi.org/10.1038/s41392-019-0068-3

31. T.M. Allen, Drug delivery systems: Entering the mainstream, *Science*, **303**(5665), 1818-1822 (2004). Doi: https://doi.org/10.1126/science.1095833

32. F. Mollaamin, M. Monajjemi, S. Mohammadi, Physicochemical characterization of antiviral phytochemicals of *Artemisia annua* plant as therapeutic potential against coronavirus disease: *In silico*–drug delivery by density functional theory benchmark, *Journal of Biological Regulators and Homeostatic Agents*, **37**(7), 3629-3639 (2023). Doi: https://doi.org/10.23812/j.biol.regul.homeost.agents.20233707.358

33. M. Monajjemi, M.T. Baie, F. Mollaamin, Interaction between threonine and cadmium cation in [Cd(Thr)] (n = 1-3) complexes: Density functional calculations, *Russian Chemical Bulletin*, **59**, 886-889 (2010). Doi: https://doi.org/10.1007/s11172-010-0181-5

34. F. Mollaamin, M. Monajjemi, *In situ* drug delivery investigation through characterization and application of carbon-based nanomaterials: A promising approach for treating viral diseases, *Journal of Biological Regulators and Homeostatic Agents*, **38**(3), 1961-1973 (2024). Doi: https://doi.org/10.23812/j.biol.regul.homeost.agents.20243803.153

35. B. Ghalandari, M. Monajjemi, F. Mollaamin, Theoretical investigation of carbon nanotube binding to DNA in view of drug delivery, *Journal of Computational and Theoretical Nanoscience*, **8**(7), 1212-1219 (2011). Doi: https://doi.org/10.1166/jctn.2011.1801

36. F. Mollaamin, Computational methods in the drug delivery of carbon nanocarriers onto several compounds in Sarraceniaceae medicinal plant as monkeypox therapy, *Computation*, **11**(4), 84 (2023). Doi: https://doi.org/10.3390/computation11040084

37. B. Khalili-Hadad, F. Mollaamin, M. Monajjemi, Biophysical chemistry of macrocycles for drug delivery: A theoretical study, *Russian Chemical Bulletin*, **60**(2), 238-241 (2011). Doi: https://doi.org/10.1007/s11172-011-0039-5

38. F. Mollaamin, M. Monajjemi, Transition metal (X = Mn, Fe, Co, Ni, Cu, Zn)-doped graphene as gas sensor for CO_2 and NO_2 detection: A molecular modeling framework by DFT perspective, *Journal of Molecular Modeling*, **29**(4), 119 (2023). Doi: https://doi.org/10.1007/s00894-023-05526-3

39. D. Pan, F. Su, H. Liu, Y. Ma, R. Das, Q. Hu, C. Liu, Z. Guo, The properties and preparation methods of different boron nitride nanostructures and applications of related nanocomposites, *The Chemical Record*, **20**(11), 1314-1337 (2020). Doi: https://doi.org/10.1002/tcr.202000079

40. S.M. Sharker, Hexagonal boron nitrides (white graphene): A promising method for cancer drug delivery, *International Journal of Nanomedicine*, **14**, 9983-9993 (2019). Doi: https://doi.org/10.2147/IJN.S205095

41. M. Penz, E.I. Tellgren, M.A. Csirik, M. Ruggenthaler, A. Laestadius, The structure of density-potential mapping. Part I: Standard density-functional theory*, ACS Physical Chemistry Au*, **3**(4), 334-347 (2023). Doi: https://doi.org/10.1021/acsphyschemau.2c00069

42. T. van Mourik, M. Bühl, M.-P. Gaigeot, Density functional theory across chemistry, physics and biology, *Philosophical Transactions of the Royal Society A: Mathematical, Physical and Engineering Sciences*, **372**(2011), 20120488 (2014). Doi: https://doi.org/10.1098/rsta.2012.0488

43. F. Mollaamin, M. Monajjemi, *In silico*-DFT investigation of nanocluster alloys of Al-(Mg, Ge, Sn) coated by nitrogen heterocyclic carbenes as corrosion inhibitors, *Journal of Cluster Science*, **34**(6), 2901-2918 (2023). Doi: https://doi.org/10.1007/s10876-023-02436-5

44. K. Bakhshi, F. Mollaamin, M. Monajjemi, Exchange and correlation effect of hydrogen chemisorption on nano V(100) surface: A DFT study by generalized gradient approximation (GGA), *Journal of Computational and Theoretical Nanoscience*, **8**(4), 763-768 (2011). Doi: https://doi.org/10.1166/jctn.2011.1750

45. F. Mollaamin, M. Monajjemi, Graphene-based resistant sensor decorated with Mn, Co, Cu for nitric oxide detection: Langmuir adsorption & DFT method, *Sensor Review*, **43**(4), 266-279 (2023). Doi: https://doi.org/10.1108/SR-03-2023-0040

46. M. Monajjemi, J. Najafpour, F. Mollaamin, $(3,3)_4$ Armchair carbon nanotube in connection with PNP and NPN junctions: *Ab Initio* and DFT-based studies, *Fullerenes Nanotubes and Carbon Nanostructures*, **21**(3), 213-232 (2013). Doi: https://doi.org/10.1080/1536383X.2011.597010

47. F. Mollaamin, M. Monajjemi, Molecular modelling framework of metal-organic clusters for conserving surfaces: Langmuir sorption through the TD-DFT/ONIOM approach, *Molecular Simulation*, **49**(4), 365-376 (2023). Doi: https://doi.org/10.1080/08927022.2022.2159996

48. F. Mollaamin, M. Monajjemi, Adsorption ability of Ga5N10 nanomaterial for removing metal ions contamination from drinking water by DFT, *International Journal of Quantum Chemistry,* **124**(2), e27348 (2024). Doi: https://doi.org/10.1002/qua.27348

49. A.D. Becke, Density-functional exchange-energy approximation with correct asymptotic behavior, *Physical Review* A, **38**(6), 3098-3100 (1988). Doi: https://doi.org/10.1103/PhysRevA.38.3098

50. C. Lee, W. Yang, R.G. Parr, Development of the Colle-Salvetti correlation-energy formula into a functional of the electron density, *Physical Review B*, **37**(2), 785-789 (1988). Doi: https://doi.org/10.1103/PhysRevB.37.785

51. L.J. Onsager, Electric moments of molecules in liquids, *Journal of the American Chemical Society*, **58**(8), 1486-1493 (1936). Doi: https://doi.org/10.1021/ja01299a050

52. C.J. Cramer, D.G. Truhlar, PM3-SM3: A general parameterization for including aqueous solvation effects in the PM3 molecular orbital model, *Journal of Computational Chemistry*, **13**(9), 1089-1097 (1992). Doi: https://doi.org/10.1002/jcc.540130907

53. M. Monajjemi, M. Khaleghian, N. Tadayonpour, F. Mollaamin, The effect of different solvents and temperatures on stability of single-walled carbon nanotube: A QM/MD study, *International Journal of Nanoscience*, **9**(5), 517-529 (2010). Doi: https://doi.org/10.1142/S0219581X10007071

54. F. Mollaamin, A. Ilkhani, N. Sakhaei, B. Bonsakhteh, A. Faridchehr, S. Tohidi, M. Monajjemi, Thermodynamic and solvent effect on dynamic structures of nano bilayer-cell membrane: Hydrogen bonding study, *Journal of Computational and Theoretical Nanoscience*, **12**(10), 3148-3154 (2015). Doi: https://doi.org/10.1166/jctn.2015.4092

55. M. Khaleghian, M. Zahmatkesh, F. Mollaamin, M. Monajjemi, Investigation of solvent effects on armchair single-walled carbon nanotubes: A QM/MD study, *Fullerenes, Nanotubes and Carbon Nanostructures*, **19**(4), 251-261 (2011). Doi: https://doi.org/10.1080/15363831003721757

56. F. Mollaamin, F. Najafi, M. Khaleghian, B. Khalili-Hadad, M. Monajjemi, Theoretical study of different solvents and temperatures effects on single-walled carbon nanotube and temozolomide drug: A QM/MM study, *Fullerenes, Nanotubes and Carbon Nanostructures*, **19**(7), 653-667 (2011). Doi: https://doi.org/10.1080/1536383X.2010.504956

57. E.M. Sarasia, S. Afsharnezhad, B. Honarparvar, F. Mollaamin, M. Monajjemi, Theoretical study of solvent effect on NMR shielding tensors of luciferin derivatives, *Physics and Chemistry of Liquids*, **49**(5), 561-571 (2011). Doi: https://doi.org/10.1080/00319101003698992

58. F. Mollaamin, M. Monajjemi, S. Salemi, M.T. Baei, A dielectric effect on normal mode analysis and symmetry of BNNT nanotube, *Fullerenes, Nanotubes and Carbon Nanostructures*, **19**(3), 182-196 (2011). Doi: https://doi.org/10.1080/15363831003782932

59. M.A.A. Zadeh, H. Lari, L. Kharghanian, E. Balali, R. Khadivi, H. Yahyaei, F. Mollaamin, M. Monajjemi, Density functional theory study and anti-cancer properties of Shyshaq plant: In viewpoint of nano biotechnology, *Journal of Computational and Theoretical Nanoscience*, **12**(11), 4358-4367 (2015). Doi: https://doi.org/10.1166/jctn.2015.4366

60. C.C. Chambers, G.D. Hawkins, C.J. Cramer, D.G. Truhlar, Model for aqueous solvation based on class IV atomic charges and first solvation shell effects, *Journal of Physical Chemistry*, **100**(40), 16385-16398 (1996). Doi: https://doi.org/10.1021/jp9610776

61. M. Monajjemi, M. Noei, F. Mollaamin, Design of fMet-tRNA and calculation of its bonding properties by quantum mechanics, *Nucleosides, Nucleotides & Nucleic Acids*, **29**(9), 676-683 (2010). Doi: https://doi.org/10.1080/15257771003781642

62. F. Mollaamin, Features of parametric point nuclear magnetic resonance of metals implantation on boron nitride nanotube by density functional theory/electron paramagnetic resonance, *Journal of Computational and Theoretical Nanoscience*, **11**(11), 2393-2398 (2014). Doi: https://doi.org/10.1166/jctn.2014.3653

63. A. Tahan, F. Mollaamin, M. Monajjemi, Thermochemistry and NBO analysis of peptide bond: Investigation of basis sets and binding energy, *Russian Journal of Physical Chemistry A*, **83**(4), 587-597 (2009). Doi: https://doi.org/10.1134/S003602440904013X

64. F. Mollaamin, M. Monajjemi, B_5N_{10} nanocarrier functionalized with Al, C, Si atoms: A drug delivery method for infectious disease remedy, *OBM Genetics*, **8**(1), 214 (**2024**). Doi: https://doi.org/10.21926/obm.genet.2401214

65. F. Mollaamin, M. Monajjemi, Bone therapy through drug delivery of chelated [bisphosphonate-metal ions] adsorbed on the surface of carbon nanotubes, *Revista Colombiana de Ciencias Químico-Farmacéuticas*, **52**(2), 741-765 (2023). Doi: https://doi.org/10.15446/rcciquifa.v52n2.110734

66. F. Mollaamin, M. Monajjemi, Harmonic linear combination and normal mode analysis of semiconductor nanotubes vibrations, *Journal of Computational and Theoretical Nanoscience*, **12**(6), 1030-1039 (2015). Doi: https://doi.org/10.1166/jctn.2015.3846

67. *A.M.Vargason, A.C. Anselmo, S. Mitragotri, The evolution of commercial drug delivery technologies, Nature Biomedical Engineering,* **5**(9), 951-967 (2021). Doi: https://doi.org/10.1038/s41551-021-00698-w

68. M.J. Frisch, G.W. Trucks, H.B. Schlegel, G.E. Scuseria, M.A. Robb, J.R. Cheeseman, G. Scalmani, *et al.*, Gaussian 16, Revision C.01, Gaussian, Inc., Wallingford CT, 2016.

69. C. Ochsenfeld, J. Kussmann, F. Koziol, *Ab initio* NMR spectra for molecular systems with a thousand and more atoms: a linear-scaling methods. *Angewante Chemie, International Edition*, **43**(34), 4485-4489 (2004). Doi: https://doi.org/10.1002/anie.200460336

70. J.A.S. Smith, Nuclear quadrupole resonance spectroscopy. General principles, *Journal of Chemical Education*, **48**(1), 39-41 (1971). Doi: https://doi.org/10.1021/ed048p39

How to cite this article

F. Mollaamin, M. Monajjemi, Drug delivery using doping of boron nitride nanosensor towards releasing chloroquine drug in the cells: A promising method for overcoming viral disease, *Rev. Colomb. Cienc. Quim. Farm.*, **53**(2), 430-454 (2024). https://doi.org/10.15446/rcciquifa.v53n2.114450

Artículo de investigación científica / https://doi.org/10.15446/rcciquifa.v53n2.114451

Composición química y actividad expectorante de las brácteas moradas de *Bougainvillea glabra*

Carmita Gladys Jaramillo Jaramillo [1a], Ana Paola Echavarria [2b], Helen Yuleisy Romero Macas [1c], Luiggi Oscar Solano Maza [1d], Jefferson Tocto León [1e], Luisa Rojas de Astudillo [3f*]

[1] Facultad de Ciencias Químicas y de la Salud, Universidad Técnica de Machala, Machala, Ecuador

[2] Facultad de Ciencias de la Ingeniería, Universidad Estatal de Milagro, Milagro, Ecuador

[3] Departamento de Química, Escuela de Ciencias, Núcleo de Sucre, Universidad de Oriente, Cumaná, Venezuela. *Autora de correspondencia.

Correos electrónicos:

[a] cjaramillo@utmachala.edu.ec, [b] ana08nov@gmail.com, [c] helenromeromacas@gmail.com, [d] losolano@utmachala.edu.ec, [e] jtocto@utmachala.edu.ec, [f] lrojas40@yahoo.com

Recibido: 30 de diciembre de 2023
Revisado: 14 de marzo de 2024
Aceptado: 18 de marzo de 2024

Resumen

Objetivo: Se evaluó la composición química y la actividad expectorante de las brácteas moradas de *B. glabra*. **Métodos**: Las concentraciones de alcaloides y saponinas se determinaron espectrofotométricamente y los compuestos químicos disueltos en cloroformo del extracto seco de las brácteas de *B. glabra* fueron identificados por cromatografía de gases acoplada a espectrometría de masas (CG-EM). Para el estudio biológico, se usaron ratones CD1, divididos en 3 grupos: Dos grupos a los cuales, respectivamente, las dosis de la solución (500 mg/kg) del extracto seco de las brácteas moradas de *B. glabra* y la del jarabe de bromhexina (25 mg/kg) como control positivo, se les administraron por vía oral y un grupo control. La actividad expectorante de cada tratamiento fue evaluada usando el método espectrofotométrico de cuantificación del rojo fenol en la secreción traqueobronquial de los ratones. **Resultados**: Los compuestos identificados, por CG-EM en el extracto seco disuelto en cloroformo fueron: la 4-hidroxi-4-metil-2-pentanona, el 2,2-dietoxi-propano, el ácido hexadecanoico y el éster etílico del ácido hexadecanoico. Las soluciones del extracto seco de las brácteas moradas de *B. glabra* y de bromhexina, respectivamente, produjeron significativamente ($P<0,05$) mayor liberación de rojo fenol en la secreción traqueobronquial de los ratones, en comparación con el control negativo.

Conclusiones: La solución del extracto seco de las brácteas moradas de *B. glabra* tuvo acción terapéutica como agente expectorante. Además, se puede inferir que, por efecto sinérgico, los compuestos químicos identificados por CG-EM y el contenido de alcaloides y saponinas potencian la actividad expectorante de las brácteas moradas de *B. glabra*.

Palabras claves: *Bougainvillea glabra*, brácteas, expectorante, composición química, ratones.

Summary

Chemical composition and expectorant activity of purple bracts of *Bougainvillea glabra*

Objective: The chemical composition and expectorant activity of the purple bracts of *B. glabra* were evaluated. **Methods** The concentrations of alkaloids and saponins were determined spectrophotometrically and the chemical compounds dissolved in chloroform of the dry extract of *B. glabra* bracts were identified by gas chromatography coupled to mass spectrometry (GC-MS). CD1 mice were used to evaluate the expectorant activity, which were divided into 3 groups: Two groups to which, respectively, the doses of the solution (500 mg/kg) of the dry extract of the purple bracts of *B. glabra* and that of the bromhexine syrup (25 mg/kg) as a positive control, were administered by orally and one control group. The expectorant activity of each treatment was analyzed by the spectrophotometric method for the quantification of phenol red in tracheobronchial secretion of mice. **Results**: The compounds identified by GC-MS in the dry extract dissolved in chloroform were: 4-hydroxy-4-methyl-2-pentanone, 2,2-diethoxy-propane, hexadecanoic acid and ethyl ester of hexadecanoic acid. The solutions of the dry extract of the purple bracts of *B. glabra* and that of bromhexine, administered orally to the mice, produced significantly ($P<0.05$) higher release of phenol red in the tracheobronchial secretion, respectively, in comparison with the negative control. **Conclusions**: The dry extract of the purple bracts of *B. glabra* had therapeutic action as an expectorant agent. It could be inferred that, due to the synergistic effect, the chemical compounds identified by GC-MS and the content of alkaloids and saponins enhance the expectorant activity of purple bracts of *B. glabra*.

Keywords: Bougainvillea glabra, bracts; expectorant, chemical composition, mice.

Resumo

Composição química e atividade expectorante das brácteas moradas de *Bougainvillea glabra*

Objetivo: Avaliar a composição química e a atividade expectorante das brácteas moradas de *B. glabra*. **Métodos:** As concentrações de alcalóides e saponinas são determinadas espectrofotometricamente e os compostos químicos dissolvidos em clorofórmio do extrato seco das brácteas de *B. glabra* são identificados por cromatografia de gases acoplada a espectrometria de massas (CG-EM). Para o estúdio biológico, use ratos CD1, divididos em 3 grupos: Dos grupos aos quais, respectivamente, as doses da solução (500 mg/kg) do extrato seco das brácteas moradas de *B. glabra* e do jarabe de bromexina (25 mg/kg) como controle positivo, é administrado por via oral e um controle de grupo. A atividade expectorante de cada tratamento foi avaliada usando o método espectrofotométrico de quantificação do fenol vermelho na secreção traqueobrônquica dos ratos. **Resultados:** Os compostos identificados, por CG-EM no extrato seco disuelto em cloroformo forte: la 4-hidroxi-4-metil--2-pentanona, o 2,2-dietoxi-propano, o ácido hexadecanoico e o éster etílico do ácido hexadecanoico. As soluções do extrato seco das brácteas moradas de *B. glabra* e de bromexina, respectivamente, produziram significativamente ($P<0,05$) maior liberação de fenol vermelho na secreção traqueobrônquica dos ratos, em comparação com o controle negativo. **Conclusões:** A solução do extrato seco das brácteas moradas de *B. glabra* tem sua ação terapêutica como agente expectorante. Além disso, pode-se inferir que, por efeito sinérgico, os compostos químicos identificados por CG-EM e o conteúdo de alcalóides e saponinas potencializam a atividade expectorante das brácteas moradas de *B. glabra*.

Palavras-chave: Bougainvillea glabra, brácteas, expectorante, composição química, ratos.

Introducción

La flema también llamada moco, producida en el tracto inferior del aparato respiratorio, es una parte crítica del sistema inmunológico y en su estado normal es un gel de baja viscosidad y elasticidad, que se transporta fácilmente por acción ciliar. Sin embargo, cuando la producción de flema excede de lo normal o aumenta su viscosidad, su eliminación se hace más difícil de las vías respiratorias. Esta alteración de la eliminación de flema provoca tos, obstrucción de las vías respiratorias y disnea [1,2]. Esta hiper-

secreción de mucosidad en las vías respiratorias es una de las características clínicas y patológicas importantes de las enfermedades inflamatorias crónicas de las vías respiratorias, incluida la enfermedad pulmonar obstructiva crónica (EPOC), el asma bronquial, las bronquiectasias y la fibrosis quística. Sus presentaciones clínicas incluyen tos recurrente y flema [3,4].

En cuanto a la EPOC, es una causa cada vez más importante de morbilidad, discapacidad, y mortalidad en todo el mundo [5]. La EPOC está incluida en el Plan de Acción Mundial para la Prevención y el Control de las Enfermedades No Transmisibles (ENT) de la Organización Mundial de la Salud (OMS) y en la Agenda 2030 para el Desarrollo Sostenible de las Naciones Unidas. Además, la OMS está tomando medidas para ampliar el diagnóstico y el tratamiento de la EPOC de varias formas [6].

En la mayoría de las EPOC se altera la secreción de mucosidad y, en algunos casos, la secreción anormal agrava la enfermedad. Por eso, mucho esfuerzo se ha dedicado a diseñar formas de tratamiento que cambien la cantidad o la calidad de moco traqueobronquial [7]. Los agentes mucoactivos han sido la medicación de elección para el tratamiento de enfermedades respiratorias en las que la hipersecreción de moco es una complicación clínica. El objetivo principal de los fármacos mucoactivos es aumentar la capacidad de expectorar el esputo y/o disminuir la hipersecreción de moco [8].

Tanto los mucolíticos como los expectorantes se utilizan para favorecer la eliminación de las secreciones bronquiales. Los mucolíticos modifican las propiedades fisicoquímicas de la secreción traqueobronquial para que la expectoración sea más eficaz y cómoda, mientras que los expectorantes estimulan los mecanismos de expulsión del moco, bien sea aumentando el movimiento ciliar o el reflejo tusígeno o el volumen hídrico. Aunque los dos mecanismos de acción son claramente distintos, en la práctica, esta separación no es tan evidente en la acción de muchos fármacos, debido a los efectos superpuestos que presentan [8,9].

En el escenario mundial, con las drogas naturales de las plantas medicinales se ha encontrado una alternativa para el tratamiento de trastornos respiratorios y varias plantas han mostrado que tienen actividad expectorante [10,11]. En relación con la planta *Bougainvillea glabra*, también llamada Flor de Papel debido a la presencia de brácteas coloridas, es la planta más común del género *Bougainvillea*, de la familia Nyctaginaceae, la cual se ha usado para el tratamiento de afecciones respiratorias y se recomienda para controlar el asma y la bronquitis [12,13]; sin embargo, no existen reportes de evaluación como expectorante de las brácteas de color morado de *B. glabra*, la más común de todas las variedades de colores de brácteas [13].

Por otra parte, hay gran interés en las brácteas de *B. glabra* por ser una fuente de compuestos polifenólicos, flavonoides y betalaínas que están relacionados con su propiedad antioxidante [13-15].

Con base a lo mencionado, en este estudio se evaluaron la composición química y la actividad expectorante en las brácteas de color morado de *Bougainvillea glabra*.

Metodología

las brácteas de *Bougainvillea glabra* de color morado fueron recolectadas, seleccionadas y clasificadas, de acuerdo con las indicaciones de la Organización Mundial de La Salud [16], en la ciudad de Machala (Latitud 3°15' 9,187" S; Longitud 79°56' 45,063" 0), Provincia El Oro, Ecuador. La identificación botánica fue realizada en el herbario Guay, de la Universidad de Guayaquil, Ecuador.

Preparación de los extractos

Se pesaron 10 g de las muestras secas y molidas de las brácteas moradas de *B. glabra*, se mezclaron con 100 mL de agua/etanol 98° (30:70). Esta mezcla fue dejada en reposo por 24 horas para luego someterla a una extracción asistida por ultrasonido [17], utilizando un baño ultrasónico (Fisher Scientific CPXH Series, Modelo 3800, Fisher Scientific, USA), durante 15 min. Posteriormente, el extracto filtrado se concentró hasta sequedad en un rotoevaporador (Laborota 4001 Efficient, Heidolph, España) acoplado a un criostato (Lauda/Alpha RA-8, Alemania) y a una bomba de vacío (VACUUBRAND PC600, Alemania). Finalmente, el extracto seco se almacenó a 4°C y protegido de la luz hasta su uso en los análisis posteriores.

Determinación de alcaloides

Se utilizó el método de Shamsa *et al.* [18], basado en la reacción del alcaloide con verde de bromocresol (BCG). Se tomaron alícuotas (0,4; 0,6; 0,8; 1,0 y 1,2 mL) de una solución estándar de atropina de 1 mg/mL y 5 mL de la solución del extracto hidroalcohólico de las brácteas de *B. glabra*, los cuales se transfirieron, cada uno, a diferentes embudos de decantación. A continuación, se añadieron 5 mL de un buffer de fosfato de pH 4,7 y 5 mL de la solución de BCG. Se agregaron volúmenes parciales (2, 2, 3 y 3 mL) de cloroformo en cada embudo de decantación y estos extractos de cloroformo se recogieron en un matraz aforado de 10 mL. La absorbancia del complejo alcaloide-BCG, disuelto en cloroformo, se midió usando un espectrofotómetro UV-Visible a 470 nm. Todo el proceso por muestra fue realizado por triplicado.

Determinación de saponinas

Basado en la propiedad de estos compuestos de producir hemólisis, para la cuantificación se usó un método modificado de Guerra *et al*. [19]. Los eritrocitos se obtuvieron a partir de 5 mL de sangre humana disuelta al 90% con citrato de sodio (36,5 g/L), centrifugados a 2 500 rpm durante 15 min, y lavados tres veces con 50 mL de suero salino fisiológico. Luego, los eritrocitos se suspendieron en una solución de citrato de sodio al 3 % para obtener una concentración de eritrocitos al 5 %.

Para la curva de calibración se usó 0,2 mg/mL de saponinas de *Quillaja saponaria* (Sigma®) disuelta con una solución buffer de KH_2PO_4 de pH 7,4. A partir de la cual se preparó una serie de patrones, con las siguientes concentraciones: 30; 25; 20; 15; 10 y 5 μg/mL, por dilución con la solución buffer, de las cuales se tomaron 6 mL de cada uno y se colocaron en los tubos de ensayo respectivos.

Del extracto hidroalcohólico se preparó una dilución 1:10 con buffer de KH_2PO_4 a pH 7,4 y de ésta se elaboraron una serie de ocho diluciones agregando desde 0,3 a 3,0 mL en diferentes tubos de ensayo y completada con agua destilada hasta un volumen total de 6 mL. Posteriormente, 6 mL de solución de citrato de sodio al 6 % y 1 mL de la solución de eritrocitos se le añadieron a cada tubo respectivo, que contenía las soluciones patrones y las diluciones de las muestras. Estos tubos se colocaron en un baño de agua a 35 °C, durante 30 min y después se centrifugaron a 2 500 rpm por cinco minutos, y se dejaron en reposo por 15 minutos antes de realizar las medidas de absorbancias, a 540 nm, en un espectrofotómetro UV-Vis (Shimadzu, mini-1240). De la misma forma, se prepararon dos controles, uno utilizando agua destilada y otro de citrato de sodio al 3 %, para determinar el 100 % y el 0 % de hemólisis, respectivamente. Con la curva de calibración (porcentaje de hemólisis vs concentración de saponinas) y los resultados de las curvas del porcentaje de hemólisis contra los volúmenes de las diluciones de cada muestra, se determinó la concentración de saponinas en las brácteas, expresada en mg equivalentes a las de *Quillaja saponaria* por gramo de material seco.

Identificación de compuestos químicos por cromatografía de gases acoplada a espectrometría de masas (CG-EM)

Para el análisis cromatográfico, se utilizó una solución disuelta al 2% en cloroformo del extracto seco de las brácteas moradas de *B. glabra*, se realizó utilizando un cromatógrafo de gases (TRACE serie 1300, Thermo Scientific) acoplado a un espectrómetro de masas de triple cuadrupolo (TSQ 8000, Thermo Scientific). Se utilizó un inyector en modo Split (1:10), a una temperatura de 280°C, equipado con un automuestreador (AI 1310, Thermo Scientific). Para la separación cromatográfica de los compuestos orgánicos se utilizó una columna capilar TG-5MS (30 m × 0,25 mm, 0,25 μm)

(Thermo Scientific). Se utilizó un programa de gradiente de temperatura, la temperatura inicial fue de 40ºC durante 5 min, seguido de un aumento a 5ºC/min hasta llegar a 310°C y permaneciendo a esta temperatura durante 10 min. Se utilizó helio como gas de arrastre, a un flujo constante de 1,0 mL/min. La corrida se realizó en modo de ionización por impacto electrónico con una energía de 70 eV. Se registró el espectro de masas en un intervalo de 50-500 m/z. Los análisis fueron realizados por triplicado. La identificación se hizo por la comparación de los espectros de masas obtenidos con los almacenados en las bases de datos de las bibliotecas del Instituto Nacional de Estándares y Tecnología (NIST) y de Wiley (9 ed.).

Evaluación de la actividad expectorante

Se emplearon ratones sanos (*Mus musculus*) de la cepa CD1, con masas de 20 a 30 gramos. La reproducción, crianza y cuidados se realizó en el Bioterio- Biomódulo- Bioterio de la Universidad Técnica de Machala, Ecuador, el cual cuenta con la acreditación del SAE (Servicio de Acreditación Ecuatoriano) y de la Entidad Nacional de Acreditación en España (ENAC), siguiendo las directrices de la *guía para el cuidado y uso* de los *animales de laboratorio* de la National Research Council [20]. El suministro de agua y comida fue *ad libitum*. Temperatura: (22 ± 3) °C y fotoperiodo 12x12 h luz/oscuridad.

Se formaron 3 grupos conformados por 5 ratones cada uno: un grupo control, al que se le administró, por vía oral, una solución salina (0,9 % de NaCl) (2 mL/kg de masa corporal del ratón) y los otros dos grupos recibieron, también por vía oral, la dosis de la solución (500 mg/kg) del extracto seco, disuelto en solución salina, de las brácteas moradas de *B. glabra* y la dosis del jarabe de bromhexina (25 mg/kg), respectivamente. Pasados 30 minutos después de la administración vía oral de cada tratamiento, a cada ratón le fue inyectado por vía intraperitoneal una solución de rojo fenol (500 mg/kg). Luego de haber transcurrido 30 min de la administración de las dosis, los animales fueron sacrificados por dislocación cervical sin dañar la tráquea. Posteriormente, se procedió a la disección y extracción de cada tráquea, desde el cartílago tiroideo hasta la arborización bronquial, la cual se introdujo en un tubo de ensayo con 1 mL de solución de NaCl al 0,9% y este tubo fue colocado en un baño ultrasónico (Fisher Scientific CPXH Series, Modelo 3800, Fisher Scientific, USA) durante 5 minuto [21]. Luego se le agregó 0,1 mL de NaOH (1 mol/L) a cada tubo y la solución resultante fue centrifugada.

Con las concentraciones, de 0,1 a 10 μg/mL, preparadas a partir de una solución de rojo fenol (20 μg/mL) y las absorbancias respectivas medidas en un espectrofotómetro UV-Vis (Shimadzu, mini-1240), a una longitud de onda de 565 nm, se obtuvo por regresión lineal una ecuación que permitió calcular la concentración promedio de rojo fenol en la solución resultante de la secreción traqueobronquial de cada tratamiento.

Se determinó el porcentaje de incremento de la excreción traqueobronquial de rojo fenol por cada solución evaluada como expectorante, fue determinado mediante la comparación del valor medio de la concentración del grupo tratado con el del grupo control.

Análisis estadístico

Se realizó un ANOVA con el método de Dunnett para determinar si los grupos con los tratamientos tuvieron actividad expectorante significativamente diferente al grupo no tratado. El nivel de confianza para todas las comparaciones fue de 95%, considerándose el valor de $P< 0,05$ como significativo.

Resultados

En relación con la composición química de las brácteas moradas de *B. glabra*, las concentraciones de alcaloides y saponinas determinadas espectrofotométricamente fueron de (0,892± 0,002) mg/g y (3,08 ± 0,02) mg/g, respectivamente.

Del análisis cromatográfico usando CG-EM del extracto seco disuelto en cloroformo, cuatro compuestos fueron identificados: 4-hidroxi-4-metil-2-pentanona (24,0%), 2,2-dietoxi-propano (13,4%), ácido hexadecanoico (12,7%) y el ácido hexadecanoico, etil éster (6,31%). Los detalles respectivos de estos compuestos bioactivos: los tiempos de retención, los nombres de los compuestos químicos, las fórmulas químicas, los porcentajes de área del pico en el cromatograma y el tipo de compuesto están dados en la Tabla 1.

Tabla 1. Compuestos químicos identificados por CG-EM en la solución disuelta en cloroformo del extracto seco de las brácteas moradas de *B. glabra*.

Tiempo de retención	Nombre del compuesto	Fórmula química	% Area del pico	Tipo de compuesto
6,23	2,2-dietoxi-propano	$C_7H_{16}O_2$	13,4	Cetona
8,90	4-hidroxi-4-metil-2-pentanona	$C_7H_{12}O_2$	24,0	Cetona
38,58	ácido hexadecanoico	$C_{16}H_{32}0_2$	12,7	Ácido graso
39,19	ácido hexadecanoico, etil ester	$C_{18}H_{36}O_2$	6,31	Ester etílico de un ácido graso

Mediante el método espectrofotométrico para la cuantificación del rojo fenol en la secreción traqueobronquial, se obtuvo la ecuación de regresión lineal: $y = 0,1524x – 0,027$, con $R^2 > 0,99$ que indica una linealidad satisfactoria entre la concentración del rojo fenol y la respuesta espectrofotométrica.

Las concentraciones de rojo de fenol en las secreciones traqueobronquiales para cada tratamiento fueron: 1,77 ± 0,59 mg/mL para el grupo con solución salina (control); 2,45 ± 0,37 mg/mL para el grupo tratado con bromhexina (control positivo) y 2,99 ± 0,79 mg/mL para el grupo tratado con la solución del extracto seco de las brácteas moradas de *B. glabra* (Fig. 1). También se puede observar (Fig. 1) que la mayor concentración de rojo fenol en las secreciones traqueobronquiales fue en los ratones tratados con la dosis oral (500 mg/kg) de la solución del extracto seco de las brácteas moradas de *B. glabra*, en comparación con los tratados por la bromhexina (control positivo) y el control negativo.

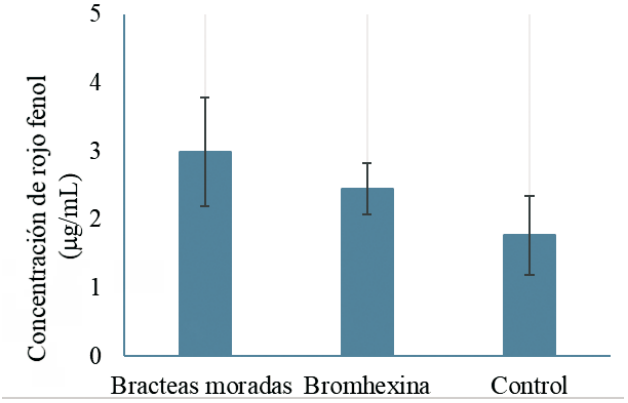

Figura 1. Concentración de rojo fenol liberada en la secreción traqueobronquial de cada tratamiento: control, bromhexina (25 mg/kg) y de la solución (500mg/kg) del extracto seco de las brácteas moradas d*e B. glabra*.

En comparación con el control, tanto el tratamiento de ratones con la bromhexina (25 mg/kg), como el de la solución (500 mg/kg) del extracto seco de las brácteas moradas de *B. glabra* aumentaron significativamente ($p<0,05$) el porcentaje de la secreción traqueobronquial de rojo fenol, en un 38,1% y 68,6%, respectivamente.

Discusión

Las brácteas moradas de *B. glabra* contienen alcaloides, como parte de sus componentes químicos, es posible que estos metabolitos secundarios sean coadyuvantes de la actividad expectorante presentes en las brácteas moradas de *B. glabra.* Otros estudios han indicado que los alcaloides evaluados muestran actividad expectorante, por sus potentes efectos como eliminadores de la flema; entre ellos, el trabajo de Wang *et al.* [22], quienes refieren que cuatro alcaloides aislados del bulbo de la especie vegetal

Fritillaria wabuensi aumentaron notablemente la producción de rojo fenol en la tráquea de los ratones y el de Liu *et al.* [23] quienes demostraron que los alcaloides de quinazolina (±)-vasicina, desoxivasicina y (±)-vasicinona, los cuales son los ingredientes activos de *Peganum harmala* L., tienen importantes actividades antitusivas, broncodilatadoras y también expectorante.

En cuanto a las saponinas, también los resultados revelaron que forman parte de los componentes químicos en las brácteas moradas de *B. glabra*, y estos metabolitos secundarios pueden favorecer a la expulsión de la mucosidad de las vías respiratorias. Se ha demostrado que las saponinas estimulan la mucosa gástrica, debido al reflejo vago, provocando un aumento de la secreción bronquial y mejorando la expectoración al diluir el esputo en los bronquios [11]. Adicionalmente, los resultados de las investigaciones en las que se evaluaron las saponinas en la raíz de *Glycyrrhiza glabra* muestran que tienen la propiedad de ayudar a aflojar la mucosidad acumulada para expulsarla más fácilmente de los pulmones [24].

Referente a los compuestos químicos solubles en cloroformo, presentes en el extracto seco de las brácteas moradas de *B. glabra* e identificados usando CG-EM, se encuentra la cetona 4-hidroxi-4-metil-2-pentanona, la cual también forma parte de la composición química de la planta *Tectona grandis* que ha sido utilizada en la medicina tradicional desde tiempos inmemoriales por tener varias actividades biológicas, entre ellas como antiinflamatoria, para tratar la bronquitis y como expectorante [25]. Igualmente, esta cetona se encuentra en otras plantas como *Lamium album* [26-27] y *Astragalus glycyphyllos* [28] que potencialmente tienen la propiedad de ser expectorantes. En relación con el ácido hexadecanoico, los estudios estructurales y cinéticos de Aparna *et al.* [29] concluyeron que este ácido graso es un inhibidor de la fosfolipasa A2, la inhibición de la fosfolipasa A2 es una de las formas de controlar la inflamación; por lo tanto, el ácido hexadecanoico es un compuesto antiinflamatorio. Estar presente la actividad antiinflamatoria en las brácteas de *B. glabra* es de mucha utilidad, dado que los fármacos que poseen propiedades antiinflamatorias, expectorantes y antitusivas simultáneas se consideran que ofrecen una protección integral contra diversos trastornos respiratorios. Debido a esta combinación de beneficios terapéuticos, existe una creciente demanda de tratamientos que abarquen estas tres propiedades para el manejo efectivo de distintos trastornos respiratorios [30].

Tres de los compuestos identificados en el extracto seco de las brácteas de *B. glabra* (éster etílico del ácido hexadecanoico, el ácido hexadecanoico, y el 2,2-dietoxipropano) también fueron encontrados en el extracto hidroetanólico de las hojas de *Trattinnickia rhoifolia* Willd que pertenece a la familia Burseraceae y esta especie es

ampliamente utilizada en las prácticas culturales etnofarmacológicas de los pueblos amazónicos, además como analgésico, antiinflamatorio y cicatrizante, también como expectorante [31].

Con base en la revisión de la literatura, no se han reportado otros estudios en los cuales se hayan identificados estos compuestos químicos por CG-EM en el extracto seco disuelto en cloroformo de las brácteas moradas de *B. glabra*.

Los resultados en este trabajo demuestran que el método *in vivo*, el cual se basa en la propiedad que tiene el rojo fenol de colorear los fluidos de tracto respiratorio y es utilizado para evaluar la actividad expectorante, fue idóneo. Además, se comprobó que la cuantificación de rojo fenol en la secreción traqueobronquial fue un ensayo rápido y de bajo costo para el descubrimiento de nuevos fármacos expectorantes [21].

La efectividad como expectorantes de las soluciones del extracto seco de las brácteas moradas de *B. glabra* y del control positivo (bromhexina), respectivamente, fue demostrada al producirse un incremento en la concentración de rojo fenol en las secreciones traqueobronquial de los ratones CD1. Aunque con la solución del extracto seco de las brácteas moradas de *B. glabra* se obtuvo mayor concentración de rojo fenol en la secreción traqueobronquial, en comparación con la bromhexina (control positivo).

El extracto seco de estas brácteas moradas puede considerarse inocuo, al no presentar efecto tóxico a la dosis de 2000 mg/kg de masa de ratón, por lo que éste puede ser una opción segura como expectorante [32]. Sin embargo, la bromhexina es un derivado de la vasicina, alcaloide de la nuez *Adhatoda vasica* y en su perfil de seguridad se han notificado mareos, cefaleas, crisis broncobstructivas (poco frecuente) y síntomas gastrointestinales [9].

Posiblemente, la solución del extracto seco de las brácteas moradas de *B. glabra* actúe como la mayoría de los fármacos expectorantes, los cuales aumentan la secreción y diluyen la flema en las vías respiratorias, de manera que con el movimiento ciliar sea fácilmente expectorada [8, 33].

Este ha sido el primer estudio de evaluación del efecto expectorante del extracto seco de las brácteas de color morado de *B. glabra* en ratones CD1, a la dosis de 500 mg/kg, siendo este resultado importante desde el punto de vista farmacológico; sin embargo, se requieren estudios clínicos y también determinar el mecanismo de la acción expectorante.

Se puede señalar que es posible que la actividad expectorante puede estar influenciada, por efecto sinérgicos, por el contenido de saponinas, alcaloides y los compuestos químicos identificados por CG-EM presentes en las brácteas moradas de *B. glabra* [34].

Agradecimientos

Los autores agradecen a Facultad de Ciencias de la Escuela Superior Politécnica de Chimborazo (ESPOCH), Ecuador, por la donación de los ratones de la cepa CD1, para su reproducción, crianza y cuidados en el Bioterio de la Universidad Técnica de Machala, Ecuador. También al Vicerrectorado y Dirección de Investigación de la Universidad Técnica de Machala, Ecuador por el financiamiento del proyecto que permitió el desarrollo de esta investigación.

Conflicto de intereses

Los autores del estudio manifestamos no presentar ningún conflicto de interés.

Referencias

1. J.V. Fahy, B.F. Dickey, Airway mucus function and dysfunction, *The New England Journal of Medicine*, **363**(23), 2233-2247 (2010). Doi: https://doi.org/10.1056/NEJMra0910061

2. A.Vinod, R.Tadmor, D. Katoshevski, E.J. Gutmark, Gels that serve as mucus simulants: A review, *Gels*, **9**(7), 555 (2023). Doi: https://doi.org/10.3390/gels9070555

3. L. Fernandez-Restrepo, L. Shaffer, B. Amalakuhan, M.I. Restrepo, J. Peters, R. Restrepo, Effects of intrapulmonary percussive ventilation on airway mucus clearance: A bench model, *World Journal of Critical Care Medicine*, **6**(3), 164-171 (2017). Doi: https://doi.org/10.5492/wjccm.v6.i3.164

4. T. Zhang, X. Zhou, Clinical application of expectorant therapy in chronic inflammatory airway diseases (Review), *Experimental and Therapeutic Medicine*, **7**(4), 763-767 (2014). Doi: https://doi.org/10.3892/etm.2014.1494

5. D. Adeloye, P. Song, Y. Zhu, H. Campbell, A. Sheikh, I. Rudan, *et al.*, Regional, and national prevalence of, and risk factors for, chronic obstructive pulmonary disease (COPD) in 2019: a systematic review and modelling analysis, *The Lancet: Respiratory Medicine*, **10**(5), 447-458 (2022). Doi: https://doi.org/10.1016/S2213-2600(21)00511-7

6. Organización Mundial de la Salud (OMS), Enfermedad pulmonar obstructiva crónica (EPOC), 2023. URL: https://www.who.int/es/news-room/fact-sheets/detail/chronic-obstructive-pulmonary-disease-(copd)

7. F. Scaglione, O. Petrini, Mucoactive agents in the therapy of upper respiratory airways infections: fair to describe them just as mucoactive?, *Clinical Medicine Insights: Ear, Nose and Throat*, **12**, 1179550618821930 (2019). Doi: https://doi.org/10.1177/1179550618821930

8. R. Balsamo, L. Lanata, C.G. Egan, Mucoactive drugs, *European Respiratory Review*, **19**(116), 127-133 (2010). Doi: https://doi.org/10.1183/09059180.00003510

9. A. Rodríguez, C. Izuibejeres, V. González, Antitusígenos y expectorantes sintéticos, *Archivos de Pediatría del Uruguay*, **92**, e809 (2021). URL: http://www.scielo.edu.uy/pdf/adp/v92nnspe2/1688-1249-adp-92-nspe2-e809.pdf

10. A.A.Haile, B.A. Tsegay, A. Seid, W. Adnew, A. Moges, Review on medicinal plants used in the management of respiratory problems in Ethiopia over a twenty-year period (2000-2021), *Evidence-Based Complementary and Alternative Medicine*, **2022**, 2935015 (2022). Doi: https://doi.org/10.1155/2022/2935015

11. S. Marchyshyn, L. Slobodianiuk, L. Budniak, L. Shostak, O. Gerush, Investigation on the expectorant effect of extracts from *Primula veris* L., *Open Access Macedonian Journal of Medical Sciences,* **10**, 1368-1372 (2022). Doi: https://doi.org/10.3889/oamjms.2022.10657

12. R. Abarca-Vargas, V.L. Petricevich, *Bougainvillea* genus: A review on phytochemistry, pharmacology, and toxicology, *Evidence-based Complementary and Alternative Medicine*, **2018**, 9070927 (2018). Doi: https://doi.org/10.1155/2018/9070927

13. H. Saleem, A. Usman, M.F. Mahomoodally, N. Ahemad, *Bougainvillea glabra* (Choisy): A comprehensive review on botany, traditional uses, phytochemistry, pharmacology and toxicity, *Journal of Ethnopharmacology*, **266**, 113356 (2021). Doi: https://doi.org/10.1016/j.jep.2020.113356

14. M. Robles-Aguilar, C. Jaramillo-Jaramillo, L. Rojas de Astudillo, Contenido de betalainas y actividad antioxidante en brácteas de *Bougainvillea glabra* Choisy, *Revista Cubana de Farmacia,* **51**(2) (2018). URL: https://revfarmacia.sld.cu/index.php/far/article/view/226/132

15. C. Jaramillo, J.C. Armijos, R. Cedeño, M. Campos, L. Rojas, Comparación de la relación de fenoles totales, flavonoides y capacidad antioxidante en brácteas de dos variedades de *Bougainvillea glabra* Choisy, *InfoAnalitica*, **91**, 167-179 (2021). Doi: https://doi.org/10.26807/ia.v9i1.203

16. Organización Mundial de la Salud (OMS), *Directrices de la OMS sobre buenas prácticas agrícolas y de recolección (BPAR) de plantas medicinales*, Ginebra, 2003, 87 p. URL: https://bit.ly/3NapVnk

17. M. Vinatoru, An overview of the ultrasonically assisted extraction of bioactive principles from herbs, *Ultrasonics Sonochemistry*, **8**(3), 303-313 (2001). Doi: https://doi.org/10.1016/s1350-4177(01)00071-2

18. F. Shamsa, H. Monsef, R. Ghamooshi, M. Verdian-Rizi, Spectrophotometric determination of total alkaloids in some Iranian medicinal plants, *Journal of Applied Horticulture*, **12**(1), 69-70, (2010). URL: http://horticultureresearch.net/jah/2010_12_1_69_70.PDF

19. J. Guerra, C. Nogueiras, R. Delgado, O. Hernández, Determinación cuantitativa de saponinas y azúcares reductores del *Agave brittoniana* T, *Revista Cubana de Química*, **13**, 37-42 (2001).

20. National Research Council (NRC), Guide for the care and use of laboratory animals, 8th ed., The National Academies Press, Washington, D.C., 2011, 246 p. URL: https://bit.ly/3MSAQ3M

21. P.M.N. Menezes, M.C. Brito, P.G.S. de Sá, L.A.A. Ribeiro, L.A. Rolim, F.S. Silva, Analytical and pharmacological validation of the quantification of phenol red in a mouse model: An optimized method to evaluate expectorant drugs, *Journal of Pharmacological and Toxicological Methods*, **98**, 106586 (2019). Doi: https://doi.org/10.1016/j.vascn.2019.106586

22. D. Wang, S. Wang, X. Chen, X. Xu, J. Zhu, L. Nie, X. Long, Antitussive, expectorant and anti-inflammatory activities of four alkaloids isolated from bulbus of *Fritillaria wabuensi*, *Journal of Ethnopharmacology*, **139**(1), 189-193 (2012). Doi: https://doi.org/10.1016/j.jep.2011.10.036

23. W. Liu, Y. Wang, D.-d. He, S.-p. Li, Y.-d. Zhu, B. Jiang, X.-m. Cheng, Z.-t. Wang, C.-h. Wang, Antitussive, expectorant, and bronchodilating effects of quinazoline alkaloids (±)-vasicine, deoxyvasicine, and (±)-vasicinone from aerial parts of *Peganum harmala L*, *Phytomedicine*, **22**(12), 1088-1095 (2015). Doi: https://doi.org/10.1016/j.phymed.2015.08.005

24. S. Wahab, S. Annadurai, S.S. Abullais, G. Das, W. Ahmad, M.F. Ahmad, G. Kandasamy, R. Vasudevan, M.S. Ali, M. Amir, *Glycyrrhiza glabra* (Licorice): A comprehensive review on its phytochemistry, biological activities, clinical evidence and toxicology, *Plants* (Basel), **10**(12), 2751 (2021). Doi: https://doi.org/10.3390/plants10122751

25. S.M.B. Asdaq, N. Nayeem, Abida, Md.T. Alam, S.I. Alaqel, M. Imran, E.-W. Elamin-Hassan, S.I. Rabbani, *Tectona grandis* Lf: A comprehensive review on its patents, chemical constituents, and biological activities, *Saudi Journal of Biological Sciences*, **29**(3), 1456-1464 (2022). Doi: https://doi.org/10.1016/j.sjbs.2021.11.026

26. A. Konarska, E. Weryszko-Chmielewska, A. Matysik-Woźniak, A. Sulborska, B. Polak, M. Dmitruk, K. Piotrowska-Weryszko, B. Stefańczyk, R. Rejdak, Histochemical and phytochemical analysis of *Lamium album* subsp. *album* L. Corolla: Essential oil, triterpenes, and iridoids, *Molecules* (Basel), **26**(14), 4166 (2021). Doi: https://doi.org/10.3390/molecules26144166

27. B. Salehi, L. Armstrong, A. Rescigno, B. Yeskaliyeva, G. Seitimova, A. Beyatli, *et al.*, *Lamium* plants- A comprehensive review on health benefits and biological activities, *Molecules* (Basel), **24**(10), 1913 (2019). Doi: https://doi.org/10.3390/molecules24101913

28. I. Stambolov, A. Shkondrov, I. Krasteva, *Astragalus glycyphyllos* L.: Phytochemical constituents, pharmacology, and biotechnology, *Pharmacia*, **70**(3), 635-641 (2023). Doi: https://doi.org/10.3897/pharmacia.70.e107989

29. V. Aparna, K.V. Dileep, P.K. Mandal, P. Karthe, C. Sadasivan, M. Haridas, Anti-inflammatory property of n-hexadecanoic acid: Structural evidence and kinetic assessment, *Chemical Biology & Drug Design*, **80**(3), 434-439 (2012). Doi: https://doi.org/10.1111/j.1747-0285.2012.01418.x

30. J.R. Hu, C.J. Jung, S.M. Ku, D.H. Jung, K.M.I. Bashir, S.K. Ku, J.S. Choi, Anti-inflammatory, expectorant, and antitussive properties of *Kyeongok-go* in ICR mice, *Pharmaceutical Biology*, **59**(1), 321-334 (2021). Doi: https://doi.org/10.1080/13880209.2021.1892155

31. A.A. de Souza, B.L.S. Ortíz, S.F. Borges, A.V.P. Pinto, R.D.S. Ramos, I.C. Pena, *et al.*, Acute toxicity and anti-inflammatory activity of *Trattinnickia rhoifolia* Willd (Sucuruba) using the *Zebrafish* model, *Molecules*, **27**(22), 7741 (2022). Doi: https://doi.org/10.3390/molecules27227741

32. C.G. Jaramillo-Jaramillo, K.A. Zambrano-Gonzaga, J.C. Armijos-Aguilar, S.A. Cuenca-Buele, M. Tocto-León, L. Rojas de Astudillo, Evaluación del contenido de alcaloides, la toxicidad aguda y antitusiva de las brácteas de dos variedades de *Bougainvillea glabra* Choisy, *Revista Científica, FCV-LUZ*, **33**(2), e33248 (2023). Doi: https://doi.org/10.52973/rcfcv-e33248

33. T. Guo, J. Qing Wei, J.P. Ma, Antitussive and expectorant activities of *Potentilla anserina*, *Pharmaceutical Biology*, **54**(5), 807-811 (2016). Doi: https://doi.org/10.3109/13880209.2015.1080734

34. H. Ali, D. Ali, B.O. Almutairi, G. Kumar, G.A. Karga, C. Masi, V.P. Sundramurthy, Synergistic effect of conventional medicinal herbs against different pharmacological activity, *BioMed Research International*, **2022**, 7337261 (2022). Doi: https://doi.org/10.1155/2022/7337261

Como citar este artículo

C.G. Jaramillo-Jaramillo, A.P. Echavarria, H.Y. Romero-Macas, L.O. Solano-Maza, J. Tocto-León, L. Rojas de Astudillo, Composición química y actividad expectorante de las brácteas moradas de *Bougainvillea glabra*, *Rev. Colomb. Cienc. Quim. Farm.*, **53**(2), 455-470 (2024). https://doi.org/10.15446/rcciquifa.v53n2.114451

Artículo de investigación científica / https://doi.org/10.15446/rcciquifa.v53n2.114452

Estudio fitoquímico y actividad biológica de *Hinterhubera imbricata* Cuatrec. & Aristeg

Ysbelia Obregón-Díaz[1a*], Luis Rojas-Fermín†[1b], Alida Pérez-Colmenares[1c], Yndra Cordero[1d], Rosa Aparicio[1e], Wilberto De Lima[2f], Johana Hernández[3g], Alfredo Usubillaga[1h]

[1] Instituto de Investigaciones "Dr. Alfredo Nicolás Usubillaga del Hierro", Facultad de Farmacia y Bioanálisis, Universidad de Los Andes, Mérida C.P. 5101. República Bolivariana de Venezuela. *Autora de correspondencia.

[2] Laboratorio de Análisis Instrumental, Núcleo Universitario Rafael Rangel, Universidad de Los Andes, Trujillo C.P. 3150. República Bolivariana de Venezuela.

[3] Laboratorio de Investigaciones en Bioquímica, Facultad de Farmacia y Bioanálisis, Universidad de Los Andes, Mérida C.P. 5101. República Bolivariana de Venezuela.

Correos electrónicos: [a] ysbeliaobregon@gmail.com, [b] rojasfermin33@gmail.com, [c] alidaperezc@gmail.com, [d] yndracprdero@gmail.com, [e] apariciorosa12@gmail.com, [f] wilberto.a@gmail.com, [g] hjohannacarolina@gmail.com, [h] usubi80@gmail.com

Recibido: 22 de diciembre de 2023
Revisado: 23 de marzo de 2024
Aceptado: 26 de marzo de 2024

Resumen

Objetivo: En la presente investigación se realizó el estudio fitoquímico de los extractos de hexano, diclorometano y metanol de las partes aéreas de *Hinterhubera imbricata* recolectada en el estado Mérida-Venezuela. **Métodos:** La purificación de los extractos y aislamiento de los metabolitos secundarios se hizo a través de cromatografía de columna. La identificación y caracterización de los compuestos fue mediante análisis de cromatografía de gases acoplada a espectrometría de masas, espectroscopía infrarrojo y de resonancia magnética nuclear. La actividad antibacteriana se evaluó *in vitro* empleando el método de difusión en agar con discos frente a cepas de referencia internacional de *Staphylococcus aureus*, *Escherichia coli*, *Enterococcus faecalis*, *Klebsiella pneumoniae* y *Pseudomonas aeruginosa*. La actividad antioxidante se determinó *in vitro* por el método del radical libre 2,2-difenil-1-picrilhidrazilo. **Resultados**: El tamizaje fitoquímico reporta la presencia en los extractos de hexano y diclorometano de las hojas-tallos de triterpenos y esteroles, y en los extractos de metanol de las hojas, tallos y flores; esteroles, compuestos fenólicos, flavonoides y cumarinas. Se aislaron cuatro compuestos que fueron identificados como 7-hidroxi-6-metoxicumarina, friedelona, friedelan-3-ol y ácido ursólico. Todos los extractos presentaron actividad frente a *S. aureus* y *K. pneumoniae* en una concentración de

1000 µg/mL, siendo los más activos los extractos de metanol (hojas-tallos y flores) con una concentración inhibitoria mínima de 250 y 125 µg/mL, respectivamente. La actividad antioxidante fue moderada, siendo la concentración efectiva media de 12,9 y 8,3 µg/mL, para el extracto de metanol de hojas-tallos y flores. **Conclusión:** Las partes aéreas de *Hinterhubera imbricata* contienen metabolitos secundarios con actividad antibacteriana y antioxidante, siendo esta especie una fuente de sustancias biológicamente activas.

Palabras clave: Asteraceae, Hinterhuberinae, *Hinterhubera imbricata*, triterpenos, cumarinas.

Summary

Phytochemical study and biological activity of *Hinterhubera imbricata* Cuatrec. & Aristeg.

Objective: The phytochemical study of the extract of hexane, dichlorometane, and methanol from the aerial parts of *Hinterhubera imbricate* collected in the State of Mérida, Venezuela was performed in this research. **Methods**: The purification of the extracts and isolation of the secondary metabolites was done through column chromatography. Compounds were identified and characterized by gas chromatography coupled to mass spectrometry, infrared spectroscopy and nuclear magnetic resonance analysis. Antibacterial activity was evaluated in vitro using the disk agar diffusion method against international reference strains of *Staphylococcus aureus*, *Escherichia coli*, *Enterococcus faecalis*, *Klebsiella pneumoniae* and *Pseudomonas aeruginosa*. Antioxidant activity was determined *in vitro* through the 2,2-diphenyl-1-picrylhidrazyl free radical method. **Results**: Phytochemical screening reports the presence in hexane and dichloromethane extracts of leaves-stems of triterpenes and sterols, and in methanol extracts of leaves, stems and flowers; sterols, phenolic compounds, flavonoids and coumarins. Four compounds were isolated and identified as 7-hydroxy-6-methoxycoumarin, friedelone, friedelan-3-ol and ursolic acid. All extracts showed activity against *S. aureus* and *K. pneumoniae* at a concentration of 1000 µg/mL, being the most active the methanol extracts (leaves-stems and flowers) with a minimum inhibitory concentration of 250 and 125 µg/mL, respectively. The antioxidant activity was moderate, being the median effective concentration of 12.9 and 8.3 µg/mL, for the methanol extract of leaves-stems and flowers.

Conclusion: The aerial parts of *Hinterhubera imbricate* contain secondary metabolites with antibacterial and antioxidant activity, being this species a source of biologically active substances.

Keywords: Asteraceae, Hinterhuberinae, *Hinterhubera imbricata*, triterpenes, coumarins.

Resumo

Estudio fitoquímico e atividade biológica de *Hinterhubera imbricata* Cuatrec. & Aristeg.

Objetivo: Na presente investigação foi realizado o estudo fitoquímico dos extratos de hexano, diclorometano e metanol das partes aéreas de *Hinterhubera imbricata* recolhidas no estado de Mérida-Venezuela. **Métodos:** A purificação dos extratos e o isolamento dos metabolitos secundários foram efetuados por cromatografia em coluna. A identificação e caraterização dos compostos foi efetuada por cromatografia gasosa acoplada a espectrometria de massa, espetroscopia de infravermelhos e análise de ressonância magnética nuclear. A atividade antibacteriana foi avaliada *in vitro* utilizando o método de difusão em disco de ágar contra estirpes de referência internacional de *Staphylococcus aureus*, *Escherichia coli*, *Enterococcus faecalis*, *Klebsiella pneumoniae* e *Pseudomonas aeruginosa*. A atividade antioxidante foi determinada *in vitro* pelo método do radical livre 2,2-difenil-1-picrilhidrazil. **Resultados:** O rastreio fitoquímico indica a presença de triterpenos e esteróis nos extractos de hexano e diclorometano das folhas e caules, e de esteróis, compostos fenólicos, flavonóides e cumarinas nos extratos de metanol das folhas, caules e flores. Quatro compostos foram isolados e identificados como 7-hidroxi-6-metoxicumarina, friedelona, friedelan-3-ol e ácido ursólico. Todos os extratos mostraram atividade contra *S. aureus* e *K. pneumoniae* a uma concentração de 1000 μg/mL, sendo os mais ativos os extratos de metanol (folhas-caules e flores) com uma concentração inibitória mínima de 250 e 125 μg/mL, respetivamente. A atividade antioxidante foi moderada, com concentrações médias eficazes de 12,9 e 8,3 μg/mL para o extrato metanólico das folhas-caules e flores. **Conclusão:** As partes aéreas de *Hinterhubera imbricata* contêm metabolitos secundários com atividade antibacteriana e antioxidante, sendo esta espécie uma fonte de substâncias biologicamente ativas.

Palavras-chave: Asteraceae, Hinterhuberinae, *Hinterhubera imbricata*, triterpenos, cumarinas.

Introducción

El género *Hinterhubera* (Asteraceae), fue determinado por Schultz Bipontinus y posteriormente publicado por Weddell (1855), siendo José Cuatrecasas (1969) quien reconoció la singular morfología de sus corolas y estableció su ubicación en la subtribu Hinterhuberinae [1, 2]. Las 8 especies de *Hinterhubera* se encuentran distribuidas en las zonas andinas de Colombia y Venezuela [3, 4]; donde dos especies (*H. nevadensis* Cuatrec. y *H. harrietae* Cuatrec.), se ubican en la Sierra Nevada de Santa Marta (Colombia) y siete en la Cordillera Andina Venezolana (*H. adenopetala* Cuatrec. & Aristeg., *H. columbica* Sch. Bip. ex Wedd., *H. ericoides* Wedd., *H. imbricata* Cuatrec. & Aristeg., *H. lanuginosa* Cuatrec. & Aristeg., *H. laseguei* Wedd. y *H. longiloba* M. Carrillo, M. Lapp *et* P. Torrecilla *sp. nov.*), siendo cinco especies endémicas en Venezuela localizadas desde el estado Mérida hasta las estribaciones andinas del estado Lara [1-5]. Algunas plantas pertenecientes a la subtribu Hinterhuberinae poseen actividades biológicas como citotóxico, antitumoral, antioxidante, antimicrobiano, hipotensor y antiinflammatorio [6-11]. Estudios previos reportan que de las partes aéreas de la especie *H. imbricata*, se logró aislar un triterpeno identificado como ácido oleanólico y tres diterpenos caracterizados como 3-hidroxi-imbricatol-valerico, 3-hidroxi-imbricatol-α-metilbutirato y 3-hidroxi-imbricatol-angelico [12]. En la presente investigación se realizó el estudio fitoquímico de las partes aéreas de *Hinterhubera imbricata*, logrando el aislamiento de cuatro compuestos los cuales fueron identificados mediantes técnicas espectroscópicas de Resonancia Magnética Nuclear (RMN) y Cromatografía de Gases acoplada a Espectrometría de Masas (CG-EM). Adicionalmente se evaluó la actividad antioxidante mediante el método de 2,2-difenil-1-picril-hidracilo (DPPH) y antibacteriana por el método de difusión en agar con pozos (Kirby-Bauer).

Materiales y métodos

Procedimiento general

Los puntos de fusión fueron determinados utilizando un instrumento digital Fisatom 430 D. Los análisis de espectroscopía ultravioleta (UV) se efectuaron con un espectrofotómetro Spectronic Genesys 10 Bio, empleando celdas de cuarzo de 1×1×1 cm y celda de cuarzo de paso fino. Los espectros infrarrojos (IR) se realizaron en un espectrofotómetro Perkin Elmer, modelo Spectrum Two, en discos de KBr. Los espectros de masas (EM) se obtuvieron en un equipo de cromatografía de gases acoplado a masas marca Hewlett Packard, modelo 5973, utilizando una columna HP-5 (30 m × 0,25 mm × 0,25 μm de i.d) y un detector de impacto electrónico (IE energía e- 70 eV). Los espectros

de Resonancia Magnética Nuclear (RMN) uni y bi dimensionales se realizaron en un equipo de RMN Bruker-Avance DRX 400. Como solventes se usaron metanol deuterado (CD_3OD) y cloroformo deuterado ($CDCl_3$).

Material vegetal

Las partes aéreas (hojas, tallos y flores) de la especie fueron recolectadas en el año 2010 en el Parque Nacional La Culata, laguna Los Guaches vía pico El Águila (2500 m.s.n.m.), en el Estado Mérida-Venezuela. Una muestra testigo fue depositada en el Herbario MERF de la Facultad de Farmacia y Bioanálisis de la Universidad de Los Andes (Voucher specimen N° YO001) e identificada como *Hinterhubera imbricata* Cuatrec. & Aristeg por el Dr. Pablo Meléndez.

Obtención de los extractos

Las partes aéreas fueron separadas en hojas-tallos y flores, posteriormente se colocaron en bandejas y se secaron en estufa a 40 °C. Luego se procedió a moler hasta la obtención de un polvo fino, obteniéndose 2450,0 g de hojas-tallos y 117,0 g de flores. El material vegetal fue sometido a maceración a temperatura ambiente con disolventes en orden de polaridad creciente (hexano, diclorometano y metanol), las soluciones provenientes de las extracciones se filtraron y se concentraron en un rotavapor a presión reducida a una temperatura no mayor a 45 °C., obteniéndose 140,0 g del extracto de hexano; 244,6 g del extracto de diclorometano y 385,1 g del extracto de metanol correspondiente a las hojas-tallos. Por otra parte, de las flores se obtuvo 8,6 g del extracto de hexano; 5,0 g del extracto de diclorometano y 13,2 g del extracto de metanol.

Estudio fitoquímico preliminar

Para la caracterización química de los metabolitos secundarios presentes en los extractos de hexano, diclorometano y metanol de las hojas-tallos y flores de *H. imbricata* se efectuó una serie de pruebas químicas cualitativas siguiendo la metodología descrita por Marcano y Hasegawa [13].

Extracción y aislamiento de los compuestos

El extracto de metanol de las hojas-tallos (EMHT; 385,1 g) se sometió a una extracción líquido-líquido usando una mezcla de acetato de etilo y agua destilada (2:1), el procedimiento se realizó cuatro veces obteniéndose las fases orgánicas FO-1 (160,5 g), FO-2 (90,2 g), FO-3 (25,2 g) y FO-4 (55,6 g). Luego de realizar el análisis de las fracciones por cromatografía de capa fina (CCF), se tomó de la fracción orgánica identificada como FO-1 11,1 g y se purificaron en un sistema de cromatografía de columna flash, utilizando como fase estacionaria sílica gel 70-230 Mesh, 60-200 mm, 60 Å y como fase móvil hexano, diclorometano y metanol en mezclas en orden de polaridad cre-

ciente, obteniendo 11 sub-fracciones (FO-1.1 - FO-1.11). La subfracción FO-1.5 al ser analizada por CCF presentó un compuesto mayoritario, el cual se purificó mediante cromatografía de columna usando como soporte Sephadex LH20 y como fase móvil diclorometano y metanol (95:5), eluyendo el compuesto 1 (Figura 1).

Por otra parte, se pesaron 100,0 g del extracto de diclorometano obtenido de las hojas y tallos (EDHT) y fue sometido a procesos de separación y purificación mediante cromatografía flash, utilizando como soporte sílica gel 60 y como fase móvil hexano, mezclas de hexano:acetato de etilo y metanol en orden de polaridad creciente. Se obtuvieron 13 fracciones (EDHT-1 a EDHT-13) las cuales se analizaron mediante CCF y se reunieron de acuerdo a sus características comunes. La fracción EDHT-2 (4,4 g) fue recristalizada con acetato de etilo obteniendo el compuesto 2 (0,3 g). Adicionalmente, la fracción EDHT-3 (1,1 g) fue sometida nuevamente a cromatografía de columna y eluida con hexano y acetato de etilo (90:10), obteniéndose el compuesto 3 (0,4 g). Finalmente, la fracción EDHT-7 (3,4 g) se purificó bajo un sistema de cromatografía de columna flash y como fase móvil: hexano y acetato de etilo en mezclas de polaridad creciente, consiguiendo aislar el compuesto 4 (0,4 g) (Figura 1).

En cuanto al extracto de metanol de las flores (EMF), se tomaron 10,0 g y se purificaron mediante cromatografía flash, utilizando como soporte sílica gel 60 y como fase móvil diclorometano y metanol en orden de polaridad creciente, luego del análisis por CCF se reunieron 20 fracciones (EMF-1 a EMF-20). En la fracción EMF-8 se obtuvo un compuesto puro (0,08 g) que al ser comparado por CCF coincide con el compuesto 1 obtenido previamente en FO-1.5 (EMHT). Por otra parte, el extracto de hexano de las flores (EHF) fue analizado por cromatografía de gases-masas evidenciando la presencia de hidrocarburos saturados, donde el nonacosano resultó ser el componente mayoritario.

La caracterización estructural de los compuestos (1-4) fue realizada utilizando técnicas de resonancia magnética nuclear uni y bidimensionales, infrarrojo y cromatografía de gases acoplada a espectrometría de masas. Para poder analizar el compuesto 4 por espectrometría de masas se procedió a realizar la metilación de la sustancia con diazometano *in situ* [14, 15]. Los datos obtenidos se compararon con los reportados previamente en la literatura.

Actividad antibacteriana

Las cepas bacterianas utilizadas fueron *Staphylococcus aureus* (ATCC 25923), *Escherichia coli* (ATCC 25922), *Enterococcus faecalis* (ATCC 29219), *Klebsiella pneumoniae* (ATCC 23357), *Pseudomonas aeruginosa* (ATCC 27853) proporcionadas por el

Cepario del Laboratorio de Microbiología de la Facultad de Farmacia y Bioanálisis de la Universidad de Los Andes.

La actividad antibacteriana se evaluó mediante el método de difusión en agar con pozos [16], el ensayo se realizó con un cultivo de 18 horas de cada microorganismo en 2,5 mL de caldo Müeller-Hinton a 37 °C. El inóculo bacteriano fue ajustado con solución salina fisiológica al patrón de turbidez de Mac Farland N° 0,5 (10^{6-8} UFC/mL). Cada inóculo se diseminó sobre la superficie de una placa que contenía agar Müeller-Hinton y luego con una pipeta Pasteur estéril invertida se realizaron los pozos, posteriormente se depositan 10 µL de las soluciones de los extractos obtenidos de las hojas-tallos (EHHT, EDHT, EMHT) y flores (EHF y EMF) a una concentración de 1000 ppm, así mismo se colocó el control negativo dimetilsulfóxido (DMSO) y los discos estándares de los antibióticos de referencias como control positivo (Amikacina® y Ampicilina®) para cada uno de los microorganismos, posteriormente se incubaron las placas por 24 horas a 37 °C en atmósfera aeróbica y se realizó la lectura de los halos de inhibición en milímetros (mm). Se consideró un resultado positivo o sensible (actividad antibacteriana) cuando se observó un halo de inhibición del crecimiento bacteriano alrededor de los pozos. El caso contrario, la ausencia de dicho halo se interpretó como negativo o resistente (sin actividad antibacteriana). En los microorganismos que mostraron zona de inhibición se determinó la concentración inhibitoria mínima (CIM) [17], disolviendo los extractos en DMSO a concentraciones de 500, 250, 125 y 62,5 mg/mL. Todos los ensayos se realizaron por duplicado.

Actividad antioxidante

La actividad antioxidante fue determinada mediante el método de cuantificación del poder captador del radical libre 2,2-difenil-1-picrilhidrazilo (DPPH•) descrito por Díaz *et al.* [18] calculando el porcentaje de inhibición del DPPH (% I_{DPPH}) por medio de la siguiente ecuación:

$$\% I_{DPPH} = (A_{DPPH} - A_M / A_{DPPH}) \times 100$$

En la que A_{DPPH} es la absorbancia del DPPH y A_M es la absorbancia de la muestra.

La cuantificación de % I_{DPPH} se realizó preparando una solución del radical DPPH 0,06 mM (23,64 mg/L) y una solución de ácido ascórbico 1 mM (176 µg/mL como patrón de referencia). Ambas soluciones se almacenaron en frascos color ámbar para protegerlos de la luz. Para el ensayo, se colocó una alícuota de 0,2 mL de los extractos de metanol y el compuesto 1 (1000 µg/mL) a analizar en tubos de ensayo por separado y se

adicionaron 2,8 mL de solución de DPPH a cada uno, se dejó en reposo por 30 minutos a temperatura ambiente y en completa ausencia de luz. Se realizaron las lecturas de las absorbancias en un espectrofotómetro UV-visible (Spectronic GENESYSTM 10 Bio) a 517 nm. Una solución de 2,8 mL de DPPH y 0,2 mL de etanol fue usada como blanco. El ácido ascórbico se trató de igual manera que la muestra en estudio.

La determinación de la concentración efectiva media (CE_{50}), se llevó a cabo en las muestras que obtuvieron un porcentaje de inhibición mayor al 50 %. La CE_{50} indica la mínima concentración necesaria de un antioxidante para reducir en un 50 % la cantidad de radicales libres presentes en el medio. Para ello se prepararon diluciones de las muestras en concentraciones en el rango de 500 - 5 μg/mL, calculándose la CE_{50} por regresión lineal. Todos los ensayos se realizaron por triplicado.

Análisis estadístico

La media y la desviación estándar de los extractos ensayados se calcularon por triplicado utilizando Microsoft Excel. Para evaluar su importancia, todos los resultados se sometieron a una prueba de Tukey (p <0,05) para análisis unidireccional (ANOVA) [19].

Resultados y discusión

El tamizaje fitoquímico de los extractos de *Hinterhubera imbricata* (Tabla 1) se realizó mediante pruebas químicas cualitativas específicas, los extractos obtenidos se colocaron en contacto con diversos reactivos y se observaron las reacciones de coloración o precipitación que determinaron la presencia de ciertos metabolitos secundarios. Los análisis de los extractos de hexano y diclorometano de las hojas-tallos y flores presentaron una coloración roja y verde en la prueba de Liebermann-Burchard, indicando la presencia de triterpenos y esteroles, de igual modo, en el extracto de metanol las hojas-tallos y flores de evidenció la presencia de compuestos fenólicos, flavonoides, cumarinas y esteroles, siendo similar la composición química de las partes aéreas analizadas de *H. imbricata.* Estos resultados corresponden con los reportados por Bohlmann *et al*. [12] en el estudio del extracto etéreo de *H. imbricata* en el cual se aislaron diterpenos y triterpenos, sin embargo, en esta investigación se analizaron extractos más polares de hojas-tallos y flores evidenciándose la presencia de otros metabolitos secundarios como flavonoides y cumarinas.

Tabla 1. Tamizaje fitoquímico de los extractos de *Hinterhubera imbricata*

Metabolitos	Pruebas	Extractos Hojas-Tallos			Extractos flores		
		EHHT	EDHT	EMHT	EHF	EDF	EMF
Alcaloides	Reacciones Dragendorf Mayer Wagner	-	-	-	-	-	-
Flavonoides	Reacción Shinoda	-	-	+	-	-	+
Compuestos Fenólicos	Reacción $FeCl_3$ (1 %)	-	-	+	-	-	+
Saponinas	Reacción Espuma	-	-	-	-	-	-
Cumarinas	Reacción Hidróxido de amonio	-	-	+ Fluorescencias azul	-	-	+ Fluorescencias azul
Triterpenos y Esteroles	Reacción de Liebermann-Burchard	Esteroles +	Triterpenos Esteroles +	Esteroles +	Esteroles +	Triterpenos Esteroles +	Esteroles +
Taninos	Prueba de gelatina	-	-	-	-	-	-

Leyenda: EHHT: Extracto de Hexano de Hojas-Tallos. **EDHT:** Extracto de Diclorometano Hojas-Tallos. **EMHT:** Extracto de Metanol Hojas-Tallos. **EHF:** Extracto de Hexano Flores. **EDF:** Extracto de Diclorometano Flores. **EMF:** Extracto de Metanol Flores.

Por otra parte, luego de sucesivas cromatografías realizadas en los diferentes extractos de *H. imbricata* se logró el aislamiento y caracterización de cuatro compuestos que fueron identificados como 7-hidroxi-6-metoxicumarina (1), friedelona (2), friedelan-3-ol (3) y ácido ursólico (4) (Figura 1), a continuación, se presentan sus características físicas y espectroscópicas:

7-hidroxi-6-metoxicumarina (1): Sólido cristalino; $C_{10}H_8O_4$; p.f. 202-204 °C; EM *m/z*: 192 (M^+, 98,8), 177 (65,5), 164 (31,1), 149 (50); IR (KBr) $\nu_{máx.}$ cm^{-1}: 3342 (OH), 3002 (-C-H sp), 1709 (C=O), 1607 (C=C), 1200 (C-O); RMN ^1H (MeOD, 300 MHz) δ: 3,90 (3H, s, H-1'), 6,19 (1H, d, *J*= 10 Hz, H-3), 6,76 (1H, s, H-8), 7,10 (1H, s, H-5), 7,84 (1H, d, *J*=10 Hz, H-4); RMN ^{13}C (MeOD, 100 MHz) δ: 164,06 (C-2), 153,99 (C-7), 151,40 (C-8a), 147,07 (C-6), 146,11 (C-4), 112,57 (C-4a), 112,51 (C-3), 109,87 (C-5), 103,94 (C-8), 56,78 (C-1').

Friedelona (2): Sólido oleoso amarillo; $C_{30}H_{50}O$; p.f. 251-253 °C; EM *m/z:* 426,4 (M^+, 41,1); 411 (11,7); 341 (64,7); 273 (61,7); 207 (55,8); IR (KBr) $\nu_{máx.}$ cm^{-1}: 2918

(C-H sp^3), 1712 (C=O), 757 (C-H); RMN ^1H ($CDCl_3$, 300 MHz) δ: 2,20 (1H, m, H-4), 1.26-2.40 (25H, m, H-1, H-2, H-6, H-7, H-8, H-10, H-11, H-12, H-15, H-16, H-18, H-19, H-21, H-22), 1,23 (3H, s, H-28), 1,14 (3H, s, H-27), 1,00 (3H, s, H-26), 0,98 (3H, s, H-29), 0,93 (3H, s, H-30), 0,89 (3H, s, H-25), 0,84 (3H, d, *J*=7 Hz, H-23), 0,64 (3H, s, H-24); RMN ^{13}C (MeOD, 100 MHz) δ: 213,3 (C-3), 59,43 (C-10), 58,19 (C-4), 53,06 (C-8), 42,74 (C-18), 42,13 (C-5), 41,50 (C-2), 41,25 (C-6), 39,66 (C-13), 39,22 (C-22), 38,26 (C-14), 37,40 (C-9), 35,97 (C-16), 35,31 (C-19), 35,58 (C-11), 35,00 (C-30), 32,73 (C-21), 32,38 (C-15), 32,06 (C-28), 31,76 (C-29), 30,48 (C-12), 29,96 (C-17), 28,14 (C-20), 22,26 (C-1), 20,24 (C-26), 18,65 (C-27), 18,20 (C-7), 17,92 (C-25), 14,63 (C-24), 6,80 (C-23).

Friedelan-3-ol (3): Sólido blanco-amarillento; $C_{30}H_{52}O$; p.f. 209-211 °C; EM *m/z:* 428,3 (M+, 14,48); 413,4 (27,86); 399 (9,65); 281 (39,62); 207 (100); IR (KBr) $\nu_{máx.}$ cm^{-1}: 3471(OH), 2983 (C-H sp^3), 1108 (C-O); RMN ^1H ($CDCl_3$, 300 MHz) δ: 3,72 (1H, m, H-3), 1,97 (2H, t, H-11), 1,72 (1H, H-18), 1,55 (2H, t, H-1), 1,53 (2H, t, H-16), 1,57 (1H, d, H-4), 1,44 (2H, m, H-2), 1,42 (2H, t, H-12), 1,38 (2H, m, H-7), 1,26 (1H, t, H-8), 1,24 (1H, s, H-29), 1,16 (1H, s, H-30), 1,00 (1H, s, H-28), 0,95 (1H, s, H-27), 0,92 (1H, s, H-25), 0,94 (1H, s, H-26), 0,85 (1H, s, H-24), 0,85 (2H, t, H-22), 0,84 (3H, d, H-23); RMN ^{13}C ($CDCl_3$, 100 MHz) δ: 72,74 (C-3), 61,30 (C-10), 53,16 (C-8), 49,13 (C-4), 42,77 (C-18), 41,68 (C-6), 39,64 (C-14), 39,25 (C-22), 38,33 (C-13), 37,79 (C-5), 37,06 (C-9), 36,04 (C-2), 35,52 (C-16), 35,30 (C-11), 35,13 (C-19), 35,01 (C-29), 32,77 (C-21), 32,29 (C-15), 32,06 (C-28), 31,77 (C-30), 30,61 (C-12), 29,99 (C-17), 28,15 (C-20), 20,10 (C26), 18,63 (C-27), 18,22 (C-25), 17,52 (C-7), 16,37 (C-24), 15,76 (C-1), 11,61 (C-23).

Ácido ursólico (4): Sólido blanco cristalino; $C_{31}H_{50}O_3$ (Metil ursolato); p.f. 209-211 °C; EM *m/z:* 470, 411, 262, 203, 133; IR (KBr) $\nu_{máx.}$ cm^{-1}: 2918 (C-H sp^3) 1712 (C=O) 1650 (C=C); RMN ^1H ($CDCl_3$, 300 MHz) δ: 5,14 (1H, t, H-12), 2,99 (1H, t, H-3), 2,65 (1H, d H-18), 1,84 (2H, m, H-11), 1,56 (2H, m, H-22), 1,52 (1H, t, H-20), 1,47 (2H, m, H-2), 1,45 (1H, t, H-9), 1,38 (2H, m, H-21), 1,02 (3H, s, H-27), 0,91 (2H, m, H-1), 0,90 (1H, t, H-19), 0,90 (3H, s, H-23), 0,88 (3H, s, H-26), 0,84 (3H, s, H-25), 0,64 (3H, s, H-24); RMN ^{13}C ($CDCl_3$, 100 MHz) δ: 206,0 (C-28), 39,8 (C-1), 27,67 (C-2), 78,55 (C-3), 39,13 (C-4), 55,18 (C-5), 18,29 (C-6), 33,08 (C-7), 41,67 (C-8), 47,55 (C-9), 36,97 (C-10), 35,58 (C-11), 121,9 (C-12), 144,0 (C-13), 42,3 (C-14), 29,58 (C-15), 35,97 (C-16), 29,96 (C-17), 42,74 (C-18), 35,31 (C-19), 28,14 (C-20), 32,67 (C-21), 39,22 (C-22), 28,11 (C-23), 17,02 (C-24), 15,27 (C-25), 27,11 (C-26), 25,84 (C-27), 31,76 (C-29), 28,11 (C-30).

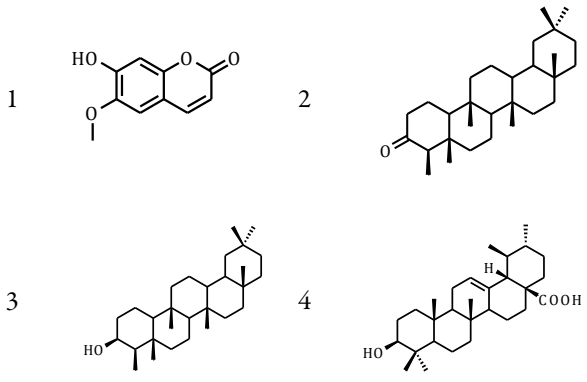

Figura 1. Estructuras de los compuestos aislados de los extractos de *Hinterhubera imbricata*.

Con respecto a la evaluación de la actividad antibacteriana (Tabla 2 y 3), todos los extractos de *H. imbricata* presentaron actividad contra *S. aureus* y *K. pneumoniae* en una concentración de 1000 µg/mL, siendo más activos los extractos de metanol con una concentración inhibitoria mínima (CIM) de 250 y 125 µg/mL, frente ambas bacterias. En tal sentido, para los metabolitos secundarios determinados en estos extractos (triterpenos, esteroles, compuestos fenólicos, cumarinas y flavonoides) se han descrito diversas actividades biológicas (antifúngica, antibacteriana y citotóxica) [20]. Siendo los compuestos fenólicos a los que se le atribuye el mecanismos de acción antibacteriano, al parecer está relacionado a la formación de complejos con las proteínas solubles y extracelulares de las células de la pared bacteriana, posiblemente mediante reacción con los grupos sulfihidrilos o por interacciones no especificas con las proteínas bacterianas [21]; por lo cual, se estima que *H. imbricata* representa una fuente de compuestos biológicamente activos. Este es el primer reporte sobre actividad antibacteriana del género *Hinterhubera*.

Tabla 2. Actividad antibacteriana de los extractos de *Hinterhubera imbricata*

		Halos de Inhibición (mm)				
Cepas Bacterias ATCC		*S. aureus* ATCC 25923	*E. faecalis* ATCC 19433	*E. coli* ATCC 25922	*K. pneumoniae* ATCC 23357	*P. aeruginosa* ATCC 27853
Extractos Hojas-Tallos 1000 µg/mL	EHHT	7,0	0,0	0,0	7,0	0,0
	EDHT	7,0	0,0	0,0	7,0	0,0
	EMHT	7,0	0,0	0,0	7,0	0,0

(*Continúa*)

Halos de Inhibición (mm)						
Cepas Bacterias ATCC		*S. aureus* ATCC 25923	*E. faecalis* ATCC 19433	*E. coli* ATCC 25922	*K. pneumoniae* ATCC 23357	*P. aeruginosa* ATCC 27853
Extractos Flores 1000 µg/mL	EHF	7,0	0,0	0,0	7,0	0,0
	EDF	7,0	0,0	0,0	7,0	0,0
	EMF	8,0	0,0	0,0	8,0	0,0
Antibióticos de referencia	PIP	-	-	24,0	27,0	26,0
	AMP	-	32,0	-	-	-
	ERI	33,0	-	-	-	-

Leyenda: EHHT: Extracto de Hexano de Hojas-Tallos. **EDHT:** Extracto de Diclorometano Hojas-Tallos. **EMHT:** Extracto de Metanol Hojas-Tallos. **EHF:** Extracto de Hexano Flores. **EDF:** Extracto de Diclorometano Flores. **EMF:** Extracto de Metanol Flores. **PIP**: Piperacilina * (100 µg). **AMP:** Ampicilina * (10 µg). **ERI:** Eritromicina * (15 µg). Los resultados son el promedio de tres mediciones por separado de los halos de inhibición (mm) ± Desviación Estándar (DE) de los extractos ensayados.

Tabla 3. Concentración inhibitoria mínima de los extractos de *Hinterhubera imbricata*

Microorganismos	CIM (µg/mL)					
	Extractos Hojas-Tallos			Extractos Flores		
	EHHT	EDHT	EMHT	EHF	EDF	EMF
S. aureus (ATCC 25923)	500	500	250	500	500	125
K. pneumoniae (ATCC 23357)	500	500	250	500	500	125

Leyenda: EHHT: Extracto de Hexano de Hojas-Tallos. **EDHT:** Extracto de Diclorometano Hojas-Tallos. **EMHT:** Extracto de Metanol Hojas-Tallos. **EHF:** Extracto de Hexano Flores. **EDF:** Extracto de Diclorometano Flores. **EMF:** Extracto de Metanol Flores. **CIM:** Concentración Inhibitoria Mínima. **NA:** No Activo. Los resultados son el promedio de tres mediciones por separado de cada concentración (mg/mL) ± Desviación Estándar (DE) de los extractos ensayados.

Con respecto al análisis de la actividad antioxidante se empleó el método del radical libre DPPH•, siendo una manera efectiva de evaluar los extractos y compuestos naturales debido a su fuerte capacidad donadora de hidrógeno. La capacidad antioxidante de los extractos de metanol (hojas-tallos y flores) y el compuesto 1 (7-hidroxi-6-metoxicumarina) se determinó a una concentración de 1000 µg/mL. Los porcentajes de inhibición (% I_{DPPH} ± DE) fueron de 92,50 ± 0,13 % para extracto de metanol de hojas-tallos; 93,05 ± 0,20% para el extracto de metanol de flores y 71,59 ± 0,25 % para el compuesto 1 (Tabla 4). Con el fin de encontrar la concentración efectiva 50 (CE_{50}), se prepararon diluciones de las muestras a concentraciones entre 500 a 5 µg/mL, calculándose la CE_{50} por regresión lineal. Todos los ensayos se realizaron por triplicado.

Tabla 4. Resultados obtenidos de la actividad antioxidante *in vitro* por el método del radical libre 2,2-difenil-1-picrilhidrazilo (DPPH•) de *Hinterhubera imbricata*.

Muestras analizadas	Concentración (µg/mL)	% I_{DPPH} ± DE	CE_{50} ± DE (µg/mL)
EMHT	1000	92,50 ± 0,13	12,9 ± 0,02
EMF		93,05 ± 0,20	8,3 ± 0,01
Compuesto 1		71,59 ± 0,25	494,3 ± 0,09
Patrón:	Ácido Ascórbico	96,51 ± 0,01	

Leyenda: EMHT: Extracto de Metanol Hojas-Tallos. **EMF**: Extracto de Metanol Flores. **Compuesto 1**: 7-hidroxi-6-metoxicumarina. Los resultados son el promedio de tres mediciones por separado del Porcentaje de Inhibición (% I_{DPPH}) ± Desviación Estándar (DE) de las muestras ensayadas.

Los resultados obtenidos reflejan que los extractos de metanol de las hojas-tallos (CE_{50}= 12,9 ± 0,02 µg/mL) y flores (CE_{50}= 8,3 ± 0,01 µg/mL) poseen mayor actividad antioxidante que la 7-hidroxi-6-metoxicumarina (compuesto 1, CE_{50}= 494,3 ± 0,09 µg/mL). Según el tamizaje fitoquímico, la composición química de ambos extractos es semejante (compuesto 1, flavonoides, triterpenos y esteroles), por lo cual se presume que hay un sinergismo entre la cumarina aislada y los otros metabolitos presentes en los extractos aumentando la actividad de los mismos. En este sentido, estudios previos reportan la actividad antioxidante de las cumarinas [22, 23] y sus derivados hemisintéticos [24, 25] determinando que la actividad captadora de radicales libres depende del número y localización de los grupos hidroxilo en la estructura del derivado fenólico, debido a la facilidad con la que el átomo de hidrógeno del grupo hidroxilo aromático puede ser donado a la especie radical, y a la estabilidad de la quinona resultante que soporta un electrón desapareado [26-28], la 7-hidroxi-6-metoxicumarina (1), posee un solo grupo hidroxilo, a lo cual puede atribuirse que la actividad es más baja en comparación a los extractos de metanol ensayados.

Conclusiones

La composición química de los extractos obtenidos de las hojas-tallos y flores de *Hinterhubera imbricata* es similar, se logró el aislamiento de cuatro compuestos que fueron identificados como 7-hidroxi-6-metoxicumarina, friedelona, friedelan-3-ol y ácido ursólico, siendo la primera vez que se reportan para el género *Hinterhubera*. Los extractos presentaron actividad antibacteriana y antioxidante a bajas concentraciones lo que cataloga esta planta como punto de partida para la búsqueda y caracterización de nuevos compuestos con actividad biológica.

Agradecimientos

Todos los autores agradecen al Consejo de Desarrollo Científico, Humanístico, Tecnológico y de las Artes (CDCHTA). Instituto de Investigaciones "Dr. Alfredo Nicolás Usubillaga del Hierro" y al Grupo de Productos Naturales y Química Medicinal de la Facultad de Farmacia y Bioanálisis, Universidad de Los Andes por su apoyo. Al Dr. Juan Manuel Amaro Luis por su apoyo y colaboración en la recolección de la especie en estudio. A la Université de Bordeaux, Institut des Sciences Moléculaires (CNRSUMR 5255) y el Institut Européen de Chimie et Biologie, por la colaboración prestada para obtener los espectros de Resonancia Magnética Nuclear (RMN) uni y bi dimensionales.

Conflicto de intereses

Los autores declaran no tener conflictos de intereses.

Referencias

1. J. Cuatrecasas, Prima Flora Colombiana. 3. *Compositae-Astereae*, *Webbia: Journal of Plant Taxonomy and Geography*, **24**(1), 1-335 (1969). Doi: https://doi.org/10.1080/00837792.1969.10669907

2. G.L. Nesom, *Aztecaster* (Asteraceae: Astereae). A new ditypic genus of dioecious shrubs from Mexico with redefinitions of the subtribes Hinterhuberinae and Baccharidinae, *Phytologia*, **75**(1), 45-54 (1993). URL: https://www.biodiversitylibrary.org/partpdf/96825

3. V. Karaman, *Phylogeny of Hinterhubera, Novenia and related genera based on the nuclear ribosomal (nr) DNA sequence data (Asteraceae: Astereae)*, Ph. D. thesis, Louisiana State University and Agricultural and Mechanical College, Baton Rouge, Louisiana, USA, 2006. 202 p. URL: https://repository.lsu.edu/gradschool_dissertations/2200/

4. A.A. Anderberg, B.G. Baldwin, R.G. Bayer, J. Breitwieser, C. Jeffrey, M.O. Dillon, P. Eldenäs, V. Funk, N. García-Jacas, P.O. Hind Karis, *et al.*, Compositae, en: J.W. Kadereit, C. Jeffrey (editores), *Flowering Plants · Eudicots: Asterales*, Springer - Verlag, Berlin Heidelberg, 2007, Vol. VIII, pp. 61-588. URL: https://link.springer.com/chapter/10.1007/978-3-540-31051-8_7

5. V. Badillo, S. Díaz-Piedrahita, C. E. Benítez, Asteraceae, en: O. Hokche, P.E. Berry, Otto Huber (editores), *Nuevo catálogo de la flora vascular de Venezuela*, Fundación Instituto Botánico de Venezuela "Dr. Tobías Lasser", Caracas, Venezuela, 2008, Vol. 28, pp. 1-44.

6. I.C. Zampini, S. Cuello, M.R. Alberto, R.M. Ordoñez, R. D'Almeida, E. Solorzano, M.I. Isla, Antimicrobial activity of selected plant species from "the Argentine Puna" against sensitive and multi-resistant bacteria, *Journal of Ethnopharmacology*, **124**(3), 499-505 (2009). Doi: https://doi.org/10.1016/j.jep.2009.05.011

7. R.E. D'Almeida, M.R. Alberto, C. Quispe, G. Schmeda-Hirschmann, M.I. Isla, Antimicrobial phenylpropanoids from the Argentinean highland plant *Parastrephia lucida* (Meyen) Cabrera, *Journal of Ethnopharmacology*, **142**(2), 407-414 (2012). Doi: https://doi.org/10.1016/j.jep.2012.05.010

8. C. Echiburu-Chau, L. Pastén, C. Parra, J. Bórquez, A. Mocan, M.J. Simirgiotis, High resolution UHPLC-MS characterization and isolation of main compounds from the antioxidant medicinal plant *Parastrephia lucida* (Meyen), *Saudi Pharmaceutical Journal*, **25**(7), 1032-1039 (2017). Doi: https://doi.org/10.1016/j.jsps.2017.03.001

9. L.S. Di Ciaccio, V.G. Spotorno, M.M. Córdoba-Estévez, D.J.L. Ríos, R.H. Fortunato, A.E. Salvat, Antifungal activity of *Parastrephia quadrangularis* (Meyen) Cabrera extracts against *Fusarium verticillioides*, *Letters in Aplied Microbiology*, **66**(3), 244-251 (2018). Doi: https://doi.org/10.1111/lam.12844

10. F. Cifuentes, J.R. Palacios, C.R. Nwokocha, J. Bórquez, M.J. Simirgiotis, I. Norambuena, M. Chiong, A. Paredes, Polyphenolic composition and hypotensive effects of *Parastrephia quadrangularis* (Meyen) Cabrera in rat, *Antioxidants* (Basel), **8**(12), 591 (2019). Doi: https://doi.org/10.3390/antiox8120591

11. S.M. Alcalde Bahamonde, M.L. Flores, A.V. Uhrich, M.D. Escobar Daza, O.L. Córdoba, *Chiliotrichum diffusum* (G. Forst.) Kuntze, en: A. Máthé, A. Bandoni (editores), *Medicinal and Aromatic Plants of South America Vol. 2: Argentina, Chile and Uruguay*, Springer, 2021, Vol 7, p. 1-60.

12. F. Bohlmann, M. Grenz, H. Schwarz, Naturally occurring terpene derivatives. XXV. New diterpenes from *Hinterhubera imbricate* [Natürlich vorkommende Terpenderivate, XXV. Neue Diterpene aus *Hinterhubera imbricata* Cuatr.], *Chemische Berichte*, **106**(8), 2479-2484 (1973). Doi: https://doi.org/10.1002/cber.19731060808

13. D. Marcano, M. Hasegawa, *Fitoquímica Orgánica*, 2ª ed., Editorial Torino, Caracas, Venezuela, 2002, 588 p.

14. W. Hartman, L. Roll, *α*-Methyl-*α*-phenylhydrazine, Organic syntheses, Collective Vol II, John Wiley & Sons, New York, 1957, p. 418. URL: https://www.orgsyn.org/Content/pdfs/procedures/cv2p0418.pdf

15. F. Arndt, Diazomethane, Organic syntheses, Collective Vol II, John Wiley & Sons, New York, 1957, p. 165. URL: https://orgsyn.org/Content/pdfs/procedures/cv2p0165.pdf

16. CLSI supplement M100, Clinical and Laboratory Standards Institute, Wayne (PA), USA, 2018, pp. 1-15. URL: https://www.nih.org.pk/wp-content/uploads/2021/02/CLSI-2020.pdf

17. D.W. Tholen, A. Kallner, J.W. Kennedy, J.S. Krouwer, K. Meier, *Evaluation of precision performance of quantitative measurement methods, Approved guideline–Second Edition*, Volume 24, Number 25, CLSI document EP05-A2, Clinical and Laboratory Standards Institute, Wayne (PA), 2004. URL: https://webstore.ansi.org/preview-pages/CLSI/preview_EP05-A2.pdf

18. L. Díaz, S. De Montijo, A.L. Medina, P. Meléndez, V. Laurence, G. Marti-Mestres, Activity of ethanolic extracts leaves of *Machaerium floribundum* against acne-inducing bacteria, and their cytoprotective and antioxidant effects on fibroblast, *Revista Peruana de Biología,* **18**(2), 153-158 (2011). URL: http://www.scielo.org.pe/pdf/rpb/v18n2/a04v18n2.pdf

19. V. Bewick, L. Cheek, J. Ball, Statistics review 9: one-way analysis of variance, *Critical Care*, **8**, 130 (2004). Doi: https://doi.org/10.1186/cc2836

20. L. Hernández-Vásquez, J. Palazon, A. Navarro-Ocaña, The pentacyclic triterpenes *α*,*β*-amyrins: A review of sources and biological activities, en: V. Rao (editor), *Phytochemicals – A Global Perspective of Their Role in Nutrition and Health*, InTechOpen, Rijeka, Croatia, 2012, pp. 487-502. URL: https://diposit.ub.edu/dspace/bitstream/2445/176113/1/267422.pdf

21. D. Domingo, M. López-Brea, Plantas con acción antimicrobiana, *Revista Española de Quimioterapia*, **16**(4), 385-393 (2003). URL: https://www.seq.es/seq/0214-3429/16/4/385.pdf

22. K.C. Fylaktakidou, D.J. Hadjipavlou-Litina, K.E. Litinas, D.N. Nicolaides, Natural and synthetic coumarin derivatives with anti-inflammatory/antioxidant activities, *Current Pharmaceutical Design*, **10**(30), 3813-33 (2004). Doi: https://doi.org/10.2174/1381612043382710

23. A. Basile, S. Sorbo, V. Spadaro, M. Bruno Maggio, N. Faraone, S. Rosselli, Antimicrobial and antioxidant activities of coumarins from the roots of *Ferulago campestris* (Apiaceae), *Molecules*, **14**(3), 939-952 (2009). Doi: https://doi.org/10.3390/molecules14030939

24. G. Tataringa, C. Stan, C. Mircea, A. Jitareanu, A.M. Zbancioc, Antioxidant evaluation of some coumarin derivatives, *Farmacia*, **64**(4), 533-538 (2016). URL: https://farmaciajournal.com/wp-content/uploads/2016-04-art-09-Tataringa_Stan_Mircea_533-538.pdf

25. Zabiulla, F.H. Al-Ostoot, Y.H.E. Mohammed, M. Jyothi, S.V. Mamatha, N.F. Khanum, S.A. Khanum, Evaluation of antioxidant activity of coumarin derivatives conjugated with benzophenone, *International Journal of Scientific Progress and Research*, **32**(90), 47-51 (2017). URL: https://www.ijspr.com/citations/v32n1/IJSPR_3201_1810.pdf

26. C.A. Rice-Evans, N.J. Miller, G. Paganga, Structure-antioxidant activity relationships of flavonoids and phenolic acids. *Free Radical Biology and Medicine*, **20**(7), 933-956 (1996). Doi: https://doi.org/10.1016/0891-5849(95)02227-9

27. G. Cao, E. Sofic, R.L. Prior, Antioxidant and prooxidant behavior of flavonoids: structure-activity relationships, *Free Radical Biology and Medicine*, **22**(5), 749-760 (1997). Doi. https://doi.org/10.1016/s0891-5849(96)00351-6

28. A.S. Pannala, T.S. Chan, P. O'brien, C. Rice-Evans, Flavonoid B-ring chemistry and antioxidant activity: fast-reaction kinetics, *Biochemical and Biophysical Research Communications*, **282**(5), 1161-1168 (2001). Doi: https://doi.org/10.1006/bbrc.2001.4705

Como citar este artículo

Y. Obregón-Díaz, L. Rojas-Fermín, A. Pérez-Colmenares, Y. Cordero, R. Aparicio, W. De Lima, J. Hernández, A. Usubillaga, Estudio fitoquímico y actividad biológica de *Hinterhubera imbricata* Cuatrec. & Aristeg, *Rev. Colomb. Cienc. Quim. Farm.*, **53**(2), 471-487 (2024). https://doi.org/10.15446/rcciquifa.v53n2.114452

Artículo de investigación clínica / https://doi.org/10.15446/rcciquifa.v53n2.114453

Nivel de implementación del programa de farmacovigilancia y sus factores asociados en instituciones de salud en el Valle del Cauca

Jobany Castro Espinosa[1a], Hernán Estupiñán Cabrera[2b], María Alejandra Gil Pineda[3c], Laura Valentina Moreno Posso[3d], María Cristina Donoso Huertas[3e], Daihana Pino Quinto[3f]

[1] Grupo de Investigación en Salud Pública (GISAP), Fundación Universitaria San Martin, Cra 122 #25-305, Santiago de Cali, Valle del Cauca, Colombia

[2] Ensalud Group, Calle 5 #39-50, Santiago de Cali, Valle del Cauca, Colombia

[3] Semillero de Investigación INNOVA, Fundación Universitaria San Martin, Cra 122 #25-305, Santiago de Cali, Valle del Cauca, Colombia

Correos electrónicos:

[a] jobany.castro@sanmartin.edu.co, [b] hernan.estupinan@yahoo.es, [c] mariaagilp28@gmail.com, [d] valentinamoreno5903@gmail.com, [e] 110211202043@est.sanmartin.edu.co, [f] diana1975quinto@gmail.com

ORCID ID:

[a] https://orcid.org/0000-0002-3476-248X, [b] https://orcid.org/0009-0007-0391-8385, [c] https://orcid.org/0009-0007-6470-4356, [d] https://orcid.org/0005-1810-2982, [e] https://orcid.org/0009-2458-223X, [f] https://orcid.org/0009-0007-6302-6207

Recibido: 25 de diciembre de 2023
Revisado: 23 de marzo de 2024
Aceptado: 26 de marzo de 2024

Resumen

Introducción: Los Eventos Adversos Medicamentosos (EAM), son vigilados por los programas de farmacovigilancia. Aunque en Colombia la legislación exige a las instituciones prestadoras de servicios de salud contar con un programa institucional de farmacovigilancia, no todas las instituciones cumplen esta regulación. **Objetivo:** Determinar el nivel de implementación del programa de farmacovigilancia y sus factores asociados en instituciones de salud del Valle del Cauca. **Metodología:** Se diseñó una encuesta basada en la escala HENRI PFv del Instituto Nacional de Vigilancia de Medicamentos y Alimentos (INVIMA). La encuesta se envió a las instituciones de salud. Se consultó información en el registro especial de prestadores de salud e información sobre el reporte en VigiFlow. **Resultados:** Participaron 80 instituciones de las que el 81% catalogaron como en implementación y el 19% como

no implementado. El ítem de menor cumplimiento fue contar con programas y estrategias de farmacovigilancia (40%) y contar con un sistema de gestión de calidad (45%) y el item de mayor cumplimiento fue la revisión de alertas y medidas sanitarias (88%). El análisis bivariado permitió establecer la asociación entre la implementación del programa y variables como la presencia de personal farmacéutico, la ubicación de la institución en un municipio grande, la duración del funcionamiento del programa de más de un año, y la percepción de que el INVIMA no envía reportes a los actores. **Conclusión:** Se determinó la implementación para cada institución. Los factores asociados a la implementación constituyen aspectos a considerar para mejorar el funcionamiento de los programas de farmacovigilancia.

Palabras clave: farmacéuticos, farmacovigilancia, investigación en farmacia, instituciones de salud, notificación.

Summary

Level of implementation of the pharmacovigilance program and its associated factors in health institutions in Valle del Cauca

Introduction: pharmacovigilance programs monitor the Adverse Drug Events (ADEs). Although Colombian legislation mandates healthcare service providers to have an institutional pharmacovigilance program, not all institutions comply with this regulation. **Objective**: Determine the level of implementation of the pharmacovigilance program and its associated factors in health institutions in Valle del Cauca. **Methodology:** A survey was designed based on the HENRI PFv scale of the National Institute for Food and Drug Surveillance (INVIMA). The survey was sent to health institutions. Information was consulted in the special registry of health providers and information on the EAM report in VigiFlow. The association between the implementation of the program and each of the factors was evaluated, using Stata version 14 software. **Results:** 80 institutions participated, of which 81% were classified as being implemented and 19% as not being implemented. The item with the lowest compliance was having pharmacovigilance programs and strategies (40%) and having a quality management system (45%), and the item with the highest compliance was the review of alerts and health measures (88%). The bivariate analysis allowed establishing the association between program implementation and variables such as the presence of pharmaceutical personnel, the institution's location in a large municipality, the program's operational duration of more than one year, and the perception that INVIMA does not send reports to stakeholders.

Conclusion: The implementation was determined for each institution. The factors associated with implementation constitute aspects to consider to improve the functioning of pharmacovigilance programs.

Keywords: pharmacists, pharmacovigilance, pharmacy research, health facilities, notification.

Resumo

Nível de implementação do programa de farmacovigilância e seus fatores associados nas instituições de saúde do Vale do Cauca

Introdução: Os Eventos Adversos Medicamentosos (EAM), são vigiados pelos programas de farmacovigilância. Embora na Colômbia a legislação exija que as instituições prestadoras de serviços de saúde contem com um programa institucional de farmacovigilância, nem todas as instituições cumprem esta regulamentação. Objetivo: Determinar o nível de implementação do programa de farmacovigilância e seus fatores associados nas instituições de saúde do Vale do Cauca. **Metodologia:** Foi desenvolvida uma consulta baseada na escala HENRI PFv do Instituto Nacional de Vigilância de Medicamentos e Alimentos (INVIMA). A consulta foi enviada às instituições de saúde. Foram consultadas informações no registro especial de discussão de saúde e informações sobre o relatório no VigiFlow. **Resultados:** Participaram 80 instituições das quais 81% foram catalogadas como em implementação e 19% como não implantadas. O item de menor cumprimento foi contado com programas e estratégias de farmacovigilância (40%) e contado com um sistema de gestão de qualidade (45%) e o item de maior cumprimento foi a revisão de alertas e medidas sanitárias (88%). A análise bivariada permitiu estabelecer a associação entre a implementação do programa e variáveis como a presença de farmacêutico pessoal, a localização da instituição em um município grande, a duração do funcionamento do programa por mais de um ano, e a percepção de que o INVIMA no envía reporta aos atores. **Conclusão:** Foi determinada a implementação para cada instituição. Os fatores associados à implementação constituem aspectos a serem considerados para melhorar o funcionamento dos programas de farmacovigilância.

Palavras-chave: farmacêuticos, farmacovigilância, investigação em farmácia, instituições de saúde, notificação.

Introducción

Los eventos adversos medicamentosos (EAM), afectan a individuos de diversa índole [1] y pueden manifestarse en grados de gravedad variables [2], llegando incluso a desencadenar consecuencias fatales, siendo considerados un evento de interés en salud pública. La farmacovigilancia se encarga de analizar los procedimientos de notificación, determinar los medicamentos sujetos a seguimiento, descubrir nuevas reacciones adversas y establecer medidas preventivas [3]. La legislación Colombiana, a través de la Resolución 1403 de 2007 del Ministerio de la Protección Social y la Red Nacional de Farmacovigilancia, requiere que las instituciones de salud implementen sus programas de farmacovigilancia y reporten los EAM en la plataforma VigiFlow, estando inscritas en la red de farmacovigilancia del Instituto Nacional de Vigilancia de Medicamentos y Alimentos (INVIMA), entidad gubernamental encargada de vigilarlos a nivel nacional. La omisión de la inscripción, reporte o implementación de dicho programa constituye una violación a esta normativa, la cual abarca aspectos relativos al personal, la documentación, las capacitaciones, los eventos adversos y sus estadísticas [4]. Por consiguiente, resulta esencial promover el desarrollo de programas de farmacovigilancia, que fomenten el uso seguro de los medicamentos. Pese a su relevancia, en numerosas instituciones no operan de manera óptima o, simplemente, no se cuenta con ellos. El objetivo de este estudio fue determinar el nivel de implementación del programa de farmacovigilancia y sus factores asociados en instituciones de salud del Valle del Cauca, Colombia.

Metodologia

La presente investigación se enmarca en un enfoque cuantitativo, observacional y transversal. Los criterios de inclusión se centraron en las instituciones de salud del Valle del Cauca, Colombia, que forman parte de la red nacional de farmacovigilancia. El INVIMA desarrolló el instrumento HENRI PFv como parte de sus esfuerzos para promover y garantizar la implementación efectiva de programas de farmacovigilancia en dichas instituciones. Este instrumento fue diseñado con el propósito de evaluar y hacer seguimiento a los programas de farmacovigilancia en las instituciones. La guía de visitas de seguimiento a la implementación de los programas de farmacovigilancia en Instituciones Prestadoras de Servicios de Salud del INVIMA, describe este instrumento como una herramienta de evaluación numérica para determinar el nivel de implementación del programa de farmacovigilancia. En este estudio, se utilizaron las preguntas de la escala HENRI PFv del INVIMA, para evaluar la implementación del programa. Esta escala consiste en una lista de verificación de 12 preguntas, con opciones de calificación como “cumple”, “cumple parcialmente” y “no cumple”, que equivalen a los valores de

1,0, 0,5 y 0,0 respectivamente. Cada pregunta tiene asignado un peso según su impacto, siendo critico=12, mayor=6 y menor=2 [5]. El cumplimiento global de cada criterio se calculó como el cociente de la suma del cumplimiento de todas las instituciones multiplicado por el peso del criterio, dividido por el denominador correspondiente al valor máximo posible, es decir, si todas las instituciones cumplieran totalmente, en cuyo caso sería el valor de uno (1) y eso multiplicado por el peso del criterio (Ecuación 1). Este cálculo se realizó de manera independiente para las instituciones del grupo "en implementación" y las "No implementadas", como se define más adelante.

$$\text{Cumplimiento global del criterio} = \frac{\left[\sum_{a}^{n}=1 \text{ cumplimiento de todas las instituciones (a)}\right] * \text{peso}}{\text{n*peso}} \quad \text{(Ec. 1)}$$

En cuanto a las preguntas sobre los factores asociados, estas se organizaron en tres categorías: aquellas relacionadas con la percepción del encuestado, la institución y el programa (un total de 24 preguntas). La información complementaria de las instituciones se obtuvo del Registro Especial de Prestadores de Servicios de Salud, mientras que los reportes en la plataforma de VigiFlow de la secretaría de salud departamental, para calcular el promedio mensual de reportes. El instrumento se elaboró utilizando Google Forms y se envió a las direcciones de correo electrónico de las instituciones. Previamente, se solicitó su consentimiento informado para participar, y una vez aceptado, procedieron a completar la encuesta. Las respuestas se exportaron a Microsoft Excel y, en función del puntaje total obtenido, cada institución se clasificó como "en implementación" si alcanzaba un puntaje igual o superior al 64%, o como "no implementado" si obtenía un puntaje menor a 64%.

La variable dependiente se definió como "en implementación", mientras que todas las demás se consideraron variables independientes. Se llevó a cabo un análisis bivariado para estimar el Odds ratio (OR) y su significancia estadística, utilizando el Intervalo de confianza al 95 % (IC 95%) y la prueba de chi cuadrado ($p<0,05$), para lo cual se empleó el software Stata versión 14. Este proyecto se adhirió a compromisos de confidencialidad establecidos con el consentimiento informado, y recibió el aval de la Fundación Universitaria San Martín (PYI-2018-001) y de la Secretaría de Salud Departamental del Valle del Cauca (Acta 8-2020).

Resultados

De las 153 instituciones que cumplían con los criterios de inclusión, participaron 80 (52,3%), mientras que 2 rechazaron la participación (1,3%) y 2 fueron descartadas por

completar la encuesta de manera inadecuada (1,3%). En la mayoría de los casos, los programas tenían más de 3 años de funcionamiento (39%) y estaban activos, realizando seguimiento farmacoterapéutico, reportes de EAM y reuniones de farmacovigilancia (85%). La mayoría de los participantes eran químicos farmacéuticos (55%), con más de 3 años de experiencia (48%), habían recibido entre 2 y 5 capacitaciones (51%), consultaban fuentes bibliográficas en sitios web (50%) y tenían una dedicación no exclusiva a farmacovigilancia, es decir tenían responsabilidades adicionales a esta (94%).

La implementación fue más alta en instituciones donde el responsable de farmacovigilancia era un Químico Farmacéutico (98%) y cuando el promedio de profesionales en el programa era mayor (7,48 vs 7,27), aunque esta diferencia no fue estadísticamente significativa (valor de p = 0,9228). Las instituciones con programas activos mostraron una mayor implementación (85% vs 58%), al igual que aquellas ubicadas en municipios grandes en comparación con municipios pequeños (88% vs 56%). La implementación aumentó en la medida que aumentaba el tiempo de funcionamiento del programa (50%, 90%, 94%), la experiencia en farmacovigilancia (57%, 67%, 73%, 95%) y las capacitaciones recibidas (44%, 83%, 96%). También fue mayor en instituciones que consultaban fuentes bibliográficas, las de mayor nivel de atención (100%), las que tenían servicio farmacéutico (83%) y que este era de media o alta complejidad (100%). Estaba más implementado entre los que tenían más capacidad instalada (medida como el promedio de la cantidad de camas) (131 vs 64), aunque esta diferencia no fue estadísticamente significativa (valor de p = 0,2103).

Las instituciones se clasificaron en cuartiles según el promedio de reportes mensuales, considerando como alto reporte aquellas del cuarto cuartil (24%). Quienes tienen el programa implementado presentaron un promedio de reportes superior a los que no lo tenían (7,51 vs 4,45), sin embargo, esta diferencia no mostró ser estadísticamente significativa (valor de p = 0,6345). Según los encuestados, la farmacovigilancia es considerada "muy importante" especialmente por el personal asistencial (78%) en comparación con el personal administrativo (66%). Respecto al INVIMA, la mayoría percibe que esta entidad lleva a cabo iniciativas de vigilancia activa de EAM (69%), pero lo que menos consideran es que esta entidad comparte los resultados de las intervenciones con las instituciones (38%). La mayoría ha visitado la página web del INVIMA y ha encontrado la información útil (85%) (Tabla 1).

Tabla 1. Caracterización y percepción de los participantes, de las instituciones y del programa según el nivel de implementación de la farmacovigilancia

Profesión del encuestado	En implementación	No implementado	Total	Porcentaje total	% en implementación
Químico Farmacéutico	43	1	44	55%	98%
Regente de Farmacia	10	4	14	18%	71%
Auxiliar de farmacia	1	0	1	1%	100%
Medico(a)	2	0	2	3%	100%
Enfermero(a)	5	6	11	14%	45%
Otro	4	4	8	10%	50%
Programa de farmacovigilancia activo	**En implementación**	**No implementado**	**Total**	**Porcentaje total**	**% en implementación**
Si	58	10	68	85%	85%
No	7	5	12	15%	58%
Tipo de municipio de la institución	**En implementación**	**No implementado**	**Total**	**Porcentaje total**	**% en implementación**
Grande	56	8	64	80%	88%
Pequeño	9	7	16	20%	56%
Tiempo funcionando el programa de farmacovigilancia	**En implementación**	**No implementado**	**Total**	**Porcentaje total**	**% en implementación**
Menos de 1 año	10	10	20	25%	50%
Entre 1 y 3 años	26	3	29	36%	90%
Más de 3 años	29	2	31	39%	94%
El encuestado es el referente de farmacovigilancia	**En implementación**	**No implementado**	**Total**	**Porcentaje total**	**% en implementación**
Si	60	13	73	91%	82%
No	5	2	7	9%	71%

(*Continúa*)

Experiencia del encuestado en farmacovigilancia	En implementación	No implementado	Total	Porcentaje total	% en implementación
Nada	4	3	7	9%	57%
Menos de 1 año	6	3	9	11%	67%
Entre 1 y 3 años	19	7	26	33%	73%
Más de 3 años	36	2	38	48%	95%
Capacitaciones recibidas del encuestado	**En implementación**	**No implementado**	**Total**	**Porcentaje total**	**% en implementación**
Ninguna	5	2	7	9%	71%
1	4	5	9	11%	44%
Entre 2 y 5	34	7	41	51%	83%
Más de 5	22	1	23	29%	96%
El encuestado hizo el curso de VigiFlow	**En implementación**	**No implementado**	**Total**	**Porcentaje total**	**% en implementación**
Si	52	13	65	81%	80%
No	13	2	15	19%	87%
Elementos exclusivos para realizar farmacovigilancia	**En implementación**	**No implementado**	**Total**	**Porcentaje total**	**% en implementación**
Computador	33	7	40	50%	83%
Correo electrónico	37	6	43	54%	86%
Teléfono	15	4	19	24%	79%
Oficina	16	6	22	28%	73%
Fuente bibliográfica para consulta en de farmacovigilancia	**En implementación**	**No implementado**	**Total**	**Porcentaje total**	**% en implementación**
Bases de datos	10	0	10	13%	100%
Bases de datos, Libro de farmacovigilancia, Sitio web	4	0	4	5%	100%
Bases de datos, Sitio web	11	0	11	14%	100%

(*Continúa*)

Fuente bibliográfica para consulta en de farmacovigilancia	En implementación	No implementado	Total	Porcentaje total	% en implementación
Libro de farmacovigilancia, Sitio web	2	1	3	4%	67%
Sitio web	30	10	40	50%	75%
Ninguno	8	4	12	15%	67%
Tipo de dedicación del encuestado para farmacovigilancia	**En implementación**	**No implementado**	**Total**	**Porcentaje total**	**% en implementación**
Exclusivo en farmacovigilancia	3	1	4	5%	75%
Farmacovigilancia y otras funciones	61	14	75	94%	81%
Sin registro	1	0	1	1%	100%
Naturaleza jurídica de la institución	**En implementación**	**No implementado**	**Total**	**Porcentaje total**	**% en implementación**
Privada	53	7	60	75%	88%
Mixta	1	0	1	1%	100%
Publica	10	7	17	21%	59%
Sin registro	1	1	2	3%	50%
La institución es una empresa Social del estado	**En implementación**	**No implementado**	**Total**	**Porcentaje total**	**% en implementación**
Si	11	7	18	23%	61%
No	27	4	31	39%	87%
Sin registro	27	4	31	39%	87%
Nivel de atención de la institución	**En implementación**	**No implementado**	**Total**	**Porcentaje total**	**% en implementación**
1	5	7	12	15%	42%
2	5	0	5	6%	100%
3	1	0	1	1%	100%
Sin registro	54	8	62	78%	87%

(*Continúa*)

Carácter territorial de la institución	En implementación	No implementado	Total	Porcentaje total	% en implementación
Departamental	6	0	6	8%	100%
Municipal	5	7	12	15%	42%
Sin registro	54	8	62	78%	87%
La institución cuenta con servicio de vacunación	**En implementación**	**No implementado**	**Total**	**Porcentaje total**	**% en implementación**
Si	33	14	47	59%	70%
No	32	1	33	41%	97%
La institución cuenta con servicio farmacéutico	**En implementación**	**No implementado**	**Total**	**Porcentaje total**	**% en implementación**
Si	54	11	65	81%	83%
No	11	4	15	19%	73%
Complejidad del servicio farmacéutico	**En implementación**	**No implementado**	**Total**	**Porcentaje total**	**% en implementación**
Alta	13	0	13	16%	100%
Media	20	0	20	25%	100%
Baja	19	10	29	36%	66%
N/A	11	4	15	19%	73%
Sin registro	2	1	3	4%	67%
Nivel de reporte	**En implementación**	**No implementado**	**Total**	**Porcentaje total**	**% en implementación**
Alto reporte (4º cuartil)	18	1	19	24%	95%
Bajo reporte (3er, 2º o 1er cuartil)	47	14	61	76%	77%
Capacidad instalada	**En implementación**	**No implementado**	**Total**	**Porcentaje total**	**% en implementación**
Mayor capacidad (Más de 50 elementos)	34	5	39	49%	87%

(*Continúa*)

Capacidad instalada	En implementación	No implementado	Total	Porcentaje total	% en implementación
Menor capacidad (50 o menos elementos)	31	10	41	51%	76%
Percepción sobre la importancia de la farmacovigilancia para el personal asistencial	**En implementación**	**No implementado**	**Total**	**Porcentaje total**	**% en implementación**
Moderadamente Importante	16	2	18	23%	89%
Muy importante	49	13	62	78%	79%
Percepción sobre la importancia de la farmacovigilancia para el personal administrativo	**En implementación**	**No implementado**	**Total**	**Porcentaje total**	**% en implementación**
Moderadamente Importante	24	3	27	34%	89%
Muy importante	41	12	53	66%	77%
Con respecto al programa nacional de Farmacovigilancia, considera que el INVIMA:	**En implementación**	**No implementado**	**Si**	**Porcentaje**	**% en implementación**
Mantiene contacto con las instituciones a través del envío periódico de informes	40	14	54	68%	74%
Comparte los resultados de las intervenciones realizadas con las instituciones	23	7	30	38%	77%
Realiza asistencia técnica a las instituciones y promueve la participación en eventos nacionales	39	8	47	59%	83%
Da o recibe soporte de otros programas institucionales	29	8	37	46%	78%
Desarrolla o participa en iniciativas de vigilancia activa de eventos adversos.	45	10	55	69%	82%

(*Continúa*)

Desarrolla programas de capacitación a la comunidad en general	38	5	43	54%	88%
Es fácil la comunicación con el INVIMA (teléfono, correo, web, etc.)	27	10	37	46%	73%
Ha visitado la página web del INVIMA y su información le ha resultado útil para el programa de farmacovigilancia	**En implementación**	**No implementado**	**Si**	**Porcentaje total**	**% en implementación**
La ha visitado y la información le ha resultado útil.	55	13	68	85%	81%
La ha visitado, pero la información no le ha resultado útil.	7	0	7	9%	100%
No he visitado la página web del INVIMA.	1	2	3	4%	33%
No sabía que el INVIMA tiene una página web	2	0	2	3%	100%

Nota: la prueba de Chi cuadrado para el promedio de reportes mensuales mostró que no se comportaba como una variable normal.

En relación a las respuestas del instrumento HENRI PFv se identificó que el 95% afirmó conocer las normas que aplicables al programa; sin embargo, menos de la mitad (49%) respondió adecuadamente a las preguntas relacionadas con estas normas. El 96% indicó que en su institución existe un procedimiento estandarizado de farmacovigilancia, siendo el análisis de causalidad el aspecto menos empleado para el reporte (79%). El 72% mencionó que el procedimiento diferencia claramente el momento de reporte para eventos serios y para los no serios. En cuanto a las estadísticas de los EAM, se encontró que el 46% lo tiene documentado de tal forma que les ha permitido detectar señales, tomar decisiones y realizar planes de mejora (46%). El 79% afirmó que está documentado la conformación del comité multidisciplinario, con actas de reunión, y el 76% indicó que conoce las publicaciones relacionadas con farmacovigilancia. En lo que respecta a actividades de uso seguro, la identificación de medicamentos LASA (del inglés: *Look*, *alike*, *sound like*, que se refiere a medicamentos con similitudes físicas o nombres parecidos) y de alto riesgo fue la práctica más común (63%). La mayoría cuenta con un programa de capacitación (61%) que incluye registros de asistencia (64%), y el 44% está certificado en gestión de calidad (Tabla 2).

Tabla 2. Preguntas de implementación del programa de farmacovigilancia, según el instrumento HENRI

Conoce las normas que aplican al programa de farmacovigilancia	**Cantidad**	**Porcentaje**
Si	72	95%
No	8	11%
Respondieron adecuadamente las respuestas sobre la normatividad	**Cantidad**	**Porcentaje**
Si	37	49%
No	43	57%
La institución posee un procedimiento de Farmacovigilancia	Cantidad	Porcentaje
Si	73	96%
No	7	9%
En el reporte en VigiFlow tiene en cuenta:	Cantidad	Porcentaje
Datos del paciente	76	100%
Datos del medicamento	73	96%
Datos del evento adverso	74	97%
Datos del reportante	61	80%
Análisis de causalidad	60	79%
El procedimiento describe el momento en el que se reportan los eventos adversos medicamentosos y los discrimina para serios y no serios.	**Cantidad**	**Porcentaje**
Describe y discrimina el momento de reportes de eventos serios y no serios	55	72%

(*Continúa*)

Describe el momento de reporte, pero no lo discrimina	18	24%
No describe el momento de reporte	7	9%
Tiene documentado la generación de estadísticas epidemiológicas y permiten la detección de señales, toma de decisiones y generación de planes de mejora.	**Cantidad**	**Porcentaje**
Documentado, pero no han permitido detectar señales, toma de decisiones y planes de mejora	14	18%
Documentado y han permitido detectar señales, toma de decisiones y planes de mejora.	35	46%
No está documentado, ni se generan estadísticas.	14	18%
Generan estadísticas, que han permitido detectar señales, toma de decisiones y planes de mejora, pero no está documentado	17	22%
Cuentan con un grupo multidisciplinario para la evaluación de los eventos adversos reportados.	**Cantidad**	**Porcentaje**
Documentado la conformación del comité y cuentan con actas de reunión.	60	79%
El comité no está conformado, pero tienen actas de reuniones.	9	12%
El comité no está conformado.	5	7%
Solo está documentado la conformación del comité.	6	8%
El encuestado conoce publicaciones para reporte, análisis de causalidad de eventos adversos, inscripción a la RNFV, entre otros temas.	**Cantidad**	**Porcentaje**
Si	61	76%
No	19	24%
Está documentada la periodicidad en la revisión de alertas y medidas sanitarias publicadas.	**Cantidad**	**Porcentaje**
Está documentada la revisión periódica de las alertas y esta se realiza.	63	79%
Está documentada la revisión periódica de las alertas, pero no se realiza	4	5%
Está documentada la periodicidad en la revisión de alertas y medidas sanitarias publicadas.	**Cantidad**	**Porcentaje**
No está documentada, pero se realiza la revisión periódica de las alertas	12	15%
No está documentada, ni se realiza la revisión periódica de las alertas	1	1%
Actividades que tienen documentadas y que se relacionan farmacovigilancia y con el uso seguro de medicamentos.	**Cantidad**	**Porcentaje**
Boletines, informes o folletos informativos.	22	33%
Guías de uso seguro de medicamentos.	24	36%
Identificación de medicamentos LASA y de alto riesgo, etc.	42	63%
Reuniones propias de Farmacovigilancia	37	55%
Fondos de pantalla en computadores de la institución con temas de interés.	1	1%
No cuenta con ninguna	9	13%

(*Continúa*)

Cuentan con programa de capacitación	Cantidad	Porcentaje
Cuentan con el programa de capacitación y se ha ejecutado	49	61%
No cuentan con el programa de capacitación y no se realiza	4	5%
No cuentan con el programa de capacitación, pero estas se han realizado.	14	18%
Cuentan con el programa de capacitación, pero no se ha ejecutado	13	16%
En relación al programa de capacitación:	**Cantidad**	**Porcentaje**
Tiene registros diligenciados de asistencia	51	64%
Tiene cronograma	44	55%
Tiene resultados de evaluación	31	39%
Está documentado el procedimiento	43	54%
No respondida	18	23%
La institución tiene certificación en algún sistema de gestión de la calidad.	**Cantidad**	**Porcentaje**
Si	35	44%
No	45	56%

El 81% de las instituciones fueron clasificadas como "en implementación", mientras que el 19% como "No implementado". En el análisis global, el aspecto con menor cumplimiento fue la presencia de programas y estrategias de farmacovigilancia (40%), mientras que la revisión de alertas y medidas sanitarias obtuvo el mayor cumplimiento (88%). Entre las instituciones clasificadas como "en implementación", los criterios con mayor cumplimiento fueron la periodicidad del reporte (0,92), la presencia de un grupo multidisciplinario (0,92) y la revisión de alertas y medidas sanitarias (0,92). En contraste, para aquellas catalogadas como "no implementado", el criterio con mayor cumplimiento fue la disponibilidad del formato de notificación (0,76) (Figura 1).

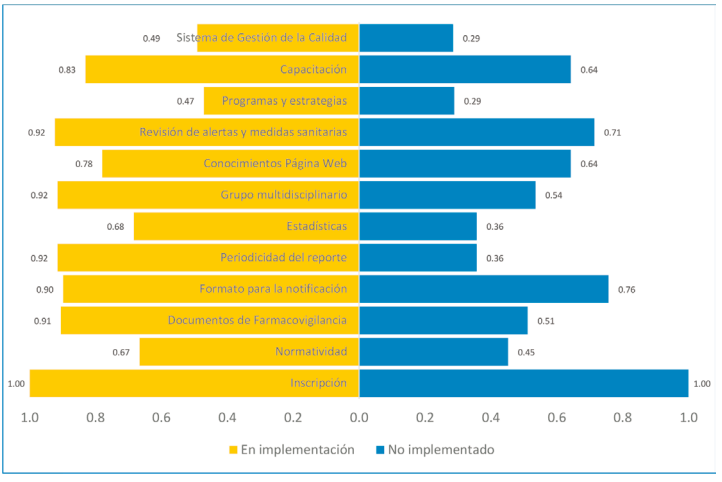

Figura 1. Cumplimiento global por criterios según el nivel de implementación

En la Tabla 3 se presentan los resultados de la asociación bivariada entre el programa "En implementación" con las demás variables.

Tabla 3. Análisis bivariado de los factores asociados a la implementación del programa de farmacovigilancia

Análisis Bivariado			
Variable	**OR**	**IC 95%**	**Valor de p**
Programa activo	4,14	0,84 a 18,57	0,0274
El encuestado es el referente	1,85	0,16 a 12,80	0,4858
Recibió capacitaciones	1,85	0,16 a 12,80	0,4858
El encuestado hizo el curso de vigiflow	0,61	0,06 a 3,31	0,551
Computador exclusivo	1,18	0,33 a 4,30	0,7745
Correo exclusivo	1,98	0,55 a 7,56	0,236
Teléfono exclusivo	0,83	0,20 a 4,08	0,7684
Oficina exclusiva	0,49	0,13 a 1,96	0,229
Desempeña otras funciones (Si)	1,45	0,02 a 19,61	0,753
Fuente bibliográfica-Base de datos	ND	ND	0,0038
Fuente bibliográfica-Libro	1,42	0,15 a 70,09	0,7514
Fuente bibliográfica-sitio web	0,95	0,19 a 3,77	0,9361
Fuente bibliográfica (si tiene)	2,59	0,48 a 11,78	0,1604
INVIMA envía informes	**0,11**	**0,00 a 0,86**	**0,0178***
INVIMA comparte resultados	0,55	0,14 a 2,10	0,3067
INVIMA realiza asistencias técnicas	1,31	0,36 a 4,71	0,6364
INVIMA da o recibe soporte	0,7	0,19 a 2,53	0,5416
INVIMA tiene iniciativas de vigilancia	1,13	0,27 a 4,20	0,8469
INVIMA desarrolla capacitaciones	2,81	0,76 a 11,59	0,0785
INVIMA fácil comunicación	0,36	0,09 a 1,31	0,0785
Contar con un farmacéutico	**8,83**	**2,19 a 38,13**	**0,0002***
Municipio grande	**8,25**	**2,03 a 34,21**	**0,0003***
Farmacovigilancia funcionando más de 1 año	**11**	**2,64 a 48,56**	**0**
Experiencia del encuestado en farmacovigilancia	3,81	4,48 a 25,31	0,0871
Importancia del personal asistencial	0,47	0,05 a 2,47	0,3456
Importancia del personal administrativo	0,43	0,07 a 1,86	0,2115
Reporta (si)	1	0,26 a 3,59	1
Reporta alto nivel (4o cuartil)	5,36	0,70 a 239,07	0,0846
Tiene servicio de vacunación	**0**	**0,00 a 0,29**	**0,006***
Tiene servicio farmacéutico	1,78	0,35 a 7,56	0,3835

*Estadísticamente significante

Discusión

Un porcentaje significativo de instituciones, de acuerdo a las respuestas dadas, calificó su programa de farmacovigilancia como "no implementado", lo que subraya la urgencia de abordar los criterios necesarios para mejorar su funcionamiento. En países como Colombia, es posible que estos programas no estén lo suficientemente desarrollados. Varios estudios han evaluado los programas de farmacovigilancia, convergiendo en resultados similares sobre la baja implementación de sus programas. Una revisión sistemática sobre el desempeño de los programas de farmacovigilancia de países en desarrollo, reveló un rendimiento deficiente en dichos sistemas [6]. Otro estudio realizado en Pakistán demostró que la mayoría de los hospitales no cumplían con los requisitos mínimos para farmacovigilancia [7]. El estudio llevado a cabo por Aagaard *et al.*, que analizó las reacciones adversas a medicamentos (ADRs) reportadas a la base de datos de la OMS, VigiBase, mostró que los países de ingresos bajos presentaban tasas más bajas de reporte [8]. El estudio de Vogler *et al.* investigó la implementación del sistema VigiFlow en Brasil en el que, si bien se observó un aumento en las tasas de informes de casos individuales de seguridad (ICSRs) después de la implementación de VigiFlow, los autores resaltaron los desafíos en la adaptación del sistema a las diferencias lingüísticas y estructurales de Brasil [9]. El trabajo de AlShamari *et al.* examinó los programas nacionales de farmacovigilancia en países árabes. A pesar de observar una mejora en estos programas en los últimos años, el estudio identificó diferencias significativas en la implementación y práctica entre los países, con factores como el apoyo gubernamental y la capacidad del personal influyendo en la madurez de los sistemas de farmacovigilancia [10]. En conjunto, estos estudios ofrecen una visión integral de los desafíos y las disparidades en la implementación de programas de farmacovigilancia a nivel mundial. Aunque cada estudio utilizó metodologías y enfoques diferentes, los resultados convergen en la necesidad de fortalecer los programas de farmacovigilancia, especialmente en países con recursos limitados, y fomentar la colaboración internacional para abordar estas brechas y garantizar la seguridad en el uso de medicamentos a nivel global.

Nuestros resultados revelan que el área en el que las instituciones presentan menor cumplimiento es en la implementación de programas y estrategias. Para abordar esta deficiencia, es crucial desarrollar actividades como campañas sobre uso seguro de medicamentos y la gestión de medicamentos de alto riesgo. Otra deficiencia común entre aquellas instituciones que no han implementado el programa es la falta de sistemas de gestión de calidad. Es sabido que estos sistemas son fundamentales para cumplir con estándares que abarcan aspectos tales como documentación, personal y equipos. La ausencia de estos sistemas de calidad puede indicar una falta de elementos necesarios para

el funcionamiento efectivo de la farmacovigilancia. Se observa una brecha importante entre el nivel de implementación y la falta de implementación en la documentación de la periodicidad de los reportes. Esta discrepancia puede atribuirse al desconocimiento de la norma, especialmente en lo referente a la notificación oportuna de eventos serios, donde el plazo máximo es de 72 horas. Es esencial que estas instituciones reciban información detallada al respecto para mejorar la oportunidad de los reportes.

Se identificó una asociación entre la implementación y el tiempo de funcionamiento del programa, lo que sugiere un mayor nivel de madurez en aquellos con programas establecidos durante más tiempo. Las instituciones que informaron que sus programas estaban inactivos, deben considerar la importancia de mantener una actividad constante para un funcionamiento efectivo. Además, se observó que las instituciones ubicadas en municipios pequeños presentaban menor implementación, posiblemente debido a su menor complejidad, menor personal a cargo, ubicación remota con acceso limitado a información de la capital y condiciones económicas menos favorables. Un estudio que comparó las tasas de notificación encontró que en países de bajos ingresos estas eran menores, lo que resalta la necesidad de investigar más a fondo el impacto de las estructuras organizativas y los recursos económicos en los centros de farmacovigilancia [8].

Menos de la mitad de los encuestados conoce la norma en torno al programa, lo que muestra la necesidad de capacitación en estos temas, sin embargo, más de la mitad manifiesta que cuentan con programa de capacitación. En este sentido, diversos estudios han señalado un bajo conocimiento y baja participación en actividades de farmacovigilancia entre los profesionales de la salud [11, 12]. Investigaciones han mostrado que el personal es consciente de su responsabilidad y de su trascendencia [13], mientras que otras han resaltado una actitud negativa frente a este [14]. Los resultados de este estudio indican que las instituciones con menor implementación, consideran que el programa es "muy importante", entonces es posible que tengan una actitud positiva hacia él, pese a ello puede que el personal no tenga suficiente tiempo para atender estas funciones. Los resultados indicaron que la mayoría de los encuestados no se dedican de forma exclusiva a actividades de farmacovigilancia, porque tienen que atender otras funciones, sin embargo esta es una responsabilidad de suma envergadura, que debe incorporarse en su rutina diaria [15], y entender que requieren dedicación de un tiempo laboral específico. Una investigación realizada en un hospital de referencia que analizó el tiempo para la gestión de EAM encontró que se requería una mediana de 69 minutos para llevar a cabo estas tareas [16].

En relación al referente del programa es fundamental que sea un profesional farmacéutico, bien sea Químico farmacéutico o Tecnólogo regente de Farmacia. A pesar que todos los profesionales de la salud pueden hacer parte de estos programas, algunos

pueden mostrar una actitud negativa [14]. Los resultados de este estudio señalan la relevancia del farmacéutico por ser el más comprometido, lo que puede deberse, por un lado, al soporte legal que lo faculta y por otro lado a su idoneidad. El soporte legal tiene que ver con que la norma colombiana que reglamenta el servicio farmacéutico, también reglamenta la farmacovigilancia y define al farmacéutico como el director técnico de este servicio, por ello su mejor competencia [4]. Con respecto a su idoneidad, algunos trabajos han señalado que entre los distintos profesionales, el farmacéutico es el más involucrado en este proceso [11, 12], mostrando una actitud positiva y reconociendo su responsabilidad [17]. A pesar de esto, en algunos casos, su conocimiento en estos temas puede ser deficiente [17, 18] y en ocasiones, incluso solo folletos pueden ser su única fuente de información para temas de medicamentos [17]. Por esta razón se reconoce la obligación de realizar capacitaciones [17], que han sido evaluadas, con resultados que muestran ser efectivas [12]. Los procesos de formación profesional también juegan un papel fundamental. Diversos autores han encontrado que los estudiantes de carreras de salud muestran un desconocimiento de la farmacovigilancia, que puede ser motivo de un desempeño deficiente más adelante cuando sean profesionales, ello hace indispensable su inclusión en los planes de estudio [17]. Las fuentes de información para la consulta también resultaron clave dado que la mayoría empleaba al menos una de ellas, que incluían bases de datos, sitios web y libros. Estudios han indicado la asociación entre el reporte y contar con referencias bibliográficas [19]. No obstante, las bases de datos deben emplearse de forma precavida porque no siempre constituyen la mejor fuente, debido a que la información puede ser insuficiente o sesgada, lo que implica escogerlas adecuadamente tal como lo indica Proy-Vega *et al.* [20]. Quienes tienen el programa implementado muestran una percepción negativa de que el INVIMA envíe reportes a los actores, esto presenta la exigencia que la entidad comunique mejor y de forma frecuente a los participantes de la red.

Una consecuencia de la baja implementación es el sub reporte, en este sentido los resultados mostraron que los de mayor implementación tenían un mayor reporte, aunque este no fue significativo. La baja notificación se puede deber a que no exista la cultura del reporte, no se ha empoderado ningún profesional para esta gestión, no se cuenta con los elementos las capacitaciones son insuficientes, la falta de cooperación, de comunicación, de tiempo, de conciencia, de personal, su alta rotación o que no sea calificado [21]. Si hay sub notificación, se estaría subestimando el impacto de los EAM, en este caso la población podría estar siendo afectada con consecuencias graves, sin que la institución o las autoridades sanitarias se enteren y tomen las medidas oportunas. Comprender la farmacovigilancia, resolver los problemas para la notificación, las intervenciones educativas, los programas centrados en el paciente, los esfuerzos para la detección de

los EAM y la implementación de equipos de cómputo y software, pueden proporcionar un sistema de farmacovigilancia exitoso [22]. En Colombia se notifica en el software VigiFlow, pero además algunas instituciones desarrollan plataformas digitales propias que pueden ser eficientes [23], sin embargo, algunos estudios han identificado barreras para el uso de este tipo de sistemas [24]. En caso de subreporte se pueden desarrollar estrategias que incrementen la cantidad de notificaciones, manteniendo los estándares de calidad, como lo desarrollado por Dittrich *et al.* [25] y las intervenciones educativas que han mostrado ser efectivas [26]. A futuro se podría llevar a cabo trabajos que identifiquen los motivos del bajo reporte, para diseñar estrategias que contribuyan a su incremento.

Este estudio tuvo como limitación la participación de un poco más de la mitad de las instituciones potenciales, no obstante, es de aclarar que en 5 ocasiones diferentes se contactó a todas, empleando para ello correo electrónico y llamadas telefónicas. Otra limitante es que los hallazgos de este estudio podrían estar sobre estimando la implementación, porque aquí se incluyeron solo instituciones inscritas a la red nacional, que es un ítem que suma a favor de la implementación.

Con estos resultados, después de identificar las instituciones de mayor implementación es posible concertar la conformación de un nodo regional de farmacovigilancia activa y centinela para hacer seguimiento a un determinado grupo de medicamentos [2, 27-29] o reacciones adversas [30], para que de manera conjunta se puedan reconocer señales [31], que contribuyan a divulgar alertas y gestionar medidas para sopesarlos, que sirva para recomendar cambios en el uso e incluso el retiro del mercado de ser necesario, como lo han mostrado algunos trabajos [27]. Por su parte en aquellas de menor implementación se recomienda que la Secretaría de salud departamental realice acompañamiento técnico, que incluyan por ejemplo capacitaciones, para el fortalecimiento de la notificación, análisis y toma de acciones para los eventos de mayor impacto. Este estudio permitió evaluar el nivel de implementación del programa de farmacovigilancia de instituciones de salud identificando cuales tenían un alto nivel de implementación y cuales un bajo nivel. También permitió identificar qué aspectos tales como no contar con un profesional farmacéutico, ubicarse en un municipio pequeño y tener poco tiempo de funcionamiento, podrían considerarse como factores de riesgo para una baja implementación. Por otro lado, se apreció que, si bien el INVIMA realiza una labor valiosa, es imprescindible que comparta los resultados de sus intervenciones con los actores de la red nacional para que haya retroalimentación permanente.

Agradecimientos

Se agradece muy especialmente a la Fundación Universitaria San Martín por haber financiado el desarrollo de este proyecto. Agradecimiento a la Secretaría de Salud Departamental del Valle del Cauca por la aprobación de este proyecto y suministrar información del reporte a través de la plataforma VigiFlow. Se agradece a cada uno de los referentes del programa de farmacovigilancia de cada una de las instituciones participantes, por el diligenciamiento adecuado del instrumento de este proyecto. También se agradece a la organización del X Encuentro Nacional de Farmacovigilancia, realizado en Bogotá D. C., el 11 y 12 de octubre de 2023, por aceptar la presentación parcial de este trabajo.

Conflicto de intereses

Los autores declaramos no tener conflicto de intereses en el desarrollo de este estudio.

Referencias

1. A.C. Brabete, L. Greaves, M. Maximos, E. Huber, A. Li, M.-L. Lê, A sex- and gender-based analysis of adverse drug reactions: A scoping review of pharmacovigilance databases, *Pharmaceuticals* (Basel), **15**(3), 298 (2022). Doi: https://doi.org/10.3390/ph15030298

2. Y.-J. Choi, S.-W. Yang, W.-G. Kwack, J.-K. Lee, T.-H. Lee, J.-Y. Jang, E.-K. Chung, Comparative safety profiles of sedatives commonly used in clinical practice: A 10-year nationwide pharmacovigilance study in Korea, *Pharmaceuticals* (Basel), **14**(8), 783 (2021). Doi: https://doi.org/10.3390/ph14080783

3. E. Montané, J. Santesmases, Reacciones adversas a medicamentos, *Medicina Clínica* (Barcelona), **154**(5), 178-184 (2020). Doi: https://doi.org/10.1016/j.medcli.2019.08.007

4. República de Colombia, Ministerio de la Protección Social, Resolución 1403 de 2007 "Por la cual se determina el Modelo de Gestión del Servicio Farmacéutico, se adopta el Manual de Condiciones Esenciales y Procedimientos y se dictan otras disposiciones", Bogotá D. C., 2007. URL: https://www.minsalud.gov.co/sites/rid/Lists/BibliotecaDigital/RIDE/DE/DIJ/Resoluci%C3%B3n_1403_de_2007.pdf

5. Instituto de Vigilancia de Medicamentos y Alimentos (INVIMA), *Guía de visitas de seguimiento a la implementación de los Programas de Farmacovigilancia en Instituciones Prestadoras de Servicios de Salud, Ministerio de la Protección Social*, República de Colombia, Bogotá D. C., URL: https://www.invima.gov.co/sites/default/files/medicamentos-productos-biologicos/Medicamentos%20de%20s%C3%ADntesis%20qu%C3%ADmica%20y%20biol%C3%B3gica/Vigilancia/Programa-Nacioal-de-Farmacovigilancia/Formatos-tramites-y-guias/2024/GU%C3%8DA%20DE%20VISITAS%20DE%20SEGUIMIENTO%20A%20LA%20IMPLEMENTACI%C3%93N%20DE%20LOS%20PROGRAMAS%20DE%20FARMACOVIGILANCIA%20EN%20IPS.pdf

6. H.Y. Garashi, D.T. Steinke, E.I. Schafheutle, A systematic review of pharmacovigilance systems in developing countries using the WHO pharmacovigilance indicators, *Therapeutic Innovation & Regulatory Science*, **56**(5), 717-743 (2022). Doi: https://doi.org/10.1007/s43441-022-00415-y

7. M.A.A. Khan, S. Hamid, T. Ur-Rehman, Z.-U.-D. Babar, Assessment of the current state of pharmacovigilance system in Pakistan using indicator-based assessment tool, *Frontiers in Pharmacology*, **12**, 789103 (2022). Doi: https://doi.org/10.3389/fphar.2021.789103

8. L. Aagaard, J. Strandell, L. Melskens, P.S.G. Petersen, E.H. Hansen, Global patterns of adverse drug reactions over a decade, *Drug Safety*, **35**(12), 1171-1182 (2012). Doi: https://doi.org/10.1007/BF03262002

9. M. Vogler, H.R. Conesa, K. de Araújo-Ferreira, F. Moreira-Cruz, F. Simioni-Gasparotto, K. Fleck, F.M. Rebelo, B. Kollross, Y. Silveira-Gonçalves, Electronic reporting systems in pharmacovigilance: The implementation of VigiFlow in Brazil, *Pharmaceutical Medicine*, **34**(5), 327-334 (2020). Doi. https://doi.org/10.1007/s40290-020-00349-6

10. T.M. Alshammari, K.A. Alenzi, S.I. Ata, National pharmacovigilance programs in Arab countries: A quantitative assessment study, *Pharmacoepidemiology & Drug Safety*, **29**(9), 1001-1010 (2020). Doi. https://doi.org/10.1002/pds.4991

11. T.M. AlShammari, M.J. Almoslem, Knowledge attitudes & practices of healthcare professionals in hospitals towards the reporting of adverse drug reactions in Saudi Arabia: A multi-centre cross sectional study, *Saudi Pharmaceutical Journal*, **26**(7), 925-931 (2018). Doi: https://doi.org/10.1016/j.jsps.2018.04.012

12. D.M. Ibrahim, M.A. Shawki, M.H. Solayman, N.A. Sabri, Pharmacovigilance education to healthcare professionals: Will it affect their performance in reporting adverse drug reactions? *The International Journal of Clinical Practice*, **75**(11), e14731 (2021). Doi: https://doi.org/10.1111/ijcp.14731

13. R. Shakya-Gurung, D. Shrestha, R. Thapa, Assessment on knowledge, attitude and practice of pharmacovigilance among the professionals in a tertiary hospital of Kathmandu, *Nepal Medical College Journal*, **21**(1), 53-59 (2019). Doi: https://doi.org/10.3126/nmcj.v21i1.24854

14. Z. Abdulrasool, The development of a pharmacovigilance system in Bahrain, *Saudi Pharmaceutical Journal*, **30**(6), 825-841 (2022). Doi: https://doi.org/10.1016/j.jsps.2022.03.009

15. A. Pérez-Ricart, E. Gea-Rodríguez, A. Roca-Montañana, E. Gil-Máñez, A. Pérez-Feliu, Integrating pharmacovigilance into the routine of pharmacy department: experience of nine years, *Farmacia Hospitalaria*, **43**(4), 128-133 (2019). Doi: https://doi.org/10.7399/fh.11169

16. G.B. McLachlan, C. Keith, C. Wood, The cost of pharmacovigilance: a time and motion study of an adverse drug reaction program, *The International Journal of Pharmacy Practice*, **29**(5), 521-523 (2021). Doi: https://doi.org/10.1093/ijpp/riab037

17. A. Atia, A. Botto, S. Alarbi, Knowledge attitudes and practices of pharmacists about pharmacovigilance, Libya, *East Mediterranean Health Journal*, **27**(7), 693-697 (2021). URL: https://applications.emro.who.int/EMHJ/V27/07/1020-3397-2021-2707-693-697-eng.pdf

18. T. Kobayashi, A. Noda, T. Obara, M. Tsuchiya, K. Akasaka, M. Yoshida, M. Matsuura, M. Sato, Y. Murai, H. Yamaguchi, F. Tsuchiya, K. Kihira, N. Mano, Knowledge, attitudes, and practice of hospital pharmacists regarding pharmacovigilance and adverse drug reaction reporting in Japan, *Hospital Pharmacy*, **56**(1), 7-16 (2021). Doi: https://doi.org/10.1177/0018578719851455

19. J. Castro-Espinosa, A.M. Jiménez-Urrego, A. Botero-Carvajal, Factors related to technical management and adverse drug event reporting in independent retail pharmacies in Cali, Colombia, *Heliyon*, **8**(3), e09016 (2022). Doi: https://doi.org/10.1016/j.heliyon.2022.e09016

20. B. Proy-Vega, N. Cano-Cuenca, J. Solis-García Del Pozo, J. Jordan, ¿Son las bases de datos bibliográficas una buena fuente de la evidencia científica en la retirada de fármacos del mercado? [Are scientific literature databases a good source of scientific evidence for discontinuing a drug from the market?], *Farmacia Hospitalaria*, **38**(4), 381-382 (2014). URL: http://www.grupoaulamedica.com/fh/pdf/7295.pdf

21. R. Kiguba, S. Olsson, C. Waitt, Pharmacovigilance in low- and middle-income countries: A review with particular focus on Africa, *British Journal of Clinical Pharmacology*, **89**(2), 491-509 (2023). Doi: https://doi.org/10.1111/bcp.15193

22. P. Abideen, Practical implications of spontaneous adverse drug reaction reporting system in hospitals - An overview, *Asian Journal of Pharmaceutical and Clinical Research*, **6**(4), 10-15 (2013). URL: https://journals.innovareacademics.in/index.php/ajpcr/article/view/463/311

23. J.S. Almenoff, G. Powell, R. Schaaf, D. Fram, J.M. Fitzpatrick, A. Pendleton, N. Payvandi, N. Yuen, Online signal management: A systems-based approach that delivers new analytical capabilities and operational efficiency to the practice of pharmacovigilance, *Drug Information Journal*, **41**(6), 779-789 (2007). Doi: https://doi.org/10.1177/009286150704100610

24. O.O. Agoro, S.W. Kibira, J.V. Freeman, H.S.F. Fraser, Barriers to the success of an electronic pharmacovigilance reporting system in Kenya: an evaluation three years post implementation, *Journal of the American Medical Informatics Association*, **25**(6), 627-634 (2018). Doi: https://doi.org/10.1093/jamia/ocx102

25. A.T.M. Dittrich, N.J.L. Smeets, E.F.M. de Jong, J.L. Kämink, Y. Kroeze, J.M.T. Draaisma, E.P. van Puijenbroek, D.M.W.M.T. Loo, Quality of active versus spontaneous reporting of adverse drug reactions in pediatric patients: Relevance for pharmacovigilance and knowledge in pediatric medical care, *Pharmaceuticals* (Basel), **15**(9), 1148 (2022). Doi: https://doi.org/10.3390/ph15091148

26. C. Pagotto, F. Varallo, P. Mastroianni, Impact of educational interventions on adverse drug events reporting, *International Journal of Technology Assessment in Health Care*, **29**(4), 410-417 (2013). Doi: https://doi.org/10.1017/S0266462313000457

27. S. Chiappini, R. Vickers-Smith, A. Guirguis, J.M. Corkery, G. Martinotti, D.R. Harris, F. Schifano, Pharmacovigilance signals of the opioid epidemic over 10 Years: Data mining methods in the analysis of pharmacovigilance datasets collecting adverse drug reactions (ADRs) reported to EudraVigilance (EV) and the FDA Adverse Event Reporting System (FAERS), *Pharmaceuticals* (Basel), **15**(6), 675 (2022). Doi: https://doi.org/10.3390/ph15060675

28. G. Pop, A. Farcaș, A. Butucă, C. Morgovan, A.M. Arseniu, M. Pumnea, M. Teodoru, F.G. Gligor, Post-marketing surveillance of statins—A descriptive analysis of psychiatric adverse reactions in EudraVigilance, *Pharmaceuticals* (Basel), **15**(12), 1536 (2022). Doi: https://doi.org/10.3390/ph15121536

29. M. Li, Q.-S. Zhang, X.-L. Liu, H.-L. Wang, W. Liu, Adverse events associated with nirmatrelvir/ritonavir: A pharmacovigilance analysis based on FAERS, *Pharmaceuticals* (Basel), **15**(12), 1455 (2022). Doi: https://doi.org/10.3390/ph15121455

30. G. di Mauro, A. Mascolo, M. Gaio, C. Rafaniello, A. De Angelis, L. Berrino, G. Paolisso, F. Rossi, A. Capuano, The reporting frequency of ketoacidosis events with dapagliflozin from the European Spontaneous Reporting System: The DAPA-KETO study, *Pharmaceuticals* (Basel), **15**(3), 286 (2022). Doi: https://doi.org/10.3390/ph15030286

31. J.-Y. Choi, J.-H. Choi, M.-G. Kim, S.-J. Rhie, Signal detection of adverse drug reactions of cephalosporins using data from a national pharmacovigilance database, *Pharmaceuticals* (Basel), **14**(5), 425 (2021). Doi: https://doi.org/10.3390/ph14050425

Como citar este artículo

J. Castro-Espinosa, H. Estupiñan-Cabrera, M.A. Gil-Pineda, L.V. Moreno-Posso, M.C. Donoso-Huertas, D. Pino-Quinto, Nivel de implementación del programa de farmacovigilancia y sus factores asociados en instituciones de salud en el Valle del Cauca, *Rev. Colomb. Cienc. Quim. Farm.*, **53**(2), 488-512 (2024). https://doi.org/10.15446/rcciquifa.v53n2.114453

Scientific research article / https://doi.org/10.15446/rcciquifa.v53n2.114454

An *in vivo* and *in silico* predictive study on the toxicological and modulatory effects of abused substances on sperm quality and testicular function in Wistar rats

Charles Obiora Nwonuma[1], Adeola Oluwaseun Adedoyin[1], Melody Onyemaka[1], Emenike Irokanulo[2], Omokolade Oluwaseyi Alejolowo[1], Inemesit Asukwo Udofia[3], Oluwafemi Adeleke Ojo[4], Deborah A. Adah[5], Funmilayo Abimbola Okeniyi[6], Omorefosa O. Osemwegie[2]

[1] Department of Biochemistry, College of Pure and Applied Sciences, Landmark University P.M.B. 1001, Omu Aran, Kwara State, Nigeria.

[2] Department of Food Science and Microbiology, College of Pure and Applied Sciences, Landmark University P.M.B. 1001, Omu Aran, Kwara State, Nigeria.

[3] Department of Chemistry, University of Lagos, Lagos State, Nigeria.

[4] Phytomedicine, Molecular Toxicology, and Computational Biochemistry Research Laboratory (PMTCB-RL), Department of Biochemistry, Bowen University, Iwo, Nigeria.

[5] Department of Veterinary Physiology and Biochemistry, University of Ilorin, Ilorin, Nigeria.

[6] Department of Animal Science, Landmark University, Omu-Aran, Nigeria.

*Corresponding author e-mail: Nwonuma.charles@lmu.edu.ng

Received: October 27, 2023

Corrected: March 23, 2024

Accepted: March 27, 2024

Summary

Introduction: Some compounds like Opioids that are commonly used may affect the biological system in addition to having a high potential for addiction. **Objective**: This study assessed the effects of commonly misused substances on sperm quality and testicular function in Wistar rats. **Material and Methods**: Twenty-five Wistar rats weighing an average of 120 ± 0.1 g were randomly assigned to five treatment groups and were orally administered with water for the control, carbonated sugar drink, 150, 300, and 300 mg/kg body weight doses of menthol, monosodium glutamate, and tramadol respectively. The rats were euthanized 24 hours after the last day of the thirty-day treatment. Biochemical assays were on carried out the plasma

and testicular homogenate. **Results**: There was a significant increase ($p<0.05$) in testosterone, FSH, LH, HDL, TG, phospholipids, glycogen, reduced glutathione concentration, sperm total count; %testicular weight change, and; there was also a significant decrease in the %tail defect, and %non-motile sperm across the treatment groups compared to the control. Contrary, there was a significant increase ($p<0.05$) in the testicular ACP and Na-K ATPases activities but MDA levels decreased significantly across treatment groups. The ouabain-α-ATPase complex's binding energy is comparable to that of the α-ATPase complexes with tramadol, glucose, menthol, and MSG, respectively. **Conclusion**: The improved sperm quality and testicular function show that these compounds were not harmful to the reproductive functions of Wistar rats. The docking analysis corroborated the effects of ATPase activity modulation on sperm motility.

Keywords: Wistar rats, Sperm Motility, Sodium Glutamate, Tramadol, Menthol, Follicle Stimulating Hormone.

Resumen

Un estudio predictivo *in vivo* e *in silico* sobre los efectos toxicológicos y moduladores de las sustancias de abuso sobre la calidad del esperma y la función testicular en ratas Wistar

Introducción: Algunos compuestos como los opioides, que se usan comúnmente, pueden afectar el sistema biológico, además de tener un alto potencial de adicción. **Objetivo:** Este estudio evaluó los efectos de sustancias comúnmente utilizadas indebidamente sobre la calidad del esperma y la función testicular en ratas Wistar. **Material y métodos:** Veinticinco ratas Wistar con un peso promedio de 120 ± 0,1 g fueron asignadas aleatoriamente a cinco grupos de tratamiento y se les administró por vía oral, agua para el control, bebida azucarada carbonatada, dosis de 150, 300 y 300 mg/kg de peso corporal de mentol, glutamato monosódico y tramadol, respectivamente. Las ratas fueron sacrificadas 24 horas después del último día del tratamiento de treinta días. Se realizaron ensayos bioquímicos sobre el plasma y el homogeneizado testicular. **Resultados:** Hubo aumento significativo ($p<0,05$) en testosterona, FSH, LH, HDL, TG, fosfolípidos, glucógeno, reducción de la concentración de glutatión, recuento total de espermatozoides, % de cambio de peso testicular, y también hubo una disminución significativa en el porcentaje de defectos en la cola y en el porcentaje de espermatozoides no móviles en los grupos de tratamiento en comparación con el control. Por el contrario, hubo un aumento significativo ($p<0,05$) en las actividades

testiculares de ACP y Na-K ATPasas, pero los niveles de MDA disminuyeron significativamente en todos los grupos de tratamiento. La energía de unión del complejo ouabaína-α-ATPasa es comparable a la de los complejos α-ATPasa con tramadol, glucosa, mentol y glutamato monosódico, respectivamente. **Conclusión:** La mejora de la calidad del esperma y la función testicular muestran que estos compuestos no fueron perjudiciales para las funciones reproductivas de las ratas Wistar. El análisis de acoplamiento corroboró los efectos de la modulación de la actividad de la ATPasa sobre la motilidad de los espermatozoides.

Palabras clave: ratas Wistar, motilidad de los espermatozoides, glutamato de sodio, tramadol, mentol, hormona folículo estimulante.

Resumo

Um estudo preditivo *in vivo* e *in silico* sobre os efeitos toxicológicos e moduladores de substâncias de abuso na qualidade do esperma e na função testicular em ratos Wistar

Introdução: Alguns compostos como os opioides, comumente utilizados, podem afetar o sistema biológico, além de apresentarem alto potencial de dependência. Objetivo: Este estudo avaliou os efeitos de substâncias comumente mal utilizadas na qualidade do esperma e na função testicular em ratos Wistar. **Material e métodos:** Vinte e cinco ratos Wistar com peso médio de 120 ± 0,1 g foram distribuídos aleatoriamente em cinco grupos de tratamento e receberam por via oral água para controle, bebida gaseificada açucarada, doses de 150, 300 e 300 mg/kg de peso corporal de mentol, glutamato monossódico e tramadol, respectivamente. Os ratos foram sacrificados 24 horas após o último dia do tratamento de trinta dias. Ensaios bioquímicos foram realizados em plasma e homogeneizado testicular. **Resultados:** Houve aumento significativo ($p<0,05$) de testosterona, FSH, LH, HDL, TG, fosfolipídios, glicogênio, redução na concentração de glutationa, contagem total de espermatozoides, % de alteração no peso testicular, e também houve diminuição significativa de a porcentagem de defeitos na cauda e a porcentagem de espermatozoides imóveis nos grupos de tratamento em comparação com o controle. Em contraste, houve um aumento significativo ($p<0,05$) nas atividades testiculares de ACP e Na-K ATPase, mas os níveis de MDA diminuíram significativamente em todos os grupos de tratamento. A energia de ligação do complexo ouabaína-α-ATPase é comparável à dos complexos α-ATPase com tramadol, glicose, mentol e glutamato monossódico, respectivamente. **Conclusão:** A melhoria da qualidade espermática e da função testi-

cular mostram que estes compostos não foram prejudiciais às funções reprodutivas de ratos Wistar. A análise de docking corroborou os efeitos da modulação da atividade da ATPase na motilidade espermática.

Palavras-chave: Ratos Wistar, motilidade espermática, glutamato de sódio, tramadol, mentol, hormônio folículo-estimulante.

Introduction

One of the prevailing public health concerns, prevalent in both affluent and impoverished nations, revolves around substance abuse [1]. Certain substances classified as "new emergent drugs of abuse" are increasingly being misused as alternatives to conventional drugs, sought for their psychoactive properties to induce feelings of boldness and pleasure. Conversely, research suggests that substance abuse can also impact male reproductive health. Men may experience infertility due to the presence of endocrine-disrupting chemicals (EDCs), which mimic natural hormones upon binding to common receptors, thus exerting a biological influence [2]. Conversely, they can directly impact sperm cells, as demonstrated by the effects of 1,3-dinitrobenzene (mDNB) on sperm motility [3]. Consequently, impaired sperm motility can hinder its ability to fertilize an egg [4, 5]. According to computer-assisted sperm analysis (CASA), the lateral head displacement is associated with the efficiency of cervical mucus penetration. At the same time, fertilization rates correlate with both the curvilinear velocity (VCL) and straight-line velocity (VSL) of sperm motility in the distal corpus epididymides and distal cauda epididymides [6]. This underscores a connection between fertility and the reduction in sperm motility induced by toxicants [7].

Research indicates that males grappling with opiate addiction tend to exhibit diminished sperm quality. Specifically, alterations in the morphology and motility of sperm are observed, accompanied by a correlation with hypogonadism [8]. Likewise, opioids can impact the functioning of the male reproductive system by decreasing the secretion of gonadotropin-releasing hormone (GnRH) within the hypothalamus of the brain [9]. Moreover, human spermatozoa membranes contain three opioid receptors [10], and endogenous opioid peptides are present in various male reproductive tracts, suggesting a potential role in reproductive processes [11]. Furthermore, sustained opiate administration in male rats has been demonstrated to adversely impact fertility [12]. Opioids can also modify male reproductive function by activating signal transduction through the opioid receptor on the plasma membrane of testicular cells [11]. In addition, studies have indicated that opioids impact male reproduction by decreasing

testosterone levels and increasing concentrations of sex hormone-binding globulin, thereby rendering the hormone inactive [9]. Recently, the emergence of new abused substances has raised significant global concerns due to their potential impact on users, particularly on their reproductive function.

Tramadol, categorized as an opioid drug, is primarily prescribed for the management of acute or chronic severe pain. Its notable feature lies in its heightened affinity for the μ-opioid receptor compared to other opioids [13-16]. Tramadol undergoes conversion by the liver enzyme CYP2D6 into its active metabolite, O-desmethyl tramadol (desmetramadol), responsible for its pharmacological effects. However, in cases where the enzyme is deficient, there might be insufficient production of the active metabolite (desmetramadol) to adequately manage pain [17]. Regulatory bodies like The Joint Committee of World Health Organization (WHO) experts and FAO consider MSG, also known as glutamic acid or its salt, to be safe but addictive. However, despite this, there is a widespread belief among the public that consuming MSG contributes to "Chinese restaurant syndrome," characterized by symptoms such as dizziness, headaches, weakness, numbness, tremors, palpitations, and nausea [18, 19]. Glutamate, a significant aminoacidergic transmitter, serves as an endogenous neurotransmitter involved in various physiological functions. These include trophic roles linked to central nervous system (CNS) ontogenesis, memory and learning processes, and stimulation of dopamine release in the striatum, a critical aspect in addiction [20, 21]. Menthol, a monoterpenoid-class organic compound, can be synthesized artificially or extracted naturally from mints such as corn mint, peppermint, or other mint varieties. The analgesic effects of menthol are attributed to its selective activation of Transient Receptor Potential (TRP) channels [22], Consequently, menthol reduces neural activity that could otherwise stimulate muscles by blocking calcium channels and voltage-sensitive sodium channels [23]. Given the limited literature regarding the impacts of these substances at elevated doses, this study was devised to assess the toxicological and modulatory effects of commonly misused substances on sperm quality and testicular function in Wistar rats. This evaluation was conducted through a combination of experimental and in-silico approaches.

Materials and methods

Procurement of the substances

Menthol, Tramadol, and monosodium glutamate were obtained from Sigma-Aldrich Company Limited, UK

Animal model

The experimental procedures on laboratory animals were done in adherence to the Guideline to the Care and Use of Experimental Animals from the National Institutes of Health (NIH). Institutional approval for the use of the animals was by the Department of Biochemistry Landmark University Animal Care and Use Committee with an Approval number LUAC/BCH/2022. Thirty Wistar rats with an average weight of 120 ± 0.1 g were procured from Animal Holdings Landmark University and were allowed to acclimatize for two weeks before the commencement of the experiment. The animals were kept in wooden cages kept in a well-ventilated animal house and were allowed access to food and water *ad libitium*.

Preparation of the chemical

The drug substances were combined in the following format: menthol with a carbonated sugar drink mixture, monosodium glutamate with a water mixture, and tramadol with a water mixture [24]. Menthol was dissolved in a sugar-carbonated drink, while tramadol and monosodium glutamate were dissolved in water.

Animal grouping, experimental design, and animal sacrifice

The Wistar rats were randomly allocated into five groups (A-E), with five rats assigned to each group:

Group A- Rats are administered 2 ml of water (negative control).

Group B- Rats are administered 2 ml of a carbonated sugar drink (positive control).

Group C- Rats are treated with 150 mg/kg body weight of menthol in 2 ml of carbonated sugar drink (psychoactive mixture) [24].

Group D- Rats are treated with 300 mg/kg body weight of monosodium glutamate in 2 ml of distilled water.

Group E- Rats are treated with 300 mg/kg body weight of 2-[(dimethylamino) methyl]-1-(3-methoxyphenyl) cyclohexanol (tramadol) in 2 ml of distilled water.

Each group received oral administration of the treatment substance daily for a period of 30 days. After a 24-hour interval following the last treatment, the rats were anesthetized using 0.5% halothane and euthanized by severing their aorta with a surgical knife. Blood samples were collected in sample bottles, and the scrotal sac was incised to extract the testes. Serum was separated from clotted blood, and homogenate was obtained from homogenized testicular tissue. Both serum and homogenate samples were then frozen and utilized in biochemical assays.

Methods for the sperm analysis

As soon as the rat was euthanized, the scrotal sac was cut open, and the epididymis was instantly removed, the surrounding fat was removed, and it was then weighed. The sperm per gram caudal epididymis was calculated using the weight of the caudal epididymis. The 2010 WHO standard served as the foundation for the reference utilized for the manual sperm examination [25]. Sperm concentration was measured using the Neubauer hemocytometer and the Epididymal Sperm Concentration was counted following the modified method described by Yokoi and Mayi [26]. Similarly, the Sperm Progressive Motility was evaluated by an earlier method by Sonmez *et al.* [27]. An Olympus light microscope equipped with a Makler counting chamber (Sefi-Medical Instruments, Haifa, Israel) was adjusted to ×100 magnification to evaluate sperm count and straight-line sperm motility. Similarly, the morphological abnormality was also estimated with an Olympus light microscope, two hundred sperm cells were examined at ×400 magnifications per animal.

Hormonal assay

LH, FSH, and testosterone levels were evaluated using the principle of solid-phase enzyme-linked immunosorbent assay (ELISA) [28].

Biochemical assays

For measuring or estimating the activity of certain biochemical parameters in both serum and testicular samples, a digital UV/VIS spectrometer (Jenway, England) was utilized. Total protein concentration was determined using the method outlined by Gornall *et al.* [29]. The activities of ACP and ALP were assessed following the procedure described by Wright *et al.* [30]. Superoxide dismutase (SOD) activity was estimated by the method detailed by Misra and Fridovich [31], while the reduced glutathione level was determined using the method described by Jollow *et al.* [32]. Measurement of MDA level (a product of lipid peroxidation) was conducted by quantifying thiobarbituric acid reactive substances (TBARS) according to the methods outlined by Satoh [33]. Acetylcholine esterase activity was evaluated by the method described by Ellman *et al.* [34]. The procedure outlined by Ronner *et al.* [35], with modifications as described by Bewaji *et al.* [36] was employed for estimating Na^+/K^+-ATPase activity. Total phospholipids were determined using the method described by Stewart [37]. Glycogen concentrations were assessed following the procedure detailed by Kemp and Van Heijningen [38], while the determination of nitric acid concentrations was conducted according to the method described by Ilavarasan *et al.* [39]. The method described by Gidez *et al.* [40] was adopted for the extraction of HDL from the tissue while the method described by Folch *et al.* [41] was adopted for the extraction of

lipids from the tissue (testes). The evaluation of the HMG-CoA/mevalonate ratio was conducted using the method described by Ramakrishnan and Rao [42].

Molecular docking simulation

The protein structure (ATPase) used in the docking simulation was obtained from the protein data bank (pdb), with the pdb code; 3A3Y (Resolution: 2.80 Å). Water molecules and the bound ligands were deleted from the X-ray crystallographic structure. Molecular docking was performed using AutoDock vina [43] with the help of PyRx [44], a graphical user interface program. The following ligand structures: Ouabain, tramadol, menthol, glucose, and sodium monoglutamate were optimized at the B3LYP/6-31Gd) level of theory before use for docking simulations. The control for the docking experiment was Ouabain (Figure 1), where energies of binding and interactions of other ligands used in the present study were compared. Since 3A3Y.pdb contains various chains with their respective binding sites, we kept the protein structure fixed while sampling the entire protein space with the ligands. The grid dimension used are as follows: center x = -34.6247; y = -55.0409 and z = 61.1613 Å while the size was: size x = 122.871241837; y = 134.560933971 and z = 189.749764137 Å. The exhaustiveness of eight was used throughout the docking experiment. Various interactions were observed for the molecular docking of the studied ligands with 3a3y.pdb file. Figure 1 shows the Ouabain ligand docked into the active site of 3a3y.pdb crystal structure.

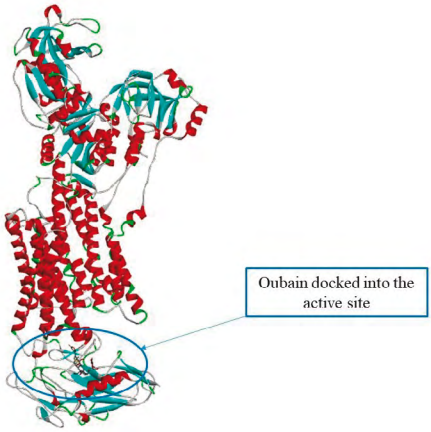

Figure 1. Ouabain ligand in the blue circle, docked in the active site of 3a3y.pdb structure between two chains, as also reported in the original manuscript of the crystal structure.

Histopathology

The standard method for tissue fixation for histological assessment was carried out using the method described by Hewitson and Darby [45]. The testes removed from the euthanized rats were instantly fixed by dropping the tissue in 10 % buffered formalin (pH 7.4) for about 12 h and later embedded in paraffin. The tissue from paraffin was subsequently sectioned (5 mm) with a microtome. Hematoxylin and eosin were used to stain the tissue, which was subsequently mounted in Canada balsam and sectioned. The stained sections were viewed under the light microscope and their histological features were captured using Sony DSC-W35. The examination checked for cell necrosis, degraded cells, cell detachment, and lymphocyte infiltration in the damaged tissues [46].

Data analysis

The results were presented as mean ± SEM. Mean comparison was performed with One Way Analysis of Variance (ANOVA) with Tukey post hoc to assess the significant difference at $p<0.05$. SPSS Statistics 22 (Statistical Package for Social Science) (SPSS Inc., Chicago, IL, USA) was used in all the statistical analyses.

Results

There was a significant increase ($p<0.05$) in testosterone levels across treatment groups compared to the control (Figure 2A). There was a significant increase ($p<0.05$) in the FSH level across the treatment groups compared to the control (Figure 2B). There was a significant decrease ($p<0.05$) in LH level in animals administered carbonated sugar drinks and carbonated sugar drinks & menthol compared to animals in the control group. Contrary, LH levels significantly increased ($p<0.05$) in animals administered MSG and tramadol (Figure 2C).

There was no significant change ($p>0.05$) in sperm volume/weight in the treatment groups compared to the control (Figure 3A). There was no significant change ($p>0.05$) in the sperm concentration count in the treatment groups except in the group administered tramadol which showed a significant increase ($p<0.05$) compared to the control (Figure 3B). Similarly, there was no significant change ($p>0.05$) in the sperm total count in the treatment groups except for the group-administered carbonated sugar drink only which showed a significant decrease ($p<0.05$) compared to the control (Figure 3B). In the % sperm morphology, there was no significant change ($p>0.05$) in the % of the normal sperm cells, % of sperm with head defects, and % of sperm with neck defects in the treatment groups compared to the control (Figure 4A). There was a significant increase ($p<0.05$) in the tail defects in the sperm cells of the animal

groups administered menthol with carbonated sugar drink and MSG while the groups administered tramadol showed a significant decrease ($p<0.05$) in tail defects compared to the control (Figure 4A). Similarly, the sperm %progressive assessment showed no significant change ($p>0.05$) in the %fast and slow-moving sperm cells across treatment groups compared to the control (Figure 4B). Meanwhile, there was a significant increase ($p<0.05$) in the %non-motile sperm cells in the treatment groups except in the group administered tramadol which showed no significant change ($p>0.05$) compared to the control (Figure 4B).

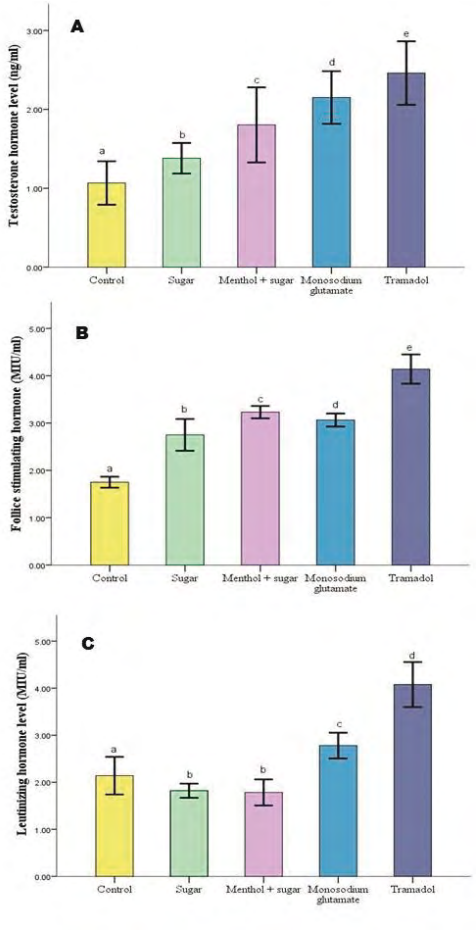

Figure 2. Effects of carbonated sugar drink, menthol and carbonated sugar drink, monosodium glutamate, and tramadol on testosterone level (A), follicle-stimulating hormone level (B), and luteinizing hormone levels (C), on male Wister rats. Data are presented as mean ± SEM; bars with a different superscript are significantly different at a confidence interval of $p<0.05$.

a

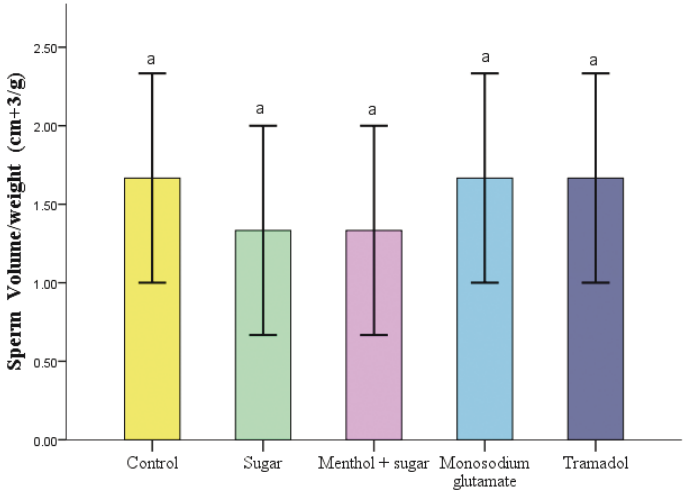

b

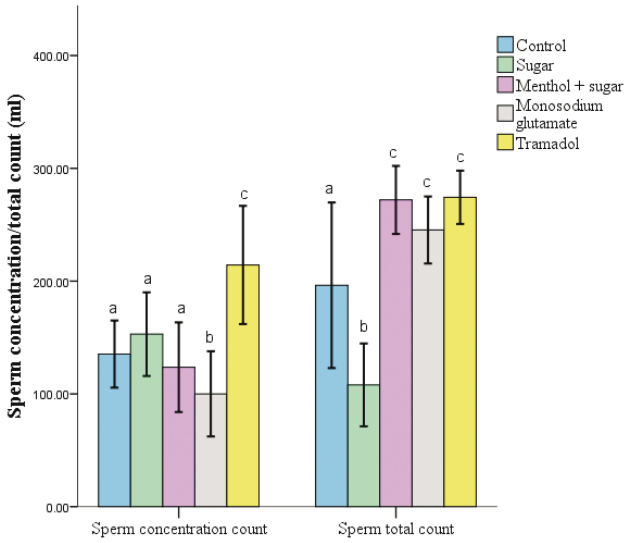

Figure 3. Effects of carbonated sugar drink, menthol+ carbonated sugar drink, monosodium glutamate, and tramadol on sperm volume/weight (A) and sperm concentration/total count (B), on Wister rats. Data are presented as mean ± SEM; bars with a different superscript are significantly different at a confidence interval of $p<0.05$.

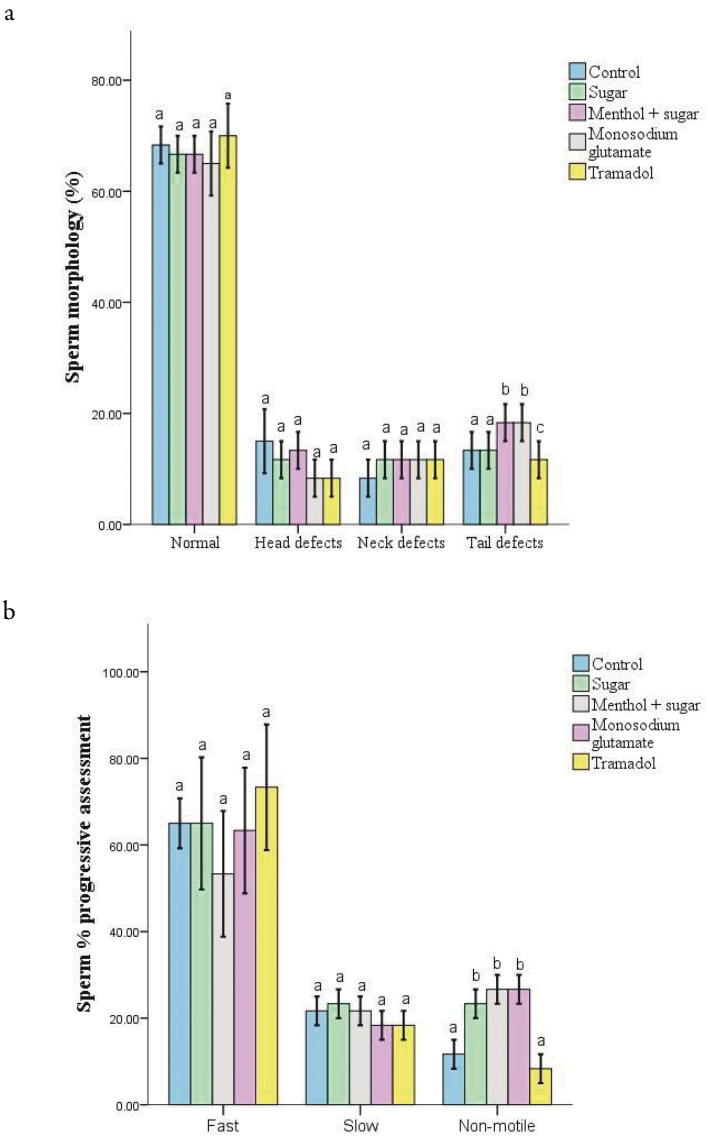

Figure 4. Effects of carbonated sugar drink, menthol+ carbonated sugar drink, monosodium glutamate, and tramadol on the total count concentration sperm morphology (A) and sperm % progressive assessment (B), in male Wister rats. Data are presented as mean ± SEM; bars with a different superscript are significantly different at a confidence interval of $p<0.05$.

There was a significant increase ($p<0.05$) in the total cholesterol concentration in the testis of rats administered carbonated sugar drink and menthol with carbonated sugar drink but there was a significant decrease ($p<0.05$) in the testis of the group administered MSG compared to the control (Figure 5A). Contrary, there was no significant change ($p>0.05$) in the cholesterol concentration in the testis of the rat treated with tramadol compared to the control (Figure 5A). Furthermore, the plasma HDL concentration increased significantly ($p<0.05$) across the treatment groups compared to the control (Figure 5B). Similarly, the treatment groups showed a significant increase ($p<0.05$) in the testicular triglyceride concentration compared to the control (Figure 5C). There was a significant increase ($p<0.05$) in phospholipid concentration in all the treatment groups except in the group administered carbonated sugar drink only which decreased significantly ($p<0.05$) when compared to the control (Figure 5D).

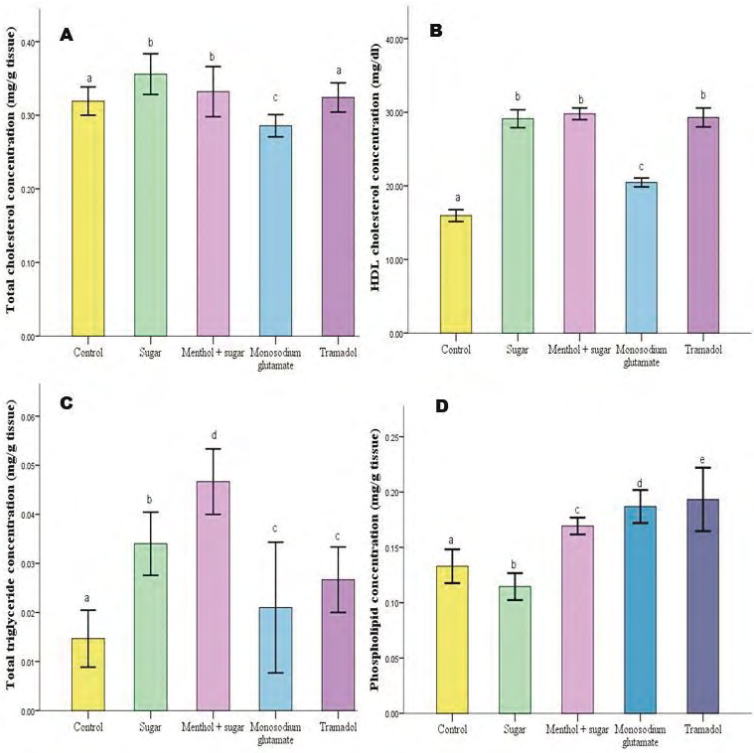

Figure 5. Effects of carbonated sugar drink, menthol+ carbonated sugar drink, monosodium glutamate, and tramadol on the total cholesterol concentration (A), plasma HDL cholesterol concentration (B), total triglyceride concentration (C), and phospholipid concentration (D), in the testis of rats. Data are presented as mean ± SEM; bars with a different superscript are significantly different at a confidence interval of $p<0.05$.

There was a significant decrease ($p<0.05$) in the catalase activity in the testis of the rats across the treatment groups compared to the control (Figure 6A). Similarly, there was a significant increase ($p<0.05$) in SOD activity in the treatment groups except for the group treated with MSG which showed a significant decrease ($p<0.05$) in the activity of SOD compared to the control (Figure 6B). There was a significant increase ($p<0.05$) in MDA concentration in the group administered menthol with carbonated sugar drink while there was a significant decrease ($p<0.05$) in MDA in the group treated with MSG compared to the control (Figure 6C). There was no significant change ($p>0.05$) in the MDA level in the testis of the rat administered carbonated sugar drink only and tramadol compared to the control (Figure 5C). Reduced glutathione levels in the testis of the treated rats increased significantly ($p<0.05$) in all the groups except in the group administered MSG which showed a significant decrease ($p<0.05$) compared to the control (Figure 6D).

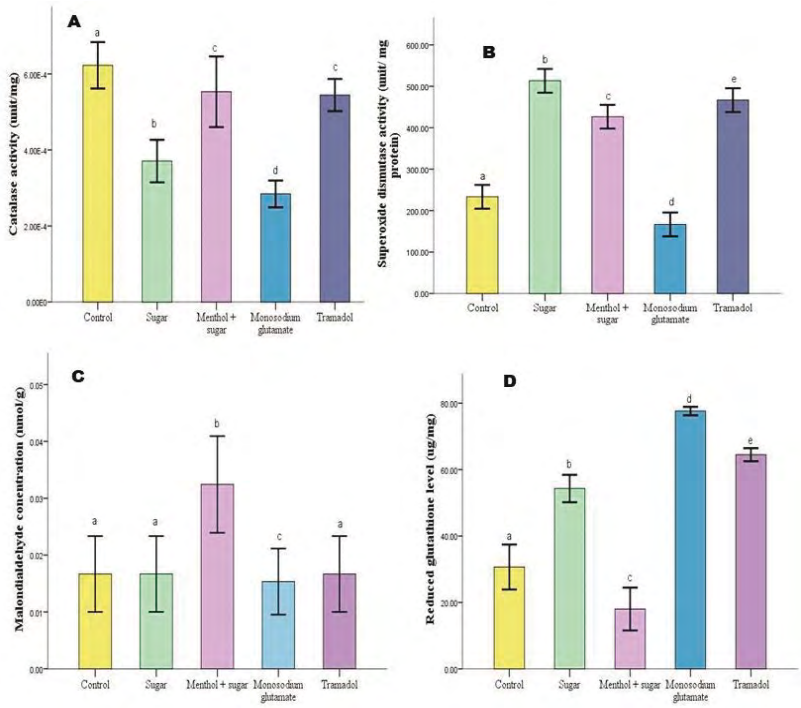

Figure 6. Effects of carbonated sugar drink, menthol+ carbonated sugar drink, monosodium glutamate, and tramadol on catalase activity (A), superoxide dismutase activity (B), malondialdehyde concentration (C), and reduced glutathione concentration (D), in the testis. Data are presented as mean ± SEM; bars with a different superscript are significantly different at a confidence interval of $p<0.05$.

There was a significant increase ($p<0.05$) in the nitric oxide level in the testis of the rats in the treated groups except for the group treated with tramadol which showed a significant decrease ($p<0.05$) in NO level compared to the control (Figure 7A). There was a significant increase ($p<0.05$) in the glycogen concentration in the treatment groups compared to the control (Figure 7B). There was a significant increase ($p<0.05$) in the % testicular weight change compared to the control (Figure 7C). The groups treated with menthol with carbonated sugar drinks and tramadol showed a significant decrease in the % organ body weight while the groups administered MSG and carbonated sugar drinks only showed an increase in organ body ratio compared to the control (Figure 7D).

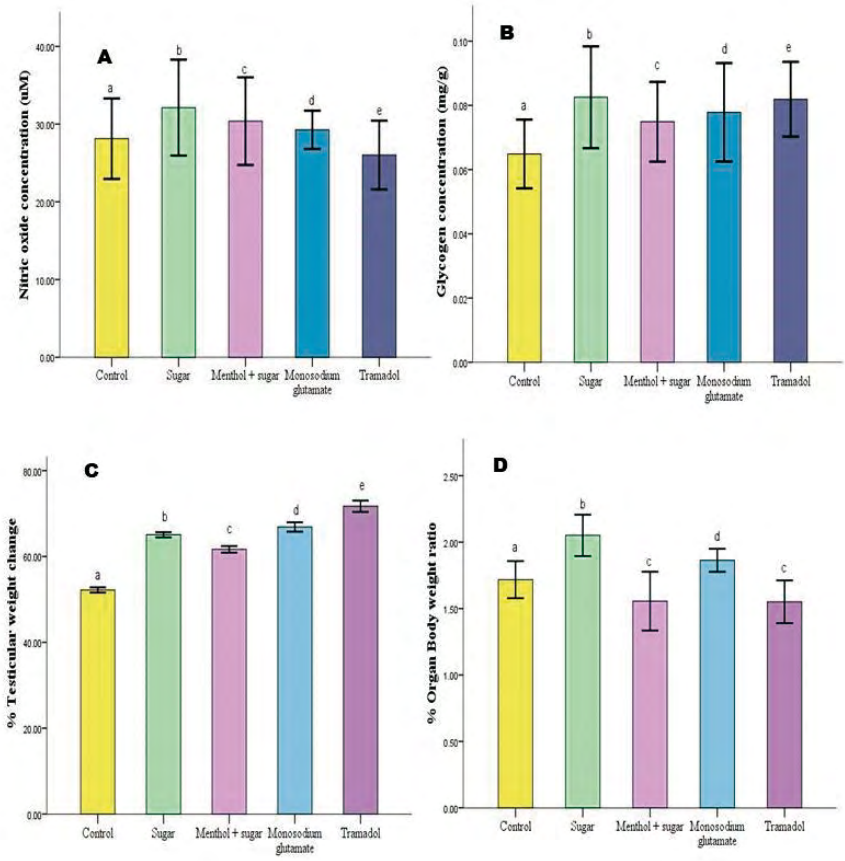

Figure 7. Effects of carbonated sugar drink, menthol + carbonated sugar drink, monosodium glutamate, and tramadol on nitric oxide concentration (A), glycogen concentration (B), % testicular weight change (C), and % organ body weight (D), of the testis. Data are presented as mean ± SEM; bars with a different superscript are significantly different at a confidence interval of $p<0.05$.

There was a significant decrease ($p<0.05$) in the HMG-CoA/mevalonate ratio in the treatment groups except for the group administered carbonated sugar drink which showed a significant increase ($p<0.05$) compared to the control (Figure 8A). There was no significant change ($p>0.05$) in Na-K ATPase activity in the treatment groups except in the group administered tramadol which showed a significant increase ($p<0.05$) compared to the control group (Figure 8B). There was a significant increase ($p>0.05$) in the acetylcholine esterase activity across the treatment groups compared to the control, however, the enzyme activity decreased significantly ($p<0.05$) in the group administered a combination of carbonated sugar drink and menthol (Figure 8C).

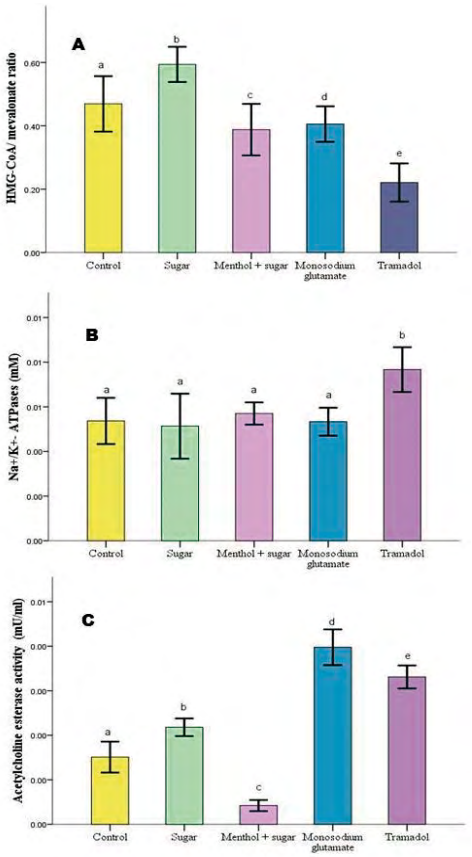

Figure 8. Effects of carbonated sugar drink, menthol+ carbonated sugar drink, monosodium glutamate, and tramadol on HMG-CoA mevalonate ratio (A), Na^+/K^+- ATPases activity (B), and acetylcholine esterase activity (C) in the testis. Data are presented as mean ± SEM; bars with a different superscript are significantly different at a confidence interval of $p<0.05$.

There was a significant increase ($p<0.05$) in the total protein concentration in the treatment groups except for the group administered MSG which showed a significant decrease ($p<0.05$) compared to the control (Figure 9A). There was a significant increase ($p<0.05$) in the acid phosphatase activity compared to the control (Figure 9B). There was a significant decrease ($p<0.05$) in alkaline phosphatase activity in the groups administered menthol with carbonated sugar drink and monosodium glutamate while the other treatment groups did not show any significant ($p>0.05$) change (Figure 9B).

The histology of the testis across the treatment groups showed normal histomorphology with a typical seminiferous tubule containing different types of germ cells; spermatogonia lying on the basement membrane with other cells proliferating in a centripetal direction when compared to the control (Figure 10).

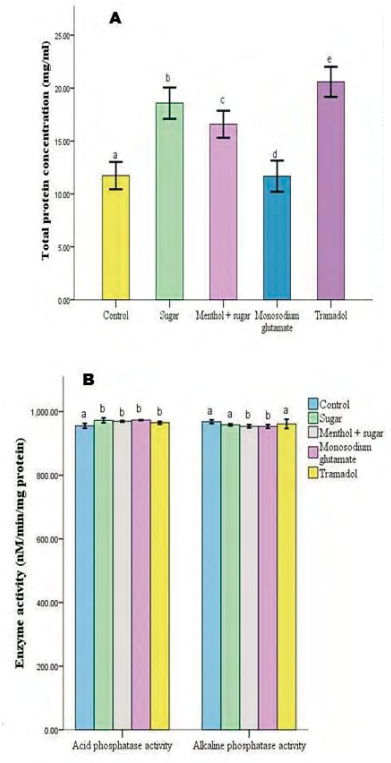

Figure 9. Effects of carbonated sugar drink, menthol+ carbonated sugar drink, monosodium glutamate, and tramadol on total protein concentration (A) and acid/alkaline phosphatase activity (B) in the testis. Data are presented as mean ± SEM; bars with a different superscript are significantly different at a confidence interval of $p<0.05$.

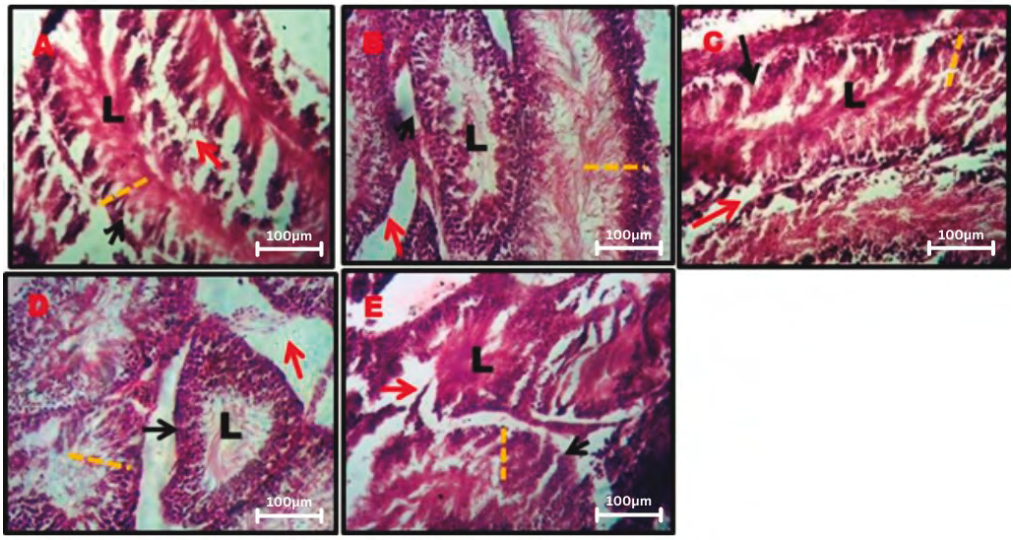

Figure 10. Photomicrograph of the testis (**H and E x100**): **Control:** The histomorphology is normal; normally, the seminiferous tubule includes several types of germ cells; at the membrane basement, other cells are lined up and grow in a centripetal orientation. Erosion at the basement membrane is afferent (A). **Carbonated sugar drink:** The histomorphology is normal; normally, the seminiferous tubule includes several types of germ cells; at the membrane basement, other cells are lined up and grow in a centripetal orientation (B). **Menthol + carbonated sugar drink:** The histomorphology is normal; normally, the seminiferous tubule includes several types of germ cells; at the membrane basement, other cells are lined up and grow in a centripetal orientation (C). **Monosodium glutamate:** The histomorphology is normal; normally, the seminiferous tubule includes several types of germ cells; at the membrane basement, other cells are lined up and grow in a centripetal orientation (D). **Tramadol:** The histomorphology is normal; normally, the seminiferous tubule includes several types of germ cells; at the membrane basement, other cells are lined up and grow in a centripetal orientation (E). (Black arrow: Basement membrane, L: lumen, Dotted line: Seminiferous epithelium).

In the course of the docking process, nine conformers were generated and the conformers with the highest binding affinities, that is, those with the highest negative values are presented in Table 1. From the docking results, the ligand with the best binding affinity is the control (Ouabain) with a value of -8.5 kcal/mol. This is not surprising since many hydroxyl moieties are used for binding at the residue. The one with the

lowest binding energy is due to monosodium glutamate (MSG) with a value of -5.1 kcal/mol. Thus, various interactions were observed for the molecular docking of the studied ligands with 3a3y.pdb file. From Figure 11A, Oubain showed only hydrogen bonding interactions; conventional and carbon. The conventional H-bond is however moderate and occurs over a distance of 2.69 Å with His B: 80, while the C-H bonds are weak and occur over a distance of 3.63 Å with Ser B: 105 and Asp A: 897. This H-bonding is greatly important in mediating the stability of a protein-ligand complex. The dominant interactions are strong conventional hydrogen bonding and moderate carbon-hydrogen bonding interactions. Interestingly, other chemical interactions played out in the Protein-Tramadol complex, as can be seen in (Figure 11B). The interactions of tramadol with the amino acid residues of the pocket are observed to be purely hydrophobic over long ranges. The strongest is the Pi-Sigma interaction and is with Val26 of chain G. The Pi-orbital mediated interaction, Pi-Pi Stacked interaction, is mainly due to chain A with the aromatic ring of tramadol. Mixed hydrogen bonding and hydrophobic interactions (mainly Alkyl and Pi-Alky) interactions were observed in the Protein-Menthol complex (Figure 11C). Hydrogen bonding interaction was observed to be strong over a distance of 2.02 Å between the hydroxyl hydrogen and Gln203 of chain B. Just like Ouabain, the interaction of 3a3y.pdb protein with Glucose is between oxygen and hydroxyl groups in the ligand structure and the amino acid residues (Figure 11D). The interaction of 3a3y.pdb protein with MSG ligand is observed to be mainly hydrogen bonding. Intramolecular interaction between Glu21 and Lys377 was also observed (Figure 11E).

Table 1. The binding free energy values of the ligands

Ligand	Binding affinity (kcal/mol)
Ouabain	-8.5
Tramadol	-6.9
Glucose	-6.0
Menthol	-5.9
Monosodium glutamate	-5.1

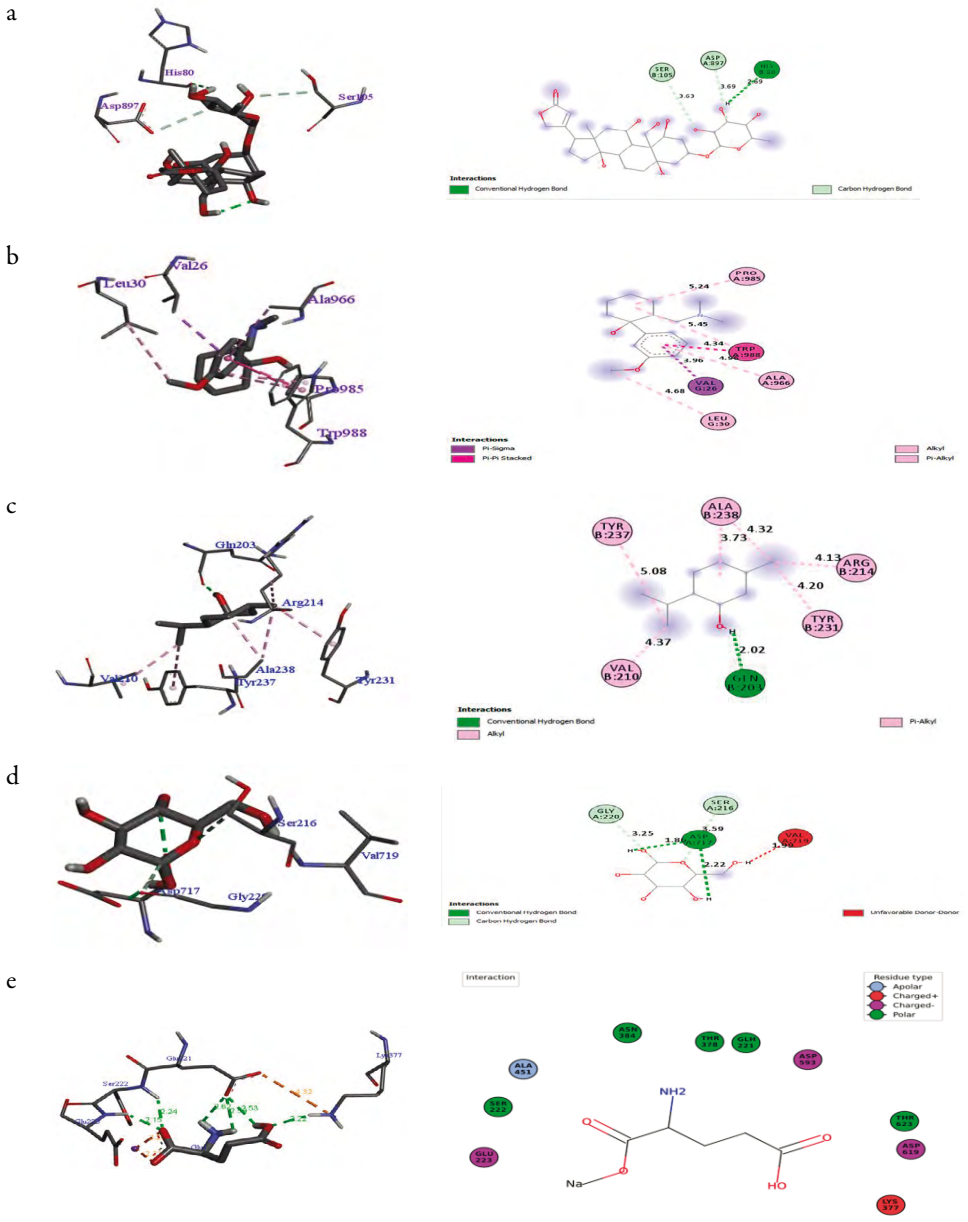

Figure 11. Interaction diagrams of Ouabain ligand (the reference inhibitor) (A), Tramadol ligand (B), Menthol ligand (C), glucose (D), and sodium monoglutamate (E), with the amino acid residues of the protein pocket (ATPase) respectively. The bond distances are given Angstrom (Å).

Discussion

Reproductive endocrine hormones trigger a series of biochemical processes in specialized testicular cells, crucial for spermatogenesis and the generation of high-quality sperm cells. Consequently, the health and integrity of testicular cells play a pivotal role in this process. Variations in the frequency of stages within the cycle of the seminiferous epithelium serve as indicators to assess the effects of treatments on spermatogenesis [47]. Sertoli cells serve as nurturing cells within the testis, creating a luminal environment essential for providing energy for spermatogenesis. Additionally, they offer crucial nutritional support for the growth and maturation of male germ cells into sperm cells [48, 49]. Furthermore, lactate is secreted by Sertoli cells as a by-product of lipid, amino acid, and glycogen metabolism [50, 51]. Similarly, When FSH binds to the Sertoli cells, it activates adenylyl cyclase and increases cytosolic cAMP, which then activates cAMP-dependent kinases and resulting in the phosphorylation of several unidentified proteins in the cell [52, 53]. When the enzymes are activated, it produces steroid, nuclear RNA, and protein synthesis, as well as steroid and protein secretion [54]. Furthermore, in the basal compartment of the testes are located Leydig cells which produce steroid hormones, primarily testosterone. The circulating luteinizing hormones (LH) secreted by the pituitary gland stimulate testosterone production in the Leydig cells [55]. Testosterone controls spermatogenesis by regulating the adhesion of round spermatids to Sertoli cells and the release of spermatids from the testis [56]. Because the generation of these hormones was normal, the chemicals did not interfere with hormone production or harm the testicular cells that serve as the source of these hormones. The interstitial germ cell required for spermatogenesis and other testicular machinery is housed in the testes. As a result, the rise in testes weight seen in rats fed these compounds may be explained by the hypertrophy or hyperplasia of the interstitial cells, without a change in the ratio of testicular to germ cells or Sertoli cells, as a result of the substance's impact [57]. Cell hypertrophy could be linked to sugar's high caloric content and an increase in food intake brought on by MSG's regulation of the brain's center for hunger. The decrease in organ body weight observed in menthol with carbonated sugar drinks and tramadol, on the other hand, may be due to an increase in metabolic activity. Additionally, these drugs may affect biochemical processes that affect the activity of germ cells or testicular cells, which could ultimately affect the quality of sperm production. The total sperm count is equal to the number of sperm in the entire ejaculate (sperm concentration times semen volume), where sperm concentration is the number of sperm per unit volume (milliliter) of semen [58]. Though no one test or sperm characteristic can predict male fertility or infertility with 100% certainty since no one sperm feature or function reflects the capacity of spermatozoa to complete the intricate processes that will result in pregnancy [59]. Due to the

descriptive nature of various sperm parameters, some studies have found a connection between IVF and motility [60], concentration [61], and normal/abnormal morphology because some of the sperm parameters are descriptive [62]. However, the current investigation demonstrated that none of the semen quality indicators were adversely affected by the medications used in the experiment; rather, it appeared that numerous semen metrics were enhanced [63], which may have been caused by the cumulative effect of chemicals with an endogenous source. An electrochemical gradient created by the electrogenic translocation of three sodium ions and two potassium ions out of the cell, mediated by the heteromeric integral membrane protein known as Na K-ATPase, resulting in the breakdown of ATP to ADP, which powers the cell [64-66]. The discovery of an α-4 isoform of Na, K-ATPase in the central region of the flagellum of spermatozoa pointed to a physiological function associated with the particular activity of these cells. This unique Na, K-ATPase isoform was crucial for sperm cell motility since blocking the α-4 isoform stops sperm from moving [67]. Because of this, the increased ATPase activity observed in this study may be proof that tramadol has the potential to increase sperm fertility. Additionally, it has been discovered that the cholinergic system is present in mammalian testicular cells like Sertoli cells and germ cells, both of which include functioning Ach receptors that are associated with sperm motility [68, 69]. The current study's elevated activity of Na K-ATPase and Ach helped to explain why there were so many sperms with fast motility and so few with slow motility or none at all.

High-density lipoprotein (HDL) serves as the principal supplier of cholesterol for steroidogenic tissue [70]. The interstitial tissue housing Leydig cells contains steroidogenic tissue equipped with specialized high-density lipoprotein-binding sites [71]. The elevation of HDL observed in this study corroborated findings indicating a correlation between heightened serum HDL levels and increased hepatic production, attributed to the demand from steroidogenic tissue [72, 73]. Evidence from both clinical and experimental sources underscores the significance of lipid metabolism in governing testicular physiology and male fertility [74]. Likewise, the function of steroidogenesis in the testis relies on either the *de novo* synthesis of cholesterol in Leydig cells or the stored cholesterol ester [75]. Cholesterol is a precursor of steroid hormones that are essential for sperm production [76, 77]. Furthermore, HMG-CoA reductase activity is required for interstitial tissue and Leydig cell homeostasis [78, 79]. Similarly, a series of biochemical reactions leads to the production of hydroxy-methyl glutaryl-CoA (HMG-CoA), which in turn leads to the production of mevalonate, which in turn leads to the production of cholesterol. The decrease in the HMG-CoA/mevalonate ratio correlates with increased activity of the reductase, which may be responsible for increased cholesterol production, steroidogenesis, and improved sperm quality, as demonstrated in this study [80]. Glycogen is found in the seminiferous tubules and

Sertoli cells, and its abundance varies at different stages of spermatogenesis. Glycogen is most likely important in the maturation of germinal cells. Despite being the primary source of ATP and sperm activity, failure of glucose uptake into the cell will result in the cell switching to glycogen metabolism as an alternative source of glucose [81-83]. The increased glycogen in this study could indicate intact testicular energy metabolism, which is required for spermatogenesis. NO is an inflammatory mediator that is produced in normal testis and has been found to regulate Leydig cell function and spermatogenic development in previous studies [84, 85]. The increased NO production and steroidogenesis in this study indicated that these emerging psychoactive substances had no negative effects on interstitial cell and spermatogenic activity [86, 87]. Phosphatidylcholine (PC) and phosphatidylethanolamine (PE) are the major phospholipids that serve as a building block of the cell membrane in the developing testis during sperm cell development [88-90]. Phospholipids are involved in sperm membrane permeability and fluidity [91-93], acrosomal reactions [94], and sperm motility [95]. The increased phospholipid level reported in this study could be linked to improved sperm quality hence these substances did alter the biochemical process for either phospholipid production or spermatogenesis. *Triacylglycerides* (TAG), membrane remodeling, and synthesis are indicators of male germ cell differentiation [96]. The final enzymatic step in TAG biosynthesis involves the joining of a long-chain fatty acid to a diacylglycerol molecule, which is mediated by the enzyme acyl-CoA: diacylglycerol acyltransferase (DGAT), which is found in most tissues' cells [97]. Similarly, the increased TAG production may be related to testicular cell differentiation vital in sperm production which is also an indication of the un-interruption of this process in the teste by these substances. Proteins present in the testis and epididymis play vital roles in regulating spermatogenesis, sperm maturation, and the differentiation of testicular cells [98]. The enhanced sperm quality and improved testicular function observed in this study may be linked to elevated total protein concentrations induced by these substances, supporting their non-toxic effects on male reproductive physiology. The abundance of long-chain and very long-chain unsaturated fatty acids in germ cell and sperm cell membranes renders them susceptible to lipid peroxidation, which is the primary cause of cellular damage [99, 100]. This damage entails alterations in germ cell membrane structure and sperm function, leading to cytopathological modifications and cell death [101-103]. The reduction in the lipid peroxide biomarker (MDA) observed in this study further underscores the non-toxic effects on both testicular and sperm cells. Additionally, lipid peroxidation, typically induced by toxicants generating ROS/free radicals, prompts the activation of antioxidant enzymes such as catalase and SOD to neutralize them. Therefore, the decreased activities of these endogenous antioxidant enzymes might be attributed to a reduced generation of radicals by the substances administered, providing further evidence for the observed low concentra-

tion of MDA in this study. Similarly, the levels of GSH indicated that these substances may not have an oxidative effect on testicular germ cells.

ACP is an appropriate biomarker for assessing prostate function [104]. ACP in semen is synthesized and secreted by the prostate [105], which is regulated by androgens [106], therefore decrease in ACP activity in plasma is an inflammatory effect on the prostate [107, 108]. The increase in the activity of ACP in this study also was an expression of an enhancement of the function of the prostate which was an indication of the safety of testicular function. Alkaline phosphatase (ALP) is found in seminal fluid and is thought to play a role in the glycolytic and fructose formation pathways in sperm [109]. Therefore in some mammals, ALP in sperm is produced in the testes or a testicular accessory organ (prostate, epididymis) [110, 111], while in some other species where the majority of semen plasma is alkaline phosphatase (SPAP), activity originates from the epididymis and testicle and can serve as an ejaculatory biomarker to distinguish azoospermia or oligospermia from ejaculatory failure [112]. The reported activity of testicular ALP in this study indicates that none of these substances could be deleterious on spermatogenesis or testicular function. The cellular architecture of the testis was normal, with no distortion or degeneration, supporting our claim that these substances which were administered at the highest daily/therapeutic did not disrupt reproductive efficiency in male rats. The last phase of the loss of testicular function, as characterized clinically, is testicular cell degeneration [113]. Reduced sperm production may also be linked to higher rates of germ cell degeneration [114, 115]. Therefore, the enhanced testicular and sperm quality in this study is indicative that these substances are not deleterious to the testicular cells.

Moreover, molecular docking facilitates a clearer comprehension of the molecular mechanisms underlying biochemical processes. The insights obtained through docking are poised to enhance the outcomes of atomic-level experiments [116-118]. Ouabain, known as a potent Na^+/K^+-ATPase inhibitor [119], exhibited a lower binding energy, supporting its stronger inhibitory effect on ATPase activity. Conversely, the higher binding energy observed with tramadol and glucose might be indicative of activity activation of Na^+/K^+-ATPase. The observed sperm progressive assessment in this study could be attributed to the activation of Na^+/K^+-ATPase activity during the acrosome reaction. The process of acrosome reaction (AR) in sperm cells involves fusion and vesiculation of the outer acrosomal membrane, which interfaces with the cell plasma membrane. This reaction is crucial for fertilization both in vivo and in vitro and necessitates preceding changes in the sperm known collectively as capacitation [1, 2]. The binding energies observed with tramadol and glucose may suggest their potential to induce sperm cell capacitation through the activity of Na^+,K^+-ATPase, with result-

ing K^+ influx being vital for mammalian sperm AR [3]. This study has demonstrated that ATPase activity serves as one of the signaling pathways in the regulation of sperm motility, capacitation, and acrosome reaction. Additional, molecular docking data in this study confirmed the previously described involvement of α-ATPase activity in sperm motility [67].

Conclusion

The development of healthy sperm cells relies on the intricate interplay between biochemical processes and hormonal effects within intact interstitial cells. Disruption of hormonal function or oxidative damage to the testicular cell membrane can impede reproductive functions or sperm integrity. Therefore, maintaining intact testicular cells and optimal levels of reproductive hormones may have contributed to the improved sperm quality observed in this study. The substances administered did not exhibit detrimental effects on testicular cells or reproductive function in male rats. Additionally, the in-silico study predicted that the enhanced sperm motility observed could be attributed to the effects of these substances on sperm cell ATPase activity.

Funding

Not Applicable

Data availability

Data will be made available on request.

Acknowledgments

Not Applicable

CRediT authorship contribution statement

Nwonuma Charles: Conceptualization, Data curation, Writing review & editing, Formal analysis, Investigation, Methodology, **Adedoyin, Adeola:** Investigation, Writing original draft, Methodology, **Inemesit. Asokwa:** Resources, Methodology. **Okeniyi Funmilayo:** Supervision, Writing review & editing. **Onyemaka Melody**: Project administration, Supervision, **Osemwegie, Omorefosa :** Writing review & editing, Ojo Adeleke: Formal analysis, Investigation, **Irokanulo Emenike:** Resources, Formal analysis **Adah, Deborah :** Formal analysis, Investigation **Alejolowo, Omokolade :** Data curation, Methodology.

Conflicts of interest

Authors declare that they have no conflicts of interest

References

1. S. Crowe, M. Utley, A. Costello, C. Pagel, How many births in sub-Saharan Africa and South Asia will not be attended by a skilled birth attendant between 2011 and 2015? *BMC Pregnancy and Childbirth*, **12**, 4 (2012). Doi: https://doi.org/10.1186/1471-2393-12-4

2. T.B. Hayes, L.L. Anderson, VR. Beasley, S.R. de Solla, T. Iguchi, H. Ingraham, P. Kestemont, J. Kniewald, Z. Kniewald, V.S. Langlois, *et al.*, Demasculinization and feminization of male gonads by atrazine: consistent effects across vertebrate classes, *The Journal of Steroid Biochemistry and Molecular Biology*, **127**(1-2), 64-73 (2011). Doi: https://doi.org/10.1016/j.jsbmb.2011.03.015

3. L. Peiris, H. Moore, Evaluation of effects of 1, 3-dinitrobenzene on sperm motility of hamster using computer assisted semen analysis (CASA), *Asian Journal of Andrology*, **3**(2), 109-114 (2001).

4. S.E. Lewis, J.M. Moohan, W. Thompson, Effects of pentoxifylline on human sperm motility in normospermic individuals using computer-assisted analysis, *Fertility and Sterility*, **59**(2), 418-423 (1993). Doi: https://doi.org/10.1016/s0015-0282(16)55708-2

5. D.M.I.H. Dissanayake, W.L.R. Keerthirathna, L.D.C. Peiris, Male infertility problem: A contemporary review on present status and future perspective, *Gender and the Genome*, **3**, 1-7 (2019). Doi: https://doi.org/10.1177/2470289719868240

6. J. McConnell, Abnormalities in sperm motility: techniques of evaluation and treatment, in: L.I. Lipshultz, S.S. Howards (editors), *Infertility in the male*, 3rd ed., Mosby Publications, New York (NY), 1997, pp. 249-267.

7. G.P. Toth, J.A. Stober, H. Zenick, E.J. Read, S.A. Christ, M.K. Smith, Correlation of sperm motion parameters with fertility in rats treated subchronically with epichlorohydrin, *Journal of Andrology*, **12**(1), 54-61 (1991). Doi: https://doi.org/10.1002/j.1939-4640.1991.tb00215.x

8. R. Singer, M. Ben-Bassat, Z. Malik, M. Sagiv, A. Ravid, B. Shohat, E. Livni, T. Mamon, E. Segenreich, C. Servadio, Oligozoospermia, asthenozoospermia, and sperm abnormalities in ex-addict to heroin, morphine, and hashish, *Archives of Andrology*, **16**(2), 167-174 (1986). Doi: https://doi.org/10.3109/01485018608986938

9. C. Vuong, S.H.M Van Uum, L.E. O'Dell, K. Lutfy, T.C. Friedman, The effects of opioids and opioid analogs on animal and human endocrine systems, *Endocrine Reviews*, **31**(1), 98-132 (2010). Doi: https://doi.org/10.1210/er.2009-0009

10. E. Agirregoitia, A. Valdivia, A. Carracedo, L. Casis, J. Gil, N. Subiran, C. Ochoa, J. Irazusta, Expression and localization of δ-, κ-, and μ-opioid receptors in human spermatozoa and implications for sperm motility, *The Journal of Clinical Endocrinology & Metabolism*, **91**(12), 4969-4975 (2006). Doi: https://doi.org/10.1210/jc.2006-0599

11. N. Subirán, L. Casis, J. Irazusta, Regulation of male fertility by the opioid system, *Molecular Medicine*, **17**(7), 846-853 (2011). Doi: https://doi.org/10.2119/molmed.2010.00268

12. T.J. Cicero, L.A. Davis, M.C. LaRegina, E.R. Meyer, M.S. Schlegel, Chronic opiate exposure in the male rat adversely affects fertility, *Pharmacology Biochemistry and Behavior*, **72**(1-2), 157-163 (2002). Doi: https://doi.org/10.1016/S0091-3057(01)00751-1

13. H.A. Shouip, *Tramadol synthesis and mechanism of action*, Faculty of Pharmacy and Pharmaceutical Industries, Sinai University, Arish, North Sinai, Egypt, 2015.

14. R.B. Raffa, H. Buschmann, T. Christoph, G. Eichenbaum, W. Englberger, C.M. Flores, T. Hertrampf, B. Kögel, K. Schiene, W. Straßburger, R. Terlinden, T.M. Tzschentke, Mechanistic and functional differentiation of tapentadol and tramadol, *Expert Opinion on Pharmacotherapy*, **13**(10), 1437-1449 (2012). Doi: https://doi.org/10.1517/14656566.2012.696097

15. S. Naveed, L. Jaweed, UV spectrophotometric assay of Ketoconazole oral formulations. *American Journal of Biology and Life Sciences*, **2**(5), 108-111 (2014). URL: http://www.openscienceonline.com/journal/archive2?journalId=704&paperId=795

16. S. Grond, A. Sablotzki, Clinical pharmacology of tramadol, Clinical Pharmacokinetics, 43(13), 879-923 (2004). Doi: https://doi.org/10.2165/00003088-200443130-00004

17. S. Alizadeh, M. Hasanzadeh, A. Irandoost, Tramadol, methadone and buprenorphine-AuNPs kit based on chemometrics tools and software, *Sensor Letters*, **18**(3), 227-235 (2020). Doi: https://doi.org/10.1166/sl.2020.4212

18. A.V. Ciurea, F.V. Edu, *Probleme de nocivitate în alimentele uzuale*, Galaxia Gutenberg, Barcelona, 2011.

19. R.K. Bush, S.L. Taylor, Reactions to food and drug additives, in: N.F. Adkinson, Jr, B.S. Bochner, A. Wesley-Burks, W.W. Busse, S.T. Holgate, R.F. Lemanske, Jr., R.E. O'Hehir (editors), *Middleton's Allergy: Principles and Practice*, 8th ed., Saunders-Elsevier Inc., 2014, pp. 1340-1356. Doi: https://doi.org/10.1016/B978-0-323-08593-9.00083-8

20. A. Buzescu, A.N. Cristea, L. Avram, C. Chiriță, The addictive behaviour induced by food monosodium glutamate: Experimental study, *Romanian Journal of Medical Practice*, **8**(4), 229-233 (2013). URL: https://rjmp.com.ro/articles/2013.4/PM_Nr-4_2013_Art-4.pdf

21. S. Nakanishi, Molecular diversity of glutamate receptors and implications for brain function, *Science*, **258**(5082), 597-603 (1992). Doi: https://doi.org/10.1126/science.1329206

22. N. Galeotti, L.D.C. Mannelli, G. Mazzanti, A. Bartolini, C. Ghelardini, Menthol: A natural analgesic compound, *Neuroscience Letters*, **322**(3), 145-148 (2002). Doi: https://doi.org/10.1016/S0304-3940(01)02527-7

23. G. Haeseler, D. Maue, J. Grosskreutz, J. Bufler, B. Nentwig, S. Piepenbrock, R. Dengler, M. Leuwer, Voltage-dependent block of neuronal and skeletal muscle sodium channels by thymol and menthol, *European Journal of Anaesthesiology*, **19**(8), 571-579 (2002). Doi: https://doi.org/10.1017/S0265021502000923

24. E.W. Dumbili, I.D. Ebuenyi, K.C. Ugoeze, New psychoactive substances in Nigeria: A call for more research in Africa, *Emerging Trends in Drugs, Addictions, and Health*, **1**, 100008 (2021). Doi: https://doi.org/10.1016/j.etdah.2021.100008

25. T.G. Cooper, E. Noonan, S. von Eckardstein, J. Auger, H.W.G. Baker, H.M. Behre, T.B. Haugen, T. Kruger, C. Wang, M.T. Mbizvo, K.M. Vogelsong, World Health Organization reference values for human semen characteristics, *Human Reproduction Update*, **16**(3), 231-245 (2010). Doi: https://doi.org/10.1093/humupd/dmp048

26. K. Yokoi, Z. Mayi, Organ apoptosis with cytotoxic drugs, *Toxicology*, **290**, 78-85 (2004).

27. M. Sönmez, G. Türk, A. Yüce, The effect of ascorbic acid supplementation on sperm quality, lipid peroxidation and testosterone levels of male Wistar rats, *Theriogenology*, **63**(7), 2063-2072 (2005). Doi: https://doi.org/10.1016/j.theriogenology.2004.10.003

28. M.A.u. Azim, M. Hasan, I.H. Ansari, F. Nasreen, Chemiluminescence immunoassay: Basic mechanism and applications, *Bangladesh Journal of Nuclear Medicine*, **18**(2), 171-178 (2015). Doi: https://doi.org/10.3329/bjnm.v18i2.35240

29. A.G. Gornall, C.J. Bardawill, M.M. David, Determination of serum proteins by means of the biuret reaction, *Journal of Biological Chemistry*, **177**(2), 751-766 (1949). Doi: https://doi.org/10.1016/S0021-9258(18)57021-6

30. P.J. Wright, P.D. Leathwood, D.T. Plummer, Enzymes in rat urine: alkaline phosphatase, *Enzymologia*, **42**(4), 317-327 (1972).

31. H.P. Misra, I. Fridovich, The generation of superoxide radical during the autoxidation of hemoglobin, *Journal of Biological Chemistry*, **247**(21), 6960-6962 (1972). Doi: https://doi.org/10.1016/S0021-9258(19)44679-6

32. D.J. Jollow, J.R. Mitchell, N. Zampaglione, J.R. Gillette, Bromobenzene-induced liver necrosis. Protective role of glutathione and evidence for 3,4-bromobenzene oxide as the hepatotoxic metabolite, *Pharmacology*, **11**(3), 151-169 (1974). Doi: https://doi.org/10.1159/000136485

33. K. Satoh, Serum lipid peroxide in cerebrovascular disorders determined by a new colorimetric method, *Clinica Chimica Acta*, **90**(1), 37-43 (1978). Doi: https://doi.org/10.1016/0009-8981(78)90081-5

34. G.L. Ellman, K.D. Courtney, V. Andres Jr., R.M. Featherstone, A new and rapid colorimetric determination of acetylcholinesterase activity, *Biochemical Pharmacology*, **7**(2), 88-95 (1961). Doi: https://doi.org/10.1016/0006-2952(61)90145-9

35. P. Ronner, P. Gazzotti, E. Carafoli, A lipid requirement for the (Ca^{2+} + Mg^{2+})-activated ATPase of erythrocyte membranes, *Archives of Biochemistry and Biophysics*, **179**(2), 578-583 (1977). Doi: https://doi.org/10.1016/0003-9861(77)90146-1

36. C.O. Bewaji, O.O. Olorunsogo, E.A. Bababunmi, Comparison of the membrane-bound (Ca^{2+} + Mg^{2+})-ATPase in erythrocyte ghosts from some mammalian species, *Comparative Biochemistry and Physiology Part B: Comparative Biochemistry*, **82**(1), 117-122 (1985). Doi: https://doi.org/10.1016/0305-0491(85)90138-5

37. J.C.M. Stewart, Colorimetric determination of phospholipids with ammonium ferrothiocyanate, *Analytical Biochemistry*, **104**(1), 10-14 (1980). Doi: https://doi.org/10.1016/0003-2697(80)90269-9

38. A. Kemp, A.J.M.K. Van Heijningen, A colorimetric micro-method for the determination of glycogen in tissues, *Biochemical Journal*, **56**(4), 646-648 (1954). Doi: https://doi.org/10.1042/bj0560646

39. R. Ilavarasan, M. Mallika, S. Venkataraman, Anti-inflammatory and free radical scavenging activity of *Ricinus communis* root extract, *Journal of Ethnopharmacology*, **103**(3), 478-480 (2006). Doi: https://doi.org/10.1016/j.jep.2005.07.029

40. L.I. Gidez, G.J. Miller, M. Burstein, S. Slagle, H.A. Eder, Separation and quantitation of subclasses of human plasma high density lipoproteins by a simple precipitation procedure, *Journal of Lipid Research*, **23**(8), 1206-1223 (1982). Doi: https://doi.org/10.1016/S0022-2275(20)38059-7

41. J. Folch, M. Lees, G.H. Sloane-Stanley, A simple method for the isolation and purification of total lipids from animal tissues, *Journal of Biological Chemistry*, **226**(1), 497-509 (1957). Doi: https://doi.org/10.1016/S0021-9258(18)64849-5

42. S. Ramakrishnan, A.V. Rao, Indirect assessment of hydroxymethylglutaryl-CoA reductase (NADPH) activity in liver tissue, *Clinical Chemistry*, **21**(10), 1523-1525 (1975). Doi: https://doi.org/10.1093/clinchem/21.10.1523

43. O. Trott, A.J. Olson, AutoDock Vina: Improving the speed and accuracy of docking with a new scoring function, efficient optimization, and multithreading, *Journal of Computational Chemistry*, **31**(2), 455-461 (2010). Doi: https://doi.org/10.1002/jcc.21334

44. S. Dallakyan, A.J. Olson, Small-molecule library screening by docking with PyRx, in: J. Hempel, C. Williams, C. Hong (editors), *Chemical Biology. Methods in Molecular Biology*, vol 1263, Humana Press, New York (NY), 2015, pp. 243-250. Doi: https://doi.org/10.1007/978-1-4939-2269-7_19

45. T.D. Hewitson, I.A. Darby, *Histology protocols*, Humana Press, Springer, 2010. Doi: https://doi.org/10.1007/978-1-60327-345-9

46. X. Peng, C. Dai, Q. Liu, J. Li, J. Qiu, Curcumin attenuates on carbon tetrachloride-induced acute liver injury in mice via modulation of the Nrf2/HO-1 and TGF-β1/Smad3 pathway, *Molecules*, **23**(1), 215 (2018). Doi: https://doi.org/10.3390/molecules23010215

47. R.A. Hess, D.J. Schaeffer, V.P. Eroschenko, J.E. Keen, Frequency of the stages in the cycle of the seminiferous epithelium in the rat, *Biology of Reproduction*, **43**(3), 517-524 (1990). Doi: https://doi.org/10.1095/biolreprod43.3.517

48. T. Lord, B. Nixon, Metabolic changes accompanying spermatogonial stem cell differentiation, *Developmental Cell*, **52**(4), 399-411 (2020). Doi: https://doi.org/10.1016/j.devcel.2020.01.014

49. C.-H. Wong, C.Y. Cheng, The blood-testis barrier: its biology, regulation, and physiological role in spermatogenesis, *Current Topics in Developmental Biology*, **71**, 263-296 (2005). Doi: https://doi.org/10.1016/S0070-2153(05)71008-5

50. M.F. Riera, S.B. Meroni, H.F. Schteingart, E.H. Pellizzari, S.B. Cigorraga, Regulation of lactate production and glucose transport as well as of glucose transporter 1 and lactate dehydrogenase A mRNA levels by basic fibroblast growth factor in rat Sertoli cells, *Journal of Endocrinology*, **173**(2), 335-343 (2002). Doi: https://doi.org/10.1677/joe.0.1730335

51. M.F. Riera, M.N. Galardo, E.H. Pellizzari, S.B. Meroni, S.B. Cigorraga, Molecular mechanisms involved in Sertoli cell adaptation to glucose deprivation, *American Journal of Physiology: Endocrinology and Metabolism*, **297**(4), E907-E914 (2009). Doi: https://doi.org/10.1152/ajpendo.00235.2009

52. A.R. Means, J.R. Dedman, J.S. Tash, D.J. Tindall, M. van Sickle, M.J. Welsh, Regulation of the testis Sertoli cell by follicle stimulating hormone, *Annual Review of Physiology*, **42**, 59-70 (1980). Doi: https://doi.org/10.1146/annurev.ph.42.030180.000423

53. J.L. Fakunding, D.J. Tindall, J.R. Dedman, C.R. Mena, A.R. Means, Biochemical actions of follice-stimulating hormone in the Sertoli cell of the rat testis, *Endocrinology*, **98**(2), 392-402 (1976). Doi: https://doi.org/10.1210/endo-98-2-392

54. A.R. Means, J.L. Fakunding, C. Huckins, D.J. Tindall, R. Vitale, Follicle-stimulating hormone, the Sertoli cell, and spermatogenesis, in: R.O. Greep (editor), *Proceedings of the 1975 Laurentian Hormone Conference, Volume 32 in Recent Progress in Hormone Research*, Academic Press, 1976, pp. 477-527. Doi: https://doi.org/10.1016/b978-0-12-571132-6.50027-0

55. P.J. O'Shaughnessy, Hormonal control of germ cell development and spermatogenesis, *Seminars in Cell & Developmental Biology*, **29**, 55-65 (2014). Doi: https://doi.org/10.1016/j.semcdb.2014.02.010

56. R.I. McLachlan, L. O'Donnell, S.J. Meachem, P.G. Stanton, D.M. De Kretser, K. Pratis, D.M. Robertson, Identification of specific sites of hormonal regulation in spermatogenesis in rats, monkeys, and man, *Recent Progress in Hormone Research*, **57**, 149-179 (2002). Doi: https://doi.org/10.1210/rp.57.1.149

57. T.L. Thompson, W.E. Berndtson, Testicular weight, Sertoli cell number, daily sperm production, and sperm output of sexually mature rabbits after neonatal or prepubertal hemicastration, *Biology of Reproduction*, **48**(5), 952-957 (1993). Doi: https://doi.org/10.1095/biolreprod48.5.952

58. M. Sigman, A. Zini, Semen analysis and sperm function assays: what do they mean? *Seminars in Reproductive Medicine*, **27**(2), 115-123 (2009). Doi: https://doi.org/10.1055/s-0029-1202300

59. K. Coetzee, T.F. Kruge, C.J. Lombard, Predictive value of normal sperm morphology: a structured literature review, *Human Reproduction Update*, **4**(1), 73-82 (1998). Doi: https://doi.org/10.1093/humupd/4.1.73

60. J.N. Robinson, G.M. Lockwood, A. Dokras, D.M. Egan, S.C. Nicholson, C. Ross, D.H. Barlow, Does isolated teratozoospermia affect performance in in-vitro fertilization and embryo transfer? *Human Reproduction*, **9**(5), 870-874 (1994). Doi: https://doi.org/10.1093/oxfordjournals.humrep.a138608

61. M.M. Biljan, C.T. Taylor, P.R. Manasse, E.C. Joughin, C.R. Kingsland, D.I. Lewis-Jones, Evaluation of different sperm function tests as screening methods for male fertilization potential--the value of the sperm migration test, *Fertility and Sterility*, **62**(3), 591-598 (1994). Doi: https://doi.org/10.1016/s0015-0282(16)56951-9

62. D.R. Grow, S. Oehninger, H.J. Seltman, J.P. Toner, R.J. Swanson, T.F. Kruger, S.J. Muasher, Sperm morphology as diagnosed by strict criteria: probing the impact of teratozoospermia on fertilization rate and pregnancy outcome in a large *in vitro* fertilization population, *Fertility and Sterility*, **62**(3), 559-567 (1994). Doi: https://doi.org/10.1016/s0015-0282(16)56946-5

63. C.O. Nwonuma, V.C. Nwatu, G. Mostafa-Hedeab, O.S. Adeyemi, O.O. Alejolowo, O.A. Ojo, S.A. Adah, O.J. Awakan, C.E. Okolie, N.T. Asogwa, I.A. Udofia, G.O. Egharevba, N.H. Aljarba, S. Alkahtani, G. El-Saber-Batiha, Experimental validation and molecular docking to explore the active components of cannabis in testicular function and sperm quality modulations in rats, *BMC Complementary Medicine and Therapies*, **22**(1), 227 (2022). Doi: https://doi.org/10.1186/s12906-022-03704-z

64. G. Blanco, R.W. Mercer, Isozymes of the Na-K-ATPase: heterogeneity in structure, diversity in function, *American Journal of Physiology – Renal Physiology*, **275**(5), F633-F650 (1998). Doi: https://doi.org/10.1152/ajprenal.1998.275.5.F633

65. J.B. Lingrel, T. Kuntzweiler, Na^+,$K(^+)$-ATPase, *The Journal of Biological Chemistry*, **269**(31), 19659-19662 (1994). URL: https://www.jbc.org/article/S0021-9258(17)32067-7/pdf

66. K.J. Sweadner, Isozymes of the Na^+/K+-ATPase, *Biochimica et Biophysica Acta (BBA) - Reviews on Biomembranes*, **988**(2), 185-220 (1989). Doi: https://doi.org/10.1016/0304-4157(89)90019-1

67. A.L. Woo, P.F. James, PF, J.B. Lingrel, Sperm motility is dependent on a unique isoform of the Na,K-ATPase, *Journal of Biological Chemistry*, **275**(27), 20693-20699 (2000). Doi: https://doi.org/10.1074/jbc.M002323200

68. M.O.R. Borges, M.L.C. Abreu, C.S. Porto, M.C.W. Avellar, Characterization of muscarinic acetylcholine receptor in rat Sertoli cells, *Endocrinology*, **142**(11), 4701-4710 (2001). Doi: https://doi.org/10.1210/endo.142.11.8465

69. C. Bray, J.-H. Son, P. Kumar, S. Meizel, Mice deficient in CHRNA7, a subunit of the nicotinic acetylcholine receptor, produce sperm with impaired motility, *Biology of Reproduction*, **73**(4), 807-814 (2005). Doi: https://doi.org/10.1095/biolreprod.105.042184

70. J.T. Gwynne, D. Mahaffee, H.B. Brewer, Jr, R.L. Ney, Adrenal cholesterol uptake from plasma lipoproteins: Regulation by corticotropin, *Proceedings of the National Academy of Sciences of the United States of America*, **73**(12), 4329-4333 (1976). Doi: https://doi.org/10.1073/pnas.73.12.4329

71. Y. Chen, F.B. Kraemer, G.M. Reaven, Identification of specific high density lipoprotein-binding sites in rat testis and regulation of binding by human chorionic gonadotropin, *Journal of Biological Chemistry*, **255**(19), 9162-9167 (1980). Doi: https://doi.org/10.1016/S0021-9258(19)70541-9

72. J.F. Henderson, Studies on fatty liver induction by 4-aminopyrazolopyrimidine, *Journal of Lipid Research*, **4**(1), 68-74 (1963). Doi: https://doi.org/10.1016/S0022-2275(20)40368-2

73. T. Shiff, P. Roheim, H. Eder, Effects of high sucrose diets and 4-aminopyrazolopyrimidine on serum lipids and lipoproteins in the rat, *Journal of Lipid Research*, **12**(5), 596-603 (1971). Doi: https://doi.org/10.1016/S0022-2275(20)39479-7

74. F.-Z. El-Hajjaji, A. Oumeddour, A.J.C. Pommier, A. Ouvrier, E. Viennois, J. Dufour, F. Caira, J.R. Drevet, D.H. Volle, S. Baron, F. Saez, J.-M.A. Lobaccaro, Liver X receptors, lipids and their reproductive secrets in the male, *Biochimica et Biophysica Acta (BBA) - Molecular Basis of Disease*, **1812**(8), 974-981 (2011). Doi: https://doi.org/10.1016/j.bbadis.2011.02.004

75. W.-J. Shen, S. Azhar, F.B. Kraemer, Lipid droplets and steroidogenic cells, *Experimental Cell Research*, **340**(2), 209-214 (2016). Doi: https://doi.org/10.1016/j.yexcr.2015.11.024

76. R.G. Parton, J.F. Hancock, Lipid rafts and plasma membrane microorganization: insights from Ras, *Trends in Cell Biology*, **14**(3), 141-147 (2004). Doi: https://doi.org/10.1016/j.tcb.2004.02.001

77. S. Yokoyama, Release of cellular cholesterol: molecular mechanism for cholesterol homeostasis in cells and in the body, *Biochimica et Biophysica Acta (BBA) - Molecular and Cell Biology of Lipids*, **1529**(1-3), 231-244 (2000). Doi: https://doi.org/10.1016/s1388-1981(00)00152-9

78. O. Kabbaj, C. Holm, M.L. Vitale, R.-M. Pelletier, Expression, activity, and subcellular localization of testicular hormone-sensitive lipase during postnatal development in the guinea pig, *Biology of Reproduction*, **65**(2), 601-612 (2001). Doi: https://doi.org/10.1095/biolreprod65.2.601

79. O. Kabbaj, S.R. Yoon, C. Holm, J. Rose, M.L. Vitale, R.-M. Pelletier, Relationship of the hormone-sensitive lipase-mediated modulation of cholesterol metabolism in individual compartments of the testis to serum pituitary hormone and testosterone concentrations in a seasonal breeder, the mink (*Mustela vison*), *Biology of Reproduction*, **68**(3), 722-734 (2003). Doi: https://doi.org/10.1095/biolreprod.102.008169

80. L. Sèdes, L. Thirouard, S. Maqdasy, M. Garcia, F. Caira, J.-M.A. Lobaccaro, C. Beaudoin, D.H. Volle, Cholesterol: a gatekeeper of male fertility? *Frontiers in Endocrinology*, **9**, 369 (2018). Doi: https://doi.org/10.3389/fendo.2018.00369

81. F. Villarroel-Espíndola, R. Maldonado, H. Mancilla, K. vander Stelt, A.I. Acuña, A. Covarrubias, C. López, C. Angulo, M.A. Castro, J.C. Slebe, J. Durán, M. García-Rocha, J.J. Guinovart, I.I. Concha, Muscle glycogen synthase isoform is responsible for testicular glycogen synthesis: Glycogen overproduction induces apoptosis in male germ cells, *Journal of Cellular Biochemistry*, **114**(7), 1653-1664 (2013). Doi: https://doi.org/10.1002/jcb.24507

82. F. Odet, S.A. Gabel, J. Williams, R.E. London, E. Goldberg, E.M. Eddy, Lactate dehydrogenase C and energy metabolism in mouse sperm, *Biology of Reproduction*, **85**(3), 556-564 (2011). Doi: https://doi.org/10.1095/biolreprod.111.091546

83. M. Dodo, H. Kitamura, H. Shima, D. Saigusa, S.M. Wati, N. Ota, F. Katsuoka, H. Chiba, H. Okae, T. Arima, K. Igarashi, T. Koseki, H. Sekine, H. Motohashi, Lactate dehydrogenase C is required for the protein expression of a sperm-specific isoform of lactate dehydrogenase A, *The Journal of Biochemistry*, **165**(4), 323-334 (2019). Doi: https://doi.org/10.1093/jb/mvy108

84. B. Jegou, C. Cudicini, E. Gomez, J.P. Stephan, Interleukin-1, interleukin-6 and the germ cell-Sertoli cell cross-talk, *Reproduction, Fertility and Development*, **7**(4), 723-730 (1995). Doi: https://doi.org/10.1071/rd9950723

85. D.B. Hales, Leydig cell-macrophage interactions: an overview, in: A.H. Payne, M.P. Hardy, L.D. Russell (editors), *The Leyding Cell*, Cache River Press, Vienna (IL), 1996, pp. 451-465.

86. K. Del Punta, E.H. Charreau, O.P. Pignataro, Nitric oxide inhibits Leydig cell steroidogenesis, *Endocrinology*, **137**(12), 5337-5343 (1996). Doi: https://doi.org/10.1210/endo.137.12.8940355

87. M.K. O'Bryan, S. Schlatt, O. Gerdprasert, D.J. Phillips, D.M. de Kretser, M.P. Hedger, Inducible nitric oxide synthase in the rat testis: evidence for potential roles in both normal function and inflammation-mediated infertility, *Biology of Reproduction*, **63**(5), 1285-1293 (2000). Doi: https://doi.org/10.1095/biolreprod63.5.1285

88. J. Dupont, M. Reverchon, M.J. Bertoldo, P. Froment, Nutritional signals and reproduction, *Molecular and Cellular Endocrinology*, **382**(1), 527-537 (2014). Doi: https://doi.org/10.1016/j.mce.2013.09.028

89. D.C. Wathes, D.R.E. Abayasekara, R.J. Aitken, Polyunsaturated fatty acids in male and female reproduction, *Biology of Reproduction*, **77**(2), 190-201 (2007). Doi: https://doi.org/10.1095/biolreprod.107.060558

90. D.R. Tocher, Metabolism and functions of lipids and fatty acids in teleost fish, *Reviews in Fisheries Science*, **11**(2), 107-184 (2003). Doi: https://doi.org/10.1080/713610925

91. J.T. Davis, R.B. Bridges, J.G. Coniglio, Changes in lipid composition of the maturing rat testis, *Biochemical Journal*, **98**(1), 342-346 (1966). Doi: https://doi.org/10.1042/bj0980342

92. A. Lenzi, M. Picardo, L. Gandini, F. Dondero, Lipids of the sperm plasma membrane: from polyunsaturated fatty acids considered as markers of sperm function to possible scavenger therapy, *Human Reproduction Update*, **2**(3), 246-256 (1996). Doi: https://doi.org/10.1093/humupd/2.3.246

93. D.S. Lin, M. Neuringer, W.E. Connor, Selective changes of docosahexaenoic acid-containing phospholipid molecular species in monkey testis during puberty, *Journal of Lipid Research*, **45**(3), 529-535 (2004). Doi: https://doi.org/10.1194/jlr.M300374-JLR200

94. N.L. Cross, Phosphatidylcholine enhances the acrosomal responsiveness of human sperm, *Journal of Andrology*, **15**(5), 484-488 (1994). Doi: https://doi.org/10.1002/j.1939-4640.1994.tb00484.x

95. J.P. Infante, V.A. Huszagh, Synthesis of highly unsaturated phosphatidylcholines in the development of sperm motility: a role for epididymal glycerol-3-phosphorylcholine, *Molecular and Cellular Biochemistry*, **69**(1), 3-6 (1985). Doi: https://doi.org/10.1007/bf00225921

96. G.M. Oresti, J. García-López, M.I. Aveldaño, J. del Mazo, Cell-type-specific regulation of genes involved in testicular lipid metabolism: fatty acid-binding proteins, diacylglycerol acyltransferases, and perilipin 2, *Reproduction*, **146**(5), 471-480 (2013). Doi: https://doi.org/10.1530/rep-13-0199

97. R. Lehner, A. Kuksis, Biosynthesis of triacylglycerols, *Progress in Lipid Research*, **35**(2), 169-201 (1996). Doi: https://doi.org/10.1016/0163-7827(96)00005-7

98. X. Liu, F. Liu, In-depth mapping of human testicular and epididymal proteins and their functional association with spermatozoa, *Molecular Medicine Reports*, **12**(1), 173-179 (2015). Doi: https://doi.org/10.3892/mmr.2015.3435

99. J. Parodi, Motility, viability, and calcium in the sperm cells, *Systems Biology in Reproductive Medicine*, **60**(2), 65-71 (2014). Doi: https://doi.org/10.3109/19396368.2013.869273

100. S.C. Sikka, Relative impact of oxidative stress on male reproductive function, *Current Medicinal Chemistry*, **8**(7), 851-862 (2001). Doi: https://doi.org/10.2174/0929867013373039

101. G. Collodel, M.G. Federico, M. Geminiani, S. Martini, C. Bonechi, C. Rossi, N. Figura, E. Moretti, Effect of trans-resveratrol on induced oxidative stress in human sperm and in rat germinal cells, *Reproductive Toxicology*, **31**(2), 239-246 (2011). Doi: https://doi.org/10.1016/j.reprotox.2010.11.010

102. E.O. Farombi, S.O. Abarikwu, A.C. Adesiyan, T.O. Oyejola, Quercetin exacerbates the effects of subacute treatment of atrazine on reproductive tissue antioxidant defence system, lipid peroxidation and sperm quality in rats, *Andrologia*, **45**(4), 256-265 (2013). Doi: https://doi.org/10.1111/and.12001

103. C.T. Leong, U.J.A. D'Souza, M. Iqbal, Z.A. Mustapha, Lipid peroxidation and decline in antioxidant status as one of the toxicity measures of diazinon in the testis, *Redox Report*, **18**(4), 155-164 (2013). Doi: https://doi.org/10.1179/1351000213Y.0000000054

104. C.O. Madu, Y. Lu, Novel diagnostic biomarkers for prostate cancer, *Journal of Cancer*, **1**, 150-177 (2010). Doi: https://doi.org/10.7150/jca.1.150

105. J.-C. Lu, F. Chen, H.-R. Xu, Y.-F. Huang, N.-Q. Lu, Preliminary investigations on the standardization and quality control for the determination of acid phosphatase activity in seminal plasma, *Clinica Chimica Acta*, **375**(1-2), 76-81 (2007). Doi: https://doi.org/10.1016/j.cca.2006.06.005

106. N.J. Bolton, R. Lahtonen, P. Vihko, M. Kontturi, R. Vihko, Androgens and prostate-specific acid phosphatase in whole tissue and in separated epithelium from human benign prostatic hypertrophic glands, *The Prostate*, **2**(4), 409-416 (1981). Doi: https://doi.org/10.1002/pros.2990020408

107. S.M. Girgis, M.K. Deinasury, M. El-Kodary, B. Metawy, M.M. Moussa, N. Momen, S.M. Saleh, Diagnostic value of determination of acid and alkaline phosphatase levels in the seminal plasma of infertile males, *Andrologia*, **13**(4), 330-334 (1981). Doi: https://doi.org/10.1111/j.1439-0272.1981.tb00057.x

108. J.P. Kavanagh, C. Darby, C.B. Costello, The response of seven prostatic fluid components to prostatic disease, *International Journal of Andrology*, **5**(5), 487-496 (1982). Doi: https://doi.org/10.1111/j.1365-2605.1982.tb00280.x

109. T. Mann, Biochemistry of stallion semen, *Journal of Reproduction and Fertility. Supplement*, **23**, 47-52 (1975).

110. T. Mann, *The biochemistry of semen and of the male reproductive tract*, John Wiley & Sons, New York (NY), 1964.

111. F.C.M. Alexander, R. Zemjanis, E.F. Graham, M.L. Schmehl, Semen characteristics and chemistry from bulls before and after seminal vesiculectomy and after vasectomy, *Journal of Dairy Science*, **54**(10), 1530-1535 (1971). Doi: https://doi.org/10.3168/jds.S0022-0302(71)86059-9

112. P.N. Olson, Clinical approach for evaluating dogs with azoospermia or aspermia, *Veterinary Clinics of North America: Small Animal Practice*, **21**(3), 591-608 (1991). Doi: https://doi.org/10.1016/s0195-5616(91)50062-0

113. T.L. Blanchard, L. Johnson, D.D. Varner, S.L. Rigby, S.P. Brinsko, C.C. Love, C. Miller, Low daily sperm output per ml of testis as a diagnostic criteria for testicular degeneration in stallions, *Journal of Equine Veterinary Science*, **21**(1), 11-35 (2001). Doi: https://doi.org/10.1016/S0737-0806(01)70228-6

114. T.L. Blanchard, L. Johnson, Increased germ cell degeneration and reduced germ cell:Sertoli cell ratio in stallions with low sperm production, *Theriogenology*, **47**(3), 665-677 (1997). Doi: https://doi.org/10.1016/s0093-691x(97)00025-3

115. A.J. Ross, K.G. Waymire, J.E. Moss, A.F. Parlow, M.K. Skinner, L.D. Russell, G.R. MacGregor, Testicular degeneration in Bclw-deficient mice, *Nature Genetics*, **18**(3), 251-256 (1998). Doi: https://doi.org/10.1038/ng0398-251

116. R.K. Hussein, H.M. Elkhair, Molecular docking identification for the efficacy of some zinc complexes with chloroquine and hydroxychloroquine against main protease of COVID-19, *Journal of Molecular Structure*, **1231**, 129979 (2021). Doi: https://doi.org/10.1016/j.molstruc.2021.129979

117. G. Munsamy, MES Soliman, Unveiling a new era in malaria therapeutics: A tailored molecular approach towards the design of plasmepsin IX inhibitors, *The Protein Journal*, **38**(6), 616-627 (2019). Doi: https://doi.org/10.1007/s10930-019-09871-2

118. T. Ogawa, T. Furuhashi, A. Okazawa, R. Nakai, M. Nakazawa, T. Kind, O. Fiehn, S. Kanaya, M. Arita, D. Ohta, Exploration of polar lipid accumulation profiles in *Euglena gracilis* using LipidBlast, an MS/MS spectral library constructed *in silico*, *Bioscience, Biotechnology, and Biochemistry*, **78**(1), 14-18 (2014). Doi: https://doi.org/10.1080/09168451.2014.877826

119. J.L. Gregersen, D. Mattle, N.U. Fedosova, P. Nissen, L. Reinhard, Isolation, crystallization and crystal structure determination of bovine kidney Na^+,K^+-ATPase, *Acta Crystallographica Section F: Structural Biology Communications*, **72**(Pt 4), 282-287 (2016). Doi: https://doi.org/10.1107/s2053230x1600279x

How to cite this article

C.O. Nwonuma, A.O. Adedoyin, M. Onyemaka, I.A. Udofia, O.O. Alejolowo, E. Irokanulo, O.A. Ojo, D.A. Adah, F.A. Okeniyi, O.O. Osemwegie, An *in vivo* and *in silico* predictive study on the toxicological and modulatory effects of abused substances on sperm quality and testicular function in Wistar rats, *Rev. Colomb. Cienc. Quim. Farm.*, **53**(2), 513-551(2024). https://doi.org/10.15446/rcciquifa.v53n2.114454

Technological research article / https://doi.org/10.15446/rcciquifa.v53n2.114455

Food designing for Covid-19 patients with the help of applied mathematical optimization technique in LINDO Software

Rakesh Yadav [1a*], Monika Sahu [1b], Ankur Bala [2c], Shekhar Wadia [3d], Manju Rani [4e]

[1]Department of Mathematics, School of Chemical Engineering & Physical Sciences, Lovely Professional University, Phagwara, Punjab, India

[2]Department of Mathematics, Government College, Hansi, India

[3]Department of Mathematics, M.N.S. Govt. College Bhiwani, India

[4]Department of Mathematics, Indra Gandhi University, Rewari, India

E-mail addresses:

[a]rakesh.21798@lpu.co.in, [b]sahumonika2507@gmail.com, [c]ankur.mathematics@gmail.com, [d]wadia97@gmail.com, [e]manju.math.rs@igu.ac.in

Received: December 18, 2023
Corrected: April 7, 2024
Accepted: April 12, 2024

Summary

Objective: Due to the alarming rise in COVID-19 cases every day in India, numerous academics are already developing a variety of math-based estimation models to forecast the pandemic future course. This paper makes use of publicly available data to anticipate certain COVID-19 trajectories in India. **Methods:** We used the Auto-Regressive Integrated Moving Average Model, a time series model, to anticipate the number of COVID-19 infected cases every day soon. People need to consume nutritious food that is well-balanced and contains the right number of calories, nutrients, as well as vitamins for strong development, bearing in mind that sustaining and repairing bodily tissues is the goal while preventing unfavorable illnesses and disease. **Results:** Recent studies have shown that healthy eating can help lower the possibilities of developing cancer, cardiovascular disease and for COVID patients. Therefore, an optimization strategy and LINDO software was used to solve the model. This study offers an exhaustive daily meal plan created especially for hospital patients, acting as a helpful resource for school administrators. With six different food choices, the diet plan makes sure that you get all the nutrients you need each day at a reasonable price. **Conclusions:** The model is solved

using LINDO software in the study, which shows how effective it is when compared to other heuristic techniques like biological algorithms. It is determined through thorough investigation that the chosen meals are both financially and nutritionally feasible to serve in ho spital settings. Hospital patients make up the study's participants, and each day's total cost comes to Rs109.34. This cost makes it possible to deliver meals that are minimally more costly but of higher quality, improving the patients' overall nutritional value.

Keywords: Menu planning, integer linear programming, optimization, mathematical modelling, decision-making.

Resumen

Diseño de alimentos para pacientes de Covid-19 con la ayuda de la técnica de optimización matemática aplicada del software LINDO

Objetivo: Debido al alarmante aumento de casos de COVID-19 cada día en la India, numerosos académicos ya están desarrollando una variedad de modelos de estimación basados en matemáticas para pronosticar el curso futuro de la pandemia. Este documento utiliza datos disponibles públicamente para anticipar ciertas trayectorias de COVID-19 en la India. **Métodos:** Utilizamos el modelo de media móvil integrada autorregresiva, un modelo de series temporales, para anticipar el número de casos de infección por COVID-19 todos los días en el corto plazo. Las personas necesitan consumir alimentos nutritivos, bien equilibrados y que contengan la cantidad adecuada de calorías, nutrientes y vitaminas para un desarrollo fuerte, teniendo en cuenta que el objetivo es mantener y reparar los tejidos corporales y, al mismo tiempo, prevenir enfermedades y dolencias desfavorables. **Resultados:** Estudios recientes han demostrado que una alimentación saludable puede ayudar a reducir las posibilidades de desarrollar cáncer, enfermedades cardiovasculares y en pacientes con COVID. Por lo tanto, se utilizó una estrategia de optimización y el software LINDO para resolver el modelo. Este estudio ofrece un plan de alimentación diario exhaustivo creado especialmente para pacientes hospitalarios, que actúa como un recurso útil para los administradores escolares. Con seis opciones de alimentos diferentes, el plan de dieta garantiza que obtenga todos los nutrientes que necesita cada día a un precio razonable. **Conclusiones:** El modelo se resuelve utilizando el software LINDO en el estudio, lo que muestra su efectividad en comparación con otras técnicas heurísticas como los algoritmos biológicos. A través de una investigación exhaustiva se determina que las comidas elegidas son viables desde el punto de

vista financiero y nutricional para servir en entornos hospitalarios. Los pacientes del hospital constituyen los participantes del estudio y el costo total de cada día asciende a 109,34 rupias. Este costo permite entregar comidas mínimamente más costosas pero de mayor calidad, mejorando el valor nutricional general de los pacientes.

Palabras clave: Planificación de menús, programación lineal entera, optimización, modelado matemático, toma de decisiones.

Resumo

Design de alimentos para pacientes com Covid-19 com ajuda de técnica de otimização matemática aplicada no software LINDO

Objectivo: Devido ao aumento alarmante de casos diários de COVID-19 na Índia, vários académicos já estão a desenvolver uma variedade de modelos de estimativa baseados em matemática para prever o curso futuro da pandemia. Este artigo utiliza dados disponíveis publicamente para antecipar certas trajetórias da COVID-19 na Índia. **Métodos:** Usamos o modelo de média móvel integrada auto-regressiva, um modelo de série temporal, para antecipar o número de casos infectados por COVID-19 todos os dias em breve. As pessoas precisam consumir alimentos nutritivos, bem balanceados e que contenham a quantidade certa de calorias, nutrientes e vitaminas para um forte desenvolvimento, tendo em mente que o objetivo é sustentar e reparar os tecidos corporais, ao mesmo tempo que se previnem doenças e enfermidades desfavoráveis. **Resultados:** Estudos recentes demonstraram que uma alimentação saudável pode ajudar a diminuir as possibilidades de desenvolvimento de cancro, doenças cardiovasculares e para pacientes com COVID. Portanto, uma estratégia de otimização e o software LINDO foram utilizados para resolver o modelo. Este estudo oferece um plano alimentar diário exaustivo criado especialmente para pacientes hospitalares, atuando como um recurso útil para administradores escolares. Com seis opções alimentares diferentes, o plano de dieta garante que você obtenha todos os nutrientes necessários todos os dias a um preço razoável. **Conclusões:** O modelo é resolvido utilizando o software LINDO no estudo, o que mostra sua eficácia quando comparado a outras técnicas heurísticas como algoritmos biológicos. Através de investigação minuciosa é determinado que as refeições escolhidas são financeiramente e nutricionalmente viáveis para serem servidas em ambientes hospitalares. Os pacientes do hospital constituem os participantes do estudo e o

custo total de cada dia chega a Rs109,34. Esse custo permite entregar refeições minimamente mais caras, mas de maior qualidade, melhorando o valor nutricional geral dos pacientes.

Palavras-chave: Planejamento de cardápio, programação linear inteira, otimização, modelagem matemática, tomada de decisão.

Introduction

Nutrition is very important in this lifestyle. Numerous socioeconomic and environmental factors have an impact on nutrition. Even if the world's diet crisis was acute during World War II, the task of supplying food for everyone in a sustainable and nutritious way will only get worse. Between 1950 and 1960, the initial analysis incorporating LP into diets was released. Jerry Cornfield developed "The Diet Problem for the Army during World War II (1941–1955) in an effort to find a cheap diet that would satisfy a soldier's nutritional requirements". This was the beginning of the hunt for diet solutions. The COVID-19 pandemic, which started rapidly and extensively spreading in late 2019, had a significant impact on food security and nutrition.

Therefore, utilize operational research and judgement to create a mathematical model to study menu planning. The issue was solved using LINDO and LP Solve programming language. LP problem can be addressed using a variety of techniques, including the graphical and simplex methods. These techniques take a long time to manually solve the LP model. The LP model is solved using the LINDO programmer in this paper's application to calculate the patient minimum meal cost. By using computer assisted menu planning and data control, for institutional feeding programmers, a multiple-phase system was created to lower the price of food. Assembling meal items for a series of days that meet the necessary structural, nutritional, compatibility requirements, and variety restrictions at fewer prices was the basis for the formulation of food management objectives, a problem that is commonly encountered by each individual and volume feeding agency. The answer was found by solving big integer programs sequentially using a newly created truncated block enumeration technique [1, 2].

The correlation in both palatable meals and satisfying nutrients is mathematically modelled and analyzed. The standard minimal-cost dietary issue is inappropriate for many uses in the pursuit of the least financial cost that leads to meals that are undesirable to individuals as well as to groups of people. This research presents a unique thought that utilizes a goal value dependent on each person food preferences. Based on this research, a computational technique for using linear programming to create individu-

ally appropriate diets is described [3-5]. Scientific proof is still required to determine which foods constitute a healthy diet in terms of the primary prevention of serious chronic diseases.

Therefore, sought to provide a thorough review of foods associated with health based on the eight years data from the EPIC-Potsdam research [6, 7]. Every patient was getting supportive treatment at the outset, such as anti-inflammatory and antiviral medications, and all patients were receiving oxygen assistance. "Nine patients experienced at least a 1-point improvement on the clinical scale by day 7 post- transfusion with convalescent plasma, and seven of those patients were discharged. On day 14 following the transfusion, 11 patients were released, and 19 (76%) patients had at least a 1-point improvement in their clinical state". No unfavorable effects of the plasma transfusion were noted. There was no association between strain genotype and disease severity found in the whole genome sequencing data [8, 9].

It is generally known that poor nutrition has an adverse effect on critically ill patients, contributing to higher mortality, longer stays in intensive care units (ICUs), impairment and general morbidity following hospitalization. Guidelines for nutritional therapy for people with SARS-CoV-2 infection were just released by "European Society for Clinical Nutrition and Metabolism (ESPEN)", and they include suggestions for patients being treated in the intensive care unit (ICU). The main goal of these suggestions is to use promotility drugs to promote gastric emptying, initiating proximal nutrition (PN) if enteral food (EN) is not tolerated, providing early EN where feasible, and utilizing EN Post Extubation if oral feeding is not tolerated [10].

The article addresses how students choose their diets, consuming certain foods to meet their daily nutritional requirements. The goal of the current investigation was to reduce the daily [11, 12]. According to the World Health Organization, as of November 14, 2020, there were more than 54 million COVID-19 cases globally, and more than 1,323,196 individuals died as a result. As a result, several countries had to declare an illness or impose a period of isolation, which had a negative effect on society, the economy, and public health in addition to slowing the COVID-19 pandemic progress. Therefore, "we provide a mathematical model for the dynamics of COVID-19 disease transmission as well as a mathematical model for the dynamics of diabetes before emphasizing the detrimental effects of quarantine on the health of diabetics [9]. One Chinese meta-analysis of 1,527 patients revealed that diabetes (9.7%, 95% CI 6.9–12.5%) and cardio-cerebrovascular disease (16.4%, 95% CI 6.6–26.1%) were the two most common cardiovascular metabolic comorbidities with COVID-19". According to this study, patients with diabetes or high blood pressure had a 2-fold increased chance of developing a serious illness or needing admission to an intensive care unit

(ICU), but patients with cardio-cerebrovascular disease had a 3-fold increased risk. In a subset of 355 COVID-19 patients in Italy who passed away, the mean number of underlying diseases was 2.7, and only 3 people were co morbidity-free [13].

At the time of corona-virus incidents, the condition damaged many people. When someone tests positive for corona-virus, they should adhere to the nutrition to boost their immunity. Therefore, the Health Department oversees creating patient diets that take food prices into account. Hospital caterers who provide the whole day food according to the given menu lists. Patients are not given the option to select their favorite dishes from the non-selective menu that is offered. This research paper main goal is to create a framework that might enable the construction of the whole day meal. We tried to meet the needs of COVID-19 patients while keeping government funding to a minimum. Additionally, we aimed to maximize variety and satisfy consumer preferences.

Therefore, it is imperative to conduct investigation into meal preparation using computational frameworks that incorporate logistic study and scientific decision-making approaches to help caterers serve healthy meals for extended periods of time while adhering to financial restrictions. A healthy diet helps ensure that the body is in the best condition to fight the infection. Researchers have discovered that there is no source of viral transmission via food or food packaging, so that to stop the virus from spreading, the system for managing food safety needs to provide staff and food safety officials with appropriate respiratory protection. However, adopting safe food practices is always advised to reduce the possibility of getting infected.

Mathematical model: This model represents an effort to investigate a portion of the real-life problem mathematically. Mathematical transformation of a physical situation under certain conditions.

Linear programming: the method of optimizing a problem that is subject to restrictions is known as linear programming. It denotes the process of maximizing or minimizing linear functions under limits imposed by linear inequality. The easiest problem to solve is the one using linear programmers.

LINDO Software: system creates software tools for modelling and optimization. Quickly and simply solve linear, nonlinear, and integer problems. LINDO Systems has committed itself to offering robust, cutting-edge optimization tools that are both adaptable and user-friendly. In 1988, LINGO, the company's first product with a full-featured modelling capability, was released. Users were able to use summations and subscripted variables to succinctly express models using the modelling language. A large-scale nonlinear solver was implemented in LINGO in 1993. The user did not have to specify which solver to use, making it special. Following a model analysis,

LINGO would automatically select the best linear or nonlinear solver. The ability to support both general and binary integer limitations was another feature exclusive to LINGO's nonlinear solver.

Data interpretation

A menu-displaying model requires different types of information. The institutionalized cost is included in the Recommended Daily Allowance (RDA), which includes the recommended daily requirement of nutritional diet for hospitalized individuals and the national budget for nutrition suppliers for each menu item. Total six supplements were taken into consideration, as indicated in Table 1, carbs, protein, fat, calories, fiber, and iron. Also, fourteen different types of meals, Egg, papaya, lentils, idly, cardamom, banana, milk, ragi porridge, fresh dates, dosa, almond, cottage cheese, curd and muskmelon were all taken into consideration in this study.

Table 1. Everyday Consumption of Food Ingredient

Food Ingredient	Everyday Consumption
Carbohydrates	185
Protein	60
Fats	50
Calories	1800
Fibber	35
Iron	20

Table 1, six supplements were taken into consideration, these are carbs, protein, fat, calories, fiber, and iron. These six supplements are making a complete diet for a human in a day. The consumption of all these supplements in different valued that is carbohydrates in a day a human can takes 185, protein 60, fats 50, calories 1800, fibber 35 and iron 20.

So that based on above table, forms a mathematical model as follows: -

Minimization $Y = d_1q_1 + d_2q_2 + d_3q_3 + \ldots + d_nq_n$

Subject to constraints:

$$p_{11}\ q_1 + p_{12}\ q_2 + p_{13}\ q_3 + \cdots + p_{1n}\ q_n \geq 185$$

$$p_{21}\ q_1 + p_{22}\ q_2 + p_{23}\ q_3 + \cdots + p_{2n}\ q_n \geq 60$$

$$p_{31}\,q_1 + p_{32}\,q_2 + p_{33}\,q_3 + \cdots + p_{3n}\,q_n \geq 50$$

$$p_{41}\,q_1 + p_{42}\,q_2 + p_{43}\,q_3 + \cdots + p_{4n}\,q_n \geq 1800$$

$$p_{51}\,q_1 + p_{52}\,q_2 + p_{53}\,q_3 + \cdots + p_{5n}\,q_n \geq 35$$

$$p_{61}\,q_1 + p_{62}\,q_2 + p_{63}\,q_3 + \cdots + p_{6n}\,q_n \geq 20$$

$$q_1 + q_2 + q_3 + \cdots + q_n \geq 1$$

Since the information is reliant on the menu supplied by the hospital administration, the LP model will be configured in accordance with the meal prices determined by the management. Here are some examples of foods for COVID sufferers that are nutrient rich.

As summarized in Table 2, there are fourteen different types of meals, that is, Egg, papaya, lentils, idly, cardamom, banana, milk, ragi porridge, fresh dates, dosa, almond, cottage cheese, curd and muskmelon were all taken into consideration in this study. The cost is also considering all the fourteen meals that is, Egg is 7 rupees, papaya is 10 rupees, lentils is 10 rupees, idly is 5 rupees, cardamom is 4 rupees, banana is 3 rupees, milk is 20 rupees, ragi porridge is 15 rupees, fresh dates is 20 rupees, dosa is 10 rupees, almond is 20 rupees, cottage cheese is 25 rupees, curd is 10 rupees and muskmelon is 15 rupees.

Table 2. Different types of foods

Code	Food item	Cost
$x1$	Cottage cheese	25
$x2$	Curd	10
$x3$	Papaya	10
$x4$	Egg	7
$x5$	Idly	5
$x6$	Milk	20
$x7$	Cardamom, banana	7
$x8$	Ragi Porridge	15
$x9$	Almond	20
$x10$	Lentils	10
$x11$	Spinach Soup	10
$x12$	Dosa	10
$x13$	Fresh Dates	20
$x14$	Muskmelon	15

Formulation of the equation

Minimize Y = 25$x1$ + 10$x2$ + 10$x3$ + 7$x4$ + 5$x5$ + 20$x6$ + 7$x7$ + 15$x8$ + 20$x9$ + 10$x10$ + 10$x11$ + 10$x12$ + 20$x13$ + 15$x14$

Table 3 summarizes that there are six supplements taken into consideration, these are carbs, protein, fat, calories, fiber, and iron. These six supplements are making a complete diet for a human in a day. Also, Table 1 is told about the consumption of all these six supplements. Table 2, is about fourteen different types of meals, that is, Egg, papaya, lentils, idly, cardamom, banana, milk, ragi porridge, fresh dates, dosa, almond, cottage cheese, curd and muskmelon were all taken into consideration in this study. Table 2 is also told about the cost of all the fourteen meals. Table 3 is the combination of Table 1 and Table 2.

Table 3. Menu contained the nutrients or the patients

Variable	$x1$	$x2$	$x3$	$x4$	$x5$	$x6$	$x7$	$x8$	$x9$	$x10$	$x11$	$x12$	$x13$	$x14$
Carbohydrates	6	4.7	30	1.1	12	12	18	32	6.1	8	7.1	15.6	5.33	8
Protein	18.3	3.5	2	13	3	8.14	1	13	6	25	7.2	2	0.17	0.8
Fat	27	3.3	0.5	11	0.1	8	0	1	14.2	1.2	2.4	5.1	0.03	0.2
Calories	265	4.7	119	72	58	122	105	354	164	147	37	133	20	34
Fiber	0	0	5	0	0.3	0	3.07	3	3.5	12	2	0.8	0.6	0.9
Iron	216	0.1	0.2	1.89	5	0	0.1	0.1	10	7.57	2.7	0	0.07	0.1

Subject to constrains:

6$x1$ + 4.7$x2$ + 30$x3$ + 1.1$x4$+ 12$x5$ + 12$x6$ + 18$x7$ + 32$x8$ + 6.1$x9$ + 8$x10$ + 7.1$x11$ + 15.6$x12$ + 5.33$x13$ + 8$x14$ ≥ 185

18.3$x1$ + 3.5$x2$+ 2$x3$ + 13$x4$ + 3$x5$ + 8.14$x6$ + $x7$ + 13$x8$ + 6$x9$ + 25$x10$ + 7.$x2x11$ + 2$x12$ + 0.17$x13$ + 0.8$x14$ ≥ 60

27$x1$ + 3.3$x2$ + 0.5$x3$ + 11$x4$ + 0.1$x5$ + 8$x6$ + $x8$ + 14.2$x9$ + 1.2$x10$ + 2.4$x11$ + 5.1$x12$ + 0.03$x13$ + 0.2$x14$ ≥ 50

$265x1 + 4.7x2 + 119x3 + 72x4 + 58x5 + 122x6 + 105x7 + 354x8 + 164x9 + 147x10 + 37x11 + 133x12 + 20x13 + 34x14 \geq 1800$

$5x3 + 0.3x5 + 3.07x7 + 3x8 + 3.5x9 + 12x10 + 2x11 + 0.8x12 + 0.6x13 + 0.9x14 \geq 35$

$216x1 + 0.1x2 + 0.2x3 + 1.89x4 + 5x5 + 0.1x7 + 0.1x8 + 10x9 + 7.57x10 + 2.7x11 + 0.07x13 + 0.1x14 \geq 20$

$q_1, q_2, q_3, \ldots, q_n$ & $x_1, x_2, x_3, \ldots, x_n$ represents same elements

As a visual help, Fig. 1 represents the process of working LINDO Software.

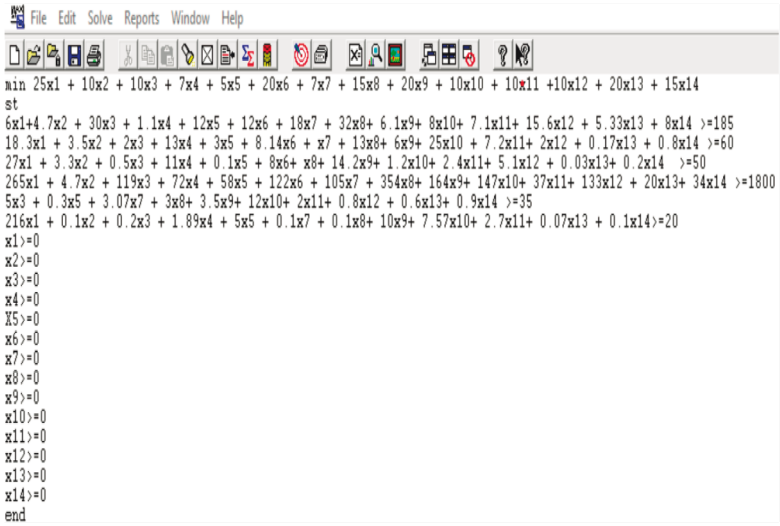

Figure 1. Process of working LINDO software

A single serving of each dish was allowed per day. The decision variables, restrictions, and parameters used in this investigation were numerous. This program was created in LINDO using LP Solve, and it took just one second to find the best solution for a one-day menu. Comparing this to alternative methods that would have required more than 4 hours or even a day, this is incredibly quick. Investigations carried out in the past have illustrated the effectiveness of the strategies in resolving this menu planning issue. These are a few sample problems that is resolved using the LINDO Software.

Lindo formulation

LINGO solution

Global optimal solution

Objective value: 109.3363

Infeasibilities: 0.000000

Total solver iteration: 6

Model class: LP

Total variable: 14

Nonlinear variable: 0

Total constraints: 20

Total variables: 14

Nonlinear variables: 0

Total constraints: 20

As a visual help Fig. 2 represents the optimum solution by using LINDO Software.

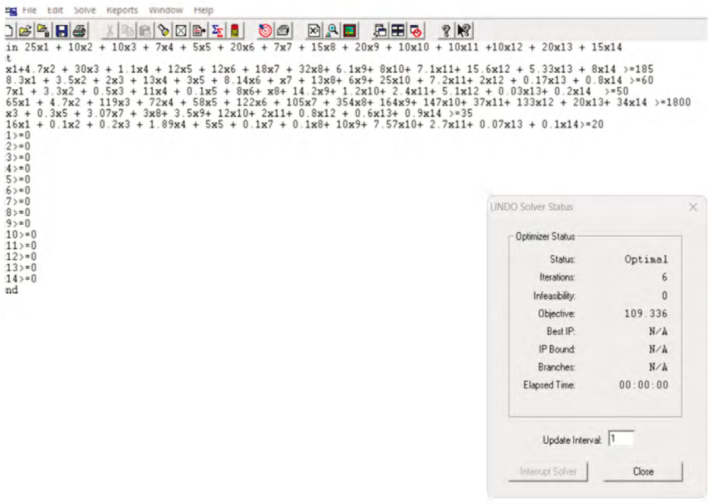

Figure 2. Optimum solution by using LINDO Software.

Using LINGO, an application of LINDO Software. Here are find a solution the problem of a diet plan of a person of a day. That is the objective value is 109.3363, Infeasibilities are 0.000000, Total solver iteration are 6, Model class is LP, Total variable is 14, Nonlinear variable is 0, Total constraints are 20, Total variables are 14, Nonlinear variables is 0 and the Total constraints are 20.

Figure 3 is an example of finding exact solution.

LP OPTIMUM FOUND AT STEP 6

OBJECTIVE FUNCTION VALUE

1) 109.3363

VARIABLE	VALUE	REDUCED COST
X1	0.015202	0.000000
X2	0.000000	7.525709
X3	2.600355	0.000000
X4	4.003656	0.000000
X5	0.000000	1.347327
X6	0.000000	11.460486
X7	0.000000	0.372815
X8	2.927621	0.000000
X9	0.000000	7.047612
X10	1.101280	0.000000
X11	0.000000	5.985193
X12	0.000000	1.648369
X13	0.000000	18.386141
X14	0.000000	12.417277

ROW	SLACK OR SURPLUS	DUAL PRICES
2)	0.000000	-0.173712
3)	63.117512	0.000000
4)	0.000000	-0.470173
5)	0.000000	-0.022079
6)	0.000000	-0.384239
7)	0.000000	-0.025057
8)	0.015202	0.000000
9)	0.000000	0.000000
10)	2.600355	0.000000
11)	4.003656	0.000000
12)	0.000000	0.000000
13)	0.000000	0.000000
14)	0.000000	0.000000
15)	2.927621	0.000000
16)	0.000000	0.000000
17)	1.101280	0.000000
18)	0.000000	0.000000
19)	0.000000	0.000000
20)	0.000000	0.000000
21)	0.000000	0.000000

NO. ITERATIONS= 6

RANGES IN WHICH THE BASIS IS UNCHANGED:

OBJ COEFFICIENT RANGES

VARIABLE	CURRENT COEF	ALLOWABLE INCREASE	ALLOWABLE DECREASE
X1	25.000000	47.881336	5.293648
X2	10.000000	INFINITY	7.525709
X3	10.000000	0.844178	3.661041
X4	7.000000	2.175130	4.989720
X5	5.000000	INFINITY	1.347327
X6	20.000000	INFINITY	11.460486
X7	7.000000	INFINITY	0.372815
X8	15.000000	2.650131	5.460338
X9	20.000000	INFINITY	7.047612
X10	10.000000	9.904737	4.535483
X11	10.000000	INFINITY	5.985193
X12	10.000000	INFINITY	1.648369
X13	20.000000	INFINITY	18.386141
X14	15.000000	INFINITY	12.417277

RIGHTHAND SIDE RANGES

ROW	CURRENT RHS	ALLOWABLE INCREASE	ALLOWABLE DECREASE
2	185.000000	62.793018	26.102392
3	60.000000	63.117512	INFINITY
4	50.000000	21.836929	42.488907
5	1800.000000	567.394531	724.040222
6	35.000000	5.107429	12.999310
7	20.000000	347.551483	3.211621
8	0.000000	0.015202	INFINITY
9	0.000000	0.000000	INFINITY
10	0.000000	2.600355	INFINITY
11	0.000000	4.003656	INFINITY
12	0.000000	0.000000	INFINITY
13	0.000000	0.000000	INFINITY
14	0.000000	0.000000	INFINITY
15	0.000000	2.927621	INFINITY
16	0.000000	0.000000	INFINITY
17	0.000000	1.101280	INFINITY
18	0.000000	0.000000	INFINITY
19	0.000000	0.000000	INFINITY
20	0.000000	0.000000	INFINITY
21	0.000000	0.000000	INFINITY

Figure 3. Finding exact solution.

Result

the findings are shown in Table 4 It lists the meals that the hospital administration will give the patients each day. Table 4 shows a variety of beverages and foods given in various forms for a single day, which covers six different meals. All of these provide hospital patients with the daily nutrition they need at a low cost. Therefore, it can be said that every meal picked is healthy and is suggested to be given to the patients. The whole cost is less than the management's allocated budget. Therefore, the hospital's administration will only pay around 200 rupees each day.

Table 4. Menu of per day

Food	Time
Papaya, milk and idly	Breakfast
Muskmelon	Morning tea
Egg, curd, lentils and ragi	Lunch
Spinach soup, almond	Evening tea
Dosa, cottage cheese	Dinner
Cardamom, banana, fresh dates	Supper

A complete and healthy diet is most important for every human on the earth, Table 4, is about menu of a day, according to this table, in breakfast, can be take, papaya, milk and idly. In morning tea, muskmelon can be taken, in lunch time, egg, curd, lentils and ragi can be eat. In evening tea, spinach soup, and almond can be taken. In dinner, can be eat dosa and cottage cheese and in super can be eat cardamom, banana, and fresh dates.

Conclusion

This article includes a useful per day diet that can serve as a manual for school administration. The foods provided in diverse way for six separate meals in a single day. These all affordably supply hospital patients with the daily nutrients they require. Consequently, it can be concluded that each meal chosen is healthful and should be served to the patients. The entire expenditure is less than the budget that the management set aside. LINDO software was used to solve the model. When compared to other methods of heuristics like biological algorithms, it yields a better result and satisfies all the study limitations. The participants in this study were hospital patients. Rs109.34 is the total cost for the day. As a result, we can provide the patients with slightly more expensive and higher-quality meals.

Declaration

Conflict of Interest: The authors report that there is no conflict of interest.

Funding: This research received no external funding.

Acknowledgement: None.

Data Availability: Data sharing not applicable to this article as no datasets were generated.

Ethical statement for human participant: Not applicable for this research.

References

1. J.L. Balintfy, A mathematical programming system for food management applications, *Interfaces,* **6**(1-part-2), 13-31 (1975). Doi: https://doi.org/10.1287/inte.6.1pt2.13

2. N.G. Khiêm, Q.M. Tuấn, L.N. An, T.T.T. Trà, Building a personalized diet proposal algorithm for Covid 19 patients' treatment at home with linear programming planning method, *VNU-HCM Journal of Engineering and Technology*, **5**(SI1), 56-61 (2022). Doi: https://doi.org/10.32508/stdjet.v5iSI1.991

3. N. Arkin, K. Krishnan, M.G. Chang, E.A. Bittner, Nutrition in critically ill patients with COVID-19: Challenges and special considerations, *Clinical Nutrition*, **39**(7), 2327-2328 (2020). Doi: https://doi.org/10.1016/j.clnu.2020.05.007

4. E.L. Ferguson, N. Darmon, A. Briend, I.M. Premachandra, Food-based dietary guidelines can be developed and tested using linear programming analysis, *The Journal of Nutrition*, **134**(4), 951-957 (2004). Doi: https://doi.org/10.1093/jn/134.4.951

5. J. Foytik, Devising and using a computerized diet: An exploratory study, *The Journal of Consumer Affairs*, **15**(1), 158-169 (1981). Doi: https://doi.org/10.1111/j.1745-6606.1981.tb00699.x

6. A. Hussain, B. Bhowmik, N.C. do Vale-Moreira, COVID-19 and diabetes: Knowledge in progress, *Diabetes Research and Clinical Practice*, **162**, 108142 (2020). Doi: https://doi.org/10.1016/j.diabres.2020.108142

7. M. Maillot, A. Drewnowski, A conflict between nutritionally adequate diets and meeting the 2010 dietary guidelines for sodium, *American Journal of Preventive Medicine*, **42**(2), 174-179 (2012). Doi: https://doi.org/10.1016/j.amepre.2011.10.009

8. H. Laarabi, A. Abta, K. Hattaf, Optimal control of a delayed SIRS epidemic model with vaccination and treatment, *Acta Biotheoretica*, **63**(2), 87-97 (2015). Doi: https://doi.org/10.1007/s10441-015-9244-1

9. R. Yadav, M. Sahu, Diet planning problems for diabetic patients by using mathematical modeling technique, *AIP Conference Proceedings*, **2800**, 020189 (2023). Doi: https://doi.org/10.1063/5.0169434

10. V.E. Smith, Linear programming models for the determination of palatable human diets, *American Journal of Agricultural Economics*, **41**(2), 272-283 (1959). URL: https://onlinelibrary.wiley.com/doi/10.2307/1235154

11. D. Sklan, I. Dariel, Diet planning for humans using mixed- integer linear programming, *British Journal of Nutrition*, **70**(1), 27-35 (1993). Doi: https://doi.org/10.1079/BJN19930102

12. R. Yadav, M. Sahu, Food intake pattern to achieve nutritional goals for Indian adults by linear programming optimization techniques, *International Journal of Health Sciences*, **16**(S2), 7346- 7352 (2022). Doi: https://doi.org/10.53730/ijhs.v6nS2.6858

13. R. Yadav, S. Wadia, Generalizing the effect of Indian populace with the help of mathematical modeling, *Journal of Physics: Conference Series*, **1531**, 012079 (2020). URL: https://iopscience.iop.org/article/10.1088/1742-6596/1531/1/012079/pdf

How to cite this article

R. Yadav, M. Sahu, A. Bala, S. Wadia, M. Rani, Food designing for Covid-19 patients with the help of applied mathematical optimization technique in LINDO software, *Rev. Colomb. Cienc. Quim. Farm.*, **53**(2), 522-536 (2024). https://doi.org/10.15446/rcciquifa.v53n2.114455

Artículo de revisión / https://doi.org/10.15446/rcciquifa.v53n2.114456

Nanopartículas: Un sistema de entrega de antifúngicos

Laura Estela Castrillón Rivera*, Alejandro Palma Ramos, Jorge Ismael Castañeda Sánchez, Violeta Espinosa Antúnez

Laboratorio de Inmunología, Departamento de Sistemas Biológicos, Universidad Autónoma Metropolitana Unidad Xochimilco, México

*Autora de correspondencia: lcrivera@correo.xoc.uam.mx

Recibido: 7 de septiembre de 2023
Revisado: 10 de abril de 2024
Aceptado: 13 de abril de 2024

Resumen

Introducción: El aumento en la incidencia de patologías en las que los hongos aparecen como patógenos emergentes, se asocia principalmente con hongos oportunistas así como con la susceptibilidad en pacientes con cierto grado de inmunodeficiencia debido a que presentan algunos factores de riesgo como son la neutropenia, diabetes, cirugías, abuso de tratamiento con antibióticos, enfermedades nosocomiales y pacientes transplantados entre otros. A la fecha la terapia antifúngica está muy lejos de ser ideal porque además de la resistencia a los antifúngicos, existe una limitación de su disponibilidad como consecuencia de su toxicidad, así como a la disminución de la efectividad del fármaco en forma libre, mínima penetración restringida a tejidos, disminución de la biodisponibilidad, pobre farmacocinética, falta de selectividad, efectos colaterales severos y baja solubilidad en agua: Por esta situación, se obliga a contar con nuevas medidas terapéuticas que sean eficientes para combatir principalmente a las micosis invasivas, de ahí el objetivo del presente trabajo de revisión para conocer el estado del arte de los diversos sistemas de entrega de antifúngicos. **Desarrollo del tema**: La presente revisión bibliográfica aborda los siguientes aspectos relacionados con: a) Tipos y estructura de los nanomateriales, b) Actividad antifúngica de nanopartículas y c) Evaluación in vivo y citotoxicidad de nanopartículas. **Conclusión:** El desarrollo de nuevas tecnologías y síntesis de nanomateriales surge como una posible alternativa para el tratamiento de las infecciones por hongos. En este este trabajo se presentan los principales avances relacionados con nanomateriales diseñados como un posible sistema de entrega de antifúngicos.

Palabras clave: Nanotecnología, nanomateriales, nanopartículas, antifúngicos.

Summary

Nanoparticles: A delivery system for antifungals

Introduction: The increase in the incidence of pathologies in which fungi appear as emerging pathogens is mainly associated with opportunistic fungi as well as susceptibility in patients with a certain degree of immunodeficiency because they present some risk factors such as neutropenia, diabetes, surgeries, abuse of antibiotic treatment, nosocomial diseases and transplant patients among others. To date, antifungal therapy is far from being ideal because in addition to resistance to antifungals, there is a limitation of their availability as a consequence of their toxicity, as well as the decrease in the effectiveness of the drug in free form, minimal restricted penetration. to tissues, decreased bioavailability, poor pharmacokinetics, lack of selectivity, severe side effects and low water solubility: Due to this situation, it is necessary to have new therapeutic measures that are efficient to combat mainly invasive mycoses, hence the objective of this review work to know the state of the art of the various antifungal delivery systems. **Development of the topic**: This bibliographic review addresses the following aspects related to: a) Types and structure of nanomaterials, b) Antifungal activity of nanoparticles and c) *In vivo* evaluation and cytotoxicity of nanoparticles. **Conclusion**: The development of new technologies and synthesis of nanomaterials emerges as a possible alternative for the treatment of fungal infections. In this work, the main advances related to nanomaterials designed as a possible delivery system for antifungals are presented.

Keywords: Nanotechnology, nanomaterials, nanoparticles, antifungals.

Resumo

Nanopartículas: um sistema de entrega antifúngico

Introdução: O aumento da incidência de patologias em que os fungos aparecem como patógenos emergentes está principalmente associado a fungos oportunistas bem como à suscetibilidade em pacientes com certo grau de imunodeficiência por apresentarem alguns fatores de risco como neutropenia, diabetes, cirurgias, abuso de tratamento com antibióticos, doenças nosocomiais e pacientes transplantados, entre outros. Até à data, a terapia antifúngica está longe de ser ideal porque além da resistência aos antifúngicos, existe uma limitação da sua disponibilidade em consequência da sua toxicidade, bem como a diminuição da eficácia do medicamento

na forma livre, penetração mínima restrita aos tecidos, diminuição da biodisponibilidade, má farmacocinética, falta de seletividade, efeitos colaterais graves e baixa solubilidade em água: Devido a esta situação, é necessário ter novas medidas terapêuticas que sejam eficientes para combater principalmente micoses invasivas, daí o objetivo deste revisar trabalhos para conhecer o estado da arte dos diversos sistemas de entrega de antifúngicos. **Desenvolvimento do tema:** Esta revisão bibliográfica aborda os seguintes aspectos relacionados a: a) Tipos e estrutura de nanomateriais, b) Atividade antifúngica de nanopartículas e c) Avaliação in vivo e citotoxicidade de nanopartículas. **Conclusão:** O desenvolvimento de novas tecnologias e síntese de nanomateriais surge como uma possível alternativa para o tratamento de infecções fúngicas. Neste trabalho são apresentados os principais avanços relacionados aos nanomateriais concebidos como um possível sistema de entrega de antifúngicos.

Palavras-chave: Nanotecnologia, nanomateriais, nanopartículas, antifúngicos.

Introducción

La nanotecnología es el estudio, diseño, creación, síntesis, manipulación y aplicación de materiales, aparatos y sistemas funcionales a través del control de la materia a nanoescala (de 1 a 100 nm) [1, 2]. Es una tecnología que manipula la estructura a nivel molecular de los materiales para cambiar sus propiedades intrínsecas y lograr comportamientos únicos, lo que ha permitido su aplicación en diversos campos industriales como son el de la construcción, electromecánica, alimentos, textil, farmacéutico y cosmético entre otros.

En el campo de la industria farmacéutica, esta tecnología tiene el potencial para optimizar los procesos industriales, crear productos innovadores y aportar soluciones a problemáticas críticas de solubilidad. Estos sistemas tienen como principal ventaja que mejoran los aspectos farmacológicos de las formulaciones convencionales, disminuyen sus efectos tóxicos y aumentan el tiempo de liberación y estabilidad porque pueden ser dosificados por diferentes vías de administración.

Los nanomateriales pueden tener diferentes tamaños, formas, naturaleza química y diferente procedencia. Estos pueden agruparse por varias categorías pero una de ellas depende de sus dimensiones, según lo siguiente [3]:

Nanomateriales de dimensión 0: Como son los fullerenos, nanopartículas metálicas como las de oro y plata, nanoarcillas, y "quantum-dots". Todas sus dimensiones se encuentran dentro de la nonoescala y se les considera como nanopartículas.

Nanomateriales unidimensionales 1D: Poseen solo dos dimensiones dentro de la nanoescala como son los nanotubos y las nanofibras de carbono, tienen la finalidad de mejorar la conductividad eléctrica en adhesivos y pinturas.

Nanomateriales bidimensionales 2D: Poseen tres dimensiones dentro de la nanoescala entre los que se encuentran como monocapas, películas multicapa y el grafeno.

Nanomateriales tridimensionales 3D: Son materiales nanoestructurados como los policristales, nanobolas, nanobobinas y nanoflores.

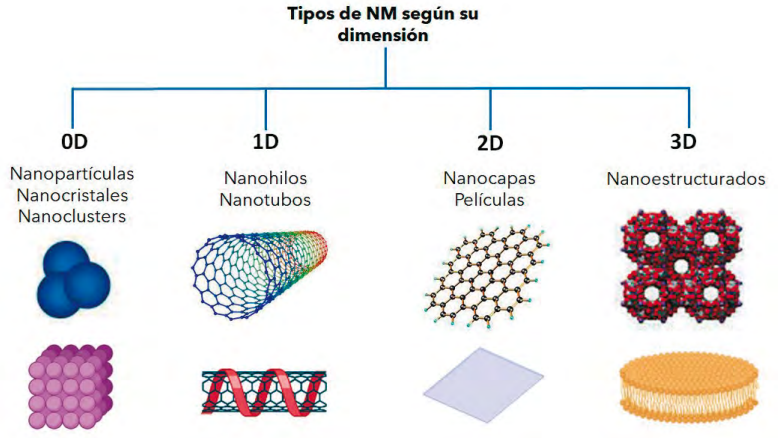

Figura 1. Clasificación de nanomateriales según su dimensión.

Fuente: Modificado de Estrada-Flores *et al.* (2023) [3].

Otra clasificación de las nanopartículas (NPs) y nanomateriales (NMs) se basa en propiedades como el área superficial, la composición química, la química de superficie, el tamaño de partícula, distribución, morfología, carga superficial, formación de aglomerados, agregados, estructura cristalina, o la solubilidad [4].

En base a estas características, la clasificación de las NPs depende de su composición química, dividiéndose en NPs orgánicas, NPs poliméricas, dendrímeros, liposomas y micelas, y NPs inorgánicas, partículas de oro, plata, óxido de hierro, sílice mesoporo y nanotubos de carbono.

Nanotransportadores

Existen aproximadamente 80 tipos de drogas antifúngicas que incluyen los polienos (anfotericina B), alilaminas, azoles (fluconazol, itraconazol, posaconazol etc.) análogos de pirimidina y equinocandinas (caspopungina, micafungina, anidulafungina) [5], sin

embargo, cada categoría tiene sus limitaciones relacionadas con su espectro de actividad, desarrollo de resistencia y toxicidad que en muchos casos está asociada con su baja solubilidad lo que puede manifestarse en una variedad de consecuencias no deseadas para la correcta administración de fármacos, afectando su biodisponibilidad, su liberación incompleta de la dosificación y la presencia de alta variabilidad de respuesta entre los pacientes.

Además del uso de las NPs mismas utilizadas como antifúngicos, la encapsulación de fármacos antimicóticos dentro de nanoestructuras utilizadas como vehículos de entrega, permite mejorar su solubilidad así como su actividad, tiempo de vida media, reducir sus efectos secundarios o adversos [5-9]. Por otra parte, la adición de antifúngicos a NPs puede beneficiar su eficacia porque aumenta su rugosidad y pueden generar daño mecánico en su célula blanco. Cuando los antifúngicos se encapsulan en NPs más que recubriéndolas se puede reducir su toxicidad como se ha demostrado con la Anfotericina B [10, 11].

Se han estudiado diferentes nanoestructuras (Figura 2) para la entrega de estos fármacos que pueden ser útiles para enfermedades de la piel y micosis sistémicas, entre los que se encuentran [8, 12, 13]: *i*) los sistemas de vesículas: liposomas, transferosomas, etosomas, transetosomas y niosomas, *ii*) Nanopartículas: NP poliméricas, NP metálicas, *iii*) nanopartículas lipídicas sólidas (SLNs) transportadores lipídicos nanoestructurados (NLCs), *iv*) nanoemulsiones, *v*) nanotubos de carbón, y *vi*) dendrímeros.

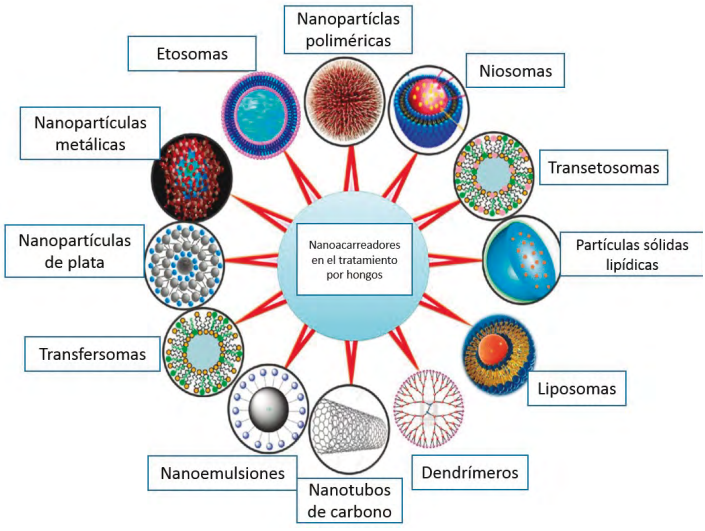

Figura 2. Nanotransportadores diseñados para el tratamiento antifúngico.

Fuente: Modificado de Vijay *et al.* (2021) [8].

Las principales formulaciones diseñadas como transportadores de antifúngicos se presentan en la Tabla 1.

Tabla 1. Antimicóticos evaluados como nanosistemas.

Nanoestructura	Mico	Eco	Keto	Clotr	Itrac	Fluc	Vori	Terb	Naft	Bute	Anfo	Nist	Sulc	Sert	Tebu	Nata	Anid	Tico
Niosomas	x	x	x	x	x	x			x			x						
SLN	x	x	x	x	x	x	x	x		x	x	x				x		
Microemulsiones	x	x	x	x	x	x	x		x									
Liposomas	x	x	x	x	x	x		x			x	x					x	
Nanoemulsiones	x	x	x									x	x					
Nanoesponjas	x	x		x														
Transferosomas	x			x	x						x							
NLC		x	x	x	x	x					x							
Etosomas		x		x		x	x				x							
Transetosomas		x					x											
Micelas poliméricas		x		x		x												
Spanlasticos			x	x	x	x					x							
Dendrímeros			x	x														
Emulgel polimérico				x		x								x				
Polimerosomas					x		x				x							
Nanopartículas sílica		x			x	x					x				x			
Microesponjas																		
Nanopartículas quitosán	x	x																x
Nanopartículas metálicas				x		x					x	x						
PLGA					x						x							

Mico: Miconazol, **Eco:** Econazol, **Keto:** Ketoconazol, **Clotr:** Clotrimazol, **Itrac:** Itraconazol, **Fluc:** Fluconazol, **Vori:** Voriconazol, **Terb:** Terbinafina, **Naft:** Naftifina, **Bute:** Butenafina, **Anfo:** Anfotericina B, **Nist:** Nistatina, **Sulc:** Sulconazol, **Sert:** Sertaconazol, **Tebu:** Tebuconazol, **Nata:** Natamicina, **Anid:** Anidulafungina, **Tico:** Ticonazol. Fuente: Younus *et al.* (2022) [10], Fernández-García *et al.* (2017) [11], Sousa *et al.* (2020) [14], Jangiou *et al.* (2022) [15], Du *et al.* (2021) [16].

Las características estructurales y funcionales de estas formulaciones son:

Liposomas:

Estas estructuras fueron los primeros nanotransportadores empleados en la clínica, son estructuras vesiculares de entre 50 y 100 nm compuestas de una doble capa de fosfolípidos como la fosfatidilcolina, fosfatidilglicerol, fosfatidiletanolamina y fosfatidilserina, ofrecen protección contra la degradación y una liberación sostenida, presentan

muy baja toxicidad, sin embargo tienen baja eficiencia en la encapsulación, se fusionan fácilmente con las membranas y presentan fuga de fármaco para evitar esta situación se ha incorporado colesterol en su superficie favoreciendo así su estabilidad. Además se ha utilizado el polietilenglicol (PEG) en su superficie para crear un escudo protector que prolonga el tiempo de vida media de estas estructuras en la circulación sanguínea, formando una capa de hidratación que retrasa el reconocimiento y captura por el sistema reticuloendotelial [17]. Se pueden sintetizar liposomas multilaminares resultado liposomas de diferentes tamaños de 20 a 300 nm, existe una relación directa entre el nivel de penetración de los liposomas y su tamaño, penetrando más cuanto menor sea su tamaño [18]. Se ha reportado que para los antifúngicos como croconazol, econazol, fluconazol, ketoconazol, hidrocloruro de terbinafina, tolnaftato y miconazol atrapados en nanoliposomas mejoran la penetración en piel y sus efectos biológicos [19].

Transferosomas

Son vesículas elásticas ultra-deformables y biocompatibles elaboradas con fosfolípidos naturales y surfactantes no iónicos. Debido a su estructura pueden "cargar" tanto moléculas hidrosolubles como liposolubles, tienen una alta velocidad de flujo y penetración a través de la piel [20].

Etosomas

Son vesículas suaves, no invasivas, maleables que permiten diseminar el fármaco en la circulación sanguínea y las capas profundas de la piel, están compuestas de lípidos, etanol (10-50%) y agua. Cuando las concentraciones de alcohol son altas, le confiere una carga negativa a la vesícula, reduciendo su tamaño y favoreciendo la biodisponibilidad terapéutica del fármaco [21].

Transetosomas

Son una combinación de transferosomas y etosomas ya que contienen fosfolípidos y alta concentración de alcohol (30-40%), emulsificantes y agua. Esta composición debilita la bicapa lipídica aumentando su deformabilidad y reduciendo la tensión interfacial favoreciendo la permeabilidad en piel por la capacidad del alcohol a intercalarse en los lípidos intercelulares aumentando la fluidez de los lípidos y disminuyendo la densidad de la capa lipídica. Se ha desarrollado una formulación con voriconazol demostrando su actividad contra *Candida albicans*, *Aspergillus flavus* y *Aspergillus fumigatus* [22].

Niosomas

Son liposomas compuestos de surfactantes de cadena simple en combinación con colesterol, son no tóxicos, biodegradables y estables forman una bicapa en medio acuoso que resultan en la liberación controlada del fármaco. Estos sistemas pueden acarrear

moléculas lipofílicas e hidrofílicas. Pueden dosificarse por vía parenteral, oral y tópica. La revisión en la literatura demuestra las ventajas de los niosomas en la entrega de antifúngicos con superioridad sobre otros sistemas de nanotransportadores [23].

Nanopartículas poliméricas

Son estructuras sólidas con propiedades coloidales de tamaño de 10-1000 nm, el fármaco se distribuye en la matriz por lo que puede ser liberado se manera sostenida. Las NPs poliméricas que se forman por cadenas de estructuras químicas idénticas llamadas monómeros que pueden ser de origen natural o sintético como son el alginato, quitosano, PGLA (ácico glicólico/ácido láctico) o por PLC (policaprolactonas) lo que les permite ser biocompatibles y biodegradables [24].

La superficie de las NPs poliméricas también es el lugar para la conjugación de ligandos, con el objetivo de apuntar a receptores específicos de tejidos y órganos. La modificación de la superficie de las NPs, con proteínas específicas, anticuerpos y otras biomoléculas, se puede utilizar para diseñar fármacos que actúen selectivamente en tejidos particulares.

El tamaño de las NPs poliméricas utilizadas como sistemas de administración de fármacos debe ser lo suficientemente grande (diámetro de ~ 100 nm) para evitar su escape rápido de los capilares sanguíneos y la filtración renal, pero lo suficientemente pequeño (NP < 50 nm) para evitar la eliminación por el sistema de fagocitos mononucleares [6].

Nanopartículas metálicas

La actividad antimicrobiana de metales como plata (Ag), cobre (Cu), oro (Au), titanio (Ti), y zinc (Zn), cada uno con varias propiedades, mecanismos y espectros de acción, ha sido utilizada desde hace siglos [25]. Son las nanoestructuras mejor evaluadas ya que presentan propiedades ópticas, magnéticas y catalíticas únicas, la morfología y tamaño son muy importantes dependiendo de la aplicación final, formadas principalmente por oro (AuNPs), plata (AgNPs), cobre (CuNPs), titanio (TiNPs), níquel (Ni/NiONPs), óxido de silicio (SiO_2NPs) y hierro (Fe_2O_3)NPs), entre otras [26]. Las NPs metálicas se han propuesto para la liberación intracelular de fármacos. Su superficie puede ser funcionalizada con anticuerpos o fármacos para promover el reconocimiento, permanencia y acumulación de estos sistemas en el órgano blanco. Adicionalmente, puede ser posible dirigirlas a un órgano o tejido determinado por acción de un campo magnético exterior, para quedar desmagnetizadas una vez que el campo sea retirado.

Nanopartículas lipídicas sólidas (SLN)

Son una forma alternativa en la administración de fármacos lipofílicos con acción de liberación sostenida, están compuestas de lípidos en fase sólida a temperatura ambiente

y de surfactantes para su emulsificación, tienen una capacidad de carga limitada, son biodegradables y con buena tolerancia. Se han utilizado para los antimicóticos azoles que son extremadamente insolubles en agua y susceptibles a la degradación por oxidación e hidrólisis lo que limita su biodisponibilidad y por tanto su efecto. Al tener lípidos conjugados con fármacos es factible cargar tanto moléculas hidrofílicas como lipofílicas [12].

Transportadores lipídicos nanoestructurados (NLCs)

La adición de lípidos líquidos en los que el fármaco es más soluble genera nuevos sistemas nanoestructurados conocidos como transportadores lipídicos nanoestructurados, están compuestos de lípidos fisiológicamente compatibles, agua y agentes emulsificantes/surfactantes/cosurfactantes como aceites (cetiol V, aceite de coco), lípidos sólidos como cera de abeja, ácido palmítico), contraiones (hexaedecil fosfato, monodecil fosfato y como agentes emulsificantes (lecitina de huevo, alcohol polivinílico). La presencia de la mezcla de lípidos genera una estructura amorfa que mejora la capacidad de carga de fármacos lipofílicos.

Nanoemulsiones

Son partículas que transportan fármacos con arreglos moleculares coloidales de tamaños de 10 a 1000 nm. El fármaco liposoluble se incorpora en la fase oleosa o en la interface aceite-agua. Pueden ser gotas de lípidos de tamaño submicrónico (20-200 nm) con baja tensión superficial, estabilizadas con surfactantes que previenen la acumulación y coalescencia en una solución acuosa. Sus ventajas permiten aumentar la velocidad de absorción, ayudan a solubilizar fármacos liposolubles y pueden ser administrados por varias rutas aumentando la biodisponibilidad, son termodinámicamente estables, reducen la dosificación frecuente y los efectos adversos. Sin embargo se ha visto que expulsan el fármaco debido a reacomodo de lípidos durante su almacenamiento. Recientemente se ha reportado la actividad de estas nanoemulsiones con anfotericina B contra biopelículas del patógeno emergente *Candida auris* sugiriendo su posible uso terapéutico [27].

Nanotubos de carbono (NTCs)

Existen diferentes tipos de NTC's en función de las capas de grafito que los forman, pueden ser nanotubos de carbono de pared sencilla (SWCN T"s por sus siglas en inglés) y nanotubos de carbono de pared múltiple (M'h'CNT 's) que pueden considerarse como capas de láminas de grafito enrolladas concéntricamente donde cada átomo de carbono está unido con otros tres mediante hibridación.

Algunos fármacos a base de proteínas necesitan ser administrados vía intravenosa ya que por vía oral el pH del estómago no es favorable para la biodistribución del fármaco. Este problema, ha servido de base en investigaciones donde los NTC's transportan este tipo de fármacos dentro de las célula. Tienen excelentes propiedades que pueden ser modificadas mediante la funcionalización química. Una de las propiedades físicas a modificar es su dispersión, lo que ayuda a que sus aplicaciones biológicas y médicas [28].

Dendrímeros

Los dendrímeros son un tipo de macromoléculas poliméricas de tamaño nanométrico que se caracterizan por presentar una estructura muy bien definida, con baja polidispersidad y un exterior multivalente con posibilidad de funcionalización. Son nanoestructuras obtenidas empleando macromoléculas como la poliamidoamina (PAMAM), polipropilenimina y poliaril-éter. Son ampliamente ramificadas con un núcleo interno. Su tamaño va de 1-100 nm. Tienen un índice de polidispersabilidad, múltiples sitios de unión, tamaño bien definido y su estructura puede modificarse fácilmente para cambiar sus propiedades. Los dendrímeros son eficientes como transportadores de fármacos antimicóticos pero también muestran acción antifúngica *per se*. Se han evaluado tioconazol, nistatina, triclosan, terbinafina, anfotericina B, itraconazol, clotrimazol y griseofluvina [29].

A la fecha, los principales reportes en donde se han desarrollado nanomateriales como transportadores de antifúngicos se han evaluado en diversos microorganismos de interés en la clínica humana y veterinaria así como en hongos fitopatógenos. La mayor parte de los estudios se han realizado con liposomas y nanopartículas metálicas como AgNPs, AuNPs, ZnONPs, CuNPs. La aparición de nuevos nanosistemas genera numerosos reportes de su actividad biológica en donde se calculan la concentración mínima inhibitoria ($MIC_{100,}$ $MIC_{50,}$ MIC_{90} o MIC_{80} mg/mL) y la concentración mínima fungicida (MFC), su actividad sobre biopelículas maduras o su capacidad de inhibición de su formación, actividad citotóxica y los posibles mecanismos de acción entre otras. Las especies fúngicas más reportadas se encuentran *Candida* y *Aspergillus*.

Actividad antifúngica de nanopartículas

Las nanopartículas presentan un mecanismo de acción totalmente diferente a los antibióticos tradicionales, proporcionando así una nueva alternativa ante la creciente resistencia y aunque la actividad antimicrobiana se ha descrito ampliamente en bacterias [30, 31], sus propiedades pueden hacerlas útiles como agentes antimicóticos y su efectividad no solo depende de su estructura sino del tipo de patógeno contra el cual están formuladas (Tabla 2) [15].

Tabla 2. Especies fúngicas donde se han evaluado diversos nanomateriales utilizados como transportadores de antifúngicos [5, 7, 15, 16, 19, 32, 33]

Género	Especies
Candida	*Candida albicans*, *Candida glabrata*, *Candida parapsilosis*, *Candida tropicalis*, *Candida krusei*, *Candida dubliniensis*, *Candida auris*, *Candida guillermondi*
Aspergillus	*Aspergillus flavus*, *Aspergillus fumigatus*, *Aspergillus terrus*, *Aspergillus niger*, *Aspergillus brasiliensis*, *Aspergillus oryzae*, *Aspergillus aculeatus*, *Aspergillus nidulans*, *Aspergillus ochraceus*
Fusarium	*Fusarium solani*, *Fusarium moniliforme*, *Fusarium oxysporum*, *Fusarium equistei*, *Fusarium graminearum*, *Fusarium culmorum*, *Fusarium poae*
Trichosporon	*Trichosporon beigelii*, *Trichosporon asahii*
Trichophyton	*Trichophyton rubrum*, *Trichopyton mentagrophytes*, *Trychopyton tonsurans*
Saccharomyces	*Saccharomyces cerevisiae*, *Saccharomyces boulardii*
Cryptococcus	*Cryptococcus neoformans*, *Cryptococcus gatti*
Microsporum	*Mycrosporus canis*, *Mycrosporum gypseum*
Penicillum	*Penicillum chrysogenum*, *Penicillum notatum*, *Penicillum expansum*, *Penicillum herquet*, *Penicillum expansum*, *Penicillum brevicompactum*
Malassezia	*Malassezia furfur*, *Malassezia pachydermatis*
Alternaria	*Alternaria alternate*, *Alternaria solani*
Cladosporium	*Cladiosporium cladosporioides*, *Cladosporium herbarum*
Otros	*Sporothrix schenkii*, *Paracoccidioides brasiliensis*, *Botrys cinerea*, *Mucor plumbeus*, *Bipolaris sorokiniana*, *Chaetomium globosum*, *Magnaporthe grisea*, *Motierella alpine*, *Rizoctonia solani*, *Stachbotrys chartarum*, *Corticum salmonicolor*, *Puccinia grammis tritci*, *Curvularia lunata*, *Botrytis cinereal*, *Rhizopus solonifer*, *Erythricium salmonicolor*, *Phythium debaryanum*, *Trichoderma harzianum*, *Sclerotium rolfsii*, *Trichotecium roesum*, *Issaechenkia orientali*

El tratamiento con NPs cargadas con antifúngicos ha demostrado ser efectivo en contraste con los antifúngicos utilizados en forma libre, ya que son capaces de mostrar capacidad citotóxica hacia hifas o levaduras y que se requieren de concentraciones bajas para alcanzar el mismo efecto.

La exposición de NPs en la pared celular del hongo produce la reducción de su superficie por encogimiento, agregación celular, formación de marcas y poros y deformación en general. Las NPs se incrustan en la pared celular durante la adsorción, las membranas internas sufren distorsión, con deposito alterado de organelos (aumentan las vesículas y vacuolas y disminuye su contenido citoplásmico).

Los principales mecanismos asociados con la actividad antimicrobiana de NPs son [32, 33]: *i*) estrés oxidativo: Las NP atraviesan la membrana y al interior celular ocurre un desbalance oxidativo elevando la concentración de radicales libres de oxígeno (ROS) y con ello el daño a la membrana y ácidos nucléicos ocasionando con la muerte celular; *ii*) iones metálicos: son liberados por las NPs y absorbidos por las membranas celulares ocasionando una alteración del pH y con ello los grupos funcionales modificando la actividad enzimática y cambios estructurales que resultan en daños fisiológicos; y, *iii*) mecanismos no oxidativos: como son la disminución en el metabolismo energético de aminoácidos, carbohidratos y nucleótidos por desregulación enzimática.

Evaluación *in vivo* de formulaciones antifúngicas con nanosistemas

La evaluación de nanosistemas con antimicóticos se ha realizado principalmente en modelos animales (murinos, rata, cobayo o conejo) para candidiasis, aspergilosis, coccidioidomicosis, mucormicosis y criptococosis [34, 35], siendo las NPs metálicas y los liposomas los mejor estudiados.

Para el caso de los reportes en humanos se han presentado con las formulaciones con anfotericina B complejo lipídico de anfotericina B (ABLC), dispersión coloidal de anfotericina B (ABCD), deoxicolato de anfotericina B (D-AmB) o anfotericina B liposomal (L-AmB) las cuales son las únicas que están disponibles en forma comercial como Fungizone®, Abelcet®, AmBisome®, Amphocil/Ampotec® [11, 14, 16, 36].

Citotoxicidad de nanopartículas

La comprensión de las propiedades de las NPs y su efecto sobre el organismo es crucial antes de su uso clínico, por tanto, la toxicidad debe ser considerada como un factor crítico que para evaluar su uso potencial [37, 38].

La toxicidad es inversamente proporcional al tamaño de las NPs porque se ha demostrado que las de menor tamaño son más tóxicas aún en concentraciones bajas, esto se debe a que tienen mayor área superficial y permite que más moléculas se expongan y por tanto, al haber mayor interacción celular se intensifica su efecto biológico pero también se pueden alcanzar concentraciones que resulten en daño celular, además existe una mayor captación transcelular a través de los epitelios [39].

La actividad y citotoxicidad de las NPs pueden afectar su comportamiento en entornos biológicos, por ejemplo, las NPs biodegradadas y pequeñas causan endocitosis sin dañar la pared celular del hongo, pueden acumularse dentro de la célula y ocasionar cambios intracelulares como alteración de la integridad de los organelos o del genoma [40], esto depende de la toxicidad intrínseca de NPs asociada con su tamaño, forma, área superficial, hidrofobicidad, grado de agregación, rugosidad, composición, partícu-

las utilizadas para su recubrimiento, liberación de la eficiencia de los iones que las forman, tipo de agentes reductores utilizados y el proceso sintético de origen entre otras.

Se ha demostrado la capacidad citotóxica de las nanopartículas de plata (Ag NPs) en diferentes líneas de mamífero reportando un elevado porcentaje de muerte sobre las células humanas THP-1 ("Human leukemia monocytic cell"), MCF7 ("breast cancer cell"), y en las células VERO (riñón de mono), MRC5 ("human fetal lung fibroblast *cells"*), HUVECs ("Human umbilical vein endotelial cells") y CHO ("Chinese hamster ovary cells") demostrando la inhibición de su crecimiento en diferentes porcentajes evitando con ello su uso para la terapéutica por lo que su aplicación clínica aún requiere de mayores estudios [5].

En los últimos años se han reportado los efectos toxicológicos, ecotoxicológicos y genotóxicos de los nanomateriales principalmente en modelos animales y en plantas, lo que genera riesgos potenciales para la salud, la agricultura y para el ambiente. Esta situación ha generado el desarrollo de una nueva disciplina científica denominada nanotoxicología [41].

Se debe reconocer que los estudios de toxicología convencional no aplican para las nanopartículas debido a sus propiedades particulares de estos materiales porque en la actualidad no se cuenta con metodologías estandarizadas que permitan conocer su distribución, eliminación y efectos colaterales asociados con su uso así como su efecto en el ambiente.

El conocimiento de los mecanismos involucrados, los efectos de la acumulación de estos materiales dependiente de su uso a largo plazo y la relación dosis-respuesta aún es desconocida, por tanto, estos nuevos materiales deben ser evaluados de manera exhaustiva que aseguren su inocuidad y actividad y en caso de presentarse efectos adversos contar con alternativas de tratamiento.

Conclusión

El desarrollo de nuevas tecnologías y síntesis de nanomateriales surge como una posible alternativa para el tratamiento de las infecciones por hongos, debido a que el principal objetivo de los sistemas nanoestructurados consiste en la reducción de los efectos indeseables que están relacionados con los sistemas farmacéuticos convencionales y que gracias a sus propiedades fisicoquímicas, permiten ya sea por la composición de sus componentes iónicos los cuales poseen capacidad citotóxica, o bien, sean utilizados como transportadores de fármacos antifúngicos controlando en consecuencia, un sistema de entrega de drogas que puede mejorar el tratamiento de las micosis sin alterar la

calidad de vida del paciente [12]. Sin embargo, como en el caso de todas las nuevas tecnologías, se deben realizar estudios profundos sobre el posible impacto en la salud que podrá tener la implementación de estas nuevas tecnologías antes de ser comercializadas [42].

Conflicto de intereses

Los autores del estudio manifestamos no presentar ningún conflicto de interés.

Referencias

1. C.G. Lizarazo-Salcedo, E.E. González-Jiménez, C.Y. Arias-Portela, J. Guaraguati-Ariza, Nanomateriales: un acercamiento a lo básico, *Medicina y Seguridad del Trabajo*, **64**(251), 109-118 (2018). URL: https://scielo.isciii.es/scielo.php?script=sci_abstract&pid=S0465-546X2018000200109

2. F. Diaz del Castillo-Rodríguez, *Lecturas de Ingeniería 20. Introducción a los nanomateriales*, Facultad de Estudios Superiores Cuautiltán Izcalli, UNAM, México, 2012, 82 p. URL: http://olimpia.cuautitlan2.unam.mx/pagina_ingenieria/mecanica/mat/mat_mec/m6/Introduccion%20a%20los%20nanomateriales.pdf

3. S.L. Estrada-Flores, C. García-Morales, C.M. Pérez-Berumen, L. Cantu-Sifuentes, Nanomateriales conceptos, aplicacion en nanoterapia y regulaciones, *Química Viva*, **22**(1), E0242 (2023). URL: http://www.quimicaviva.qb.fcen.uba.ar/v22n1/E0242.html

4. T.P.J. Linsinger, G. Roebben, C. Solans, R. Ramsch, Reference materials for measuring the size of nanoparticles, *TrAC Trends in Analytical Chemistry*, **30**(1), 18-27 (2011). Doi: https://doi.org/10.1016/j.trac.2010.09.005

5. T. Huang, X. Li, M. Maier, N.M. O'Brien-Simpson, D.E. Heath, A.J. O'Connor, Using inorganic nanoparticles to fight fungal infections in the antimicrobial resistant era, *Acta Biomaterialia*, **158**, 56-79 (2023). Doi: https://doi.org/10.1016/j.actbio.2023.01.019

6. S. Onoue, S. Yamada, H.-K. Chan, Nanodrugs: pharmacokinetics and safety, *International Journal of Nanomedicine*, **9**, 1025-1037 (2014). Doi: https://doi.org/10.2147/IJN.S38378

7. S. Nami, A. Aghebati-Maleki, L. Aghebati-Maleki, Current applications and prospects of nanoparticles for antifungal drug delivery, *EXCLI Journal*, **20**, 562-584 (2021). Doi: https://doi.org/10.17179/excli2020-3068

8. M. Vijay, M. Singh, Y. Mishra, N. Charbe, P. Nayak, K. Sudhakar, A.A. Aljabali, H.S. Shahcheraghi, H. Bakshi, A. Serrano-Aroca, *et al.*, Nanoarchitectures in management of fungal diseases: An overview, *Applied Sciences*, **11**(15), 7119 (2021). Doi: https://doi.org/10.3390/app11157119

9. S. Alcalá-Alcalá, D. Quintanar-Guerrero, La terapia a nanoescala: ensamble de estructuras liberadoras de fármacos, *Mundo Nano*, **7**(12), 32-48 (2014). URL: https://www.scielo.org.mx/pdf/mn/v7n12/2448-5691-mn-7-12-32.pdf

10. I. Younus, J.S. Khan, S. Maqbool, Z. Begum, Antifungal therapy via incorporation of nanostructures: A systematic review for new dimensions, *Physica Scripta*, **97**, 012001 (2022). Doi: https://doi.org/10.1088/1402-4896/ac445d

11. R. Fernández-García, E. de Pablo, M.P. Ballesteros, D.R. Serrano, Unmet clinical needs in the treatment of systemic fungal infections: The role of amphotericin B and drug targeting, *International Journal of Pharmaceutics*, **525**(1), 139-148 (2017). Doi: https://doi.org/10.1016/j.ijpharm.2017.04.013

12. L.E. Castrillón-Rivera, A. Palma-Ramos, Actividad antimicótica de nanopartículas, *Mundo Nano*, **7**(12), 6-18 (2014). URL: http://www.mundonano.unam.mx/ojs/index.php/nano/article/view/49099/44150

13. S. Vermaa, P. Utrejab, Vesicular nanocarrier based treatment of skin fungal infections: Potential and emerging trends in nanoscale pharmacotherapy, *Asian Journal of Pharmaceutical Sciences*, **14**(2), 117-129 (2019). Doi: https://doi.org/10.1016/j.ajps.2018.05.007

14. F. Sousa, D. Ferreira, S. Reis, P. Costa, Current insights on antifungal therapy: Novel nanotechnology approaches for drug delivery systems and new drug from natural sources, *Pharmaceuticals*, **13**(9), 248 (2020). Doi: https://doi.org/10.3390/ph13090248

15. A. Jangjou, Z. Zareshahrabadi, M. Abbasi, A. Talaiekhozani, H. Kamyab, S. Chelliapan, A. Vaez, A. Golchin, L. Tayebi, E. Vafa, *et al.*, Time to conquer fungal infectious diseases: Employing nanoparticles as powerful and versatile antifungal nanosystems against a wide variety of fungal species, *Sustainability*, **14**(19), 12942 (2022). Doi: https://doi.org/10.3390/su141912942

16. W. Du, Y. Gao, L. Liu, S. Sai, C. Ding, Striking back against fungal infections: The utilization of nanosystems for antifungal strategies, *International Journal of Molecular Sciences*, **22**(18), 10104 (2021). Doi: https://doi.org/10.3390/ijms221810104

17. M.L. Immordino, F. Dosio, L. Cattel, Stealth liposomes: Review of the basic science, rationale and clinical applications, existing and potential, *International Journal of Nanomedicine*, **1**(3), 297-315 (2006). URL: https://www.tandfonline.com/doi/pdf/10.2147/DIJN.1.S633

18. A. Jersoka, O. Orwar, Liposomes: Technologies and analytical applications, *Annual Review of Analytical Chemistry*, **1**, 801-832 (2008). Doi: https://doi.org/10.1146/annurev.anchem.1.031207.112747

19. P. Asadi, A. Mehravaran, N. Soltanloo, M. Abastabar, J. Akhtari, Nanoliposome-loaded antifungal drugs for dermal administration: A review, *Current Medical Mycology*, **7**(1), 71-78 (2021). Doi: https://doi.org/10.18502/cmm.7.1.6247

20. B. Das, K.A. Nayak, S. Mallick, Chapter 7: Transferosomes: a novel nanovesicular approach for drug delivery, en: A.K. Nayak, M.S. Hasnain, T.M. Aminabhavi, V.P. Torchilin (editores), *Systems of Nanovesicular Drug Delivery*, Academic Press, 2022, pp. 103-114. Doi: https://doi.org/10.1016/B978-0-323-91864-0.00022-X

21. M.K. Bhalaria, S. Naik, A.N. Misra, Ethosomes: a novel delivery system for antifungal drugs in the treatment of topical fungal diseases, *Indian Journal of Experimental Biology*, **47**(5), 368-375 (2009). URL: https://nopr.niscair.res.in/bitstream/123456789/4209/1/IJEB%2047%285%29%20368-375.pdf

22. M. Farooq, F. Usman, S. Zaib, S.H. Shah, Q.A. Jamil, F.A. Sheikh, A. Khan, S. Rabea, S.A.A. Hagras, G.E.-S. Batiha, *et al.*, Transethosomes for enhancing antifungal and antileishmanial activity, *Molecules*, **27**(10), 3347 (2022). Doi: https://doi.org/10.3390/molecules27103347

23. M. Osanloo, S. Assadpour, A. Mehravaran, M. Abastabar, J. Akhtari, Niosome-loaded antifungal drugs as an effective nanocarrier system: A mini review, *Current Medical Mycology*, **4**(4), 31-36 (2018). Doi: https://doi.org/10.18502/cmm.4.4.384

24. S. Wu, W. Guo, B. Li, H. Zhou, H. Meng, J. Sun, R. Li, D. Guo, X. Zhang, R. Li, W. Qu, Progress of polymer-based strategies in fungal disease management: Designed for different roles, *Frontiers in Cellular and Infection Microbiology*, **13**, 1142029 (2023). Doi: https://doi.org/10.3389/fcimb.2023.1142029

25. C. Malarkodi, S. Rajeshkumar, K. Paulkumar, M. Vanaja, G. Gnanajobitha, G. Annadurai, Biosynthesis and antimicrobial activity of semiconductor nanoparticles against oral pathogens, *Bioinorganic Chemistry and Applications*, **2014**, 347167 (2014). Doi: https://doi.org/10.1155/2014/347167

26. M.K. Gregorio-Jáuregui, J.E. Rivera-Salinas, H. Saade-Caballero, G.R. López-Campos, L.J. Martínez-Hernández, A. Ilina, *Las nanopartículas magnéticas y sus múltiples aplicaciones*, Universidad Autónoma de Coahuila, México, pp. 397-411. URL: https://ciqa.repositorioinstitucional.mx/jspui/bitstream/1025/494/1/Las%20nanopart%C3%ADculas%20magn%C3%A9ticas%20y%20sus%20m%C3%BAltiples%20aplicaciones.pdf

27. G.D. Marena, A. Ruiz-Gaitán, V. Garcia-Bustos, M.A. Tormo-Mas, J.M. Pérez-Royo, A. López, P. Bernarbe, M.D. Pérez Ruiz, L. Zaragoza-Macian, C. Vicente-Saez, *et al.*, Nanoemulsion increases the antifungal activity of Amphotericin B against four *Candida auris* clades: *In vitro* and *in vivo* assays, *Microorganisms*, **11**(7), 1626 (2023). Doi: https://doi.org/10.3390/microorganisms110716264

28. M.L. Andrade-Cuel, L.I. López-López, A. Sáenz-Calindo, Nanotubos de carbono: funcionalización y aplicaciones biológicas, *Revista Mexicana de Ciencias Farmacéuticas*, **43**(3), 9-18 (2012). URL: https://www.scielo.org.mx/pdf/rmcf/v43n3/v43n3a2.pdf

29. T.D. Mlynarczyk, J. Dlugaszewska, A. Kaluzna-Mlynarczyk, T. Goslinski, Dendrimers against fungi - A state of the art review, *Journal of Controlled Release*, **330**, 599-617 (2021). Doi: https://doi.org/10.1016/j.jconrel.2020.12.021

30. L. Wang, C. Hu, L. Shao, The antimicrobial activity of nanoparticles: present situation and prospects for the future, *International Journal of Nanomedicine*, **12**, 1227-1249 (2017). Doi: https://doi.org/10.2147/IJN.S121956

31. J.Y. Slavin, J. Asnis, U.O. Hafeli, H. Bach, Metal nanoparticles: understanding the mechanisms behind antibacterial activity, *Journal of Nanobiotechnology*, **15**, 65 (2017). Doi: https://doi.org/10.1186/s12951-017-0308-z

32. M. Nagpal, M. Kaur, Nanomaterials for skin antifungal therapy: An updated review, *Journal of Applied Pharmaceutical Science*, **11**(Supp 1), 15-25 (2021). Doi: https://doi.org/10.7324/JAPS.2021.11s102

33. A.R. Cruz-Luna, H. Cruz-Martínez, A. Vásquez-López, D.I. Medina, Metal nanoparticles as novel antifungal agents for sustainable agriculture: Current advances and future directions, *Journal of Fungi*, **7**(12), 1033 (2021). Doi: https://doi.org/10.3390/jof7121033

34. M.A. Hady, A.B. Darwish, M.S. Abdel-Aziz, O.M. Sayed, Design of transfersomal nanocarriers of nystatin for combating vulvovaginal candidiasis; A different prospective, *Colloids and Surfaces B: Interfaces*, **211**, 112304 (2022). Doi: https://doi.org/10.1016/j.colsurfb.2021.112304

35. L.A. Buitimea, J.A. Garza-Cervantes, D.Y. Gallegos-Alvarado, M. Osorio-Concepción, J.R. Morones-Ramirez, Nanomaterial-based antifungal therapies to combat fungal diseases aspergillosis, coccidioidomycosdis, mucormycosis, and candidiasis, *Pathogens*, **10**(10), 1303 (2021). Doi: https://doi.org/10.3390/pathogens10101303

36. A. Voltan, G. Quindós, K. Alarcón, A.M. Fusco-Almeida, M.J. Mendes-Giannini, M. Chorilli, Fungal diseases: Could nanostructured drug delivery be a novel paradigm for therapy? *International Journal of Nanomedicine*, **11**, 3715-3730 (2016). Doi: https://doi.org/10.2147/IJN.S93105

37. Y.N. Slavin, H. Bach, Mechanisms of antifungal properties of metal nanoparticles, *Nanomaterials* (Basel), **12**(24), 4470 (2022). Doi: https://doi.org/10.3390/nano12244470

38. A.C.O. Souza, A.C. Amaral, Antifungal therapy of systemic mycosis and the nanobiotechnology era: Improving efficacy, biodistribution and toxicity, *Frontiers in Microbiology*, **8**, 336 (2017). Doi: https://doi.org/10.3389/fmicb.2017.00336

39. R.A. Petros, J.M. Desimone, Strategies in the design of nanoparticles for therapeutic applications, *Nature Reviews Drug Discovery*, **9**(8), 615-627 (2010). Doi: https://doi.org/10.1038/nrd2591

40. N. Lewinski, V. Colvin, R. Drezek, Cytotoxicity of nanoparticles, *Small*, **4**(1), 26-49 (2008). Doi: https://doi.org/10.1002/smll.200700595

41. A. Zielińska, B. Costa, M.V. Ferreira, D. Miguéis, J.M.S. Louros, A. Durazzo, M. Lucarini, P. Eder, M.V. Chaud, M. Morsink, *et al.*, Nanotoxicology and nanosafety: Safety-by-design and testing at a glance, *International Journal of Environmental Research and Public Health*, **17**(13), 4657 (2020). Doi: https://doi.org/10.3390/ijerph17134657

42. M. Mogharabi, M. Abdollahi, M.A. Faramarzi, Toxicity of nanomaterials; an undermined issue, *DARU Journal of Pharmaceutical Sciences*, **22**(1), 59 (2014). Doi: https://doi.org/10.1186/s40199-014-0059-4

Como citar este artículo

L.E. Castrillón-Rivera, A. Palma-Ramos, J.I. Castañeda-Sánchez, V. Espinosa-Antúnez, Nanopartículas: Un sistema de entrega de antifúngicos, *Rev. Colomb. Cienc. Quim. Farm.*, **53**(2), 537-555 (2024). https://doi.org/10.15446/rcciquifa.v53n2.114456

Abstracts of the V Ibero-American Pharmacometrics Network (RedIF) Congress, Bogotá D.C., Colombia, April 24th - 26th, 2024

Organized by:

Universidad Nacional de Colombia and the Ibero-American Pharmacometrics Network (RedIF)

Scientific Committee

Dr. Bibiana Verlindo, Professor, Universidade Federal do Rio Grande do Sul (Brasil)

Dr. Darlene Santiago, Professor, Puerto Rico University (Puerto Rico)

Dr. Gonzalo Suárez, Professor, Universidad de la República (Uruguay)

Dr. Manuel Ibarra, Professor, Universidad de la República (Uruguay)

Dr. Marcela Aragón, Professor, Universidad Nacional de Colombia (Colombia)

Dr. Mauricio García, Professor, Pontificia Universidad Católica de Chile (Chile)

Dr. Teresa Dalla Costa, Professor, Universidade Federal do Rio Grande do Sul (Brasil)

Dr. Victor Mangas, Professor, Universidad de Valencia (España)

Organizing Committee

Dr. Marcela Aragón, Professor, Universidad Nacional de Colombia (Colombia)

Dr. Bibiana Verlindo, Professor, Universidade Federal do Rio Grande do Sul (Brasil)

Dr. Maritza Rojas, Professor, Universidad Nacional de Colombia (Colombia)

Dr. Izabel Almeida Alves, Professor, Universidade Federal de Bahia (Brasil)

Dr. Paola Cárdenas, Independed consultant

Dr. Gina Domínguez, Professor, Universidad del Atlántico (Colombia)

Dr Andrés Zuluaga, Professor, Universidad de Antioquia (Colombia)

Dr. Diana Sinuco, Professor, Universidad Nacional de Colombia (Colombia)

Dr. Constain H. Salamanca, Professor, Universidad Nacional de Colombia (Colombia)

MSc. Sandra Echeverry, PhD. Student, Universidad Nacional de Colombia (Colombia)

Miss. Karen Lancheros, Pharmacist

Oral presentations

Piperacillin/tazobactam target attainment in neonatal intensive care unit patients

Frida Sofía Boer Pérez[1]*, Silvia Romano Moreno[1], Ma. Victoria Lima Rogel[2], Susanna Edith Medellín Garibay[1], Ana Ruth Mejía Elizondo[2], Paula Schaiquevich[3], Ana Socorro Rodríguez Baez[1], Cristian Jazmín Rodríguez Pinal[1], Rosa del Carmen Milán Segovia[1]

[1] Facultad de Ciencias Químicas, Universidad Autónoma de San Luis Potosí, San Luis Potosí, México

[2] Hospital Central "Dr. Ignacio Morones Prieto", San Luis Potosí, México

[3] Hospital Pediátrico Dr. Juan P. Garrahan, Buenos Aires, Argentina

*E-mail: A239034@alumnos.uaslp.mx.com

Summary

Piperacillin/tazobactam has been used extensively for late-onset neonatal sepsis treatment, although safety and pharmacokinetic (PK) data in this population are limited [1]. The present work aims to evaluate the pharmacokinetic/pharmacodynamic (PK/PD) target attainment of piperacillin/tazobactam in preterm and term Mexican neonates with severe infections. A total of 65 piperacillin concentrations from 25 neonatal intensive care unit (NICU) patients were determined by liquid chromatography/tandem mass spectrometry (LC/MS/MS). The overall median value (range) postnatal age, gestational age, and body weight were 14 (8-28) days, 34.2 (28-41.1) weeks, and 1760 (995-3430) grams, respectively. The attainment of the PK/PD target (70% fT>MIC, free drug concentration above minimum inhibitory concentration during 70% of the dosing interval) was evaluated for different MICs using the individual Bayesian estimates method in NONMEM VII. A significant difference was found in piperacillin concentrations observed at 70% of the dosing interval between the very preterm (49.8 mg/L) and term neonates (23.7 mg/L) (p=0.041). 72% and 88% of preterm and term neonates achieved the PK/PD target for a MIC of 16 mg/L, however, of each category, respectively, 56% and 12% attained the PK/PD target for a MIC of 32 mg/L. Potential toxicity piperacillin concentration >150 mg/L was observed in 44% of our population [2]. In neonates with life-threatening infections, the rapid pathophysiological fluctuations and organic immaturity can difficult to achieve the PK/PD target. The importance

of this study lies in the necessity to monitor the piperacillin plasma concentrations in NICU patients to optimize antibiotic therapy and minimize the risk of toxicity.

Ethical approval

The present study was approved by the Comité en Ética e Investigación del Hospital Central "Dr. Ignacio Morones Prieto" with the registration code: CONBIOETICA-24- CEI-001-20160227.

Financial support and acknowledgements

This project is supported by Mexico's Consejo Nacional de Ciencia y Tecnología through the student grant number: 745752.

References

1. C.I.B. Barker, K. Kipper, D.O. Lonsdale, K. Wright, G. Thompson, M. Kim, M.A. Turner, A. Johnston, M. Sharland, J.F. Standing, The neonatal and paediatric pharmacokinetics of antimicrobials study (NAPPA): Investigating amoxicillin, benzylpenicillin, flucloxacillin and piperacillin pharmacokinetics from birth to adolescence, *J. Antimicrob. Chemother.*, **78**, 2148-2161 (2023). Doi: https://doi.org/10.1093/jac/dkad196

2. M.C. Quinton, S. Bodeau, L. Kontar, Y. Zerbib, J. Maizel, M. Slama, K. Masmoudi, A.S. Lemaire-Hurtel, Y. Bennis, Neurotoxic concentration of piperacillin during continuous infusion in critically ill patients, *Antimicrob. Agents Chemother.*, **61**, 614 (2017). Doi: https://doi.org/10.1128/aac.00654-17

Guiding methotrexate rescue therapy through a population pharmacokinetic model in brazilian pediatric patients with osteosarcoma

Laura Ben Olivo[1]*, Pricilla de Oliveira Henz[1], Sophia Wermann[1], Bruna Bernar Dias[1], Gabriel Osorio Porto[1], Amanda Valle Pinhatti[2,3], Lauro José Gregianin[3], Teresa Dalla Costa[1], Bibiana Verlindo de Araújo[1,2]

[1] Pharmacokinetics and PK/PD Modeling Laboratory, Pharmaceutical Sciences Graduate Program, Federal University of Rio Grande do Sul, 2752 Ipiranga Ave., Santana, RS 90610-000 Porto Alegre, Brazil

[2] Medical Sciences Graduate Program, Federal University of Rio Grande do Sul, Porto Alegre, Brazil

[3] Pediatric Oncology Service, Hospital de Clínicas de Porto Alegre, Department of Pediatrics, Federal University of Rio Grande do Sul, Porto Alegre, Brazil

*E-mail: lauraolivo96@gmail.com

Summary

Methotrexate (MTX) is part of the Brazilian Osteosarcoma Treatment Group protocol. Itpresents high interindividual variability and is subject to therapeutic drug monitoring (TDM) [1, 2]. The administration of MTX is associated with several cases of toxicity which have been diminished due to the concomitant administration with leucovorin rescue therapy [3]. This work aimed to develop a population pharmacokinetic model (POPPK) of MTX in Brazilian children with osteosarcoma (OS) to support the prevention of several adverse effects. Pediatric patients with OS who received MTX as part of cancer treatment were included in the study. The model was developed using retrospective data from TDM, NONMEM 7.4 (Icon®), ADVAN3 TRANS4 and FOCE-I. Interindividual (IIV) and interoccasion (IOV) variabilities were analyzed between subjects. Several demographic and biochemical covariates were tested to explain variabilities. Data fitted in a two-compartment model, using 216 MTX cycles from 32 patients (5-18 y.o) with OS. Serum creatinine was added in clearance to explain the variabilities associated with this parameter. Body surface area was added in peripheral volume as a covariate. Clearance estimate was 15.6 L/h and intercompartmental clearance was 0.208 L/h. The volume of the central compartment was 87.1 L and for the peripheral volume was 5.89 L.

The model adequately describes MTX exposure in Brazilian children with OS. The model was used to predict MTX plasma concentrations, guide rescue therapy, and prevent toxicity exposure.

Ethical approval

The study was approved by the Ethics Committee in Human Research of Hospital de Clínicas de Porto Alegre (4.260.110 in 10/21/2021).

Financial support and acknowledgements

This work was financed in part by the Coordenação de Aperfeiçoamento de Pessoal de Nível Superior—Brasil (CAPES, Finance Code 001) and by the PPSUS/FAPERGS, Rio Grande do Sul, Brazil (#21/2551–0000065-1). Acknowledgments to Coordination for the Improvement of Higher Education Personnel (CAPES) and Hospital de Clínicas de Porto Alegre (HCPA).

References

1. A.S. Petrilli, B. de Camargo, V.O. Filho, P. Bruniera, A.L. Brunetto, R. Jesus-Garcia, O.P. Camargo, W. Pena, P. Péricles, A. Davi, J.D. Prospero, M.T.S. Alves, C.R. Oliveira, C.R.D. Macedo, W.L. Mendes, M.Teresa A. Almeida, M.L. Borsato, T.M. dos Santos, J. Ortega, E. Consentino, Results of the Brazilian osteosarcoma treatment group studies III and IV: prognostic factors and impact on survival, *J. Clin. Oncol.*, **24**, 1161-1168 (2006). Doi: https://doi.org/10.1200/JCO.2005.03.5352

2. A.A. Senerchia, C.R. Macedo, S. Ferman, M. Scopinaro, W. Cacciavillano, E. Boldrini, V.L. Lins de Moraes, G. Rey, C.T. de Oliveira, L. Castillo, M.T. Almeida, M.L. Borsato, E. Lima, D. Lustos, J.H. Barreto, T. El-Jaick, S. Aguiar, A. Brunetto, L. Greggiani, H. Cogo-Moreira, A. Atallah, A.S. Petrilli, Results of a randomized, prospective clinical trial evaluating metronomic chemotherapy in nonmetastatic patients with high-grade, operable osteosarcomas of the extremities: A report from the Latin American Group of Osteosarcoma Treatment, *Cancer*, **123**, 1003-1010 (2017). Doi: https://doi.org/10.1002/cncr.30411

1. K.R. Crews, T. Liu, C. Rodriguez-Galindo, M. Tan, W.H. Meyer, J.C. Panetta, M.P. Link, N.C. Daw, High-dose methotrexate pharmacokinetics and outcome of children and young adults with osteosarcoma, *Cancer*, **100**, 1724-1733 (2004). Doi: https://doi.org/10.1002/cncr.20152

Population pharmacokinetics of meropenem in critically ill children and young adults

Ronaldo Morales Junior[1*], Tomoyuki Mizuno[1,2], Kelli Paice[1,3], Kathryn Pavia[1,3], Peter Tang[2], Rhonda Jones[3], Abigayle Gibson[3], Erin Stoneman[3], Calise Curry[4], Jennifer Kaplan[2,3], Sonya Tang Girdwood[1,2,4]

[1] Division of Clinical Pharmacology, Cincinnati Children's Hospital Medical Center, Cincinnati, OH, USA

[2] Department of Pediatrics, University of Cincinnati College of Medicine, Cincinnati, OH, USA

[3] Division of Critical Care Medicine, Cincinnati Children's Hospital Medical Center, Cincinnati, OH, USA

[4] Division of Hospital Medicine, Cincinnati Children's Hospital Medical Center, Cincinnati, OH, USA

*E-mail: ronaldo.moralesjunior@cchmc.org

Summary

Meropenem, a β-lactam antibiotic widely prescribed for severe infections, poses dosing challenges in critically ill patients due to highly variable pharmacokinetics. We aim to develop a population pharmacokinetic model of meropenem for critically ill pediatric and young adult patients. Pediatric intensive care unit patients receiving meropenem 20-40 mg/kg Q8h as a 30-minute infusion were prospectively followed for clinical data collection and scavenged opportunistic plasma sampling [1]. Meropenem concentrations were measured using high-performance liquid chromatography. Nonlinear mixed effects modeling was conducted using Monolix®. Allometric body weight scaling was included with fixed exponents to account for body size differences. Data from 48 patients, aged 1 month to 30 years, with 296 samples, were described using a two-compartment model with first-order elimination. Inter-individual variabilities were estimated for clearance (CL) and central volume of distribution (V1), but could not be estimated for intercompartmental clearance (Q) or peripheral volume (V2). Creatinine clearance and percentage of fluid overload were identified as covariates on CL and V1, respectively. The maturation function for glomerular filtration rate [2] was incorporated to accommodate

developmental changes in renal clearance. The final parameters were estimated with good precision: CL 13.22 L/h/70 kg$^{0.75}$, Q 1.78 L/h/70 kg$^{0.75}$, V1 16.45 L/70 kg, and V2 7.66 L/70 kg. The goodness-of-fit plots showed no model misspecification. Bootstrap results confirmed the final model's stability. In conclusion, a meropenem PK model for critically ill pediatric patients was successfully developed accounting for patients' renal function, fluid status, body size- and age-related development. It will be applied for optimal dosing simulations and model-informed precision dosing.

Ethical approval

The study was approved by the Cincinnati Children's Hospital Medical Center Institutional Review Board, which granted a waiver of consent (Protocol 2018-3245).

Financial support and acknowledgements

This work was supported by the National Institute of General Medical Sciences of the National Institute of Health under award number R35GM146701-01.

References

1. S.C. Tang Girdwood, P.H. Tang, M.E. Murphy, A.R. Chamberlain, L.A. Benken, R.L. Jones, E.M. Stoneman, J.M. Kaplan, A.A. Vinks, Demonstrating feasibility of an opportunistic sampling approach for pharmacokinetic studies of β-lactam antibiotics in critically ill children, *J. Clin. Pharmacol.*, **61**, 565-573 (2020). Doi: https://doi.org/10.1002/jcph.1773

2. M.M. Rhodin, B.J. Anderson, A.M. Peters, M.G. Coulthard, B. Wilkins, M. Cole, E. Chatelut, A. Grubb, G.J. Veal, M.J. Keir, N.H.G. Holford, Human renal function maturation: a quantitative description using weight and postmenstrual age, *Pediatr. Nephrol.*, **24**, 67-76 (2009). Doi: https://doi.org/10.1007/s00467-008-0997-5

Model-informed development of gastroretentive furosemide formulations with physiologically based biopharmaceutics modeling

María Luisa Rodríguez[1]*, Santiago Palma[2], Pietro Fagiolino[1], Manuel Ibarra[1]

[1] Pharmaceutical Sciences Department, Faculty of Chemistry, Universidad de la República, Uruguay

[2] Pharmaceutical Sciences Department, Faculty of Chemical Sciences, Universidad Nacional de Córdoba, Argentina

*E-mail: mluisar@fq.edu.uy

Summary

Furosemide is a potent diuretic widely used in clinical practice; however, it has a narrow absorption window restricted to the upper part of the gastrointestinal tract. To improve its oral bioavailability and diuretic effect, controlled-release gastroretentive systems are being developed [1]. In this study, we employed physiologically based biopharmaceutics modeling (PBBM) to predict the *in vivo* behavior of gastroretentive formulations, aiming to aid the development of effective furosemide pharmaceutical dosage forms. This includes integrating formulation parameters estimated from *in vitro* dissolution testing into a PBPK model [2]. A validated PBPK model for furosemide in dogs [3] was adapted to humans in PK-Sim® and MoBi® [4], utilizing literature pharmacokinetic data post intravenous and oral administration [5]. The model was optimized for plasma and urinary excretion profiles based on individual sex. Model predictions were validated with published plasma pharmacokinetic profiles post immediate and modified dosage forms in men and women [6-9]. The PBBM approach described furosemide pharmacokinetics and product performance in both men and women. The model was applied to simulate the performance of multiple-unit floating drug delivery systems developed, System I (SI) and System II (SII), and compare it to the immediate-release reference formulation after a single 40 mg oral dose. The predicted Test/Reference GMR for AUC in men (n=1000) were 1.00 for AUC0-inf (90%CI 0.89-1.14) for SI and 1.30 for AUC0-inf (90%CI 1.17-1.50) for SII. *In silico* predictions suggest that the developed SII would exhibit higher bioavailability relative to the immediate release reference formulation of furosemide, making it a promising candidate for further *in vivo* studies.

Financial support and acknowledgements

Postgraduate student María Luisa Rodríguez receive funding from the CAP (Postgraduate Academic Committee) postgraduate scholarship (UdelaR) and the economic rate for postgraduate students of the Basic Sciences Development Program (PEDECIBA).

References

1. F. Mentre, CPT: Pharmacometrics & Systems Pharmacology 2.0, *CPT Pharmacometrics Syst. Pharmacol.*, **8**, 197 (2019). Doi: https://doi.org/10.1002/psp4

2. C. Valiante *et al.*, Tesis de maestría, Universidad de la República, Uruguay, 2022.

3. Open Systems Pharmacology. URL: http://www.open-systems-pharmacology.org. Accessed 14 Dec 2023

4. H. Britz, N. Hanke, M.E. Taub, T. Wang, B. Prasad, É. Fernandez, P. Stopfer, V. Nock, T. Lehr, Physiologically based pharmacokinetic models of probenecid and furosemide to predict transporter mediated drug-drug interactions, *Pharm. Res.*, **37**, 250 (2020). Doi: https://doi.org/10.1007/s11095-020-02964-z

5. L. Magallanes, P. Fagiolino, M. Vázquez, N. Fotaki, M. Ibarra, M. Lorier, V. Bértola, A. Barindelli, Influence of food and sex on the pharmacokinetics and pharmacodynamics of furosemide, *Curr. Topics Pharmacol.*, **20**, 45-56 (2016).

6. Y. Akiyama, N. Nagahara, E. Nara, M. Kitano, S. Iwasa, I. Yamamoto, J. Azuma, Y. Ogawa, Evaluation of oral mucoadhesive microspheres in man on the basis of the pharmacokinetics of furosemide and riboflavin, compounds with limited gastrointestinal absorption sites, *J. Pharm. Pharmacol.*, **50**, 159-166 (1998). Doi: https://doi.org/10.1111/j.2042-7158.1998.tb06171.x

7. E.A. Klausner, E. Lavy, D. Stepensky, E. Cserepes, M. Barta, M. Friedman, A. Hoffman, Furosemide pharmacokinetics and pharmacodynamics following gastroretentive dosage form administration to healthy volunteers, *J. Clin. Pharmacol.*, **43**, 711-720 (2003). Doi: https://doi.org/10.1177/0091270003254575

8. M. Neumann, C. Heimhardt, K. Seidlitz, M. Koziolek, F. Schneider, C. Schiller, U. Hanke, M. Anschütz, C. Knopke, F. Donath, R. Thoma, C. Brätter, B. Schug, H. Franke, W. Weitschies, Development of a furosemide-containing expandable system for gastric retention, *J. Control Release*, **338**, 105-118 (2021). Doi: https://doi.org/10.1016/j.jconrel.2021.08.026

Physiologically-based pharmacokinetics modelling to predict drug concentration in human milk: a contribution from the conception project

Julia Macente[1]*, Nina Nauwelaerts[1], Justine Marine Badée[2], Rodolfo Hernandes Bonan[3], Miao-Chan Huang[1], Martje Van Neste[1], Karel Allegaert[1], Frederico Severino Martins[1], Pieter Annaert[1,3]

[1] KU Leuven, Leuven, Belgium

[2] Novartis Institutes for BioMedical Research, Basel, Switzerland

[3] BioNotus GCV, Niel, Belgium

*E-mail: julia.macente@kuleuven.be

Summary

Physiologically-based Pharmacokinetic (PBPK) modelling emerges as a highly valuable tool to predict drug concentration in human milk, and estimates the daily infant dosage (DID), and subsequently, the infants systemic exposure [1]. This study aimed to develop and evaluate the performance of lactation PBPK models to predict drug concentrations in human milk and the relative infant dose (RID, %) of sertraline, sildenafil, nevirapine and valproic acid. An adult healthy volunteer (HV) PBPK model was developed, reproduced or adapted [2-4] and validated using Simcyp v21 software. The validated adult HV model was extended to lactating women. Drug transfer into human milk was parameterized using the perfusion-limited model, with the milk-to-plasma ratio calculated using log-transformed phase distribution model by Atkinson and Begg [5]. The DID (mg/kg/day) received via breastfeeding and the RID, was calculated relying on the average (C_{ave}, milk) predicted concentration in human milk. The adult HV models established exhibited a good prediction (<2-fold) compared to observed data, qualifying as base for lactating women's PBPK models. The lactation PBPK models resulted in good prediction for the selected drugs. The RID was low (<10%) for all compounds. In addition, the DID was compared to the common therapeutic infant dosage, revealing <10% when compared to the therapeutic usage. The PBPK models effectively describe plasma and milk concentrations, simulations revealed a low infant systemic exposure compared to maternal exposure. Ongoing efforts to establish a non-clinical

workflow for (*in vitro*, and) PBPK-based predictions (permeability-limited model) of drug transfer into human milk are in progress.

Financial support and acknowledgements

This work has received support from the EU/EFPIA (Innovative Medicines initiative). Joint Undertaking ConcePTION grant No. 821520. The research leading to these Results was conducted as part of the ConcePTION consortium. This abstract only reflects the personal views of the stated authors.

References

1. N. Nauwelaerts, J. Macente, N. Deferm, R. Hernandes Bonan, M.C. Huang, M. Van Neste, D. Bibi, J. Badee, F.S. Martins, A. Smits, K. Allegaert, T. Bouillon, P. Annaert. Generic workflow to predict medicine concentrations in human milk using physiologically-based pharmacokinetic (PBPK) Modelling-A contribution from the ConcePTION project, *Pharmaceutics*, **15**, 1469 (2023). Doi: https://doi.org/10.3390/pharmaceutics15051469

2. A. Almurjan, H. Macfarlane, R.K.S. Badhan, The application of precision dosing in the use of sertraline throughout pregnancy for poor and ultrarapid metabolizer CYP 2C19 subjects: A virtual clinical trial pharmacokinetics study, *Biopharm. Drug Dispos.*, **42**, 252-262 (2021). Doi: https://doi.org/10.1002/bdd.2278

3. J. Macente, N. Nauwelaerts, F.M. Russo, J. Deprest, K. Allegaert, B. Lammens, R. Hernandes Bonan, J.M. Turner, S. Kumar, A. Diniz, F.S. Martins, P. Annaert, PBPK-based dose finding for sildenafil in pregnant women for antenatal treatment of congenital diaphragmatic hernia, *Front. Pharmacol.*, **14**, 1068153 (2023). Doi: https://doi.org/10.3389/fphar.2023.1068153

4. T.M. Conner, V.C Nikolian, P.E. Georgoff , M.P. Pai, H.B. Alam, D. Sun, R.C. Reed, T. Zhang, Physiologically based pharmacokinetic modeling of disposition and drug-drug interactions for valproic acid and divalproex, *Eur. J. Pharm. Sci.*, **111**, 465-481 (2018). Doi: https://doi.org/10.1016/j.ejps.2017.10.009

5. E.J. Begg, H.C. Atkinson, Modelling of the passage of drugs into milk, *Pharmacol. Ther.*, **59**, 301-310 (1993). Doi: https://doi.org/10.1016/0163-7258(93)90072-l

Enhancing tacrolimus precision dosing with multimodel methods

Martin Umpiérrez[1]*, Cecilia Maldonado[1], Oscar Noboa[2], Sebastian Wicha[3], Manuel Ibarra[1]

[1] Pharmaceutical Sciences Department, Faculty of Chemistry- Universidad de la República, Montevideo, Uruguay

[2] Nephrology Center, Faculty of Medicine- Universidad de la República, Montevideo, Uruguay

[3] Department of Clinical Pharmacy, University of Hamburg, Hamburg, Germany

*E-mail: martinumpierrezbattaglino@gmail.com

Summary

Tacrolimus (FK), an essential immunosuppressant, demands dose titration due to its narrow therapeutic index and high intra- and inter-individual variability [1, 2]. In this context, Model-Informed Precision Dosing (MIPD) [3] holds the potential of overcoming limitations of traditional therapeutic drug monitoring. However, the effectiveness of this approach can be hindered by significant inter-model variability. Utilizing a single model for a target population, either developed in-house or adopted from the literature, may fail to account for individual variations. Here, we explored multi-model approaches, Model Selection Algorithm (MSA) and Model Averaging Algorithm (MAA) [4] for FK MIPD. These methods use a single-model (MSA) or a combined-model forecast (MAA) for each patient, using a weighed selection based on the fit of individual models to observed data. Twenty-one population pharmacokinetic models were selected through systematic review and implemented in TDMxR [5].The accuracy and precision of single-models, MSA and MAA predictions were evaluated using data from 49 renal transplant patients (328 observations) collected in 6 occasions. Metrics such as relative bias (rBIAS) and mean absolute prediction error (MAPE) [6] were implemented. MSA and MAA consistently outperformed individual models in both precision and accuracy. Remarkably, MSA and MAA combining the five models with the poorest individual performance with data up to the first occasion yielded lower rBIAS (-15.2 and -10.6%) relative to individual models which showed results as high as 66.9% (Vadcharavivad) [7] or -55.9% (Han) [8]. Our study highlights the potential of these algorithms in replacing traditional approaches for implementing MIPD with FK, alleviating resource-intensive processes of in-house model development and external evaluation.

Ethical approval

This work was approved by the Ethics Committee of the Hospital de Clínicas Dr. Manuel Quintela (Approved 03/2021)

Financial support and acknowledgements

This work is supported by the Agencia Nacional de Investigación e Innovación and by Comisión Sectorial de Investigación Científica Investigación + Desarrollo (CSIC 1+D).

References

1. R. Venkataramanan, A. Swaminathan, T. Prasad, A. Jain, S. Zuckerman, V. Warty, J. McMichael, J. Lever, G. Burckart, T. Starzl, Clinical pharmacokinetics of tacrolimus, *Clin. Pharmacokinet.*, **29**, 404-430 (1995). Doi: https://doi.org/10.2165/00003088-199529060-00003

2. C.E.Staatz, S.E. Tett, Clinical pharmacokinetics and pharmacodynamics of tacrolimus in solid organ transplantation, *Clin. Pharmacokinet.*, **43**, 623-653 (2004). Doi: https://doi.org/10.2165/00003088-200443100-00001

3. R.J. Keizer, R.T. Heine, A. Frymoyer, L.J. Lesko, R. Mangat, S. Goswami, Model-informed precision dosing at the bedside: scientific challenges and opportunities, *CPT Pharmacometrics Syst. Pharmacol.*, 7, 785-787 (2018). Doi: https://doi.org/10.1002/psp4.12353

4. D.W. Uster, S.L. Stocker, J.E. Carland, J. Brett, D.J.E. Marriott, R.O. Day, S.G. Wicha, A model averaging/selection approach improves the predictive performance of model-informed precision dosing: Vancomycin as a case study, *Clin. Pharmacol. Ther.*, **109**, 175-183 (2021). Doi: https://doi.org/10.1002/cpt.2065

5. S.G. Wicha, M.G. Kees, A. Solms, I.K. Minichmayr, A. Kratzer, C. Kloft, TDMx: a novel web-based open-access support tool for optimising antimicrobial dosing regimens in clinical routine, *Int. J. Antimicrob. Agents*, **45**, 442-444 (2015). Doi: https://doi.org/10.1016/j.ijantimicag.2014.12.010

6. C.Y. Zhao, Z. Jiao, J.J. Mao, X.Y. Qiu, External evaluation of published population pharmacokinetic models of tacrolimus in adult renal transplant recipients, *Br. J. Clin. Pharmacol.*, **81**, 891-907 (2016). Doi: https://doi.org/10.1111/bcp.12830

7. S. Vadcharavivad, S. Praisuwan, N. Techawathanawanna, W. Treyaprasert, Y. Avihingsanon, Population pharmacokinetics of tacrolimus in Thai kidney transplant patients: comparison with similar data from other populations, *J. Clin. Pharm. Ther.*, **41**, 310-328 (2016). Doi: https://doi.org/10.1111/jcpt.12396

8. N. Han, S. Ha, H.Y. Yun, M.G. Kim, S.I. Min, J. Ha, J.I. Lee, J.M. Oh, I.W. Kim, Population pharmacokinetic-pharmacogenetic model of tacrolimus in the early period after kidney transplantation, *Basic Clin. Pharmacol. Toxicol.*, **114**, 400-406 (2014). Doi: https://doi.org/10.1111/bcpt.12176

Poster presentations

Relative bioequivalence of ivermectin 1%: single vs. combined formulation with fluazuron 12.5% by subcutaneous administration on cattle

Diego Robaina[1]*, Gonzalo Suárez[1]

[1] Departmento de Clínica y Hospital Veterinario, Universidad de la República, Montevideo, Uruguay

*E-mail: diego.robaina@fvet.edu.uy

Summary

Ivermectin (IVM) is the first Macrocyclic Lactone developed for animals. Differences in formulations account for changes in plasma kinetics and parasite exposure [1]. The objective of this study was to check for IVM bioequivalence using two formulations. Six Hereford cows (weight 372 ± 34 kg) and six Hereford heifers (weight 295 ± 33 kg) were randomized into two groups (three cows and three heifers per group). Group A (IVM 1 %, 0.2 mg/kg) and group B (a combined formulation of IVM and Fluazuron [IVM 1%, 0.2 mg/kg + Fluazuron 12.5%, 12.5 mg/kg]), both by subcutaneous route on the side of the neck (single dose). Blood samples were collected until 29 days after dosing. Non-compartmental approach showed bioequivalence for IVM between formulations, with Cmax ratio of 1.1 (CI90: 1.00 – 1.21, ANOVA, P = 0.077) and AUC0-t ratio of 0.99 (CI90: 0.93 – 1.05, ANOVA, P = 0.85) with Tmax (2.5 ± 2.3 and 1.6 ± 0.8 days (Mann-Whitney U test, P = 0.79) for A and B, respectively). The pharmacokinetic model has one compartment, linear elimination with first-order absorption and lag time; formulation was added as covariable for the absorption rate and lag time, weight was covariable on volume of distribution. We conclude that both IVM 1% formulations (alone or combined with fluazuron 12.5%), are bioequivalent in cattle. Carrying out bioequivalence studies are of great importance to ensure interchangeability between formulations.

Ethical approval

The experimental study was approved by the Comisión Honoraria de Experimentación Animal, Universidad de la República, Uruguay (CHEA, No. 506-1493294137).

Financial support and acknowledgements

Financial Support was granted from Universidad de la República.

References

1. D. Robaina, S. Alvariza, G. Suárez, Bioequivalence of two novel formulations of ivermectin 1% combined with fluazuron 12.5% for subcutaneous administration in cattle, *J. Pharm. Pharmacogn. Res.*, **9**, 88-97 (2021).

Modeling and simulation focusing on the chronopharmacokinetics of gentamicin in dogs

Karina Krauss Ferraz Vasconcelos[1]*, Kevellyn Silveira Gomes Martins[1], Naira Fernanda Dias da Silva[1], Lillian Pereira Gouvêia[1], Sibely Aiva Flores[1], Lucas Wamser Fonseca Gonzaga[1]

[1] Faculdade de Zootecnia e Medicina Veterinária, Universidade Federal de Lavras, Lavras, Minas Gerais, Brazil

*E-mail: karina.ferraz2007@gmail.com

Summary

Gentamicin is an aminoglycoside used to treat dogs with sepsis and bacterial infections, with chronotherapy being an alternative to increase efficacy and reduce side effects considering the impact of the circadian rhythm on pharmacokinetics (PK) [1]. The objective was to build a PK model to optimize gentamicin doses according to the administration schedule. The model was built using the Monolix2023 software based on plasma concentration data, at two different times, obtained from a chronopharmacokinetic study [2]. The best-fitting model was exported to the Simulix2023 software, in which different protocols were simulated (2, 4, 6 and 8 mg/kg) for both times. An MIC range of 0.016 to 32 μg/mL and the PK/PD index of Cmax/MIC=10 [3] were used to calculate the probability of target attainment (PTA). A 2-compartment intravenous linear elimination model was efficient in predicting plasma concentration. Administration time was inserted as a categorical covariate, correlating with clearance and volume of the peripheral compartment. For bacterias with a MIC of up to 0.5 μg/mL, all protocols achieved a PTA ≥ 90. The dose of 6 mg/kg and 8 mg/kg, recommended for sepsis in dogs [4], reached a PTA ≥ 90 for bacterias with MIC of up to 2 μg/mL at both administration times. For MICs up to 4 μg/mL, the nighttime dose of 8mg/kg was the only one that reached the PTA. Therefore, the model was efficient in predicting the ideal dose according to the MIC of the bacteria and the time of administration.

Ethical approval

Since this is an *in silico* study, no animals were used.

Financial support and acknowledgements

This study was funded by Coordenação de Aperfeiçoamento de Pessoal de Nível Superior (CAPES) and by Conselho Nacional de Desenvolvimento Científico e Tecnológico (CNPq).

References

1. Y. Yang, L.A. Lindsey-Boltz, C.M. Vaughn, *et al.*, Circadian clock, carcinogenesis, chronochemotherapy connections, *J. Biol. Chem.*, **297**, 101068 (2021). Doi: https://doi.org/10.1016/j.jbc.2021.101068

2. N. Widerhon, D. Díaz, E. Picco, M. Rebuelto, T. Encinas, J.C. Boggio, Chronopharmacokinetic study of gentamicin in dogs, *Chronobiology International*, **22**, 731-739 (2005). Doi: https://doi.org/10.1080/07420520500179738

3. G. Santana, *et al.*, *Manual de Terapêutica em Animais Domésticos*, Manole, 2021.

4. D.C. Plumb, *Plumb's Veterinary Drug Handbook*, 6th ed., Wiley Blackwell, 2008.

Physiology-based pharmacokinetic modeling of dexmedetomidine in healthy dogs

Lillian Pereira Gouvêia[1]*, Lucas Wamser Fonseca Gonzaga[1], Karina Krauss Ferraz Vasconcelos[1], Naira Fernanda Dias da Silva[1], Sibely Aiva Flores[1], Marcos Ferrante[1]

[1] Faculdade de Zootecnia e Medicina Veterinária, Universidade Federal de Lavras, Lavras, Minas Gerais, Brazil

*E-mail: gouveialillian@gmail.com

Summary

Pharmacokinetic modeling based on physiology (PBPK) aims to estimate the concentration of drugs in the blood and other tissues [1]. Dexmedetomidine has been used intravenously as an adjunct to anesthesia in dogs [2]. Therefore, the objective was to develop a physiologically-based pharmacokinetic (PB/PK) model to predict the plasma concentration after intravenous administration of dexmedetomidine in dogs. The model was developed with the assistance of PK-SIM® software (OPEN SYSTEMS PHARMACOLOGY), version 11.2. Plasma profiles of dexmedetomidine previously published in the literature were employed. The drug's physicochemical data were obtained from the PubChem database. Pharmacokinetic data were divided into a construction group and a validation group. The model was refined based on observed data from pharmacokinetic studies and evaluated using the geometric mean fold error (GMFE), calculated based on area under the curve from the first to the last point (AUCt-end) values. A sensitivity analysis was conducted to identify the impact of model parameters on AUCt- end and maximum concentration (Cmax) and suggest possible future adjustments. The model demonstrated satisfactory predictive performance with a GMFE value of 1.95, indicating acceptable accuracy under a double-error criterion [3]. Four datasets were used, two for model construction and two for validation. In the sensitivity analysis, changes in hepatic clearance, muscle volume, and hematocrit variables were observed to affect AUCt-end and Cmax values, suggesting potential future applications for the model. The model efficiently predicted the pharmacokinetics of dexmedetomidine in dogs, making it applicable for various purposes in the future.

Ethical approval

Since this is an *in silico* study, no animals were used.

Financial support and acknowledgements

This study was funded by Coordenação de Aperfeiçoamento de Pessoal de Nível Superior (CAPES), and by Fundação de Amparo à Pesquisa de Minas Gerais (FAPEMIG).

References

1. L. Kuepfer, C. Niederalt, T. Wendl, J.-F. Schlender, S. Willmann, J. Lippert, M. Block, T. Eissing, D. Teutonico, Applied concepts in PBPK modeling: How to build a PBPK/PD model, *CPT Pharmacometrics Syst. Pharmacol.*, **5**, 516-531 (2016). Doi: https://doi.org/10.1002/psp4.12134

2. O.L. Levionnois, A. Barbarossa, A. Barhi, J. Siegenthaler, T.F. Pleyers, M. Guidi, C. Spadavecchia, M. Raillard, Enantiospecific pharmacokinetics of intravenous dexmedetomidine in beagles, *J. Vet. Pharmacol. Therap.*, **45**, 366-372 (2022). Doi: https://doi.org/10.1111/jvp.13063

3. L. Kovar. A. Weber, M. Zemlin, Y. Kohl, R. Bals, B. Meibohm, D. Selzer, T. Lehr, Physiologically-based pharmacokinetic (PBPK) modeling providing insights into fentanyl pharmacokinetics in adults and pediatric patients, *Pharmaceutics*, **12**, 908 (2020). Doi: https://doi.org/10.3390/pharmaceutics12100908

PBPK modeling for propofol dose optimization in dogs with hepatic impairment

Lucas Wamser Fonseca Gonzaga[1]*, João Bosco Costa Coelho[1], Beatriz Monte Egito[1], Lillian Pereira Gouveia[1], Frederico Severino Martin[2], Marcos Ferrante[1]

[1] Faculdade de Zootecnia e Medicina Veterinária, Universidade Federal de Lavras, Lavras, Minas Gerais, Brazil

[2] Faculdade de ciências farmacêuticas da Universidade de São Paulo, São Paulo, Brazil

*E-mail: lucaswamserfg@gmail.com

Summary

A PBPK model allows predicting the concentration of a medication in different tissues over time and can be used to simulate and optimize various therapeutic protocols in both healthy and diseased individuals [1]. With this objective, a PBPK model was created to predict propofol doses in dogs with hepatic dysfunction. The model was developed using PK-SIM® software (OPEN SYSTEMS PHARMACOLOGY), version 11.2, based on pharmacokinetic data obtained from the literature. Physicochemical data of the drug were sourced from the PubChem database. The model's evaluation was based on the geometric mean fold error (GMFE) of the area under the curve (AUCt-end). Individuals with hepatic impairment were simulated by reducing hepatic clearance to mimic 20%, 40%, 60%, and 80% reductions in hepatic function. Populations were simulated, and adjustments to the protocols were made based on the area under the curve from 0 to 3 hours (AUC0-3) [2]. The model for healthy dogs showed good predictive performance, evidenced by the GMFE ranging from 0.8 to 1.25, meeting the double error criterion [3]. The simulated regimen for healthy dogs of 5mg/kg (administered as a bolus) followed by continuous infusion at a rate of 0.13mg/kg/min was sufficient and ensured that all simulated subjects reached the target plasma concentration. Dogs with 80% and 60% hepatic impairment required adjustments in the infusion rate to ensure that individuals did not exceed the therapeutic window. The results presented in the manuscript demonstrate the effectiveness and practicality of a PBPK model for propofol in dogs, with a particular focus on hepatic impairment.

Ethical approval

Since this is an *in silico* study, no animals were used.

Financial support and acknowledgements

This study was funded by Coordenação de Aperfeiçoamento de Pessoal de Nível Superior (CAPES), and by Fundação de Amparo a Pesquisa de Minas Gerais (FAPEMIG).

References

1. L. Kuepfer, C. Niederalt, T. Wendl, J.-F. Schlender, S. Willmann, J. Lippert, M. Block, T. Eissing, D. Teutonico, Applied concepts in PBPK modeling: How to build a PBPK/PD model, *CPT Pharmacometrics Syst. Pharmacol.*, **5**, 516-531 (2016). Doi: https://doi.org/10.1002/psp4.12134

2. P.L. Toutain, A. Autefage, M. Oukessou, M. Alvinerie, Pharmacokinetics of methylprednisolone succinate, methylprednisolone, and lidocaine in the normal dog and during hemorrhagic shock, *J. Pharm. Sci.*, **76**, 528-534 (1987). Doi: https://doi.org/10.1002/jps.2600760708

3. L. Kovar. A. Weber, M. Zemlin, Y. Kohl, R. Bals, B. Meibohm, D. Selzer, T. Lehr, Physiologically-based pharmacokinetic (PBPK) modeling providing insights into fentanyl pharmacokinetics in adults and pediatric patients, *Pharmaceutics*, **12**, 908 (2020). Doi: https://doi.org/10.3390/pharmaceutics12100908

Pharmacokinetic modeling applied to the optimization of methadone dosing regimen in dogs

Naira Fernanda Dias da Silva[1]*, Karina Krauss Ferraz Vasconcelos[1], Lillian Pereira Gouvêia[1], Sibely Aiva Flores[1], Kevellyn Silveira Gomes Martins[1], Lucas Wamser Fonseca Gonzaga[1]

[1] Faculdade de Zootecnia e Medicina Veterinária, Universidade Federal de Lavras, Lavras, Minas Gerais, Brazil

*E-mail: nairafernandadias@gmail.com

Summary

Methadone is a widely used opioid analgesic in the management of pain in small animals [1]. However, there are few studies relating its analgesic effect to its plasma concentration over time. Therefore, the aim was to create a pharmacokinetic (PK) model for intravenous methadone administration in dogs, in order to establish more effective drug dosing regimens for this species. Plasma concentration data for methadone from *in vivo* studies were used to construct the PK model [2-4]. The model was developed using "Monolix 2023R1 software, Lixoft SAS, a Simulations Plus Company", by testing different models; the structural model choice relied on graphical analysis within the program. The analgesic duration of methadone for different doses and repetitions was predicted using "Simulx 2023R1 software, Lixoft SAS, a Simulations Plus Company", based on methadone concentration values that remained above the minimum plasma concentration (17 $ng{\cdot}ml^{-1}$) for analgesia obtained from an *in vivo* study [5]. The PK model fell within the 90% prediction interval, allowing the correlation of drug dose to plasma concentration over time and the estimation of analgesic effect duration from the model in the Simulx software. The intermittent administration protocol of 0.3 mg/kg every 3 hours kept the population at a dosage near or above the minimum concentration for analgesia, taking into account the half-life interval of approximately 2 hours for reduced exposure. Thus, this model can be employed for simulating different doses of methadone and assessing its analgesic effect, as well as exploring dosing regimen possibilities in dogs.

Ethical approval

Since this is an *in-silico* study, no animals were used.

Financial support and acknowledgements

This study was funded by Coordenação de Aperfeiçoamento de Pessoal de Nível Superior (CAPES).

References

1. T. Elwell-Cuddy, M. Li, B. KuKanich, Z. Lin, The construction and application of a population physiologically based pharmacokinetic model for methadone in Beagles and Greyhounds, *J. Vet. Pharmacol. Ther.*, **41**, 670-683 (2018). Doi: https://doi.org/10.1111/jvp.12676

2. C. Ingvast-Larsson, A. Holgersson, U. Bondesson, A.S. Lagerstedt, K. Olsson, Clinical pharmacology of methadone in dogs, *Vet. Anaesth. Analg.*, **37**, 48-56 (2010). Doi: https://doi.org/10.1111/j.1467-2995.2009.00476.x

3. B. Kukanich, B.D.X. Lascelles, M.G. Papich, Pharmacokinetics of morphine and plasma concentrations of morphine-6-glucuronide following morphine administration to dogs, *J. Vet. Pharmacol. Ther.*, **28**, 371-376 (2005). Doi: https://doi.org/10.1111/j.1365-2885.2005.00661.x

4. N. Schmidt, K. Brune, K.M. Williams, G. Geisslinger, Stereoselective pharmacokinetics of methadone in beagle dogs, *Chirality*, **6**, 492-495 (1994). Doi: https://doi.org/10.1002/chir.530060608

5. T. Amon, S.B.R. Kästner, M. Kietzmann, J. Tünsmeyer, Plasma levels of a methadone constant rate infusion and their corresponding effects on thermal and mechanical nociceptive thresholds in dogs, *BMC Vet. Res.*, **17**, 35 (2021). Doi: https://doi.org/10.1186/s12917-020-02735-3

PBPK modeling to predict *in vivo* performance of floating 3D printed inks containing ricobendazole in dogs

Marianela Lorier[1]*, María Eugenia Barberis[2], Juan Pablo Real[2], Manuel Ibarra[1]

[1] Department of Pharmaceutical Sciences, Faculty of Chemistry, Universidad de la República, Montevideo, Uruguay

[2] Research and Development Unit in Pharmaceutical Technology (UNITEFA), CONICET and Department of Pharmacy, Faculty of Chemical Sciences. Universidad Nacional de Córdoba, Córdoba, Argentina

*E-mail: mlorier@fq.edu.uy

Summary

Ricobendazole is a widely used antiparasitic which exhibits low oral bioavailability due to poor solubility at intestinal pH. Floating formulations may increase Ricobendazole gastric residence time enhancing its dissolution. This study aimed to simulate the *in vivo* performance of floating printlets to identify a suitable candidate for a pilot pharmacokinetic study in dogs and subsequently validate the predictions with the experimental data. A PBPK model was developed in PK-Sim® 11.1 using previously published pharmacokinetic data for oral powder formulations as a training dataset [1]. The model was further refined with data obtained after the administration of a micronized powder, the selected 3D printed floating formulation (T1), and a capsule containing the ink (DS1), to six dogs. Gastro-floating was implemented by setting Tablet Delay Factor to a value close to cero. T1 was selected for the pilot study due to its higher predicted bioavailability. Dissolution of DS1 and T1 was characterized by a varying pH *in vitro* study. Optimization of the drug's pH-dependent solubility profile was necessary to describe *in vivo* plasma concentration levels. The developed PBPK model adequately predicted the mean relative area under the curve and maximum plasma concentration between T1 and DS1 (1.66 vs. 1.56 and 1.48 vs. 1.50, respectively). DS1 and T1 exhibited better *in vivo* performance than initially predicted. This may be primarily attributed to enhanced solubility at gastric and intestinal pH levels, as well as extended gastric residence time. Gastroretention would lead to a 20% increase in bioavailability.

Ethical approval

Animal procedures and management protocols were approved by the Catholic University of Cordoba (UCC) Ethical Committee and were in compliance with the guidelines of the US National Research Council's for the Care and Use of Laboratory Animals (NRC-USA, 2011).

References

1. A. J. Paredes, N.M. Camacho, L. Schofs, A. Dib, M.P. Zarazaga, N. Litterio, D.A. Allemandi, S. Sánchez Bruni, C. Lanusse, S.D. Palma, Ricobendazole nanocrystals obtained by media milling and spray drying: Pharmacokinetic comparison with the micronized form of the drug, *Int. J. Pharm.*, **585**, 119501 (2020). Doi: https://doi.org/10.1016/j.ijpharm.2020.119501

Covariates affecting potassium bromide apparent clearance in dogs

Silvana Alvariza[1]*, Vernadette Bianchinotti[1], Micaela Sturchio[1], Diego Robaina[1], Gonzalo Suárez[1]

[1] Pharmacology and Therapeutics Unit, School of Veterinary Medicine, Universidad de la República,

Montevideo, Uruguay

*E-mail: silvana.alvariza@fvet.edu.uy

Summary

Potassium bromide KBr is a first line drug for treatment of canine epilepsy, demanding precise dosage control due to its narrow therapeutic window. Monitor its serum levels is crucial for effective treatments. Our study analyzed thirty predose serum samples from dogs treated with KBr alone or in conjunction with phenobarbital. In this study, we analyzed thirty predose serum samples from dogs receiving KBr alone or with phenobarbital, using Monolix® software to investigate factors influencing KBr elimination clearance. We examined the impact of age, sex, phenobarbital consumption, body weight (WT), serum urea (sUr), and creatinine concentration (sCr) on apparent clearance (CL/F). Employing a one-compartment model with fixed absorption rate constant and volume of distribution, WT, sex, and Ur were found to significantly affect CL/F of KBr ($p< 0.001$, $p<0.05$, and $p<0.001$ respectively). Our findings suggest that CL/F increases with higher WT and sUr levels and decreases in male dogs, with males exhibiting a 26% lower CL/F than females. The correlation between CL/F and sUr may stem from bromide's tubular excretion and reabsorption processes, with glomerular filtration playing a minor role in elimination.

Ethical approval

This research was approved by the Committee of Ethics in the Use of Animals (CEUA-FVET) of the School of Veterinary Medicine – Protocol number 799

Financial support and acknowledgements

Financial Support: funds from the Pharmacology and Therapeutics Unit

References

1. P.A. March, M. Podell, R.A. Sams, Pharmacokinetics and toxicity of bromide following high-dose oral potassium bromide administration in healthy Beagles, *J. Vet. Pharmacol. Ther.*, **25**, 425-432 (2002). Doi: https://doi.org/10.1046/j.1365-2885.2002.00440.x

2. J.H. Rossmeisl, K.D. Inzana, Clinical signs, risk factors, and outcomes associated with bromide toxicosis (bromism) in dogs with idiopathic epilepsy, *J. Am. Vet. Med. Assoc.*, 234, 1425-1431 (2009). Doi: https://doi.org/10.2460/javma.234.11.1425

Pharmacokinetic and pharmacodynamic modeling for *in vitro* evaluation of cloxacillin against *Corynebacterium pseudotuberculosis*

Marcos Ferrante[1]*, Larissa Alexsandra Felix[1], Maria Leticia Carneiro Rodrigues[2], Ana Milena César Lima[2], Viviane Maria Dias Costa[2], Patrícia Yoshida Faccioli-Martins[2]

[1] Faculdade de Zootecnia e Medicina Veterinária, Universidade Federal de Lavras, Lavras, Minas Gerais, Brazil

[2] Embrapa Caprinos e Ovinos, Sobral, Ceará, Brazil

*E-mail: marcos.ferrante@ufla.com

Summary

Current treatment of *Corynebacterium pseudotuberculosis* does not result in bacteriological cure and has low biosafety, making it necessary to develop new therapeutic strategies. Therefore, the objective of this study was to determine the epidemiological cutoff point and the PK/PD index of cloxacillin against *C. pseudotuberculosis* based on the *in vitro* bacterial time-kill curve. The minimum inhibitory concentration (MIC) and the time-kill curve were studied in the Cation-adjusted Miller Hinton broth. The epidemiological cut-off point was determined from the MIC distribution [1]. A sigmoid E_{max} model was used to determine the PK/PD index that best described the dose-response profile observed in the time-kill curves. PK/PD (PDT) values were established for bacteriostatic (E=0), bactericidal (E= 3 log10) and eradication (E= -4 log10) activity [2]. The MIC distribution of 35 isolates ranged from 4 to 16 μg/mL with an ECOFF of 16 μg/mL (IC 99.9%). Cloxacillin showed a time-dependent profile represented by the PK/PD indice T>MIC, that is the time that the concentration was above MIC (R^2=0.92). However, in this study the PDT value was established for the area under the curve divided by MIC (AUC/MIC) too. PDT values for the %T>MIC bactericidal (E= 3 log10) and eradication activity were 39% and 51%, respectively, and, for the AUC/MIC were 33.65 h and 46.07 h. This study is a necessary step towards the development of more effective drugs with less emergence of antimicrobial resistance.

Ethical approval

Since this is an *in silico* study, no animals were used.

Financial support and acknowledgements

This study was funded by a Coordenação de Aperfeiçoamento de Pessoal de Nível Superior (CAPES), Conselho Nacional de Desenvolvimento Científico e Tecnológico (CNPq - 448011/2014-0), FAPEMIG - APQ-01168-21, FUNCAP BP5-0197-00148.01.00/22, DCR-CNPq/Funcap 04854900/2022 and EMBRAPA (SEG 20.20.03.002.00.00).

References

1. J. Turnidge, G. Kahlmeter, G. Kronvall, Statistical characterisation of bacterial wild-type MIC value distributions and the determination of epidemiological cut-off values, *Clin. Microbiol. Infect.*, **12**, 418-425 (2006). Doi: https://doi.org/10.1111/j.1469-0691.2006.01377.x

2. Y.F. Zhou, Z. Sun, R.L. Wang, J.G. Li, C.Y. Niu, X.A. Li, Y.Y. Feng, J. Sun, Y. H. Liu, X.P. Liao, Comparison of PK/PD targets and cutoff values for danofloxacin against *Pasteurella multocida* and *Haemophilus parasuis* in piglets, *Front. Vet. Sci.*, **9**, 811967 (2022). Doi: https://doi.org/10.3389/fvets.2022.811967

Pharmacokinetic and pharmacodynamic integration of enrofloxacin in broiler for colibacillosis treatment

Larissa Alexsandra Felix[1]*, Beatriz Monte Egito[1], Bruna Christina Fernandes Soares[1], Diego Diaz[2], Sheila Rezler Wosiack[3], Marcos Ferrante[1]

[1] Faculdade de Zootecnia e Medicina Veterinária, Universidade Federal de Lavras, Lavras, Minas Gerais, Brazil

[2] Faculty of Veterinary Science, Universidad Nacional del Litoral, Santa Fe, Argentina

[3] Departamento de Medicina Veterinária, Universidade Estadual de Maringá, Umuarama, Paraná, Brazil

*E-mail: felix_larissaa@outlook.com

Summary

Enrofloxacin is widely used in poultry production for the treatment of respiratory and enteric infections [1]. The aim of this study was to perform a pharmacokinetic/pharmacodynamic (PK/PD) integration to establish therapeutic protocols for enrofloxacin in broilers for the treatment of colibacillosis. A PK model of enrofloxacin in broilers was constructed using Monolix 2023R1 software based on literature data [2]. The best-fit model was used as the basis for PK/PD integration, with the area under the curve divided by the minimum inhibitory concentration (AUC/MIC) as the PK/PD index. The target values (PDT) were 9.74, 21.29 and 32.13, considering bacteriostatic, bactericidal and eradication action, respectively [3]. A MIC range of 0.004 to 256 μg/mL was used [4-7]. Three doses of enrofloxacin were simulated: 10, 20 and 50 mg/kg, single dose, by gavage. The probability of target achievement (PTA) for each of the protocols was assessed according to a distribution of MICs. The recommended dose of 10 mg/kg achieves a PTA ≥ 90 only for bacteria with an MIC up to 0.06μg/mL for eradication. However, the 20 mg/kg dose could achieve a PTA of 94% for bacteria with a MIC of 0.125 μg/mL for eradication. This is still a preliminary model, but it has already demonstrated the need for dose adjustment in the face of increasing MICs due to antimicrobial resistance.

Ethical approval

Since this is an *in silico* study, no animals were used.

Financial support and acknowledgements

This study was funded by a Coordenação de Aperfeiçoamento de Pessoal de Nível Superior (CAPES), Conselho Nacional de Desenvolvimento Científico e Tecnológico and Undergraduate Research Scholarship Program of UFLA.

References

1. R. Temmerman, L. Pelligand, W. Schelstraete, G. Antonissen, A. Garmyn, M. Devreese, Enrofloxacin dose optimization for the treatment of colibacillosis in broiler chickens using a drinking behaviour pharmacokinetic model, *Antibiotics* (Basel), **10**, 604 (2021). Doi: https://doi.org/10.3390/antibiotics10050604

2. M.C. Kruse, Thesis, 2008.

3. X. Xiao, X. Chen, K. Yan, L. Jiang, R. Li, Y. Liu , M. Wang, Z. Wang, PK/PD integration and pharmacodynamic cutoff of cefquinome against cow mastitis due to *Escherichia coli*, *J. Vet. Pharmacol. Ther.*, **45**, 83-91 (2022). Doi: https://doi.org/10.1111/jvp.13012

4. T.M. Huang, T.L. Lin, C.C. Wu, Antimicrobial susceptibility and resistance of chicken *Escherichia coli*, *Salmonella* spp., and Pasteurella multocida isolates, *Avians Dis.*, **53**, 89-93 (2009). Doi: https://doi.org/10.1637/8268-021608-Reg.1

5. M. Vanni, V. Meucci, R. Tognetti, P. Cagnardi, C. Montesissa, A. Piccirillo, A.M. Rossi, D. Di Bello, L. Intorre, Fluoroquinolone resistance and molecular characterization of gyrA and parC quinolone resistance-determining regions in *Escherichia coli* isolated from poultry, *Poult. Sci.*, **93**, 856-863 (2014). Doi: https://doi.org/10.3382/ps.2013-03627

6. K. Sang, H.H. Hao, L.L. Huang, X. Wang, Z.H. Yuan,Pharmacokinetic-pharmacodynamic modeling of enrofloxacin against *Escherichia coli* in broilers, *Front. Vet. Sci.*, **2**, 80 (2016). Doi: https://doi.org/10.3389/fvets.2015.00080

7. R. Temmerman, A. Garmyn, G. Antonissen, G. Vanantwerpen, M. Vanrobaeys, F. Haesebrouck, M. Devreese, Evaluation of fluoroquinolone resistance in clinical avian pathogenic Escherichia coli isolates from Flanders (Belgium), *Antibiotics* (Basel), **9**, 800 (2020). Doi: https://doi.org/10.3390/antibiotics9110800

Population modeling to study the pharmacokinetics of rutin in an extract of calyces from *Physalis peruviana* in New Zealand white rabbits

Gina Paola Domínguez Moré[1,2]*, Cláudia Maria Oliveira Simões[3], Diana Marcela Aragón[1]

[1] Departamento de Farmacia, Universidad Nacional de Colombia, Bogotá, D.C, Colombia

[2] Facultad de Química y Farmacia, Universidad del Atlántico, Puerto Colombia, Atlántico, Colombia

[3] Programa de Pós-Graduação em Farmácia, Universidade Federal de Santa Catarina, Florianópolis, SC, Brazil

*E-mail: ginadominguez@mail.uniatlantico.edu.co

Summary

A hydroethanolic extract of calyces from *P. peruviana* rich in rutin (quercetin-*3-O*-rutinoside), has shown hypoglycemic activity [1] and produced significant changes in the pharmacokinetics of the pure compound, in rats [2]. This work aimed to study the pharmacokinetics of rutin in the extract, compared to that of the pure compound, in New Zealand White rabbits, a non-rodent species, using population pharmacokinetics (popPK) modeling. The animals (n = 5) received intravenous or oral doses (0.37 to 500 mg/kg) of either the extract or pure rutin. Blood samples were collected for up to 48 h, and the plasma concentrations of rutin and quercetin (rutin metabolite) were quantified using a validated bioanalytical method [3]. The popPK modeling was carried out in Monolix 2019R, incorporating the rutin source as a covariate. The intravenous rutin profile was fitted to a model of two compartments with first-order elimination. The population parameters values for volume of central compartment and elimination rate constant increased (β 0.678 and 0.625, respectively), but the distribution to peripherical compartment rate constant decreased (β –0.634), due to the extract. Orally, the dominant compound in plasma was quercetin which exhibited a double absorption profile with two absorption rate constants, ka1 and ka2. The model showed that the extract produces a decrease of ka1 and an increase of ka2 (β –0.949 and 3.53, respectively). The two popPK models

developed effectively characterized rutin and quercetin pharmacokinetics in the extract (AIC< 1300) and confirmed the variability of the parameters with respect to the pure compound in animal species.

Ethical approval

The study was approved by the ethics committee of the science faculty of the Universidad Nacional de Colombia (Act 06, 2015, project 40831, 22 June 2015).

Financial support and acknowledgements

Authors thanks Universidad Nacional de Colombia and Universidad del Atlántico (Colombia) for their financial support.

References

1. S. Echeverry, I.H. Valderrama, G.M. Costa, L.F. Ospina-Giraldo, D.M. Aragón, Development and optimization of microparticles containing a hypoglycemic fraction of calyces from *Physalis peruviana*, *J. App. Pharm. Sci.*, **8**, 10-18 (2018). Doi: https://doi.org/10.7324/JAPS.2018.8502

2. D. Moré, G. Paola, M.I. Cardona, P.M. Sepúlveda, S.M. Echeverry, C.M. Oliveira Simões, D.M. Aragón, Matrix effects of the hydroethanolic extract of calyces of *Physalis peruviana* L. on rutin pharmacokinetics in Wistar rats using population modeling, *Pharmaceutics*, **13**, 535 (2021). Doi: https://doi.org/10.3390/pharmaceutics13040535

3. G. Domínguez, *Estudio farmacocinético de quercetina-3-O-rutinósido a partir de un extracto estandarizado de cálices de Physalis peruviana en dos modelos animales*, Ph. D. thesis, Universidad Nacional de Colombia, 2020.

Sex, drugs, & PBPK: an assessment of relevant men-women physiologic differences representation in PK-Sim and GastroPlus

Marianela Chavarría-Rojas[1,2]*, Marianela Lorier[3], Manuel Ibarra[3]

[1] Graduate Program in Chemistry, Faculty of Chemistry, Universidad de la República, Montevideo, Uruguay

[2] Industrial Pharmacy Department, Faculty of Pharmacy, Universidad de Costa Rica, San José, Costa Rica

[3] Department of Pharmaceutical Sciences, Faculty of Chemistry, Universidad de la República, Montevideo, Uruguay

*E-mail: marianela.chavarria@ucr.ac.cr

Summary

Physiologically based pharmacokinetic (PBPK) modelling is well-established in model- informed drug development [1]. Its integration in biopharmaceutical applications, involving drug products *in vitro* characterization is gaining traction in generic and controlled-release formulations development. Additionally, it supports risk assessment and alternative bioequivalence approaches in regulatory submissions [2, 3]. While PBPK models enable the evaluation of intrinsic and extrinsic factors affecting drug exposure, the impact of sex-related differences in gastrointestinal tract (GIT) physiology on bioavailability and bioequivalence remains underexplored [1, 2]. This work includes a comprehensive review of sex-related differences impacting pharmacokinetics, particularly drug absorption. Through literature and software revision, we assessed how these differences are represented in predefined anatomical and physiological parameters in PK-Sim® and Gastroplus® PBPK models for virtual populations of Caucasian men and women aged 18-50. Finally, we explore how these differences might affect pharmacokinetic predictions. Key physiological factors with reported sex-related differences, such as GIT pH, transit times, and enzyme and transporters expression, were found to be inadequately reflected in PBPK platforms. For instance, reported gastric pH values (2.16±0.09 for men, 2.79±0.18 for women) [4] are not differentiated in PK-Sim (pH=2.00) and Gastroplus (pH=1.30). Similar discrepancies exist between reported duodenal pH (6.75±0.63 for men, 7.16±0.29 for women) [4] and the included value (pH=6) in both platforms. These parameters

can be manually defined, considering that failing to incorporate sex-related differences may lead to simulation errors, particularly for females, impacting bioavailability and bioequivalence predictions. This research emphasizes the importance of refining PBPK models to better reflect sex-related disparities in GIT physiology, enhancing predictive accuracy and applicability across populations.

Financial support and acknowledgements

Financial support MCR is funded by a scholarship from the Universidad de Costa Rica, granted through the Office of International Affairs and External Cooperation (OAICE) under the contract OAICE-33-2023.

References

1. A. Golhar, M. Pillai, P. Dhakne, N. Rajput, T. Jadav, P. Sengupta, Progressive tools and critical strategies for development of best fit PBPK model aiming better *in vitro-in vivo* correlation, *Int. J. Pharm.*, **643**, 123267 (2023). Doi: https://doi.org/10.1016/j.ijpharm.2023.123267

2. C.G. Wilson, L. Aarons, P. Augustijns, J. Brouwers, A.S. Darwich, T. De Waal, G. Garbacz, S. Hansmann, D. Hoc, A. Ivanova, M. Koziolek, C. Reppas, P. Schick, M. Vertzoni, J.A. García-Horsman, Integration of advanced methods and models to study drug absorption and related processes: An UNGAP perspective, *Eur. J. Pharm. Sci.*, **172**, 106100 (2022). Doi: https://doi.org/10.1016/j.ejps.2021.106100

3. S. Subhani, C. Kim, P. Muniz, M. Rodriguez, S. van Os, E. Suarez, R. Cristofoletti, S. Schmidt, V. Vozmediano, Application of physiologically based absorption and pharmacokinetic modeling in the development process of oral modified release generic products, *Eur. J. Pharm. Biopharm.*, **176**, 87-94 (2022). Doi: https://doi.org/10.1016/j.ejpb.2022.05.007

4. A.C. Freire, A.W. Basit, R. Choudhary, C.W. Piong, H.A. Merchant, Does sex matter? The influence of gender on gastrointestinal physiology and drug delivery, *Int. J. Pharm.*, **415**, 15-28 (2011). Doi: https://doi.org/10.1016/j.ijpharm.2011.04.069

Can inhaled cannabis users accurately evaluate impaired driving ability? A PKPD model

Nicolas Simon[1], Bibiana Cardozo[1]*, Sarah Hartley, Islam Amine Larabi, Jean Claude Alvarez

[1] Department of Clinical Pharmacology, Aix Marseille University, SESSTIM

*E-mail: bibiana.cardozo@etu.univ-amu.fr

Summary

The aim of this investigation is to study the effect of inhaled cannabis on self-assessed predicted driving ability and its relation to reaction times and driving ability on a driving simulator. Participants: 30 healthy males aged 18–34, divided into 15 chronic (1–2 joints/day) and 15 occasional (1–2 joints/week) users. Assessments included self-rated driving confidence (visual analog scale), vigilance (Karolinska), reaction time (mRRT, psychomotor vigilance test), driving ability (SDLP on a York driving simulator), and blood THC concentrations. Measurements were taken before and at intervals after controlled inhalation of placebo, 10mg, or 30mg of THC mixed with tobacco in a cigarette. A population pharmacokinetic/pharmacodynamic analysis was conducted using non-linear mixed-effects modeling in NONMEM version 7.4.1 (26) with the gfortran 4.6.0 compiler. The Wings for NONMEM version 743 served as a "front end" for the NONMEM program [Holford]. Graphical analysis utilized R software version 3.4.2. The first order conditional estimate (FOCE) method with the interaction option was used. Cannabis consumption (at 10 and 30mg) led to a marked decrease in driving confidence over the first 2 h which remained below baseline at 8 h. Driving confidence was related to THC dose and to THC concentrations in the effective compartment with a low concentration of 0.11 ng/ml for the EC50 and a rapid onset of action (T1/2 37min). Driving ability and reaction times were reduced by cannabis consumption. Driving confidence was shown to be related to driving ability and reaction times in both chronic and occasional consumers. Cannabis consumption leads to a rapid reduction in driving confidence which is related to reduced ability on a driving simulator.

Ethical approval

Data used for medialization were obtained from the Study of the Relationship Between Dose-concentration-effect of Delta-9-tetrahydrocannabinol (THC) and the Ability to Drive in Chronic or Occasional Cannabis Users (VIGICANN).

The study was approved by the local Ethics Commitee (CPP Ile-de-France XI: NP 13039), all participants gave their accord to participate in the study by signing an informed consent. Clinical trial registration: ClinicalTrials.gov, identifier: NCT02061020.

Financial support and acknowledgements

Financial Support: Funding for the Ph.D. thesis was provided by the Ministry of Sciences of Colombia. Additional support came from Aix-Marseille University, Faculty of Medicine, SESSTIM group.

References

5. S. Hartley, N. Simon, B. Cardozo, I.A. Larabi, J.C. Alvarez, Can inhaled cannabis users accurately evaluate impaired driving ability? A randomized controlled trial, *Frontiers in Public Health*, **11**, 1234765 (2023). Doi: https://doi.org/10.3389/fpubh.2023.1234765

Application of a pharmacometrics model by assessing the efficacy of amphotericin B deoxycholate

Laiz Campos Pereira [1,2]*, Valdeene Vieira dos Santos[1,2], Matheus Antônio da Hora Borges[1,2], Jackeline Marley dos Santos Araújo[1,2], Luisa Oliveira Samtos[1,2], Rafaela Ferreira Santos Marques[1], Izabel Almeida Alves[1], Francine Johansson Azeredo[2,3]

[1] Laboratory of Pharmacokinetics and Pharmacometrics, Faculty of Pharmacy, Federal University of Bahia, Salvador, Brazil

[2] Pharmacy Graduate Program, Federal University of Bahia, Salvador, Brazil

[3] Center for Pharmacokinetics & System Pharmacology, Department of Pharmaceutics, University of Florida, Orlando, Florida, United States of America

*E-mail: laiz.campos08@gmail.com

Summary

Amphotericin B (AmB) is a drug used to treat invasive candidiasis, and it is considere one of the oldest antifungals employed in clinical practice [1, 2]. In Brazil, AmB deoxycholate is more cost-effective, and only this formulation is provided by the Public Health System [3]. A better understanding of the pharmacokinetic/pharmacodynamic (PK/PD) parameters of AmB deoxycholate is needed to optimize the treatment with this antifungal [4]. The study aims to develop a pharmacokinetic-pharmacodynamic (PK/PD) model to delineate the efficacy of AmB deoxycholate against *Candida albicans*. The modeling was carried out using the Monolix ® software, with the analyzed data obtained from studies featuring static time-kill curves previously conducted by our research group. Among the models evaluated to characterize the antifungal effect of AmB, the modified Emax model was the most descriptive, in which a parameter (*alpha*) was added to signify the delay in the growth of *C. albicans*, both in the presence and absence of the drug. From this model, the parameters related to the potency (kmax) and effectiveness (EC50) of the AmB were obtained. The results were as follows: k0 = 5.52 ± 0.2 h^{-1}; kmax = 0.42 ± 0.11 h^{-1}; EC50 = 0.2 ± 0.06 μg/mL and *alpha* = 1.11 ± 0.29. These results demonstrate that the model employed was considered the best to describe the fungicidal activity of AmB. Therefore, it can be used as a tool for simulating alternative dosage regimens and contribute significantly to optimizing AmB dosage.

Financial support and acknowledgements

Financed by the Coordenação de Aperfeiçoamento de Pessoal de Nível Superior – Brasil (CAPES) – Finance Code 001. CNPq Grant number 407600/2016-7.

References

1. A.M. Tortorano, A. Prigitano, G. Morroni, L. Brescini, F. Barchiesi, Candidemia: Evolution of drug resistance and novel therapeutic approaches, *Infect. Drug Resist.*, **14**, 5543-5553 (2021). Doi: https://doi.org/10.2147/IDR.S274872

2. A. Lemke, A.F. Kiderlen, O. Kayser, Amphotericin B, *Appl. Microbiol. Biotechnol.*, **68**, 151-162 (2005). Doi: https://doi.org/10.1007/s00253-005-1955-9

3. H.H. Lobo Borba, L.M. Steimbach 1, B. Salgado Riveros, F. Stumpf Tonin, V. Lins Ferreira, B.A. de Queiros Bagatim, G. Balan, R. Pontarolo, A. Wiens, *Mycoses*, **61**, 754-763 (2018). Doi: https://doi.org/10.1111/myc.12801

4. N.J. Onufrak, A. Forrest, D. Gonzalez, Pharmacokinetic and pharmacodynamic principles of anti-infective dosing, *Clin. Therap.*, **38**, 1930-1947 (2016). Doi: https://doi.org/10.1016/j.clinthera.2016.06.01

Simulation of pharmacokinetic properties of naringenin, curcumin and β-carotene

Jessica Cruz-Mora[1]*, Marisín Pecchio[2], Johant Lakey-Beitia[1,3]

[1] Center for Biodiversity and Drug Discovery, Instituto de Investigaciones Científicas y Servicios de Alta Tecnología (INDICASAT AIP), Clayton, City of Knowledge, Panama City 0843-01103, Panama

[2] Center for Academic Affairs and Collaboration, Instituto de Investigaciones Científicas y Servicios de Alta Tecnología (INDICASAT AIP), Clayton, City of Knowledge, Panama City 0843-01103, Panama

[3] Sistema Nacional de Investigación (SNI), SENACYT, Panama City 0816-02852, Panama

*E-mail: jessicacruzmora128@gmail.com

Summary

Naringenin, curcumin and β-carotene are natural products that in recent years have demonstrated a wide range of potential therapeutic properties such as neuroprotective activity, anti-aggregation and antioxidants [1-4]. Our research group is interested in improving the neuroprotective activity of these 3 compounds through synthetic modification of their structures. The aim of this study was to predict *in silico* the physicochemical properties and to simulate the pharmacokinetic behavior of each compound after an oral administration of 10 mg. SwissADME and ADMET Predictor software were used to predict the physicochemical properties. The estimated logP for naringenin, curcumin and β-carotene were 2.42, 3.62 and 9.75, respectively. The ADMET parameters (absorption, distribution, metabolism, excretion and toxicity) of the compounds were estimated with ADMET Predictor. The bioavailable fraction values for naringenin, curcumin and β-carotene were 93.5%, 85.1% and 0.065%. The low bioavailability estimated with β-carotene is consistent with the insolubility in water reported in the literature [5]. In addition, half-life results were obtained for naringenin (5 h), curcumin (8 h) and β-carotene (30 h). The participation of the hepatic enzyme CYP3A4, Caco-2 cells and albumin are highly involved in the pharmacokinetic processes of these compounds [1-3]. This project allowed us to validate a workflow that will be used for the understanding of

the ADMET properties of synthetic compounds in association with the knowledge of pharmacological potency, will support us in the identification of pharmacokinetically more acceptable derivatives for future *in vivo* studies.

Financial support and acknowledgements

We are grateful for the support of SENACYT for project FID23-003 and the National Research System (SNI).

References

1. J. Adiwidjaja, A.J. McLachlan, A.V. Boddy, Curcumin as a clinically-promising anti-cancer agent: pharmacokinetics and drug interactions, *Expert Opin. Drug Metab. Toxicol.*, **13**, 953-972 (2017). Doi: https://doi.org/10.1080/17425255.2017.1360279

2. R. Joshi, Y.A. Kulkarni, S. Wairkar, Pharmacokinetic, pharmacodynamic and formulations aspects of Naringenin: An update, *Life Sciences*, **215**, 43-56 (2018). Doi: https://doi.org/10.1016/j.lfs.2018.10.066

3. T. Bohn, C. Desmarchelier, S.N. El, J. Keijer, E. van Schothorst, R. Rühl, P. Borel, β-Carotene in the human body: metabolic bioactivation pathways - from digestion to tissue distribution and excretion, *Proc. Nutr. Soc.*, **78**, 68-87 (2019). Doi: https://doi.org/10.1017/S0029665118002641

4. Z. Nouri,Fakhri, F.F. El-Senduny, N. Sanadgol, G.E. Abd-ElGhani, M.H. Farzaei, J.T. Chen, On the neuroprotective effects of naringenin: Pharmacological targets, signaling pathways, molecular mechanisms, and clinical perspective, *Biomolecules*, **9**, 690 (2019). Doi: https://doi.org/10.3390/biom9110690

5. National Center for Biotechnology Information, PubChem Compound Summary for CID 5280489, Beta-Carotene, URL: https://pubchem.ncbi.nlm.nih.gov/compound/Beta-Carotene. Accessed 2024.

PD modeling of artesunate-mefloquine association effect in mice

Valdeene Vieira Santos[1]*, Laiz Campos Pereira[1], Aline Morena Lourenço dos Santos Miranda[2], Helenita Costa Quadros[3], Mariana da Cruz Borges Silva[2], Diogo Rodrigo de Magalhães Moreira[2], Francine Johansson Azeredo[3]

[1] Pharmacy Post Graduate Program, College of Pharmacy, Federal University of Bahia, Salvador, Bahia, Brazil

[2] Instituto Gonçalo Moniz, Fundação Oswaldo Cruz, Salvador, Bahia, Brazil

[3] Center for Pharmacometrics & System Pharmacology, College of Pharmacy, University of Florida, Orlando, Florida, United States of America

*E-mail: valdeene.vieira@ufba.br

Summary

The artesunate-mefloquine (ARMQ) association treats malaria caused by *Plasmodium falciparum* [1]. Pharmacokinetic/pharmacodynamic (PK/PD) modeling for drug association establishes the effect-time relationship, analyzing the interaction of drugs administered together [2]. To compose the PK/PD model, preclinical PD studies and modeling can be used to describe the concentration-effect relationship of drugs. With this, time-to-event analysis (TTE) and determination of parasitemia were performed. The efficacy of the ARMQ association was evaluated using survival (TTE) and the Thompson test in mice infected with *P. berghei* after administration of 100 mg/kg and 55 mg/kg of AR and MQ, respectively (n=6/group). For TTE analysis, untreated AR and ARMQ groups of animals were observed for 30 days. Survival analysis was performed using the MonolixSuite™ software, using treatment as a covariate. The Thompson test determined parasitemia using flow cytometry on days 5, 6, 7, 8, and 9 after infection. As a result, in the TTE analysis, the Weibull model was chosen as it better describes the survival curve of the data, and the covariate analysis identified that the ARMQ is significant in the Te_pop parameter, with an estimate of 13.66 h, p_pop 4.39 and beta Te_ARMQ of 0.77 h. The probability of survival after treatment with ARMQ for 7, 15, and 30 days was 94.4%, 88.9%, and 14.9%, respectively. Parasitemia in the ARMQ group decreased when compared to the untreated group. Therefore, it can be concluded that the ARMQ association increases survival and reduces parasitemia of infected animals.

Ethical approval

All procedures were reviewed and approved by the Committee on Ethics in the Use of Animals of Instituto Gonçalo Moniz (015/2022).

Financial support and acknowledgements

We thank CNPq for grant number 440227/2022-4S and FAPESB for the scholarship support.

References

1. Brasil, Guia de tratamento da malária no Brasil 2º edição, Ministério da Saúde, 2021.

2. M.J. Brill, A.N. Kristoffersson, C. Zhao, E.I. Nielsen, L.E. Friberg, Semi-mechanistic pharmacokinetic-pharmacodynamic modelling of antibiotic drug combinations, *Clin. Microbiol. Infect.*, **24**, 697-706 (2018). Doi: https://doi.org/10.1016/j.cmi.2017.11.023

PBPK modeling in drug development for rare diseases: A systematic review of FDA approvals

Karen Dayana Lancheros Porras[1], Diana Marcela Aragón Novoa[1]*

[1] Department of Pharmacy, Universidad Nacional de Colombia, Bogotá D.C., Colombia

*E-mail: dmaragonn@unal.edu.co

Summary

Currently, there are more than 10,000 rare diseases worldwide, and the majority represent an unmet medical need [1, 2]. However, due to the nature of these diseases and limited number of patients, it is impractical to develop new drugs using traditional models [3]. Physiologically Based Pharmacokinetic (PBPK) modeling is presented as a valuable tool for drug development in this context, enabling the prediction of systemic drug exposure by integrating *in vitro* information, the physicochemical properties of the drug, and physiological factors [4]. The aim of this work was to assess the use of PBPK in the U.S Food and Drug Administration agency (FDA) applications for novel orphan drugs from 2018 to 2023. Data on yearly approved drugs were sourced from the FDA's novel drug approvals annual reports. For each drug, the Application Review Files available in the FDA's approved drug database were reviewed, focusing on the PBPK modeling section. It was found that 50 orphan drugs employed PBPK modeling in their approval process, and after the FDA review, only 5 models were considered completely inadequate, mainly because of a lack of validation data and uncertainty regarding the enzymatic contribution. The primary approved use (60%) was for the treatment of oncological diseases, particularly those with specific genetic variations, and the main application of PBPK modeling was to predict drug interactions mediated by enzymes (63%). PBPK modeling supported studies at the clinical trial stage, fulfilling a crucial role in both the development and regulatory approval processes for new treatments in rare diseases.

Financial support and acknowledgements

Acknowledgements to the Universidad Nacional de Colombia for making possible the development of the present review and to the professors involved for their guidance and support.

References

1. Global Genes. Rare diseases: Facts and statistics, 2023. URL: http://globalgenes.org/rare-diseases-facts- statistics/. Accessed November 18, 2023.

2. P. Kaufmann, A.R. Pariser, C. Austin, From scientific discovery to treatments for rare diseases - the view from the National Center for Advancing Translational Sciences - Office of Rare Diseases Research, *Orphanet J. Rare Dis.*, **13**, 196 (2018). Doi: https://doi.org/10.1186/s13023-018-0936-x

3. M.J. Field, T.B. Boat, *Rare diseases and orphan products: Accelerating research and development*, Institute of Medicine (US) Committee on Accelerating Rare Diseases Research and Orphan Product Development, 2010. Doi: https://doi.org/10.17226/12953

4. F. Wu, Y. Mousa, K. Raines, C. Bode, Y. Chung Tsang, R. Cristofoletti, H. Zhang, T. Heimbach, L. Fang, F. Kesisoglou, A. Mitra, J. Polli, M.J. Kim, J. Fan, B.S. Zolnik, D. Sun, Y. Zhang, L. Zhao, Regulatory utility of physiologically-based pharmacokinetic modeling to support alternative bioequivalence approaches and risk assessment: A workshop summary report, *CPT Pharmacometrics Syst. Pharmacol.*, **12**, 585-597 (2023). Doi: https://doi.org/10.1002/psp4.12907

Two-step *in vitro-in vivo* correlation for development a predictive flow through cell dissolution method for carbamazepine modified release tablet

Laura Carvajal Barbosa[1], Marcela Aragón Novoa[1]*

[1] Department of Pharmacy, Universidad Nacional de Colombia, Bogotá D.C., Colombia

*E-mail: dmaragonn@unal.edu.co

Summary

The development of an *in vitro-in vivo* correlation (IVIVC) aims to use *in vitro* dissolution data to predict the *in vivo* performance of a drug product [1]. This correlation is not only useful for achieving a biowaiver in bioequivalence (BE) studies but also for successful generic drug product development [2]. The aim of this work was to develop an *in vivo* predictive flow-through cell dissolution method for a modified release carbamazepine tablet (Tegretol® Retard) in a local pharmaceutical company. For this purpose, an experimental design was employed to optimize the dissolution method minimizing the prediction error of the Area Under the Curve (AUC_{0-t}) and Cmax. Three factors at three levels were evaluated: sodium lauryl sulfate concentration in dissolution media, the amount of glass beads, and flow rate. The IVIVC was developed using a deconvolution with the Wagner-Nelson equation, followed by a two-step scaling approach, and a reconvolution [3]. The two-step approach was carried out by constructing a Levy plot, scaling up the dissolution profiles and plotting them against the absorption profile. The obtained IVIVC models were then used to predict the absorbed fractions. Fifteen dissolution profiles and IVIVC models were obtained under different conditions, with AUC_{0-t} and Cmax prediction errors ranging from -64% to -8%. With the optimized dissolution method, an IVIVC was achieved with an r^2= 0.9905, predicting errors of -6.08% for the AUC_{0-t} and -1.93% for Cmax. The developed and optimized dissolution method was challenged with immediate-release carbamazepine tablets (Tegretol® IR) and proved to be discriminative. In conclusion, an *in vivo* predictive flow-through cell dissolution method was developed in a local pharmaceutical company as a tool for the development of generic modified release carbamazepine products.

Financial support and acknowledgements

Pharmacy Department of the Universidad Nacional de Colombia and Pharmetique Labs.

References

1. Y. Lu, S. Kim, K. Park, *In vitro-in vivo* correlation: Perspectives on model development, *Int. J. Pharm.*, **418**, 142148 (2011). Doi: https://doi.org/10.1016/j.ijpharm.2011.01.010

2. B. Sánchez-Dengra, I. González-García, M. González-Álvarez, I. González-Álvarez, M. Bermejo, Two-step *in vitro-in vivo* correlations: Deconvolution and convolution methods, which one gives the best predictability? Comparison with one-step approach, *Eur. J. Pharm. Biopharm.*, **158**, 185-197 (2021). Doi: https://doi.org/10.1016/j.ejpb.2020.11.009

3. M.C. Gohel., R.K. Parikh, P.Y. Aghara, S.A. Nagori, R.R. Delvadia, M.R. Dabhi, Application of simplex lattice design and desirability function for the formulation development of mouth dissolving film of salbutamol sulphate, *Curr. Drug Deliv.*, **6**, 486-494 (2009). Doi: https://doi.org/10.2174/156720109789941696

Evaluation of the dissolution behavior of etodolac tablets using a physiologically based biopharmaceutics modeling approach

Larissa Lopes Rodrigues Gomide[1], Marcelo Dutra Duque[1]*

[1] Universidade Federal de São Paulo - UNIFESP, Institute of Environmental, Chemical and Pharmaceutical Sciences, Diadema, São Paulo, Brazil

*E-mail: marcelo.duque@unifesp.br

Summary

Etodolac is an acidic molecule (pKa 4.65) with pH-dependent solubility and classified as a BCS class II drug [1]. Due to its low solubility, it is important to understand if different dissolution media could lead to different results on its predicted bioavailability. In order to evaluate such influence, a Physiologically Based Biopharmaceutics Model (PBBM) was developed and validated. Methods: Experimental dissolution tests were carried out using the reference drug product in Brazil, Flancox 400mg, at four different dissolution pH values 5.5, 6.0, 6.4 and 6.8 using USP apparatus II at 50 rpm and a PBBM for etodolac using GastroPlus® version 9.8.3. The *in vitro* dissolution profiles were modeled in GastroPlus® using the Z-factor dissolution model, and virtual bioequivalence (VBE) studies were run in comparison to Lodine, FDA's etodolac reference drug product. As expected, for each pH different dissolutions profiles were observed, as well as different Z-factor values. These values were used to run ten VBE trials for each pH condition, and all were within the 0.8 -1.25 acceptance criteria. These results showed similar predicted *in vivo* dissolution behavior of the evaluated drug product, with high probability to be bioequivalent to the FDA's reference drug product, Lodine. Although etodolac is a BCS class II drug, under pH conditions above its pKa, it behaves as a BCS class I drug, according to the predictions and virtual bioequivalences.

Financial support and acknowledgements

The authors would like to thank Simulations Plus Inc., (Lancaster, CA, USA) for providing GastroPlus® software.

References

1. X. Hu, Y. Gong, Z. Cao, Z. Huang, J. Sha, Y. Li, T. Li, B. Ren, Solubility, Hansen solubility parameter and thermodynamic properties of etodolac in twelve organic pure solvents at different temperatures, *J. Mol. Liq.*, **316**, 113779 (2020). Doi: https://doi.org/10.1016/j.molliq.2020.113779

Physiology-based pharmacokinetic evaluation of tafenoquine drug-drug interactions

Luisa Oliveira Santos[1]*, Francine Johansson Azeredo[1,2]

[1] Graduate Program in Pharmacy, Federal University of Bahia, Salvador, Bahia, Brazil

[2] Center for Pharmacometrics & Systems Pharmacology, Department of Pharmaceutics, College of Pharmacy, University of Florida, Orlando, Florida, FL, United States of America

*E-mail: santos.luisa@ufba.br

Summary

Physiology-Based Pharmacokinetics (PBPK) uses models and simulations combining physiology, population, drug substance, and product characteristics to mechanistically describe the pharmacokinetic behaviors of a drug [1]. PBPK has become a promising tool for drug interaction potential evaluation [2]. Malaria is an acute febrile infectious disease transmitted by the bite of the female Anopheles mosquito [3]. In South America, 77% of the global cases accumulate, most related to the etiological agent *Plasmodium vivax*. This species has evolutionary forms that remain dormant in the liver [4, 5]. Tafenoquine (TQ) is an 8-aminoquinoline analog of primaquine that appears promising due to its administration in a single dose. However, being a prodrug, there are concerns regarding its drug-drug interactions [6]. A PBPK model for TQ was developed in the PK-SIM® software (v.11) utilizing previously published studies. The model was created based on a healthy male European individual considering CYP2D6 as the predominant metabolizing enzyme. For some parameters that could not be informed from experimental data or were present to be relevant after sensitivity analyses, parameter identification based on plasma concentration-time profiles was performed using a subset of the available clinical studies (training dataset) for model optimization. The predicted Cmax value fell within the 2-fold acceptance criteria with an overall geometric mean fold error (GMFE) of 1.09. The mean relative deviations (MRD) for all plasma concentration was 1.29 falling within 2-fold of the corresponding concentration observed. Model still needs improvement and training with different doses so then it can be used for drug interaction evaluation regarding the CYP2D6 enzyme.

Financial support and acknowledgements

Financed by the Fundação de Amparo à Pesquisa do Estado da Bahia – Finance code 916/2023.

References

1. FDA, The Use of Physiologically Based Pharmacokinetics Analyses, 2020. URL: https://www.fda.gov/regulatory-information/search-fda-guidance-documents/use-physiologically-based-pharmacokinetic-analyses-biopharmaceutics-applications-oral-drug-product, Accessed 2024.

2. C. Wagner, Y. Pan, V. Hsu, V. Sinha, P. Zhao, Predicting the Effect of CYP3A Inducers on the pharmacokinetics of substrate drugs using physiologically based pharmacokinetic (PBPK) modeling: An analysis of PBPK submissions to the US FDA, *Clin. Pharmacokinet.*, **55**, 475-483 (2016). Doi: https://doi.org/10.1007/s40262-015-0330-y

3. E.M. Braga, *et al.*, *Livro Parasitologia Humana*, 13 ed., Atheneu, 2016.

4. WHO, World Malaria Report, 2023. URL: https://www.who.int/teams/global-malaria-programme/reports/world-malaria-report-2023. Accessed 2024.

5. Brasil, Guia de tratamento da malária no Brasil, 2021. URL: https://www.gov.br/saude/pt-br/centrais-de-conteudo/publicacoes/svsa/malaria/tratamento. Accessed 2024.

PBPK modeling of 3D-printed benznidazole formulations for individualized Chagas disease treatment

Patricia Rega[1,2*], María Sol Magi[3,4], Lucía Lopez-Vidal[3,4], Álvaro Jimenez Kairuz[4], Santiago Daniel Palma[3,4], Juan Pablo Real[3,4], Manuel Ibarra[1]

[1] Department of Pharmaceutical Sciences, Faculty of Chemistry. Universidad de la República. Montevideo, Uruguay

[2] Postgraduate Program, Faculty of Chemistry, Universidad de la República, Montevideo, Uruguay

[3] Investigation Unit and Pharmaceutical Technology Development, CONICET. Universidad Nacional de Córdoba, Argentina

[4] Department of Pharmaceutical Sciences, Faculty of Chemical Sciences, Universidad Nacional de Córdoba, Argentina

*E-mail: patriciarega@fq.edu.uy

Summary

Benznidazole (BNZ) is a first-line drug used against Chagas disease, a neglected tropical disease associated with ten thousand deaths and seven million annual infections. The treatment implies the administration of high doses of BNZ over extended periods, often leading to the appearance of severe adverse events that compromise patient adherence. Consequently, the development of innovative technologies, such as 3D-printed solid pharmaceutical forms, emerges as a promising strategy to individualize the pharmacotherapy and improve BNZ safety and efficacy. 3D inks advantages includes providing specific drug release properties and enabling a customized dose [1]. This work aimed to inform decision-making in the preclinical development stage by predicting the pharmacokinetic performance of two printlets (immediate release and extended release) in dogs, and subsequently projecting a third formulation containing a mixture of both inks. A physiologically based pharmacokinetic model (PBPK) for BNZ in dogs was developed using reported data including *in vitro* drug dissolution and *in vivo* pharmacokinetics after administration of Abarax® (immediate release formulation) and a modified release formulation based on ionic polymers combination (IPC) [2], which were later used in the production of one

of the inks. Sensitivity analyses were conducted to evaluate variables affecting BNZ bioavailability, including *in vivo* dissolution profile, absorption time, and a gastro-retentive delivery system implementation. Single and multiple dose plasma profiles were simulated for the formulation of interest. The combination of gastro-retention and IPC as a solubility enhancer was predicted to improve BNZ bioavailability, resulting in a desirable therapeutic profile. This formulation strategy holds promise for personalized medicine design.

Financial support and acknowledgements

Financial support was received from the National Postgraduate Scholarship Program of ANII (Agencia Nacional de Innovación e Investigación-Uruguay), grant POS_NAC_2022_1_174151).

References

1. J. Goole, K. Amighi, 3D printing in pharmaceutics: A new tool for designing customized drug delivery systems, *Int. J. Pharm.*, **499**, 376-394 (2016). Doi: https://doi.org/10.1016/j.ijpharm.2015.12.071

2. M.C. García, M.L. Guzman, M.A. Himelfarb, N.J. Litterio, M.E. Olivera, A. Jimenez-Kairuz, Preclinical pharmacokinetics of benznidazole-loaded interpolyelectrolyte complex-based delivery systems, *Eur. J. Pharm. Sci.*, **122**, 281-291 (2018). Doi: https://doi.org/10.1016/j.ejps.2018.07.005

Physiology-based pharmacokinetic modeling to optimize intravenous lidocaine infusion in dogs with hemorrhagic shock

Sibely Aiva Flores[1]*, Bárbara Fernandes Dorante[1], Vivian Aparecida Malta[1], Bruna Christina Fernandes Soares[1], Lucas Wamser Fonseca Gonzaga[1], Marcos Ferrante[1]

[1] Faculdade de Zootecnia e Medicina Veterinária, Universidade Federal de Lavras, Lavras, Minas Gerais, Brazil

*E-mail: sibelyaflores@gmail.com

Summary

Lidocaine, when administered intravenously, can promote analgesia in dogs [1]. Eventually, patients in critical condition may present other conditions adjacent to the pain, such as hemorrhagic shock, leading to the need to adjust the dose of analgesics in this situation [2]. This study aims to create a physiologically based pharmacokinetic model (PBPK) to optimize the lidocaine infusion protocol for dogs in hemorrhagic shock. The model was developed in the PK-SIM® software (OPEN SYSTEMS PHARMACOLOGY), version 11.2 based on pharmacokinetic data obtained in the literature. Physicochemical data of the drug were obtained from the PubChem database. The model was evaluated by the geometric mean fold error (GMFE) of the area under the curve (AUCt-end) [3]. Therefore, it was resized to predict doses in patients with hemorrhagic shock based on a pharmacokinetic study [2]. The administration of a 2 mg/kg/h infusion was simulated to compare and adjust the infusion rate based on the area under the curve values from 0 to 3 hours (AUC0-3h) of the two individuals. A GMFE value of 1.42 was observed, indicating a good predictive value when considering a double error criterion. The simulated protocols revealed AUC0-2h values of 473.56 μmol·min/L for healthy patients and 850.7 μmol·min/L for shock patients. When adjusting the infusion rate to 1.1 mg/kg/h, the AUC0-2h value of shock patients was reduced to 467.89 μmol·min/L. With this model, it was possible to suggest an adjustment in the lidocaine infusion rate for patients in shock to minimize possible adverse effects of lidocaine.

Ethical approval

Since this is an in silico study, no animals were used.

Financial support and acknowledgements

This study was funded by Coordenação de Aperfeiçoamento de Pessoal de Nível Superior (CAPES) and by Fundação de Amparo a Pesquisa de Minas Gerais (FAPEMIG).

References

1. P. Raušer. H. Němečková, M. Mrázová, J. Václavíková, L. Novák, Influence of fentanyl, ketamine, and lidocaine on tear production in healthy conscious dogs, *Top Companion Anim. Med.*, **46**, 100615 (2022). Doi: https://doi.org/10.1016/j.tcam.2021.100615

2. P. L. Toutain. A. Autefage, M. Oukessou, M. Alvinerie, Pharmacokinetics of methylprednisolone succinate, methylprednisolone, and lidocaine in the normal dog and during hemorrhagic shock, *J. Pharm. Sci.*, **76**, 528-534 (1987). Doi: https://doi.org/10.1002/jps.2600760708

3. L. Kovar. A. Weber, M. Zemlin, Y. Kohl, R. Bals, B. Meibohm, D. Selzer, T. Lehr, Physiologically-based pharmacokinetic (PBPK) modeling providing insights into fentanyl pharmacokinetics in adults and pediatric patients, *Pharmaceutics*, **12**, 908 (2020). Doi: https://doi.org/10.3390/pharmaceutics12100908

Evaluation of the dissolution behavior of the lysosomotropic drug amlodipine using physiologically based biopharmaceutics modeling (PBBM)

Jose Perez-Urizar[1,2*], Porfirio de La Cruz[1], Larissa Lopes Rodrigues Gomide[3], Marcelo Dutra Duque[3]

[1] Facultad de Ciencias Químicas, Universidad Autónoma de San Luis Potosí, San Luis Potosí, México [2] FS Scientia Pharma S.A. de C.V., San Luis Potosí, México

[3] Department Pharmaceutical Sciences, Universidade Federal de São Paulo-UNIFESP, Institute of Environmental, Chemical and Pharmaceutical Sciences, Diadema, São Paulo, Brazil

*E-mail: jpurizar@uaslp.mx

Summary

Amlodipine (AML) is a weak base drug (pKa 9.1) classified as a BCS class I drug. The aim of this study was to develop and validate a PBBM to evaluate the dissolution behavior of AML when administered orally. GastroPlus® software was used to build a compartmental pharmacokinetic (PK) model based on intravenous (IV) and oral administration data. Lysosomal trapping of the drug was evaluated using MembranePlus™ software by testing different pHs in the lysosomes. The model was validated by comparing the obtained PK data with different literature data, and it was used to evaluate different dissolution profiles [1, 2] of the reference drug product Norvasc® 5 mg. The predicted/observed (P/O) ratio values for Cmax, Tmax and AUC, were within the 0.8-1.25 acceptance range for the IV 10 mg infusion and for the 5 mg tablet used to build the model, and for 5 mg and 10 mg tablets from different literature. AML showed to be trapped by the lysosomes, with a fraction unbound to the enterocytes of 1.3%. The calculated Z-factor values for the dissolution profiles of Norvasc® 5 mg tablets were 4.98E-4, 4.05E-4, and 4.96E-4 mL/mg/s, for pH 1.2, 4.5, and 6.8, respectively. The results showed that lysosomal trapping is responsible for the long Tmax (>6h) of AML, and the three dissolution test conditions evaluated can be used as biopredictive, since similar predicted *in vivo* behavior was observed independent of the dissolution profile used in the model.

Financial support and acknowledgements

The authors would like the thank Simulations Plus Inc., (Lancaster, CA, USA) for providing the software GastroPlus® and MembranePlus™ as academic license, and to Consejo Potosino de Ciencia y Tecnología for financial support via FME/2023/SE-08/17 project.

References

1. A.N. Zaid, S. Natur, A. Qaddomi, M. Abualhasan, R. Al-Ramahi, N. Shraim, S. Khammash, N. Jaradat, Formulation and bioequivalence of two Valsartan/Amlodipine immediate release tablets after a single oral administration, *Pak. J. Pharm. Sci.*, **27**, 755-762 (2014).

2. A.N. Zaid, N. Shraim, A. Radwan, N. Jaradat, S. Hirzallah, I. Issa, A. Khraim, Does GastroPlus support similarity and dissimilarity factors of *in vitro-in vivo* prediction in biowaiver studies? A lower strength amlodipine as a model drug, *Drug Res.* (Stuttg), **68**, 625-630 (2018). Doi: https://doi.org/10.1055/a-0611-4927

Advancing horizons in PBPK modeling: A review of patent from 2013 to 2024

Brian Sebastian Correa Barrera[1], Karen Lancheros[1], Izabel Almeida Alves[2], Diana Marcela Aragón Novoa[1]*

[1] Departamento de Farmacia, Universidad Nacional de Colombia, Bogotá D.C., Colombia

[2] Faculdade de Farmácia, Universidade Federal de Bahia, Salvador-BA, Brazil

*E-mail: dmaragonn@unal.edu.co

Summary

Physiologically-Based Pharmacokinetic (PBPK) models have emerged as a powerful mathematical framework integrating physiological and pharmacological insights to predict PK profiles across diverse compounds [1, 2]. Despite advancements, accurately characterizing substance behavior and translating findings to human contexts remains a challenge due to inter-individual variabilities and substance complexities [3]. This study aims to evaluate recent patents concerning PBPK modeling. Data were retrieved from the Espacenet patents database spanning 2000 to 2023 using the keyword "PBPK" Screening criteria encompassed titles, summaries, and content pertinent to PBPK modeling. Sixteen patents were identified, primarily applied in toxicology, bioequivalence, and drug development decision support. Notably, 44% of PBPK patents focused on enhancing *in vitro* test understanding and *in vivo* extrapolation, while 25% addressed toxic risk assessment and 13% targeted anticancer drugs. PBPK models proved beneficial for drugs with narrow therapeutic margins or inadequate *in vitro* data, facilitating predictive physiological and metabolic insights using *in vitro* information. This study underscores PBPK modeling's adaptability in predicting physiological and metabolic responses to diverse compounds, particularly those with toxic potential, thereby enhancing drug development decision-making processes.

Ethical approval

This study did not involve experimentation on cells, animals, or human subjects.

Financial support and acknowledgements

Acknowledgments to Universidad Nacional de Colombia for making possible the development of this research.

References

1. D. Deepika, V. Kumar, The role of "Physiologically Based Pharmacokinetic Model (PBPK)" new approach methodology (NAM) in pharmaceuticals and environmental chemical risk assessment, *Int. J. Environ. Res. Public Health*, **20**, 3473 (2023). Doi: https://doi.org/10.3390/ijerph20043473

2. K.D. Lancheros, I.A. Alves, D.M. Aragon, PBPK modeling as an alternative method of interspecies extrapolation that reduces the use of animals: A systematic review, *Current Medicinal Chemistry*, **31**, 102-126 (2024). Doi: https://doi.org/10.2174/0929867330666230408201849

3. H. Jones, K. Rowland-Yeo, Basic concepts in physiologically based pharmacokinetic modeling in drug discovery and development, *CPT Pharmacometrics Syst. Pharmacol.*, **2**, e63 (2013). Doi: https://doi.org/10.1038/psp.2013.41

Prediction of *in vivo* behaviour of metformin-loaded PLGA nanoparticles

Dalia Elena Lopera[1,2]*, Marisin Pecchio[1,2]

[1] Facultad de Farmacia, Universidad de Panamá, Ciudad de Panamá, Panamá

[2] Instituto de Investigaciones Científicas y Servicios de Alta Tecnología AIP (INDICASAT AIP), Ciudad de Panamá, País de Panamá

*E-mail: daliamariafar@gmail.com

Summary

Metformin is the drug of first choice in the treatment of type II diabetes. To maintain effective concentrations of metformin in plasma, repeated doses are necessary. Nanoparticles appear to be able to improve the pharmacokinetics of many substances, and in many cases have the ability to efficiently cross biological barriers. Therefore, applying this new technology in the administration of drugs such as metformin points to improvements in their therapeutic profile [1]. A PK model was developed from a physiological model with the use of the *in silico* program, PK-Sim® [2, 3], using data from *in vitro* dissolution of three metformin -loaded PGLA nanoparticle with a size of less than 300 nm, obtained from the *in vitro* dissolution profile, achieving predictions for absorption, distribution, metabolism and excretion (ADME). The first priori predictions were made, to human population, in normal Mexican adult women, without modifying the transporter systems and enzymes responsible for metabolism in man. Simulations were performed with simple and advanced administration protocols. The most favorable simulations were obtained with the advanced administration protocol, at an initial dose of 5000 mg, orally, with three repetitions. The results suggest that the prepared nanoparticles could be promising for oral administration of metformin. The application of this approach physiologically based pharmacokinetic (PK) modeling is very interesting to describe the development of a new PGLA metformin nanoparticle formulation without resorting to *in vivo* assays. Changes that have the greatest impact on single-dose administration and elimination half-life can be predicted.

References

1. G.G. Graham, J. Punt, M. Arora, R.O. Day, M.P. Doogue, J.K. Duong, T.J. Furlong, J.R. Greenfield, L.C. Greenup, C.M. Kirkpatrick, J.E. Ray, P. Timmins, K.M. Williams, Clinical pharmacokinetics of metformin, *Clin. Pharmacokinet.*, **50**, 81-98 (2011). Doi: https://doi.org/10.2165/11534750-000000000-00000

2. PK-SIM® y MOBI® para PBPK, GitHub. Open-Systems-Pharmacology, 2019.

3. L. Kuepfer, C. Niederalt, T. Wendl, J.F. Schlender, S. Willmann, J. Lippert, M. Block, T. Eissing, D. Teutonico, Applied concepts in PBPK modeling: How to build a PBPK/PD model, *CPT Pharmacometrics Syst. Pharmacol.*, **5**, 516-531 (2016). Doi: https://doi.org/10.1002/psp4.12134

Impact of the differences *in vitro* dissolution on the albendazole pharmacokinetics parameters

Nelly Norma Castro-Torres[1]*, Iliana González-Hernández[1], Lourdes Mayet-Cruz[2], José Becerril-Vega[2], Helgi Jung-Cook[2]

[1] Laboratorio de Neurobioquímica y conducta, Instituto Nacional de Neurología y Neurocirugía MVS, Ciudad de México, México

[2] Laboratorio de Biofarmacia, División de Estudios de posgrado Facultad de química, Universidad Nacional Autónoma de México, Ciudad de México, México

*E-mail: nelly.castro@innn.edu.mx

Summary

Except for Brazil and Mexico, in Latin America a bioequivalence study is not required for generic albendazole products, however they must comply with a dissolution requirement. The aim of the present study was to evaluate if differences in the *in vitro* dissolution of albendazole tablets could be related to *in vivo* pharmacokinetic differences. For the *in vitro* evaluation 3 Mexican generic products containing 200 mg of albendazole (ALB) and the innovator product, were selected. Study was performed according to the Mexican Pharmacopeia [1]. Differences were found in the mean dissolution time (MDT) and in the f2 test. For the *in vivo* study, the product with the lowest similarity factor was selected. Study was performed in 12 healthy volunteers who received a dose of 400 mg of ALB in a crossover design. ALB and its main metabolite albendazole sulfoxide (ALBSO) were determined using a previously validated LC/MS/MS assay. A high interindividual variability was found both for the reference and the test products. No significant differences ($P<0.05$) were found in maximum concentration (Cmax) and area under the curve (AUC) for ALB or ALBSO, and therefore a relation *in vitro-in vivo* was not found. To explain the variability, a nonlinear mixed-effects modeling approach was employed using Monolix 2021R1 software. The best model was a one compartment with double absorption peaks and lag time. Results showed that due to the high variability in albendazole absorption and the double peak phenomena, the pharmacopeia dissolution test would not be representative of the *in vivo* behavior of the drug products.

Ethical approval

Protocol 19/18 approved by the Investigation Committee of the Instituto Nacional de Neurologia, MVS.

Financial support and acknowledgements

Financial Support. The authors thankfully acknowledge Facultad de Química, UNAM (grant number PAIP 50009137) and CONACYT (grant number 229785) for providing financial support.

References

1. Farmacopea de los Estados Unidos Mexicanos, Undécima edición, México, Secretaría de Salud, Vol III, 2018, pp. 2095-2097.

Mechanistic insights into amlodipine oral absorption

Porfirio de la Cruz Cruz[1]*, Mauricio García Alcalde[2], Ángel Antonio Vértiz Hernández[3], José Trinidad Pérez Urizar[4,5]

[1] Doctorado Institucional en Ingeniería y Ciencia de Materiales, Universidad Autónoma de San Luis Potosí, San Luis Potosí, México

[2] Departmento de Farmacia, Escuela de Química y Farmacia, Facultad de Química y de Farmacia, Pontificia Universidad Católica de Chile, Santiago, Chile

[3] Coordinación Académica Región Altiplano, Universidad Autónoma de San Luis Potosí, San Luis Potosí, México

[4] Facultad de Ciencias Químicas, Universidad Autónoma de San Luis Potosí, San Luis Potosí, México

[5] FS Scientia Pharma S.A. de C.V., San Luis Potosí, México

*E-mail: porfirio1104@hotmail.com

Summary

Amlodipine (AML) is the only dihydropyridine with a slow absorption, resulting in prolonged Tmax (6-8 h), most likely due to its basic pKa=9.1. Although models have been successfully developed, they overlooked the mechanisms behind this phenomenon. Even though this could be explained by the recently introduced lysosomal trapping (Hypothesis 1: H1), it may also relate to a potential slow intestinal permeability (Hypothesis 2: H2). In this work, we developed and validated a PBPK model using GastroPlus® to assess H1 and H2. Lukacova's method was used to model AML distribution, calculating the blood- to-plasma ratio from published equations [1, 2]. Renal clearance was fit to 1.6 L/h [3]. CYP3A4 Km and Vmax were simultaneously fit to match intravenous profiles, while CYP3A5 Vmax was set to 10% that of CYP3A4 [4]. For H1, permeability (Peff=1.9x10^{-4} cm/s) was calculated from ka [5] and fraction trapped was calculated to 1.17% using Henderson-Hasselbach. For H2, Peff was decreased to target a borderline An=0.85 assuming no trapping. Both internal and external validations showed r^2>0.94 and RMSE <9.17. After oral dose simulation, neither approach correctly predicted Tmax (1.1 and 2.0 h, H1 and

H2, *vs* 8.0 h observed). Nonetheless, H2 performed comparatively better than H1 in predicting Cmax (prediction errors of 53 and 284%, respectively). Results suggest that deeper mechanistic understanding is needed to model AML oral absorption, although the H2 seemed to provide closer predictions. Therefore, further knowledge on regional absorption may be to improve predictions for this and other similar drugs.

Financial support and acknowledgements

The authors would like the thank Simulations Plus Inc., (Lancaster, CA, USA) for providing the software GastroPlus® as academic license, and to Consejo Potosino de Ciencia y Tecnología for financial support via FME/2023/SE-08/17 project.

References

1. C. Tannergren, H. Jadhav, E. Eckernäs, J. Fagerberg, P. Augustijns, E. Sjögren, Physiologically based biopharmaceutics modeling of regional and colon absorption in humans, *Eur. J. Pharm. Biopharm.*, **186**, 144-159 (2023). Doi: https://doi.org/10.1016/j.ejpb.2023.03.013

2. A.P. Beresford, D. McGibney, M.J. Humphrey, P.V. Macrae, D.A. Stopher, Metabolism and kinetics of amlodipine in man, *Xenobiotica*, **18**, 245-254 (1988). Doi: https://doi.org/10.3109/00498258809041660

3. J.K. Faulkner, D. McGibney, L.F. Chasseaud, J.L. Perry, I.W. Taylor, The pharmacokinetics of amlodipine in healthy volunteers after single intravenous and oral doses and after 14 repeated oral doses given once daily, *Br. J. Clin. Pharmacol.*, **22**, 21-25 (1986). Doi: https://doi.org/10.1111/j.1365-2125.1986.tb02874.x

4. Y. Zhu, F. Wang, Q. Li, M. Zhu, A. Du, W. Tang, W. Chen, Amlodipine metabolism in human liver microsomes and roles of CYP3A4/5 in the dihydropyridine dehydrogenation, *Drug Metab. Dispos.*, **42**, 245-249 (2014). Doi: https://doi.org/10.1124/dmd.113.055400

5. J.T. Flynn, M.C. Nahata, J.D. Mahan Jr, R.J. Portman, Population pharmacokinetics of amlodipine in hypertensive children and adolescents, *J. Clin. Pharmacol.*, **46**, 905-916 (2006). Doi: https://doi.org/10.1177/0091270006289844

Novel and simple method to back-calculate plasma concentrations in two-compartmental models

Mauricio A. García[1]*, Pablo M. González[2]

[1] Departamento de Farmacia, Escuela de Química y Farmacia, Facultad de Química y de Farmacia, Pontificia Universidad Católica de Chile, Santiago, 7820436, Chile

[2] Innovation and Biopharmaceutical Evaluation Center (IBECenter), Recoleta, Santiago, Chile

*E-mail: magarci3@uc.cl

Summary

Pharmacometrics is the discipline that quantifies the interaction between the drug product and the patient through modelling. Among pharmacokinetic (PK) models, compartmental are the simplest and perhaps most used in pharmaceutical industry. Level A *in vivo-in vitro* correlation (IVIVC) is the highest standard were fraction dissolved and absorbed are correlated point-by-point. Although mechanistical PBPK software have recently emerged, compartmental deconvolution is still highly used due to its simplicity and fewer number of assumptions. Validation of the IVIVC requires reconstructing plasma profiles from *in vitro* dissolution. In 2005, Gohel *et al.* [1] published one equation for one- compartment PK. However, no method was reported two-compartment cases. In this poster, we derived a novel and simple method to reconstruct plasma profiles after Loo- Riegelman's deconvolution, which can be easily solved. Validation was achieved by both numerical back-calculation of plasma profiles and applicating the equation to a real IVIVC case for levonorgestrel as model drug. Back-calculation of plasma levels was not only accomplished, but also this method was successfully applied to correlate *in vitro* dissolution and *in vivo* absorption of two contraception formulations with levonorgestrel and ethynyl estradiol, which failed the bioequivalence for the former drug. Prediction errors (PE) for Cmax and AUC parameters were below 15% for each formulation, with average PE being below 10%, thus fulfilling the regulatory requirements for IVIVC validation. This tool may be a valuable asset for small generic companies that not always can afford expensive software.

Ethical approval

Clinical trial was approved by the Independent Ethics Committee (IEC) (protocol HP8814-03, Version: 2 .0, and date of approval 04 December 2021), in accordance with the Declaration of Helsinki.

Financial support and acknowledgements

Financial Support was received from "Proyecto de Inserción Académica (PIA)" no 3915-1004-301-81, Pontificia Universidad Católica de Chile.

References

1. J.C. Loo, S. Riegelman, New method for calculating the intrinsic absorption rate of drugs, *J. Pharm. Sci.*, **57**, 918-928 (1968). Doi: https://doi.org/10.1002/jps.2600570602

Approximation to the population PK/PD model of a self-emulsifying delivery system of an extract from *Physalis peruviana*

Cristian Sneyder Castellanos Sánchez[1], Maria Isabel Cardona[1], Gina Paola Domínguez Moré[1,2], Diana Marcela Aragón[1]*

[1] Departamento de Farmacia, Facultad de Ciencias, Universidad Nacional de Colombia, Bogotá, Colombia

[2] Centro de servicios farmacéuticos y monitoreo de fármacos. Programa de Farmacia, Facultad de Química y Farmacia, Universidad del Atlántico, Puerto Colombia, Colombia

*E-mail: dmaragonn@unal.edu.co

Summary

The hydroalcoholic extract of *Physalis peruviana* has poor oral bioavailability due to low solubility and permeability [1, 2]. To improve the bioavailability and hypoglycemic activity of rutin, the major flavonoid on the extract, a self-emulsifying delivery system (SEDDs) was developed. This study aims to conduct population pharmacokinetic and pharmacodynamic (PK/PD) modeling of the extract formulated with SEDDs and evaluated through an oral glucose test in Wistar rats. The PK/PD model, developed using Monolix software (Lixoft®, Paris, France) was chosen based on the observation of graphs, Akaike information criterion (AIC) values and precision of the estimated parameters. The final popPK exhibit two compartments, dual uptake of order 1 and order 0, a time delay for the second uptake, and Michaelis-Menten elimination. These results could be explained because high plasma levels of rutin (from extracts) after oral administration of SEDDs cause changes in the rate of metabolic processes such as transport into the intestinal lumen and active tubular secretion may become saturated [3, 4]. Our pharmacodynamic model suggests an indirect stimulation mechanism for rutin, sice rutin stimulate calcium channels to promote glucose reuptake into muscles [5, 6]. SEDDs significantly enhance extract bioavailability, with 12 times greater potency than unformulated extract.

Ethical approval

The study was approved by the Ethics Committee of the Science Faculty of Universidad Nacional de Colombia (Act 06, 2015, project 40831, 22 June 2015).

Financial support and acknowledgements

To the Universidad Nacional de Colombia and Lixoft for the academic license of Monolix software.

References

1. G.P. Domínguez Moré, M.I. Cardona, P.M. Sepúlveda, S.M. Echeverry, C.M. Oliveira Simões, D.M. Aragón, *Pharmaceutics*, **13**, 535 (2021). Doi: https://doi.org/10.3390/pharmaceutics13040535

2. M.I. Cardona. G.P. Dominguez, S.M. Echeverry, I.H. Valderrama, A. Bernkop-Schnürch, M. Aragón, Enhanced oral bioavailability of rutin by a self-emulsifying drug delivery system of an extract of calyces from *Physalis peruviana*, *J. Drug Deliv. Sci. Technol.*, **66**, 102797 (2021). Doi: https://doi.org/10.1016/j.jddst.2021.102797

3. D. Muñoz-Reyes. A.I. Morales, M. Prieto, Transit and metabolic pathways of quercetin in tubular Cells: Involvement of its antioxidant properties in the kidney, *Antioxidants* (Basel), **10**, 909 (2021). Doi: https://doi.org/10.3390/antiox10060909

4. X. Chen, O.Q.P. Yin, Z. Zuo, M.S.S. Chow, Pharmacokinetics and modeling of quercetin and metabolites, *Pharm. Res.*, **22**, 892-901 (2005). Doi: https://doi.org/10.1007/s11095-005-4584-1

5. V. D. Kappel, L. Zanatta, B.G. Postal, F.R.M. Barreto Silva, Rutin potentiates calcium uptake via voltage-dependent calcium channel associated with stimulation of glucose uptake in skeletal muscle, *Arch. Biochem. Biophys.*, **532**, 55-60 (2013). Doi: https://doi.org/10.1016/j.abb.2013.01.008

6. M.A. Felmlee, M.E. Morris, D.E. Mager, Mechanism-based pharmacodynamic modeling, *Computational Toxicology*, **1**, 583-600 (2012).

Improvement type 2 diabetes treatment with vildagliptin using population pharmacokinetic and pharmacodynamic modeling

Bruna Bernar Dias[1]*, Laura Ben Olivo[1], Bibiana Verlindo de Araújo[1]

[1] Pharmaceutical Sciences Graduate Program, Federal University of Rio Grande do Sul, Brazil

*E-mail: b.bernardias@gmail.com

Summary

Diabetes is a chronic metabolic disease [1, 2]. Previous studies demonstrated vildagliptin (VDG) concentration in plasma in healthy and diabetic animals are the same, but tissue penetration in healthy subjects is reduced compared to diabetic rats [3, 4]. To understand VDG distribution and PK/PD we used a population-based approach via NONMEM®v.7.4. PK/PD analysis simulated free tissue concentrations in diabetic patients after doses of 25, 50 and 100 mg once and twice daily with DPP-4 inhibition described by an Emax model. Four-compartment model with linear elimination described data, with bidirectional transport between tissues and central compartment, diabetes influencing Q1 and Qout,liver, with CL: 2.7 L/h/kg (5%RSE), V1: 1.1 L/kg (9%RSE), Q1,healthy: 0.338 L/h/kg (21%RSE), Q1,diabetic: 2.61 L/h/kg (21%RSE), V2: 1.85 L/kg (12 %RSE). Tissue parameters were: Vmuscle: 2.5L/kg (26%RSE), Qin,muscle: 2.0 L/h/kg (0.8%RSE), Qout,muscle: 14.3 L/h/kg (23 %RSE) and Vliver: 2.2 L/kg (48 %RSE), Qin,liver: 1.38 L/h/kg (31 %RSE), Qout,liver,healthy: 218 L/h/kg (53 %RSE), Qout,liver,diabetic: 19.7 L/h/kg (49 %RSE). Model was translated from mice to humans using data from previously published model developed for humans [5]. Muscle and liver Qin and Qout were used to simulate the prediction expected tissue levels in patients. Free tissue concentrations following once-daily dosing did not cause DPP-4 inhibition across all dosing intervals, whereas 50 and 100 mg twice-daily dose produced sufficient DPP-4 inhibition for adequate hypoglycemic effect during the whole interval of dose. This first investigation of free tissue exposure and effect of VDG demonstrate plasma concentrations are not useful to predict tissue effect of VDG and dose administered twice daily can lead to better treatment results in type 2 diabetes.

Ethical approval

This study was approved by the Ethics Committee in Animal Use from the Federal University of Rio Grande do Sul (UFRGS/CEUA #20352).

Financial support and acknowledgements

The authors acknowledge Coordination of Superior Level Staff Improvement (CAPES) for the scholarship.

References

1. Y. Zheng, S.H. Ley, F.B. Hu, Global aetiology and epidemiology of type 2 diabetes mellitus and its complications, *Nat. Rev. Endocrinol.*, **14**, 88-98 (2017). Doi: https://doi.org/10.1038/nrendo.2017.151

2. M.A. Nauck, J. Wefers, J.J. Meier, Treatment of type 2 diabetes: challenges, hopes, and anticipated successes, *Lancet Diabetes Endocrinol.*, **9**, 525-544 (2021). Doi: https://doi.org/10.1016/S2213-8587(21)00113-3

3. C. De Andrade, Dissertação de mestrado, UFRGS, 2013.

4. C. de Andrade, G. de Araújo Lock, M.C. Pigatto, S.E. Haas, T. Dalla Costa, B. Verlindo de Araújo, Validation of LC-MS/MS method applied to evaluation of free tissue concentrations of vildagliptin in diabetic rats by microdialysis, *Biomed. Chromatogr.*, **28**, 1722-1727 (2014). Doi: https://doi.org/10.1002/bmc.3212

5. C.B. Landersdorfer, Y.L. He, W.J. Jusko, Mechanism-based population pharmacokinetic modelling in diabetes: vildagliptin as a tight binding inhibitor and substrate of dipeptidyl peptidase IV, *Br. J. Clin. Pharmacol.*, **73**, 391-401 (2012). Doi: https://doi.org/10.1111/j.1365-2125.2011.04108.x

A software tool for a priori model-informed dose selection of tacrolimus for solid organ transplant recipients

Yannick Hoffert[1]*, Nada Dia[1], Erwin Dreesen[1]

[1] KU Leuven, Department of Pharmaceutical and Pharmacological Sciences, Leuven, Belgium

*E-mail: yannick.hoffert@kuleuven.be

Summary

Tacrolimus concentrations are not available before start of therapy and in resource-limited settings, preventing *a posteriori* model-informed precision dosing (MIPD). Still, population pharmacokinetics (popPK) models can be used for *a priori* (covariate-based) model-informed dosing. PopPK models were collected in a systematic literature review and code was reconstructed. For each graft type, the model with the highest sample/patient ratio was selected. The tool was developed into a web application using the *Shiny* package in R (v1.7.4), where simulations are performed using the *mrgsolve* package (v4.3.0). Four models were integrated, covering a broad range of covariates [1–4]. After selecting a popPK model and providing dosing details, the user can determine the clinical relevance of covariates using a novel and rational probability of target attainment (PTA)- based approach, including PTA *versus* covariate plots and receiver operating characteristic (ROC) curves. Dose finding can be guided by a user-defined PTA target and the area under the ROC curve (AUROC). An AUROC >0.5 indicates clinical relevance of the covariate, hence covariate-based dosing may be investigated. User- specified virtual patients (*i.e.*, covariates sets) can be inspected using predicted tacrolimus exposure and PTA over time plots. Results were cross-validated against NONMEM. The beta version of the tool can be accessed at https://hyannick.shinyapps.io/app_tac_simulator/. Our tool provides an objective and efficient framework for simulation-based assessment of the clinical relevance of covariates for *a priori* popPK model-informed dosing of tacrolimus. It enables the investigation of individualized dosing right from the first dose and is useful in settings where MIPD is not routinely/frequently performed.

Financial support and acknowledgements

Yannick Hoffert is supported by a doctoral research grant from the Research Foundation – Flanders, Belgium (1SHAA24N).

References

1. X. Cai. H. Song, Z. Jiao, H. Yang, M. Zhu, C. Wang, D. Wei, L. Shi, B. Wu, J. Chen, Population pharmacokinetics and dosing regimen optimization of tacrolimus in Chinese lung transplant recipients, *Eur. J. Pharm. Sci.*, **152**, 105448 (2020). Doi: https://doi.org/10.1016/j.ejps.2020.105448

2. R. Kirubakaran, S. Hennig, B. Maslen, R.O. Day, J.E. Carland, S.L. Stocker, Evaluation of published population pharmacokinetic models to inform tacrolimus dosing in adult heart transplant recipients, *Br. J. Clin. Pharmacol.*, **88**, 1751-1772 (2022). Doi: https://doi.org/10.1111/bcp.15091

3. J.Y. Lee, H.J. Hahn, I.J. Son, K.S. Suh, N.J. Yi, J.M. Oh, W. G. Shin, Factors affecting the apparent clearance of tacrolimus in Korean adult liver transplant recipients, *Pharmacotherapy*, **26**, 1069-1077 (2006). Doi: https://doi.org/10.1592/phco.26.8.1069

4. Z. Lu, P. Bonate, J. Keirns, Population pharmacokinetics of immediate- and prolonged-release tacrolimus formulations in liver, kidney and heart transplant recipients, *Br. J. Clin. Pharm.*, **85**, 1692-1703 (2019). Doi: https://doi.org/10.1111/bcp.13952

A quantitative systems pharmacology model of valproic acid-induced hyperammonemia for pediatric and adult patients

Alejandra Schiavo[1,2]*, Cecilia Maldonado[1], Marta Vázquez[1], Pietro Fagiolino[1], Iñaki F. Trocóniz[3,4], Manuel Ibarra[1]

[1] Department of Pharmaceutical Sciences, Faculty of Chemistry, Universidad de la República, Montevideo, Uruguay

[2] Graduate Program in Chemistry, Faculty of Chemistry, Universidad de la República, Montevideo, Uruguay

[3] Pharmacometrics and Systems Pharmacology Research Unit, Department of Pharmaceutical Technology and Chemistry, School of Pharmacy and Nutrition, University of Navarra, Pamplona, Spain

[4] IdiSNA, Navarra Institute for Health Research, Pamplona, Spain

*E-mail: schiavoma@fq.edu.uy

Summary

Valproic acid (VPA) induces hyperammonemia (HA) in adults and pediatric patients. We aimed to enhance a previous Quantitative Systems Pharmacology model of VPA developed in Simulx® [1], focusing on characterizing age- and sex-related differences in VPA-induced HA. A virtual population (n=2000) aged 0 to 40 years was created in PK- Sim®. Individual patients were categorized into three groups: i) toddlers (0-2 y/o); ii) children (3-14 y/o); iii) adults (15-40 y/o, 50% women). Following literature reports, sex and age were introduced as covariates affecting VPA clearance and inputs of carnitine, ammonia, and fatty acid. We simulated the pharmacokinetic profiles of a delayed-release (Reference) and an extended-release (Test) formulations containing VPA. Model extrapolation to the pediatric population was assessed comparing predicted outputs with reported data [2-4]. HA incidence was predicted for each formulation under a 500q12 VPA, further stratifying by age. Our findings supported Test's objective to achieve a lower HA incidence compared to Reference (odds ratio = 0.88). They also indicated that VPA treatment was safer in pediatric patients. Interestingly, only these patients received preventive L-carnitine supplementation (CS). Moreover, women exhibited 15% higher HA incidence than men when receiving Reference. We conclude that admin-

istering an L- carnitine dose equal to double the VPA dose, with the same inter-dose interval, effectively maintains ammonia levels at baseline for adults and pediatrics. This supplementation does not significantly impact unbound VPA concentrations, indicating that the treatment efficacy should not be affected. This conclusion aligns with the preventive CS practice implemented at the Uruguayan pediatric Hospital Pereira Rossell.

References

1. A. Schiavo, C. Maldonado, M. Vázquez, P. Fagiolino, I.F. Trocóniz, M. Ibarra, Quantitative systems pharmacology Model to characterize valproic acid-induced hyperammonemia and the effect of L-carnitine supplementation, *Eur. J. Pharm. Sci.*, **183**, 106399 (2023). Doi: https://doi.org/10.1016/j.ejps.2023.106399

2. B.B. Serrano, M.J. García Sánchez, M.J. Otero, D.S. Buelga, J. Serrano, A. Domínguez-Gil, Valproate population pharmacokinetics in children, *J. Clin. Pharm. Therap.*, **24**, 73-80 (1999). Doi: https://doi.org/10.1046/j.1365-2710.1999.00202.x

3. J.C. Cloyd, An overview of antiepileptic drug therapy, *Am. J. Hosp. Pharm.*, **50**(12 SUPPL. 5), S3-S4 (1993).

4. E. Yukawa, T. Honda, S. Ohdo, S. Higuchi, T. Aoyama, Detection of carbamazepine-induced changes in valproic acid relative clearance in man by simple pharmacokinetic screening, *J. Pharm. Pharmacol.*, **47**, 751-756 (1997). Doi: https://doi.org/10.1111/j.2042-7158.1997.tb06106.x

Population pharmacokinetics of tenofovir/emtricitabine among transwomen at HIV risk on oral prep and feminizing hormone therapy: Analysis of potential interactions on prep

Vitória Berg Cattani[1]*, Emilia Jalil[1], Thiago Torres[1], Sandra Cardoso[1], Leonardo Eksterman[1], Cristiane Castro[1], Bruna Bernar Dias[2], Laila Monteiro[1], Erin Wilson[3], Bibiana Araujo[2], Valdilea Veloso[1], Beatriz Grinsztejn[1], Rita Estrela[1]

[1] Evandro Chagas National Institute of Infectious Diseases INI Fiocruz, Rio de Janeiro, Brazil

[2] Pharmacy Graduate Program, Federal University of Rio Grande do Sul, Porto Alegre, Brazil

[3] Department of Epidemiology and Biostatistics, University of California, San Francisco, United States

*E-mail: vitoria.berg@ini.fiocruz.br

Summary

Interactions between feminizing hormone therapy (FHT) and oral pre-exposure prophylaxis (PrEP): tenofovir disoproxil fumarate (TFV) and emtricitabine (FTC) could negatively affect PrEP outcomes among transwomen [1]. We aimed to develop a PopPK model using TFV and FTC plasma PK data from our trans-specific oral PrEP study (PrEParadas) to evaluate the impact of FHT on oral PrEP PK and to estimate TFV- diphosphate and FTC-triphosphate intracellular levels. PK data (24 h) from two groups of participants (using PrEP only and using PrEP plus FHT) from the PrEParadas study was used [2]. The popPK analysis employed the software NONMEM. The final model was expanded to the peripheral blood mononuclear cell compartment using formation and elimination rate constant of metabolites previously published [3]. The model was applied to estimate TFV-diphosphate and FTC-triphosphate intracellular levels for transwomen on daily oral PrEP. A two-compartment model with first-order absorption/elimination with lag time was the best model to describe TFV and FTC PK. TFV clearance (CL/F) and volume of distribution (V/F) estimated by the model were 62.5L/h (residual standard error [RSE]: 4%) and 300L (RSE 13%), respectively. Body mass index was a significant covariate influencing CL/F. FTC CL/F and V/F estimated by the model were 21.9L/h (RSE 4%) and 80.6L (RSE 8%), respectively, and body mass index and age

were significant covariates influencing CL/F. The simulated intracellular through concentrations of TFV- DP (mean: 61 fmol/10^6 cells) was of the same order as previously published for transwomen on PrEP [3]. This suggests the potential use of this model to estimate intracellular metabolite levels among transwomen on PrEP.

Ethical approval

Institutional Review Board INI/Fiocruz (CAAE: 08405912.9.1001.5262)

Financial support and acknowledgements

CNPq; FAPERJ; Brazilian Ministry of Health (SVS-MS).

References

1. J. Yager, P.L. Anderson, Pharmacology and drug interactions with HIV PrEP in transgender persons receiving gender affirming hormone therapy, *Expert Opin. Drug Metab. Toxicol.*, **16**, 463-474 (2020). Doi: https://doi.org/10.1080/17425255.2020.1752662

2. V.B. Cattani, E.M. Jalil, L. Eksterman, T. Torres, S. Wagner Cardoso, C.R.V. Castro, L. Monteiro, E. Wilson, L. Bushman, P. Anderson, V. Gonçalves Veloso, B. Grinsztejn, R. Estrela, Impact of feminizing hormone therapy on tenofovir and emtricitabine plasma pharmacokinetics: a nested drug-drug interaction study in a cohort of Brazilian transgender women using HIV pre-exposure prophylaxis, *J. Antimicrob. Chemother.*, **77**, 2729-2729 (2022). Doi: https://doi.org/10.1093/jac/dkac229

3. A. Tanaudommongkon, A. Chaturvedula, C.W. Hendrix, E.J. Fuchs, E. Shieh, R.P. Bakshi, M.A. Marzinke, Population pharmacokinetics of tenofovir, emtricitabine and intracellular metabolites in transgender women, *Br. J. Clin. Pharmacol.*, **88**, 3674-3672 (2022). Doi: https://doi.org/10.1111/bcp.15310

New insights into the effect of VKORC1 polymorphisms on model-informed precision dosing of warfarin in Caribbean Hispanics: External validation of a population PK/PD model

Karine Rodríguez-Fernández[1], Gledys Reynaldo[2], Stephanie Reyes-González[3], Camila de las Barreras[2], Leyanis Rodríguez[4], Jorge Duconge[3]*, Victor Mangas-Sanjuan[5]

[1] Dept. of Pharmacy, Pharmaceutical Technology & Parasitology, University of Valencia, Valencia, Spain

[2] Institute of Pharmacy and Foods, University of Havana, Havana, Cuba

[3] Dept. of Pharmaceutical Sciences, School of Pharmacy, University of Puerto Rico, San Juan, PR, USA

[4] Department of Pharmaceutics, College of Pharmacy, University of Florida, Orlando, FL, USA

[5] Interuniversity Research Institute for Molecular Recognition and Technological Development, Polytechnic University of Valencia-University of Valencia, Valencia, Spain

*E-mail: jorge.duconge@upr.edu

Summary

Warfarin, an oral anticoagulant, has been used for decades to prevent thromboembolic events. The complex interplay between *CYP2C9* and *VKORC1* genotypes on warfarin PK and PD properties is not fully understood in special sub-groups of patients. This study aimed to externally validate a population pharmacokinetic/pharmacodynamic (PK/PD) model for the effect of warfarin on international normalized ratio (INR) and to evaluate optimal dosing strategies based on the selected covariates in Caribbean Hispanic patients [1]. INR, and *CYP2C9* and *VKORC1* genotypes from 138 patients were used to develop a population PK/PD model in NONMEM. The structural definition of a previously published PK and PD models for warfarin and INR, respectively, were implemented. Simulations were conducted to determine optimal dosing strategies for each genotype combination, focusing on achieving therapeutic INR levels. Findings revealed elevated IC50 for G/G,

G/A, and A/A *VKORC1* haplotypes (11.76, 10.49, and 9.22 mg/L, respectively), in this population compared to previous reports. The model-informed precision dosing analysis recommended daily warfarin doses of 3-5 mg for most genotypes to maintain desired INR levels, although subjects with combination of *CYP2C9* and *VKORC1* genotypes *2/*2-, *2/*3- and *2/*5-A/A would require only 1 mg daily. This research underscores the potential of population PK/PD modeling to inform personalized warfarin dosing in populations typically underrepresented in clinical studies, potentially leading to improved treatment outcomes and patient safety [2]. By integrating genetic factors and clinical data, this approach could pave the way for more effective and tailored anticoagulation therapy in diverse patient groups.

Ethical approval

The study was conducted following Helsinki's declaration for human subject protection in clinical surveys (IRB approval #A4070109).

Financial support and acknowledgements

NASA EPSCoR grant # 80 NSSC19M0148, and NIGMS-NIH grant #1R16 GM149372. We want to thank the patients for voluntarily participating in the original study where data used in this analysis were gathered.

References

1. S. Reyes-González, C. de Las Barreras, G. Reynaldo, L. Rodríguez-Vera, C. Vlaar, V. Lopez Mejia, J.C.M. Monbaliu, T. Stelzer, V. Mangas, J. Duconge, Genotype-driven pharmacokinetic simulations of warfarin levels in Puerto Ricans, *Drug Metabolism and Personalized Therapy*, **35**, 4 (2020). Doi: https://doi.org/10.1515/dmdi-2020-0135

2. K. Rodríguez-Fernández, G. Reynaldo-Fernández, S. Reyes-González, C. de Las Barreras, L. Rodríguez-Vera, C. Vlaar, J.C.M. Monbaliu, T. Stelzer, J. Duconge, V. Mangas-Sanjuan, New insights into the role of VKORC1 polymorphisms for optimal warfarin dose selection in Caribbean Hispanic patients through an external validation of a population PK/PD model, *Biomed. Pharmacother.*, **170**, 115977 (2023). Doi: https://doi.org/10.1016/j.biopha.2023.115977

Predictive performance of different published models for warfarin using a Bayesian forecasting in Mexican patients with atrial fibrillation and valve replacement

Omar Rodríguez Pérez[1]*, Juan Manuel López Quijano[2], Antonio Augusto Gordillo Moscoso[3], Rodrigo Velarde Salcedo[1], Silvia Romano Moreno[1], Rosa del Carmen Milán Segovia[1], Úrsula Fabiola Medina Moreno[2], Susanna Edith Medellín Garibay[1]

[1] Facultad de Ciencias Químicas, Universidad Autónoma de San Luis Potosí, México

[2] Cardiology Department, Hospital Central "Dr. Ignacio Morones Prieto", México

[3] Facultad de Medicina, Universidad Autónoma de San Luis Potosí, México,

*E-mail: omarloops54@gmail.com

Summary

Warfarin stands out as one of the main anticoagulant drugs used in outpatients with atrial fibrillation (AF) and valve replacement (VR) [1]. Due to its high variability, multiple population models have been published to reduce the occurrence of adverse effects and improve therapeutic target attainment [2]. Most models are built using data from European and Asian populations, evidencing the lack of models with Latin-American populations. The objective of this study was to evaluate the predictive performance of different population pharmacokinetic models using Bayesian forecasting with Abbotbase PKS v1.1.0. Seven population pharmacokinetic (PK) models reporting typical PK parameters and interindividual variability were included. Warfarin plasma concentrations were monitored in 22 outpatients (14 female) aged from 33 to 72 years with aortic and mitral valve replacement (86%) and atrial fibrillation (14%). A total of 41 warfarin plasma concentrations were measured using High Performance Liquid Chromatography (mean ±SD=2.35 ± 0.94 μg/mL). *A priori* concentration estimates were calculated for all models. Mean relative prediction error (rPE) values on each model ranged from 55% to 88% and root mean square errors (RMSE) ranged from 1.31 to 2.03 μg/mL The best fitting model was reported by Lane *et al.* (2012) [3] using age and gender as covariates. Most models showed poor predictive performance when applied to the studied population. This suggests the need to build a specific model for the Mexican population since none has yet been published.

Ethical approval

The present work was approved by: "Comité de ética en Investigación y Docencia de la Facultad de Ciencias Químicas (CEID-FCQ)" with code CEID2021-014-S and "Comité Estatal de ética en Investigación en Salud" with code SLP/09-2021.

Financial support and acknowledgements

This work was promoted by the Technological Research Council of Science for a master's fellowship (781982).

References

1. X. Li, D. Li, J.C. Wu, Z.Q. Liu, H.H. Zhou, J.Y. Yin, Precision dosing of warfarin: open questions and strategies, *Pharmacogenomics J*., **19**, 219-229 (2019). Doi: https://doi.org/10.1038/s41397-019-0083-3

2. A.K. Hamberg, M. Wadelius, J.D. Lindh, M.L. Dahl, R. Padrini, P. Deloukas, A. Rane, E.N. Jonsson, A pharmacometric model describing the relationship between warfarin dose and INR response with respect to variations in CYP2C9, VKORC1, and age, *Clin. Pharmacol. Therap.*, **87**, 727-734 (2010). Doi: https://doi.org/10.1038/clpt.2010.37

3. S. Lane, S. Al-Zubiedi, E. Hatch, I. Matthews, A.L. Jorgensen, P. Deloukas, A.K. Daly, B.K. Park, L. Aarons, K. Ogungbenro, F. Kamali, D. Hughes, M. Pirmohamed, The population pharmacokinetics of R- and S-warfarin: effect of genetic and clinical factors, *Br. J. Clin. Pharmacol.*, **73**, 66-76 (2012). Doi: https://doi.org/10.1111/j.1365-2125.2011.04051.x

Pharmacokinetic characterization of isoniazid and rifampicin treatment in tuberculosis patients from Uruguay

Andrés Baptista[1,2*], Yessica Imbriago[1,2], Patricia Rega[1,2], Marianela Lorier[1], Nicolás Dell'Oca[3], Carla Molles[3], Fernanda Domínguez[3], Daniela Guicheney[4], Camila Urroz[4], Marcia Velázquez[4], Natalia Morena[4], Mercedes Perendones[4], Mercedes Corral[5], María Buroni[5],Susana Cabrera[6], Mónica Hernández[7], Mariela Contrera[7], Eduardo Reséndiz[8], Paolo Denti[8], Manuel Ibarra[1]

[1] Department of Pharmaceutical Sciences, Faculty of Chemistry, Universidad de la República, Uruguay.

[2] Graduate Program in Chemistry, Faculty of Chemistry, Universidad de la República, Uruguay

[3] Department of Genetics, Faculty of Medicine, Universidad de la República, Uruguay

[4] Medical Clinical 2, Hospital Pasteur, Administración de los Servicios de Salud del Estado, Uruguay

[5] Intensive Care Unit, Hospital Español, Administración de los Servicios de Salud del Estado, Uruguay

[6] Infectious Diseases Department, Hospital de Clínicas, Administración de los Servicios de Salud del Estado, Uruguay

[7] Comisión Honoraria para la Lucha Antituberculosa y Enfermedades Prevalentes, Uruguay

[8] Division of Clinical Pharmacology, Department of Medicine, University of Cape Town, Cape Town, South Africa

*E-mail: abaptista@fq.edu.uy

Summary

Isoniazid (INH) and rifampicin (RMP) are first-line drugs for tuberculosis (TB) treatment which exhibit high intra- and interindividual pharmacokinetic variability and potentially severe adverse effects. In Uruguay, TB has a moderately rising incidence. Delayed diagnosis, among other causes, results in high hospitalization rates and a prolonged anti- TB drug regimen [1]. In this work, we aimed to characterize INH and RMP exposure by leveraging reported population pharmacokinetic (popPK) models for INH and RMP as prior information for conducting empiric Bayesian estimation of popPK parameters. We collected plasma concentrations of INH and RMP from 97 hospitalized patients (19 critically ill) under standard treatment using a limited sampling strategy (2 samples within 1-3 and 4-6 post-dosing hours). Additionally, NAT2 gene polymorphism was determined. A two-compartment model with transit compartment absorption and linear elimination, incorporating body weight and NAT2 phenotype as covariates, was found to best describe INH concentrations [2], while a one-compartment delayed first-order absorption and linear elimination, with bodyweight as covariate, best described RMP concentrations [3]. For INH, 73% of patients achieved an AUC within the target range, with a mean value of 15.9 μg·h/mL, and 46% of patients achieved a Cmax within the range, with a mean value of 3.76 μg/mL. Meanwhile, for RMP, 92% of patients achieved an AUC within the range, with a mean value of 27.0 μg·h/mL, and 20% of patients achieved a Cmax within the range, with a mean value of 6.1 μg/mL. This represents the initial phase in implementing model-informed precision dosing to optimize anti-TB treatment in Uruguay.

Ethical approval

The study was conducted according to the ICH-GCP and the normative from the Public Health Ministry from Uruguay (decree 158/2019). Additionally, the study was done following the recommendations from the World Medical Association.

Financial support and acknowledgements

The project "Evaluación farmacoterapéutica del tratamiento antituberculoso actual con rifampicina e isoniazida en pacientes críticos y moderados" is supported by the program CSIC I+D 2020, Universidad de la República.

References

1. CHLA-EP, Situación de la tuberculosis en Uruguay, 2022, 2023.

2. P. Denti, K. Jeremiah, E. Chigutsa, D. Faurholt-Jepsen, G. PrayGod, Pharmacokinetics of isoniazid, pyrazinamide, and ethambutol in newly diagnosed pulmonary TB patients in Tanzania, *PLoS One*, **10**, e0141002 (2015). Doi: https://doi.org/10.1371/journal.pone.0141002

3. N. Rockwood, G. Meintjes, M. Chirehwa, L. Wiesner, H. McIlleron, R.J. Wilkinson, P. Denti, HIV-1 coinfection does not reduce exposure to rifampin, isoniazid, and pyrazinamide in South African tuberculosis outpatients, *Antimicrob. Agents Chemother.*, **60**, 6050-6059 (2016). Doi: https://doi.org/10.1128/AAC.00480-16

Pharmacokinetic model of lamotrigine in bipolar disease patients

Priscilla Navarro Medina[1], Elba Margarita Romero Tejeda[2], Claudia Verónica Palacios Magaña[2], Edy David Rubio Arellano[3], Jaime Carmona Huerta[3,4], Nicte Selene Fajardo Robledo[2*]

[1] Doctorado en Farmacología, CUCS, Universidad de Guadalajara, Guadalajara, Jalisco, México

[2] Departamento de Farmacobiología, CUCEI, Universidad de Guadalajara, Guadalajara, Jalisco, México

[3] Departamento de Fisiología, CUCS, Universidad de Guadalajara, Guadalajara, Jalisco, México

[4] Instituto Jaliscience de Salud Mental, Guadalajara, Jalisco, Mexico

*E-mail: nicte.fajardo@academicos.udg.mx

Summary

Lamotrigine (LMT), a phenyltriazine derivative approved as anticonvulsant drug [1]. In bipolar disease (BD), the interest of LMT is as a mood stabilizer, and came from limited but robust evidence of its efficacy in the prevention of mood relapses. However, as the molecular pathogenesis and mechanistic basis of mood stabilizer strategies of BD are poorly understood [2] it is important to know course of the drug for better comprehension. In our study we included nineteen ongoing patients, Mexican women from the psychiatry service of the Mental Health Institute (SALME), the mean age was 36.4 ± 9.94 years old. They were diagnosed with Bipolar Disease type I according to the DMS IV criteria. We obtain a total of thirty-one blood samples from different times in a period of 1-3 months after treatment with 200 mg standard dose of LMT. The model was developed using MONOLIX v. 2021R1. The final model described a one- compartment model with an absorption and elimination first-order process. The residual error model was described as proportional. Given the trough steady-state, we could estimate the following parameters and RSE%. V/F = 91.33 L (13.0%) weight was added as a covariate, CL/F = 3.98 L/h (78.9%), while the absorption rate constant (ka) was set at literature values of 3.5 h^{-1} [3]. As the pharmacokinetic profile, this drug has been studied

as an epileptic drug, it is essential to propose a pharmacokinetic model of LMT in patients with bipolar disease that helps to describe and comprehend the course of the drug in this disease.

Ethical approval

This study was approved by the ethics committee "Comité de Ética en Investigación del Instituto Jalisciencie de Salud Mental" under registration number 198.

Financial support and acknowledgements

This study was developed with the financial support of the "Programa de Apoyo a la Mejora en las Condiciones de Producción de los Miembros del Sistema Nacional de Investigadores y del Sistema Nacional de Creadores de Arte (SNCA) de la Universidad de Guadalajara".

References

1. J.P. Rissardo, A.L. Fornari-Caprara, Lamotrigine-associated movement disorder: A literature review, *Neurol. India*, **69**, 1524-1538 (2021). Doi: https://doi.org/10.4103/0028-3886.333440

2. S.I. Rapoport, M. Basselin, H.W. Kim, J.S. Rao, Bipolar disorder and mechanisms of action of mood stabilizers, *Brain Res. Rev.*, **61**, 185-209 (2009). Doi: https://doi.org/10.1016/j.brainresrev.2009.06.003

3. V. Chan, R.G. Morris, K.F. Ilett, S.E. Tett, Population pharmacokinetics of lamotrigine, *Ther. Drug Monit.*, **23**, 630-635 (2001). Doi: https://doi.org/10.1097/00007691-200112000-00006

Population pharmacokinetic model of cefepime in adults with hematological malignancies and febrile neutropenia after chemotherapy

Daniel S. Parra[1*], José C. Álvarez[2,3], Sonia I. Cuervo[2,3,4#], Edelberto Silva[1,3], Jorge A. Díaz[1,3,5], Lorena L. Jiménez[3,4], Julio C. Gómez[3,4], Ricardo Sánchez[2,3,4], Jorge A. Cortés[2,5]

[1] Departamento de Farmacia, Facultad de Ciencias, Universidad Nacional de Colombia, Bogotá, Colombia

[2] Facultad de Medicina, Universidad Nacional de Colombia, Bogotá, Colombia

[3] Grupo en Enfermedades Infecciosas en Cáncer y Alteraciones Hematológicas (GREICAH), Universidad Nacional de Colombia, Bogotá, Colombia

[4] Instituto Nacional de Cancerología (INC)—Empresa Social del Estado, Bogotá, Colombia

[5] Grupo de Investigación en Enfermedades Infecciosas, Facultad de Medicina, Universidad Nacional de Colombia, Bogotá, Colombia

[*]E-mail: dsparrag@unal.edu.co; [#]E-mail: sicuervom@unal.edu.co

Summary

Chemotherapy-induced febrile neutropenia (CIFN) induces physiological alterations with potential implications for antibiotic pharmacokinetics (PK), possibly resulting in suboptimal drug exposure and reduced effectiveness. The pharmacokinetics of cefepime (FEP) was investigated in an open-label, non-randomized, observational study. Patients with CIFN received cefepime in a dose of 2 g IV every 8 hours as 30-minute infusions. Plasma concentrations of FEP were determined using a microbiological assay. A two-compartment population PK model appropriately described the data, ith individual clearance dependent on serum creatinine levels. Monte Carlo simulation was employed to evaluate and compare various dosing regimens with different minimum inhibitory concentration (MIC) values, related to resistance cut-off points for Enterobacteriaceae. According to the simulations, increasing the daily dose of cefepime beyond 6 g daily was unnecessary to achieve a probability of target attainment (PTA) ≥ 90%. Cumulative fraction of response

(CFR) with intermittent dosing was suboptimal for empirical therapy regimens against *K. pneumoniae* and *P. aeruginosa*. Continuous infusions could be utilized in this setting to maximize exposure. Patients with high serum creatinine levels were more likely to achieve predefined pharmacokinetic/pharmacodynamic (PK/PD) targets compared to patients with low levels.

Ethical approval

All participants provided informed consent before joining the study. The research adhered to the Declaration of Helsinki and was approved by the Ethics Committee of the Faculty of Medicine at Universidad Nacional de Colombia (code: CE-005/024-14, approved on 10 April 2014) and the Institutional Review Board of Instituto Nacional de Cancerología (code: INT-OFI-006567-2014, approved on 17 September 2014).

Financial support and acknowledgements

We received support from the National Cancer Institute and obtained project funding from Inversión Nación, identified with SAP code C41030110-012. Additionally, the National University of Colombia provided resources for the project through an inter-institutional agreement between two state public institutions.

References

1. O. Lortholary, A. Lefort, M. Tod, A.M. Chomat, C. Darras-Joly, C. Cordonnier, Pharmacodynamics and pharmacokinetics of antibacterial drugs in the management of febrile neutropenia, *The Lancet: Infectious Diseases*, **8**, 612-620 (2008). Doi: https://doi.org/10.1016/S1473-3099(08)70228-7

Noncompartmental pharmacokinetic analysis of isosorbide-5-mononitrate in healthy Mexican volunteers

Ivette Guadalupe Herrera Pérez[1]*, Malena Veloz Domínguez[1], Juan Luis Gutiérrez Velázquez[1], Luis Eligio Chable Cen[1], Juan Ernesto Dávila Romero[1], Héctor Manuel González Martínez[1]

[1] Department of development and validation, Unidad Analítica, Laboratorio Cinasi S. A. de C. V., Tlaquepaque, Jalisco, México

*E-mail: ivette.hpz96@gmail.com

Summary

Oral formulations of isosorbide-5-mononitrate (5-ISMN) emerge as a treatment option for patients with angina pectoris to minimize the problems associated with isosorbide dinitrate, such as a longer elimination half-life, no first-pass metabolisms, and it has prolonged therapeutic effects and reproducible clinical effects [1, 2]. This study aimed to develop and validate a UPLC-MS/MS method for quantifying 5-ISMN in human plasma and demonstrate its application in a pilot study through noncompartmental pharmacokinetic (PK) analysis. The method adhered to national [3] regulations. This method was successfully applied to determine 5-ISMN in samples from six healthy Mexican volunteers after an oral single- dose of 60 mg. Noncompartmental PK analysis, executed with Phoenix WinNonlin software. The media ± standard deviation or median (interval) values of Cmax, Tmax, AUC0∞, clearance, half-life and elimination constant were 620.80 ± 159.35 ng/mL, 3.83 ± 0.81 h, 9560.00 ± 2693.00 (h·ng/mL), 6.84 (6.18 – 10.01) L/h and 0.1015 (0.07 – 0.11) h^{-1}, respectively. Before initiating a crucial bioequivalence study, it is advisable to conduct a preliminary investigation known as a pilot study. This preliminary study serves multiple purposes, including validating analytical methods, evaluating variability in PK, determining the required sample size for sufficient statistical power, and refining the timing of sample collection intervals. In conclusion, this information can be used to establish pharmacokinetic profiles to assess new formulations and facilitate the development of a bioequivalence study.

Ethical approval

The present work was approved by "Comité de ética en investigación y comité de investigación" with registration CONBIOETICA-19-CEI-009-20160729.

Financial support and acknowledgements

This project did not receive financial support from any institution.

References

1. T. Kosoglou, J.E. Patrick, A. Cohen, E. Radwanski, D. Christopher, M.B. Affrime, Pharmacokinetics of isosorbide-5-mononitrate after oral administration of an extended-release mononitrate formulation versus a standard dinitrate formulation, *Journal of Clinical Therapeutics*, **17**, 241-251 (1995). Doi: https://doi.org/10.1016/0149-2918(95)80022-0

2. Y. Zhou, A. Liu, R. Jia, M. Wu, N. Wu, C. Liu, Z. Han, H. Hu, H. Wang, Q. He, Determination of isosorbide-5-mononitrate in human plasma by high-performance liquid chromatography-tandem mass spectrometry and its application to a bioequivalence study, *Journal of Analytical Methods in Chemistry*, **2020**, 1753265 (2020). Doi: https://doi.org/10.1155/2020/1753265

3. Secretaría de salud, Diario Oficial de la Federación, México, 2013.

Impact of chromosomal translocations and transporter polymorphisms on population pharmacokinetics of methotrexate in children with acute lymphoblastic leukemia

Fausto Zaruma Torres[1*], Maritza Ochoa Castro[1], Enmanuel Guerrero[2,3], Andrés Andrade[2,3], Adriana Orellana[2], Catherine Acurio[4], Soledad Jiménez[4], Geovanny Barrera[5] Rodrigo Caroca[5]

[1] College of Chemical Sciences – Universidad de Cuenca, Cuenca, Ecuador

[2] College of Medical Sciences, Universidad de Cuenca, Ecuador, Cuenca, Ecuador

[3] Cancer Fighting Society Institute, Cuenca, Ecuador

[4] Cancer Fighting Society Institute, Loja, Ecuador

[5] Department of Biology, Universidad del Azuay, Cuenca, Ecuador

*E-mail: fausto.zaruma@ucuenca.edu.ec

Summary

Acute lymphoblastic leukemia (ALL) stands as the most prevalent malignant neoplasm within the pediatric population in Ecuador [1-3]. Its treatment requires high doses of methotrexate (HDMTX), whose pharmacokinetics might be influenced by chromosomal translocations (ChTr) and transporter polymorphisms. The aim of this research is to ascertain the correlation between chromosomal translocations and transporter polymorphisms with methotrexate pharmacokinetics (MTX) [2-4]. A prospective study was conducted involving 48 children (aged 1 to 17 years) diagnosed with ALL, who were treated at SOLCA Hospitals in Cuenca, Loja and Machala. These patients received HDMTX through slow infusion over 24 hours during the maintenance phase. Chromosomal translocations *12/21, 1/19* were identified using karyotype analysis, while genetic polymorphisms ABCB1*rs1128503, rs*1045642 were assessed through qPCR. Plasma concentrations of MTX were determined using enzyme immunoassay. Population pharmacokinetic (PopPK) analysis was performed using Monolix_Suite v2023R1 software, assessing the impact of covariates on intercompartmental clearance (CL), central distribution volume (V1), and peripheral distribution volume (V2). The structural two-compartment model was employed, and covariates related to both translocations

and polymorphisms did not influence. However, gender had an impact on V1 (L) = 0.59, CL (L/h) =1.02, Q (L/h) =0.04, V2 (L) = 0.0005. The results obtained indicated no association with *rs1045642*, consistent with findings in other studies [5-8], although some suggest a decrease in CL. Regarding chromosomal translocations, there are no studies related to PopPk of MTX. No association was found between the mentioned polymorphisms or ChTr and the PopPk of methotrexate. Only V1 was associated with gender, which should be considered for dose adjustments.

Ethical approval

This study was approved by the Research Ethics Committee on Human Subjects of the University of San Francisco De Quito, Quito-Ecuador (approval 2017-106E).

Financial support and acknowledgements

This work was carried out within the framework of funding provided by the University of Cuenca (UCuenca). We acknowledge the participation and support of SOLCA – Cuenca, SOLCA – Machala, SOLCA – Loja.

References

1. M. Lejman, A. Chałupnik, Z. Chilimoniuk, M. Dobosz, Genetic biomarkers and their clinical implications in B-cell acute lymphoblastic leukemia in children, *Int. J. Mol. Sci.*, **23**, 2755 (2022). Doi: https://doi.org/10.3390/ijms23052755

2. D. Bhojwani, N.D. Sabin, D. Pei, J.J. Yang, R.B. Khan, *et al.*, Methotrexate-induced neurotoxicity and leukoencephalopathy in childhood acute lymphoblastic leukemia, *J. Clin. Oncol.*, **32**, 949-959 (2014). Doi: https://doi.org/10.1200/JCO.2013.53.0808

3. G. Gervasini, S. Mota-Zamorano, Clinical implications of methotrexate pharmacogenetics in childhood acute lymphoblastic leukaemia, *Curr. Drug Metab.*, **20**, 313-330 (2019). Doi: https://doi.org/10.2174/1389200220666190130161758

4. L. Zhan, J. Lian, H. Jin, S. Wang, J. Ding, Z. Shao, ABCB1 polymorphisms and childhood acute lymphoblastic leukemia risk: A meta-analysis, *Crit. Rev. Eukaryot. Gene Expr.*, **27**, 173-181 (2017). Doi: https://doi.org/10.1615/CritRevEukaryotGeneExpr.2017019077

5. M. Hegyi, A. Arany, A.F. Semsei, K. Csordas, O. Eipel, A. Gezsi, N. Kutszegi, M. Csoka, J. Muller, D.J. Erdelyi, P. Antal, C. Szalai, G.T. Kovacs, Pharmacogenetic analysis of high-dose methotrexate treatment in children with osteosarcoma, *Oncotarget*, **8**, 9388-9398 (2017). Doi: https://doi.org/10.18632/oncotarget.11543

6. Y. Cheng, M.H. Chen, Q. Zhuang, B.J Lin, Y.Y. Chen, L. Yang, M.B. Liu, W.C Que, H.Q. Qiu, Genetic factors involved in delayed methotrexate elimination in children with acute lymphoblastic leukemia, *Pediatr. Blood Cancer*, **68**, e28858 (2021). Doi: https://doi.org/10.1002/pbc.28858

7. Radtke, O. Zolk, B. Renner, M. Paulides, M. Zimmermann, A. Möricke, M. Stanulla, M. Schrappe, T. Langer, Germline genetic variations in methotrexate candidate genes are associated with pharmacokinetics, toxicity, and outcome in childhood acute lymphoblastic leukemia, *Blood*, **121**, 5145-5153 (2013). Doi: https://doi.org/10.1182/blood-2013-01-480335

8. B. Faganel Kotnik, I. Grabnar, P. Bohanec Grabar, V. Dolžan, J. Jazbec, *Eur. J. Clin. Pharmacol.*, **67**, 993-1006 (2011). Doi: https://doi.org/10.1007/s00228-011-1046-z

A posteriori pharmacokinetic analysis in pediatric patients with acute lymphoblastic leukemia at high-dose methotrexate. Proof of concept

Juan Antonio Garzón Lamarque[1]*, Monzerrat Pardo Zepeda[2], Ana Rosa Rincón Sánchez[1], Hugo Romo Rubio[2], Fernando Sánchez Zubieta[2], Elba Margarita Romero Tejeda[3]

[1] University Center of Health Sciences (CUCS), University of Guadalajara, Guadalajara, Jalisco, Mexico

[2] Pharmacological Research Laboratory, Pediatric Oncology and Hematology Service, Hospital Civil de Guadalajara "Juan I. Menchaca" (HCJIM), Guadalajara, Jalisco, Mexico

[3] University Center of Exact Sciences and Engineering, University of Guadalajara, Guadalajara, Jalisco, Mexico

*E-mail: juan.garzon9902@alumnos.udg.mx

Summary

Methotrexate (MTX) is used to treat a variety of diseases, including lupus, arthritis, and acute lymphoblastic leukemia (ALL) [1]. The therapeutic range of MTX is highly narrow; therefore, it is necessary to maintain therapeutic concentrations to avoid the induction of hepatic and pulmonary abnormalities and myelosuppression [2]. A previously established population pharmacokinetic (popPK) model was utilized to describe the drug's time course in our patients, and a posteriori method was used to estimate typical parameters due to the limited data reported by the Hematology-oncology service of the HCJIM. Retrospective, observational, and descriptive study was performed to determine pediatric patients' clinical and anthropometric characteristics. Available concentrations of MTX infused at 2-5 g/m^2 in the plasma of 25 patients with ALL between 24 to 72 hours post-dose were determined using the ELISA technique. Sixty-six concentrations of MTX were recovered from clinical records from 2018 to 2022.The a posteriori analysis was performed with the program Monolix 2023R1 (Lixoft, France), based on the two-compartment model described by Oliveira (Cl = 7.66 L/h, V1 = 26.8 L, V2 = 8.47 L, Q = 0.218 L/h) that include as covariates renal function and factors related to body size [3]. Visual prediction checks and individual prediction graphs were performed.

Our patients' concentrations were within the 90% confidence interval of the predictions, concluding that the model's covariates improved its performance. Future prospective studies are required to develop a popPK approach in our patients to explain the time course of the drug's process in the body and link it to its therapeutic effects using a PK/PD model.

Ethical approval

This study received approval from the Ethics, Research, and Biosafety Committees of CUCS opinion CI-06323 and HCJIM with registration number 0650/23 HCJIM/2023.

Financial support and acknowledgements

We thank the Hospital Civil de Guadalajara "I. Menchaca" for providing the financial, human resources, and infrastructure necessary to implement this work.

References

1. F. Karami, S. Ranjbar, Y. Ghasemi, M. Negahdaripour, Analytical methodologies for determination of methotrexate and its metabolites in pharmaceutical, biological and environmental samples, *Journal of Pharmaceutical Analysis*, **9**, 373-391 (2019). Doi: https://doi.org/10.1016/j.jpha.2019.06.001

2. Z.L. Taylor, J. Vang, E. Lopez-Lopez, N. Oosterom, T. Mikkelsen, L.B. Ramsey, Systematic review of pharmacogenetic factors that influence high-dose methotrexate pharmacokinetics in pediatric malignancies, *Cancers*, **13**, 2837 (2021). Doi: https://doi.org/10.3390/cancers13112837

3. P. Oliveira-Henz, A. Valle-Pinhatti, L.J. Gregianin, M. Martins, M. Curra, B. Verlindo de Araújo, T. Dalla-Costa, *Pharmaceutical Research*, **40**, 1777-1787 (2023) Doi: https://doi.org/10.1007/s11095-023-03544-7

Population pharmacokinetics of tacrolimus after long-term use in adult transplant recipients in Colombia

Ivone E. Jimenez[1], Andrés Hincapié[1], María A. Montoya-Giraldo[1], Andres F. Zuluaga[1]*

[1] Departamento de Farmacologia y Toxicologia, Laboratorio Integrado de Medicina Especializada, Facultad de Medicina, Universidad de Antioquia, Medellín, Colombia

*E-mail: andres.zuluaga@udea.edu.co

Summary

Tacrolimus, an immunosuppressant used after organ transplantation, exhibits significant pharmacokinetic variability. Population pharmacokinetic (pop-PK) models have been established to study this variability, but most focus on early liver and renal transplants. This study aimed to address the gap in knowledge by developing a nonparametric pop-PK model for tacrolimus in adult patients four and two-thirds years post-transplant. The model development utilized intensive sampling data (6 samples per day) from 9 patients. A three-compartment model with first-order absorption best described the data. Body mass index (BMI), hematocrit, time since transplant, and CYP3A5 and ABCB genotypes were identified as significant covariates influencing drug clearance and distribution volumes (allometrically scaled to BMI). The final model yielded an R-squared of 0.37, indicating a moderate fit between predicted and observed values. Additionally, the model exhibited a bias of 0.151 and an imprecision of 2.05. The final mean parameter estimates included apparent clearance (CL/F) of 0.03 L/h, apparent central volume (V/F) of 0.12 L, apparent peripheral volume (Vp/F) of 3.86 L, relative bioavailability, and absorption rate constant (Ka) of 0.42 h. While this model demonstrates potential for individualized dosage predictions, further validation with additional data and prospective evaluation are necessary.

Ethical approval

The ethical committee of the Hospital Alma Mater of Antioquia approved the study

Financial support and acknowledgements

This study was supported by MINCIENCIAS, grant number 111589786169

References

1. A. Åsberg, K. Midtvedt, M. van Guilder, E. Størset, S. Bremer, S. Bergan, R. Jelliffe, A. Hartmann, M.N. Neely, Inclusion of CYP3A5 genotyping in a nonparametric population model improves dosing of tacrolimus early after transplantation, *Transplant International*, **26**, 1198-1207 (2013). Doi: https://doi.org/10.1111/tri.12194

2. O. Campagne, D.E. Mager, K.M. Tornatore, Population pharmacokinetics of tacrolimus in transplant recipients: What did we learn about sources of interindividual variabilities? *J. Clin. Pharmacol.*, **59**, 309-325 (2019). Doi: https://doi.org/10.1002/jcph.1325

Population pharmacokinetic modeling of oral acetaminophen in healthy adults with and without obesity in Medellin, Colombia

Andres F. Zuluaga[1]*, Ivone Jiménez[1], Andrés Hincapié[1], Héctor Pérez[1], Maria A. Montoya[1], Carolina Rosero[1], Laura Vargas[1]

[1] Departamento de Farmacología y Toxicología, Laboratorio Integrado de Medicina Especializada (LIME), Facultad de Medicina, Universidad de Antioquia, Medellín, Colombia

*E-mail: andres.zuluaga@udea.edu.co

Summary

Acetaminophen remains a first-line analgesic for children and adults. Clearance (CL) and volume of distribution (Vd), which determine dosage, may differ in obese compared to non-obese individuals, suggesting at least two subpopulations better described by non-parametric approaches. We aimed to determine the population pharmacokinetics of acetaminophen in adults with and without obesity after an oral dose of 1000 mg, evaluating whether body composition affects drug kinetics. Twenty-four adults were recruited. Blood samples were collected at 0, 15, 30, 60, 90, 120, and 360 minutes after acetaminophen administration. Plasma concentrations were measured using a validated high-performance liquid chromatographic assay with ultraviolet detection. Data were analyzed using Pmetrics. A total of 144 samples were used, resulting in 21 support points. A two-compartment pharmacokinetic model with first-order elimination better described drug kinetics (R2 = 0.96 for individual obs-pred plot). Several subpopulations were identified comparing obese and non-obese populations. Fat mass was the best covariate to describe acetaminophen CL, which was 48.3 L/h/70 kg. Volume of central and peripheral compartments were 4.3 and 71.2 L, respectively. Absorption lag time and bioavailability were 13 minutes and 86%, respectively. Fat mass was an important covariate for describing acetaminophen pharmacokinetics. Dosing of acetaminophen in obese patients should consider population pharmacokinetic parameters.

Ethical approval

The protocol adhered to the principles of the Declaration of Helsinki and was reviewed, approved, and supervised by the Hospital Universitario San Vicente Fundación Ethics Committee.

Financial support and acknowledgements

This project was funded by Minciencias (Colombian Ministry of Science and Technology), grant 111589786169, and by the University of Antioquia, grant 2020-36930

References

1. J.D. Morse, I. Stanescu, H.C. Atkinson, B.J. Anderson, *Eur. J. Drug Metab. Pharmacokin.*, **47**, 497-507 (2022). Doi: https://doi.org/10.1007/s13318-022-00766-9

2. M.N. Neely, M.G. van Guilder, W. Yamada, A. Schumitzky, R. Jelliffe, Accurate detection of outliers and subpopulations with Pmetrics, a nonparametric and parametric pharmacometric modeling and simulation package for R, *Ther. Drug Monit.*, **34**, 467-476 (2012). Doi: https://doi.org/10.1097/FTD.0b013e31825c4ba6

In-vitro study of red blood cell-plasma partitioning of first-line anti-tuberculosis drugs and its relevance for model-informed precision dosing through dried blood spot sampling

Rodrigo Velarde Salcedo[1]*, Ivette Guadalupe Herrera Pérez[1], Cristian Jazmín Rodríguez Pinal[1], Arturo Ortiz Álvarez[2], Rosa del Carmen Milán Segovia[1], Silvia Romano Moreno[1], Susanna Edith Medellín Garibay[1]

[1] Facultad de Ciencias Químicas, Universidad Autónoma de Potosí, San Luis Potosí, SLP., México

[2] Hospital Central "Dr. Ignacio Morones Prieto", San Luis Potosí, SLP., México

*E-mail: rvelardesal@gmail.com

Summary

Model-informed precision dosing (MIPD) plays a key role in the success of tuberculosis (TB) treatment with first-line drugs (rifampicin – RIF, isoniazid – INH, ethambutol – ETB and pyrazinamide – PZA). While MIPD is traditionally performed with plasma drug concentrations, Dried Blood Spots (DBS) quantification is an increasingly popular alternative. However, plasma and DBS concentrations are non-concordant [1] and plasma therapeutic targets cannot be used to interpret DBS concentrations, limiting its applications in MIPD. Nonetheless, differences between DBS and plasma concentrations can be explained by drug partitioning between red blood cells and plasma. In this study the red blood cell / plasma partition coefficient ($K_{rbc/p}$) of first-line anti-TB drugs was estimated *in-vitro* to correct DBS concentrations. Spiked whole blood samples were incubated at 37 °C for 2 hours to obtain $K_{rbc/p}$ values through LC-MS/MS analysis [2]. Mean $K_{rbc/p}$ values were 1.02 ± 0.49 for RIF, 1.30 ± 0.33 for INH, 2.75 ± 0.37 for ETB and 1.05 ± 0.12 for PZA. $K_{rbc/p}$ was concentration-dependent for ETB and hematocrit- dependent for RIF. Drug concentrations were quantified on plasma and DBS samples from 15 TB patients and $K_{rbc/p}$ values were used to correct DBS concentrations [3]. Assessment with Bland-Altman plots showed good agreement between corrected DBS concentrations and plasma concentrations. Passing-Bablok regressions revealed concordance between concentrations in both matrices (except for RIF). This improvement in agreement indicates that $K_{rbc/p}$ estimation is important for pharmacometrics applications of DBS sampling, particularly for substituting plasma sampling for MIPD purposes.

Ethical approval

This study protocol was approved by the Research Committee and Ethics in Research Committee of *Hospital Central "Dr. Ignacio Morones Prieto"* (Registration number: 67- 21).

Financial support and acknowledgements

A doctorate fellowship was awarded to Rodrigo Velarde Salcedo (Grant No, 834558) by Mexico's National Council of Humanities, Science and Technology (CONAHCyT).

References

1. I.G. Herrera-Pérez, A.S. Rodríguez-Báez, A. Ortiz-Álvarez, R. Velarde-Salcedo, F.J. Arriaga-García, C.J. Rodríguez-Pinal, S. Romano-Moreno, R.C. Milán-Segovia, S.E. Medellín-Garibay, Standardization and validation of a novel UPLC-MS/MS method to quantify first line anti-tuberculosis drugs in plasma and dried blood spots, *Journal of Chromatography B*, **1228**, 123801 (2023). Doi: https://doi.org/10.1016/j.jchromb.2023.123801

2. S. Yu, S. Li, H. Yang, F. Lee, J.T. Wu, M.G. Qian, A novel liquid chromatography/tandem mass spectrometry based depletion method for measuring red blood cell partitioning of pharmaceutical compounds in drug discovery, *Rapid Communications in Mass Spectrometry*, **19**, 250-254 (2005). Doi: https://doi.org/10.1002/rcm.1777

3. C. Linder, K. Wide, M. Walander, O. Beck, L.L. Gustafsson, A. Pohanka, Comparison between dried blood spot and plasma sampling for therapeutic drug monitoring of antiepileptic drugs in children with epilepsy: A step towards home sampling, *Clinical Biochemistry*, **50**, 418-424 (2017). Doi: https://doi.org/10.1016/j.clinbiochem.2016.12.008

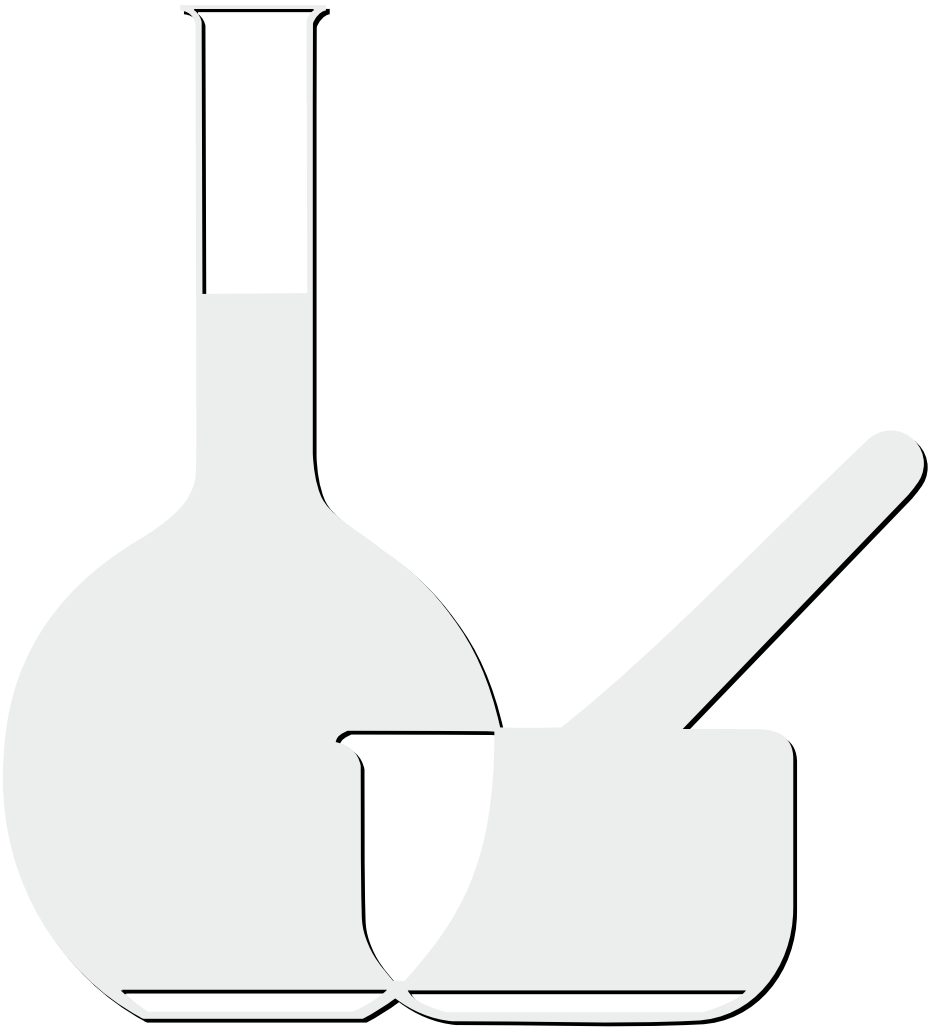

NORMAS PARA PUBLICACIÓN

La Revista Colombiana de Ciencias Químico Farmacéuticas es editada por el Departamento de Farmacia de la Universidad Nacional de Colombia (Sede Bogotá), con una periodicidad cuatrimestral y tiene como objetivo publicar artículos originales de diversos tópicos relacionados con las ciencias farmacéuticas como recursos naturales, atención farmacéutica, evaluación clínica y preclínica, y los relacionados con la industria farmacéutica, la salud y los medicamentos.

Además de artículos completos, la revista acepta revisiones, comunicaciones breves y cartas al Editor. Las contribuciones pueden enviarse en español, portugués o inglés, en letra Times New Roman, tamaño 12, al correo electrónico rccquifa_fcbog@.unal.edu.co o a través del sistema OJS en el sitio web: https://revistas.unal.edu.co/index.php/rccquifa.

Todo el material propuesto para publicación será revisado por el Comité Editorial, y luego de su aceptación para evaluación, será sometido a revisión por pares académicos. Las evaluaciones recibidas por el Comité Editorial serán remitidas al autor para que se realicen los ajustes sugeridos. Los autores tendrán un lapso de tres semanas para responder cada una de las observaciones, introducir en el texto las modificaciones del caso y retornar el documento corregido al Comité Editorial. Después de que los evaluadores o el Comité Editorial lleven a cabo una segunda revisión del manuscrito, la revista comunicará a los autores la decisión sobre la publicación o no del mismo. Los manuscritos deberán acompañarse de una carta firmada por todos los autores en la cual se declare que el trabajo es inédito; es decir, que el artículo ni parte de este ha sido publicado o está en vía de publicación en otra revista, y en la que se responsabilizan por la información publicada. Se entiende claramente que los trabajos enviados no están siendo considerados para su publicación en otros medios.

Criterios para la presentación de manuscritos

- La fuente de los manuscritos debe ser Times New Roman tamaño 12.
- No se admiten notas a pie de página.
- Título, centrado y en minúscula.
- Autor(es) con su respectiva filiación institucional y correo electrónico del autor principal.
- Resumen, *Summary* o Resumo. Incluye la justificación del estudio y los principales hallazgos y conclusiones, debe tener entre 50 y 200 palabras. Se debe incluir el título del artículo y el resumen en inglés (*Summary*) independiente del idioma del manuscrito.
- *Keywords* (debajo de *Summary*) y Palabras clave (debajo del Resumen) o Palavras chave (debajo de Resumo). De tres a seis palabras en minúscula, excepto la primera, y separadas por coma y espacio. Preferiblemente tomadas del Index

Medicus (http://www.nlm.nih.gov/mesh/meshhome.htm).

- En los manuscritos en español y portugués se empleará la coma (,) como separador decimal, en inglés se utilizará el punto (.).
- Los artículos se dividirán en las siguientes secciones: Introducción, Metodología, Resultados y Discusión, Conclusiones (si las hay), Agradecimientos, Conflicto de intereses y Referencias. Los títulos deben estar separados por dos espacios en sus partes superior e inferior, centrados y en negrilla. Los detalles acerca de la metodología experimental utilizada deberán ser lo suficientemente claros como para repetir la experimentación.
- Las tablas deben llevar numeración arábiga de acuerdo con el orden de aparición en el texto. El título debe ir en su parte superior y las notas en la parte inferior. En los encabezamientos de las columnas se deben anotar los símbolos de las unidades utilizadas.
- Las fotografías, gráficas, dibujos y esquemas se denominan 'figuras' y deben llevar numeración arábiga de acuerdo con el orden de aparición en el texto. El título debe ir debajo de las figuras.

De otro lado, los artículos relacionados con experimentación con animales deben ajustarse plenamente a los lineamientos éticos trazados por la Organización Mundial de la Salud. Los extractos o fracciones evaluados *in vitro* o *in vivo* deben definirse químicamente, cuando menos en cuanto a la clase de constituyente. El material vegetal deberá estar clasificado botánicamente.

Las abreviaturas de pesos y medidas serán las indicadas por la Farmacopea de los Estados Unidos en su edición oficial o unidades SI. Los datos espectroscópicos se deben presentar de la siguiente manera:

UV λ max (solvente ε) nm (log ε). Ej.: UV λ max (MeOH) 275 (log ε 2,94).

IR ν max (medio) cm^{-1}. Ej.: IR ν max (KBr) 1740, 1720 cm^{-1}.

EM *m/z* (% intensidad relativa). Ej.: em *m/z* (%): 340 (M^+, 100), 295 (10), 134 (26) ...

RMN ^1H (solvente, frecuencia de registro) δ ppm (integración, multiplicidad, J en Hz, asignación). Ej.: RMN ^1H ($CDCl_3$, 400 MHz) 3,84 (1H, *d*, J = 10,3 Hz, H-30).

RMN ^{13}C (solvente, frecuencia de registro) δ ppm (multiplicidad, asignación). Ej.: RMN ^{13}C ($CDCl_3$, 600 MHz) 16,60 (t, C-12).

Las abreviaturas usadas para describir la multiplicidad de las señales en RMN son: *s* = singlete, *d* = doblete, *t* = triplete, *m* = multiplete, *dd* = doble de dobletes, *ddd* = doble de doble de dobletes.

Las abreviaturas para los solventes y reactivos más comúnmente usados son: EtOH= etanol, MeOH = metanol, $CHCl_3$ = cloroformo, C_6H_6 = benceno, AcOEt = acetato de etilo, EP = éter de petróleo, Me_2CO = acetona, DMSO = dimetilsulfóxido, AcOH = ácido acético.

Se evitará el uso excesivo de tablas y figuras que estarán numeradas y que se anexarán en hojas separadas con su respectiva descripción

Referencias en los manuscritos

Las referencias se citarán en el texto con su respectiva numeración. Solo se pueden citar tesis y libros o artículos que hayan sido publicados. Deben incluir: autor(es), título de la publicación, año, volumen y páginas, así:

Revistas: Iniciales del nombre y apellido completo de todos los autores, título completo del artículo, nombre abreviado o nombre completo de la revista dependiendo si aparece en el Chemical Abstract o en índices equivalentes. El nombre de la *revista debe ir en letra itálica*, **volumen en negrilla**, páginas inicial y final, y año entre paréntesis. Ej.:

1. H.P. Baden, L.A. Goldsmith, B. Fleming, A comparative study of the physicochemical properties of human keratinized tissues, *Bioch. Biophys. Acta*, **322**, 269-278 (1973).

Comunicaciones personales: Iniciales del nombre, apellido completo e institución, seguido por las palabras comunicación personal y el año. Ej.:

2. A.J.M. Leeuwenberg, Agricultural University, Wageningen, Holanda, comunicación personal, 1984.

Libros: Iniciales del nombre y apellido completo de los autores, título del libro entre comillas, editorial, ciudad, año, volumen y página. Ej.:

3. D.R. Morris, "The Biochemistry of Disease", Morris et Marton Eds., London, 1981, Vol. 8, p. 223.

Capítulos de libros escritos por varios autores: Iniciales del nombre y apellido completo del autor, título del capítulo, seguido de: En: título del libro entre comillas, editores, editorial, ciudad, año, volumen, páginas. Ej.:

4. A.D. Elbein, R.J. Molyneux, The chemistry and biochemistry of simple indolizidine and related polyhydroxy alkaloids. En: "Alkaloids: Chemical and Biological Perspectives", Ed. por S.W. Pelletier, Wiley, New York, 1987, Vol. 5, pp. 1-54.

Tesis: Iniciales del nombre y apellido completo de los autores, *título en cursiva*, Tesis de..., institución, ciudad, año, páginas. Ej.:

5. F. Salcedo, *Contribución al estudio de las Cinchonas colombianas*, Tesis de Grado, Universidad del Valle, Cali, 1983, pp. 14-16.

Referencias de Internet: Iniciales del nombre y apellido completo del autor, título del documento, dirección URL y fecha de revisión. Ej.:

6. Lipidat, Lipid thermotropic phase transition database, Ohio State University, URL: http://www.lipidat.chemistry.ohio-state.edu, consultado en septiembre de 2001.

La correspondencia puede enviarse a la siguiente dirección o al correo de la revista *rcciquifa_fcbog@unal.edu.co*

Comité Editorial

Revista Colombiana de Ciencias Químico-Farmacéuticas
Departamento de Farmacia
Facultad de Ciencias
Universidad Nacional de Colombia

Cra. 30 N.° 45-03
Fax: 57-1-3165060

Bogotá - Colombia
Correo electrónico:
rcciquifa_fcbog@unal.edu.co

Dirección WEB:
http://www.revistas.unal.edu.co/index.php/rccquifa

Revista Colombiana
de Ciencias Químico-Farmacéuticas, 53(2)
se terminó de editar en Proceditor,
en mayo de 2024.
Bogotá, D. C., Colombia.